DESIGN AND SYNTHESIS OF NOVEL CNS BIOLOGICAL PROBES

By

Tamara Vasiljevikj

Submitted to the graduate degree program in Medicinal Chemistry and the Graduate Faculty of the University of Kansas in partial fulfillment of the requirements for the degree of Doctor of Philosophy.

_____

Chairperson: Dr. Thomas E. Prisinzano

_____

Dr. Brian S. J. Blagg

_____

Dr. Michael F. Rafferty

_____

Dr. Jon A. Tunge

_____

Dr. Jeffrey P. Krise

Date Defended: September 19, 2013

The Dissertation Committee for Tamara Vasiljevikj certifies that this is the approved version of the following dissertation:

DESIGN AND SYNTHESIS OF NOVEL CNS BIOLOGICAL PROBES

_____

Chairperson: Dr. Thomas E. Prisinzano

Date approved: September 19, 2013

ABSTARCT

Agents that exert their effects in the central nervous system are among the most important in medicinal practice. One in three Americans will have a disease affecting the nervous system in their lifetime exceeding $600 billion dollars per year in cost. Side effects, lack of efficacy, and lack of selectivity hamper their clinical use. Thus, additional agents need to be developed and new chemical tools are needed to further elucidate the mechanisms of CNS disorders.

Salvinorin A, the main component of the hallucinogenic mint *Salvia divinorum* is a novel and potent κ opioid (KOP) receptor agonist that is the first naturally occurring opioid ligand that lacks a basic nitrogen atom. In efforts to attain a greater understating for the interatctions of the furan ring binding pocket within the KOP receptor, several modifications were made at the C-13 position of the salvinoirn A scaffold. Pharmacological evaluations of the synthesized analogues indicated that there is a prefferred orientation of the furan *O*-atom in that the *cis* alkene analogue (**236**) had a greater binding affinity than the *trans* alkene analogue (**235**). However, despite its similar binding affinity to that of salvinorin A the *cis* analogue showed to 34-fold less active than salvinorin A.

It was also hypothesized that a combination of the salvinorin A scaffold with a similar terpene based family of marine natural products, namely the nakijiquinones, will alter the biological activity of salvinorin A and yield a useful biological probe. With this hypothesis in mind, several quinone containing salvinoirn A analogues were synthesized and upon pharmacological evaluation it was determined that these analogues did not exhibit any significant KOP receptor activity, indicative of a change in the biological activity of the salvinorin A

scaffold. Furthermore, these analogues proved to be the first salvinorin A based analogues that exhibit antiproliferative activity.

In the search for novel CNS biological probes, the aminoalkylindole class of synthetic cannabinoids was also investigated. Due to its cannabinoid 1 receptor (CB1R) antagonist activity, JWH-073-M4 was shown to be a valuable lead molecule. The hypothesis was that the design and synthesis of JWH-073-M4 based analogues would lead to compounds with dual CB1R antagonist/CB2R agonist activity that may have potential as alcohol abuse therapies. Upon *in vitro* pharmacological investigation, two analogues **461** and **444** were shown to have the most promise and were further subjected to *in vivo* pharmacological evaluation in animal models of alcohol abuse, namely ethanol self-administration and ethanol conditioned place preference. From these studies it was determined that analogues **461** and **444** exhibit dual CB1R antagonist/CB2R agonist activity and represent potential leads in the ongoing search for novel alcohol abuse therapies.

ACKNOWLEDGEMENTS

I would like to thank Dr. Prather and Dr. Fantegrossi from the University of Arkansas Medical Center for allowing me to come down to Arkansas and be involved in the pharmacological evaluation of my own compounds as well as to experience the entire loop from synthesis to biology and pharmacology. I would also like to thank their lab members and my roommate Ben for showing me Little Rock and making my experience very enjoyable. Additional thanks to Dr. Richard B. Rothman and Christina M. Dersch as well as Dr. Navarro and his colleagues for performing many pharmacological evaluations on compounds herein. Thanks to Dr. Justin T. Douglas, Dr. Victor W. Day, and Dr. Todd Williams from the Molecular Structures Group for their extensive help with both NMR and mass spectroscopy and X-ray crystallography. Also I want to thank both Dr. Fantegrossi and Dr. Prather for being very instructive and helpful throughout our collaboration. Furthermore, I would like to thank the University of Kansas, especially the Medicinal Chemistry Department, all its faculty and staff for allowing me to become a member of the KU Med Chem team and for making my experinec at KU very memorable. Finally, I would like to thank my committee for their their time and insightfull comments throughtout my carreer at KU.

I have been blessed with the opportunity to visit many places and meet many great people that I have stayed friends over the years. Many thanks to my collegues from Regis University and Dickinson State University for all the good times we have shared over the years. A special thanks goes to Dr. Paula Martin, my college mentor for helping me take the next step in my education. Life in graduate school and in general would not have been the same without my colleagues from the Medicinal Chemistry Department, for which no words can explain the impact that they have had on my life, especiallyWilma nd Eva. A super very special thanks goes to Anthony, Nicolette, Chris, Denise, Kim, Karrie, Mike, Rachel, Andrew, Kurt, Marci, and Mark for making coming to lab an exciting adventure. I would like thank my mentor Tom and his lovely family for taking me in and becoming my family away from home. Thank you for the many holiday feasts and TV desert night and for making me a part of your family. And Boss, thank you for your help, support, encouragement throughout the years, and for allowing me to be who I am. Lastly, I would like to thank my parents Dragan and Vesna for their endless love and support and for encouraging me to pursue my dreams, even though that meant moving very far away from home. I cannot forget my little brother Uki, without whom I would not be the person I am today.

TABLE OF CONTENT

LIST OF TABLES

LIST OF FIGURES

LIST OF SCHEMES

CHAPTER 1: INTRODUCTION

Drug Development for CNS Disorders

Disorders of the central nervous system (CNS) represent some of the most devastating and widespread disorders worldwide. Presently over 1.5 billion people worldwide are affected by disorders of the CNS.[1] This accounts for a third of the global disease burden.[1] It has been projected that within the first 50 years of this millennium, the worldwide population of persons older than 65 years will raise from 6.9% of the total population to a staggering 15.9%.[2] This increase will equal to an extra billion elderly individuals worldwide, thus increasing the need for CNS pharmaceuticals for the treatment of chronic neurological disorders. It was estimated by the Pharmaceutical Research and Manufacturers of America Foundation (PhRMA) that the cost of serious mental illnesses has reached $317 billion annually in the Unites States alone, which includes health care expenses, disability benefits and lost wages.[3] The numbers are expected to increase considerably over the next few decades. For instance, the occurrence of Alzheimer's disease (AD) will increase by over 100% in the United States and Western Europe and by more than 300% in Latin America, China, and India.[3, 4]

Despite the growing need for CNS therapeutics, the success rate for CNS drug candidates in the clinic is relatively low compared to the industry average across other therapeutic areas. Only 8% of CNS drugs that enter clinical trials are approved by the Food and Drug Administration (FDA).[5] Some of the reasons for the poor representation of CNS therapeutics on the market are the immense complexity of the CNS itself, as well as the longer development time needed for the candidates to reach the drug market.[4, 6] The extended period needed for the development of a CNS drug candidates is due to the utter complexity of the brain; the

predisposition of CNS drugs to cause unwanted CNS-mediated side effects, and the presence of the blood-brain barrier (BBB).[4]

One of the greatest challenges that CNS researches face in the development of CNS therapeutics is the vast complexity of the human brain. An inter-connected network of circuits and subcircuits connects over 100 billion neurons and a trillion glial cells whose actions are mediated through electrochemical transmission across 10^{14} synapses.[6] Additional factor to the decreased success of CNS therapeutics is the challenge of penetration through the BBB in order to reach their therapeutic target. Only about 2% of CNS drug therapeutics can cross the BBB and reach their target within the CNS, which greatly constrains their potential of becoming successful in the clinic.[7]

Challenges in CNS Drug Discovery

There are several protective barriers around the CNS that shield the brain from foreign xenobiotics, while maintaining homeostasis. Two of those include the BBB and the blood-cerebrospinal-fluid barrier (BCSFB).[8] The brain requires a vast amount of energy that comes in the form of oxygen and glucose and is delivered by a great network of blood vessels. These blood vessels are comprised of endothelial cells that contain tight intercellular junctions that control any passage of foreign substances through the BBB making it very difficult for CNS therapeutics to reach their intended target. The presence of these tight junctions leads to minimal paracellular transport and negligible pinocytosis making it very challenging for small molecules to pass through.[9, 10] As a second line of defense aside from the tight junctions, these cells are

also equipped with uptake and efflux transporters.[8] The most prevalent efflux transporter is the P-glycoprotein (P-gp) transporter. Pgp, a 170 kDa protein, is a member of the adenosine

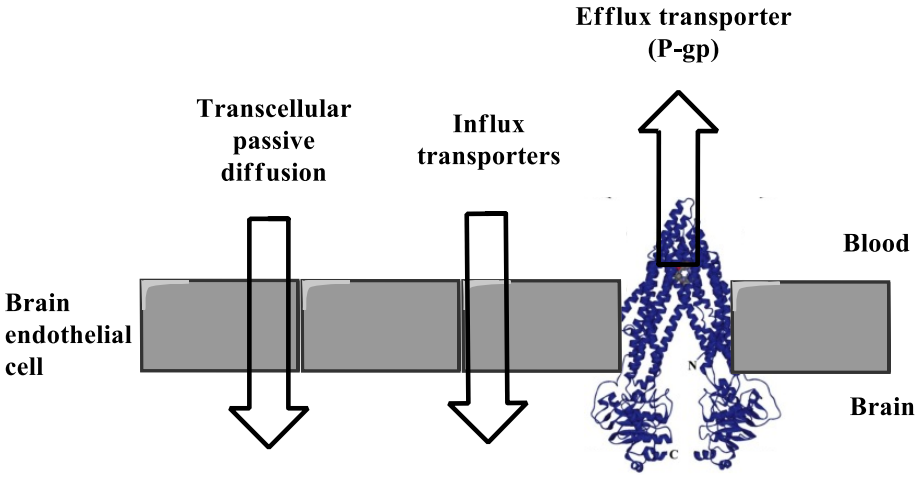

Figure 1. Mechanisms for BBB penetration[9]

triphosphate (ATP)-binding cassette (ABC) superfamily and it represents an additional obstacle to small molecules attempting to enter the CNS and obtain appreciable concentration at their target site (**Figure 1**).[11]

There are several concepts that have to be taken into account for successful brain penetration and CNS drug discovery. One of the essential concepts in *in vivo* pharmacology is the free drug hypothesis, which consists of two parts.[12] The first part of the hypothesis conditions that pharmacological activity is directly correlated to the free (unbound) drug concentration at the site of action, and the second part states that when no drug transporters are present, the free drug concentration at state is equal across all biomembranes.[7, 12] Because of the difficulty of measuring free drug concentrations in the brain, several surrogate measures have been employed to estimate the free drug concentration and use it to elucidate the pharmacological effect.[13] The second concept of importance to brain penetration is the unbound

brain-to-plasma ratio ($K_{p,uu}$). This parameter is of importance because with it one can evaluate the presence of distribution equilibrium between blood and brain compartments and because it is also reflective of the collective influence of BBB passive permeability and transporters.[7] When a compound is at a distribution equilibrium between plasma and brain compartments, the $K_{p,uu}$ value is near 1 and this is indicative of a compound that has good passive permeability and is not a substrate for transporters.[7] If a compound has a value that is significantly less than 1 that indicates that the compound in question is a substrate for efflux transporters. On the other hand, when a compound has a $K_{p,uu}$ value that is higher than 1 it is suggestive of a compound that is involved in active process and is a substrate for influx transporters.[7] When evaluating the unbound brain-to-plasma ratio, one should refrain from using total brain-to-plasma ratio because this ratio is mainly directed by nonspecific binding to lipids and/or proteins in the plasma and brain and it can lead to misleading conclusions regarding the biological activity.[9] The third concept of importance to brain penetration is the fraction unbound (f_u). This measurement is valuable in CNS drug discovery because it allows for the conversion of total drug concentration to unbound concentration in plasma or brain and it does not modify the unbound drug concentration *in vivo* for orally administered drugs.[7] BBB passive permeability (P_{app}) is the fourth concept of importance to brain penetration in CNS drug discovery. It is characterized by the rate across the BBB due to passive diffusion but not the extent of brain penetration.[7] Rapid establishment of distribution equilibrium between plasma and brain compartments is anticipated when BBB passive permeability is high; however this high BBB permeability is not indicative of a high unbound drug concentration within the brain.[7] In contrast, a low BBB passive permeability reduces the extent of brain penetration, which is due to limited diffusion absorption into the brain. However, when the P_{app} is extreme, that could be detrimental for CNS drugs

because a high BBB permeability is indicative of high lipophilicity, which could lead to non-specific binding, toxicity, rapid metabolism and low unbound drug concentration in the brain.[12, 14] Efflux ratio (ER) is the fifth and last concept of importance to brain penetration and CNS drug discovery. It is reflective of the potential of a compound to be pumped out of the brain by BBB efflux transporters like P-gp. It is very difficult to predict the unbound drug concentration of an efflux transporter substrate in the brain, thus making it dangerous for the advancement of such compound further in the drug discovery process.[7]

Understanding the challenges that are present in CNS drug development and discovery will allow us to better design molecules that will have a higher degree of success in the clinic. In addition, the concepts discussed represent critical parameters that may not be overlooked when designing CNS active molecules.

Target Product Profile of a CNS Drug Candidate

In order for successful CNS drug discovery, several physicochemical properties have to be taken into account when designing molecules. The physicochemical and biological properties of a molecule play a fundamental role in the successful absorption, distribution, metabolism, and excretion (ADME) profile of a molecule. **Table 1** lists the various physicochemical properties that should be considered in CNS drug development and are based on CNS orally active drugs.

Table 1. List of physicochemical properties for a CNS drug candidate.[6]

Physicochemical properties of a CNS drug candidate	Target profile
Desired potency at molecular target (nM)	<10
Selectivity over other targets	>30
Molecular weight (D)	<450
Aqueous solubility	>60μg/mL
pKa	Neutral or basic (7.5-10.5)
Lipophilicity	*c*logP < 4
Presence of N-atoms	At least one
Number of linear chains	<7
Volume of molecule	740-940 $Å^3$
Polar surface area	<70 $Å^2$
H-bond donors	<3
H-bond acceptors	<7
Molecular flexibility	<8 rotatable bonds
Protein binding	K_D for serum albumin binding <30 μM
Metabolic stability	>80% remaining after one hour
Solvent accessible surface area	460-580 $Å^2$
CYP 450 enzyme inhibition	<30% at 30 μM
CYP2D6 metabolism	Minimal
CYP3A4 induction	No induction
P-gp activity	No substrate activity
BBB passive permeability	**High**: P_{app} >10 x 10^{-6} cm/s **Moderate**: P_{app} 2-10 x 10^{-6} cm/s
Pharmacokinetics	%F/Cl_p/MRT **Excellent**: >50/<25% Q_H/2-4 hours **Viable**: %F 10-50/25-75% Q_H/0.5-2 hours
*h*ERG inhibition (hERG IC_{50} and effective unbound plasma concentration)	>30 fold

The molecular weight (MW) of CNS drugs was seen to be significantly reduced as compared to the MW of non-CNS therapeutics. It has been suggested that the MW should be below 450 Da with the objective of achieving acceptable brain penetration and to facilitate oral absorption.[15, 16] Lipophilicity is an important characteristic of a drug molecule and it directly relates to the ability of a molecule to cross the BBB and reach its target. Hansch and coworkers found that for several classes of CNS drugs, optimal BBB penetration is achieved when the

*c*logP is in the range of 1.5-2.7.[17] Hydrogen-bond (H-bond) acceptors are defined as heteroatoms that possess one or more lone pairs of electrons and that the ideal number of H-bond acceptors is less than 7.[6, 18] On the other hand, H-bond donors are defined as heteroatoms with one or more hydrogen atoms and the ideal number of H-bond donors for viable BBB penetration is less than 3.[6, 18] It was reported that a sum of all heteroatoms in a molecule should be less than 10 for suitable CNS penetration.[19] Increased hydrogen bonding both through H-bond donors and H-bond acceptors such as the hydrogen bonding seen in larger peptides is detrimental to CNS penetration and decreases BBB passive diffusion.[20] The degree of polarity of a given molecule can also be predicted through polar surface area (PSA) calculations and it has been used as a predictor of BBB penetration by many CNS drug discovery programs. Generally, CNS active drugs tend to have lower PSA (60-70 $Å^2$) when compared to other classes of therapeutics.[16, 21] The flexibility of a drug molecule refers to the number of rotatable bonds present and it goes along with another parameter, namely the molecular volume, which takes into account all of the accessible conformations available under physiological conditions.[15] The ideal molecular volume for a CNS active compound is in the range of 740-970 $Å^3$ and the ultimate number for rotatable bonds in a molecule is less than 8.[6, 15] There is a well acknowledged fact regarding pKa of CNS active compounds, which is that CNS active molecules have a basic center.[22] From an analysis of 119 marketed CNS drugs and 108 Pfizer CNS drug candidates, it was determined by Wager and coworkers that the mean pKa for a CNS active compound is 8.4.[22] As mentioned above, P-gp efflux transporters represent one of the challenges in BBB penetration and delivery of drug to target. Because of its role as a gatekeeper, P-gp is very promiscuous against numerous chemical structures. It has been very difficult to foresee whether a compound will be a P-gp substrate; however a rule of 4 was formulated to predict P-gp efflux liability.[23] The rule of 4

suggests that a compound with MW of less than 400 Da, total number of nitrogen and oxygen atoms less than 4, and whose pKa is less than 8 will not be a P-gp substrate.[23] Although some molecules that are CNS active may exceed one of these criteria, the rule of 4 may be used as an indicator of approaches that can be applied to decrease efflux by P-gp.

Rapid metabolism by the liver and intestines represents one of the main reasons for compounds not achieving satisfactory systemic levels. Low metabolic stability of a compound is indicative of high clearance rates and short half-life. The ideal metabolic stability is considered to be greater than 80% remaining at 60 minutes when evalated in a microsome test system.[15] The major metabolizing family of enzymes responsible for biotransformation of drugs and their pharmacological and toxicological effects is the cytochrome P450 superfamily. There are several isoforms that are responsible for the majoring of xenobiotic metabolism and they include CYP3A4, CYP2C9, CYP2D6, CYP1A2, and CYP2C19.[24] Concentration between 10 and 30 μM of drug that inhibits the metabolic activity by less than 50% is considered an acceptable level of CYP inhibition.[6, 15] In order for a compound to be a successful CNS drug and to maximize oral absorption it must have no significant CYP2D6 metabolism and not be an inducer of CYP3A4.[15] Being highly protein bound is unfavorable for a CNS drug because high protein binding will likely affect efficacy. Human serum albumin (HSA) and α_1-acid glycoprotein (AGP) are the plasma proteins most often bound by weakly basic molecules.[15] A successful CNS molecule should exhibit K_d lower than 30 μM.[6] A critical property for the unsuccessful drug discovery of any compound is the interference with the human ether-a-go-go related gene (*h*ERG). This gene encodes for a cardiac potassium channel and upon inhibition there is a risk of ventricular tachyarrhythmia also known as prolongation of the QT interval or torsade de pointes (TdP).[25] In order for a compound to avoid interactions with the *h*ERG channel, a greater than 30-fold margin

between *h*ERG IC_{50} and the drugs effective plasma concentration must be achieved.[25] Passive apparent permeability (P_{app}) is a measure of the permeability across the BBB and it is usually attained using the MDCK cell line, which is an epithelial cell line that spontaneously forms confluent polarized monolayer of cells.[22] A highly permeable molecule is considered to have $P_{app} > 10 \times 10^{-6}$ cm/s, whereas a moderately permeable molecule has a passive apparent permeability of $2.5 < P_{app} \leq 10 \times 10^{-6}$ cm/s.[22]

The target product profile for a CNS drug candidate consists of complex parameters all of which can be applied in the modification and SAR of drug candidates with the intention of enhancing the successful development of future CNS therapeutics.

Central Nervous System Disorders and Treatments

The quality of life for those affected by CNS disorders is profoundly reduced.[1] It has been projected than by year 2020, the total global burden of CNS disorders will rise from 11% seen in 1990 to 15%, a value that represents a proportionally larger increase than that projected for cardiovascular disease.[26] CNS disorders can be divided into two broader categories: CNS disorders that cause neurodegeneration and CNS disorders that do not cause neurodegeneration.[1]

Neurodegeneration causing CNS disorders are characterized by the gradual and progressive loss of cells from the spinal cord and brain and include chronic neurodegenerative disorders that cause dementia, Alzheimer's disease, multi-infarct dementia, frontotemporal lobar degeneration, Lewy body dementia, Parkinson's disease, amyotrophic lateral sclerosis and Huntington's disease.[1] In this group of CNS disorders are also demyelinating disorders such as

multiple sclerosis. Additionally, acute neurodegenerative disorders of the CNS are furthermore part of this group and include stroke, traumatic brain and spinal cord injury, as well as infectious meningitis and meningoencephalitis.[1]

CNS disorders that do not cause prominent neurodegeneration represent a diverse group of disorders and include obesity, neuropathic pain, as well as acute and chronic pain, migraine, anxiety, depression, bipolar disorder, schizophrenia, epilepsy, drug abuse, substance abuse, attention deficit hyperactivity disorder (ADHD), insomnia, and autism.[1]

Neurodegenerative CNS disorders

Alzheimer's disease

The International Alzheimer's Disease Society has reported that approximately 36 million people worldwide were living with dementia in 2010.[27] Dementia is detrimental to the people that suffer from it as well as their caregivers and families. It represents one of the major causes of disability and dependence among the aging population worldwide.[28] This number of people suffering is expected to increase to 66 million by the year 2030 and staggering 115 million people by the year 2050.[27] One of the most common causes of dementia is Alzheimer's disease. Alzheimer's disease (AD) was first described by Dr. Alois Alzheimer in 1907.[29] This form of dementia is characterized by several pathological markers in the brain such as formation of amyloid plaques, neurofibrillary tangles, and neuronal cell loss.[30] Hardy and Higgins suggested the amyloid cascade hypothesis that states that the deposition of amyloid plaques is the causative agent of Alzheimer's pathology.[30] The neurofibrillary tangles, cell loss, dementia

follow as a direct consequence of the amyloid plaque deposition.[30] Several treatments for AD are currently available on the market. **Table 2** includes the current treatments for AD and their mechanism of action and **Figure 2** contains the structures of the current AD treatments.[31]

Table 2. Current Alzheimer's disease treatments

Compound	Commercial name	Mechanism of action	Effect
Donepezil	Aricept®	Acetylcholinesterase inhibitor	Increases cortical acetylcholine (ACh) through selective reversible inhibition of hydrolysis of acetylcholine by acetylcholinesterase (AChE)
Galanthamine	Reminyl®	Acetylcholinesterase inhibitor	Increases ACh by reversible, competitive inhibition of AChE. Also, acts as an allosteric modulator of nicotinic acetylcholine receptors
Rivastigmine	Exelon®	Acetylcholinesterase inhibitor	Increases Ach by reversible inhibition of AChE. Inhibitor of butylcholineserase
Memantine	Ebixa®	NMDA glutamate receptor inhibitor	Reduces activity of glutamergic system through non-competitive inhibition of glutamergic NMDA receptors

As represented in **Table 2**, three out of the four treatments currently available on the market are acetylcholinesterase (AChE) inhibitors and they do not specifically target the underlying pathology of the disease. The reason for this is that cholinergic function is compromised in AD patients following early damage of basal forebrain cholinergic neurons.[32] Several disease-modifying candidates are currently ongoing clinical trials, however the need for novel approaches in treating AD is on the rise.[32]

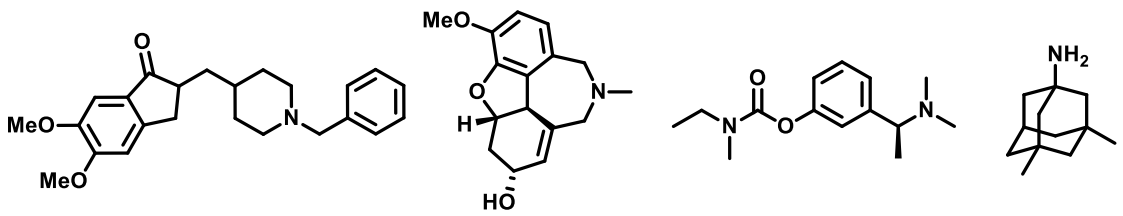

1 Donepezil **2** Galanthamine **3** Rivastigmine **4** Memantine

Figure 2. Structures of currently used AD treatments

Parkinson's disease

Parkinson's disease (PD) was first described as a neurological illness by James Parkinson in 1817.[33] Today, it is the second most common neurodegenerative disease affecting 1% of people over 60 years in developed countries.[34] Parkinson's disease employs debilitating symptoms that include resting tremors, rigidity, bradykinesia, and postural problems in younger patients.[35] Degeneration of dopamine neurons in the substantia nigra, as well as alterations to the striatum and frontal cortex are believed to be the underlying causes for the symptoms seen in PD patients.[35] The neurodegeneration observed has been linked to oxidative stress, excitotoxicity, apoptosis, inflammation, and mitochondrial dysfunction.[33] Manifestation of motor symptoms is seen with the degeneration of 60-80% of dopaminergic neurons and is considered a late stage diagnosis because the damage of the neurons has already occurred. There are several treatments available on the market for the treatment of PD, however the need for early detection of PD development in patients before pronounced loss of neurons still persists.[35]

Table 3. Currently available representative PD therapies[6]

Compound	Commercial Name	Mechanism of action	Effect
Levodopa (L-Dopa)/Carbidopa	Sinemet®	DA precursor/aromatic L-amino acid decarboxylase inhibitor	Increase dopamine (DA) concentration/decrease peripheral DA side effects
Apomorphine	Apokyn®	Non-selective D_1, D_2 receptor agonist	Increase DA concentration and reduction of L-Dopa induced dyskinesia
Trihexyphenidyl	Artane®	Antimuscarinic	Muscarinic receptor antagonist
Rasagiline	Azilect®	MAO-B irreversible inhibitor	Inhibition of the breakdown of DA in the mitochondria
Pramipexole	Mirapex®	D_2, D_3, D_4 receptor agonist	Restoring DA signals by stimulation of underfunctioning DA receptors in the striatum
Tolcapone	Tasmar®	Cathechol-O-metyl transferase inhibitor	Strengthen dopaminergic neurotransmission
Bromocriptine	Parlodel®	D_2 receptor agonist	Activation of DA receptors

Treatments currently (**Table 3**) present on the market employ several mechanisms of action the most common being the use of dopamine (DA) receptor agonists to counteract the seen DA loss in PD patients.

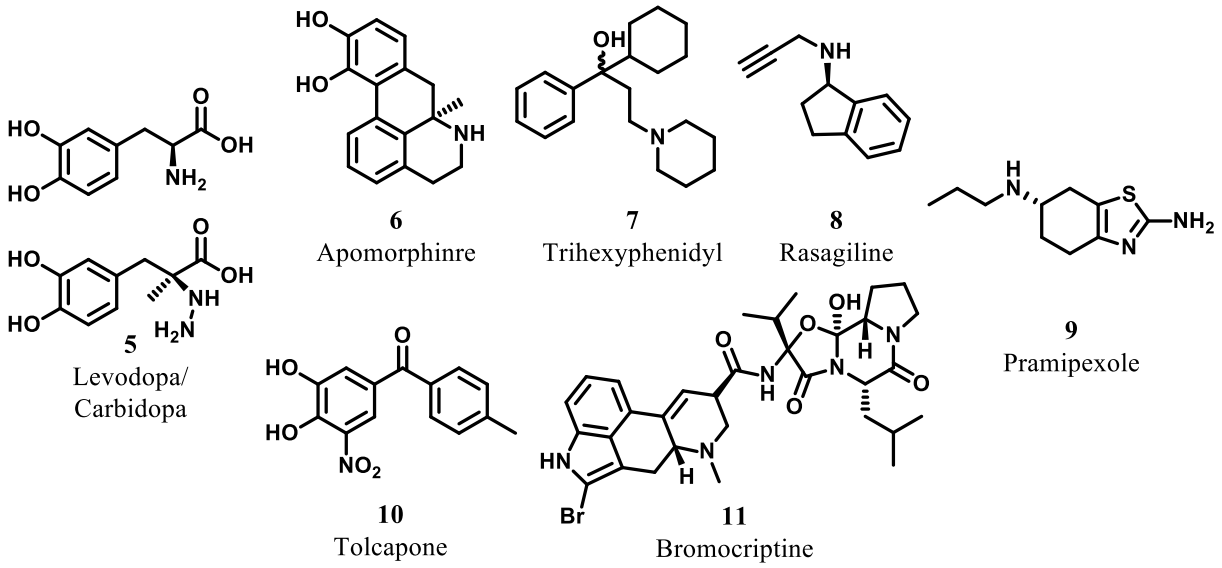

Figure 3. Representative structures of currently used PD treatments

The most effective treatment in controlling the motor symptoms presented with PD is the drug combination Sinimet®, which contains the DA precursor Levodopa (**5**) and the aromatic-amino acid decarboxylase inhibitor Carbidopa (**5**, **Figure 3**).[35] Other treatments include monoamine oxidase inhibitors, such as rasagiline (**8**). These inhibitors can be recognized as useful disease-modifying agents, because of the effect that they have on the stabilization of mitochondria, as well as the induction of the expression of neurotrophic factors.[36] The present treatments offer some comfort and provide symptom relief for patients suffering from PD, nonetheless early diagnosis that identifies the development of PD before degeneration arises is necessary.

Amyothrophic Lateral Sclerosis

Alongside Alzheimer's and Parkinson's disease, Amyothrophic lateral sclerosis (ALS), also known as Lou Gehrig's disease, is one of the major neurodegenerative CNS disorders.[37] ALS is very progressive neurodegenerative disease that leads to the dysfunction and death of

motor neurons in both the motor cortex and spinal cord.[38] One in every 100,000 individuals worldwide has been affected by ALS.[38] Of those affected, 90% of the cases are classified as sporadic (sALS) and the other 10% are classified as familial (fALS).[38] ALS is an extremely progressive disease with 50% of affected patents dying within 3 years of onset.[37] Currently, only one drug, riluzole (**13**, **Figure 4**) is available on the market for the treatment of ALS (**Table 4**).

Table 4. Currently available treatments for ALS

Compound	Commercial Name	Mechanism of action	Effect
Riluzole	Rilutek®	Sodium channel blocker	Reduction of Ca^{2+} influx which indirectly prevents stimulation of glutamate receptors

Riluzole is a neuroprotective drug that slows down the progression of ALS with the blockade of voltage-gated sodium channels and NMDA-receptor mediated responses, thus preventing excess calcium ion influx into neurons.[39, 40] Mutations of the superoxide dismutase (SOD) protein have been shown to be the cause of 10-20% of all familial ALS cases.[41] Arimoclomol has shown to delay disease progression and extend the lifespan of mice with a SOD mutation, a model for ALS.[41] Arimoclomol (**13**) is currently in phase III clinical trials as a heat-shock protein coinducer.[38] Another compound, edaravone (**16**) a free radical scavenger, is also currently in phase III clinical trials. It was demonstrated that in ALS mouse models it slowed disease progression, motor neuron degeneration and reduced abnormal SOD1 deposition.[42] Ceftriaxone (**15**), a β–lactam antibiotic was shown to increase brain expression of the glutamate transporter, GLT1 and its biochemical and functional activity, important features because these transporters are important in preventing glutamate neurotoxicity.[43] In addition to

the agents already discussed cholesterol like compound olesoxime (**14**), is also currently in clinical trials for the treatment of ALS and spinal muscular atrophy. It was determined that this compound targets proteins of the mitochondrial membrane, which in turn prevents permeability transition pore opening mediated by oxidative stress.[44] Progress has been made and there are several agents currently in phase III clinical trials, however further research into the palliative care and symptom control is still of significance for the enhancement of the quality of life for those patients suffering from ALS.[37]

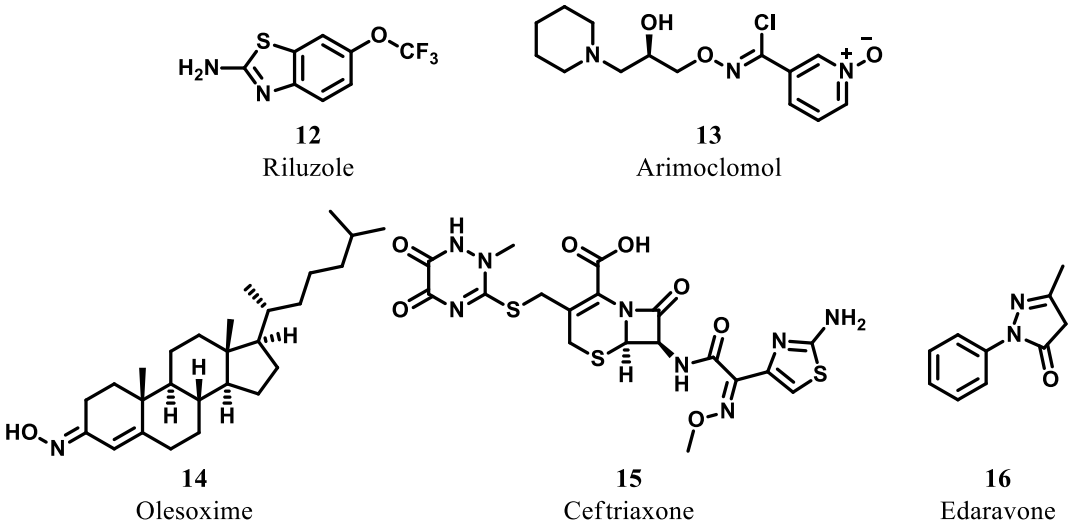

Figure 4. Commercially available ALS treatment, Riluzole and several phase III clinical trial candidates

Huntington's Disease

Huntington's disease (HD) is an autosomal, dominant neurodegenerative disorder that is caused by the expression of the anomalous Huntingtin protein. Huntingtin is a protein that is expressed in all humans; however in HD patients this protein contains an atypically lengthened polyglutamine region near its *N*-terminus.[45, 46] HD is characterized by very devastating set of

symptoms which include progressive motor dysfunction, emotional disturbance, dementia, and weight loss.[47] The incidence of HD worldwide is 5 to 10 cases per every 100,000 individuals.[48] The symptoms of HD are such that treatment is personalized for each patient and cannot be generalized for all individuals affected by HD.[49] Currently, there is no cure for HD, but there are several agents that can be used to relieve the severity of the symptoms presented with HD (**Table 5**).

Table 5. Agents used to treat symptoms of HD

Compound	Commercial Name	Mechanism of action	Symptom
Adamantine	Symmetrel®	NMDA antagonist/DA reuptake blocker	Chorea
Remacemide	Acovia®	NMDA antagonist	Chorea
Tetrabenazine	Xenazine®	VMAT inhibitor	Chorea
Mirtazapine	Remeron®	α_2 adrenergic receptor antagonist	Depression
Selisistat	Clinical trials	SIRT1 inhibitor	Neuroprotection
Cysteamine bitartrate	RP103/Clinical trial	–	–

Chorea is part of a group of neurological disorders, known as dyskinesia, and is characterized by uncontrolled involuntary movements of the body and is a symptom of HD. Several agents, adamantine (**17**), ramacemide (**18**), and tetrabenazine (**19**) are currently available for the treatment of HD chorea as seen in **Table 5** and as represented in **Figure 5**. Currently, there are several agents in clinical trials for the relief of the symptoms of HD. AMR101 is currently in phase III clinical trials and is a pro drug of eicosapantenoic acid.[50] Its mechanism of action for the treatment of HD is currently unknown.[50] Sirtuin1 (SIRT1) is a NAD-dependent deacetylase that has been implicated in the deacetylation of huntingtin.[51] Selisistat, a candidate in phase II clinical trials has been reported to be the first-in-class inhibitor of the SIRT1

deacetylase and was demonstrated to possess protective effects against HD in cellular and animal models of HD and has also been suggested to increase mutant huntingtin clearance.[52] The progress with animal models and present symptomatic treatments provide for optimism for patients and families affected by HD.

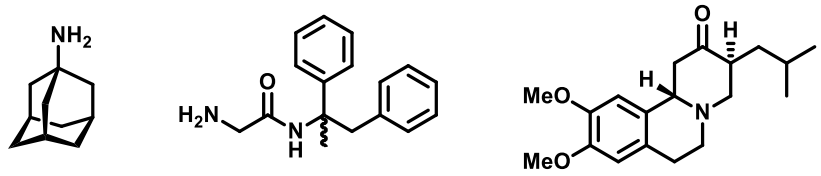

17 Adamantine **18** Remacemide **19** Tetrabenazine

Figure 5. Representative structures of currently used HD treatments

Non-neurodegenerative CNS Disorders

Schizophrenia

Schizophrenia, a non-neurodegenerative CNS disorder is among the world's top ten causes of long-term disability.[53] The incidence of schizophrenia is 0.2-0.4 per every 1000 individuals, with and onset of the disease in the early adulthood in both men and women.[54] Psychosis, apathy, social withdrawal, and cognitive impairment, hallucinations, delusions represent several of the characteristics of this disorder.[53] These characteristics lead to impaired functioning in everyday life for patents affected by schizophrenia. Schizophrenia is the most incapacitating disorder among all of the psychiatric disorders and it necessitates an unbalanced share of mental health service.[53] For instance, it was estimated that that the total cost of schizophrenia in the United States alone is $62.7 billion, which includes $22.7 billion focused on direct healthcare costs.[55] Additionally, in the United States the total cost of schizophrenia

exceeds the cost of all cancers combined.[56] Great advances have been made in the treatment of schizophrenia and there are several drugs on the market that are used to treat the symptoms of the disease permitting patients to lead more fruitful lives (**Table 6**).

Table 6. Currently available treatments for schizophrenia[6]

Compound	Commercial Name	Class	Mechanism of action
Quetiapine	Seroquel®	Atypical antipsychotic	DA, 5-HT_{1A}, adrenergic, histamine and muscarinic receptor antagonist
Clozapine	Clozaril®	Atypical antipsychotic	5-HT and DA receptor antagonist
Risperidone	Riserdal®	Atypical antipsychotic	DA, 5-HT, adrenaline and histamine (H1) receptor antagonist
Olanzapine	Zyprexa®	Atypical antipsychotic	5-HT and DA receptor antagonist
Aripiprazole	Abilify®	Atypical antipsychotic	Partial agonist at DA and 5-HT_{1A} receptors and 5-HT_{2A} receptor antagonist
Ziprasidone	Geodon®	Atypical antipsychotic	Non-selective DA, 5-HT receptor, and adrenergic receptor antagonist
Perphenazine	–	Typical antipsychotic	Non-selective D1, D2 receptor antagonist

The most widely used drugs for the treatment of schizophrenia are antipsychotic drugs, because they decrease the hallucinations and delusions of patient suffering from schizophrenia and other neuropsychiatric disorders.[57] There are two main classes of antipsychotic drugs, typical and atypical. There are several ways to distinguish and classify the two classes of antipsychotic drugs but the most commonly used is the functional classification based on liability to cause extrapyramidal side effects (EPS). The extrapyramidal system is part of the motor system and is involved in involuntary reflexes and movement as well as modulation of movement.[58] With the use of antipsychotic drug, this system becomes affected and leads to the development of EPS, which were documented immediately after the introduction of

antipsychotic drugs as clinically used agents.[59] Four common EPS syndromes are recognized and the include: tardive dyskinesia, dystonia, akathisisa, and parkinsonism.[60] The atypical antipsychotic agents produce a markedly lower incidence of EPS and are now more widely used in the clinic. However, treatment with atypical antipsychotics has been associated with increase in body mass index and development of metabolic syndrome.[61] In addition to the treatments available on the market some of which include: quetiapine (**20**), clozapine (**21**), risperidone (**22**), olanzapine (**23**), aripiprazole (**24**), perphenazine (**25**), and ziprasidone (**26**), numerous novel atypical antipsychotic agents are in various stages of development (**Figure 6**). Consequently, efforts toward designing improved treatments for individuals suffering from this neurological disorder have markedly increased.

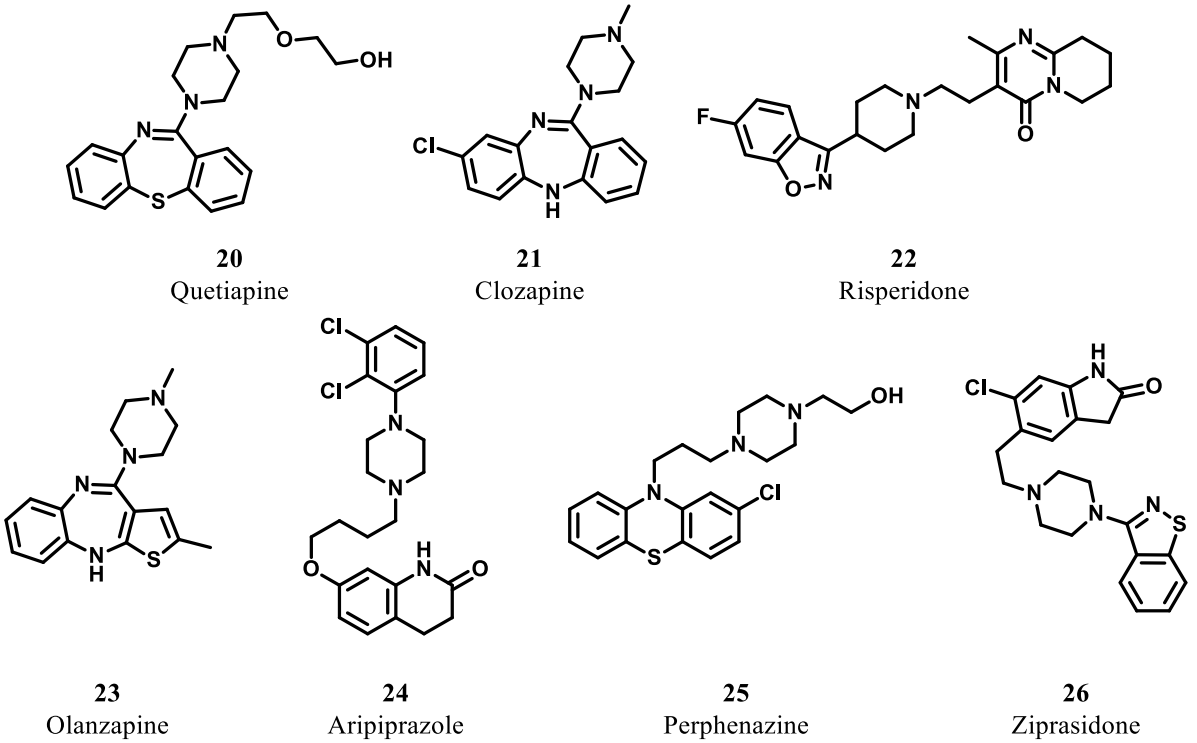

Figure 6. Representative structures of currently available treatments for schizophrenia

Epilepsy

Epilepsy is a brain disorder categorized by an lasting tendency to generate epileptic seizures.[62] This family of neurologic disorders arises with a projected frequency of around 50 per 100,000 individuals a year, mainly seen in infants and elderly people.[63, 64] If not treated timely, epilepsy leads to progressively impaired cognition and function, brain damage, and other neurologic deficits.[65]

Table 7. Currently available representative treatments for epilepsy[6]

Compound	Commercial Name	Class	Mechanism of action
Phenytoin	Dilantin®	Antiepileptic	Na^+ channel blocker
Gabapentin	Neurontin®	Antiepileptic	Neuronal Ca^{2+} channel blocker
Valproic acid	Depakote®	Anticonvulsant	Indirect agonist of $GABA_A$ receptor
Pregabalin	Lyrica®	Anticonvulsant	Neuronal Ca^{2+} channel blocker
Levetiracetam	Keppra®	Anticonvulsant	Indirect agonist of $GABA_A$ receptor
Topiramate	Topamax®	Anticonvulsant	Na^+ channel blocker
Carbamazepine	Tegretol®	Anticonvulsant	Na^+ channel blocker

Excessive and synchronous neuronal activity in the brain is the cause for an epileptic seizure.[66] Epileptic seizures are normally treated with antiepileptic drugs, which continue to be the main treatments for epilepsy. Despite their wide use, antiepileptic drugs are only effective in 60-70% of patients and their objective is to regulate seizures as quickly as possible without any adverse effects.[67]

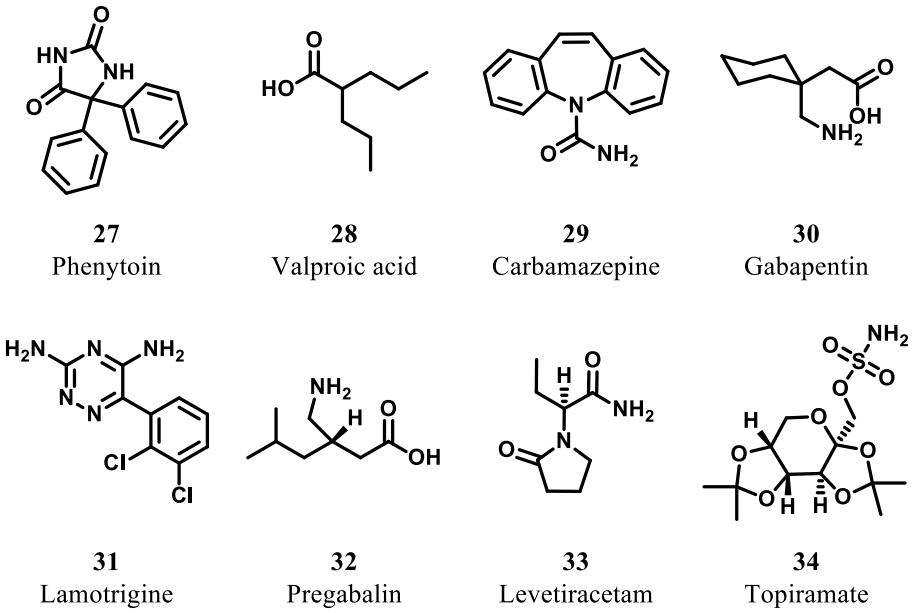

Figure 7. Structures of currently used epilepsy treatments

Antiepileptic drugs are used to prevent burst-firing of neurons, decrease excitation, and increase inhibition. Antiepileptics (**Figure 7**) widely used in the clinic include: phenytoin (**27**), valproic acid (**28**), carbamazepine (**29**), gabapentin (**30**), lamotrigine (**31**), pregabalin (**32**), levetiracetam (**33**), and topiramate (**34**). These currently used treatments for epilepsy involve compounds with various mechanisms of action, affecting different systems such as the GABAergic system, sodium and calcium ion channels.[62] Despite the fact that more than 20 antiepileptic drugs are licensed worldwide, about a third of patients suffering from epilepsy continue to experience seizures.[68] For these individuals, the only hope for improving seizure control is to be exposed to antiepileptic drugs that they haven't been exposed to before. Development of new agents is underway and great efforts are being focused at disease modification and symptom control.

Depression

The World Health Organization projected that by 2020, major depressive disorder (MDD) will become the second leading cause of disability worldwide.[69] Depression is a debilitating and life-threating mood disorder and it has been estimated that the burden for depression and related mood disorders is over $100 billion in the United States and €105 billion in the European Union (EU).[70] The prevalence rates of depression amount to 16% in the United States and around 30 million people in the EU.[71, 72] MDD is clinically characterized as heterogeneous mental illness with varying symptoms such as: anhedonia, feelings of helplessness, sadness and despair which can be caused from a combination of genetic and environmental factors.[73] Current treatments mainly target the reuptake and breakdown of monoamines (**Table 8, Figure 8**). This treatment strategy is based on the monoamine hypothesis of depression, which indicates that neurochemical imbalance directly causes the core of the symptoms seen in patients suffering from MDD.[74]

Table 8. Currently available treatments for MDD[6]

Compound	Commercial Name	Class	Mechanism of action
Bupropion	Wellbutrin®	Atypical antidepressant	Norepinephrine (NE) and DA uptake inhibitor
Fluoxetine	Prozac®	Antidepressant	Selective serotonin reuptake inhibitor (SSRI)
Venlafaxine	Effexor®	Antidepressant	Serotonin and norepinephrine reuptake inhibitor (SNRI)
Nortriptyline	Pamelor®	Tricyclic antidepressant	Norepinephrine inhibitor
Mirtazapine	Remeron®	Antidepressant	Adrenergic (α_2) receptor inhibitor
Trazadone	Desyrel®	Antidepressant	Serotonin antagonist and reuptake inhibitor
Sertaline	Zoloft®	Antidepressant	SSRI
Duloxetine	Cymbalta®	Antidepressant	SNRI

Since the development of the presently available antidepressant, the therapy for MDD has been revolutionized, however not all patients can benefit from the present treatments, especially those

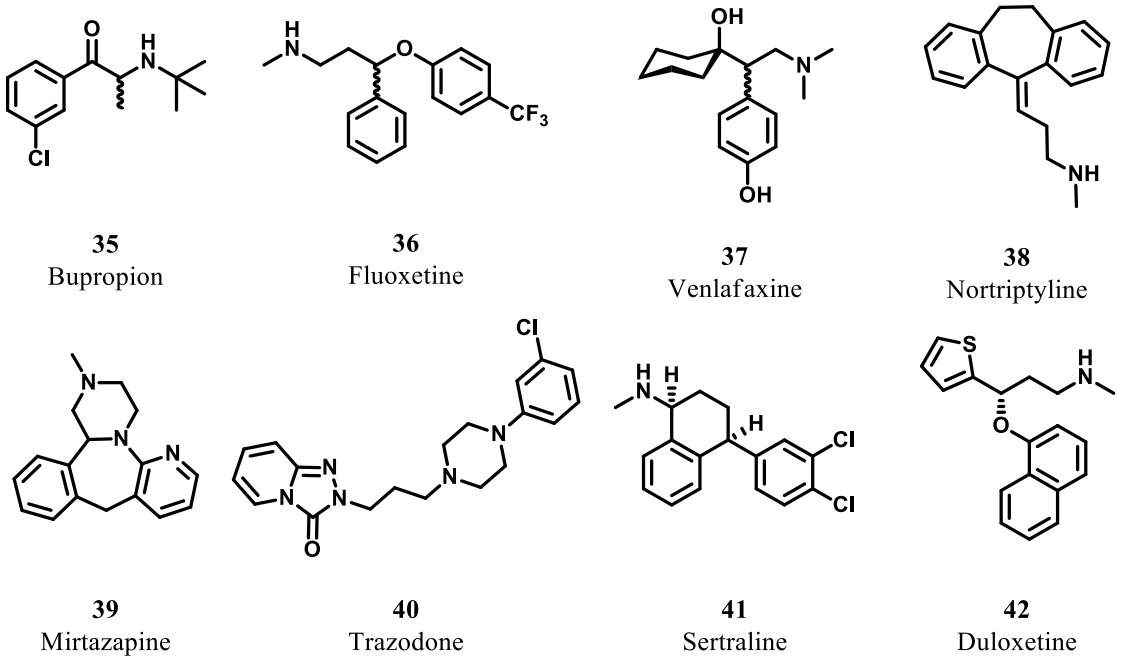

Figure 8. Representative structures of currently available treatments for MDD

those that suffer from treatment-resistant depression. Several additional drawbacks have been described for the antidepressants currently used in the clinic mainly bupropion (**35**), fluoxetine (**36**), venlafaxine (**37**), nortriptyline (**38**), mirtazapine (**39**), trazodone (**40**), sertraline (**41**), and duloxetine (**42**). They are characterized with a very slow onset of action requiring more then 3-4 weeks of treatment in order for mood improvements to be observed. Additionally, only about 30-50% of patients respond to the initial regimen indicating poor efficacy, 30% of patients are resistant to a series of treatments currently available, and many adverse effects have been reported from the use of the currently available antidepressants.[75-77] There is a growing effort in the discovery and development of agents that do not affect the monoaminergic system; in particular recent reports have introduced the glytaminergic system as a prominent target for the development of faster acting antidepressants.[70, 78]

Pain Management

One of the greatest medical challenges worldwide is pain management. For instance, in the United States alone, pain affects 116 million people, reducing quality of life with a burden of at least $636 billion annually.[79] Furthermore, pain affects more Americans than diabetes, heart disease and cancer combined; making it the most common reason for access to the health system.[80] Pain can be classified in four major categories: acute nociception, neuropathic pain, dysfunctional pain, and postoperative pain.[81] Acute, postoperative pain and several types of chronic pain are caused by the activation of the nociceptor, sensory receptor mainly found in the periphery that responds to noxious stimuli.[82] Being present in all tissues, nociceptors can be affected and can respond to several stimuli, such as mechanical, thermal, or chemical mediators

that are released from the surrounding tissue.[82] Taken together, these facts identify that the manifestation of pain is not only affected by the CNS, but can also stem from factors such as the environment, various life experiences, and gender.[82]

Non-steroidal anti-inflammatory drugs (NSAIDs) have been an important class of analgesic agents whose use has spanned for several centuries since the introduction of aspirin on the market in 1860.[83] The main use for NSAIDs has been for the treatment against inflammatory diseases, rheumatoid arthritis, osteoarthritis, dysmenorrhea, ischemic cerebrovascular disorders, and pain resulting from certain types of cancer.[84] In the early 1970s, John Vale reported the mechanism by which 'aspirin-like drugs' act, listing the inhibition of prostaglandin synthesis as their mechanism of action, a system believed to be involved with inflammation and pain.[85] In particular, the traditional NSAID agents were shown to be nonselective inhibitors of cyclooxygenase (COX) activity (**Table 9**, **Figure 9)**.

Table 9. NSAIDs used in the clinic

Compound	Commercial name	Class	Mechanism of action
Acetylsalicylic acid	Aspirin®	Salicylate	Non-selective COX-1/2 inhibitor
Diclofenac	Aclonac®	Arylacetic acid	Non-selective COX-1/2 inhibitor
Ibuprofen	Advil®	Aryl proprionic acid	Non-selective COX-1/2 inhibitor
Indomethacin	Indocin®	Heteroarylacetic acid	Non-selective COX-1/2 inhibitor
Celecoxib	Celebrex®	Coxib	Selective COX-2 inhibitor
Etoricoxib	Arcoxia®	Coxib	Selective COX-2 inhibitor
Lumiracoxib	Prexige®	Coxib	Selective COX-2 inhibitor

There are three main types of COX enzymes, COX-1 which is constitutively expressed throughout the body, COX-2, which is induced in response to inflammation and the recently

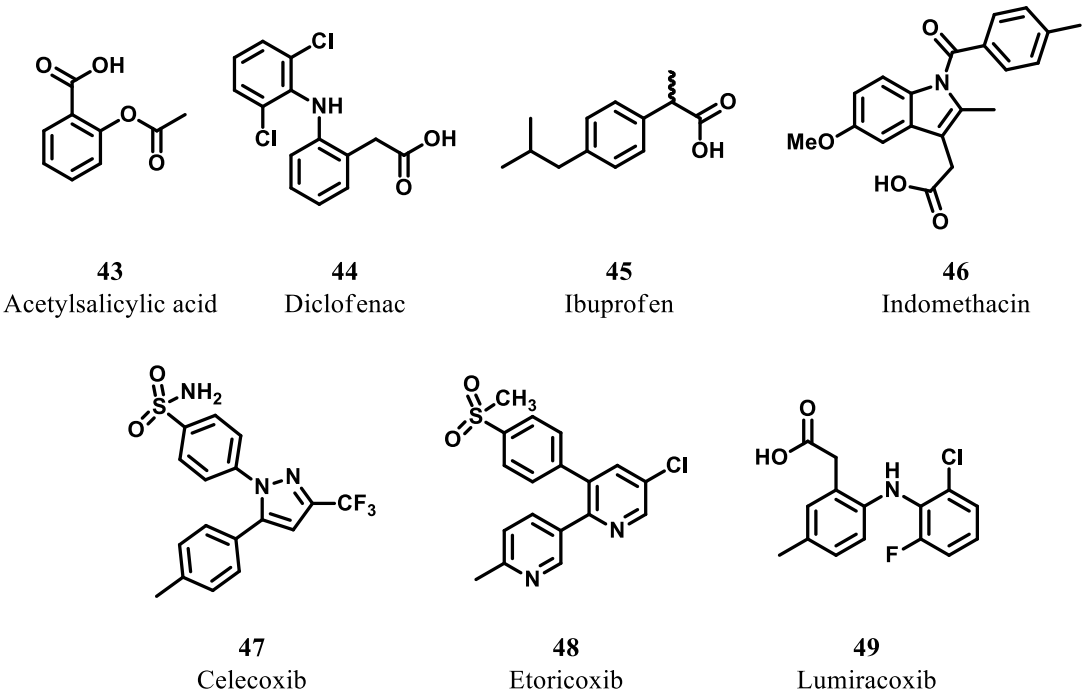

Figure 9. Structures of currently used NSAIDs

described COX-3, which is represented as an alternate splice variant of COX-1.[86-88] Because the traditional NSAIDs such as aspirin (**43**), diclofenac (**44**), ibuprofen (**45**), and indomethacin (**46**) are nonselective inhibitors of COX-1/2, long term use of these agents leads to severe gastrointestinal side effects.[89] The discovery of the inflammation inducible COX-2 isoform of cyclooxygenase has led to the development of selective COX-2 NSAIDs that have limiting gastrointestinal side effects. Members of the COX-2 selective class of NSAIDs currently available on markets worldwide include celecoxib (**47**), etoricoxib (**48**), and lumiracoxib (**49**).[90] Despite the better gastrointestinal adverse effect profile seen with the use of COX-2 selective agents, the use of these agents has been associated with cardiovascular side effects, thus

increasing the need for novel NSAIDs with more site-specific mechanism and reduced occurrence of unwanted side effects.[84, 91]

Opioid analgesics, in particular morphine and its derivatives, have been considered the "gold standard" for the treatment of severe acute or chronic pain and are generally used once primary treatment with NSAIDs does not lead to better pain management.[92] The use of morphine (**51**, **Table 10**), the principal agent responsible for the effects of the opium poppy, for the treatment of pain has been known for millennia.[93, 94] Despite its popularity, the structure of morphine, the active component of *Papaver somniferum* L. (Papaveraceae) was not proposed until 1923 by Gulland and Robinson.[95, 96] The structure of morphine was later confirmed with a total synthesis published by Gates and Tschudi in 1953.[97, 98]

Table 10. Examples of clinically used opioids

Compound	Commercial name	Class	Mechanism of action
Morphine	Contin®	Analgesic	MOP receptor agonist
Codeine		Analgesic/Antitussive	MOP receptor agonist
Hydromorphone	Dilaudid®	Analgesic	MOP receptor agonist
Oxycodone	OxyContin®	Analgesic	Non-selective opioid receptor agonist
Meperidine	Demerol®	Analgesic	MOP receptor agonist
Fentanyl	Sublimaze®	Analgesic/Anesthetic	Highly potent MOP receptor agonist
Methadone	Methadose®	Analgesic	MOP receptor agonist
Pentazocine	Fortral®	Analgesic	MOP antagonist/KOP agonist
Tapentadol	Nucynta®	Atypical analgesic	MOP agonist/NE and 5-HT reuptake inhibitor

Opioid ligands act at opioid receptors, which are G-protein-coupled receptors. There are three main types of opioid receptors: μ opioid (MOP) receptors, κ opioid (KOP) receptors, and δ

opioid (DOP) receptors.[99, 100] In general, the opioid receptors have been shown to couple to $G_{i/o}$ proteins, which results in a decrease in cAMP production resulting from inhibition of adenylate cyclase and decrease in intracellular calcium.[101, 102] It has been shown that in addition to various biological responses, each opioid receptor subtype has an effect on antinociception.[103] Each receptor differs in their density, distribution, and endogenous ligands.[104] Conversely, despite being the gold standard for pain management, physicians have become disinclined to prescribe opioids because of concerns concerning the serious and potentially life threatening adverse effects produced from long term opioid treatment.[92]

Alterations of the nervous, respiratory and gastrointestinal systems are among the most common side effects.[105] The most serious adverse effects seen with opioid analgesics use include constipation, respiratory depression, tolerance, and dependence and are thought to be associated with their agonist activity at the MOP receptors.[94] Nonetheless, opioids such as morphine (**50**), codeine (**51**), hydromorphone (**52**), oxycodone (**53**), fentanyl (**54**), methadone (**55**), and meperidine (**56**) still continue to be used as main prescription drug therapy for the treatment of pain and as antitussive agents (**Figure 10**). As seen in **Table 10**, most of the clinically used opioids exert their analgesic effect mainly through interactions with the MOP receptor. Thus, mixed agonist/antagonist ligands active at two distinct receptors can be thought to have a reduced risk for serious side effects such as those seen with MOP receptor agonist treatment. Pentazocine (**57**) is an opioid ligand exhibiting mixed agonist/antagonist activity interacting as an antagonist for the MOP receptors and an KOP receptor agonist that has a better side effect profile due to its antagonist activity at MOP receptors.[106] Tapentadol (**58**) is another mixed activity ligand that was recently approved for use in the clinic for the treatment for moderate to severe pain. It exerts its effects through MOP agonism and through the reuptake

inhibition of monoamines serotonin and norepinephrine.[107] With the intention of producing analgesics less attractive for non-oral abuse, pharmaceutical companies are investing in abuse deterrent of tamper-resistant formulations.[108] Such preparations include barriers to tampering that comprise of agonist-antagonists formulations, preparations that became increasingly viscous upon tampering, or modifying-release formulations.[108, 109] In addition to such formulations, antagonists can be used to reverse the effects of an drug overdose or to reverse the effects of postoperative sedation, an example of which is naloxone (**59**).[94] Moreover, peripherally active opioid antagonists are currently undergoing evaluation for treatment of constipation and other gastrointestinal effects associated with the use of opioid receptor agonists.[94]

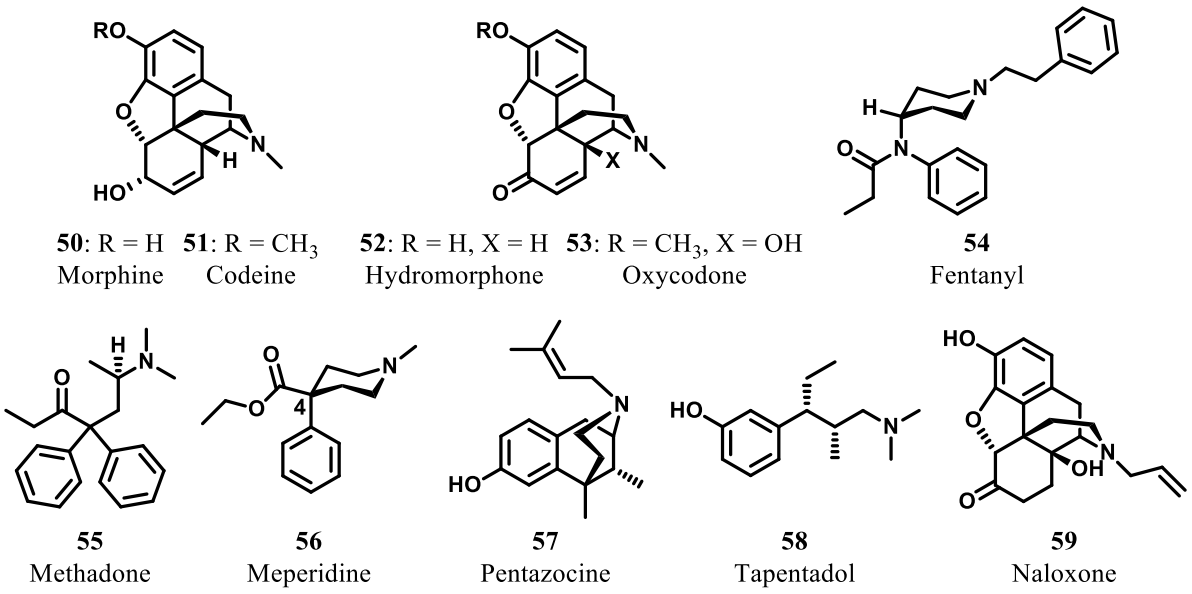

50: R = H **51**: R = CH_3 **52**: R = H, X = H **53**: R = CH_3, X = OH **54**

Morphine Codeine Hydromorphone Oxycodone Fentanyl

55 **56** **57** **58** **59**

Methadone Meperidine Pentazocine Tapentadol Naloxone

Figure 10. Examples of clinically used opioids.

Substance Addiction

Addiction represents a chronic, often relapsing brain disorder that causes compulsive drug seeking and affects all aspects of one's life. In the United States alone, the cost of drug and substance abuse, which includes health, crime related cost as well as productivity, is estimated at more than $600 billion annually, where $386 billion are attributed to illicit drugs and tobacco and $235 billion are attributed to alcohol abuse.[110-113]

The production of positive reinforcing effects that results from neurochemical actions after repeated drug use gradually lead to neurological changes in the brain reward circuits and behaviors characteristic of addiction: tolerance, sensitization, dependence, withdrawal and craving.[114] Tolerance and dependence often result from chronic use of opioids.[94] When continuous drug exposure leads to decreased effectiveness, a larger dose is required to achieve the same effect, thus leading to tolerance.[115] Physical dependence on the other hand, is a physiologically active state and its characterized by the presence of withdrawal symptoms upon abrupt cessation or significant reduction in dose.[115] Physical dependence and addiction should not be confused and interchanged. While physical dependence is defined by the appearance of withdrawal symptoms, addiction is defined as a chronic, compulsive and/or uncontrolled drug use despite significant harm to one's health and well-being.[115] Aside from alcohol, nicotine, and caffeine the most widely abused substances worldwide are the CNS stimulants cocaine and methamphetamine.[116] The use of these substances usually leads to considerable social decline, increase in crime rates as well as emergency room visit, and elevated rates of HIV, hepatitis B and C infections.[117]

Several treatments for drug and substance abuse are currently available on the market. These include nicotine replacement therapy, bupropion, and varenicline as treatments for

nicotine abuse; naltrexone, acamprosate, and disulfiram as therapy for alcohol abuse; and buprenorphine, methadone (**55, Figure 10**), naltrexone, and naloxone (**59, Figure 10**) as therapy for opioid abuse (**Table 11, Figure 11**).[118] Prominent efforts are being made in the discovery and development of novel treatments for substance abuse. Recent studies have explored the use of KOP ligands, in particular KOP receptor agonist as potential stimulant abuse therapeutics.[119] In addition to the KOP receptors as a target for the development of substance abuse therapy, research into sigma-1 receptors as potential target for substance abuse treatment has been on the rise.[120] Evidence has shown that the endocannabinoid system may play a role in the drug-seeking behaviors as well as in the mechanism that involves relapse, thus the endocannabinoid system represents another promising target for development of novel drug addiction therapy.[121, 122]

Table 11. Medications currently approved for substance abuse

Compound	Commercial name	Class	Mechanism of action
Bupropion	Wellbutrin®/ ®	Antidepressant/smoking cessation aid	DA reuptake inhibitor
Varenicline	Chantix®	Smoking cessation	Nicotinic receptor partial agonist
Naltrexone	Revia®	Alcohol dependence	Nonselective opioid antagonist
Acamprosate	Campral®	Alcohol dependence	NMDA receptor inhibitor and $GABA_A$ receptor agonist
Disulfiram	Antabuse®	Alcohol dependence	Aldehyde dehydrogenase
Buprenorphine	Buprenex®	Opioid addiction	MOP/KOP partial agonist, DOP antagonist

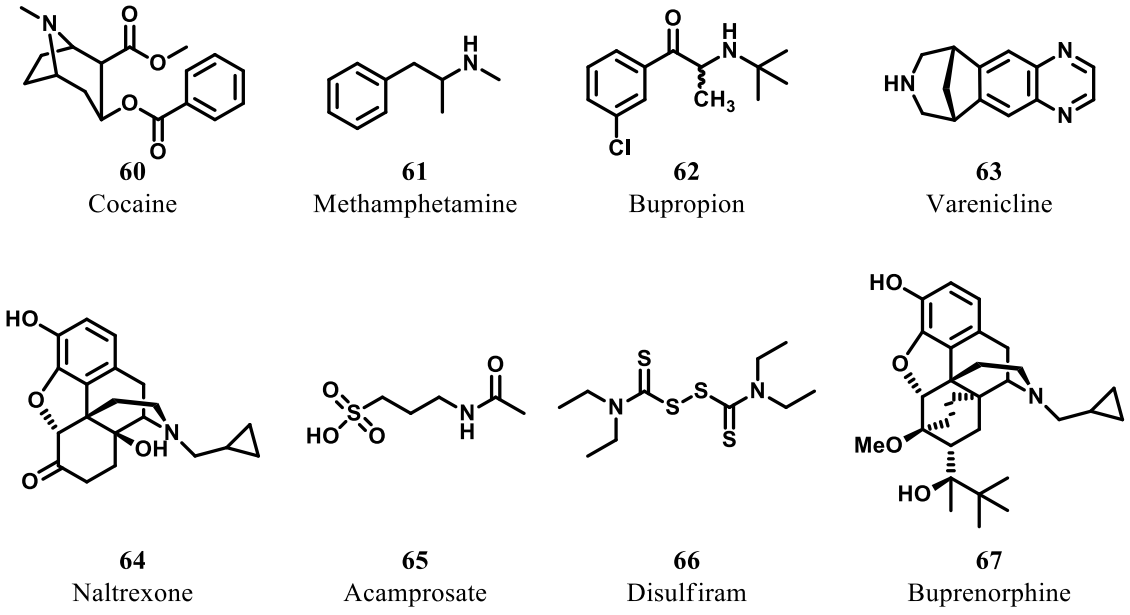

Figure 11. CNS stimulants cocaine and methamphetamine and currently available medications for the treatment of drug abuse and substance abuse

CNS disorders affect the lives of many individuals worldwide and can have devastating consequences to those affected and their families. Great efforts are being made in the discovery and development of novel CNS active agents that have potential to be utilized as CNS therapeutics. One area of research that offers great scaffold diversity is the area of natural products chemistry. Natural products have been used for centuries for their medicinal and spiritual purposes and evidence of their use as medicines dates back to the Mesopotamian pharmacopeia in 668-628 B.C.[123] Recent research has implicated salvinorin A, a KOP receptor agonist as a promising natural product for the development of CNS therapeutics for the treatment of pain and drug abuse.[124]

CHAPTER 2: SALVINORIN A

PART I: DESIGN AND SYNTHESIS OF STERICALLY CHALLENGED SALVINORIN A ANALOGUES

Natural Products as Traditional Medicines

Records indicate that humans have been using natural products for their medicinal, spiritual, and recreational purposes since ancient times.[125] The earliest records for the use of natural products in ethnomedicinal traditions date back to the ancient Mesopotamian civilizations.[126] Several of the Mesopotamian civilizations, namely the Babylonians and Assyrians were known to have outside pharmacies where clay-like tablets from natural product infusions and extracts were being dispersed to the ailing.[126] Evidence of trade dating back to 3000 B.C.E. linking Mesopotamia, Egypt, and southern Arabia involves aromatic woods, spices, aromatic gums, and myrrh all of which were used as medicines.[126] Additional evidence from other ancient cultures, such as China and India supports the notion that natural products had wide spread use in the ethnomedicinal traditions of many cultures. For instance, there are numerous references to a plant called *soma* that was used in rituals in ancient India.[127] Furthermore, ginseng and ephedra are the most well-known ethnobotanicals used in ancient Chinese medicinal practices and are still currently used to treat a variety of illnesses.[128] One of the most recognized medical documents is the *materia medica*, a text that was originally composed by a military physician under the Roman Empire in the 1st century AD, which contained the medicinal use of hundreds of plants was well preserved and copied with minor variations for centuries.[129] Lastly, the native aboriginal residents of the territories now known as Mexico recorded their use of

mind-altering natural substances from the dried leaves of the peyote cactus in their spiritual practices.[130] Evidence that natural products are still being used as ethnomedicines today lies in the fact that more than 80% of people worldwide still depend on traditional medicines.[131]

Natural Products and Modern Medicine

Plant species have been well documented for their medicinal use for thousands of years. Prior to the advent of pharmaceuticals, clay tablets and oils from various species such as *Cupressus sempervirens* (Cypress), *Commiphora* (myrrh), and *Glycyrrhiza glabra* (licorice) were used to treat coughs, colds, infections, and inflammation.[132] Natural products are secondary metabolites synthesized by many organisms in response to external stimuli such as stress, temperature, nutritional changes, infection and competition.[133] Natural products have played an important role in early drug discovery. For instance, the value of natural products as pharmaceuticals was originally realized with the discovery of penicillin (**68**) in 1928 (**Figure 12**).[133]

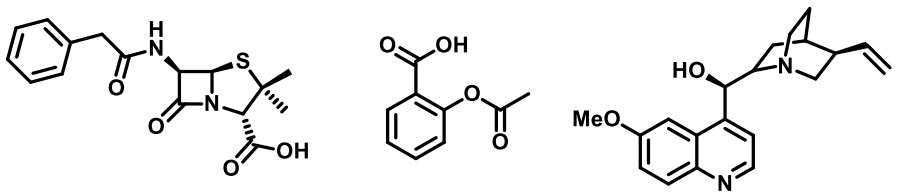

68
Penicillin G

69
Aspirin

70
Quinine

Figure 12. Representative traditional medicines still utilized in the clinic

Additionally, the isolation of the natural product salicin from the willow tree bark, eventually granted us with the discovery of aspirin (**69**), an anti-inflammatory agent that is still

widely used in the clinic.[134] Another example of the importance of natural products in current medicine was the isolation of the alkaloid morphine (**50**, **Figure 10**) from the opium poppy (*Papaver somniferum* L.), a natural product currently used for the treatment of severe pain.[135] Furthermore, the 1820 isolation of quinine from the *Cinchona* bark led to the development of additional antimalarial agents that together with quinine (**70**) are still used in the clinic to treat malaria.[136]

Natural products have greatly influenced modern medicine and the discovery and development of novel agents. In a study done by Newman and Cragg it was reported that out of the 1073 small molecule new chemical entities described from 1981-2010, 709 were natural products, natural product derived or influenced by natural products.[137] In 2008 alone, 225 natural products and natural product derivatives were in various stages of development, including preclinical, clinical and preregistration.[138] Natural products have also significantly assisted with our understanding for biologic pathways and therapeutic targets and they continue to further influence the pharmaceutical industry. The biosynthesis of natural products which can be produced by a variety of terrestrial and marine organisms is the key to the diversity of the chemical structures represented in natural products most of which possess an array of biological activities.[135] Natural products research has had an influence on the development of various biological agents including: (1) antimicrobials; (2) anti-cancer agents; (3) antimalarial; and (4) agents for pain management.

The discovery of penicillin G (**68**, **Figure 12**) by Alexander Fleming in 1928, initiated the golden age for antibacterial agents.[139] The discovery of penicillin's and sulfonamides in the 1930s led to dramatically reduced mortality rates related to bacterial infections, thus

revolutionizing medical practices.[140, 141] Despite the marvelous discovery, penicillin wasn't introduced in the clinic until 1941, followed by a large number of antibacterial agents such as various other penicillin derivatives, cephalosporins (**71**), aminoglycosides (**72**), macrolides (**73**), and glycopeptides (**Figure 13**).[139, 142] The discovery of antibiotics has greatly improved the fight against infectious diseases as well as the quality of life of those affected and continuous efforts are being made in the future development of antibacterial agents that will overcome the drawbacks of the currently available treatments, namely resistance.[143]

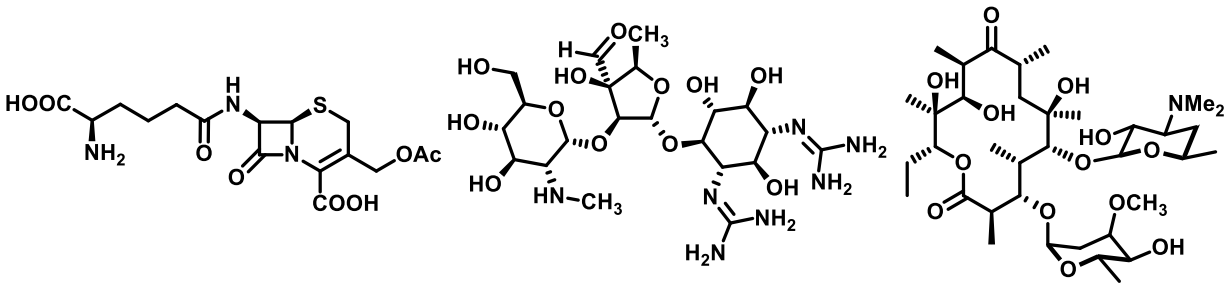

71
Cephalosporin C

72
Aminoglycoside
streptomycin

73
Macrolide
Erythromycin

Figure 13. Structures of representative antibiotic classes

Another area of medicine where natural products research has had an immense role is the area of anti-cancer therapeutics. Cancer relates to a group of devastating diseases with an estimated 1.7 million new cases to be reported in 2013 alone.[144] It was reported that approximately 80% of the cancer drugs on the market from 1981-2006 were natural products or natural product derivatives.[145] Anticancer compounds can act by several mechanisms such as induction of apoptosis, topoisomerase inhibition, tubulin polymerization and by alkylation.[138, 146] They belong to several structural classes of natural products some of which include: anthracyclines, polyketide macrolides, enediynes, isoprenoids, etc.[138] Examples include

paclitaxel (**74**), vinblastine (**75**), doxorubicin (**76**), camptothecin (**77**), and various others (**Figure 14**).[147] In addition to being highly potent anticancer agents, these natural products have helped our understanding of various cancer pathologies as well as unknown biological pathways that can be explored for discovery and development of novel and improved anticancer therapeutics.

A different area of medicine where natural products have played a great role is malaria research. Malaria is caused by *Plasmodium* parasites and it was estimated in 2010 that there were more than 219 million cases of malaria and over 660,000 deaths.[148] Furthermore, over 3.3 billion people worldwide were at risk of contracting malaria in 2011 as estimated by the World

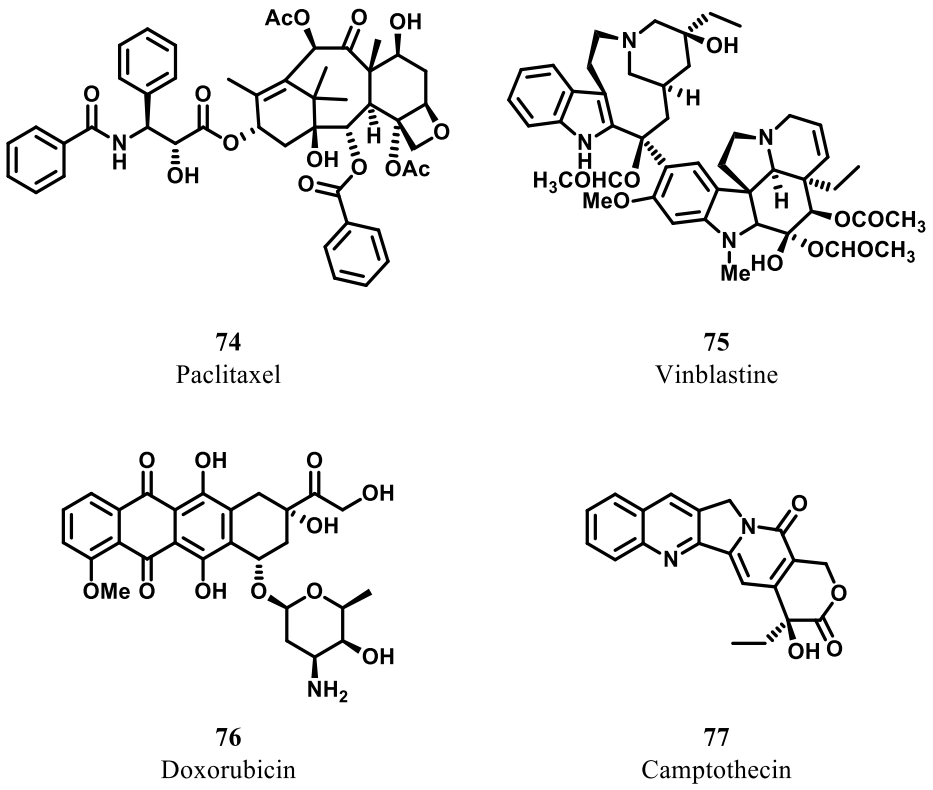

Figure 14. Stuctures of representative antibiotics

Health Organization.[149] Use of the *Cinchona* bark to treat malaria was first reported in the 1800s when the British began cultivating the plant.[134] Quinine (**70**, **Figure 12**) isolated from the

Cinchona succirubra Pav. Ex Klotsch, was approved as an antimalarial agent in the United States in 2004.[135] Efforts to synthesize quinine led to the discovery and development of chloroquine (**78**), which has been the mainstay for the treatment of malaria for the last 50 years (**Figure 15**).[150] Its great success in treating malaria and heavy use worldwide gave rise to resistance in the species responsible for malaria in humans.[151] Natural sources have helped in the discovery of novel antimalarial agents with diverse scaffolds such as artemisinin (**79**), and will continue to aid in the fight against malaria resistance.[152]

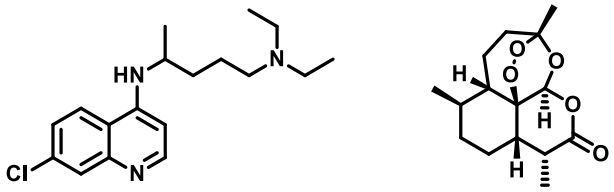

78
Chloroquine

79
Artemisinin

Figure 15. Natural products and derivatives as treatments for malaria

Natural products can be divided into groups depending on their biosynthetic pathway in such a way that the acetate pathway gives rise to fatty acids and polyketides; the shikimate pathway gives rise to amino acids and phenylpropanoids; and the mevalonate pathway gives rise to terpenoids and steroids.[153] In addition to the natural products biosynthesized by the mentioned pathways, natural products can also be divided into alkaloids and carbohydrates.[153]

Terpenes

Terpenes are a class of natural products that possess great structural and stereochemical diversity and are found in all forms of life.[154] More than 55,000 terpenoids have been isolated to

date.[154, 155] Terpenes are of interest to many researchers because of their structural complexity, structural diversity as well as their unique biological profiles. In fact, several therapeutic agents currently available on the market are members of the terpene class of natural products, for instance the antimalarial agent artemisinin and the anticancer agent paclitaxel.[138] Terpenes are secondary metabolites that are composed of isoprene units, a 5 carbon unit, whose biosynthesis stems from the mevalonate pathway.[156, 157] Classification of the terpene class of natural products is founded on the number of isoprene units present in the carbon skeleton.[156] There are several classes of terpenes that possess from one to six isoprene units and are classified into hemiterpenes, monoterpenes, sesquiterpenes, diterpenes, sesterterpenes, and triterpenes, respectively.[158] Terpenes containing more than six isoprene units are also known as tetraterpenes and they comprise of eight isoprene units.[156] Furthermore, terpenes composed of isoprene chains have also been isolated and are known as polyterpenes.[156] There are several subclasses that follow in this classification system.[156]

Specifically concentrating on the diterpene class, the classification system is further divided and there are over 50 subclasses of diterpenes, many of which are known to have biological activity.[158] Some of the best known are labdanes, kauranesa, gibberellins, taxanes, beyeranes, aphidicolins, cembranes, and abietanes.[158] For instance, natural products research on the *Turrheantus* species resulted in the isolation of labdanes that have anti-plasmodial activity; research on *Boswellia serrate* yielded an cembrane diterpene with anti-protozoal activity; studies done on *Podocarpus macrophyllus* afforded an abietane with cytotoxic activity; research on the South American plant *Smallanthus sonchifolius* has afforded an kaurane with anti-diabetic activity are just a few examples of the structural diversity and pronounced biological activity seen with the diterpene class of natural products.[159-162]

Another diterpene subclass that is abundant throughout Nature in a variety of plants, microorganisms and fungi is the clerodane class, a subclass also known for its biological activity.[163] For a diterpene to be considered a clerodane it has to be composed of four isoprene units and have four contiguous stereocenters that are present on a *cis* or *trans* decalin fused system.[163] A larger portion of clerodene diterpenes, 75%, contain the *trans* ring fusion and the natural product clerodin (**80**) is an example (**Figure 16**).

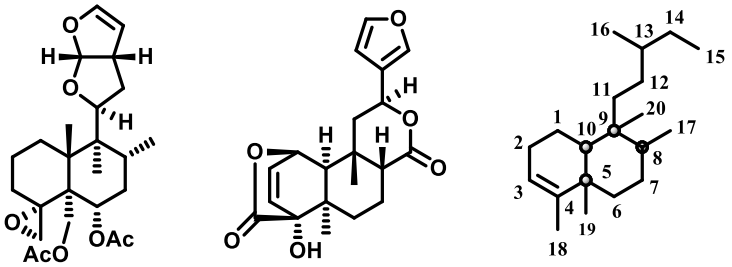

80 Clerodin **81** Columbin **82** Clerodane Skeleton

Figure 16. Examples of clerodane diterpenes

This natural product was originally isolated in 1936 from *Clerodendrum infortunatum* L. (Lamiaceae), has shown activity as an antifeedant that can potentially be used as a pesticide.[164] The other 25% of clerodanes have the *cis* ring fusion as seen in columbin (**81**). Columbin was isolated from *Tinspora bakis* (Menispermaceae), a Sudanese native species that was traditionally used for the treatment of headache and rheumatism and is currently being investigated as a potential anti-inflammatory agent.[165] Alongside with the relative configuration of the *cis*/*trans* decalin ring fusion, the clerodanes are further classified by the relative stereochemistry at the C-8 and C-9 carbons (**82**, **Figure 16**).[163] This added classification produces additional four types of clerodane skeletons which are defined with respect to their ring fusion and their stereochemistry at the C-8 and C-9 carbons: *cis*-*cis* (CC), *trans*-*trans* (TT), *cis*-*trans* (CT), and *trans*-*cis* (TC).[163]

They can be also be classified by their absolute stereochemistry; compounds that have the same absolute stereochemistry as clerodin are named neoclerodanes and compounds that are enantiomers of clerodin are referred to as *ent*-neoclerodanes.[166, 167]

Their intriguing scaffolds and extensive biological profiles have led many researchers to focus on the neoclerodane subclass of diterpenes. This interest has yielded many total synthesis efforts, which have led to structure-activity relationships (SAR) studies and pharmacological evaluations. Despite the great interest in this subclass, however, the high structural complexity that these natural products possess has shown to be the cause for complications for completion of SAR studies.[168] Additionally, these molecules are often polyfunctionalized and contain many stereocenters making it difficult for reaction development and analogues synthesis. Despite these challenges, pronounced interest has been focused on several neoclerodane diterpenes, in particular salvinorin A.

Salvia divinorum and Salvinorin A

Salvia divinorum Epling & Jativa-M. (Lamiaceae) is a psychoactive mint originally discovered in 1962 by Wasson and Hofmann.[169] This plant was also locally known as "ska Maria Pastora" because of a belief that *S. divinorum* represents a reincarnation of the Virgin Mary.[170] Its psychoactive properties were utilized in divination practices by the Mazatec Indian shamans of Oaxaca, Mexico.[171] Aside from its spiritual traditions, *S. divinorum* was also used to treat a variety of illnesses such as anemia, headache, rheumatism, and diarrhea. There are several traditional ways for administration of *S. divinorum*: chewing and swallowing of the leaves; smoking the leaves, and pulverizing the leaves into a juice and then consuming the

liquid.[172, 173] Because of the rapid onset of hallucinations and vivid "out-of-body" experiences, *S. divinorum* has become very popular among recreational users, which administer *S. divinorum* by smoking inhalation or by chewing on the leaves.[174, 175] *Salvia* has been labeled as a "drug of concern" by the Drug Enforcement Agency (FDA); however it is not a controlled substance under the Controlled Substance Act of 1970.[176]

The principal active component of *S. divinorum* is the neoclerodane diterpene salvinorin A (**83**, **Figure 17**). Salvinorin A is a *trans-cis* tricyclic neoclerodane that was originally isolated in 1984 by Valdes.[171] Salvinorin A is a potent hallucinogen that exhibits similar potency to that of known hallucinogens LSD (**84**) and DOB (**85**).[172, 177] Salvinorin A was shown not to exert its activity through the serotonin 5-HT_{2A} receptor system, the mechanism of action of many of the known hallucinogens.[172, 178] In fact, in 2002 salvinorin A was shown to exert its actions as a potent agonist of the KOP receptor.[124] With its unique non-nitrogenous structure, salvinorin A was identified as the first natural product that has high affinity and efficacy for the KOP receptors with a scaffold structurally different than that the known hallucinogens and other KOP receptor ligands like JDTic (**86**), U-50,488 (**87**), or bremazocine (**88**).[124]

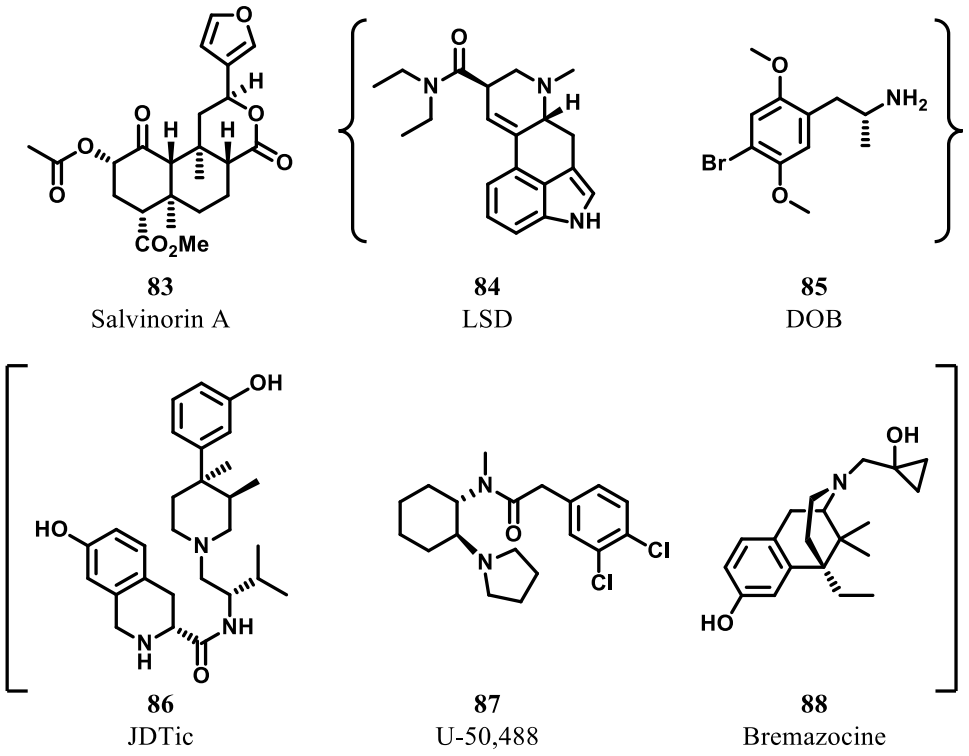

Figure 17. Reprsentative examples of KOP receptor ligands [bracket] and classical hallucinogens {braces} compared to salvinorin A

It was originally believed that a basic nitrogen atom was required for opioid receptor activity because of a binding hypothesis that suggested that the nitrogen atom interacts with an aspartate residue of the third transmembrane domain of the receptor.[179-181] The elucidation of the X-ray crystal structures for the opioid receptors eloquently accomplished by Granier and coworkers (DOP receptor), Manglik and coworkers (MOP receptor), Wu and coworkers (KOP receptor), and Thompson and coworkers (NOP/ORL-1) will allow for further exploration and validation of the *N*-atom binding hypothesis at the opioid receptors.[182-185] Furthermore, the outstanding efforts made into the elucidation of the X-ray crystal structures of the opioid receptors could be further utilized in molecular modeling studies that will aid in the development of SAR studies for further evaluation of the interactions between opioids and their receptors.[182-

[185] Due to its unique structure and activity, salvinorin A has become a primary target for further SAR development and pharmacological evaluation.

Opioid Receptors

Opioids exert their activity through the opioid receptors. With the use of radiolabeled opioid ligands, study reported by Martin and coworkers, the presence of opioid receptors was observed in the human brain. There are three main types of opioid receptors: μ (MOP), κ (KOP), and δ (DOP) receptors.[186, 187] The basis for the nomenclature of the opioid receptors lies in several observations: the ligands used for characterization, ketocyclazocine (**95**) (KOP receptor); the best known agonist, morphine (**50**, **Figure 10**) (MOP receptors), and a high affinity enkephalin receptor found in the mouse vas deferens (DOP receptors) (**Figure 19**).[100, 188] It has been proposed that a there is a possibility of receptor subtypes, however genomal evidence has not supported this notion and is now believed that receptor subtypes are actually posttranslational modifications of the opioid receptors.[189]

Opioid receptors are members of the G-protein coupled receptor (GPCR) superfamily. In *in vitro* models, it has been demonstrated that opioid receptors couple to $G_{i/o}$ proteins, but there is additional evidence that suggest that they may couple to the G_s proteins as well.[190, 191] In general, coupling to the $G_{i/o}$ proteins leads to inhibition of adenylyl cyclase, event that is the result of the decrease in the cAMP production and intracellular calcium levels.[101, 102] Additional effects are caused with the dissociation of the βγ complex, whose interaction with potassium causes additional intracellular effects.[102]

89	Met-enkephalin	Tyr-Gly-Gly-Phe-Met
90	Leu-enkephalin	Tyr-Gly-Gly-Phe-Leu
91	Dynorphin A	Tyr-Gly-Gly-Phe-Leu-Arg-Arg-Ile-Arg-Pro-Lys-Leu-Lys
92	-endorphin	Tyr-Gly-Gly-Phe-Met-Thr-Ser-Glu-Lys-Ser-Gln-Thr-Pro-Leu-Val-Thr-Leu-Phe-Lys-Asn-Ala-Ile-Ile-Lys-Asn-Ala-His-Lys-Lys-Gly-Glu

Figure 18. Endogenous opioid ligands and ligands used for receptor characterization

Despite the 60% amino acid sequence identity between the opioid receptors, they differ in their body distribution, receptor density and their respective endogenous ligands.[104, 192] Shortly after the discovery of the opioid receptors, endogenous ligands for each of the receptors were reported. Two pentapeptides that differ only in one amino acid were the first isolated peptides from brain tissue and were determined to be DOP receptor agonist.[193] The activity of methionine-enkephalin (**89**, Met-enkephalin) and leucine-enkephalin (**90**, Leu-enkephalin) was determined thorough a naloxone (**59**, **Figure 10**) antagonism study (**Figure 18**).[193] In 1981, the endogenous ligand for KOP receptors, dynorphin A (**91**) was isolated from porcine pituitary glands by Goldstein and colleagues.[194] Finally, the endogeneous ligand for the MOP receptors, β-endorphin (**92**), was characterized from camel pituitary glands in1976 by Li and coworkers.[195]

The three different opioid receptors were characterized in the early 1970s; however it wasn't until twenty years later that they were cloned and purified.[196] The first opioid receptor to be cloned was the DOP receptor, which was simultaneously achieved by two groups in 1992.[196, 197] The cloning and purification of the other two opioid receptors was also accomplished; for KOP receptors by Meng and coworkers in 1993 and for MOP receptor by Wang and coworkers in 1994.[198, 199]

Opioids have been used for centuries for the treatment of various ailments. However, specifically focusing on MOP receptor active ligands, the risk of serious side-effects has encouraged the search for structurally diverse opioid ligands that are selective for the other opioid receptors. The identification of such ligands would lessen the risk for a negative side effect profile and would limit drug abuse liability. One example of such ligands includes KOP receptor selective compounds, which have been implicated in the treatment of various diseases, such as drug abuse, mood regulation, and pain management.[94, 200-202] KOP ligands are not without drawbacks, the biggest one of which is occurrence of dysphoria upon activation of the receptors.[203] However, efforts are being made in the development of KOP ligands that will have antinociceptive effects without the occurrence of dysphoria.

Available treatments for moderate to severe pain management are mainly based on opioids, in particular opioids that exert their activity through the MOP receptors. However, despite the use of opioids for the treatment of pain for centuries, these ligands come with a severe set of negative side effects among which respiratory depression and drug abuse liability are the most life threatening.[202] As previously stated, KOP receptor selective ligands with analgesic properties would be a great replacement for MOP based pain therapy, however these ligands are not without drawbacks.[124, 203-205] Nevertheless, KOP receptor selective ligands still represent a great target for pain management because of the presence of KOP receptors in the periphery.[201, 202] For the stimulation of pain, several animal models have been established that study various types of pain; thermal, chemical, electrical, and mechanical.[202] KOP receptor agonists have shown great promise in several of these models of pain. For instance, in the inflammatory model of pain, where inflammatory agents are injected into the animal paw, KOP receptor agonists were shown to significantly diminish the antinociceptive actions and decrease

formalin-induced edema.[206] Additionally, in the sciatic nerve ligation model, a model for neuropathic pain, Xu and coworkers demonstrated that endogenous dynorphin produces both antinociceptive and pronociceptive effects in mice.[207] Furthermore, in the visceral pain model, where visceral pain is stimulated by stretching or distension of the visceral muscle, KOP receptor agonists have been shown to be effective.[202, 208] As demonstrated above, KOP ligands were shown to be a promising target for the treatment of various types of pain. Further investigations into the KOP receptor system will help us gain a better understanding of the relationship between KOP receptor system and the mechanisms of pain.

Evidence proposes that KOP receptor agonists and antagonists may modulate the activity of dopaminergic neurons and modify the neurochemical and behavioral effects of cocaine.[209] Drug and stimulant abuse represents a major problem worldwide. It is characterized by compulsive drug-seeking, and continued drug abuse despite of the socioeconomic and health consequences.[121, 210] Currently there are no FDA approved agents for the treatment of drug abuse. Stimulation of the brain's reward system, which originates in the ventral tegmental area (VTA) area and extends to the nucleus accumbens (NAc) is the primary mechanism that drives most forms of drug addiction.[211] It has been demonstrated that the KOP receptor system has an inhibitory effect on the rewarding function of the brain through the suppression of dopamine release from the mesolimbic and nigrostriatal pathways.[212-214]

It has been demonstrated that KOP receptor agonists have an effects on cocaine self-administration, place preference and behavioral sensitization.[215] Dynorphin A, the endogenous KOP receptor ligand, blocked the formation of conditioned place preference; decreased basal dopamine levels, and diminished locomotion induced by 15 mg/kg of cocaine in mice.[216] It was

demonstrated by Koob and coworkers as well as by Xi and coworkers that KOP receptor agonist U-50,488 (**87**) failed to substitute for heroin self-administration in rats, unlike with MOP receptor agonists (**Figure 18**).[217, 218] Rather, KOP receptor agonists U-50,488 and spiradoline dose-dependently decreased morphine and cocaine self-administration in mice and rats.[219, 220] On the other hand, administration of an KOP receptor antagonist nor-BNI (**102**), had no effect on morphine and cocaine self-administration in monkeys and rats (**Figure 20**).[218, 219, 221] Moreover, intravenous cocaine (**60**) and morphine (**50**) administration in rats was significantly reduced with the administration of U-50,488 (**Figure 10**, **11**).[222] Another KOP receptor agonist, U-69,593 (**93**) decreased cocaine self-administration and also inhibited the reinstatement of extinguished drug-taking behavior in response to experimenter administered cocaine (**Figure 17**).[223] Schenk and coworkers also reported that U-69,593 was able to reduce the ability of a high dose of cocaine (20 mg/kg) in the production of drug-seeking behaviors.[223] Moreover, they observed that U-69,593 was able to have an effect in the decrease of cocaine self-administration when the doses of cocaine were administered in a descending order as opposed to ascending order.[223]

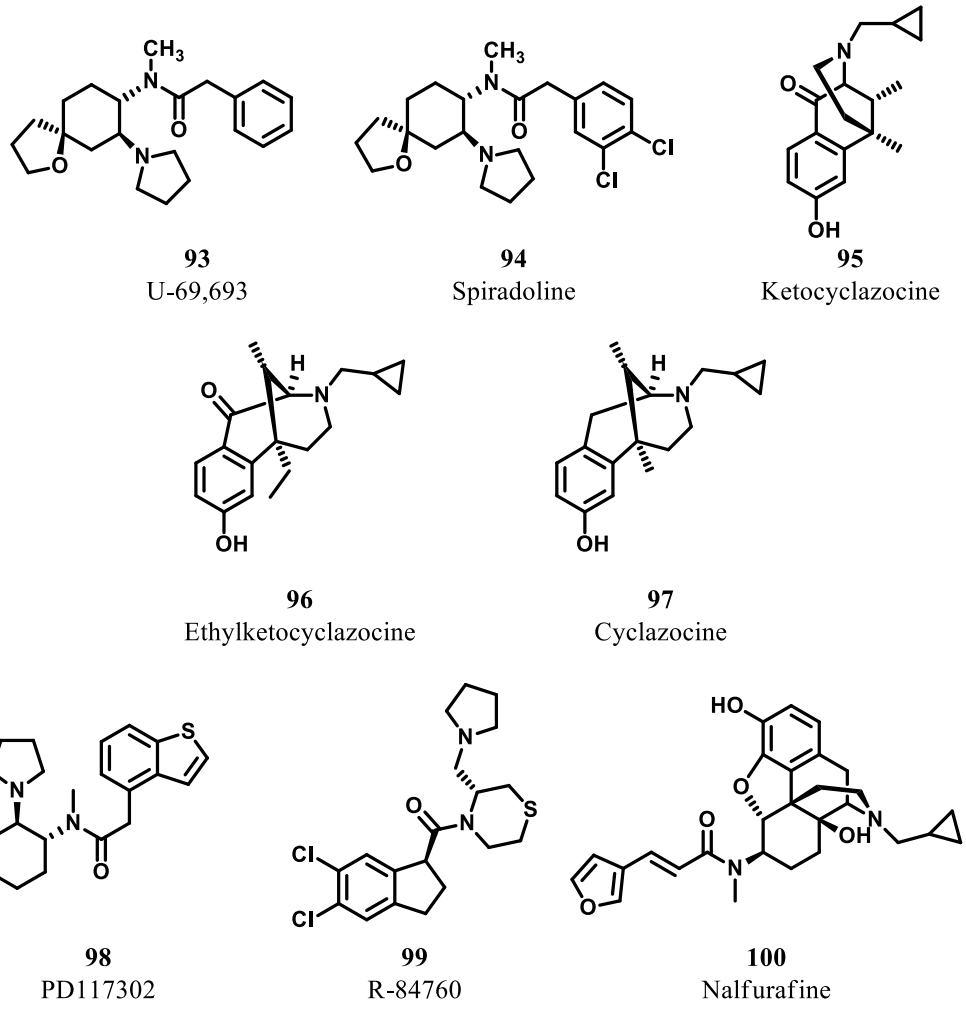

Figure 19. Pharamacologically relevant KOP receptor ligands

Validation studies of the effects of KOP receptor agonists on cocaine self-administration were also completed in non-human primates.[224, 225] It has also been reported that higher efficacy KOP receptor agonists such as U-50,488, U-69,593, ethylketocyclazocine (**96**), and bremazocine (**88**) may be more effective in decreasing cocaine-seeking behavior than lower efficacy KOP receptor agonists such as cyclazocine (**97**), PD117302 (**98**), and spiradoline (**94**) (**Figure 19**).[209]

In addition to the self-administration studies, KOP receptor agonists have been strongly investigated in conditioned place preference studies, and results suggest that agonists such as U-

50,488, U-69,593 and salvinorin A induce conditioned place aversion in rodents.[214] This effect was blocked by the KOP receptor antagonist nor-BNI.[226] In a study done by Suzuki and coworkers, it was reported that U-50,488, a selective KOP receptor agonist and naltrexone, a non-selective opioid receptor antagonist both produced conditioned place aversion.[227, 228] In a combination study completed by Suzuki and coworkers, it was identified that both U-50,488 and naltrexone blocked cocaine conditioned place preference. In addition to U-50,488, U-69,593 was similarly shown to prevent the development of sensitization to the conditioned rewarding effects of cocaine, a study completed by Shippenberg and coworkers.[229] Moreover, 0.1mg/kg of the arylacetamide R-84760 (**99**) displayed the ability to block cocaine-induced conditioned place preference and to significantly decrease cocaine-induced locomotion.[230] Unlike the other arylacetamides U-50,488 and U-69,593, R-84760 did not produce conditioned place aversion.[230] Nalfurafine (**100**) is an epoxymorphinan and high-affinity KOP receptor agonist. It has been described that induction of conditioned place aversion is observed with an administration of a high dose of nalfurafine (80 μg/kg).[231] In addition, similarly to the other KOP receptor agonists described, nalfurafine was likewise able to lessen the rewarding and locomotor effects of morphine in mice.[232] The prevention of the effects seen with an increase in the extracellular dopamine levels that is achieved as a result of recurrent administration of cocaine is also successfully treated with the administration of KOP receptor agonists.[229] Funada and colleagues demonstrated that pretreatment with KOP receptor agonists U-50,488 and E-2078, a dynorphin derivative, led to a decrease in morphine-induced conditioned place preference and it also decreased the elevated dopamine metabolites in the limbic forebrain.[233]

Evidence points to a possible role for KOP receptors in the development of morphine tolerance. It has been demonstrated that co-administration of the KOP receptor agonist U-

50,488, is capable of preventing morphine tolerance.[234-236] Also, of interest is the notion that KOP receptors are able to modulate MOP receptors by opposing their actions.[237, 238] In rodent models of tail-flick and hot plate pharmacological tests, it was observed that administration of the endogenous KOP receptor ligand, dynorphin A or the KOP receptor agonist U-50,488 dose-dependently antagonized morphine antinociception.[234, 235, 239-241]

KOP receptor antagonists have been implicated to have a potential utility in the treatment of drug abuse due to their modulation of a certain component of stress-induced drug craving, a model for relapse.[242] It has been demonstrated that states of depression and stress can be probable motivating factors and lead to cocaine relapse.[243] The development of the first highly selective KOP receptor antagonist, JDTic (**86**, **Figure 17**), raised interest for the determination of its actions in stress-induced models of relapse in rodents.[244] It was reported by Beardsley and coworkers that JDTic dose-dependently blocked stress-induced reinstatement of extinguished cocaine-reinforced responding in the footshock-induced relapse model.[245] Additionally, it was demonstrated that JDTic also showed antidepressant-like activity in the forced swim test.[245]

Despite the positive developments seen with KOP receptor agonists in the quest of drug abuse therapies, dysphoria, a characteristic of KOP receptor agonists remains a significant side effect.[246] Moreover, it has been demonstrated that KOP receptor agonists when under stress conditions, will also potentiate the rewarding effects of cocaine in stress-induced reinstatement in animals with a history of exposure to KOP receptor agonists.[247, 248] In such animals, it is likely that the prolonged activation of the KOP receptor system may be the cause for the seen success of KOP receptor antagonists have on the reduction in the increased cocaine intake.[238, 249] Thus, in a state where the KOP receptor system is suppressed such as addiction, KOP receptor

antagonists may be a prospective target for the treatment of drug addiction. Another potential target for the treatment of drug addiction are partial KOP receptor agonists. Such agents will likely be without the psychotomimetic side effects seen with KOP receptor full agonists and have the potential to antagonize the effects of CNS stimulants in a similar manner to that of KOP receptor full agonists.[178]

Ventral tagmental area, nucleus accumbens, and the prefrontal cortex are brain regions that are involved in the regulation of mood and motivation and it has been shown that the KOP receptor system is enriched in these areas.[250] KOP receptor activation in these regions of the brain has been demonstrated to lead to a decrease in dopamine levels and transmission. The seen reduction in DA transmission has been implicated in certain symptoms of depression. Thus, deactivation of the KOP receptor system with the use of KOP receptor antagonists may be a potential target for the treatment for depression. Additionally, increased levels of the transcription factor cAMP-response-element-binding protein (CREB) in the NAc as a result of stress have been related to depressive-like effects in rodents, which can be attenuated by KOP receptor antagonists.[246, 251, 252] Several KOP receptor antagonists have been investigated for antidepressant effects. Pliakas and coworkers demonstrated that nor-BNI (**101**) was able to block the swim stress-induced immobility in rats (**Figure 20**).[253] A structurally different KOP antagonist, GNTI (**102**) was also tested for antidepressant effects. It was demonstrated that a single i.c.v. treatment with GNTI showed antidepressive effects with a more potent activity than that seen with nor-BNI.[246] ANTI (**103**), a slightly more lipophilic KOP receptor antagonist was also shown to have antidepressant effects in the forced swim test after systemic administration.[246] It has been proposed that a possible mechanism for the seen antidepressive effects of KOP

receptor antagonists may be due to the blockage of the inhibitory actions that the KOP receptor system generally employs in the VTA dopaminergic neurons.[254]

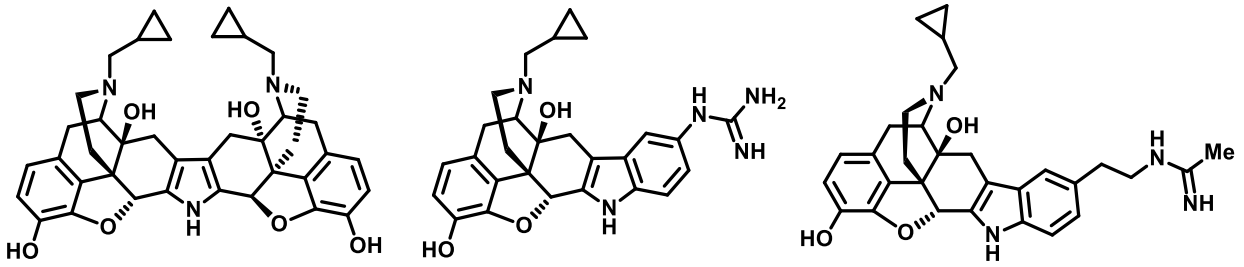

101
nor-BNI

102
GNTI

103
ANTI

Figure 20. Pharamacologically relevant KOP receptor ligands as potential treatments for depression

Despite these promising results, studies of KOP receptor antagonists are somewhat hindered by the atypically long duration of action that is seen with the treatment of these agents in rodents, non-human primates and humans.[255] Thus, the necessity and search for selective KOP receptor antagonists with improved pharmacokinetic and pharmacodynamics properties continues.

Salvinorin A *in vitro* Studies

It was identified in 2002 that salvinorin A is a highly selective and potent KOP receptor agonist.[124] This was done through a screen of a large panel of human GPCRs, transporters and ligand-gated ion channels obtained from NIMH-PDSP of a 10 μM concentration of both salvinorin A and the classical hallucinogen LSD. From this screen it was clear that salvinorin A inhibited only the [^{3}H]-bremazocine –labeled KOP receptors and did not significantly bind to neither of the two opioid receptors nor any of the other 48 molecular targets available in the screen. Results from the screen determined that the K_i value of salvinorin A for cloned KOP

receptor is 16 nM, whereas no significant binding was observed for either the MOP or DOP receptors (>10,000 nM). In the functional assay of adenylate cyclase inhibition it was determined that salvinorin A is potent agonist of the KOP receptors with an EC_{50} value of 1.05 nM, a value comparable to that of the known KOP receptor agonist U-69,593 (EC_{50} = 1.2 nM). Furthermore, in the [^{35}S]GTP-γ-S assay it was found that salvinorin A is also a potent agonist with an EC_{50} value of 235 nM, a value again comparable to that of U-69,593 (EC_{50} = 377 nM).

The results discussed above were independently reproduced and confirmed by Chavkin and coworkers using [^{3}H]-bremazocine and inhibition of adenylate cyclase assay.[256] In addition, they also determined that salvinorin A is a full agonist in a calcium mobilization assay where it was tested against other well-known KOP receptor agonists and it had comparable potency (salvinorin A, EC_{50} = 7 nM, U-50,488, EC_{50} = 24 nM, U-69,593, EC_{50} = 13 nM). It is believed that down-regulation and internalization of receptors are largely responsible for the development of tolerance and it was shown that known KOP receptor agonists down-regulate and internalize KOP receptors to a variable degree. Wang and coworkers utilized fluorescence flow cytometry and FLAG-*h*KOP receptor transfected cells to determine if salvinorin A was able to promote internalization of the *h*KOP receptor which was observed, however with a much lower potency than U-50,488.[257]

Salvinorin A *in vivo* Studies

Salvinorin A and KOP receptor Mediated Effects

In order to fully understand the observed KOP receptor activity of salvinorin A, drug discrimination studies were undertaken. These behavioral studies involve subjects being trained to respond to a drug and are then tested with other drugs to see their ability to generalize to, or "substitute" for the training drug.[258] Butelman and coworkers reported the first behavioral set of studies done with salvinorin A in non-human primates and the first drug discrimination studies of salvinorin A, where it was reported that salvinorin A does substituted for U-69,583.[259] The highest dose of subcutaneously administered salvinorin A (0.032 mg/kg) did not alter the responding rate and caused only mildsedation-like effects. Salvinorin A showed a fast onset of action, (5 minutes), and duration of action of 60 minutes. The discriminatory and neuroendocrine effects of salvinorin A were blocked by quadazocine (**109**), an opioid antagonist (**Figure 21**). They also determined in a separate drug discrimination experiment that U-69,583 did not substitute for ketamine, an anesthetic and NMDA receptor antagonist. An extension of these studies was completed in rats by Willmore-Fordham and coworkers. They determined that at the doses administered (1-3 mg/kg, i.p.) salvinorin A fully substituted for U-69,593 without modifying response rates.[260] Furthermore, it was determined that the KOP selective antagonist nor-BNI was able to entirely block the effects of salvinorin A. Sluggish and uncoordinated motor performance was observed with 3-10 mg/kg administration of salvinorin A, an experiment done with drug naïve animals that confirmed the results reported in mice by Fantegrossi and coworkers and Zhang and coworkers.[226, 261] A study reported by Baker and coworkers, extended these results with the determination that both U-69,593 and U-50,488 substituted for salvinorin A in rats trained to discriminated salvinorin A from saline.[262] Additionally, they determined that two active analogues of salvinorin A, salvinorin B ethoxymethyl ether (**104**) and salvinorin B methoxymethyl ether (**105**), substituted completely for U-69,593 (**Figure 21**).

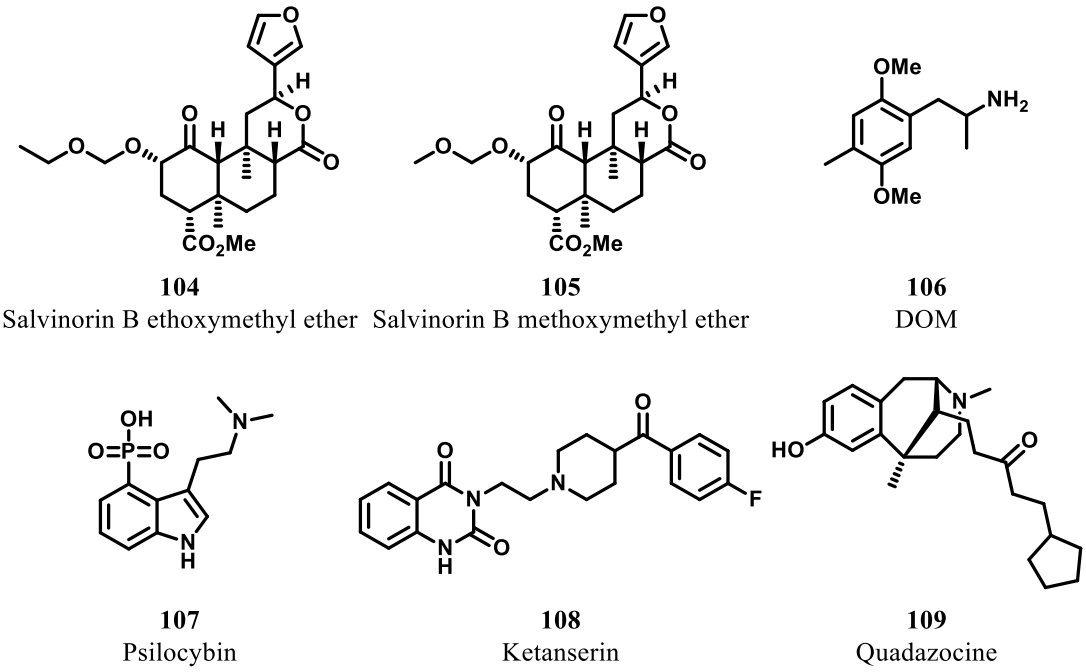

Figure 21. Pharamacologically relevant CNS ligands in determination of the KOP receptor-mediated effects of salvinorin A

Reports of the hallucinogenic effects exhibited with salvinorin A administration prompted additional studies of comparison with known hallucinogens. The study discussed above done with ketamine and salvinorin A was broadly extended by Li and coworkers.[263] In this study done on rhesus monkeys trained to discriminate DOM, a 5-HT_{2A} receptor agonist that exhibits hallucinogenic effects in humans, it was observed that neither salvinorin A nor U-50,488 substituted for DOM (**106**). Butelman and coworkers conducted the first drug discrimination study in which rhesus monkeys were trained to discriminate salvinorin A from saline.[264] It was determined that structurally diverse KOP receptor agonists, bremazocine, U-69,593, and U-50,488 were all able to substitute for salvinorin A. However, psilocybin (**107**), a 5-HT_{2A} receptor agonist and a compound with pronounced hallucinogenic/psychotomimetic effects in humans did not substitute for salvinorin A. Furthermore, the 5-HT_{2A} antagonist ketanserin (**108**) did not block the discriminative effects of salvinorin A, an effect that was successfully blocked

by the opioid antagonist quadazocine again confirming the notion that the behavioral effects of salvinorin A are indeed due to centrally acting KOP receptors (**Figure 21**).

Salvinorin A and Behavioral Studies

As discussed previously, the opioid receptor system has been implicated in various disease states. Consequently, investigation of salvinorin A and its analogues for their effects in various centrally mediated phenomena, such as pain modulation, mood and reward regulation, has been carried out by researchers worldwide.

Salvinorin A and Regulation of Mood, Stress and Reward

Disruption of dopamine function within the NAc has been believed to cause ahedonia, which is a trademark sign of clinical depression.[200] Additionally, elevated stress increases the activity of CREB within the NAc and as a result, it increases immobility behavior when tested in the forced swim test (FST), a model used to study depression.[265] The elevated levels of CREB within the NAc are believed to be in part due to the fact that CREB regulates the transcription of dynorphin, the endogenous KOP receptor ligand leading to decrease DA function. CREB-regulated transcription of dynorphin leads to increased activation of KOP receptors within the NAc that causes a decrease in the level of local dopamine function, thus triggering depressive-like effects.[200] As discussed above, KOP receptor antagonists are known to exhibit antidepressive effects in rats. In light of these finding several studies have investigated the effects of salvinorin A in the area of mood regulation. Utilizing two models of depressive-like behavior, the FST and intracranial self-stimulation (ICSS) tests, Carlezon and coworkers examined the effects of salvinorin A in rats.[200] In the FST test they found that salvinorin A exerts effects opposite of those seen with currently used antidepressants. Furthermore, salvinorin

A (0.25-2.0 mg/kg) dose-dependently increased the occurrence of immobility and also caused significant decrease in the occurrence of swimming, however no effects were seen on climbing or diving behaviors. Conversely, no effects were observed on locomotor activity in an open field at any of the doses tested. In 1953, ICSS was originally described by Olds and Milner as an operant model where animals learn to deliver brief electrical pulses into their own brain, specifically in regions believed to regulate natural reward pathways.[266, 267] Changes in lever pressing, which is learned by the animal, can be used to determine the effects that different drugs have on ICSS. Decrease in the ICSS threshold is indicative of an increase of the reward value of the stimulation, which occurs because a smaller amount of electrical stimulation is needed to recognize the stimulation as rewarding. On the other hand, the opposite is true when increase in the ICSS threshold is observed. In the ICSS assay completed by Carlezon and coworkers, salvinorin A dose-dependently increased the ICSS threshold, thus reducing the rewarding effects of the medial forebrain bundle stimulation, an observation opposite from the one seen with stimulant drugs such as cocaine.[200] This reduced sensitivity to rewarding stimuli has been shown to be a sigh of ahedonia, one of the hallmark clinical symptoms of depression. Furthermore, utilizing microdialysis, it was demonstrated that 1.0 mg/kg salvinorin A reduced dopamine activation in the mesolimbic dopamine system; however no effects were observed on serotonin concentrations in this region. Taken together, these results provide evidence of depressive-like effects of salvinorin A.

An extension of the results reported by Carlezon were the experiments completed by Ebner and coworkers, where they choose to investigate the temporal effects of a 2.0 mg/kg dose of salvinorin A on phasic dopamine release in the NAc core and shell, as well as the effects of salvinorin A on motivated behavior in ICSS and sucrose-reinforcing responding.[268] Fast scan

cyclic voltammetry was used to evaluate the effects of salvinorin A on the phasic dopamine release in the NAc core and shell and it was observed that salvinorin A significantly decreased dopamine release in both the NAc core and shell as compared to vehicle. However, no effect on dopamine reuptake was observed in either part of the brain. In the ICSS assay, it was demonstrated that a 2.0 mg/kg maximal dose of salvinorin A dose- and time-dependently increased ICSS thresholds, which is in accordance with Carlezon and coworkers. In the sucrose-reinforced responding assay, animals are trained to press a lever to obtain a sucrose pellet; the progressive ration of responding determines the motivation of the subject to respond by gradually increasing the number of lever presses necessary to receive the sucrose reward. It was determined that salvinorin A significantly decreased the breakpoint in responding and it also blocked the rate of lever-responding, both of which are indicative of a decrease in motivation. These results confirm the previously published reports that salvinorin A has depressive-like effects and decreases the dopamine concentration in the NAc.

Results reported above were further expanded by Braida and coworkers, who evaluated the effects of salvinorin A in rodent models of emotional behavior at doses lacking motor impairments.[269] Such effects were evaluated in the elevated plus maze paradigm, FST, and the tail suspension test. The elevated plus maze is a rodent model for anxiety and the device used consists of an open- and closed-arm. A compound that elicits a greater amount of time spent in the open-arm and a greater percentage of open-arm entries may be considered an anxiolytic. Rats pre-treated with 0.1-160 μg/kg dose of salvinorin A were shown to make more open-arm entries and spent more time in the open-arms than vehicle-injected rats, a result similar to that of the clinically used anxiolytic diazepam (1.0 mg/kg, i.p.), indicating that salvinorin A may have some anxiolytic effects. Mixture of the KOP receptor antagonist nor-BNI and the CB1R

antagonist AM251 were able to completely block the effects seen with salvinorin A. In the tail suspension test, where animals are suspended by their tails and the time spent between immobility and agitation is recorded, it was shown that salvinorin A (0.001-1.0 μg/kg) produced a significant decrease in the time spent in immobility. The seen effects were once again completely blocked with pretreatment of both nor-BNI and AM251, administered alone or in combination. The antidepressive effects of salvinorin A were further confirmed in the FST, where doses of 0.001 to 10 μg/kg salvinorin A dose-dependently decreased the occurrence of immobility and increased swimming, however did not have an effect on climbing behavior. Again pretreatment with either nor-BNI or AM251 completely blocked the seen effects. These results, contradict with data previously reported by Carlezon and coworkers and Ebner and coworkers. However, the difference in the dosing regimens between the different groups was suggested as a factor for the differences seen between the studies. The two other studies used higher salvinorin A doses, whereas the present authors used relatively small doses of salvinorin A. They stated that a dose of 1 mg/kg of salvinorin A did produce depressant-like effects, however these data were not reported. Based on this finding it is possible that small doses of salvinorin A produce antidepressant like effects, whereas larger repeat doses produce depressant-like effects.

These studies were further extended by Harden and coworkers, where they used animals previously exposed to a variety of mild stressors over the course of several weeks.[270] This paradigm termed chronic mild stress (CMS), produces behaviors that model anhedonia, which can be detailed in rats by measuring the relative consumption of sweet water as compared to regular drinking water.[271, 272] Various stressors were used over the testing period including 16 hour food depravation, 16 hour water depravation, 12 hour of 45° angle cage tilt, 36 hours of

continuous illumination from room light, etc. From this CMS experiment it was determined that indeed a state of ahedonia was observed in the tested rats, which was reversed in stressed animals by administration of 1 mg/kg of salvinorin A, indicating antidepressant effects of salvinorin A. There are several hypothesis that may explain these contradictive results, however additional research has to be conducted for a greater understanding of the mechanism by which salvinorin A may produce both antidepressant and pro-depressive effects.

Salvinorin A and Antinociception Studies

The documented use of *S. divinorum* as a treatment of various ailments, including rheumatism and headaches, prompted studies to evaluate of the antinociceptive effects of salvinorin A in animal models. Utilizing the KOP receptor agonists salvinorin A, TRK-820, and 3FLB, Wang and coworkers developed a study to examine the antipyretic and antinociceptive effects of these compounds in mice.[257] In a scratching assay induced by the pruritogen compound 48/80, only compound TRK-820 showed dose-dependent inhibition in the scratching behavior whereas salvinorin A and 3FLB were ineffective. Similarly, in the acetic acid writhing test, salvinorin A (15-50 mg/kg) was inactive. These results are in conflict with the results published by Harding and coworkers, where they demonstrated that salvinorin A was as potent as morpheine in the tail-flick assay as well as the *p*-phenylquinone (PPQ) writhing assay with ED_{50} values of 1.98 mg/kg and 0.59 mg/kg, respectively.[273] Additionally, they also tested the activity of salvinorin A in the hot plate assay, however no antinociceptive activity was observed. Subsequently, McCurdy and coworkers tested the effects of salvinorinA in several antinociception assays.[274] In the tail-flick assay they demonstrated that salvinorin A displayed dose- and time-dependent antinociceptive effects, produced 10-15 minutes after drug

administration, an effect that was completely reversed with nor-BNI pretreatment. They also tested the effects of salvinorin A in a hotplate and acetic acid writhing assays, where it was demonstrated that salvinorin A at doses of 1.0 mg/kg and 1.0-2.0 mg/kg, respectively, exhibited dose dependent antinociceptive effects. The authors note that in all of the experiments salvinorin A exhibited fairly short duration of action for salvinorin A with a peak at 10 minutes, which may explain the results reported by Wang and coworkers where no antinociceptive effects were observed when salvinorin A was administered 20 minutes prior to the irritant. John and coworkers further extended these results and confirmed the antinociceptive effects of salvinorin A.[275] An intrathecal (i.t.) administration of salvinorin A displayed antinociceptive effects in a tail-flick assay, effects reversed by administration of the KOP receptor antagonist nor-BNI, but not by the MOP receptor antagonist β-FNA or the DOP receptor antagonist naltrindole. Fichna and coworkers evaluated the antinociceptive effects of salvinorin A even further, however in a different animal models, namely models for colitis.[276] These models focus on the inflammation caused by bowel disease and it was determined that a 3 mg/kg dose of salvinorin A significantly attenuated the effects of 2,4,6,-trinitorbenzene sulfonic acid (TNBS)-induced colitis. These effects of salvinorin A were reversed by nor-BNI but not by the CB1R and CB2R antagonists AM251 and AM630. Lastly, Ansonoff and coworkers tested the antinociceptive and hypothermic effects of salvinorin A in KOP receptor knockout mice.[277] Intracerebroventricular (i.c.v.) injection of salvinorin A (7.5 μg) produced antinociceptive effects, which were not present in KOP receptor knockout mice. These results indicate that the antinociceptive effects of salvinorin A are indeed KOP receptor regulated. Hypothermic effects were only observed at much higher doses (50μg) of i.c.v. administered salvinorin A.

Effects of Salvinorin A in Non-Human Primates and Human Subjects

Prolactin is a hormone synthesized in the anterior pituitary gland and several neurotransmitter systems in the CNS regulate its actions.[278] The opioid receptor system modulates prolactin secretion, which has been used in non-human primates to evaluate the potency, receptor selectivity and efficacy of various opioid ligands.[278] Butelman and coworkers designed a neuroendocrine biomarker study to evaluate the effects of salvinorin A in non-human primates.[279] In this study, the experiments were set up as follows: rhesus monkeys were injected with salvinorin A, vehicle, or U-69,593 at doses of 0.0032-0.056 mg/kg i.v. and samples were collected at set intervals for 120 minutes; in antagonism experiment, the antagonist to be tested was administered 30 minutes before salvinorin A and the same collection procedure was followed. It was determined that both salvinorin A and U-69,593 dose- and time-dependently increased prolactin levels. The effects of salvinorin A were observed as soon as the 5 minute time period, but were shorter acting than those seen with U-69,593. In addition to the i.v. administration route used in this study, the authors tested the neuroendocrine effects of s.c. administered salvinorin A. It was observed that salvinorin A had much smaller effects of prolactin secretion than i.v. administered salvinorin A and a slower onset of action was also observed. More robust effects of salvinorin A on prolactin levels were observed in female monkeys in both the s.c. and i.v. experiments. The actions of salvinorin A on the KOP receptors were tested with a pretreatment of nalmefene, a universal opioid receptor antagonist and ketanserin, a 5-HT_2 receptor antagonist. In these antagonist studies it was shown that only nalmefene (0.1 mg/kg) was able to completely antagonize the effects of salvinorin A (0.032 mg/kg, i.v.), confirming the notion that salvinorin A acts through the KOP receptor system.

In a subsequent study Butelman and coworkers designed a set of experiments to determine the unconditioned behavioral effects of salvinorin A in non-human primates and the fast onset and entry into the CNS.[280] U-69,593 (0.01, 0.32, and 0.056 mg/kg, i.v.) or salvinorin A (0.032 and 0.1 mg/kg, i.v.) were administered as a single bolus injection in rhesus monkeys and behavior was observed at various time points with an end time of 90 minutes. The behavioral effects were characterized utilizing two rating scales that measured sedation and posture, and it was observed that both salvinorin A (peak at 5 minutes, decline at 30 minutes) and U-69,593 (peak at 5 minutes, decline at 60 minutes) produced a dose-dependent increase in sedation and postural changes, with U-69,593 having a longer duration of action than salvinorin A. The authors also monitored facial relaxation and ptosis. It was observed that salvinorin A at the doses mentioned produced a time- and dose-dependent increase in facial relaxation and ptosis with very rapid onset of action (1-2 minutes after i.v. administration). U-69,593 (0.01 and 0.032 mg/kg, i.v.) also produced an increase in facial relaxation and ptosis, however with an unclear timeline and longer duration of action. The opioid receptor antagonist nalmefene (0.01 or 0.1 mg/kg, s.c.) was able to completely inhibit the effects of salvinorin A on sedation and posture as well as facial relaxation and ptosis. In contrast, pretreatment with neither CB1R antagonist rimonabant nor the 5-HT_2 receptor antagonist ketanserin, were effective in modulating the effects of salvinorin A. Experiments also confirmed the rapid entry of salvinorin A into the brain of Hooker and coworkers.[281] Salvinorin A was observed in the brain immediately after i.v. injection with a peak value at 2 minutes and decreasing gradually up to 30 minutes.

In 2011, Johnson and coworkers reported preliminary findings of the basic physiological, behavioral and subjective effects of salvinorin A in human subjects.[282] In this double blind, placebo controlled experiments, 16 doses of salvinorin A were used ranging from 0.375-21

μg/kg and administered by vaporization and inhalation. Blood pressure and heart rate were measured throughout the duration of the study and participants were asked to rate the drug strength every 2 minutes for 60 minutes after drug administration. To gain a better understanding of the subjective effects of salvinorin A, the subjects were asked to complete two questionnaires, The Hallucinogen Rating Scale (HRS, 99 items) and the Mysticism Scale (M scale, 32 items). It was observed that the peak drug strength was at 2 minutes post administration and decreased gradually such that at 20 minutes indication of "possible mild" effect was noted. The study found no physiological changes in heart rate or blood pressure and no tremors were observed, indicating that salvinorin A was physiologically and psychologically well tolerated at the doses tested. Doses of salvinorin A in the range of 4.5-21 μg/kg were rated as significantly stronger than placebo; this outcome was found to correspond to the answers given in the HRS and M scale questionnaires all of which resemble results seen with classical hallucinogens.

A double-blind, placebo study of the behavioral and psychological effects of salvinorin A was reported by Addy in 2012, in which a larger group of subjects (30) was used.[283] In this study the participants smoked either a dose of 1,076 mg of salvinorin A deposited on 25 mg of dried *S. divinorum* leaves. The control was unaltered plant leaf material that was presumed not to be psychoactive (≤100 mg of salvinorin A). The participant's vitals were taken one hour after drug administration. As reported by Johnson and colleagues, no dose-related physiological changes were observed during the study and the drug was well tolerated by the participants. After 60 minutes post administration, each participant was asked to fill out an HRS, and behaviors recorded during the first 20 minutes after administration were used for further analysis. It was observed that after salvinorin A inhalation, the participants displayed increased laughing,

talking, and movement as compared to placebo and also displayed paranoid ideation and physical contact with the monitor. From the completed HRS questionnaire, it was reported that salvinorin A produced an effect significantly different than that of placebo with 43% of the participants describing it as similar to that of dreaming. Additionally, 50% of the participants reported that the present experience was unlike any other experience of an altered state of consciousness that they had encountered before. The study included an 8 week follow-up session, in which 87% of the participants reported that the effects of salvinorin A lasted less than 24 hours and 70% reported after effects lasting more than 24 h, in particular up to 3 days. Despite the undesirable after effects, no participant would refuse salvinorin A in the future.

An additional double-blind, placebo controlled, randomized, crossover study was designed by Ranganathan and coworkers to assess the behavioral and subjective effects of salvinorin A (doses 8 and 12 mg/kg).[284] Ten subjects participated in this study in which subjective feelings were measured with a self-reported visual analog scale (VAS) and psychotomimetic symptoms were measured with the Positive and Negative Syndrome Scale (PANSS) and the Psychotomimetic States Inventory (PSI). All subjects were monitored for physiological changes and EEGs were obtained after drug administration by inhalation. No changes in heart rate and blood pressure were noted throughout the duration of the study. However, salvinorin A did cause a decrease in the resting state of the EEG spectral power. It was observed that salvinorin A significantly elevated both cortisol and prolactin levels, which returned to baseline 60 minutes after administration. As previously reported, salvinorin A had short duration of action with a peak at 10 minutes post administration with a return to baseline within 30 minutes of administration.

A recent publication by MacLean and colleagues investigated the dose-related effects of salvinorin A in a double-blind, placebo controlled study.[285] Doses of salvinorin A (0.375-21 μg/kg) were administered in an ascending order, with a placebo session inserted randomly. All participants completed 20 sessions (16 different salvinorin A doses and 4 placebo doses) where salvinorin A was administered by a slow inhalation lasting 40s. As in their preliminary study, data was collected every 2 minutes for 60 minutes after drug administration, which included collection of blood pressure and heart rate, drug strength ratings and rating of drug effects. Effects of salvinorin A on recall and recognition were also assessed by an auditory memory task where salvinorin A produced a decrease in word recall and recognition. At the end of each session, the participants were asked to complete several questionnaires to obtain the subjective effects of salvinorin A. Consistent with previous results, time- and dose-related response was observed with rated drug strength peaking at 2 minutes and gradually decreasing toward pre administration levels. No physiological changes and no kinetic tremors were observed in the subjects during the experiment. The end of session measures confirmed the known hallucinogenic and dissociative effects of salvinorin A and they also provided evidence of possible abuse liability. Follow-up assessments showed no evidence of lasting negative effects and confirmed the notion that salvinoin A produces unique effects. Additional studies are necessary in order to further characterize the unique effects of salvinorin A and other KOP receptor agonists.

Salvinorin A and Drug Abuse

In 2008, study designed by Chartoff and coworkers aimed at examining the effects of acute activation of KOP receptor system on the behavioral effects of cocaine.[286] They hypothesized that acute activation of the KOP receptor system would decrease the behavioral effects of cocaine and that prior exposure to repeated activation of the KOP receptor system would potentiate the behavioral effects of cocaine. Acute administration of salvinorin A five minutes before cocaine challenge in rats was found to block the locomotor stimulant effects of cocaine. It was also demonstrated that acute salvinorin A blocked the locomotor effects of SKF 82958, a dopamine D_1 receptor agonist. Prior exposure to repeated administration of salvinorin A was shown to potentiate the locomotor response to a subsequent cocaine challenge in rats and was likewise shown to potentiate the effects of the dopamine agonist SKF 82958. Furthermore, increase of c-Fos expression (indicative of second messenger activation) in the NAc and dorsal striatum among others was observed during acute salvinorin A administration. However, during chronic administration of salvinorin A prior to cocaine challenge, no change in c-Fos expression was noted in the dorsal striatum. Collectively, this study demonstrated that salvinorin A has an effect on the locomotor stimulant effects of cocaine, effect likely caused by dopamine facilitation in the dorsal striatum.

As an extension to the above study, in 2009, Morani and colleagues reported the effects of several KOP receptor agonists on cocaine-induced drug-seeking in rats.[287] As previously reported for other KOP receptor agonists, salvinorin A was able to dose-dependently attenuate cocaine-induced cocaine seeking, at doses 0.3 and 1.0 mg/kg, i.p. Doses of 0.3 and 1.0 mg/kg salvinorin A failed to significantly decrease sucrose-reinforced responding.

Metabolism of Salvinorin A

In 2005, Schmidt and coworkers reported that the primary metabolite of salvinorin A ex vivo in both human and rhesus monkey plasma, as well as rhesus monkey cerebrospinal fluid (CSF) was salvinorin B, a C-2 deacetylated derivative of salvinorin A (**110**, **Figure 22**). It was observed that in all samples that the concentration of salvinorin B gradually increased as salvinorin A concentrations decreased.[288] As an extension of their previous work, Schmidt and colleagues reported another experiment in which they described the first *in vivo* pharmacokinetics experiment of salvinorin A in non-human primates.[289] Four (2 males and 2 females) rhesus monkeys were injected with an intravenous 0.032 mg/kg dose of salvinorin A, and upon administration blood samples were collected at selected intervals (0, 1, 5, 15, 30, and 60 minutes). The elimination $t_{1/2}$ of salvinorin A was determined to be 57 minutes, however gender variations were observed. The authors found that the concentration of salvinorin B did not increase over time and that it was below detectable levels, which could be indicative of rapid clearance of salvinorin B or its accumulation in other tissues. Kutrzeba and colleagues, utilizing various microorganisms (fungi) and brain homogenates came to the same conclusion that salvinorin B is the major metabolite of salvinorin A.[290] A human volunteer study reported by Pichini and coworkers developed a method for the quantification of salvinorin A (administered via inhalation) in blood, urine, sweat and saliva samples.[291] They determined that only 0.59 mg (1.2%) of the total administered dose was excreted in urine.

Teksin and coworkers designed a study where they looked at the *in vitro* metabolism of salvinorin A using recombinant human CYP450 and UGT2B7 enzymes.[292] In this study, a series of specific human CYP450 isoforms were used and incubation of salvinorin A (5 and 50 μM) with CYP2D6, CYP1A1, CYP2C18, and CYP2E1 resulted in a significant decrease in the remaining concentration of salvinorin A. Salvinorin A was also co-incubated with UGT2B7

enzyme and similarly to the results seen with CYP450 incubation, reduction of remaining salvinorin A concentration was once again observed. Moreover, the authors noted that there was evidence pointing to a saturable metabolism, in which lower concentrations are metabolized more efficiently than higher concentrations. Together, these studies suggest that several CYP450 as well as UGT2B7 enzymes are involved in the metabolism of salvinorin A.

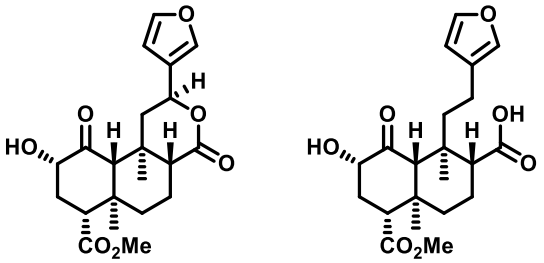

110
Salvinorin B

111

Figure 22. Metabolites of salvinorin A

Lastly, Tsujikawa and coworkers reported an *in vitro* study of salvinorin A metabolism and stability on rat plasma.[293] In this study, they aimed to characterize the esterases responsible for salvinorin A metabolism by using selective esterase inhibitors (5). In control experiments where salvinorin A was incubated for 24 hours at 37 °C, production of degradation products was not observed. Additionally, addition of sodium fluoride (NaF), an esterase inhibitor, inhibited metabolism of salvinorin A to salvinorn B. Two of the inhibitors tested showed concentration-dependent inhibition of metabolism of salvinorin A by hydrolytic inactivation, specifically sodium *bis*-*p*-nitrophenyl phosphate (BPNP), an inhibitor selective for carboxyesterases (CES) and phenylmethylsulfonyl fluoride (PMSF), selective serine esterase inhibitor. These findings support the fact that CES may be involved in salvinorin A metabolism, because CES is a serine

esterase. The authors also report an additional major metabolite of salvinorin A (**111**, **Figure 22**), which was obtained with incubation of NaF with rat plasma.

SAR Studies on Salvinorin A

Its unique non-nitrogenous structure has prompted many investigations into developing SAR studies to identify the pharmacophore required for binding at KOP receptors. The overall summary of the current SAR of salvinorin A is presented in **Figure 24**.[294]

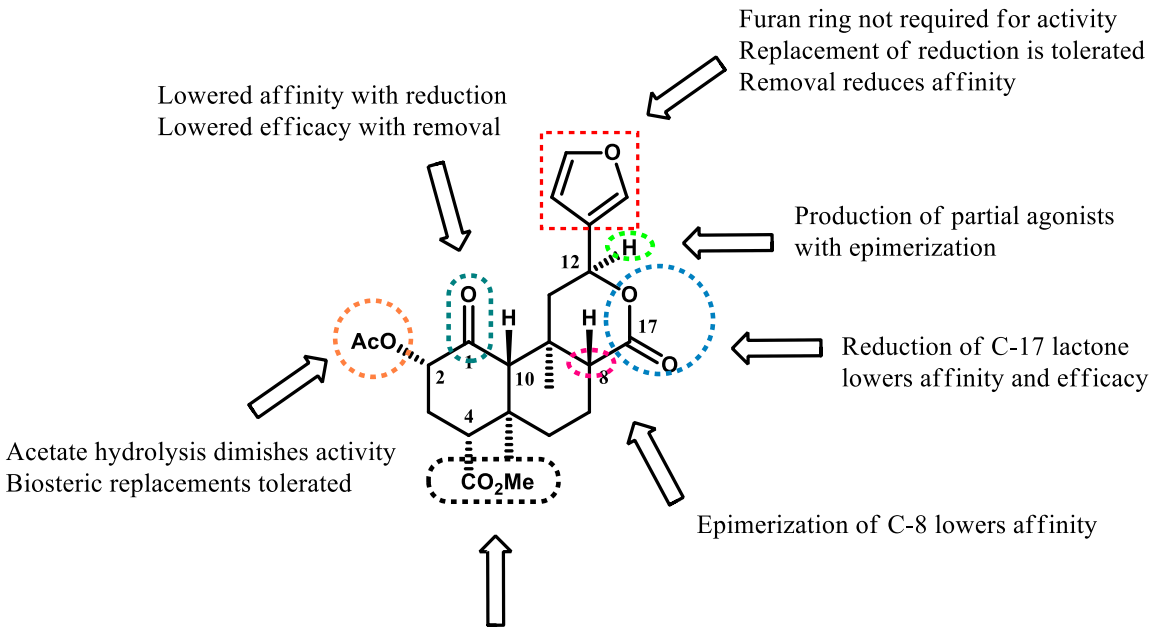

Figure 23. Overall summary of the SAR of salvinorin A analogues

Epimerization at C-8 carbon leads to lowered affinity whereas epimerization at C-12 leads to formation of partial agonists at KOP receptors. The furan ring is not necessary for activity and reduction or replacement are tolerated, however complete removal leads to loss in

affinity. Lowered affinity and efficacy are the result with reduction of C-17 lactone, additionally removal of C-1 ketone leads to lowered efficacy and reduction of the C-1 ketone leads to lowered affinity. The ester moiety at C-4 position is necessary for KOP receptor affinity since reduction of affinity is seen with reduction or hydrolysis of the methyl ester. Hydrolysis of the acetate at the C-2 position leads to complete loss of activity; however bioisosteric replacements such as amides, carbamates, carbononates, sulfonates and thisoesters are well tolerated at this position as are ethers and amides, as well as esters other than acetate.

Furan Ring Modifications

The furan ring of salvinorin A has been the focus of various modifications in order to assess the binding within the KOP receptor pocket and elucidate SAR at this position, which would assist in the development of enhanced pharmacokinetic properties at this position of salvinorin A. Furthermore, furan ring modification will assist in the development of compounds with potential therapeutic potential for treatment of KOP receptor system related CNS disorders. The various furan modifications reported thus far have yielded many analogues with very diverse pharmacological profiles.

Reduction of the furan ring afforded tetrahydrofuran analogue (**112**) of salvinorin A (**Figure 24**).[295, 296] Different values have been reported for the KOP receptor affinity of the racemate of **112** most likely due to different methods of screening.[295, 296] The C-13R epimer of **112** was separated from the mixture using HLPC conditions to yield a full KOP receptor agonists with 3.7 nM binding affinity, however the observed efficacy was 17-fold less than salvinorin A.[296] The retained activity of **112** at the KOP receptors indicates that an aromatic group at the C-

12 position may not be necessary for activity. However, complete removal of a substituent at this position in the ring (**113**) resulted in a 1700-fold decrease in KOP receptor affinity *(K_i* = 3400 nM vs. K_i = 1.9 nM).[296, 297]

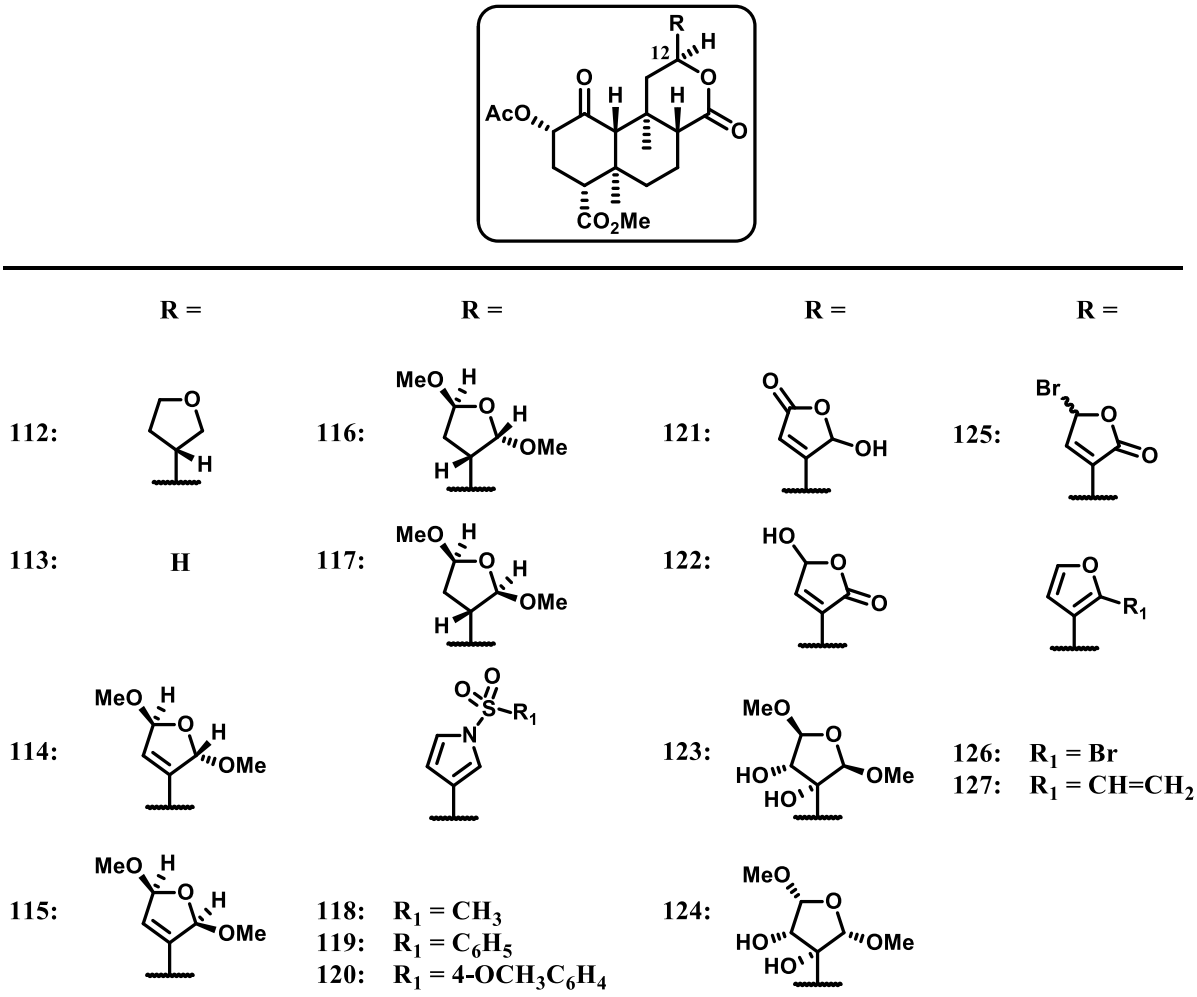

Figure 24. Previous furan ring modifications - I

When salvinorin A is combined with bromine, *trans* (**114**) and *cis* (**115**) 2,5-dimethoxydihydrofuran isomers were synthesized.[296, 298] These isomers were separated by HPLC and upon pharmacological testing it was observed that these isomers have reduced KOP

receptor affinity compared to salvinorin A (1.9 nM) of 480 nM and 180 nM, respectively.[296] Moreover, these analogues were found to be weak nonselective opioid receptor antagonists.

Hydrogenation of isomers **114** and **115** with Rh/C in a mixture of DCM and MeOH, resulted in dimethoxytetrahydrofuran derivatives **116** and **117**.[296] Compound **116** exhibited similar affinity to that of salvinorin A of 25 nM, whereas analogues **117** exhibited slightly lower affinity for KOP receptors of 125 nM. Despite the similar affinity, analogue **116** was 52-fold less efficacious at KOP receptors than salivnorin A.[296] Reaction of the racemic mixture of **119** and **119** with the appropriate sulfonamide afforded *N*-sulfonylpurroles **118**, **119**, and **120**.[297] These analogues had significantly reduced affinity compared to salvinorin A, however in the [^{35}S]GTP-γ-S functional assay they were found to be partial agonists with E_{max} values of 70%, 60%, and 60%, respectively.[297] Subjection of salvinorin A to photoxidation in the presence of sunlight resulted in the natural products salvidivins A and B, **121**, and **122**, respectively.[296] Salvidivin A showed to have antagonist activity at MOP and KOP receptors with K_e values of 760 nM and 440 nM, respectively.[296] Selective oxidation of **115** over its diastereomer **114** resulted in the formation of salvinicin A (**123**) and salvinicin B (**124**), natural products present in *S. divinorum*.[298, 299] Salvinicin A displayed KOP affinity of 390 nM and it exhibited partial KOP receptor activity with an EC_{50} of 4.1 μM and E_{max} = 80% relative to U-50,488. Salvinicin B on the other hand, displayed KOP receptor affinity of 7 μM and MOP receptor antagonist activity with a K_e of 1.9 μM.[294, 299] Reacting salvinorin A with bromine afforded dihydrofuran analogue **125** as a mixture of C-15 α and β isomers, though the C-15 β isomer was found to be more stable.[298] Treatment of salvinorin A with NBS affords bromo-salvinorin A **126**.[296, 298, 300] Bromo-salvinorin A showed to be a potent KOP receptor agonist with K_i value of 3 nM and an EC_{50} = 50 nM.[294] Exposure of bromo-salvinorin A (**126**) to Stille-coupling conditions afforded

analogue **127**, which well tolerated at KOP receptors as a full agonist with K_i = 7.1 nM and EC_{50} = 4.6 nM.[300]

Furan rings are well known to undergo Diels-Alder reaction, where the furan ring acts as the 4 π diene.[301] Thus, the Diels-Alder reaction was used to synthesize analogues that would explore the steric requirements for binding at the KOP receptors.[301] Treatment of salvinorin A with benzyne afforded analogue **128** (**Figure 25**).[301] This cycloadduct exhibited low KOP receptor affinity of 790 nM. Exposure of salvinorin A to various alkynes resulted in the synthesis of analogues **129** – **132**.[301] Despite the interesting chemistry that led to these cycloadducts, it was shown that all of these analogues have lower affinity for KOP receptors than salvinorin A, with K_i values of 120 nM (ED_{50} = 2150 nM) 60 nM (ED_{50} = 980 nM), 1900 nM, and 1900 nM, respectively.[301] Submission of analogue **128** to $Fe_2(CO)_9$ led to a reductive elimination of water and subsequent aromatization to yield compound **133**.[301] This compound was found to be inactive at the opioid receptors. Reaction of salvinorin A with selected trienones resulted to the formation of cycloadducts **134** and **135**, whose affinity at the KOP receptors was determined to be very poor, with K_i values of >13,000 nM and 290 nM, respectively.[301] Exposure of bicycles **129** – **132** to $Fe_2(CO)_9$ once again underwent similar reaction as proposed for analogue **133** to yield aromatic analogues **136** – **139**, respectively. These non-heterocyclic aromatic analogues exhibited reduced affinity at KOP receptors when compared to salvinorin A.[301]

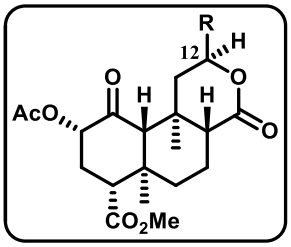

R =

128:

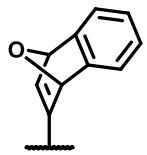

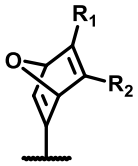

129: $R_1 = CO_2Et$, $R_2 = CO_2Et$
130: $R_1 = CO_2Me$, $R_2 = CO_2Me$
131: $R_1 = CO_2Et$, $R_2 = CF_3$
132: $R_1 = CF_3$, $R_2 = CO_2Et$

R =

133:

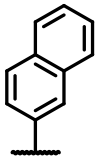

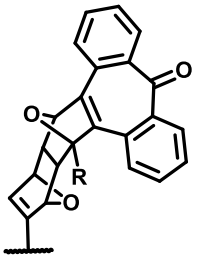

134: R = H
135: $R = CH_3$

R =

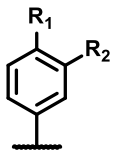

136: $R_1 = CO_2Et$, $R_2 = CO_2Et$
137: $R_1 = CO_2Me$, $R_2 = CO_2Me$
138: $R_1 = CO_2Et$, $R_2 = CF_3$
139: $R_1 = CF_3$, $R_2 = CO_2Et$

140:

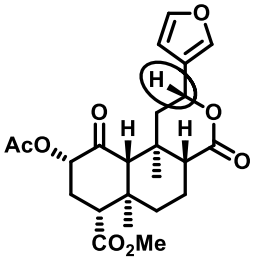

Figure 25. Previous furan ring modifications - II

12-*epi*-salvinorin A (**140**), has been synthesized utilizing several methods by both Beguin and coworkers and Lovell and colleagues.[300, 302] Lovell and coworkers reported KOP receptor affinity for 12-*epi*-salvinorin A very similar to that of salvinorin A (K_i = 17 nM vs. K_i = 7.4 nM), however that difference was slightly larger in the hands of Beguin and coworkers (K_i = 41 nM vs. K_i = 2.5 nM).[300, 302] Although 12-*epi*-salvinorin A exhibited similar affinity to that of salvinorin A, it was 18-fold less potent than salvinorin A at KOP receptors (EC_{50} = 720 nM vs. EC_{50} = 40 nM).[302]

Oxidative degradation of salvinorin A with $NaIO_4$ affords salvinorin A acid **141**, a valuable intermediate (**Figure 26**). Besides being an exceptionally valuable intermediate, salvinorin A acid retains both affinity and efficacy at KOP receptors with K_i = 55 nM and EC_{50} = 167 nM, respectively.[294] Exposure of acid **141** to thioesterification results in salvinorin A thiophenol intermediate **142**.[302] Intermediate **142** was subjected to Liebesking-Srogl coupling reaction to afford analogues **143** – **160**.[302] All of the aromatic ketones synthesized exhibited affinity for KOP receptors, among those in the low nanomolar range are analogues **143** (K_i = 70 nm, EC_{50} = 2280 nM, E_{max} = 74%), **150** (K_i = 40 nM, EC_{50} = 730 nM, E_{max} = 92%), **154** (K_i = 80 nM, EC_{50} = 2130 nM, E_{max} = 92%), **155** (K_i = 36 nM, EC_{50} = 1630 nM, E_{max} = 95%), and **157** (K_i = 31 nM, EC_{50} = 620 nM, E_{max} = 88%).[302] In addition to the functional [^{35}S]GTP-γ-S assay, compound **150** was also subjected to fluorescent Ca^{2+} mobilization assay and an EC_{50} value of 75 nM was determined.[302] Utilizing Stille coupling conditions, Beguin and coworkers also synthesized analogues **143**, **154**, and **155**.[300] Analogue **143** exhibited similar affinity and potency to that reported by Lovell and coworkers.[300] Once again utilizing acid **141** to create an acid chloride in situ and with exposure to various aryltributyl tin reagents, Beguin and coworkers were able to synthesize analogues **161** – **163**.[300] Analogues **162** and **163** presented to be full agonists at KOP receptors with K_i values of 83 nM and 20 nM, respectively; and EC_{50} values of 195 nM and 36 nM, respectively, whereas analogue **161** displayed no activity at KOP receptors.[300]

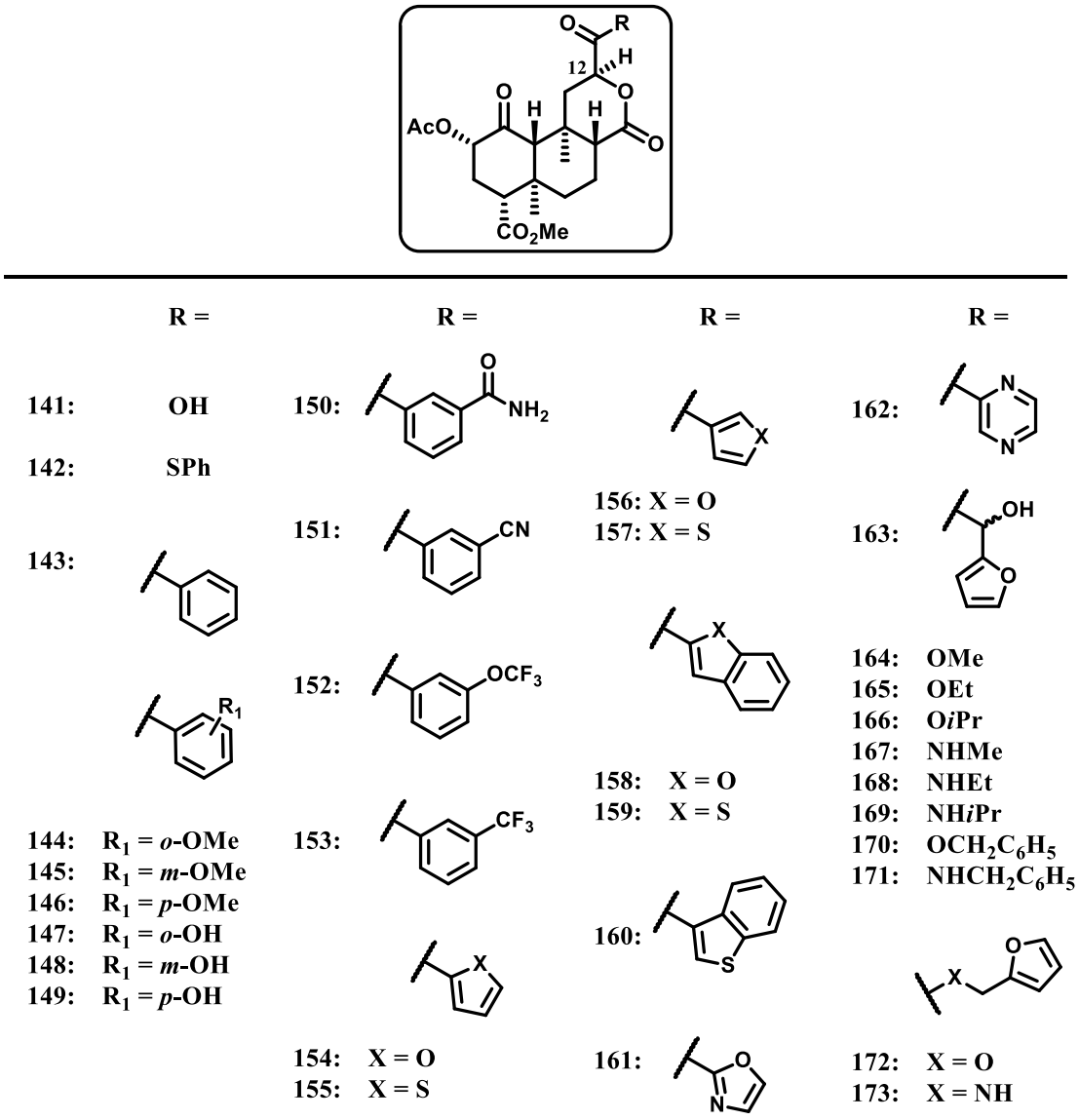

Figure 26. Previous furan ring modifications - III

Synthesis of ester and amide analogues **164** – **173** can involve several different routes as reported by Beguin and coworkers.[300] The synthesized esters exhibited moderate affinity for KOP receptors with K_i values in the range of 109 to 196 nM for esters **164** through **166**, respectively, however increase in size of esters **170** and **172** resulted in complete lack of affinity. Salvinorin A amide analogues were completely devoid of activity at the KOP receptors.[300]

Carboxylic acid **141** can also be employed in the synthesis of analogues **174** and **175** utilizing either ethanolamine or L-serine methyl ester hydrochloride and amide bong coupling conditions, which is followed up by a cyclization with bis(2-methoxyethyl)aminosulfur trifluoride (Deoxo-Fluor) (**Figure 27**).[296, 297] Oxazoline **174** exhibited moderate affinity of 300 nM for KOP receptor however that is 157-fold less than salvinorin A (K_i = 1.9 nM).[296] Conversion of **175** to compound **176** was accomplished using base, however this analogue exhibited no activity for the KOP receptors.[297] Carboxylic acid **141** was again used as the starting material towards the synthesis of various oxadiazoles (**177** – **183**) together with the appropriate amidoximes.[296, 297, 300, 303] Simpson and coworkers reported that oxadiazole **177** exhibited affinity of 59 nM at KOP receptors, and it was also demonstrated that this analogue is a functional antagonist at MOP and KOP receptors with K_e values of 430 nM and 360 nM, respectively.[296] Conversely, no activity was observed for these oxadiazoles (**177** – **183**) in the assays reported by Beguin and coworkers.[300]

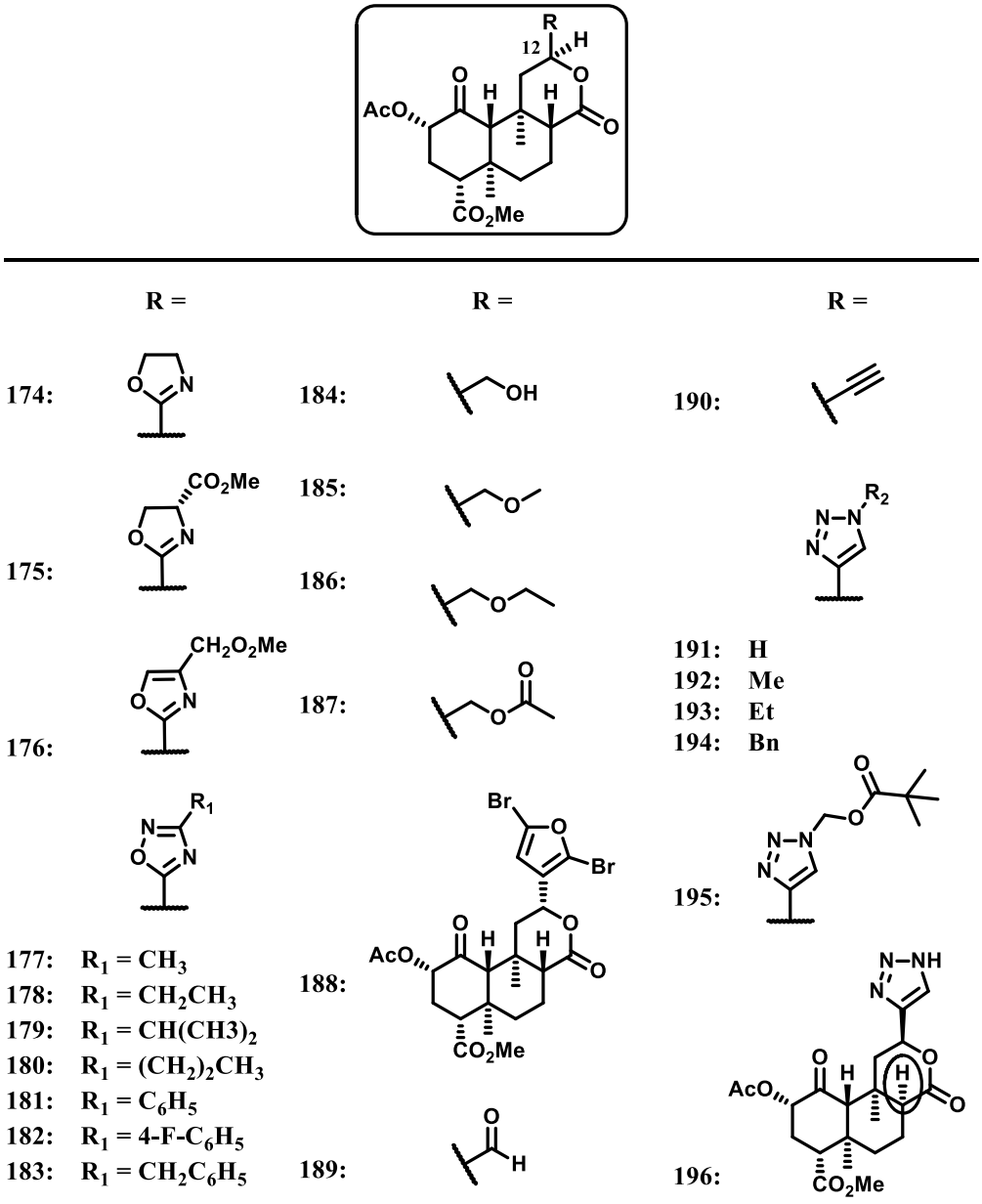

Figure 27. Previous furan ring modifications - IV

Carboxylic acid **141** has been proven to be one valuable intermediate and it was once again used by Beguin and coworkers for the synthesis of analogue **184**, which was accomplished with reduction of the acid with borane.[300] Compound **184** was then used in the synthesis of analogues **185** and **186**, which were prepared in the presence of silver oxide and either,

iodomethane or iodoethane, respectively.[300] Acetylation of compound **184** afforded analogue **170**. Reduction of carboxylic acid **141** to afford alcohol **184** resulted in complete loss of activity, whereas analogues **185** – **187** retained some affinity for KOP receptors.[300] 12-*epi*-salvinorin A was the starting material used in the synthesis of analogue **188**, which was accomplished with NBS and chloroform.[304] This analogue displayed similar affinity and activity for KOP receptors as 12-*epi*-salvinorin A.[304]

Oxidation of analogue **184** with Dess-Martin periodate afforded aldehyde **189**, which was then subjected to Seyferth-Gillbert homologation conditions which provided alkyne analogues **190**.[303] This alkyne intermediate was coupled with various azides under copper (I)-catalyzed click reaction conditions to yield analogues **191** – **194**.[303] Despite the interesting chemistry, the analogues synthesized were inactive at the opioid receptors.[303] Alkyne **190** was subjected to azidomethyl pivalate and copper sulfate condition to afford pivalyl triazole **195**, which did not exhibit any activity at the opioid receptors.[303] Treatment of analogue **195** with base and subsequent acetylation at the C-2 position afforded 8-*epi*-**191** (**196**), which did not show any activity at opioid receptors.[303]

Synthesis of salvinoirn A analogues **197** – **222** (**Figure 28**) was achieved utilizing carboxylic acid **141** and appropriate amines or alcohols in the presence of amide coupling reagents.[305] The prepared amides and esters were shown to display very poor affinity at KOP receptors with the best affinity seen with analogues **215** and **221** with K_i values of 140 nM and 160 nM, respectively.[305] In the [^{35}]GTP-γ-S functional assay, analogues **215** and **221** were found to be 100-fold less efficacious as ligands at KOP receptors, with compound **221** showing partial agonist characteristics (E_{max} = 57%).[305]

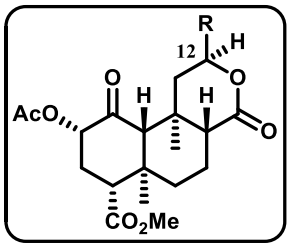

R =

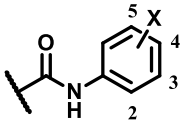

197: X = H
198: X = 2-Br
199: X = 3-Br
200: X = 4-Br
201: X = 2-OMe
202: X = 3-OMe
203: X = 4-OMe
204: X = 3-OMe, 5-OMe
205: X = 2-OMe, 4-OMe
206: X = 3-OMe, 4-OMe
207: X = 2-OMe, 4-OMe

208: 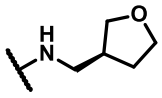

209: 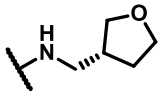

210: 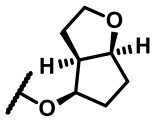

R =

211: 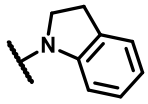

212: 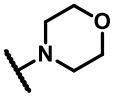

213: 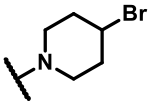

214: 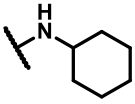

215: 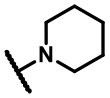

216: 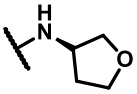

R =

217: 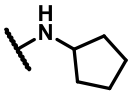

218: 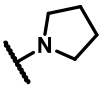

219: 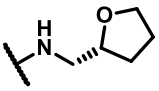

220: 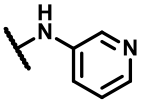

221: 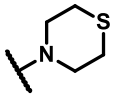

222: 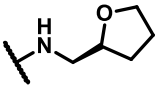

R =

223: 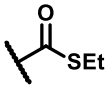

224: 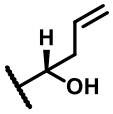

225: 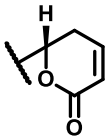

226: 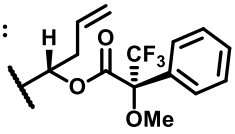

227: 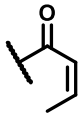

228: 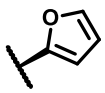

Figure 28. Previous furan ring modifications - V

Thioester analogue **223** was a valuable intermediate in the synthesis of salvinorin A aldehyde **189**.[305] Aldehyde **189** was asymmetrically allylated using B-allyl-(10*S*)-(trimethylsilyl)-9-borabicyclo[3.3.2.]decane, to afford analogue **224**.[305] Compound **224** showed to be a versatile analogue that can undergo several different conditions such as esterification to

yield Mosher ester **226** (used to determine the stereochemistry of the allylic alcohol **224**) and acylation followed by ring closing metathesis with 2nd generation Grubb's catalyst to afford analogue **225**.[305] Analogue **225** was determined to be inactive at KOP receptors.[305] Liebesking-Srogl coupling reaction was employed to afford analogue **227** from salvinorin A thiophenol ester **142** (**Figure 26**), which was then subjected to oxidative conditions with SeO_2 to yield the cyclized 2-furan analogue of salvinorin A (**228**).[302] It was determined that these analogues exhibited affinity for KOP receptors, K_i = 320 nM and K_i = 30 nM, respectively.[302] Although the similar affinity to salvinorin A, 2-furan **228** was showed to be 3.5-fold less potent at KOP receptors determined with the [^{35}]GTP-γ-S functional assay.[302] Conversely, utilizing the fluorescent Ca^{2+} mobilization assay, analogue **228** displayed efficacy only 2-fold lower than that of salvinorin A.[302]

Salvinorin A's unique structure has been of interests to many researchers, and many derivatives have been synthesized, especially focusing at the C-13 and C-2 positions in the scaffold.[168, 294, 306] The various derivatives synthesized exhibited interesting pharmacological profiles that will help us better understand the SAR that lead to activity at the KOP receptors.[295-305] Additional furan ring modifications that introduce steric bulk and examine the favored oxygen atom position will help us better understand the furan binding pocket at the KOP receptor.

Rationale and Specific Aims

Despite the great therapeutic potential of salvinorin A, there are several disadvantages that need to be addressed before savinorin A can become a valuable therapeutic agent. The presence of hallucinations and dysphoria with salvinorin A administration are two of the drawbacks that need optimization if salvinorin A were to ever become a useful therapeutic agent. Poor pharmacokinetic properties that salvinorin A exhibits represent another difficulty in the development of salvinorin A as a useful agent. Typically, pharmacokinetics are referred to and known as ADMET, which stands for Absorption, Distribution, Metabolism, Excretion and Toxicity. ADMET properties are important for every clinical candidate and are assessed early in drug discovery, normally through total synthesis efforts or semi-synthetic modifications of the molecule of interest.

Teucrin A (*Teucrium chamaedrys L.*), a neoclerodane diterpene structurally similar to salvinorin A was reported to cause hepatic necrosis.[307] This hepatotoxicity was attributed to the formation of reactive metabolites produced by CYP450 bioactivation. Interestingly, a tetrahydrofuran analogue of teucrin A (**229**, **Figure 29**) was showed not to produce any hepatotoxicity in mice. In 2006, Druckova and Marnett proposed that the toxic side effects of teucrin, the major constituent of germander are due to the formation of an enedial metabolite that arises from formation of an epoxide intermediate.[308, 309] Furthermore, aflatoxin B_1 (**230**), a difuranyl containing natural product has also been associated with hepatotoxicity due to the formation of a similar enedial species through CYP450 bioactivation.[310] Salvinorin A is a neoclerodane diterpene that possesses similar structural characteristics with teucrin A and aflatoxin B_1, a structural feature that may not be viable for medicinal use. Modification of the

furan ring through semi-synthetic efforts may lead to salvinorin A analogues without the risk for hepatotoxicity. However, before such studies are undertaken, additional information into the furan binding pocket of the KOP receptor must be obtained.

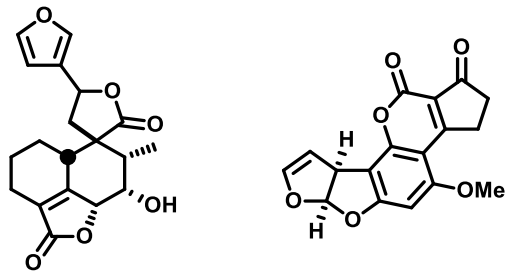

229
Teucrin A

230
Aflatoxin B_1

Figure 29. Furan containing natural products with associated toxicity

Our hypothesis is that further investigation into the SAR will assist in identifying novel salvinorin A analogues with improved pharmacological profiles that could have potential as clinical therapies. Our knowledge of the chemistry and pharmacology of salvinorin A would be facilitated with the proposed specific aims.

Specific Aim 1: Prepare selected salvinorin A analogues that will assist in the determination of the favored oxygen atom position of the furan ring at the KOP receptors, as well as explore the steric requirements at the C-13 position.

Evidence suggests that furan containing natural products may have the potential to be hepatotoxic, examples of this include aflatoxin B_1 and teucrin A, diterpenes structurally similar to salvinorin A.[307, 310] While further modifications of the furan ring will identify compounds with reduced risk for hepatotoxicity, additional information into the furan ring binding pocket must be initially obtained. Analogues that explore the addition of steric bulk, the required

conformation of the furan oxygen atom for activity at the KOP receptors, and the optimal distance between the furan ring and the salvinorin A core will be synthesized. This additional SAR will assist in demonstrating that modification at the C-13 position of salvinorin A are well tolerated at the KOP receptors and that opioid receptor selectivity can be obtained.

Specific Aim 2: Evaluate C-13 salvinorin A analogues for opioid receptor affinity and efficacy.

Compounds generated from Specific Aim 1 will be evaluated for their pharmacological profile at the opioid receptors. Where applicable radioligand binding assay that measures the displacement of the opioid ligands [^{3}H]DAMGO (MOP), [^{3}H]U-69,593 (KOP), and [^{3}H]DADLE (DOP) will be used to determine affinity for the opioid receptors. Selected ligands will then be evaluated in one of two functional screens; [^{35}S]GTP-γ-S functional assay or inhibition of adenylate cyclase activity assay. Characterization of the pharmacological behavior for selected analogues synthesized in Specific Aim 1 will be accomplished with the proposed assays.

Completion of the proposed specific aims will help us probe and increase our understanding of the furan binding pocket at the KOP receptor. Rational design of said analogues will allow us to explore the steric potential, the ideal position for binding of the furan oxygen atom, as well as the optimal distance between the furan ring and the core of the molecule. Completion of these studies will also afford us with novel opioid receptor analogues that can be further utilized as biological probes with a potential as clinical therapies. The results of these studies will be presented and discussed.

Results and Discussion

Introduction

In order to further investigate the furan binding pocket in the KOP receptor and the SAR of salvinorin A at the opioid receptors, additional salvinorin A analogues were designed and synthesized. The analogues prepared were designed to explore the changes at the C-13 position of the molecule and their effect on the activity at the KOP receptors. These modifications were designed to attain the optimal distance between the furan ring and the salvinorin A core, the steric requirements necessary for binding and activity at this position, the necessity of an aromatic substituent at the C-13 position, as well as the preferred orientation of the furan ring oxygen atom (**Figure 30**). Utilizing olefination and hydrogenation chemistry, several analogues were synthesized to test the proposed goals. The two carbon homologated analogues of salvinorin A were designed to test the steric requirements for activity at the KOP receptors, as well as to determine the preferred orientation of the furan oxygen atom, since the analogues were locked in a given conformation that came from the olefination process. Reduction of the set double bond would allow free rotation around the C-13 and examine the preferred orientation of the C-13 substituent. Furthermore, overall reduction of the implemented double bond and furan ring will examine both the preferred orientation of the substituent, as well as the necessity of an aromatic substituent at this position. Lastly, reduction of the furan ring of salvinorin A will further assess the necessity of aromatic substituents at the C-13 position for activity at KOP receptors.

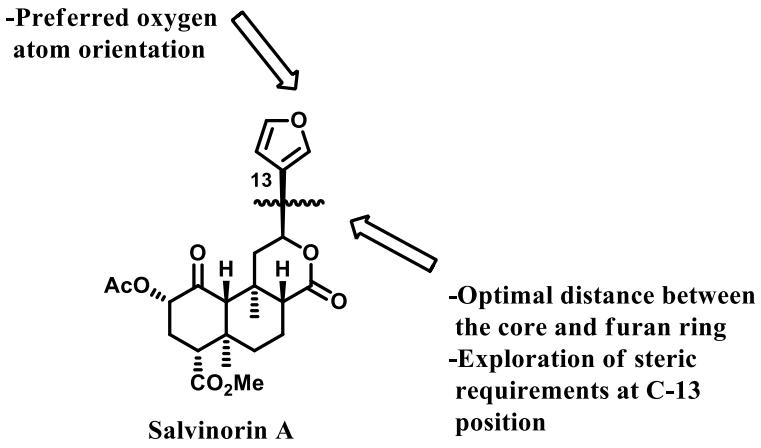

Figure 30. Rationale for proposed SAR of salvinorin A

Synthesis

To further understand the SAR of salvinorin A at KOP receptors, several analogues were synthesized. As reported previously, salvinorin A (**83**) was extracted from commercially available dried *S. divinorum* leaves.[311] Synthesis of the homologated C-13 salvniroin A analogues began with the synthesis of the Julia-Kocienski precursor as represented in **Scheme 1**. To obtain the needed Julia-Kocienski precursor, synthesis was initiated with 3-furaldehyde **231** that was reduced with $NaBH_4$ to yield the corresponding alcohol **232** in 88% yield. Alcohol **232** was then displaced with bromine in 45% yield (**233**) and treated with ammonium heptamolybdatetetrahydrate-peroxide complex to afford the Julia-Kocienski precursor **234** in 86% yield.[312] Julia-Kocineski olefination was chosen as the preferable method of homologation after several other procedures were attempted. Wittig olefination and Horner-Wadsworth-Emmons olefination conditions were ineffective due to low yields, difficulties in purification, and ultimately aldehyde degradation. Selective olefination of **83** was envisioned by introduction of an aldehyde at C-13, exploiting the reactivity of the aldehyde relative to the other four carbonyls present in **83**.

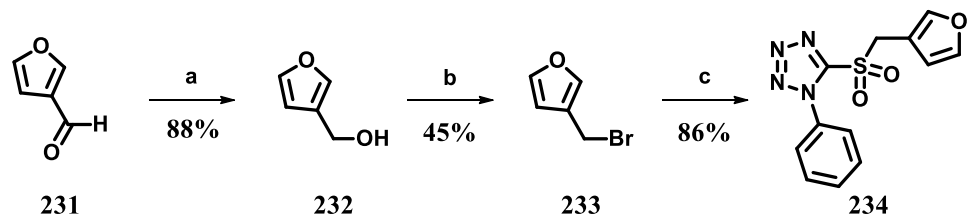

Scheme 1. Synthesis of Julia-Kocienski olefination precursor. *Reagents and Conditions:* a) $NaBH_4$, I_2, THF, 0°C; b) PBr_3, THF, 0°C; c) 1-phenyl-1*H*-tetrazole-5-thiol, Et_3N, H_2O_2, $(NH_4)_6Mo_7O_{24}{\cdot}4H_2O$, DCM

Aldehyde **189** was achieved following our previously published methods (**Scheme 2**).[298, 313] Briefly, oxidative degradation with $NaIO_4$ and catalytic $RuCl_3{\cdot}H_2O$ of salvinorin A (**83**) afforded carboxylic acid **141** in 74% yield. This valuable intermediate was then subjected to thioesterification with 2-chloro-4,6-dimethoxy-1,3,5-triazine (CDMT), *N*-methylmorpholine (NMM) and ethanethiol at ambient temperature to produce salvinorin A thioester **225** in 88% yield. Thioester **224** was then subjected to a reduction with triethylsilane and Pd/C to afford salvinorin A aldehyde **188** in 82% yield. Julia-Kocienski olefination conditions are applicable for use with base-sensitive aldehydes and are milder than previously attempted olefination conditions. The reaction of **189** and **234** in the presence of KHMDS afforded alkenes **235** and **236** in overall reaction yield of 25%. The individual isomers were isolated by flash column chromatography followed by additional HPLC purification in a 2:1 ratio of **235** to **236**.

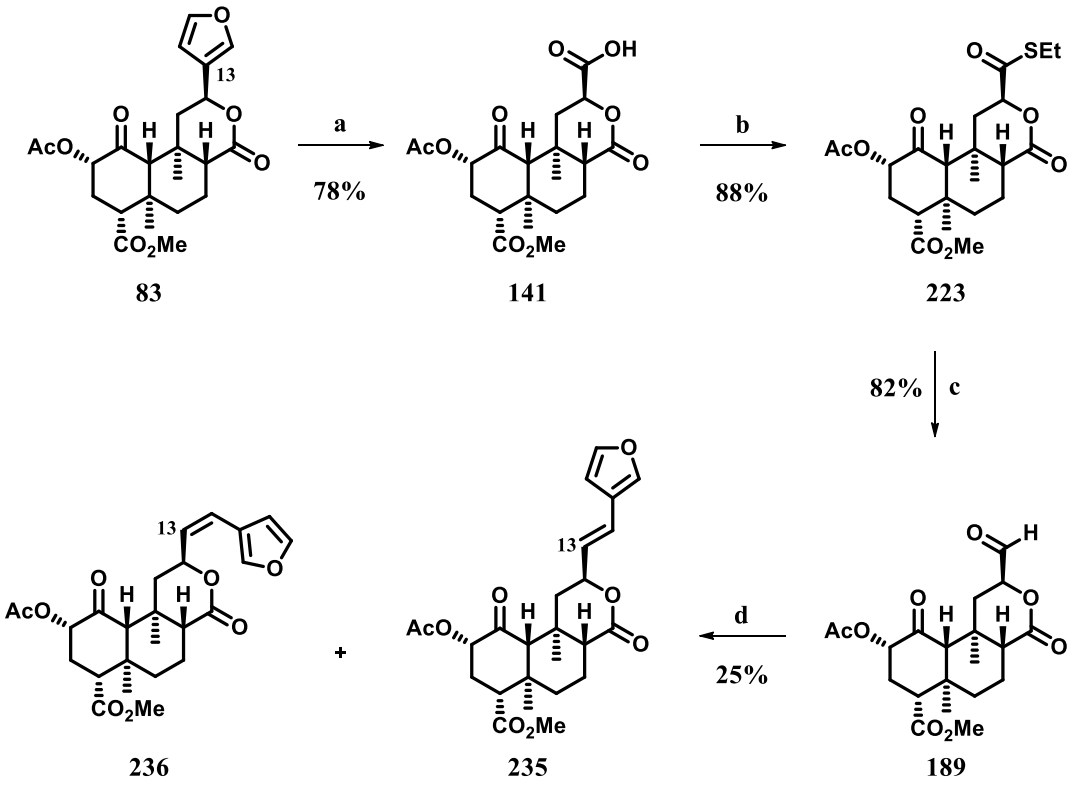

Scheme 2. Synthesis of *cis* and *trans* C-13 derivatives. *Reagents and Conditions:* a) $NaIO_4$, $RuCl_3 \cdot 3H_2O$, $CH_3CN/CCl_4/H_2O$; b) CDMT, NMM, EtSH, DCM; c) Pd/C, Et_3SiH, DCM; d) **234**, KHMDS, THF, -78°C

Analogues **235** and **236** were combined and subjected to hydrogenation conditions, where palladium on carbon, and EtOAc were utilized to afford analogue **237** in 40% yield (**Scheme 3**). Furthermore, analogues **235** and **236** were combined and again subjected to hydrogenation conditions, however with a higher quantity of palladium catalysts to afford all reduced alkane **238** in 39% yield. Salvinorin A (**83**) was additionally subjected to hydrogenation conditions utilizing a different metal catalyst, rhodium on carbon in a mixture of MeOH and DCM to produce all reduced furan **239** in 25% yield. Stereochemistry at the C-13 of analogue **239** was in accordance with previously published reports by Simpson and coworkers.[296]

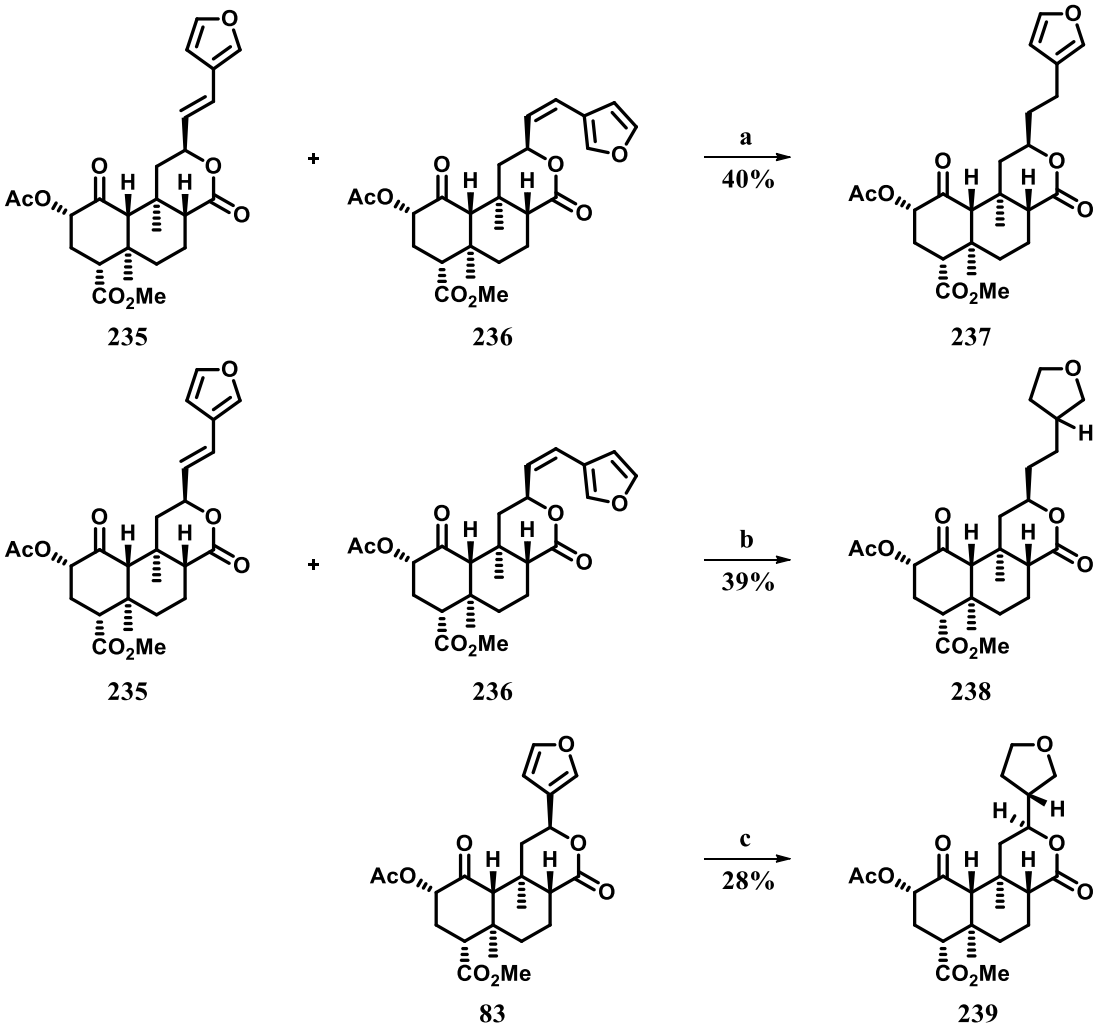

Scheme 3. Synthesis of two carbon homologated and all reduced C-13 analogues. *Reagents and Conditions:* a) Pd/C (10%, 0.03 equiv), EtOAc; b) Pd/C (10%, 0.06 equiv), EtOAc; c) Rh/C (5%), H_2, MeOH:DCM

Pharmacological Evaluation

In vitro Binding and Functional Assays

Analogues synthesized were then subjected for pharmacological testing. Analogues **235** and **236** were subjected to radioligand binding studies using methodology described previously (**Table 12**).[314] As represented in **Table 12**, it was found that the *cis* analogue **236** had almost 40-

fold higher affinity for the KOP receptor compared to the *trans* analogue **235** (K_i = 30 ± 4 nM vs. K_i = 1,120 ± 30 nM).

Table 12. Opioid receptor binding affinity for C-13 *cis* and *trans* salvinorin A analogues

	K_i ± SD, nM				
Cmpd	**[^{3}H]DAMGO (MOP)**	**[^{3}H]DADLE (DOP)**	**[^{3}H]U69,593 (KOP)**	**MOP/KOP**	**DOP/KOP**
83[a]	–	–	7.4 ± 0.7	N.D.[c]	N.D.[c]
235[b]	> 1,700	> 5,000	1,120 ± 30	> 1.5	> 4
236[b]	2,600 ± 140	> 5,000	30 ± 4	87	> 165

[a]Data from Lozama A. *et al*. *J. Nat. Prod*. **2011**, *74*, 718-726.
[b]Receptor binding was performed in CHO cells which express the human MOP, DOP or KOP receptors. All results are n = 3
[c]ND = not determined

Cis salvinorin A analogue (**236**) was also subjected to a functional assay to determine its activity at the KOP receptors using the [^{35}]GTP-γ-S assay (**Table 13**).[315] Despite the high affinity of *cis* analogue **236**, it was shown to be 34-fold less potent than **83** in the [^{35}]GTP-γ-S assay with an ED_{50} of 1,370 ± 180 nM while maintaining activity as a full agonist (E_{max} = 105 ± 4%).

Table 13. [^{35}S]GTP-γ-S KOP receptor potency for analogue **236**

Cmpd	**KOP ED_{50} ± SD[a]**	**KOP E_{max} ± SD[b]**
83[c]	40 ± 10	120 ± 2
236	1,370 ± 180	105 ± 4

[a]ED_{50} = Effective dose for 50% maximal response
[b]E_{max} is % which compound stimulates binding compared to (-)-U-50,488 (500 nM) at KOP receptors. n = 3
[c]Data from Lozama A. *et al*. *J. Nat. Prod*. **2011**, *74*, 718-726.

Analogues **237**, **238**, and **239** were subjected to pharmacological testing, utilizing the calcium mobilization assay (**Table 14**).[316] It was determined that the analogues did retain potency at KOP receptors. However, not all compounds exhibited high potency at the KOP receptors. Analogue **239** displayed potency at KOP receptors with an EC_{50} of 17 nM, compound

238 exhibited potency with an EC_{50} value of 229 nM and compound **237** displayed KOP receptor potency with an EC_{50} of 43 nM. Simpson and coworkers reported in 2007 the activity of analogue **239** in the [^{35}S]GTP-γ-S functional assay to be much lower than that seen for salvinorin A (EC_{50} = 750 nM vs. EC_{50} = 45 nM).[296] The differences seen in the potencies of this analogue could be due to the different conditions the two functional assays were performed. These results indicate that the interactions of the all reduced analogue **238** with the KOP receptor pocket are not as favorable as the ones seen with the homologated furan analogue **237**. Additionally, comparison of salvinorin A **83** and tetrahydrofuran **239** suggests that an aromatic substituent at the C-13 position is not necessary for activity at the KOP receptors. Although some of the analogues were not as potent as salvinorin A, modifications at the C-13 carbon are well tolerated and were all demonstrated to be full agonists at the KOP receptors.

Table 14. Analysis of potency of analogues **237** – **239** in the Ca^{2+} mobilization functional assay

Cmpd	KOP EC_{50} ± SEM (nM)[a]	KOP E_{max} ± SEM[b]
83	1.7 ± 0.6	103 ± 2
237	43.0 ± 7.1	124 ± 2
238	229 ± 12	98 ± 3
239	17.8 ± 1.6	111 ± 2

[a] EC_{50} = Effective concentration for 50% maximal response.
[b] Emax is % which compound stimulates binding compared to (-)-U-69,593 at KOP receptors. n = 3

Conclusions

C-13 Modified analogues of salvinorin A were designed and synthesized in order to further explore the SAR of the furan ring binding pocket. The analogues synthesized were

designed to address several key features including: (**a**) the optimal distance between the furan ring and the salvinorin A core and the steric requirements at this position; (**b**) the preferred orientation of the furan ring oxygen atom; and (**c**) the necessity of an aromatic substituent at the C-13 position of the molecule.

Upon completion of the synthesis, the designed analogues were subjected to pharmacological evaluation. Pharmacological evaluation of the *cis* and *trans* constricted alkene analogues of salvinorin A revealed a preferential conformation for activity at the KOP receptors as seen with the activity profile exhibited by the *cis* alkene conformer. Further, the C-13 two carbon homolog of salvinorin A was well tolerated at the KOP receptors. Moreover, a preferred furan ring *O*-atom orientation for activity at the KOP receptors was indeed observed in that the orientation of the *O*-atom in the *cis* conformer was more favored for binding at the KOP receptors than the orientation exhibited by the *O*-atom in the *trans* conformer. From the present study it can be concluded that a two carbon homolog at the C-13 position of salvinorin A is well tolerated at the KOP receptors, however additional studies need to be completed in order to determine the optimal distance between the furan ring and the diterpene core. Additionally, two carbon furan and tetrahydrofran homologs of salvinorin A were also well tolerated at the KOP receptor; nonetheless additional analogues need to be designed to determine the definite steric requirements at this position. Lastly, it was determined that an aromatic substituent at the C-13 position of the salvinorin A scaffold is not necessary for activity at the KOP receptors.

Future Directions

It is essential that the SAR exploration of the salvinorin A scaffold continue, especially at the furan ring position and the interactions of a C-13 substituent with the KOP receptor. The homologated furan ring analogues revealed that there may be features within the KOP receptor furan ring binding pocket that have yet to be explored. In this regard, a series of analogues with varying alkyl chain length could be used to determine the optimal length between the terpene core and the furan ring that would retain affinity and activity at the KOP receptors. The use of the Arndt-Eistert homologation reaction could be utilized as one of the strategies for the synthesis of such a series of analogues. A different series of analogues should also be designed to further test the steric requirements at this position, some of which could include the incorporation of various substituents off of the furan ring of a homologated analogue. This could be achieved utilizing Suzuki coupling reaction conditions employing bromo furan salvinorin A analogue **126** as the starting material. Based on the results reported above, a $\pi - \pi$ interaction is not necessary for activity at the KOP receptors and could be used as the basis for a series of different analogues that could be used to further probe the furan ring binding pocket. Such a series of analogues should explore the addition of various cycloalkyl substituents at the C-13 position in the molecule. Such prospective studies would help to further elucidate the SAR of the C-13 position in the salvinorin A scaffold.

The introduction of the X-ray crystal structures of the opioid receptors opened many opportunities for molecular modeling studies where the resolved structures can be implemented in the design of novel salvinorin A analogues. Despite the use of a KOP receptor antagonist to resolve the structure of the KOP receptor, one could implement such molecular modeling study as guidance towards the synthesis of novel salvinorin A analogues.

CHAPTER 2: SALVINORIN A

PART II: QUINONE CONTAINING SALVINORIN A ANLOGUES

Introduction to Marine Natural Products

The foremost traditional sources of drug molecules that have been the key players in the development of the pharmaceutical industry are natural products, specifically those derived from terrestrial sources, such as plants and microbes.[317] Agrochemicals, modern pharmaceuticals, traditional medicines, as well as herbal medicines were discovered through terrestrial bioprospecting, a search for biologically active substances from nature that has generated many structurally diverse bioactive molecules.[318] Despite the fact of the very successful and valuable terrestrial biodiversity that has and will certainly continue to provide us with valuable new bioactive molecules, the significance of exploration of novel ecosystems of molecular diversity continues to be indispensable.[318] This will allow for the discovery of exceptional structures with continuous scaffold diversity, however without previously being exposed to any known drug resistance mechanisms, a problem that has threatened the use of current therapies for various conditions.[318]

Oceans cover more than 70% of our planet's surface.[319] It has been estimated that certain marine ecosystems, such as coral reefs or the deep sea floor, contain a greater biological diversity than that seen in tropical rain forests. The ability of marine organisms to synthesize toxic compounds or attain them from other marine microorganisms, which are then used as a defense mechanism, lies in their sedentary life style and soft physical appearance.[319]

Consequently, the oceans represent an area of huge biological diversity that may lead to various novel structurally diverse bioactive compounds with potential for use in the clinic.

The first report of marine biologically active natural products was described by Bergmann and Feeney in 1950, where they reported the isolation of a mixture of nucleosides, spongothymidine and spongouridine from the Caribbean sponge *Tethya crypta*.[320] Their discovery led to the development of the antileukemic agent Ara-C (**240**) and its derivative Ara-A (**241**), an antiviral agent (**Figure 31**).[321] The introduction of scuba diving techniques allowed for a more comprehensive collection method of marine source organisms.[317]

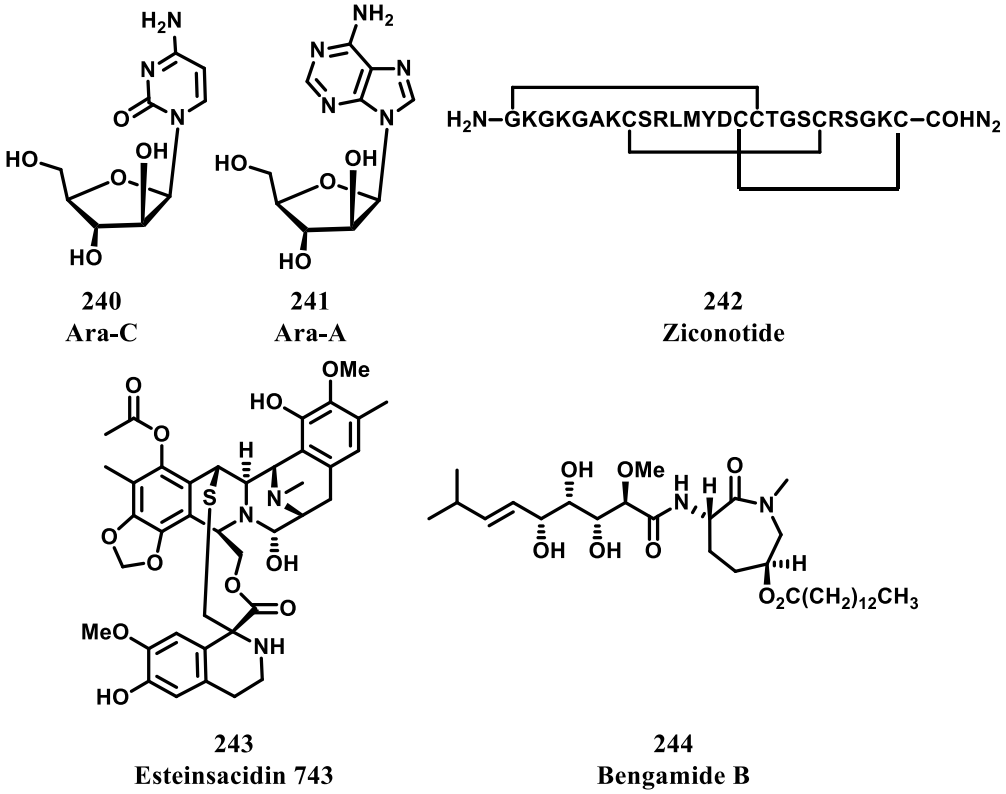

Figure 31. Representative marine bioactive natural products

Several interdisciplinary research areas such as ecology, biology, biochemistry, organic chemistry and pharmacology have been integral in the development of drug discovery from

marine organisms and to date there are many marine natural products and derivatives in the clinic or undergoing clinical trials. For instance, ziconotide (**242**) is a 25 amino acid derivative of the conotoxin peptide MVIIA isolated from a cone snail that is currently used as treatment for chronic pain; ecteinascidin 743 (**243**) is the first marine natural product that has reached the market as an anticancer drug and was isolated from a carribean tunicate; bengamide B, isolated from Jaspidae sponges has been investigated for its antihelminthic activity (**Figure 31**).[317, 321] These are just few examples of the pronounced structural diversity and diverse biological profiles of marine natural products that indicate the great potential of marine bioprospecting in drug discovery.

Introduction to Nakijiquinines

In the center of many ancient civilizations and their ethnomedicinal traditions and spiritual practices were natural products. Stress from competition, changes in environmental factors such as temperature, growth, infection and competition are the sort of stimuli that lead to the formation and production of natural products as secondary metabolites.[322] As previously mentioned, natural products have played an enormous role in the development of many pharmaceuticals and in the growth of the pharmaceutical industry.[145] Natural products and natural product derivatives represent one third of the top selling drugs worldwide, thus confirming their role in the development of clinical agents.[322] Natural products have found their niche in various diseases and to date natural products have contributed to the development of anti-cancer agents, anti-infectives, antichlolesterolemics, and various other, some of which are still currently used in the clinic.[143] Therefore, further investigation into natural products, both

terrestrial and marine, will provide us with novel scaffold with intriguing strictures that have potential to be therapeutic agents and biological probes.

Nakijiquinones are marine sesquiterpene quinones from the Spongiidae family that were isolated from an Okinawan sponge in the early 1990s.[323] To date, there are eighteen nakijiquinones all isolated from an Okinawan marine sponge (**Figure 32**). The original isolation of nakijiquionones A and B was completed by Shigemori and coworkers in 1994, where they reported the isolation and structure of the two new sesquiterpenoids.[323] They also described the rarity of such aminoquinone species from natural sources, though reports of such compounds isolated from marine sponges have been reported.[324-326] In 1995, Kobayashi and coworkers further extended their work on the Okinawan sponge and isolated nakijiquinones C and D as red amorphous solids.[327] Interestingly, the natural products isolated in the early 1990s were all monomer quinones, and it was not until 2009 when Kobayashi and coworkers isolated nakijiquinones E and F, isolated as dimer quinones.[328]

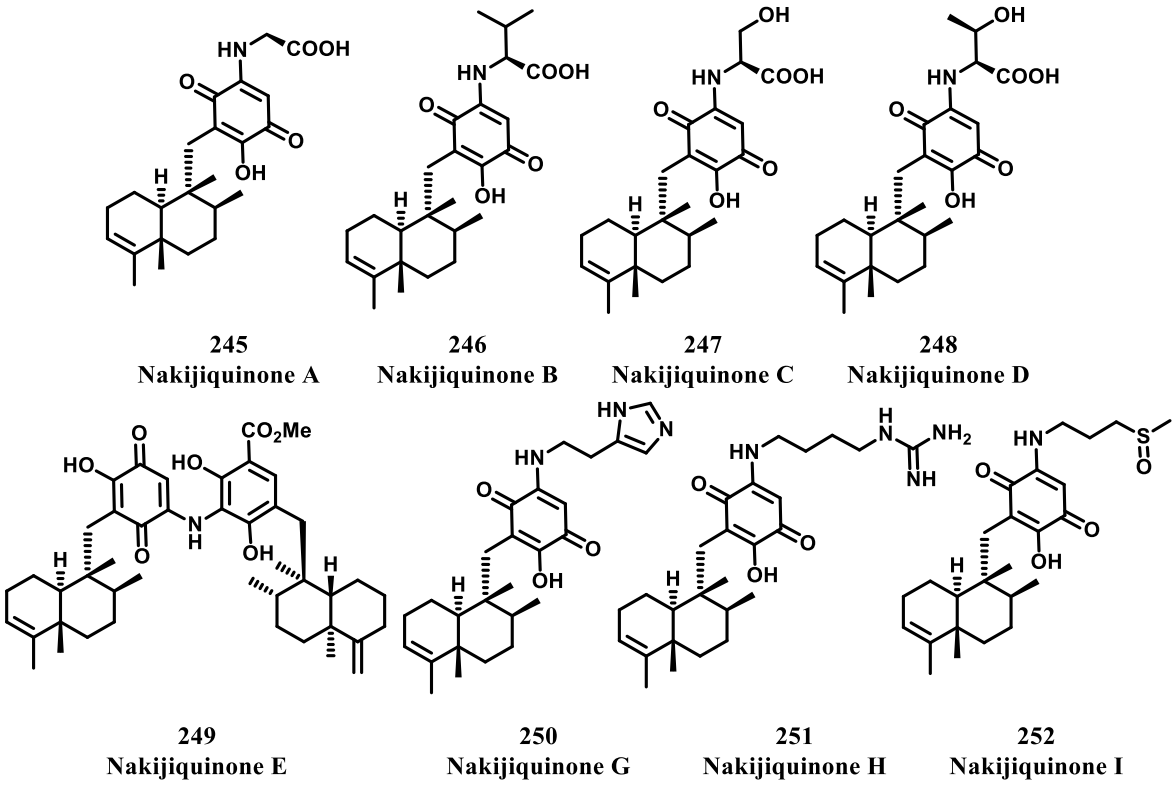

Figure 32. Structures of nakijiquinones A - I

Nakijiquinones A – F possess natural amino acid side chains off of the quinone ring and it was not until the discovery of nakijiquinones G, H, and I that other substituents were discovered at that position.[329] Nakijiquinone G and F contain side chains that are derived from amino acids, like histidine and arginine, respectively, whereas nakijiquinone I contains an interesting substituent, namely a methyl sulfoxide group.[329] Several other nakijiquinones were also isolated from two different collections of Okinawan marine sponges by Takanashi and coworkers in 2010 (**Figure 33**).[330] The newly isolated nakijiquinones J – R contained various quinone side chains, however these side chains were mainly aliphatic and only one resembled an amino acid side chain (nakijiquinones P and Q).[330] In addition to the isolated quinones, several other previously reported sesquiterpenoid quinones were also isolated from the collections of the

Okinawan marine sponge, such as the isospongiaequinone and mamanuthaquinone (**Figure 33**).[330]

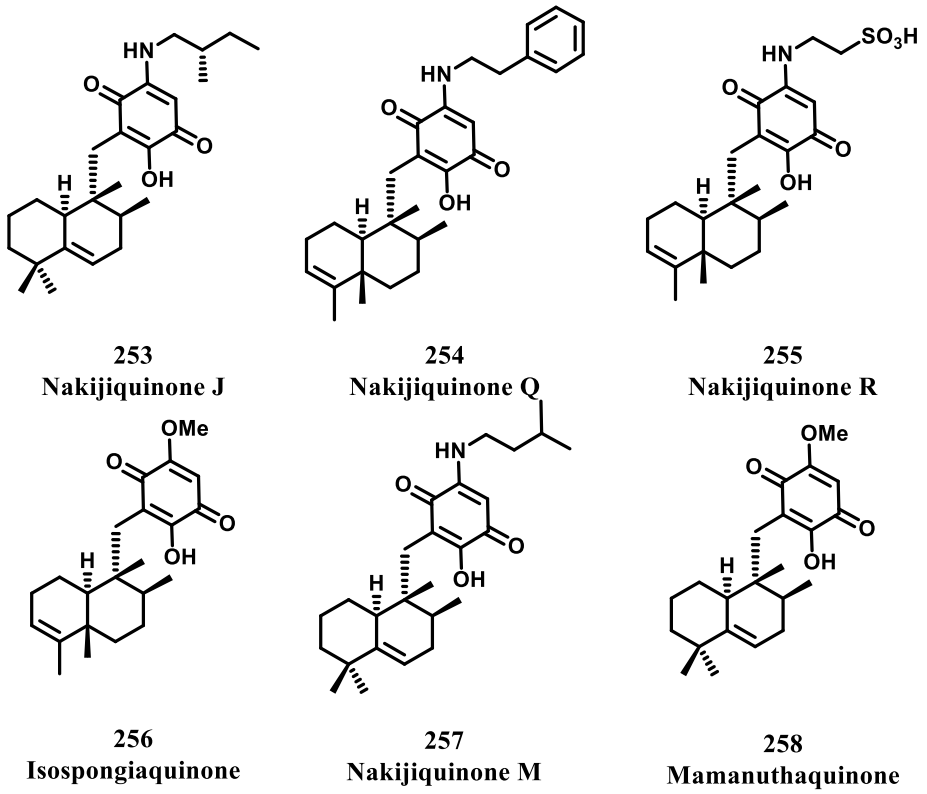

Figure 33. Structures of nakijiquinones J, K, R, M, isospongiaquinone, and mamanuthaquinone

This family of natural products possesses three structural elements: a diterpene core, an amino acid side chain, and a central *p*-quinoid moiety.[331] Upon their isolation, this family of quinones showed to be the first naturally occurring inhibitors of the Her-2/Neu receptor tyrosine kinase.[327] Nakijiquinones C and D exhibited activity against Her-2/Neu tyrosine kinase D of 26 μg/mL and 29 μg/mL, respectively.[327] The nakijiquinones were tested for their cytotoxic activity against several different cancer cell lines, specifically the L1210 murine leukemia cells, KB human epidermoid carcinoma cell line, and the P388 murine leukemia cell line. Most of the nakijiquinones tested exhibited cytotoxic activity with IC_{50} values in the range of 1.2 μg/mL –

8.5 μg/mL (**Table 15**).[323, 327, 329] Of the marine quinones tested, the most potent against KB human epidermoid carcinoma line was nakijiquinone D, with an IC_{50} of 1.2 μg/mL; against L1210 murine leukemia cell line, nakijiquinone I exhibited the highest activity with an IC_{50} value of 2.4 μg/mL; lastly the highest cytotoxic activity exhibited by any nakijiquinone against the P388 murine leukemia cell line was that of nakijiquinone H, with an IC_{50} value of 2.4 μg/mL.[323, 327, 329]

Table 15. Cytotoxic activities of najikiquinones A – I

	IC_{50} (μg/mL)[a]			
Cmpd	**L1210 murine leukemia cells**	**KB human epidermoid carcinoma cells**	**P388 murine leukemia**	**Her2/Neu**
Nakijiquinone A	3.5	4.0	–	–
Nakijiquinone B	4.0	3.2	–	–
Nakijiquinone C	5.8	6.2	–	26.0
Nakijiquinone D	8.1	1.2	–	29.0
Nakijiquinone E	>10	>10	>10	–
Nakijiquinone F	>10	>10	>10	–
Nakijiquinone G	2.9	4.8	3.2	–
Nakijiquinone H	8.5	>10	2.4	–
Nakijiquinone I	2.4	5.6	2.9	–

[a] IC_{50} = Inhibitory concentration for 50% maximal response

In addition to the seen cytotoxic activity of these marine natural products, several of the nakijiquinones exhibited antimicrobial and antifungal activity against various gram positive, gram negative microorganisms and yeast strains. Nakijiquinones A and B exhibited antimicrobial activity against the yeast strain *C. albicans* with MIC values of 2.5 and 33 μg/mL, respectively, as well as against *A. niger* with MIC values of 5.0 and 133 μg/mL, respectively (**Table 16**).[323] Nakijiquinones G, H, and I were also subjected to testing for their antimicrobial and antifungal activity and it was determined that nakijiquinone H was the most active of the

three and it excited activity against *C. neoformans* (MIC = 8.35 μg/mL), *M. luteus* (MIC = 16.7 μg/mL), *C. albicans* (MIC = 8.35 μg/mL), and *A. niger* (MIC = 16.7 μg/mL) (**Table 17**).[329]

Table 16. Antamicrobial activities of nakijiquinones A and B

	MIC ((μg/mL)[a]	
Cmpd	***C.albicans***	***A. niger***
Nakijiquinone A	2.5	5.0
Nakijiquinone B	33.0	133.0

[a]MIC = Minimal inhibitory concentration for 50% maximal response

Table 17. Antimicrobial activities of nakijiquinones G – I

	MIC (μg/mL)[a]						
Cmpd	***S. aureus***	***C. neoformans***	***B. subtilus***	***E. coli***	**M. luteus**	**C. albicans**	**A. niger**
Nakijiquinone G	33.3	>33.3	33.3	>33.3	33.3	>33.3	>33.3
Nakijiquinone H	33.3	8.35	33.3	>33.3	16.7	8.35	16.7
Nakijiquinone I	>33.3	>33.3	>33.3	>33.3	33.3	>33.3	>33.3

[a]MIC = Minimal inhibitory concentration for 50% maximal response

Due to their interesting activity, the nakijiquinone family of natural products has been of interest to many researchers. Structure-activity relationship studies as well as total synthesis efforts have been undertaken for the nakijiquinones and similar scaffolds, namely avarol and avarone.[331-335]

Rationale and Specific Aims

Nakijiquinones are a family of diterpene natural products isolated from a marine sponge that exhibit significant cytotoxic activity in various cancer cell lines. One can envision that the quinone moiety present in the molecule may be responsible for the cytotoxic activity exhibited

by these natural products. Salvinorin A possesses a diterpene core similar to the nakijiquinone family of marine natural products. Interestingly, salvinorin A has been shown to cross the BBB and have a fast onset of action.[280] It was determined in a non-human primate study conducted by Butelman and coworkers that a 0.032 mg/kg dose of salvinorin A elicited a response after only 1 minute of intravenous administration, thus confirming the fast BBB penetration of salvinorin A.[280] It was hypothesized that a combination of the nakijiquinone and salvinorin A scaffolds would yield a molecule with potential as a biological probe and a diagnostics tool for brain tumors. Thus, quinone containing salvinorin A analogues were designed and synthesized. To this end, the following specific aims were proposed:

Specific Aim 1: Prepare quinone containing salvinorin A analogues for biological evaluation through semi-synthesis.

A series of quinone containing analogues were prepared through modification of salvinorin A. Analogues that explore free rotation around the C-13 carbon of the salvinorin A core will be synthesized in addition to analogues that explore different positions of substitution on the quinone moiety now present in the salvinorin A scaffold. Such analogues will provide additional SAR for salvinorin A at KOP receptors and demonstrate that this scaffold can be manipulated in a way that will lead to novel biological activity.

Specific Aim 2: Evaluate quinone containing salvinorin A analogues KOP receptor activity and antiproliferative potential.

Analogues proposed and synthesized in Specific Aim 1 will be evaluated for activity at the KOP receptors utilizing a known calcium mobilization assay protocol.[316] This assay will be utilized because of its simpler format and definitive data and the lack of radiolabeled ligand use.

Analogues prepared from Specific Aim 1 will also be subjected to an antiproliferative assay to determine their activity in two cancer breast cell lines, MCF7 and SKBr3. The purpose of these assays is to determine the activity of the chimeric compounds at the KOP receptors as well as to attain their antiproliferative activity *in vitro*.

The studies presented in the above specific aims are intended to investigate the hypothesis that a combination of two natural products scaffold will be a useful biological probe and represent an extension in the development of novel CNS diagnostic tools. Completion of these studies will further extend the SAR of the salvinorin A scaffold at the KOP receptors and will represent the first report of salvinorin A analogues with antiproliferative activity. The results of these studies will be presented and discussed.

Results and Discussion

Introduction

In an effort to elucidate the ability of salvinorin A as a biologic probe, several quinone containing analogues of salvinorin A were synthesized. These compounds were meant to investigate the possibility of changing the biological activity of the salvinorin A core. The similarity between the two natural products, both diterpene natural products, represented an opportunity for exploration of a combination of the two in one single molecule (**Figure 34**). As previously determined reports have stated, nakijiquinones exhibit cytotoxic activity, likely do to the quinone moiety present in the scaffold. Similarly, salvinorin A whose interesting biological

activity has also been determined was shown to pass through blood-brain-barrier, making it a prime target for the development of a biological probe.

The combined scaffold analogues were synthesized to examine the hypothesis that quinone barring salvinorin A analogues may have a potential as a diagnostic tools and biological probes. Several analogues were synthesized with the purpose of examining the ability for free rotation within the active site and the quinone substituents necessary for antiproliferative activity.

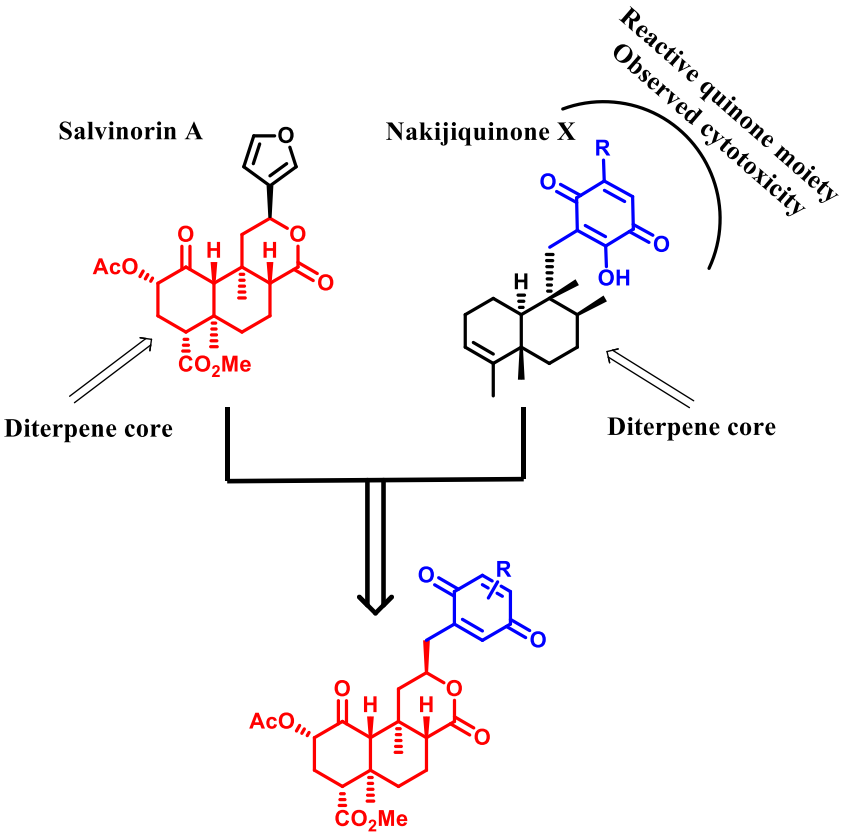

Figure 34. Rationale for quinone containing salvinorin A analogues with potential antiproliferative activity

Synthesis

Salvinorin A (**83, Scheme 5**) was isolated from *S. divinorum* leaves as previously described and the synthesis of quinone containing salvinorin A analogues begun with the synthesis of several boronic acids (**Scheme 4**).[311] The main carbon-carbon bond cross-coupling reaction was the Leiebeskind-Srogl reaction which was chosen based on the recent discovery by our laboratory that the mild coupling conditions of this reaction, which utilize bis(dibenzylideneacetone)palladium(0), copper (I) thiophene carboxylate and triethylphosphite at ambient temperature are well tolerated by the salvinorin A scaffold.[302] However, prior to the use of the Lebeskind-Srogl coupling reaction, several boronic acids were prepared, which was accomplished following previously published reports. 2,3,4,5-Tetramethoxyphenyl boronic acid was synthesized following slightly modified conditions proposed by Tremblay and coworkers.[336] The synthesis began with commercially available 2,3,4-trimethoxybenzaldehyde **259**, which was subjected to oxidation conditions with hydrogen peroxide to yield intermediate **260** in 84% yield (**Scheme 5**). This intermediate was then subjected to methylation conditions using iodomethane and potassium carbonate to afford compound **261** in 67% yield. 2,3,4,5-Trimethoxyphenyl boronic acid **262**, was synthesized from intermediate **261** in 52% yield. 2,4,5-Trimethoxyphenyl boronic acid was prepared following conditions proposed by Sutherland and coworkers.[337] Briefly, commercially available 1,2,4-trimethoxybenzene **263** was used as the starting material for the synthesis of intermediate **264** utilizing bromine in 96% yield. Intermediate **264** was then subjected to lithium-halogen exchange and in the presence of trimethyl borate compound **265** was synthesized in 38%.

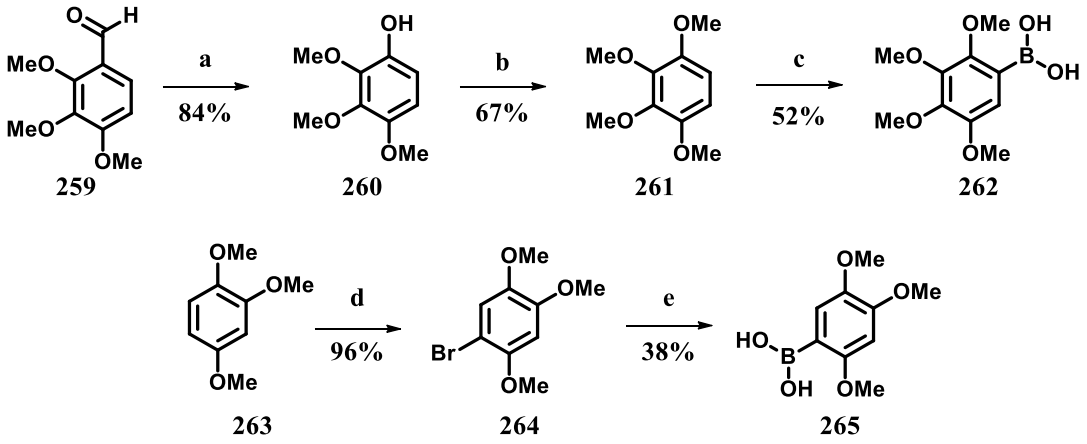

Scheme 4. Synthesis of boronic acids for Liebeskind-Srogl coupling. *Reagents and Condition:* (a) H_2O_2, H_2SO_4:MeOH; (b) K_2CO_3, MeI, acetone; (c) *n*-BuLi, $B(OMe)_3$, THF, -78°C to rt; (d) Br_2, DCM, 0°C; (e) *n*-BuLi, trimethyborate, THF, -78°C

Intermediate **141** was synthesized according to our previous reports in 74% yield (**Scheme 5**).[298] This intermediate was then subjected to esterification with thiophenol to yield salvinorin A thioester **142** in 60% yield. Compound **142** was used as the starting material in the cross-coupling reaction with several different boronic acids to yield aromatic ketones **266**, **267**, and **268** in 48%, 79%, and 90% yield, respectively (**Scheme 5**). The next step towards the synthesis of the desired analogues was a deoxygenation reaction that would ultimately yield a CH_2 homolog from a ketone starting material. Several different methods were attempted for a transformation that would produce the CH_2 homolog directly from its ketone precursor, however they demonstrated to unsuccessful because they all produced a hydroxyl product instead the desired CH_2 product (**Table 18**). In the end the Corey-Bakshi-Shibata reduction was chosen because of the higher yields and the mild conditions. Intermediates **266**, **267**, and **268** were then subjected to Corey-Bakshi-Shibata reduction condition to yield compounds **269**, **270**, and **271** in 90%, 89%, and 64% yield, respectively. Utilizing trimethylsilane and boron trifluoride diethyl etherate, compounds **269**, **270**, and **271** were subjected to a deoxygenation reaction to afford

intermediates **272**, **273**, and **274** in 36%, 55%, and 56%, respectively. Intermediates **272**, **273** and **274** were further oxidized utilizing CAN to yield final compounds **275**, **276**, and **277** in 39%, 28%, and 72% yield, respectively.

Table 18. Conditions attempted towards the synthesis of the deoxygenated intermediate

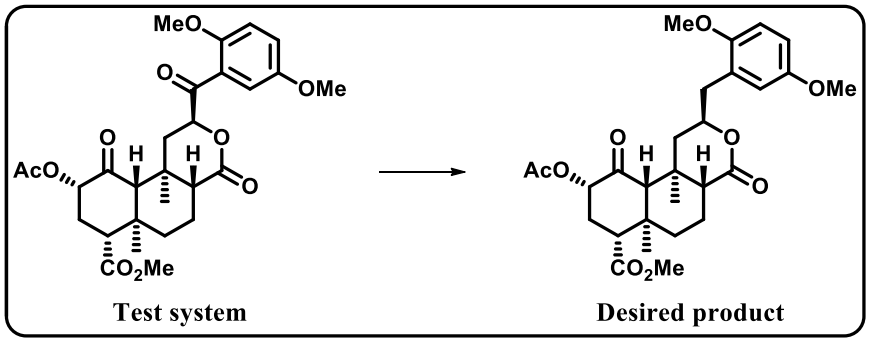

Test System	Conditions Used	Desired Product	Product Formed
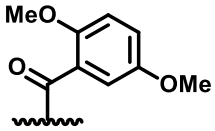	$InCl_3$, Ph_2SiH, DCM	None	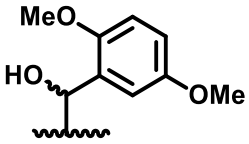
	[1,5-HDRhCl]$_2$, β-cyclodextrin, THF	None	
	$ZnCl_2$, Et_3SiH, DCE	None	
	$PdCl_2$, Et_3SiH, EtOH	None	
	TFA, Et_3SiH	None	
	$B(C_6F_5)_3$, Et_3SiH, DCM	None	
	$B(C_6F_5)_3$, Ph_2SiH, DCM	None	
	$GaCl_3$, Me_2ClSiH, DCM	None	

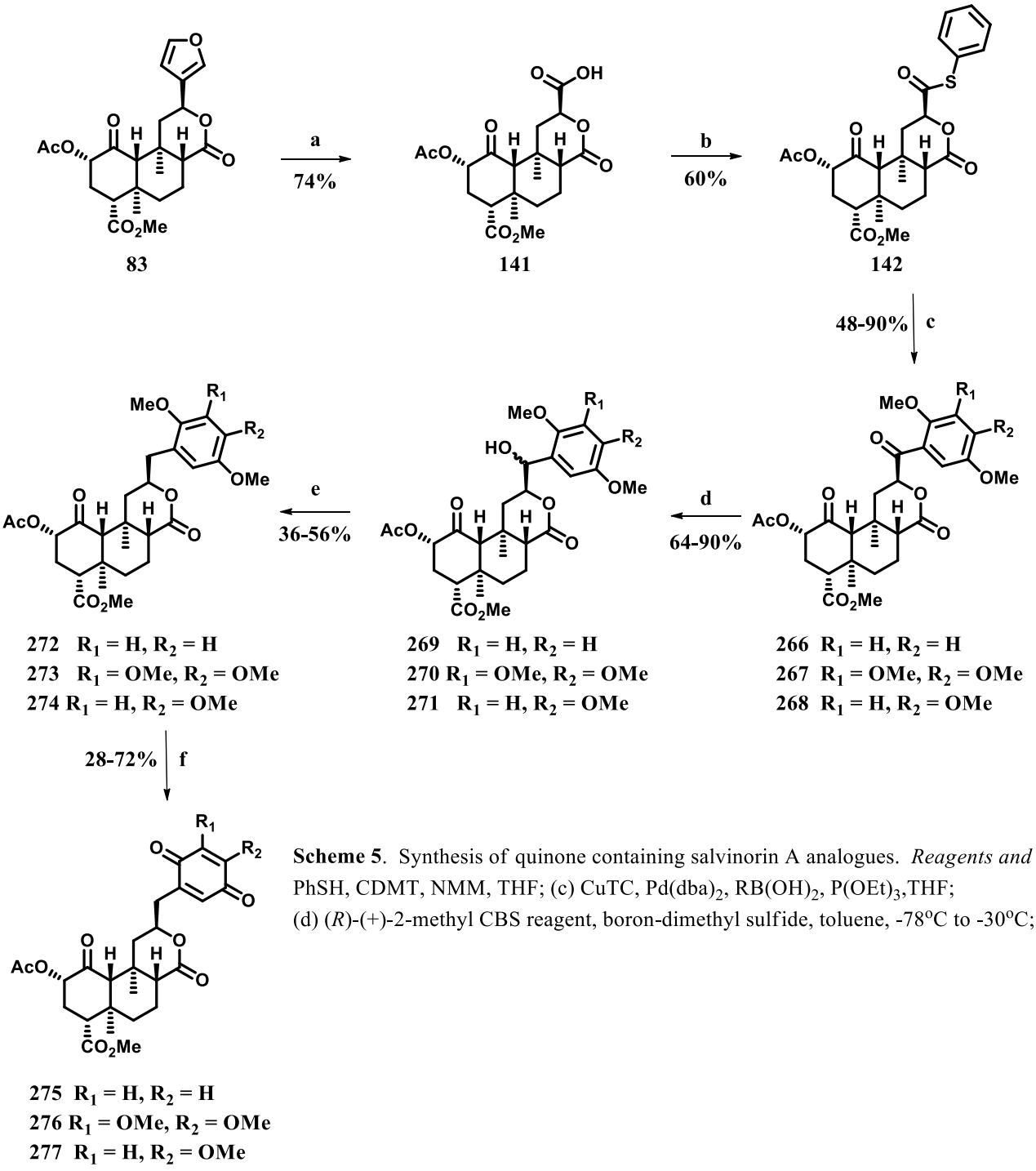

Scheme 5. Synthesis of quinone containing salvinorin A analogues. *Reagents and Conditions:* PhSH, CDMT, NMM, THF; (c) CuTC, $Pd(dba)_2$, $RB(OH)_2$, $P(OEt)_3$,THF; (d) (*R*)-(+)-2-methyl CBS reagent, boron-dimethyl sulfide, toluene, -78°C to -30°C; (e) Et_3SiH, l

Pharmacological Evaluation

***In vitro* Functional Assay**

Quinone containing analogues of salvinorin A were subjected to pharmacological testing to determine their activity at the KOP receptors as well as their antiproliferative properties. Analogues **275** – **277** were subjected to a calcium mobilization assay, which is a functional assay that will determine their activity at the KOP receptors. As expected, the majority of the analogues tested showed to be inactive at the KOP receptors, with the exception of analogue **275**, which displayed an EC_{50} value of 2.5 μM and was observed to be a partial agonist with an E_{max} value of 27% (**Table 19**).

Table 19. Analysis of potency of analogues **275** – **267** in the Ca^{2+} mobilization functional assay

Cmpd	KOP EC_{50} ± SEM (nM)[a]	KOP E_{max} ± SEM[b]
83	1.7 ± 0.6	103 ± 2
275	2500 ± 900	27 ± 4
276	>10,000	N.D.[c]
277	>10,000	N.D.[c]

[a] EC_{50} = Effective concentration for 50% maximal response.
[b] Emax is % which compound stimulates binding compared to (-)-U-69,593 at KOP receptors. n = 2
[c] N.D. = not determined

In vitro Antiproliferation Assay

The analogues synthesized were also tested in an antiproliferative assay to determine their effects in several cancer cell lines, particularly breast cancer cell lines MCF7 and SKBr3, (**Table 20**). As expected, the quinone containing salvinorin A analogues did indeed show antiproliferative effects in the cancer cell lines tested. It was determined that analogues **275** – **277** exhibited low to moderate antiproliferative activity, with analogue **276** showing the most promise in the MCF7 and SkBr3 breast cancer cell line with an EC_{50} value of 4.5 μM and 8.3 μM, respectively. Analogues **275** and **277** also exhibited antiproliferative activity with EC_{50}

values of 8.3 μM in the MCF7 cancer cell line and 14 μM and 23 μM, respectively in the SKBr3 cancer cell line. Though the analogues synthesized displayed low to moderate antiproliferative activity, they were not as active as geldanamycin (GDA) in this assay. The present results indicate that a double substitution of the quinone ring in these analogues is better tolerated than a single substitution or no substitution of the quinone ring. However, additional information is needed before a conclusion of an optimal substitution pattern for the quinone ring can be reached.

Table 20. Antiproliferative activity of compounds **275**– **277**

Cmpd	MCF7 EC_{50} ± SEM (μM)[a,b]	SKBr3 EC_{50} ± SEM (μM)[a,b]
GDA[c]	0.05 ± 0.03	0.01 ± 0.02
275	8.28 ± 0.72	13.9 ± 0.21
276	4.53 ± 1.78	8.34 ± 0.41
277	8.25 ± 0.89	23.0 ± 1.66

[a] EC_{50} = Effective concentration for 50% maximal response.
[b] Values represent mean ± standard deviation for at least two separate experiments performed in triplicate
[c] Data from Khandelwal, A. *et al*. *J. Org. Chem*. **2013**, *78*, 7859-7884.

Conclusions

The similarity between two natural products, a plant derived terpene salvinorin A and the marine sponge derived nakijiquinone family of terpene natural products, prompted an idea that a combination of the two scaffolds may yield a biological probe that could have potential as a diagnostic tool. Several compounds were synthesized with similarities to both scaffolds, mainly as salvinorin A analogues that possess a quinone moiety instead of the furan ring of salvinorin A.

Upon synthesis, the designed analogues were subjected to pharmacological testing for their activity at the KOP receptors. As expected, the quinone containing analogues of salvinorin A exhibited negligible activity at the KOP receptors. Furthermore, the analogues reported were also subjected to an antiproliferative assay to determine their activity against several breast cancer cell lines. It was determined that the analogues exhibited low to moderate antiproliferative activity, indicating their possible use as a biological probes in the diagnosis of certain brain cancer ailments. To the best of our knowledge, this represents the first report of salvinorin A analogues that exhibit antiproliferative activity.

Future Directions

Aside from possessing a quinone moiety, the nakijiquionone family of natural products also contains various amino acid-like side chains which are appended to the quionone ring. In order for a more complete SAR representation for this chimeric scaffold, additional quinone containing salvinorin A analogues need to be synthesized with side chains resembling those or derivatives of the original natural products. Furthermore, the *in vitro* activity of these analogues for the KOP receptors needs to be correlated with their ability to pass through the BBB. There are several methods that could assess the ability of a compound to pass through the BBB, including *in vitro*, in silico and *in vivo* models.[338] One of the most versatile and high throughput *in vitro* assays used in drug discovery is the parallel artificial membrane permeability assay for the blood-brain barrier (PAMPA-BBB), where the rate of transcellular passive diffusion of a drug across the BBB is accomplished by measuring the effective permeability of an artificial lipid membrane.[339] Moreover, analogues that contain fluorescent ligands in place of the quione

moiety could be beneficial in determining the mechanism of action of these salvinorin A derived ligands in brain tissue. In addition to the mentioned assays, the analogues synthesized as well as any additional analogues should also be examined for their activity at the other opioid receptors.

CHAPTER 3: EXPERIMENTAL PROCEDURES FOR SALVINORIN A ANALOGUES

PART I: DESIGN AND SYNTHESIS OF STERICALLY CHALLENGED SALVINORIN A ANALOGUES

Chemistry

General Procedures. Unless otherwise indicated, all reagents were purchased from commercial suppliers and were used without further purification. Melting points were determined on a Thomas-Hoover capillary melting apparatus. NMR spectra were recorded on a Bruker DRX-400 with qnp probe or a Bruker AV-500 with cryoprobe using δ values in ppm (TMS as internal standard) and *J* (Hz) assignments of ^{1}H resonance coupling. High resolution mass spectrometry data were collected on either a LCT Premier (Waters Corp., Milford, MA) time of flight mass spectrometer or an Agilent 6890 N gas chromatograph in conjunction with a quarto Micro GC mass spectrometer (Micromass Ltd, Manchester UK). Thin-layer chromatography (TLC) was performed on 0.25 mm plates Analtech GHLF silica gel plates using ethyl acetate/*n*-hexanes, in 1:1 ratio as the solvent system unless otherwise noted. Spots on TLC were visualized by UV (254 or 365 nm), if applicable, and phosphomolybdic acid in ethanol. Column chromatography was performed with Silica Gel (32 – 63 μ particle size) from MP Biomedical (Solon, OH). Analytical HPLC was carried out on an Agilent 1100 Series Capillary HPLC system with diode array detection at 209.4 nm on an Agilent Eclipse XDB-C18 column (250 × 10 mm, 5 μm) with isocratic elution in 60% CH_3CN/40% H_2O at a flow rate of 5.0 mL/min unless otherwise noted, or on a Phenomenex Luna column (250 × 4.5 mm, 5 μm) with

isocratic elution in 60% CH_3CN/40% H_2O unless otherwise noted. The systematic name for salvinorin A (1) is (2*S*,4a*R*,6a*R*,7*R*,9*S*,10a*S*,10b*R*)-methyl 9-acetoxy-2-(furan-3-yl)-6a,10b-dimethyl-4,10-dioxo-dodecahydro-1*H*-benzo[*f*]iso-chromene-7-carboxylate. Salvinorin A was isolated from *S. divinorum* as previously described.[340]

(4aR,6aR,7R,9S,10aS,10bR)-methyl 9-acetoxy-2-((E)-2-(furan-3-yl)vinyl)-6a,10b-dimethyl-4,10-dioxododecahydro-1H-benzo[f]isochromene-7-carboxylate (235) and (4aR,6aR,7R,9S,10aS,10bR)-methyl 9-acetoxy-2-((Z)-2-(furan-3-yl)vinyl)-6a,10b-dimethyl-4,10-dioxododecahydro-1H-benzo[f]isochromene-7-carboxylate (236). KHMDS (1.64 mL of a 0.5 M solution in toluene, 0.83 mmol) was added in a dropwise manner to a cooled (-78 °C) solution of 8[312](263 mg, 0.91 mmol) in THF (9 mL). After 30 min, a cooled solution of aldehyde 5 (300 mg, 0.761 mmol) in THF (20 mL) was added in a dropwise manner over 3 minutes. The reaction mixture was stirred at -78 °C for 2 hours or until completion reaction and then it was diluted with EtOAc (9 mL) and quenched by the addition of H_2O (10 mL). After warming to room temperature over 30 min, the phases were separated and the aqueous phase was extracted with EtOAc (2 × 10 mL). The combined organic extracts were washed with brine (2 × 10 mL) and dried over Na_2SO_4. Filtration and concentration under reduced pressure afforded **235** and **236** as a 2:1 mixture, which was separated by flash column chromatography to afford, in order of elution, major isomer **236** as a white solid and the minor isomer **236** also as a white solid. The minor isomer was further purified by HPLC (40% ACN/60% H_2O) on an Agilent Eclipse XDB-C18 column (250 × 10 mm, 5 μm) at a flow rate of 5 mL/min.

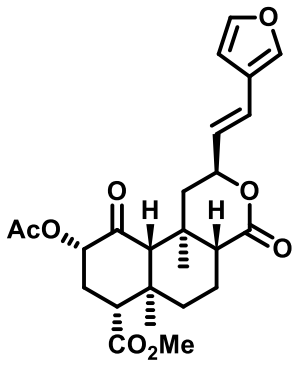

235: Isolated as an off-white solid (25 mg, 7.2% yield) of *trans* isomer after purification; mp = 192 – 194°C. ^{1}H NMR (500 MHz, $CDCl_3$) δ 7.45 (s, 1H), 7.39 (s, 1H), 6.51 (d, *J* = 13.0 Hz, 2H), 5.88 (dd, *J* = 6.3, 15.8Hz, 1H), 5.15 (d, *J* = 9.7Hz, 2H), 3.76 (s, 3H), 2.77 (d, *J* = 8.1Hz, 1H), 2.43 (d, *J* = 8.3Hz, 1H), 2.34 (d, *J* = 9.9Hz, 2H), 2.20 (s, 3H), 2.18 (s, 1H), 2.05 (s, 1H), 1.84 (s, 1H), 1.63 (s, 3H), 1.45 (s, 3H), 1.14 (s, 3H). ^{13}C NMR (126 MHz, $CDCl_3$) δ 201.85, 171.38, 171.06, 169.84, 143.57, 141.07, 126.66, 122.82, 121.74, 107.15, 77.40, 74.92, 63.96, 53.46, 51.82, 51.17, 42.89, 41.96, 38.05, 35.17, 30.56, 20.40, 17.95, 16.19, 15.04. HRMS (m/z): [M+Na] calcd for $C_{25}H_{30}O_8Na$, 481.1838; found, 481.1832. HPLC t_R= 8.832 min; purity = 98.2%.

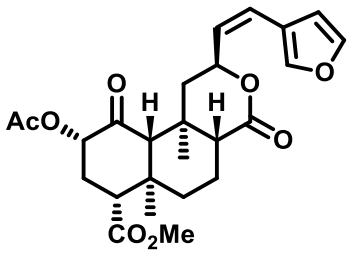

236: Isolated as a white solid (11.7 mg, 3.4 % yield) of *cis* isomer after purification; mp = 182 – 184 °C. ^{1}H NMR (500 MHz, $CDCl_3$) δ 7.52 (s, 1H), 7.45 (s, 1H), 6.45 (s, 1H), 6.40 (d, *J* =

11.2Hz, 1H), 5.54 (d, *J* = 11.2Hz, 1H), 5.47 – 5.41 (m, 1H), 5.20 – 5.15 (m, 1H), 3.76 (s, 3H), 2.81 – 2.75 (m, 1H), 2.34 (d, *J* = 9.9Hz, 4H), 2.20 (s, 3H), 2.18 (s, 1H), 2.09 – 2.04 (m, 1H), 1.84 – 1.79 (m, 1H), 1.63 (s, 3H), 1.45 (s, 3H), 1.14 (s, 3H). ^{13}C NMR (126 MHz, $CDCl_3$) δ 202.14, 171.81, 171.47, 170.21, 143.76, 142.04, 128.49, 124.02, 121.01, 110.94, 75.23, 74.12, 64.36, 53.84, 52.23, 51.65, 43.04, 42.30, 38.44, 35.70, 30.99, 20.83, 18.36, 16.65, 15.52. HRMS (m/z): [M+Na] calcd for $C_{25}H_{30}O_8Na$, 481.1838; found, 481.1830. HPLC t_R= 8.691 min; purity = 100.0%.

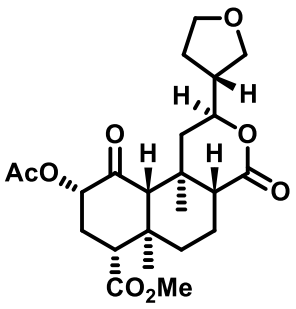

(2S,6aR,7R,9S,10bR)-methyl 9-acetoxy-6a,10b-dimethyl-4,10-dioxo-2-(tetrahydrofuran-3-yl)dodecahydro-1H-benzo[f]isochromene-7-carboxylate (239). Salvinorin A was dissolved in a 1:1 mixture of DCM:MeOH and Rh/C (5%, 0.5 g, 4..95 mmol, 5 equiv) was then added. The flask was then charged with H_2 and the resulting mixture was allowed to stir at ambient temperature for 24 hrs. Upon completion (TLC monitoring), the rection mixture was filtered through a pad of Celite and thoroughly washed with DCM (150 mL) and concentrated under reduced pressure. The resulting residue was purified by silica gel column chromatography using DCM/MeOH to afford 0.12g (28% yield) as a white solid. mp = 173-175 °C. TLC system: 10% MeOH/90% DCM. ^{1}H NMR (500 MHz, $CDCl_3$) δ 5.15 (dd, *J* = 11.6, 8.4 Hz, 1H), 4.51 – 4.33 (m, 1H), 3.96 (dd, *J* = 9.1, 7.5 Hz, 1H), 3.85 (dd, *J* = 4.9, 3.5 Hz,

1H), 3.81 – 3.74 (m, 1H), 3.73 (s, 3H), 3.55 (dd, J = 9.0, 6.7 Hz, 1H), 2.78 – 2.69 (m, 1H), 2.48 – 2.40 (m, 1H), 2.39 – 2.23 (m, 3H), 2.18 (s, 3H), 2.12 (d, J = 4.6 Hz, 1H), 2.10 – 2.02 (m, 1H), 1.94 (tdd, J = 12.9, 6.1, 3.6 Hz, 2H), 1.87 – 1.73 (m, 2H), 1.59 – 1.52 (m, 2H), 1.36 (s, 3H), 1.30 – 1.19 (m, 1H), 1.10 (s, 3H). ^{13}C NMR (126 MHz, $CDCl_3$) δ 202.03, 202.01, 171.54, 171.52, 171.30, 171.09, 169.96, 169.93, 79.34, 78.22, 74.98, 70.42, 68.86, 68.07, 67.97, 64.12, 64.08, 53.58, 53.56, 51.99, 51.43, 51.41, 45.65, 45.10, 42.08, 42.06, 41.98, 41.20, 38.15, 38.13, 35.14, 35.10, 30.79, 28.26, 28.20, 20.61, 18.16, 16.36, 15.13. HRMS (m/z): [M+K] calcd for $C_{23}H_{32}O_8K$, 475.1734; found, 475.1714. HPLC t_R= 4.855 min; purity = 95.0%.

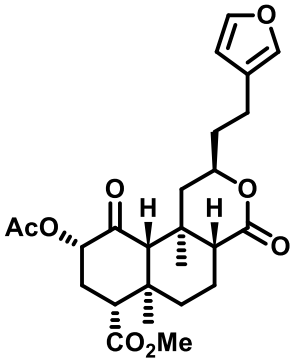

(2R,6aR,7R,9S,10bR)-methyl 9-acetoxy-2-(2-(furan-3-yl)ethyl)-6a,10b-dimethyl-4,10-dioxododecahydro-1H-benzo[f]isochromene-7-carboxylate (237). (2S,6aR,7R,9S,10bR)-methyl 9-acetoxy-2-(2-(furan-3-yl)vinyl)-6a,10b-dimethyl-4,10-dioxododecahydro-1*H*-benzo[*f*]isochromene-7-carboxylate synthesized as described above for compounds **235** and **236**) and Pd/C (10%, 0.004 g, 0.0033 mmol, 0.03 equiv) were placed in around bottom flask and charged with H_2 and EtOAc (5 mL). The resulting mixture was allowed to stir at ambient temperature until completion (TLC monitoring). Upon completion, the resulting mixture was filtered through pad of Celite and thoroughly washed with EtOAc and

concentrated under reduced pressure. The resulting residue was purified by silica gel column chromatography using 35% EtOAc/65 % pentane to afford 0.02g (40% yield) as a white solid, mp = 149-151 °C.. TLC system: 60% EtOAc/40% *n*-hexanes. ^{1}H NMR (500 MHz, $CDCl_3$) δ 7.35 (t, *J* = 1.7 Hz, 1H), 7.23 (t, *J* = 1.3 Hz, 1H), 6.26 – 6.23 (m, 1H), 5.17 – 5.09 (m, 1H), 4.51 (td, *J* = 7.6, 4.2 Hz, 1H), 3.72 (s, 3H), 2.78 – 2.69 (m, 1H), 2.62 (ddd, *J* = 14.7, 9.4, 5.2 Hz, 1H), 2.57 – 2.49 (m, 1H), 2.34 – 2.22 (m, 3H), 2.18 (s, 3H), 2.17 – 2.11 (m, 2H), 1.95 (dd, *J* = 11.7, 3.1 Hz, 1H), 1.91 – 1.83 (m, 1H), 1.82 – 1.74 (m, 2H), 1.66 – 1.56 (m, 2H), 1.34 (s, 3H), 1.28 – 1.21 (m, 2H), 1.09 (s, 3H). ^{13}C NMR (126 MHz, $CDCl_3$) δ 202.05, 171.56, 171.47, 170.01, 142.98, 139.04, 123.63, 110.79, 76.44, 75.08, 64.18, 53.62, 51.98, 51.39, 42.75, 42.11, 38.24, 37.14, 35.13, 30.75, 20.60, 20.23, 18.17, 16.36, 15.15. HRMS (m/z): [M+K] calcd for $C_{23}H_{32}O_8K$, 499.1734; found, 499.1728. HPLC t_R= 10.264 min; purity = 95.0%.

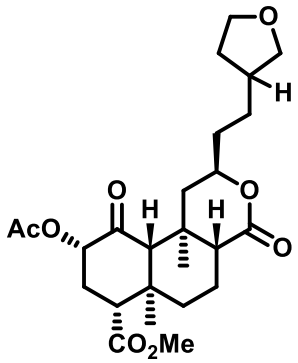

(2R,6aR,7R,9S,10bR)-methyl 9-acetoxy-6a,10b-dimethyl-4,10-dioxo-2-(2-(tetrahydrofuran-3-yl)ethyl)dodecahydro-1H-benzo[f]isochromene-7-carboxylate (238). (2S,6aR,7R,9S,10bR)-methyl 9-acetoxy-2-(2-(furan-3-yl)vinyl)-6a,10b-dimethyl-4,10-dioxododecahydro-1H-benzo[f]isochromene-7-carboxylate synthesized as described above for compounds **235** and **236**) and Pd/C (10%, 0.007 g, 0.0065 mmol, 0.06 equiv) were placed in

around bottom flask and charged with H_2 and EtOAc (5 mL). The resulting mixture was allowed to stir at ambient temperature until completion (TLC monitoring). Upon completion, the resulting mixture was filtered through pad of Celite and thoroughly washed with EtOAc and concentrated under reduced pressure. The resulting residue was purified by silica gel column chromatography using 60% EtOAc/40 % pentane to afford 0.02g (39% yield) as a white solid, mp = 82-85 °C. TLC system: 60% EtOAc/40% *n*-hexanes. ^{1}H NMR (500 MHz, $CDCl_3$) δ 5.17 – 5.10 (m, 1H), 4.53 – 4.45 (m, 1H), 3.89 (ddd, *J* = 8.7, 7.2, 1.9 Hz, 1H), 3.84 (td, *J* = 8.4, 4.7 Hz, 1H), 3.77 – 3.71 (m, 4H), 3.31 (ddd, *J* = 8.4, 7.3, 1.3 Hz, 1H), 2.79 – 2.68 (m, 1H), 2.34 – 2.21 (m, 4H), 2.21 – 2.09 (m, 7H), 2.03 (ddq, *J* = 11.8, 7.7, 3.9 Hz, 1H), 1.93 (dd, *J* = 11.7, 3.1 Hz, 1H), 1.78 (dt, *J* = 13.1, 2.5 Hz, 1H), 1.64 – 1.57 (m, 2H), 1.48 (dq, *J* = 11.9, 7.8 Hz, 1H), 1.36 (s, 3H), 1.22 (t, *J* = 12.5 Hz, 1H), 1.09 (s, 3H), 0.92 – 0.82 (m, 1H), ^{13}C NMR (126 MHz, $CDCl_3$) δ 202.08, 171.55, 171.49, 170.02, 75.08, 73.23, 67.93, 64.18, 53.62, 51.99, 51.38, 42.72, 42.11, 39.08, 39.05, 38.23, 35.62, 35.12, 32.33, 30.76, 28.38, 20.61, 18.15, 16.37, 15.15. HRMS (m/z): [M+K] calcd for $C_{25}H_{36}O_8K$, 503.2047; found, 503.2019. HPLC (50% CH_3CN/50% H_2O) t_R= 10.982 min; purity = 95.1%.

Binding and Efficacy Studies

Radioligand Binding Studies.[314] MOP receptor binding sites were labeled using [^{3}H]D-Ala^2-MePhe^4,Gly-ol^5]-enkephalin ([^{3}H]DAMGO, SA = 44 – 48 Ci/mmol) while DOP receptor binding sites were labeled using [^{3}H][D-Ala^2, D-Leu^5]-enkephalin ([^{3}H]DADLE, SA = 40 – 50 Ci/mmol) in rat brain homogenates. KOP receptor binding sites were labeled using [^{3}H]*N*-methyl-2-phenyl-*N*-[(5*R*,7*S*,8*S*)-7-(pyrrolidin-1-yl)-1-oxaspiro[4.5]dec-8-yl]acetamide

([^{3}H]U69,593, SA = 50 Ci/mmol). On the day of the assay, cell pellets were thawed on ice for 15 minutes followed by homogenization with a polytron in 10 mL/pellet of ice-cold 10mM Tris-HCl, pH 7.4. The membranes were centrifuged at 30,000 × g for 10 minutes, then resuspended in 10 mL/pellet ice-cold 10mM Tris-HCl, pH 7.4 followed again by centrifugation at 30,000 × g for 10 minutes. Membranes were then resuspended in 25°C 50 mM Tris-HCl, pH 7.4 (~100 mL/pellet *h*MOP-CHO, 50 mL/pellet *h*DOP-CHO, and 120 mL/pellet *h*KOP-CHO). All assays were performed in 50 mM Tris-HCl, pH 7.4 in a final assay volume of 1.0 mL, with a protease inhibitor cocktail: bacitracin (100 μg/mL), bestatin (10 μg/mL), leupeptin (4 μg/mL) and chymostatin (2 μg/mL). Drug dilution curves were determined with buffer containing 1 mg/mL BSA. 20 μM levallorphan ([^{3}H]DAMGO and [^{3}H]DADLE) or 10 μM (-)-U69,593 (for [^{3}H]U69,593 binding) was used to account for nonspecific binding. [^{3}H]Radioligands were used at concentrations of approximately 2 nM. After 2 hours of incubation at 25°C, triplicate samples were filtered with Brandell Cell Harvesters (Biomedical Research & Development Inc., Gaithersburg, MD), over Whatman GF/B filters. The filters were the punched into 24-well plates in which 0.6 mL of LSC-cocktail (Cytoscint) was added. After an overnight extraction, the samples were counted in a Trilux liquid scintillation counter at 44% efficiency. Approximately 30 μg protein was used in each assay tube for the opioid binding assays. The inhibition curves were determined by displacing a single concentration of radioligand by 10 concentrations of drug.

[^{35}S]GTP-γ-S Functional Assay.[315] The [^{35}S]GTP-γ-S assays were conducted as previously described. Buffer A is 50 mM Tris-HCl, pH 7.4, containing 100 mM NaCl, 10 mM $MgCl_2$, 1 mM EDTA and buffer B is buffer A with the addition of 1.67 mM dithiothreitol (DTT)

and 0.15% bovine serum albumin (BSA). On the day of the assay, cells were thawed on ice for 15 min and homogenized using a polytron in 50 mM Tris-HCl, pH 7.4, containing a protease inhibitor cocktail: bacitracin (100 μg/mL), bestatin (10 μg/mL), leupeptin (4 μg/mL) and chymostatin (2 μg/mL). The homogenate was centrifuged at 30,000 × g for 10 minutes at 4°C, and the supernatant discarded. The membrane pellets were then resuspended in buffer B and used for [^{35}S]GTP-γ-S binding assays. 50 μL of buffer A plus 0.1% BSA, 50 μL of GDP in buffer A/0.1% BSA (final concentration = 40 μM), 50 μL of drug in buffer A/0.1% bovine serum albumin, 50 μL of [^{35}S]GTP-γ-S in buffer A/0.1% BSA (final concentration = 50 pM), and 300 μL of cell membranes (50 μg of protein) in buffer B were added in test tubes. Final concentrations of reagents in the assay were: 50 mM Tris-HCl, pH 7.4, containing 100 mM NaCl, 10 mM $MgCl_2$, 1 mM EDTA, 1 mM DTT, 40 μM GDP, and 0.1% BSA. Media was incubated at 55°C for 3 hours. Non-specific binding was accounted for and determined using GTP-γ-S (40 μM). Vacuum filtration through Whatman GF/B filters separated bound and free [^{35}S]GTP-γ-S. The filters were punched into 24-well plates followed by the addition of 0.6 mL of liquid scintillation media (Cytoscint). An overnight extraction was performed and samples were counted in a Trilux liquid scintillation counter at an efficiency of 27%.

Calcium Mobilization Assay.[316] All cells were maintained in F-12 nutrient medium (Ham), supplemented with 10% fetal bovine serum (FBS), 1% penicillin and streptomycin (p/s), and 0.2% normocin. Cell culture supplies were from Invitrogen (Carlsbad, CA) unless otherwise specified. Chinese hamster ovary (CHO) cells stably expressing MOP-, KOP-, DOP-receptors, or CB1-Gαq16 were removed from their flasks using Versene and quenched with the Ham media, centrifuged and re-suspended in media. Cells were counted with a Cellometer Auto T4

(Nexcelom Bioscience, Lawrence, MA) and 30,000 cells were transferred to each well of a black Costar 96-well optical bottom plate (Corning Corporation, Corning, NY). Each plate was incubated at 37°C/5% CO_2 overnight to confluence. The culture media was removed from the plates and cells were subsequently loaded with a fluorescent calcium probe (Calcium 5 dye, Molecular Devices, Sunnyvale, CA) in an HBSS-based buffer containing 20 mM HEPES, 0.25% BSA, 1% DMSO (or 0.5% DMSO + 0.5% EtOH for CB1-expressing cells), and 10 μM probenecid (Sigma) in a total volume of 225 μL. Cells were incubated at 37°C/5% CO_2 for 1 h and then stimulated with DMSO solutions of DAMGO, U-69,593, DPDPE, ethanol solutions of CP-55,940 or DMSO solutions of test compounds at various concentrations using a Flexstation 3 plate-reader, which automatically added 25 μL of the compounds at 10X concentration to each well after reading baseline values for ~17 sec. Agonist-mediated change in fluorescence (485 nm excitation, 525 nm emission) was monitored in each well at 1.52 sec intervals for 60 sec and reported for each well. Data were collected using Softmax version 4.8 (MDS Analytical Technologies) and analyzed using Prism software (GraphPad, La Jolla, CA). Nonlinear regression analysis was performed to fit data and obtain maximum response (E_{max}), EC_{50}, correlation coefficient ($r2$) and other parameters. All experiments were performed at least 2 times to ensure reproducibility and data reported as mean ± standard error, unless noted otherwise.

Salvinorin A extraction from S. divinorum leaves.[311] Briefly, dried *Salvia divinorum* leaves (1.5 kg), obtained commercially from Ethnogens.com, were ground to a fine powder and percolated with acetone (5 x 4 L). The acetone extract was concentrated under reduces pressure to afford a crude green gum (93 g), which was subjected to column chromatography on silica

gel; with elution in *n*-hexanes containing increasing amounts of EtOAc. Fractions eluting in 20% *n*-hexanes/EtOAc contained salvinorin A (TLC) and other minor diterpenes and some pigmented material. These fractions were pooled and concentrated under reduced pressure to give a green gum (24 g). A mixture of the crude green gum, acetic anhydride (50 mL, 530 mmol) and DMAP (0.2 g) in DCM (250 mL) was stirred at ambient temperature overnight. The DCM solution was dried over Na_2SO_4 and the solvent was removed under reduced pressure to afford a yellow-green gum (23 g). The resulting gum was subjected to column chromatography on silica gel and elution was performed with mixtures of *n*-hexanes/EtOAc in 1 L fraction aliquots in increments of 10% EtOAc with the final elution in 100% EtOAc. Fractions eluting in 30% *n*-hexanes/EtOAc and subsequent fractions were pooled and the solvent removed under reduced pressure to afford salvinorin A (7.5 g, 0.5%) as a green powder.

CHAPTER 3: EXPERIMENTAL PROCEDURES FOR SALVINORIN A ANALOGUES

PART II: QUINONE CONTAINING SALVINORIN A ANALOGUES

Chemistry

General Methods. Unless otherwise indicated, all reagents were purchased from commercial sources and were used without further purification. Melting points were determined on a Thomas-Hoover capillary melting apparatus. NMR spectra were recorded on a Bruker DRX-400 with qnp probe or a Bruker AV-500 with cryoprobe using δ values in ppm (TMS as internal standard) and *J* (Hz) assignments of ^{1}H resonance coupling. High resolution mass spectrometry data were collected on either a LCT Premier (Waters Corp., Milford, MA) time of flight mass spectrometer or an Agilent 6890 N gas chromatograph in conjunction with a quarto Micro GC mass spectrometer (Micromass Ltd, Manchester UK). Thin-layer chromatography (TLC) was performed on 0.25 mm plates Analtech GHLF silica gel plates using ethyl acetate/*n*-hexanes, in 50%:50% ratio as the solvent unless otherwise noted. Spots on TLC were visualized by UV (254 or 365 nm), if applicable, and phosphomolybdic acid in ethanol. Column chromatography was performed with Silica Gel (40-63 μ particle size) from Sorbent Technologies (Atlanta, GA). Analytical HPLC was carried out on an Agilent 1100 Series Capillary HPLC system with diode array detection at 254 nm on an Agilent Eclipse XDB-C18 column (250 x 10 mm, 5 μm) with isocratic elution in 60% CH_3CN/40% H_2O unless otherwise specified.

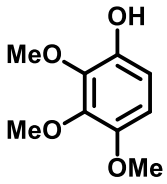

2,3,4-trimethoxyphenol (260). To a solution of 2,3,4-benzaldehyde **259** (6 g, 30.58 mmol) in H_2SO_4/MeOH (1:100 v/v), at 0 °C under an argon atmosphere was added 30% H_2O_2 (8 mL, 78.29 mmol). After completion (24 hrs), the reaction mixture was diluted with Et_2O and washed successively with H_2O, brine, dried over Na_2SO_4, filtered, and concentrated under reduced pressure. The crude mixture was purified by flash column chromatography (20% EtOAc/80% *n*-hexanes) to afford 4.72 g (84% yield) as a clear oil. Spectral data matched previously reported data.[336]

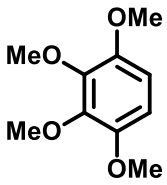

1,2,3,4-tetramethoxybenzene (261). To a stirred solution of phenol **260** and K_2CO_3 in acetone was added MeI. The reaction mixture was stirred at reflux overnight and upon completion, the mixture is allowed to cool to ambient temperature and filtered. Filtrate was washed with H_2O, brine, dried over Na_2SO_4, filtered and concentrated under reduced pressure. The crude mixture was purified by flash column chromatography (20% EtOAc/80% *n*-hexanes) to afford 3.38 g (67% yield) as a white solid. Spectral data matched previously reported data.[336]

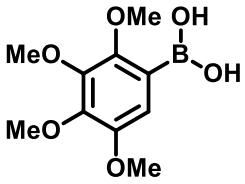

(2,3,4,5-tetramethoxyphenyl)boronic acid (262). To s stirred solution of benzene **261** (0.78 g, 3.94 mmol) in THF at ambient temperature under an argon atmosphere, *n*-BuLi (1.6 M, 2.7 mL, 4.33 mmol) was added dropwise. The mixture was stirred for 15 minutes and then cooled to -78 °C, upon which trimethyl borate (2.64 mL, 23.64 mmol) was added dropwise. Reaction mixture allowed to slowly warm up up to ambient temperature. Upon completion (TLC monitoring), reaction mixture was cooled in an ice bath and quenched with 1 N HCl and allowed to warm up to ambient temperature. After 2 hours the solution was diluted with Et_2O (50 mL) and washed successively with 1N HCl, brine, dried over Na_2SO_4, filtered and concentrated under reduced pressure. The crude mixture was purified by flash column chromatography (20% EtOAc/80% *n*-hexanes) to afford 0.46 g (52% yield) as a clear oil. Spectral data matched previously reported data.[336]

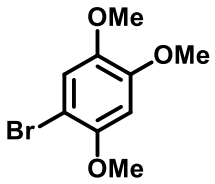

1-bromo-2,4,5-trimethoxybenzene (264). Bromine (0.64 mL, 12.49 mmol) in DCM (10 mL) was added dropwise to a solution of benzene **263** (2g, 1.77 mL, 11.89 mmol) in DCM (35 mL) at 0 °C and allowed to stir at that temperature until completion (TLC monitoring). Upon completion, the reaction mixture was washed successively with sodium sulfite, $NaHCO_3$, H_2O,

and brine, dried over Na_2SO_4, filtered and concentrated under reduced pressure to afford 2.81 g (96% yield) as a white solid that was used without further purification.[337]

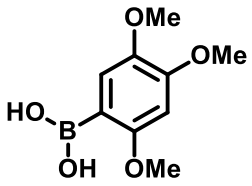

(2,4,5-trimethoxyphenyl)boronic acid (265). To a solution of bromobenzene **264** (2.81 g, 11.37 mmol) in THF (20 mL) at -78 °C was added *n*-BuLi (1.6 M, 7.1 mL, 12.51 mmol) dropwise over a period of 10 minutes. The solution was allowed to stir for 30 minutes and trimethyl borate (1.42 mL, 12.51 mmol) was added dropwise keeping the temperature at -78 C. The mixture was stirred at -78 °C until completion (TLC monitoring) and upon completion quenched with aq. NH_4Cl. Water was then added to the mixture and extracted with DCM. Organic extracts were then washed with brine, dried over Na_2SO_4, filtered and concentrated under reduced pressure. The crude mixture was purified by flash column chromatography (45% EtOAc/55% *n*-hexanes) to afford 0.91 g (38% yield) as a clear oil. Spectral data matched previously reported data.[337]

General Procedure A: Liebskind-Srogl coupling reaction. Salvinorin A thiophenol ester (1 equiv), appropriate boronic acid (3 equiv), bis(dibenzylideneacetone)palladium (0) (5 mol%), copper (I) thiophene carboxylate (1.5 equiv) were placed in a 100 mL round bottom flask and flushed with argon (2x). Anhydrous THF was then added and immediately after triphenylphosphite was also added (20 mol%, color change from red to green with a brown tint).

Reaction allowed to stir at ambient temperature and upon completion (TLC monitoring) the reaction was diluted with 30 mL of Et_2O and washed successively with sat. $NaHCO_3$, brine, dried over Na_2SO_4, filtered and concentrated under reduced pressure. The resulting residue was purified by flash chromatography on silica gel using mixtures of EtOAc/*n*-hexanes.

General Procedure B: CBS reduction. Aromatic ketone (1 equiv) was placed in a round bottom flask and flushed with argon (3x). (*R*)-(+)-2-Methyl-CBS-oxazaborolidine solution (1 M in toluene, 1 equiv) was added at -78 °C and allowed to stir for 5 minutes. Boron-dimethyl sufide (2 M in diethyl ether, 1 equiv) was then added dropwise at -78 °C and the reaction mixture was warmed up to -30 °C and allowed to stir at that temperature until completion (TLC monitoring). Upon completion, 1 mL of MeOH, 0.5 mL of H_2O and 5 mL Et_2O were added to quench the reaction, which was allowed to warm up to room temperature over a period of 1 hour. To the reaction mixture were then added 20 mL of H_2O and 20 mL of Et_2O. The aqueous layer was wased with Et_2O (2x) and the combined organic layers were washed with brine, dried over Na_2SO_4, filtered and concentrated under reduced pressure. The resulting residue was purified by flash chromatography on silica gel using mixtures of EtOAc/*n*-hexanes.

General Procedure C. Deoxygenation procedure. Alcohol (1 equiv, 0.21 mmol) was placed in a round bottom flask and flushed with argon before being dissolved in DCM (10 mL) and cooled to 0 °C. Triethylsilane (2 equiv) was then added and after a 2 minute period boron trifluoride diethyl etherate (2 equiv) was the added in a dropwise manner. The reaction mixture was allowed to stir at 0 °C overnight until completion (TLC monitoring). Upon completion,

reaction was quenched with H_2O and allowed to warm up to ambient temperature. The mixture was then extracted with EtOAc (3x), dried over Na_2SO_4, filtered and concentrated under reduced pressure. The resulting residue was purified by flash chromatography on silica gel using mixtures of EtOAc/*n*-hexanes.

General Procedure D. Quinone formation. To a solution of salvinorin A derivative (1 equiv, 0.21 mmol) in acetonitrile (7 mL) was added an aqueous solution of cerium (IV) ammonium nitrate, 2-3 equiv, 0.42 mmol, 1.4 mL). Reaction was allowed to stir at ambient temperature until completion (TLC monitoring) and upon completion 20 mL of DCM were added and successively washed with H_2O and brine, dried over Na_2SO_4, filtered and concentrated under reduced pressure. The resulting residue was purified by flash chromatography on silica gel using mixtures of EtOAc/*n*-hexanes.

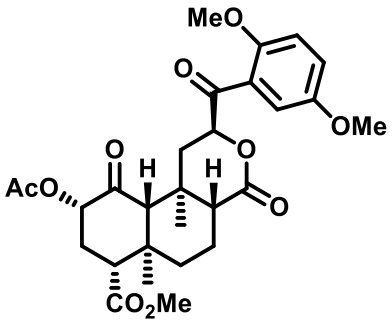

(**2*S*,4a*R*,6a*R*,7*R*,9*S*,10a*S*,10b*R***)-methyl 9-acetoxy-2-(2,5-dimethoxybenzoyl)-6a,10b-dimethyl-4,10-dioxododecahydro-1*H*-benzo[*f*]isochromene-7-carboxylate (**266**). Compound **266** was synthesized from compound **144** using general procedure A and 2,5-dimethoxyphenyl boronic acid to afford 0.250 g (48% yield) isolated as a white solid, mp = 97-100 °C. TLC system 45% EtOAc/55% *n*-hexanes. ^{1}H NMR (500 MHz, $CDCl_3$) δ 7.36 (d, *J* = 3.2 Hz, 1H),

7.10 (dd, *J* = 9.0, 3.2 Hz, 1H), 6.93 (d, *J* = 9.0 Hz, 1H), 5.95 (t, *J* = 8.1 Hz, 1H), 5.13 – 5.03 (m, 1H), 3.90 (s, 3H), 3.80 (s, 3H), 3.71 (s, 4H), 2.78 – 2.66 (m, 2H), 2.31 – 2.22 (m, 2H), 2.19 – 2.07 (m, 7H), 1.80 – 1.60 (m, 3H), 1.54 (td, *J* = 13.4, 3.8 Hz, 1H), 1.42 (s, 3H), 1.40 – 1.32 (m, 1H), 1.07 (s, 3H). ^{13}C NMR (126 MHz, $CDCl_3$) δ 201.84, 196.68, 171.61, 169.78, 153.78, 153.42, 124.04, 122.28, 114.45, 113.45, 79.12, 74.86, 65.02, 56.20, 55.84, 53.31, 51.96, 49.45, 42.04, 38.04, 37.88, 35.58, 30.75, 20.64, 18.31, 16.68, 16.05. HRMS (*m/z*): [M+Na] calcd for $C_{28}H_{34}NaO_{10}$, 553.2050; found 553.2063.

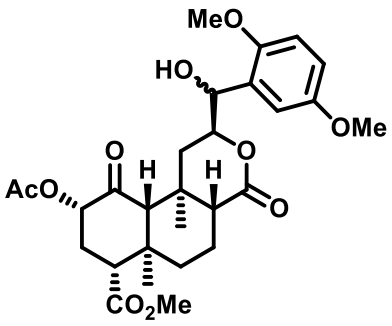

(2*S*,4a*R*,6a*R*,7*R*,9*S*,10a*S*,10b*R*)-methyl 9-acetoxy-2-((2,5-dimethoxyphenyl)(hydroxy)methyl)-6a,10b-dimethyl-4,10-dioxododecahydro-1*H*-benzo[*f*]isochromene-7-carboxylate (269). Compound **269** was synthesized from compound **266** using general procedure B to afford 0.31 g (90% yield) isolated as a white solid, mp = 125-128 °C. ^{1}H NMR (500 MHz, $CDCl_3$) δ 6.96 (dd, *J* = 11.1, 2.5 Hz, 1H), 6.85 – 6.70 (m, 2H), 5.27 (dd, *J* = 5.2, 3.1 Hz, 1H), 5.12 (dd, *J* = 12.4, 7.5 Hz, 1H), 3.78 – 3.76 (m, 5H), 3.72 (d, *J* = 4.7 Hz, 3H), 2.80 – 2.70 (m, 2H), 2.35 – 2.19 (m, 2H), 2.19 – 2.09 (m, 5H), 2.02 (dd, *J* = 11.5, 3.3 Hz, 1H), 1.87 (dd, *J* = 13.2, 6.1 Hz, 1H), 1.75 (dt, *J* = 10.1, 2.9 Hz, 1H), 1.60 – 1.52 (m, 3H), 1.30 (s, 3H), 1.06 (d, *J* = 6.0 Hz, 3H). ^{13}C NMR (126 MHz, $CDCl_3$) δ 202.16, 172.13, 171.67,

169.60, 153.82, 150.10, 127.29, 113.79, 113.21, 111.26, 78.80, 74.92, 70.54, 64.28, 55.92, 55.72, 53.44, 51.94, 50.56, 42.13, 38.10, 34.85, 34.81, 30.91, 20.60, 18.18, 16.15, 15.21. HRMS (*m/z*): [M+Na] calcd for $C_{28}H_{36}NaO_{10}$, 555.2206; found 555.2217.

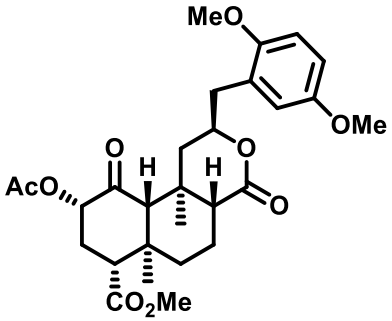

(2*S*,4a*R*,6a*R*,7*R*,9*S*,10a*S*,10b*R*)-methyl 9-acetoxy-2-(2,5-dimethoxybenzyl)-6a,10b-dimethyl-4,10-dioxododecahydro-1*H*-benzo[*f*]isochromene-7-carboxylate (272). Compound **272** was synthesized from compound **269** using general procedure C to afford 0.11 g (36% yield) isolated as a white solid, mp = 96-98 °C. TLC system: 40% EtOAc/60% *n*-hexanes. ^{1}H NMR (500 MHz, Chloroform-*d*) δ 6.79 – 6.73 (m, 3H), 5.12 (dd, *J* = 11.6, 8.4 Hz, 1H), 4.76 (dq, *J* = 11.3, 5.6 Hz, 1H), 3.76 (s, 3H), 3.75 (s, 3H), 3.72 (s, 3H), 2.91 (dd, *J* = 5.8, 2.7 Hz, 2H), 2.73 (dd, *J* = 11.7, 5.2 Hz, 1H), 2.33 – 2.23 (m, 3H), 2.17 (s, 3H), 2.14 – 2.06 (m, 2H), 1.92 – 1.83 (m, 1H), 1.79 – 1.71 (m, 1H), 1.59 – 1.49 (m, 2H), 1.33 (s, 3H), 1.08 (s, 3H). ^{13}C NMR (126 MHz, $CDCl_3$) δ 202.11, 171.61, 171.58, 169.88, 153.31, 151.83, 125.67, 117.47, 112.57, 111.30, 75.05, 64.20, 55.79, 55.73, 53.58, 51.96, 51.23, 42.25, 42.15, 38.22, 37.22, 35.08, 30.81, 20.60, 18.16, 16.31, 15.18. HRMS (*m/z*): [M+Na] calcd for $C_{28}H_{36}NaO_{9}$, 539.2257; found 539.2269.

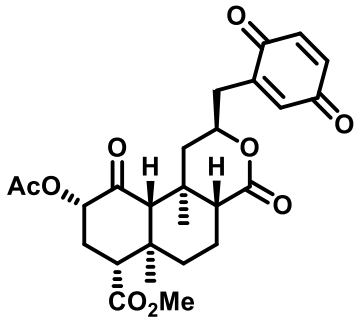

(2*S*,4a*R*,6a*R*,7*R*,9*S*,10a*S*,10b*R*)-methyl 9-acetoxy-2-((3,6-dioxocyclohexa-1,4-dien-1-yl)methyl)-6a,10b-dimethyl-4,10-dioxododecahydro-1*H*-benzo[*f*]isochromene-7-carboxylate (275). Compound **275** was synthesized from compound **272** using general procedure D to afford 0.04 g (39% yield) isolated as a yellow solid, mp = decomp at 212-214 °C. ^{1}H NMR (500 MHz, $CDCl_3$) δ 6.80 – 6.72 (m, 2H), 6.70 (dd, *J* = 2.3, 1.2 Hz, 1H), 5.14 (dd, *J* = 11.5, 8.5 Hz, 1H), 4.69 (dddd, *J* = 11.9, 9.6, 4.9, 3.2 Hz, 1H), 3.73 (s, 3H), 2.81 – 2.70 (m, 2H), 2.60 – 2.50 (m, 1H), 2.39 (dd, *J* = 13.3, 4.8 Hz, 1H), 2.34 – 2.25 (m, 2H), 2.18 (s, 3H), 2.12 (d, *J* = 3.7 Hz, 1H), 1.97 (dd, *J* = 11.5, 3.1 Hz, 1H), 1.81 – 1.74 (m, 1H), 1.65 – 1.57 (m, 1H), 1.53 (s, 1H), 1.35 (s, 3H), 1.32 – 1.22 (m, 1H), 1.09 (s, 3H). ^{13}C NMR (126 MHz, $CDCl_3$) δ 201.91, 187.17, 187.10, 171.50, 170.74, 170.00, 143.61, 136.61, 136.59, 135.20, 75.11, 75.03, 64.04, 53.60, 52.00, 51.41, 43.04, 42.09, 38.14, 36.78, 35.26, 30.75, 20.59, 18.12, 16.37, 15.17. HRMS (*m/z*): [M+K] calcd for $C_{26}H_{30}KO_9$, 525.1527; found 525.1528. HPLC t_R = 6.424; purity = 99.2%.

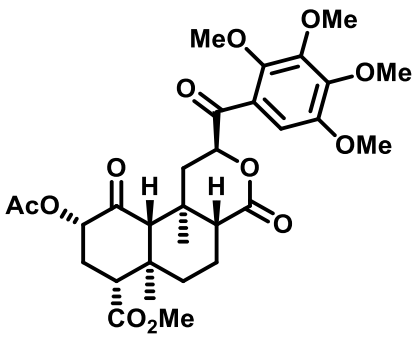

(2*S*,4a*R*,6a*R*,7*R*,9*S*,10a*S*,10b*R*)-methyl 9-acetoxy-6a,10b-dimethyl-4,10-dioxo-2-(2,3,4,5-tetramethoxybenzoyl)dodecahydro-1*H*-benzo[*f*]isochromene-7-carboxylate (267). Compound **267** was synthesized from compound **144** using general procedure A and 2,3,4,5-tetramethoxyphenyl boronic acid to afford 0.57 g (79% yield) isolated as an amorphous solid. TLC system: 45% EtOAc/55% *n*-hexanes. ^{1}H NMR (500 MHz, $CDCl_3$) δ 7.06 (s, 1H), 5.88 (t, *J* = 8.2 Hz, 1H), 5.13 – 5.04 (m, 1H), 3.98 (s, 3H), 3.94 (s, 3H), 3.90 (s, 3H), 3.86 (s, 3H), 3.72 (s, 3H), 2.71 (ddd, *J* = 12.1, 8.3, 2.5 Hz, 2H), 2.28 (td, *J* = 9.5, 2.2 Hz, 2H), 2.18 – 2.17 (m, 3H), 2.14 – 2.13 (m, 3H), 2.12 (s, 1H), 1.76 (dt, *J* = 13.4, 3.2 Hz, 1H), 1.72 – 1.58 (m, 2H), 1.43 (s, 3H). 1.07 (s, 3H). ^{13}C NMR (126 MHz, $CDCl_3$) δ 201.81, 196.30, 171.58, 171.37, 169.80, 149.46, 148.77, 148.54, 146.62, 122.46, 107.23, 78.79, 74.89, 64.92, 62.02, 61.25, 56.16, 53.38, 51.97, 49.51, 42.07, 38.38, 37.91, 35.55, 30.95, 30.71, 20.60, 18.29, 16.51, 16.05. HRMS (*m*/*z*): [M+Na] calcd for $C_{30}H_{38}NaO_{12}$, 613.2261; found 613.2289.

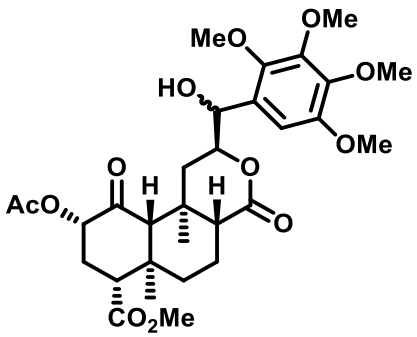

(2*S*,4a*R*,6a*R*,7*R*,9*S*,10a*S*,10b*R*)-methyl 9-acetoxy-2-(hydroxy(2,3,4,5-tetramethoxyphenyl)methyl)-6a,10b-dimethyl-4,10-dioxododecahydro-1H-benzo[f]isochromene-7-carboxylate (270). Compound **270** was synthesized from compound **267** using general procedure B to afford 0.78 g (89% yield) isolated as a white solid, mp = 104-107 °C. TLC system: 55% EtOAc/44% n-hexanes. 1H NMR (500 MHz, $CDCl_3$) δ 6.65 (s, 1H), 5.26 (dd, J = 4.7, 2.9 Hz, 1H), 5.11 (dd, J = 12.2, 7.7 Hz, 1H), 4.73 (ddd, J = 11.5, 5.8, 3.0 Hz, 1H), 3.93 (s, 3H), 3.90 (s, 3H), 3.83 (d, J = 5.1 Hz, 6H), 3.72 (s, 3H), 2.96 (s, 1H), 2.88 (s, 1H), 2.74 (dd, J = 12.7, 4.1 Hz, 1H), 2.65 (d, J = 4.9 Hz, 1H), 2.31 – 2.22 (m, 2H), 2.17 (s, 2H), 2.12 (s, 3H), 1.97 (td, J = 13.2, 12.6, 7.0 Hz, 2H), 1.81 – 1.74 (m, 1H), 1.31 (s, 3H), 1.06 (s, 3H). ^{13}C NMR (126 MHz, $CDCl_3$) δ 202.18, 171.89, 171.55, 169.53, 149.68, 146.51, 144.04, 142.65, 125.54, 104.67, 79.77, 74.90, 70.07, 64.23, 61.07, 61.05, 60.99, 56.33, 53.51, 51.91, 50.64, 42.19, 38.14, 34.81, 34.62, 30.82, 20.50, 18.12, 16.15, 15.14. HRMS (*m/z*): [M+Na] calcd for $C_{30}H_{40}NaO_{12}$, 615.2418; found 615.2435.

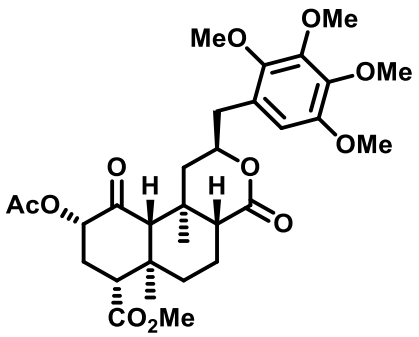

(2S,4aR,6aR,7R,9S,10aS,10bR)-methyl 9-acetoxy-6a,10b-dimethyl-4,10-dioxo-2-(2,3,4,5-tetramethoxybenzyl)dodecahydro-1H-benzo[f]isochromene-7-carboxylate (273). Compound **273** was synthesized from compound **270** using general procedure C to afford 0.42 g (55% yield) isolated as a white solid, mp = 91-94 °C. TLC system: 45% EtOAc/55% n-hexanes. 1H NMR (500 MHz, $CDCl_3$) δ 6.45 (s, 1H), 5.12 (dd, J = 11.5, 8.4 Hz, 1H), 4.71 (dq, J = 11.3, 5.5 Hz, 1H), 3.92 (s, 3H), 3.88 (s, 3H), 3.80 (d, J = 9.0 Hz, 6H), 3.72 (s, 3H), 2.88 (qd, J = 13.8, 5.9 Hz, 2H), 2.77 – 2.70 (m, 1H), 2.33 – 2.22 (m, 3H), 2.16 (s, 3H), 2.10 (d, J = 3.9 Hz, 2H), 1.87 (dd, J = 11.6, 3.1 Hz, 1H), 1.80 – 1.72 (m, 1H), 1.59 – 1.49 (m, 2H), 1.34 (s, 3H), 1.30 – 1.24 (m, 1H), 1.08 (s, 3H). 13C NMR (126 MHz, CDCl3) δ 202.14, 171.58, 171.49, 169.85, 149.22, 146.94, 145.69, 141.92, 123.97, 108.53, 77.69, 75.05, 64.12, 61.15, 61.06, 61.04, 56.23, 53.57, 51.97, 51.28, 42.28, 42.14, 38.20, 36.72, 35.07, 30.78, 20.58, 18.17, 16.33, 15.18. HRMS (*m/z*): [M+Na] calcd for $C_{30}H_{40}NaO_{11}$, 599.2468; found 599.2459.

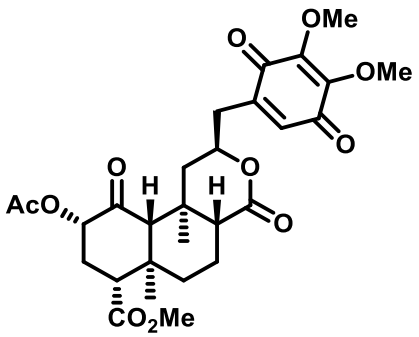

(2*S*,4a*R*,6a*R*,7*R*,9*S*,10a*S*,10b*R*)-methyl 9-acetoxy-2-((4,5-dimethoxy-3,6-dioxocyclohexa-1,4-dien-1-yl)methyl)-6a,10b-dimethyl-4,10-dioxododecahydro-1*H*-benzo[*f*]isochromene-7-carboxylate (276). Compound **276** was synthesized from compound **273** using general procedure D to afford 0.11 g (28% yield) isolated as an orange solid, mp = 102-104 °C. TLC system: 55% EtOAc/45% *n*-hexanes. ^{1}H NMR (500 MHz, $CDCl_3$) δ 6.55 – 6.48 (m, 1H), 5.14 (dd, *J* = 11.7, 8.3 Hz, 1H), 4.68 (dddd, *J* = 11.7, 9.5, 4.7, 3.2 Hz, 1H), 4.02 (s, 3H), 4.00 (s, 3H), 3.73 (s, 3H), 2.80 – 2.70 (m, 2H), 2.54 (ddd, *J* = 14.6, 9.3, 1.1 Hz, 1H), 2.38 (dd, *J* = 13.3, 4.9 Hz, 1H), 2.34 – 2.26 (m, 2H), 2.18 (s, 3H), 2.14 – 2.09 (m, 2H), 2.00 – 1.93 (m, 1H), 1.81 – 1.75 (m, 1H), 1.60 – 1.51 (m, 2H), 1.34 (s, 3H), 1.30 – 1.21 (m, 1H), 1.09 (s, 3H). ^{13}C NMR (126 MHz, $CDCl_3$) δ 201.92, 183.85, 183.80, 171.51, 170.80, 169.98, 145.04, 144.87, 141.74, 133.24, 75.19, 75.02, 64.01, 61.31, 61.24, 53.58, 52.00, 51.38, 42.97, 42.08, 38.12, 36.43, 35.25, 30.74, 20.59, 18.11, 16.36, 15.17. HRMS (*m*/*z*): [M+Na] calcd for $C_{28}H_{34}NaO_{11}$, 569.1999; found 569.1960. HPLC t_R = 6.959; purity = 98.1%.

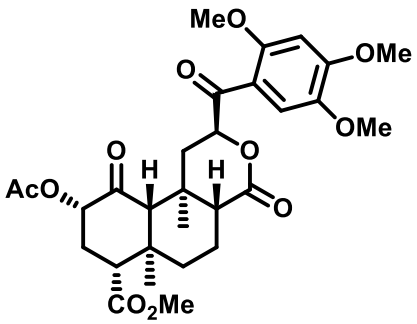

(2*S*,4a*R*,6a*R*,7*R*,9*S*,10a*S*,10b*R*)-methyl 9-acetoxy-6a,10b-dimethyl-4,10-dioxo-2-(2,4,5-trimethoxybenzoyl)dodecahydro-1*H*-benzo[*f*]isochromene-7-carboxylate (268). Compound **268** was synthesized from compound **144** using general procedure A and 2,4,5-trimethoxyphenyl boronic acid to afford 1.01 g (90% yield) isolated as a white solid, mp = 103-106°C. TLC system: 60% EtOAc/40% *n*-hexanes. ^{1}H NMR (500 MHz, $CDCl_3$) δ 7.47 (s, 1H), 6.47 (s, 1H), 5.94 (dd, *J* = 8.8, 7.3 Hz, 1H), 5.07 (ddd, *J* = 10.8, 9.3, 1.0 Hz, 1H), 3.96 (s, 3H), 3.94 (s, 3H), 3.87 (s, 3H), 3.70 (s, 3H), 2.78 (dd, *J* = 13.7, 8.8 Hz, 1H), 2.72 – 2.65 (m, 1H), 2.30 – 2.22 (m, 2H), 2.21 – 2.07 (m, 6H), 1.74 (dt, *J* = 12.9, 3.1 Hz, 1H), 1.65 (ddd, *J* = 14.8, 11.6, 3.3 Hz, 1H), 1.57 – 1.49 (m, 1H), 1.42 (s, 3H), 1.35 – 1.27 (m, 1H), 1.06 (s, 3H). ^{13}C NMR (126 MHz, $CDCl_3$) δ 201.89, 171.94, 171.63, 169.81, 155.64, 155.37, 143.68, 118.18, 114.77, 112.83, 96.12, 78.93, 74.89, 65.22, 56.30, 56.26, 56.20, 53.30, 51.95, 49.16, 42.07, 38.37, 37.88, 35.62, 30.76, 20.66, 18.35, 16.95, 16.00. HRMS (*m/z*): [M+K] calcd for $C_{29}H_{36}KO_{11}$, 599.1895; found 599.1903.

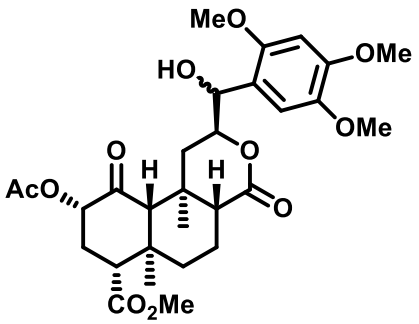

(2*S*,4a*R*,6a*R*,7*R*,9*S*,10a*S*,10b*R*)-methyl 9-acetoxy-2-(hydroxy(2,4,5-trimethoxyphenyl)methyl)-6a,10b-dimethyl-4,10-dioxododecahydro-1*H*-benzo[*f*]isochromene-7-carboxylate (271). Compound **271** was synthesized from compound **268** using general procedure B to afford 0.78 g (64% yield) isolated as a white solid, mp = 133-136 °C. TLC system: 60% EtOAc/40% *n*-hexanes. ^{1}H NMR (500 MHz, $CDCl_3$) δ 6.92 (s, 1H), 6.49 (s, 1H), 5.28 (dd, *J* = 5.0, 2.8 Hz, 1H), 5.15 – 5.05 (m, 1H), 4.75 (ddd, *J* = 11.6, 5.8, 3.0 Hz, 1H), 3.90 (s, 3H), 3.83 (s, 3H), 3.80 (s, 3H), 3.71 (s, 3H), 2.74 (dd, *J* = 12.7, 4.2 Hz, 1H), 2.63 (d, *J* = 5.2 Hz, 1H), 2.32 – 2.19 (m, 2H), 2.14 (d, *J* = 19.1 Hz, 5H), 2.02 – 1.94 (m, 1H), 1.91 (dd, *J* = 13.2, 5.8 Hz, 1H), 1.80 – 1.72 (m, 1H), 1.58 – 1.50 (m, 2H), 1.30 (s, 3H), 1.05 (s, 3H). ^{13}C NMR (126 MHz, $CDCl_3$) δ 202.19, 172.04, 171.63, 169.55, 150.16, 149.20, 143.24, 117.56, 111.01, 96.89, 79.36, 74.93, 69.90, 64.31, 56.73, 56.12, 56.02, 53.56, 51.94, 50.67, 42.23, 38.20, 34.85, 34.74, 30.89, 20.55, 18.18, 16.18, 15.19. HRMS (*m/z*): [M+K] calcd for $C_{29}H_{38}KO_{11}$, 601.2051; found 601.2029.

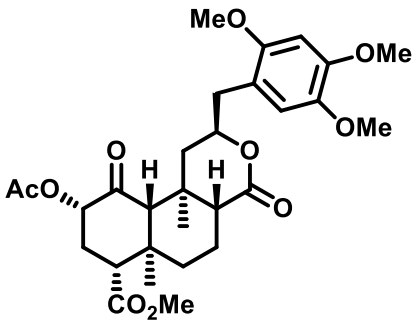

(2*S*,4a*R*,6a*R*,7*R*,9*S*,10a*S*,10b*R*)-methyl 9-acetoxy-6a,10b-dimethyl-4,10-dioxo-2-(2,4,5-trimethoxybenzyl)dodecahydro-1*H*-benzo[*f*]isochromene-7-carboxylate (274). Compound **274** was synthesized from compound **271** using general procedure C to afford 0.42 g (56% yield) isolated as a white solid, mp = 108-111 °C. TLC system: 55% EtOAc/45% *n*-hexanes. ^{1}H NMR (500 MHz, $CDCl_3$) δ 6.70 (s, 1H), 6.51 (s, 1H), 5.15 – 5.01 (m, 1H), 4.71 (dd, *J* = 11.4, 5.5 Hz, 1H), 3.89 (s, 3H), 3.81 (s, 3H), 3.78 (s, 3H), 3.71 (s, 3H), 2.96 – 2.80 (m, 2H), 2.76 – 2.67 (m, 1H), 2.32 – 2.21 (m, 3H), 2.17 (s, 3H), 2.07 (d, *J* = 11.7 Hz, 2H), 1.85 – 1.71 (m, 2H), 1.57 – 1.46 (m, 2H), 1.32 (s, 3H), 1.20 (dd, *J* = 13.5, 11.6 Hz, 1H), 1.07 (s, 3H). ^{13}C NMR (126 MHz, $CDCl_3$) δ 202.13, 171.65, 171.60, 169.89, 151.77, 148.48, 142.77, 115.84, 115.16, 97.43, 77.47, 75.07, 64.24, 56.62, 56.18, 56.15, 53.60, 51.95, 51.20, 42.18, 41.92, 38.23, 36.07, 35.02, 30.80, 20.60, 18.15, 16.32, 15.20. HRMS (*m/z*): [M+K] calcd for $C_{29}H_{38}KO_{10}$, 585.2102; found 585.2084.

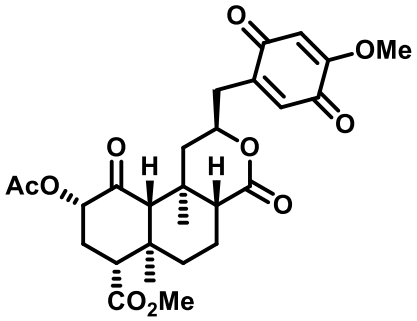

(2*S*,4a*R*,6a*R*,7*R*,9*S*,10a*S*,10b*R*)-methyl 9-acetoxy-2-((4-methoxy-3,6-dioxocyclohexa-1,4-dien-1-yl)methyl)-6a,10b-dimethyl-4,10-dioxododecahydro-1*H*-benzo[*f*]isochromene-7-carboxylate (277). Compound **277** was synthesized from compound **274** using general procedure D to afford 0.50 g (72% yield) isolated as a yellow solid, mp = 127-130 °C. TLC system: 60% EtOAc/40% *n*-hexanes. ^{1}H NMR (500 MHz, $CDCl_3$) δ 6.63 (t, *J* = 1.1 Hz, 1H), 5.93 (s, 1H), 5.14 (dd, *J* = 11.6, 8.4 Hz, 1H), 4.70 (dddd, *J* = 14.6, 8.6, 4.8, 3.3 Hz, 1H), 3.83 (s, 3H), 3.73 (s, 3H), 2.83 – 2.71 (m, 2H), 2.56 (ddd, *J* = 14.4, 9.2, 1.0 Hz, 1H), 2.38 (dd, *J* = 13.3, 4.9 Hz, 1H), 2.34 – 2.28 (m, 2H), 2.18 (s, 4H), 2.11 (d, *J* = 4.1 Hz, 2H), 2.00 – 1.94 (m, 1H), 1.82 – 1.75 (m, 1H), 1.54 (d, *J* = 12.9 Hz, 1H), 1.35 (s, 3H), 1.27 (t, *J* = 12.5 Hz, 1H), 1.09 (s, 3H). ^{13}C NMR (126 MHz, $CDCl_3$) δ 201.90, 187.00, 181.77, 171.52, 170.77, 169.98, 158.75, 144.44, 133.15, 107.66, 75.35, 75.02, 64.04, 56.31, 53.59, 52.00, 51.40, 43.01, 42.08, 38.14, 36.65, 35.26, 30.76, 20.60, 18.11, 16.37, 15.17. HRMS (*m/z*): [M+K] calcd for $C_{27}H_{32}KO_{10}$, 555.1633; found 555.1678. HPLC t_R = 6.049; purity = 95.4%.

Cell Culture[341]

The media for each cell line was supplemented with streptomycin (500 μg/mL), penicillin (100 units/mL), and 10% FBS. MCF7 and SKBr3 cells were maintained in Advanced DMEM/F12 (1:1; Gibco) supplemented with L-glutamine (2 mM). Cells were grown in a humidified atmosphere (37 °C, 5% CO_2) and passaged when confluent.

Anti-proliferation Assay[341]

Cells were grown to confluence, seeded (2000 cells/well, 100 μL total media) in clear, flat-bottom 96-well plates and allowed to attach overnight. Compound or geldanamycin at varying concentrations in DMSO (1% DMSO final concentration) was added. Cells were returned to the incubator for an additional 72 h. After 72 h, cell growth was determined using an MTS/PMS cell proliferation kit (Promega) per the manufacturer's instructions. Cells incubated in 1% DMSO were used as 100% proliferation (i.e. DMSO = 100% growth) and the relative growth for each compound concentration was compared to 1% DMSO. IC_{50} values were calculated from two separate experiments performed in triplicate using GraphPad Prism 6.0.

CHAPTER 4: SYNTHETIC CANNABINOIDS AND THEIR POTENTIAL AS ALCOHOL ABUSE TREATMENTS

Cannabis sativa L.

One of the oldest psychotropic drugs, whose use dates back to the Neolithic period is cannabis.[342] Originating in Central Asia, cannabis has been cultivated and consumed even before the appearance of writing.[342] Its medicinal, recreational, and spiritual use by many ancient cultures dates back to 4000 B.C.[343] Chinese, Indian, and Tibetan ancient cultures have utilized the seeds and fruit of cannabis to treat a variety of ailments such as pain of childbirth, gastrointestinal disorders, seizures, malaria, snake bites and various others.[343] Besides its medicinal use, cannabis has been also used in the spiritual practices and religious ceremonies of many cultures where such practices were conducted by Tantric Buddhists, Hindus and ancient shamans.[344]

It is believed that the properties and therapeutic uses of cannabis were originally described by the Emperor of China, Shen Nung, who also discovered tea and ephedrine, and inscribed it in his compendium of Chinese medicinal herbs.[345] The extent of the numerous therapeutic effects of cannabis resulted in its fast migration to many cultures and from 2000 to 1400 B.C., its use spread to India, Egypt, Persia, and Syria.[346] Furthermore, evidence suggests that cannabis was used as incense as well as medicinally by the Assyrians as early as 9th century B.C.[347] Additionally, aside from its therapeutic applications, the ancient Greek and Roman cultures valued the plant for its ropelike qualities.[346] Introduction of cannabis to the Western civilizations however, didn't occur until 1830s when Irish physician W. B. O'Shaughnessy

presented the traditional Eastern medicine in his paper about the "Indian hemp", where he recommended cannabis for various conditions including spasticity, pain, vomiting, and convulsions.[346, 348] Cannabis is found in several species and among the most relevant are *Cannabis sativa*, *Cannabis indica*, and *Cannabis ruderalis*. Of the three, *Cannabis sativa* is the most represented and is found in both tropical and temperate climates.[342] Aside from its uses as a medicinal agent and psychoactive component of spiritual practices and tradition, cannabis has been exploited as a recreational drug worldwide.[347]

With the beginning of the 20th century, use of cannabis as a medicinal agent significantly decreased even though reports from the late 19th century supported its medicinal values.[343] In the Unites States in particular, the passing of the Harrison Act of 1914, which grouped cannabis with other illicit drugs and the earlier introduction of the Pure Food and Drug Act of 1906, which advocated for improved safety of food and medicine, initiated the significant decrease in the use and marketing of cannabis derived products.[343, 349] Increase in the recreational use of cannabis was observed as a result of the decrease in marketing and production of cannabis derived products.[343] The introduction of the Marijuana Tax Act of 1937 was implemented with the intent to reduce the increased recreational use of cannabis.[349] However, although illegal the use of cannabis has been steadily increasing and today it has been estimated that approximately 50% of the population in the United States reported to have tried cannabis at least once in their life.[350]

Despite its immense popularity worldwide, it was not until 1964 when Gaoni and Mechoulan elucidated the structure of the principal psychoactive compound in *Cannabis sativa*, Δ^9-tetrahydrocannabinol (Δ^9-THC) (**Figure 35**). Sixty different cannabinoids have been isolated

from *Cannabis* and selected examples are Δ^8-tetrahydrocannabinol (Δ^8-THC), cannabinol (CBN), cannabidiol (CBD), and cannabichromene (CBC).[153, 342]

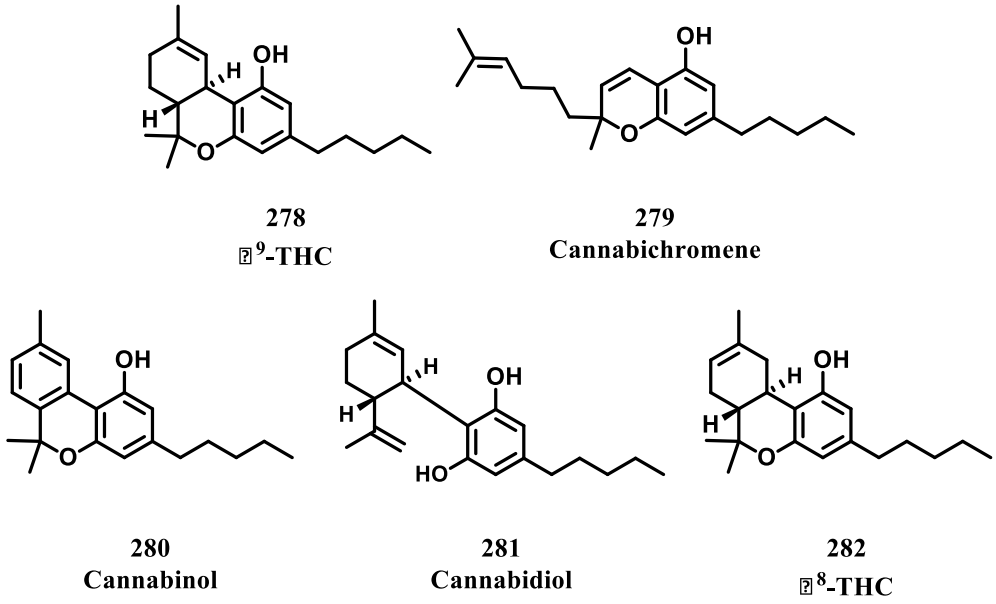

Figure 35. Structures of representative cannabinoids from *Cannabis sativa*

The Endocannabinoid System

Δ^9-THC and related cannabinoids exert their effects on cannabinoid receptors. There are two main types of cannabinoid receptors: CB1Rs and CB2Rs.[343] The principal demonstration of the presence of a cannabinoid binding site in the rat brain was demonstrated by Devane and coworkers in early 1988.[351] However, conclusive evidence of the existence of a cannabinoid receptor was provided in 1990 by Matsuda and coworkers when they reported the isolation of a cDNA of a cannabinoid receptor from a rat cerebral cortex, which was named CB1 receptor (CB1R).[352] A few years after the isolation and characterization of the CB1R, Munro and colleagues reported the cloning of a second cannabinoid receptor, found in the periphery and

termed CB2R.[353] Both of the cannabinoid receptors are members of the G-protein coupled receptor superfamily (GPCRs) and share 44% sequence identity.[354] A greater sequence similarity is seen between the clones of human, rat and mice CB1Rs, whereas the CB2Rs are much more divergent among the three species.[355] Activation of both receptors leads to the inhibition of adenylate cyclase leading to reduction of cAMP levels, as well as activation of the mitogen-activated protein kinase (MAPK), events accomplished with the coupling to the α-subunit of the $G_{i/o}$ protein family.[354, 356] Particularly for the CB1Rs, lowering the level of cAMP causes an enhancement of voltage-sensitive outwardly rectifying K^+ channels, which is caused as a result from the decreased phosphorylation of the K^+ channel protein by A-kinase.[357] Moreover, CB1Rs have been shown to interact and couple to G_o.[356] CB1Rs but not CB2Rs have been shown to also couple to G_s proteins under certain conditions.[358] Several other systems that act as intracellular mediators and are also utilized by CB1Rs and occur from activation of $G_{i/o}$: inhibition of N-type Ca^{2+} channels and expression of immediate early genes such as *Krox*-24.[357] Together, both CB1Rs and CB2Rs recruit the signaling mechanism of activation of MAPK and expression of *Knox*-24 presumably through the activation of the G-protein βγ subunit.[354] Activation of CB1Rs has also been shown to modulate the production of nitric oxide, inhibit 5-HT_3 ion channels, activate the Na^+/H^+ transporter and alter the conductance of the sodium channel.[354] Besides the two main cannabinoid receptors CB1R and CB2R, there is evidence that points to the presence of additional cannabinoid receptors. In 2007, Ryberg and coworkers identified that an orphan receptor GRP55 expressed in the CNS and various peripheral tissues binds a range of endogenous, plant-derived, and synthetic cannabinoids and it was shown to activate the G_{13} proteins.[359] Furthermore, Brown reported GRP119 as an additional cannabinoid receptor that is expressed predominately in the pancreas and gastrointestinal tract and activates

the G_s proteins.[360] However, additional evidence is necessary to determine the connection of these novel receptor subtypes to the endocannabinoid system.[354]

CB1 Receptors

CB1Rs are located mainly in the CNS in both neural and non-neural tissues and to a lesser extent are expressed in peripheral tissues. The CB1Rs are the most abundant receptors in the brain with high density seen in the basal ganglia, substantia nigra pars reticulate, cerebellum, and the external segment of the globus palladis, hippocampus, and putamen.[354, 357] In the periphery, the CB1Rs are localized in the adrenal gland, adipose tissue, heart, liver, lung, prostate, ovary, testes, bone marrow, thymus, tonsils, and presynaptic nerve terminals.[354] The activation of the CB1Rs present in presynaptic nerve termini leads to the inhibition of neurotransmitter release, which is a result of the decreasing calcium conductance and by the increase in the potassium conductance.[354, 361]

CB2 Receptors

CB2Rs on the other hand are mainly localized in tissues of the immune system, such as the spleen, tonsils, and thymus. B cells, T4 and T8 cells, mast cell, macrophages, natural killer cells, and microglial cells are the types of immune cells where localization of CB2Rs is high and out of those natural killer cells have the highest expression levels of CB2Rs. Recently, studies disputed previous reports of CB2Rs absence in the CNS and it has now been demonstrated that CB2Rs are also present in the CNS and are found on the dorsal root ganglia, the lumbar spinal cord, and sensory neurons.[362, 363] When CB2Rs expressed immune cells are activated they can modulate the migration of immune cells and cytokine release both outside and within the brain.[356]

Cannabinoid Ligands

The term cannabinoid was originally coined for any compound isolated from *Cannabis*.[364] However, today it refers to any compound that demonstrates similar pharmacology to that of Δ^9-THC.[343] There have been several classes of ligands found to have affinity at the CBRs. These include the endocannabinoid ligands, classical, non-classical cannabinoids, and synthetic cannabinoids.

Endocannabinoid Ligands

The discovery of the cannabinoid receptors prompted the notion which suggested that there are endogenous ligands that exert their physiological activity upon binding to these receptors.[357] One of the first endocannabinoids isolated form porcine brain extracts was anandamide (*N*-arachidonoylethanolamine, AEA, **283**, **Figure 36**), whose discovery was based on the hypothesis that the endogenous ligands of the cannabinoid receptors should be lipophilic like the classical exogenous cannabinoids.[365] It was determined (using transfected *h*CB1R and *h*CB2R CHO cells) that anandamide has affinity for both CB1R and CB2R with K_i values of 89 nM and 371 nM, respectively.[366] In 1995, shortly after the isolation of anandamide, Mechoulam and coworkers reported the canine gut isolation of 2-arachidonoylglycerol (2-AG, **284**), a non-amidic derivative of arachidonic acid.[367] Similarly to AEA, 2-AG also interacts with both cannabinoid receptors and has a binding affinity of 58 nM for CB1R and 145 nM for CB2R.[366] This endocannabinoid was also found to be present in the spleen and brain.[368, 369] Interestingly, 2-AG release was demonstrated to be Ca^{2+} dependent and its concentration can reach up to 170-fold higher than that of anandamide in the brain.[357, 368] Several other endocannabinoids have been isolated since the original discovery of AEA and 2-AG and they include: noladin ester,

vriodhamine (**285**), *N*-arachidonoyldopamine (NADA, **286**), oleamide, *N*-oleoyl dopamine, *N*-dihomo-γ-linolenoylethanolamine, and *N*-docosatetraenoylethanolamine (**287**); however not much is known about the endocannabinoid-like properties of these ligands (**Figure 36**).[354, 370]

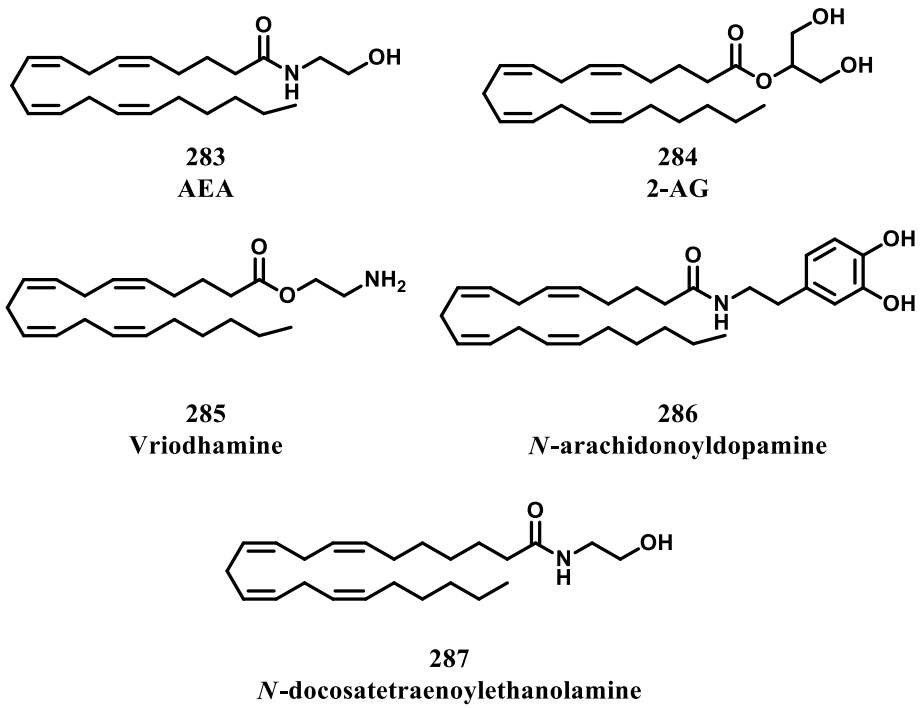

Figure 36. Structures of representative endocannabinoids

Activity-dependent or receptor-stimulated cleavage of membrane phospholipid precursors are the most common mechanisms by which the endocannabinoids are normally produced, generally on demand.[354] Because of their high lipophilic character, endocannabinoids are released immediately after their biosynthesis and endocannabonoid signaling is regulated by their synthesis, release, uptake and degradation.[354] Activation of the enzymatic processes that lead to the cleavage of membrane phospholipid precursors and consequent biosynthesis of endocannabinoids can be initiated through several processes, namely membrane depolarization, increase in the intracellular calcium levels or receptor stimulation.[354] Several different enzymes

are involved in the biosynthesis of AEA and 2-AG, specifically calcium-independent *N*-acyl-transferase, phospholipase C, and diacylglycerol lipase.[354, 371] Upon biosynthesis, endocannabinoid signaling is limited by degradation of the endocannabinoids. Enzymes involved in the efficient degradation of the endocannabinods have been well characterized and include fatty-acid amide hydrolase (FAAH) and monoacylglycerol lipase (MGL).[372] FAAH a membrane bound enzyme is involved in the hydrolysis of AEA whereas MGL, a serine hydrolase, is involved in the hydrolysis of 2-AG.[373-375]

Classical Cannabinoids

Compounds resembling the structure of Δ^9-THC that contain a tricyclic terpenoid scaffold bearing a benzopypan moiety are considered classical cannabinoids (**Figure 37**).[357] Numerous compounds isolated from *Cannabis* are members of this class of cannabinoids. Many SAR studies were undertaken on this class of cannabinoids at both CB1R and CB2Rs, however to much greater extent at the CB1Rs. The SAR developed for classical cannabinoids at CB1Rs goes as follows: (**a**) the absolute stereochemistry present in Δ^9-THC is necessary for activity at CB1Rs; (**b**) the alkyl side chain appended at the C-3 carbon is necessary for activity, the optimal length being between five to eight carbon atoms; (**c**) presence of a dimethylheptyl side chain maximizes CB1R activity and the presence of a *gem*dimethyl group either at the C-1' carbon or C-1', C-2'-dimethyl substituent enhances CB1R affinity; (**d**) a hydroxyl group at the C-1 carbon is necessary for binding at CB1Rs but a hydroxyl substituent ate the C-11 position can also be a replacement for hydrogen bonding interaction with the receptor; (**e**) phenolic group at the C-1 carbon can also be substituted with an amine group but not a thiol moiety in order to attain CB1R affinity; (**f**) the pyran oxygen atom can be substituted for a nitrogen atom leading to preserved

CB1R affinity; and (**g**) substituents other than methyl at the C-9 position are generally accepted and a hydroxyl group at either the C-11 or the C-9 improves CB1R affinity.[357, 376]

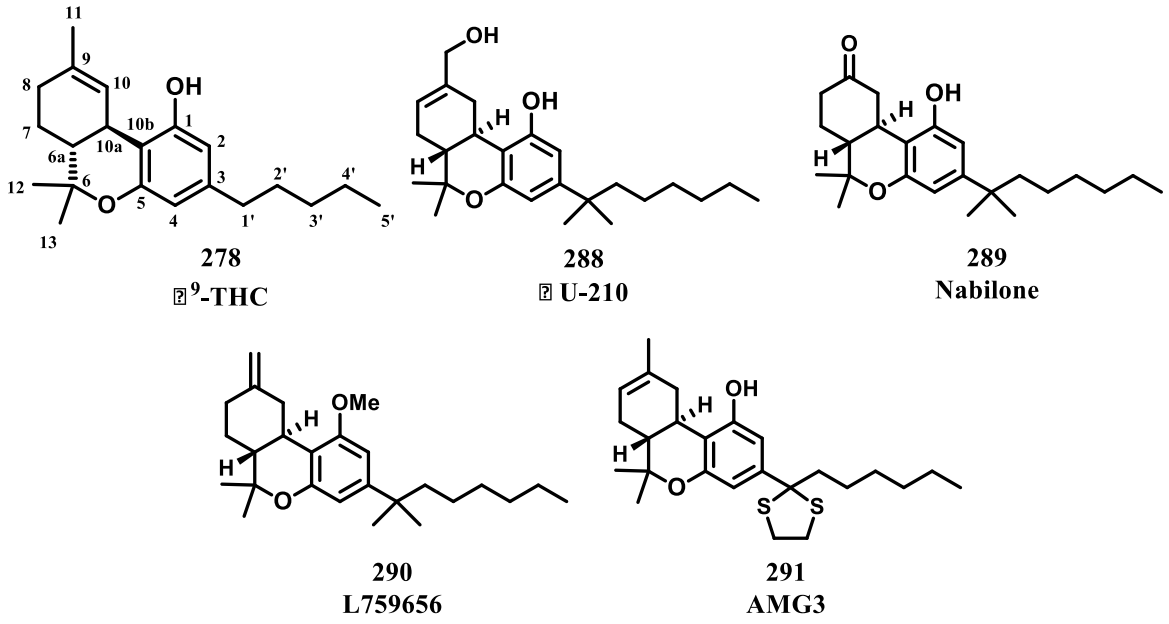

Figure 37. Structures of representative classical cannabinoids

The SAR of the classical cannabinoids at the CB2R is less developed but it encompasses the following: (**a**) for optimal activity and selectivity at the CB2Rs, the phenolic group at the C-1 carbon must be replaced with a hydrogen atom; (**b**) additionally, a methoxy group at C-1 alters affinity at CB2Rs; (**c**) as mentioned C-11 and C-9 hydroxyl groups enhance CB1R and CB2R affinity; and (**d**) with no hydroxyl on the C-1 carbon, the length of the C-3 carbon alkyl substituent does not affect CB2R affinity.[376] Thus far, not much has been revealed regarding the SAR and the effects of different substituents at the C-1 and C-9 carbons and the alkyl side chain in the scaffold.[376]

Non-Classical Cannabinoids

A molecular dissection approach was undertaken by Pfizer researchers in order to gain a better understanding of the pharmacophore of Δ^9-THC for binding at the cannabinoid receptors and discovered that a compound (CP-55,940) lacking the pyran ring retained activity at the cannabinoid receptors (**Figure 38**).[357, 377] This class of compounds includes various bicyclic as well as tricyclic analogues. Both the classical and non-classical cannabinoid have very similar SAR in that the aliphatic chain off of the C-3 carbon is necessary for activity.[377] Furthermore, similar to the SAR of classical cannabinoids, the phenolic hydroxyl moiety on C-1 carbon is necessary for activity of non-classical cannabinoids.[377] Elimination of the C-9 hydroxyl moiety resulted in decreased affinity, whereas complete removal of the cyclohexyl ring leads to complete loss of activity at the cannabinoid receptors.[377] Decreasing the size of the cyclohexyl group to a five membered ring resulted in a decrease in affinity, whereas increasing the size of this substituent to a cyclohephtyl, or adamantyl ring causes a slight increase in affinity.[377] Heteroatom substitution of the cycloalkyl group results in significantly diminished activity at both cannabinoid receptors.[377] Addition of different alkyl substituents off of the cyclohexyl ring in the molecule generally lead to a small to moderate decrease of affinity.[377] Substitution of the C-1 hydroxyl moiety with a ketone moiety resulted in a switch of activity from CB1Rs to CB2Rs.[378] It has been also demonstrated that unsaturation in the scaffold leads to a decrease in affinity.[377] Selective CB2R activity for the non-classical cannabinoids was attained with a methoxy substitution at the C-1 carbon, as well as the addition of a tertiary alcohol moiety at the C-10a carbon.[377]

In addition to the classical and non-classical cannabinoids, researchers have attempted to synthesize compounds that represent a hybrid of both scaffolds. Several groups succeeded in the development of such analogues (**296**, **Figure 38**) and established valuable SAR. Thakur and

colleagues synthesized a hybrid cannabinoid that possesses an alkyl hydroxyl group at the C-6a, seen in CP-55,940, which is conformationally constrained with a pyran ring and a double bond.[379] It was determined that both isomers are potent cannabinoid receptor ligands, exhibiting subnanomolar affinity for both recepotrs.[379] Additionally, the optimal length for the hydroxyalkyl moiety at the C-6 position was determined to be between 1 and 3 carbon atoms.[380] Iodoalkyl or alkyl chain appended at the C-6 position are both well tolerated and exhibit similar cannabinoid receptor affinity to that of the original classical and non-classical cannabinoids.[381] A C-11 or a C-9 hydroxyl groups are both well tolerated and do not cause any significant change in the affinity at the cannabinoid receptors.[380] Bourne and coworkers synthesized several Δ^9-THC/anandamide hybrid cannabinoids, which demonstrated equal or higher affinity at both cannabinoids receptors to that of the parent compounds.[382]

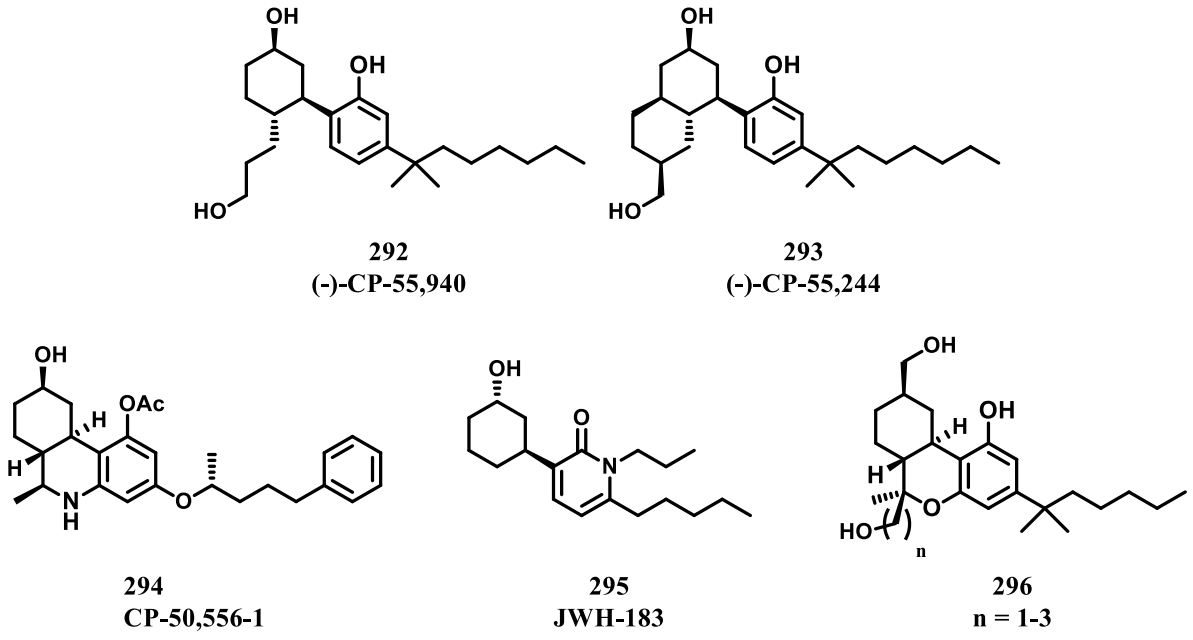

Figure 38. Structures of representative non-classical and hybrid cannabinoids

Synthetic Cannabinoids - Aminoalkylidoles

In 1992, during a developmental study for a non-steroidal anti-inflammatory drug (NSAID), a group of scientists at Sterling-Winthrop synthesized pravadoline (**297**, **Figure 39**), an aminoalkylindole (AAI).[383] In addition to exhibiting prostaglandin inhibition, it was also shown to inhibit contractions of the electrically stimulated mouse vas deferens.[384, 385] During their investigation and pharmacological testing, it was observed that pravadoline was shown to interact with cannabinoid CB1Rs and exhibit classical cannabinoid pharmacology *in vivo*.[383, 386] Its interesting pharmacology prompted many researchers into the development of preliminary SAR for the interaction of pravadoline derivatives with the cannabinoid receptors. From this primary search, D'Ambra and coworkers developed and synthesized a novel aminoalkylindole derivative, WIN-55,212-2 (**298**), a ligand with high potency for both cannabinoid receptors, whose tritiated form has extensively been used in many pharmacological investigations of this group of cannabinoid ligands since its discovery.[383]

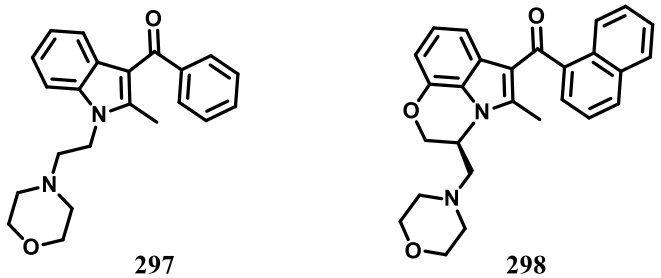

Figure 39. Structures of two original aminoalkylindole cannabinoids

Investigations into the SAR of the aminolakylindoles continued and in 1994, Huffman and Dai reported the synthesis and pharmacological testing of several acyl indoles derived from the WIN-55,212-2 structures (**Figure 40**).[387] It was determined that a naphthalene ring or a

bulkier substituent at this position may be necessary for affinity at the cannabinoid receptors. Additionally, analogues containing an alkyl chain consisting of 4-6 carbon atoms appended from the *N*-atom of the indole ring exhibited similar *in vitro* and *in vivo* pharmacology to that of Δ^9-THC and WIN-55,212-2, a finding similar to that observed for the classical cannabinoid Δ^9-THC.

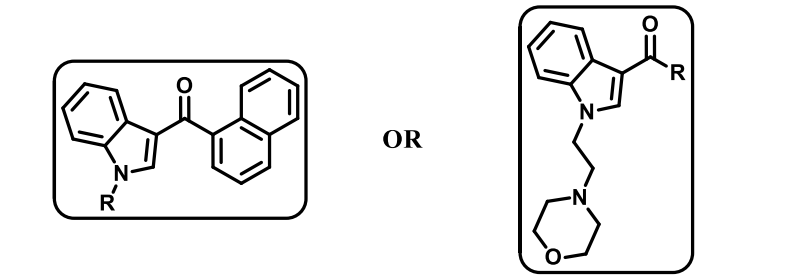

R =	R =
299: 2-phenylethyl	**306:** CH_3
300: 2-cyclohexylethyl	
301: *n*-propyl	
302: *n*-butyl	
303: *n*-pentyl	
304: *n*-hexyl	**307:** 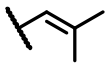
305: *n*-heptyl	

Figure 40. Representative modifications of the aminoalkylindole scaffold reported by Huffman and Dai

An extension to the Huffman study, Eissenstat and coworkers, researchers from the Sterling Winthrop laboratory, reported additional analogues of the novel aminoalkylindole class of cannabinoid ligands that were products of several modeling studies (**Figure 41**).[388] They determined that a bulky substituent is needed at the C-3 position of the indole core confirming previous studies of Huffman and Dai. Furthermore, they determined that for activity at the

cannabinoid receptors, a small substituent of preferably a hydrogen atom at the C-2 position of the indole core is necessary. Additionally, an ethylmorpholine or other aminoethyl substituents at the *N*-1 position of the indole yielded compounds with high activity at the cannabinoid receptors.

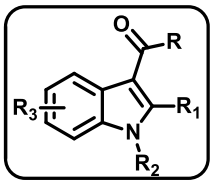

	R =	R_1 =	R_2 =	R_3 =
308:	***o*-OCH_3Ph**	**CH_3**	**$(CH_2)_2$morpholinyl**	**H**
309:	***p*-OCH_3Ph**	**CH_3**	**CH_2COOH**	**H**
310:	***p*-OCH_3Ph**	**CH_3**	**$(CH_2)_2NMe_2$**	**H**
311:	***p*-OCH_3Ph**	**CH_3**	**$(CH_2)_2$piperidinyl**	**H**
312:	***p*-OCH_3Ph**	**CH_3**	**$(CH_2)_2$morpholinyl**	**5-CH_3**
313:	***p*-OCH_3Ph**	**CH_3**	**$(CH_2)_2$pyrrolidinyl**	**H**
314:	***p*-OCH_3Ph**	**CH_3**	**$(CH_2)_2$piperazinyl**	**H**
315:	***p*-OCH_3Ph**	**CH_3**	**$(CH_2)_2$thiomorpholinyl**	**H**
316:	***p*-OCH_3Ph**	**H**	**$(CH_2)_2$morpholinyl**	**6-Br**
317:	***p*-OCH_3Ph**	**CN**	**$(CH_2)_2$morpholinyl**	**H**
318:	**1-naphthyl**	**CH_3**	**$(CH_2)_2$morpholinyl**	**H**
319:	***m*-ClPh**	**CH_3**	**$(CH_2)_2$morpholinyl**	**H**
320:	**4-CH_3-1-naphthyl**	**H**	**$(CH_2)_2$morpholinyl**	**H**
321:	**1-naphthyl**	**H**	**$CH(CH_3)CH_2$morpholinyl**	**H**
322:	**2-quinolinyl**	**CH_3**	**$(CH_2)_2$morpholinyl**	**H**
323:	**1-naphthyl**	**CH_3**	**$(CH_2)_2$morpholinyl**	**7-OCH_3**
324:	**6-quinolinyl**	**CH_3**	**$(CH_2)_2$morpholinyl**	**H**
325:	**8-quinolinyl**	**CH_3**	**$(CH_2)_2$morpholinyl**	**H**
326:	**4-benzofuryl**	**H**	**$(CH_2)_2$morpholinyl**	**H**
327:	**7-benzofuryl**	**CH_3**	**$(CH_2)_2$morpholinyl**	**H**
328:	**1-anthracenyl**	**CH_3**	**$(CH_2)_2$morpholinyl**	**H**
329:	**1-naphthyl**	**CH_3**	**$(CH_2)_2$2-Me-morpholinyl**	**H**
330:	**9-phenanthrenyl**	**CH_3**	**$(CH_2)_2$morpholinyl**	**H**

Figure 41. Representative modifications WIN-derived aminoalkylindoles reported by Eissenstat and coworkers

The above report described AAI analogues in which the heterocyclic amine nitrogen atom is attached to the indole ring nitrogen via a carbon chain. As an extension to that work the authors also synthesized AAI analogues, however with a different connectivity from the one described above.[389] In particular, this series of AAI analogues contained a series of compounds where the heterocyclic amine is attached to the indole ring via a carbon atom of the heterocycle rather than the nitrogen atom of the heterocycle (**Figure 42**).[389]

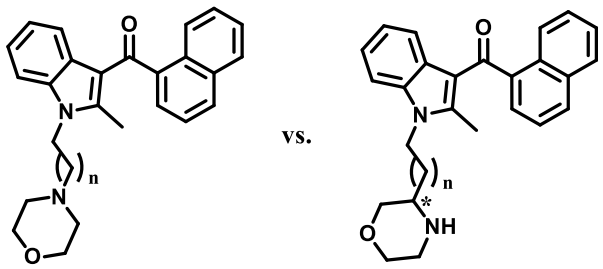

Figure 42. *N*-attached vs. C-attached aminoalkylindole derivatives

From this study it was determined that ideal carbon linker between the indole *N*-atom and the heterocyclic *N*-atom is two carbons (**Figure 43**).[389] On the other hand, attachment of the heterocycle directly to the indole moiety was not favorable, despite the two carbon distance between the heterocycle *N*-atom and the indole *N*-atom. Various heterocycles are well tolerated as substituents, which was not the case of the *N*-attached analogues synthesized previously, where only morpholine and thiomorpholine heterocycles proved active at the cannabinoid receptors. Similarly to results seen with the *N*-attached analogues, it was observed that a small substituent preferably a hydrogen atom at the C-2 position of the indole ring was also necessary for activity in the C-attached analogue series. *N*-alkyl substituents of the heterocycle side chain resulted in a significant decrease in activity.

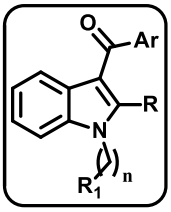

	Ar =	R =	R_1=	n =
331:	***p*-OCH_3Ph**	**CH_3**	**2-(1-methyl-piperidinyl)**	**1**
332:	***p*-OCH_3Ph**	**CH_3**	**3-(1-methyl-piperidinyl)**	**0**
333:	***p*-OCH_3Ph**	**CH_3**	**2-(1-methyl-pyrrolidinyl)**	**1**
334:	***p*-OCH_3Ph**	**CH_3**	**3-(4-methyl-morpholinyl)**	**1**
335:	***p*-OCH_3Ph**	**CH_3**	**3-(4-methyl-thiomorpholinyl)**	**1**
336:	**1-naphthyl**	**H**	**4-morpholinyl**	**2**
337:	**1-naphthyl**	**CH_3**	**2-(1-methyl-pyrrolidinyl)**	**1**
338:	**1-naphthyl**	**H**	**2-(1-methyl-piperidinyl)**	**1**
339:	**1-naphthyl**	**H**	**3-(4-methyl-morpholinyl)**	**1**
340:	**1-naphthyl**	**H**	**2-(1,4-dimethyl-piperazinyl**	**1**

Figure 43. Representative modifications of C-attached aminoalkylinodoles

In 1998, Wiley and coworkers reported further SAR of the aminoalkylindoles with a study done on indole- and pyrrole-derived compounds (**Figure 44**).[390] In the course of their study, in the three series that were synthesized, it was determined that a methyl group off of the indole ring substituted for the original ethylmorpholine group led to complete inactivity at the CB1Rs. However, affinity was regained with the extension of carbon atoms with the ultimate alkyl substituent being a *N*-pentyl group in the C-2 carbon substituted derivatives and in the C-2 non-substituted analogues the ultimate length was between four and six carbon atoms. On the other hand, in the C-2 substituted pyrrole analogues, *N*-pentyl was also the optimal chain length however not as active as the the indole series. In general, pyrrole-derived analogues exhibited lower activity at the CB1Rs then their indole-derived counterparts. Substitution of the alkyl chain with double bond barring substituents yielded compounds slightly less active at the CB1Rs, which was also the case with cycloalkyl *N*-side chains off of the indole core.

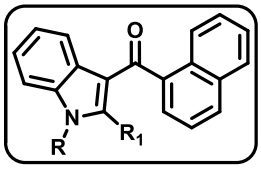

OR

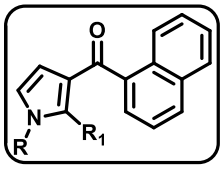

OR

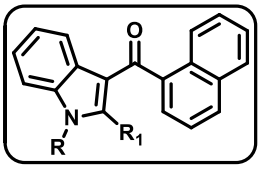

	R =	R_1 =
341:	*n*-methyl	CH_3
342:	*n*-butyl	CH_3
343:	*n*-heptyl	CH_3
344:	*n*-ethyl	H
345:	*n*-pentyl	H
346:	*n*-hexyl	H

	R =	R_1 =
347:	*n*-methyl	H
348:	*n*-ethyl	H
349:	*n*-pentyl	H
350:	*n*-hexyl	H
351:	*n*-heptyl	H

	R =	R_1 =
352:	(*E*)-2-pentenyl	CH_3
353:	allyl	CH_3
354:	4-pentenyl	H
355:	2-phenylethyl	CH_3
356:	cyclohexylethyl	CH_3
357:	(*E*)-2-pentenyl	H

Figure 44. Representative modifications of indole- and pyrrole-derived aminoalkylindoles

In order to test the possibility that the activity of the aminoalkylindole derived cannabinoids and classical cannabinoids for the cannabinoid receptors could come from one pharmacophore, Huffman and coworkers designed a hybrid molecule to test this hypothesis.[391] This hybrid cannabinoid (**358**) combined the hydroxybenzopyran ring system of the classical cannabinoid Δ^9-THC with the 1-pentylindole moiety present in most potent aminoalkylindole derivatives lacking an aminoalkyl group (**Figure 45**). It was determined that this hybrid cannabinoid exhibits similar affinity for the CB1R to that of Δ^9-THC, Δ^8-THC, WIN-55,212-2, and JWH-007. It whoever is slightly less potent *in vivo* than WIN-55,212-2 and JWH-007, but it does represent a unique probe for further investigations of cannabinoid ligands at the CB1Rs.

With the intention of developing aminoalkylindoles that are potent analogues at the CB1R and are also easily iodine radioisotope labeled, Deng and coworkers designed and synthesized a group of compounds that could be suitable for biochemical and imaging studies (**Figure 45**).[392] From their analysis of the compounds synthesized, it was determined that a potent non-selective iodinated aminoalkylindole ligand (**359**) was synthesized with high affinity

for both cannabinoid receptors with K_i values of 1.80 nM and 2.2 nM, respectively. Despite the lack of selectivity, this class of ligand will provide excellent probes for further radiolabeled imaging investigations.

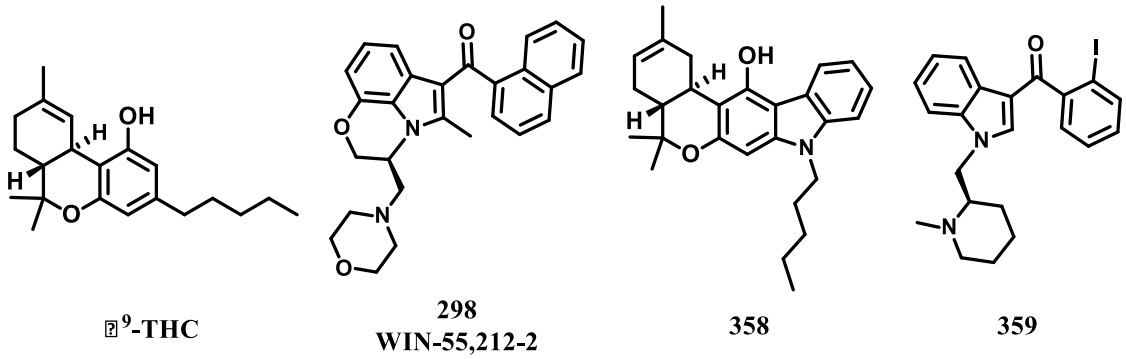

Δ⁹-THC **298 WIN-55,212-2** **358** **359**

Figure 45. Structures of Δ⁹-THC, WIN-55,212-2, the hybrid cannabinoid **358**, and the radioiodonated ligand **359**

Utility of positron emission tomography (PET) in the design and pharmacological testing of potential cannabinoid ligands and their interactions with the cannabinoid receptors is on the rise, and a suitable PET ligand is necessary.[393] In order for a ligand to be suitable for PET and single photon emission computed tomography (SPECT) imaging one has to have lower lipophilicity than the original aminoalkyindoles and relatively high binding affinity for its target.[393] With these criteria in mind, Willis and colleagues synthesized a group of aminolakylindole derivatives with lower lipophilicity (logD in the range of 2.7-4.5) and increased affinity (**Figure 46**).[393] Most of the analogues exhibited high affinity in the low nanomolar range for the CB1Rs. Out of the analogues synthesized, one compound exhibiting a K_i of 0.7 nM was chosen to be labeled with positron emitting isotope and subjected to *in vivo* mice model studies, where it was determined that this analogue specifically labels CB1Rs in the mouse brain and could be a useful tool further PET radioligand studies.

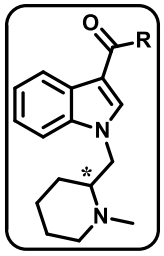

	R =	$cLogD_{7.4}$
360:	**4-Me-1-naphthoyl**	**4.0**
361:	**4-Br-1-naphthoyl**	**4.5**
362:	**4-OH-1-naphthoyl**	**3.3**
363:	**4-CN-1-naphthoyl**	**3.3**
364:	**4-(2-hydroxyethyl)-1-naphthoyl**	**2.7**
365:	**6-OH-1-naphthoyl**	**2.8**
366:	***N*-decahydroquinoline**	**2.1**
367:	***N*-naphthylamine**	**3.0**
368:	**4-NO_2-1-naphthoyl**	**3.5**
369:	**2-iodophenyl**	**3.0**
370:	**4-OMe-1-naphthoyl**	**3.6**

Figure 46. Representative analogues with potential PET capabilities

The SAR for the aminoalkylindoles continued and in 2010, the Russo group reported several new indole-based analogues (**Figure 47**).[394] They performed molecular modeling and dynamic studies on the compounds synthesized and they also subjected the synthesized analogues for antinociceptive assays in mouse models. Most of the analogues showed to have affinity for the CB1Rs, however only one analogue exhibited similar affinity for CB1Rs as WIN-55,212-2. In the antinociceptive assay, the formalin test, several of the compounds exhibited moderate antinociceptive activity. These indole 2,3-dione derivatives of the aminoalkylindole class of cannabinoids could be used as the starting point for further analogue design.

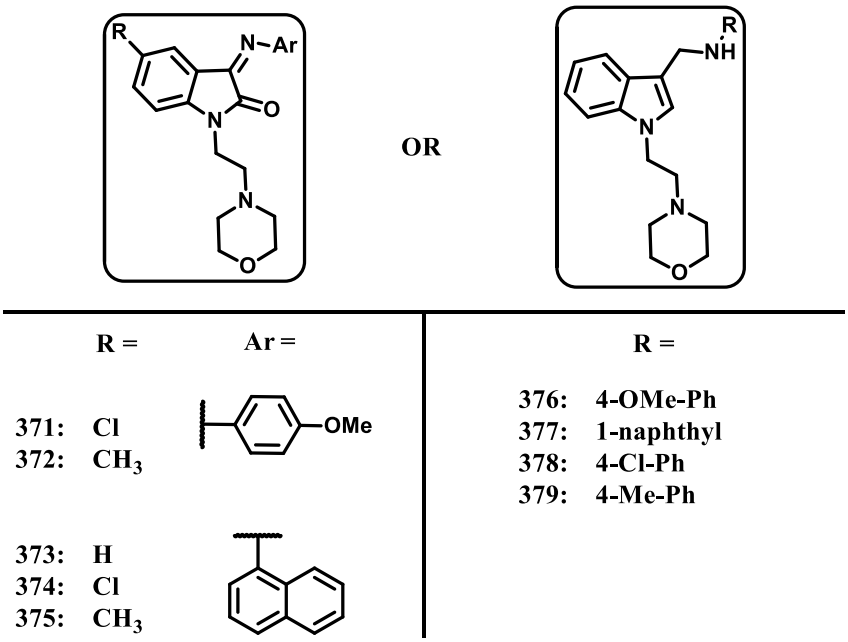

Figure 47. Representative modifications of indole-based cannabinoids

A further extension of the SAR studies of aminolakylindole cannabinoid was reported by Frost and coworkers in 2010, where they synthesized several series of analogues focusing of various indole *N*-atom substitutions and C-3 carbon ketone derivatives (**Figure 48**).[395] From their study they established that several CB2R selective compounds were synthesized with high affinity for the CB2R.[395] From their SAR they determined that an amino cycloalkyl group is not well tolerated as an indole *N*-atom substituent.[395] Additionally, aromatic side chain at the *N*-1 position are well tolerated as well as non-amine alkyl and cycloalkyl substituents.[395] In agreement with previously reported data, they also found that aminoethyl side chain at the *N*-1 position was optimal for activity.[395] They also observed a stereochemical effect where one isomer produced higher selectivity for the CB2R than the other.[395] Furthermore, changes in polarity of the *N*-1 side chain were tolerated, however carboxylic acid side chain proved to be inactive at both cannabinoid receptors.[395] The preliminary results of the *in vitro* affinity of the synthesized analogues were further confirmed in a functional calcium mobilization assay

(FLIPR).[395] The prepared compounds allow for better understating of the SAR of the aminoalkyindole class for the cannabinoid receptors.

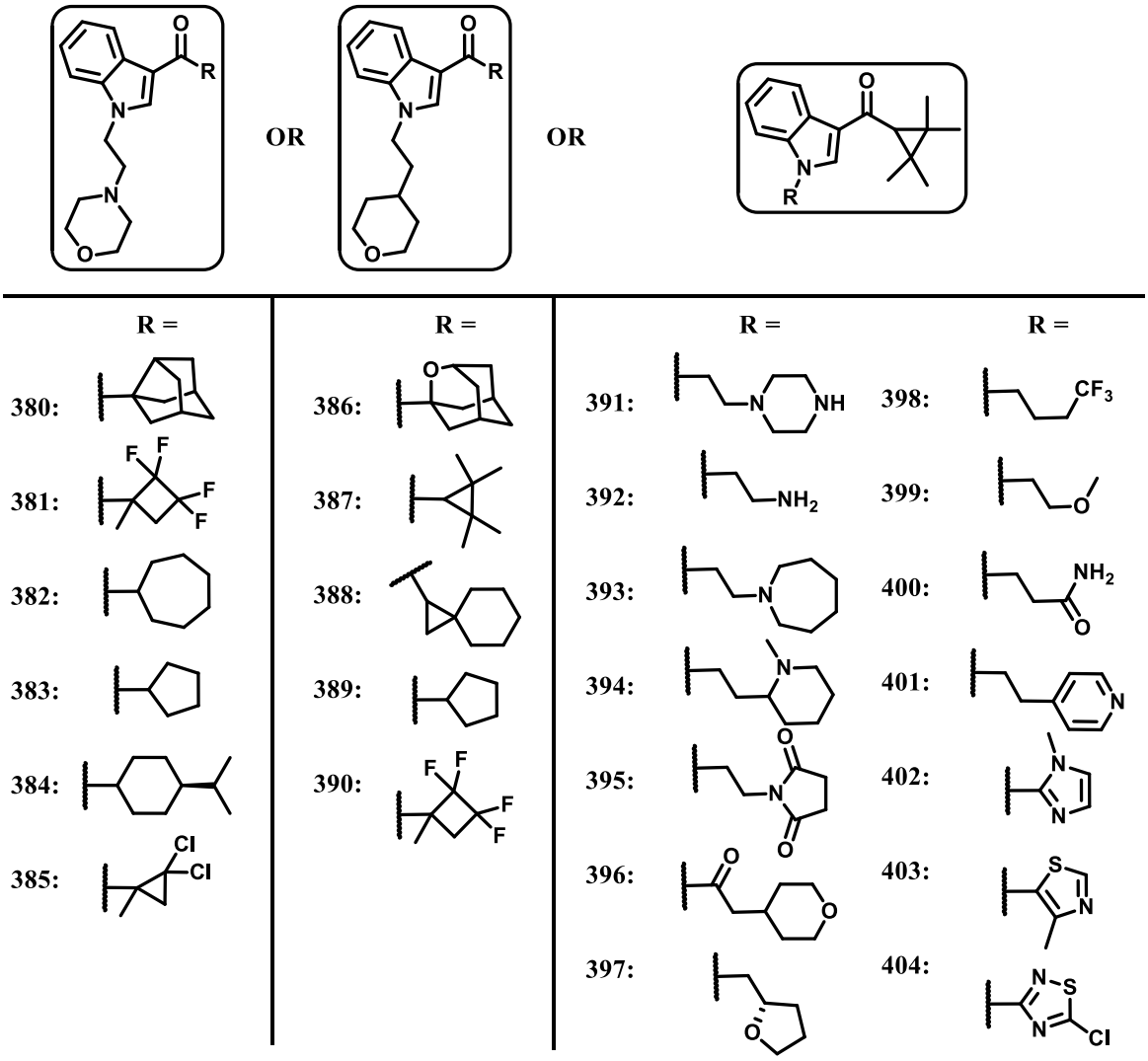

Figure 48. Representative analogues with potential CB2R selectivity - I

In addition to the CB2R selective analogues designed and synthesized in this series, Makriyannis and coworkers reported an aminoalkylindole (AM1241, **405**) that is highly selective for the CB2Rs with potential for modulation of neuropathic pain (**Figure 49**).[396] To accompany this report, Hynes and coworkers from Bristol-Myers Squibb laboratories, designed and

synthesized several additional CB2R selective analogues (**Figure 49**) with C-3 amido-indole structural characteristics.[397] From this study they established that there is only limited substitution tolerability at the C-3 position of the indole core apart from ester substituents. A C-3 amido indole analogue with acceptable K_i value for the CB2R was selected for further SAR development that yielded several analogues with anti-inflammatory characteristics in a murine model of acute inflammation. Together these studies demonstrate that the aminoalkylindole scaffold can be modulated to produce receptor selective ligands.

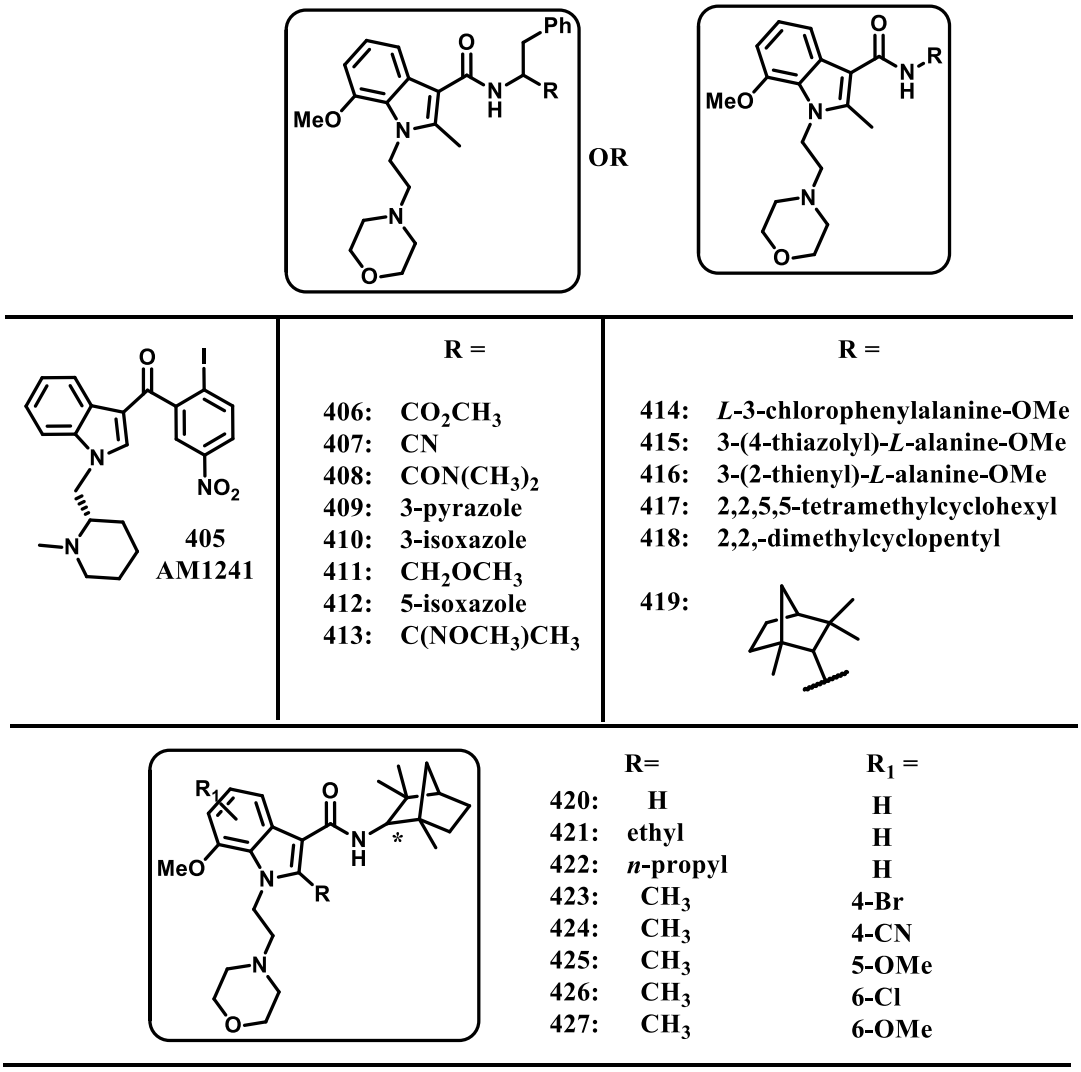

Figure 49. Representative analogues with potential CB2R selectivity - II

Therapeutic Potential of Cannabinoids

The therapeutic potential of *Cannabis* has been known and well utilized throughout many centuries. With the widespread distribution of the cannabinoid receptors within the CNS as well as in the periphery, one can envision that the endocannabinoid receptor system may be involved in various physiological processes.[398] The SAR of all the classes of cannabinoid ligands has generated compounds with very interesting pharmacological profiles that highlight the potential of the cannabinoids in a wide variety of clinical disorders.[399] These include multiple sclerosis, pain, drug abuse, obesity, and alcohol abuse.

Cannabinoids and Multiple Sclerosis

In 1868, Charcot described what is today known as multiple sclerosis (MS), the most common demyelinating disease worldwide.[400] The hallmark of this CNS disease is the formation of sclerotic plaques in the white matter of the spinal cord, as well as in other CNS structures.[401] The formation of plaques may be caused by several mechanisms such as inflammation, edema, demyelination and remyeination, oligodendrocyte depletion, astroliosis, and neuronal death.[400] The disease is characterized by muscle rigidity (spasticity), painful muscle cramps, chronic pain, tingling and prickling of the fingers, and blindness.[342] The Multiple Sclerosis Society estimates that approximately 2.1 million people worldwide are affected with MS.[402] MS affects more females than males and in an age range of 20 to 50 years.[402] There is no cure for MS, however there are several effective disease-modifying agents currently used as MS treatments.[403]

It has been demonstrated that endocannabinoids are elevated in tissues that are undergoing inflammation, suggesting that such endocannabinoid accumulation represents an adaptive attempt of the body to alleviate inflammation.[404] Furthermore, the difference in the concentration of anandamide from a post mortem healthy brain and a brain affected with MS has been reported to be 3.7 fold higher in the MS affected brain.[405] Originally, it was believed that only the CB2Rs were responsible for modulation of immune function, however it has been validated that the CB1Rs can also modify inflammation and therefore play an important role in modulating neuroinflammation.[406]

Initial evidence of the involvement of the cannabinoid system in MS has come from several experiments with animal models of this disease, including experimental autoimmune encephalomyelitis (EAE), Theiler's murine encephalomyelitis virus (TMEV), and chronic relapsing experimental allergic encephalomyelitis (CREAE). These models arise from the induction of MS-like demyelination produced by injection with Theiler's murine encephalomyelitis virus or inoculation with mixtures containing material such as CNS tissue or myelin basic protein.[407] Non-selective, as well as selective cannabinoid receptor agonists have been shown to ameliorate the signs of motor dysfunction exhibited by EAE, TMEC, and CREAE animals.[407] These results were observed with single or repeated administration of the said agonists in pre or post infected animals.[407] Accompanying evidence reported by Maresz and coworkers and Xu and coworkers supports the hypothesis that activation of CB1Rs on centrally located neurons will ameliorate signs of spasticity associated with MS, and that CB2Rs expressed on T-cell within the CNS will decrease inflammation associated with MS and possibly slow the progression of the disease.[407, 408]

Given the preclinical data, several clinical trials have been undertaken to evaluate the effects of cannabinoid in MS. The clinical trials have focused on several aspects of the disease, mainly alleviation of symptoms, such as pain, incontinence, motor control, and spasticity.[398] Despite several reports of positive findings, general results are of mixed nature; nevertheless they are promising for future research of the role of the endocannabinoid system in MS.[398, 403]

Cannabinoids and Neuroprotection

One of the most serious public health problems in the United States is traumatic brain injury (TBI), a condition that accounts for an estimated 2 million cases per year.[409] TBI represents one of the leading causes of mortality and disability in young individuals throughout the world and currently no treatments are available.[409, 410] It is characterized by numerous neurological and cognitive changes and by the release of various chemical mediators, whose release can reveal weakening of brain ionic homeostasis and release of immense glutamate concentrations from presynaptic terminals.[409] Additionally, release of reactive oxygen species has also been reported together with the release of endothelium-derived active mediators whose release can lead to ischemia and late hyperemia.[411, 412] It has been demonstrated that activation of presynaptic CB1Rs by 2-AG may modify neurotransmission and inhibit glutamate release, which would in turn limit its excitotoxicity.[409]

Utilizing animal models of brain injury, Muthian and coworkers determined that anandamide concentration is increased during transient, focal cerebral ischemia.[413] Additionally, utilizing similar animal models of brain trauma, Panikashvili and colleagues determined that in mice after a closed head injury (CHI), the concentration of 2-AG was found to be 10-fold higher

in the injured hemisphere and persisting for 24 hours.[414] Furthermore, treatment of mice with exogenous 2-AG given 1 hour after CHI was proven to be very effective as seen by the reduction in edema formation, decrease in clinical recovery, and decline of infarct volume.[414] Differences in species were noted with the report by Hansen and colleagues that in young rats, anandamide and not 2-AG concentrations were increased as a response to brain injury.[415] In support of previously published results, van der Stelt and coworkers reported that the volume of formed edema in neonatal rats using the ouabain-induced excitotoxicity model was significantly lowered than that of untreated rats.[416] Marsicano and coworkers focused their research efforts on the hypothesis that one of the important roles of the endocannabinoid system is to protect against neuronal excitotoxicity.[417] In order to test this hypothesis they used two mouse models: CB1R (-/-) deficient animals and animals lacking CB1Rs in the principal glutamatergic (excitatory) neurons of the forebrain. During the study it was observed that both types of animals exhibited more severe seizures after kainic acid treatment than control animals. This effect was blocked by the CB1R antagonist rimonabant, which was not successful however in decreasing seizures in mice lacking CB1RS in principal neurons. Reports of CB1R antagonists as neuroprotective agents were also reported by Hansen and coworkers, Amantea and colleagues and Muthian and coworkers.[413, 418, 419]

These contradictory reports may be better understood when one considers that endocannabinoids can act as anticonvulsants and proconvulsants in different situations.[420] This comes from the notion that endocannabinoids may be inhibitory by blocking glutamate release or excitatory by blocking GABA release in different neuronal circuits.[421] Despite the conflicting results, there is no doubt that the endocannabinoid receptor system plays a role as a defense

system against excitotoxic damage in the brain; however further research is needed to identify the exact mechanism of this action.[420]

Cannabinoids and Pain

The use of cannabinoids as treatments for pain is known for many centuries. Specifically, in ancient China *Cannabis* and cannabinoids were used as surgical anesthesia; in ancient Israel they were used to decrease the pain during childbirth; throughout the middle ages in Asia they were used as valuable analgesics and the many Western civilizations used cannabis as treatment for many painful ailments during the 1800s.[422]

One of the earliest reported animal studies in which it was demonstrated that cannabinoids block pain response was done by Walter Dixon in 1899 in which he demonstrated that either inhaled cannabis or subcutaneously injected cannabis were able to suppress canine reactions to pin pricks.[422] Since then various other animal models for both acute and chronic pain have been used to demonstrate the effectiveness of cannabinoids in the production of antinociception. Several models of acute pain or postoperative pain are utilized in the analysis of cannabinoid modulation of acute pain such as mechanical stimuli or incision to the hindpaw of rats.[423] Δ^9-THC, WIN-55,212-2, CP-55,940 as well as anandamide have been shown to have antinociceptive effects in various animal models.[423] The actions of these ligands was blocked by the pretreatment with CB1R antagonists rimonabant and AM251 and no antinociceptive effects were observed in CB1R knockout mice, indicative of a CB1R mechanism.[423] There are also examples of CB2R agonists exciting antinociceptive effects such as AM1241, HU308, JWH-133,

and GW405833, however these results are less consistent when compared to CB1R mediated antinociceptive effects.

In addition to the antinociceptive effects of cannabinoids in animal models of acute pain, the effects of cannabinoids in animal models of chronic pain have also been well studied. Utilizing the carrageenan-induced inflammatory animal model it was determined that WIN-55,212-2 reduced and mechanical hyperalgesia, actions blocked by both the CB1R antagonist rimonabant and the CB2R antagonist SR144528.[423] Additionally, cannabidiol was shown to exhibit time- and dose-dependent antinociceptive effects in inflammation induced by intraplantar injection of carrageenan in rats.[424] The synthetic cannabinoid nabilone exhibited similar results as those observed with cannabidiol.[425] The ability of CB2R antagonists AM630 and SR144528 to block the effects of the agonist AM1241, which caused reduction in mechanical and thermal hypersensitivity produced by a carrageenan intraplantar injection, indicating a CB2R related mechanism of antinocicpetion.[423] Peripheral administration of anandamide reduced hyperalgesia and it also inhibited the formation of oedema in the capsaicin-induced inflammatory model, an effect blocked by the CB1R antagonist rimonabant.[423] Similar results were seen with AM1241, however mediated via CB2Rs.[423] In the complete Freund's adjuvant (CFA) rat animal model of inflammation, an intrathecal administration of HU-210 caused a reduction of mechanical allodynia and thermal hyperalgesia, effects blocked by the CB1R antagonist AM251.[426] Similar results in the CFA rodent model were observed with the CB2R agonist GW405833.[427] Along with chronic pain models, Δ^9-THC and WIN-55,212-2 have been screened in various neuropathic pain models, the most common of which include chronic constriction injury, partial sciatic nerve ligation and the spinal nerve ligation, where they were shown to be very effective.[423]

With the numerous positive preclinical results for the effects of cannabinoids on pain modulation, several human clinical trials were undertaken to determine their efficacy in human volunteers.[428, 429] Briefly, in healthy volunteers low doses of smoked Δ^9-THC were seen to reduce the pain induced by intradermal capsaicin.[430] Additionally, inhaled Δ^9-THC was shown to effectively relieve chronic neuropathic pain from HIV-induced sensory neuropathy.[431] In patients suffering from advanced cancer, Δ^9-THC and cannabindiol significantly reduced pain.[432] Many other clinical trials with Δ^9-THC and related cannabinoids regarding various forms of pain have been carried out, indicating the great potential of cannabinoids in the treatment of pain.

Cannabinoids and Drug Abuse – Psychostimulants

The ventral tegmental area (VTA), the medial forebrain bundle (MFB), nucleus accumbens (NAc), ventral pallidum (VP) and the prefrontal cortex (PFC) are brain neuron strictures that encompass the brain reward system, which controls and regulates behaviors by inducing pleasurable effects.[433] These structures are part of the mesolimbic pathway, the major rewarding pathway, whose primary neurotransmitter is dopamine.[433] Because of the involvement with formation of reward-associated memories and the location of the perikarya of the mesolimbic neurons, the NAc and the VTA, respectively, play a critical role in addiction.[433]

As mentioned previously, drug addiction represents a complex and chronic brain disorder, which is characterized by multifaceted processes that lead to drug seeking and loss of control over drug consumption.[434] Activation of the cannabinoid receptors with cannabinoids leads to the production of several physiological effects, mainly through the CB1Rs, that activate the same mesolimbic reward pathway as drugs of abuse.[433] These effects can be blocked with

CB1R antagonist and with the use of CB1R knock out animals further confirming the involvement of the endocannabinoid system in the reward pathway.[433]

Utilizing the self-administration model one can assess the rewarding actions of drugs of abuse, mainly cocaine.[435] Pre-treatment with rimonabant failed to modulate cocaine self-administration in rats and squirrel monkeys.[435] Additionally, CB1R knockout mice can be trained to self-administer cocaine, indicating that the endocannabinoid system does not mediate cocaine reward.[436] Conversely, treatment with exogenous cannabinoids was shown to modulate cocaine self-administration.[435] Pre-treatment with WIN-55,212-2 was demonstrated to decrease intravenous cocaine self-administration in rats, an event mediated by CB1Rs, and blocked by rimonabant.[437] However, rimonabant was unable to affect the behavior maintained by cocaine when administered alone, indicating that endocannabinoid system modulation of cocaine self-administration may be indirect.[437, 438]

Reinstatement of self-administration is a known model of drug relapse that can be correlated to individuals that are cocaine dependent.[435] De Vries and coworkers demonstrated that pre-treatment with rimonabant was able to reduce reinstatement of cocaine seeking promoted by cocaine-associated clues or injections, but was unable to however reverse stress-induced reinstatement.[439] Additionally, rimonabant was also able to block the reinstatement of methamphetamine-seeking behavior in rats.[440] The authors also demonstrated that HU-210, a potent cannabinoid, dose-dependently promoted the reinstatement of cocaine-seeking behavior.[439] Moreover, the systematic administration of the CB1R antagonist AM251 was shown to selectively inhibit cocaine-induced reinstatement of reward-seeking behavior, by a glutamate-defendant mechanism.[441] Conditioned place preference (CPP) is an animal model that

is utilized to evaluate the perception of the rewarding value of the reinforcer.[442] It was demonstrated that co-administration of rimonabant with cocaine during the conditioning phase eliminated the CPP of cocaine in rats.

The recent reports indicating the presence of CB2Rs in certain parts of the brain such as the cerebral cortex, the cerebellum, the hippocampus, the striatum, the brainstem and the anterior olfactory nucleus have prompted researchers to re-examine the role of CB2Rs in drug reward and drug addiction.[443] Recently, Xi and colleagues determined that systematic administration of the CB2R selective agonist JWH-133 dose-dependently inhibited intravenous cocaine self-administration and it also inhibited cocaine-induced locomotion.[443] These effects were further mimicked by another selective ligand, GW405833 and blocked by AM630, a selective CB2R antagonist, an effect not exhibited with the selective CB1R antagonist AM251, all of which is suggestive of a CB2R mechanism.[443] Conformation of brain acting CB2Rs came from an experiment where they showed that an intranasal microinjection of JWH-133 once again dose-dependently inhibited intravenous cocaine self-administration, which was not seen with an intravenous microinjection of the agonist. Furthermore, Aracil-Fernandez and colleagues recently reported the adaptive effects of cocaine of mice overexpressing CB2Rs.[444] They established that CB2R overexpressing mice showed reduced motor response to acute cocaine compared to WT mice; displayed reduced motor sensitization induced by chronic cocaine administration; and exhibited cocaine-induced conditioning place aversion; exhibited reduced cocaine self-administration, a few of the results seen in CB2R overexpressing mice.[444] Collectively, these findings indicate that inhibition of CB1Rs and/or activation of CB2Rs can affect psychostimulant-induced behaviors, thus establishing the cannabinoid receptor system as target for ligands with possible use as treatments for drug abuse.

Cannabinoids and Obesity

Obesity represents a global epidemic that significantly threatens the health of those affected.[445] In 2008, according to the World Health Organization (WHO), nearly 1.5 billion adults, 20 years or older were overweight.[446] Furthermore, more than 40 million children under the age of 5 were overweight in 2011.[446] In the United States alone approximately 65% of adults are overweight, 30% of those are obese and 5 % are morbidly obese.[446] Overall, these facts suggest that obesity is a multifactorial disease with increasing occurrence worldwide.[447]

The hypothalamus is one of the areas involved in the regulation of energy balance, in which the endocannabinoids and the CB1R are produced and expressed.[448] Despite the low CB1R expression in the hypothalamus, activation of these receptors leads to profound effects.[448] One of the first reports that suggested a role between the endocannabinoid system in the hypothalamus and its role in control and food intake came from Trojniar and Wise in 1991, where they demonstrated that the systematic administration of Δ^9-THC facilitated eating which was elicited by electrical stimulation of the lateral hypothalamus.[449] Moreover, it was demonstrated that fasting raises the endocannabinoid levels in the limbic forebrain structures, including the NAc, a structure of the reward system, which is also linked to the 'liking' and 'wanting' behaviors associated with availability and variety of food.[450] Additionally, increase in food intake through a CB1R dependent manner was observed after a direct administration of 2-AG into the NAc shell, an area directly linked to eating motivation.[450] Aside from centrally regulating food intake, the endocannabinoid system was shown to also peripherally regulate food intake, by the activation of peripheral sensory terminals in the gastrointestinal tract.[451] Despite being exposed to a similar caloric intake as WT mice, CB1R knockout mice were demonstrated

to be resistant to high fat diet-induced obesity.[452] Additionally, CB1R knockout mice were shown to be leaner than their WT littermates and blockage of the CB1Rs was shown to also reduced food intake in mice.[452, 453] Consequently, the endocannabinoid system plays a significant role in food intake, energy balance and metabolism through both the central and peripheral nervous systems.[451]

With the seen actions of endocannabinoid system and cannabinoid agonists on food intake and energy balance, several human clinical trials have been conducted on CB1R antagonists to determine their therapeutic potential in obesity. After successful animal model studies, the putative CB1R antagonist/inverse agonist, rimonabant was advanced to human clinical trial where treatment with rimonabant for 7 days and later 16 weeks led to significant reduction of food and calorie intake and weight.[454] Despite the great success of rimonabant and its analogue taranabant in successfully reducing weight gain and diminishing related metabolic processes, peripheral and CNS-related side effects related to their inverse agonist activity led to their withdrawal from clinical applications and the market.[455] Research efforts are being made in the design and synthesis of true neutral antagonists or peripherally constrained CB1R antagonists, which will limit the seen side effect profile and preserve the antiobesity effects.[456]

Cannabinoids and Alcohol Abuse

One of the oldest substances abused by man is alcohol.[457] Alcohol dependence is a costly and socially devastating disorder and problems related to alcohol dependence cost the United States economy alone up to $185 billion per year.[458] Alcohol consumption causes multidimensional and complex effects on the health of those affected and the effects seen on the

mortality, morbidity and disability are overwhelming.[459] According to the WHO, approximately 2.5 million people die of alcohol abuse each year among which 320,000 young adults between the ages of 15 and 29 die from alcohol-related causes.[460]

The original link between the neurophysiological effects of cannabinoids and alcohol was demonstrated in the early 1970s, when evidence of cross-tolerance to ethanol amongst cannabis users was reported.[458] In 1994, Hungund and coworkers were the first to report that demonstrated the modulating effects of alcohol on the biosynthesis of endocannabinoids when it was revealed that chronic exposure of ethanol in mice up-regulated the activity of phospholipase A_2 (PLA_2), one of the enzymes in the biosynthetic pathway of AEA.[461] Shortly thereafter, reports followed of the decreased expression and function of CB1Rs in mice chronically exposed to ethanol vapor and the increase in the levels of AEA and 2-AG in cultured cells chronically exposed to ethanol.[462, 463] In 2003, Wang and coworkers eloquently demonstrated that the high preference for ethanol of C57BL/6J mice was completely reversed by rimonabant.[464] Additionally, in agreement with previous findings, rimonabant was also able to reduce ethanol drinking in WT mice but not in CB1R knockout, indicative of CB1R involvement.[464] As an extension to this study, Hungund and colleagues reported that mice lacking the CB1R consumed considerably less ethanol than their wild type littermates.[465]

The role of cannabinoid CB1R system in animal models of alcoholism is further evident by the effective reduction of alcohol drinking in rats with a history of ethanol dependence as well as alcohol-preferring Marchigian Sardinian (msP) rats by rimonabant.[466, 467] CB1R antagonism of rimonabant and surinabant was also related to the decrease in alcohol deprivation effect and cue-induced reinstatement on alcohol preferring msP rats.[467, 468] Acute administration of the

CB1R agonist CP-55,940 or WIN-55-212,2 on the other hand, significantly increased the motivation to consume alcohol of Wistar rats or alcohol-preferring msP rats, an effect reversed with the pretreatment of rimonabant.[469, 470] Additional behavioral effects were seen with WIN-55,212-2 administration, where it was shown to have an increase in alcohol relapse during a period of alcohol deprivation in rats.[471] Recent reports have indicated the role of the CB2R in alcohol-related behaviors. In 2007, Ishiguro and coworkers reported that downregulation of *Cb2* gene expression in the midbrain was related to ethanol reinforcement in that mice experiencing higher ethanol preference exhibited reduced *Cb2* gene expression.[457] Collectively, these studies suggest that targeting the central cannabinoid signaling system has potential in treating alcohol dependence.

Rationale and Specific Aims

The great interest in the SAR of the synthetic cannabinoids, in particular the aminoalkylindoles, and their activity at the cannabinoid receptors has yielded various analogues with very interesting pharmacological activity. Specifically, the work of Huffman and colleagues from 1998, describes a series of aminolalkylindole analogues with very potent activity at the cannabinoid receptors, with potencies greater than that of the classical cannabinoid Δ^9-THC while exhibiting psychotropic effects similar to those seen with Δ^9-THC.[390] Their non-regulated nature and pronounced pharmacological similarity to Δ^9-THC made several of these analogues popular as ingredients to the widely abused incense blends known as Spice/K2.[343] Among the most common components of K2/Spice are JWH-018, JWH-073, JWH-200, and CP-47,497 (**Figure 50**).[472]

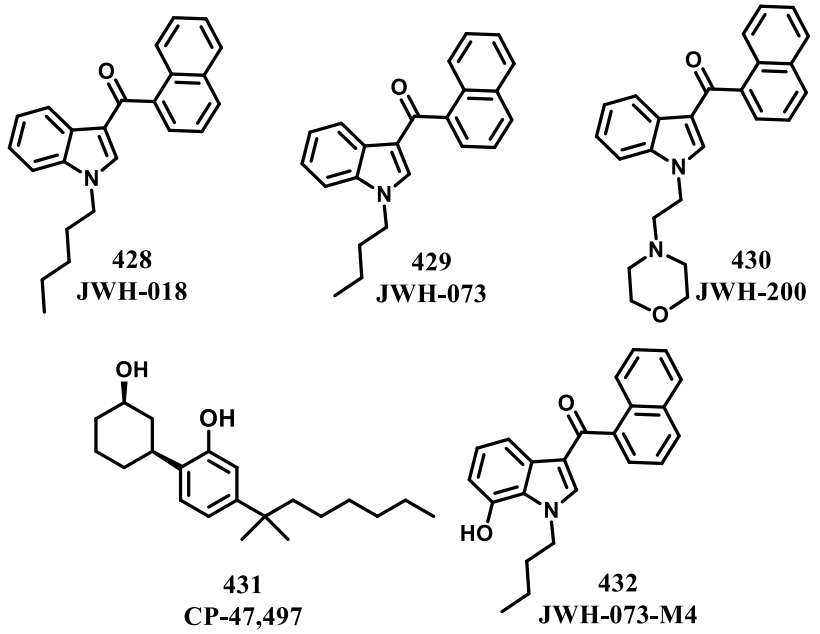

Figure 50. Structures of the most common aminoalkylindoles found in Spice/K2 and the active metabolite of JWH-073-M4

Despite the recreational popularity of these commercial preparations, very little is known regarding K2/Spice metabolism, pharmacology, and toxicity. It was recently reported that a mono-hydroxylated metabolite of aminoalkylidole JWH-073, compound JWH-073-M4 (**432**, **Figure 50**), retains relatively high affinity for CB1Rs, but lacks intrinsic activity when examined in the [^{35}S]GTP-γ-S functional assay.[473] Additionally, it was determined that JWH-073-M4 antagonizes JWH-018-induced hypothermia *in vivo*, indicative of antagonistic mechanism of activity for this metabolite.[473]

With the new found neutral antagonistic activity seen with the metabolite of JWH-073 and the widely demonstrated therapeutic potential of CB1R antagonists, principally as prospective therapy for alcohol abuse, it was hypothesized that utilizing the JWH-073-M4 scaffold as the lead for further SAR modifications would identify novel indole-based analogues with improved pharmacological profiles.

Specific Aim 1: Prepare analogues based on the JWH-073-M4 scaffold with dual CB1R antagonist/CB2R agonist activity that have potential as alcohol abuse therapies.

Modifications of the JWH-073-M4 scaffold and further exploration into the SAR of this compound will allow us to gain a better understating for its interactions with the cannabinoid receptors and lead us to the structural elements responsible for its activity. A series of analogues will be synthesized that will explore different structural features of the JWH-073-M4 scaffold such as the introduction of rotational bond, exploration of electronic potential at various positions in the molecule, and assessment of the optimal distance between the indole core and the substituent. These represent a few of the modifications to the lead scaffold that will be undertaken in order for a greater understanding of the SAR of this scaffold for the cannabinoid receptors. These modifications are intended to show that alterations of this scaffold is well tolerated at the cannabinoid receptors and that such analogues will retain and improve upon the antagonistic activity of the lead molecule.

Specific Aim 2: Evaluate JWH-073-M4 analogues for their cannabinoid receptor affinity and efficacy.

Compounds generated from Specific Aim 1 will be evaluated for their pharmacological profile at the cannabinoid receptors *in vitro*. Initially, analogues will be subjected to a radioligand binding screen to determine their affinity at the CB1R and CB2Rs. Compounds were selected for further testing if a 1 μM concentration produced over 50% displacement of a 0.2 nM concentration of [^{3}H]CP-55,940, indicating a relatively high sub-micromolar affinity. Such compounds were then subjected to a functional screen for inhibition of adenylate cyclase (AC) activity utilizing a 10 μM concentration of each test compound and comparing it to the

inhibition of AC-activity seen with the non-selective CB1R/CB2R agonist CP-55,940. Analogues exhibiting weak partial agonist to antagonist activity would then be subjected to further examination and determination of their affinity for the cannabinoid receptors by determining their K_i values. The final assay in the pharmacological testing of analogues synthesized in Specific Aim 1 will be to determine their potency at the cannabinoid receptors by calculating their IC_{50} values using inhibition of AC-activity assay.

Specific Aim 3: Evaluate selected JWH-073-M4 analogues for their behavioral effects in vivo.

Selected analogues generated in Specific Aim 1 with promising *in vitro* activity generated in Specific Aim 2 will be subjected to *in vivo* pharmacological testing to determine their activity against alcohol abuse-related behaviors in mice. Compounds will be subjected to initial thermoregulation assay to determine their *in vivo* cannabinoid receptor activity. With the successful completion of the thermoregulation assay, analogues will be subjected to two animal models of alcohol-abuse; the ethanol self-administration assay (SA) and ethanol-conditioned place preference assay (CPP). The proposed studies will further characterize and evaluate the pharmacology of indole-based JWH-073-M4 derived analogues.

The purpose of the proposed studies in the presented specific aims is to provide a greater insight into the SAR of the JWH-073-M4 scaffold required for activity at the cannabinoid receptors. The ability to develop novel cannabinoid ligands based on the JWH-073-M4 structure suggests that the aminoalkyindole class of synthetic cannabinoids represent a useful scaffold for the construction of molecules with activity for the cannabinoid receptors. Completion of these

studies will also afford us with novel indole-derived analogues that could have the potential as alcohol abuse therapies. The results of these studies will be presented and discussed.

Results and Discussion

Introduction

In order to elucidate the structural requirements needed for activity at the cannabinoid receptors, a series of analogues based on the JWH-073-M4 scaffold were designed and synthesized. Compounds were intended to investigate the SAR of this scaffold at the cannabinoid receptors. In our quest for novel dual activity compounds with CB1R neutral antagonist/CB2R agonist properties, twenty-seven analogues were prepared using step-wise molecular investigation of the elements present in the scaffold. The analogues prepared were designed to investigate the SAR at several positions on the scaffold of interest. Firstly, we wanted to examine the necessity of the carbonyl moiety as well as the optimal length of the linker from the indole core to the naphthalene ring. We also sought out to explore the possibility for addition of rotational bonds at this position of the molecule. Secondly, we set to explore the requirement of the naphthalene ring through selective introduction of electron withdrawing and electron donating groups. Our initial design strategy was to limit the use of charged species and keep steric demands to a minimum. We also sought out to explore a different substitution at the *N*-atom of the indole core with a substituent with greater pharmacokinetic properties. Lastly, we wanted to investigate the positioning of the hydroxyl moiety around the indole core and its necessity for activity at CBRs (**Figure 51**). The analogues proposed were synthesized utilizing

N-alkylation, Friedel-Crafts like acylation, Suzuki coupling reaction, reduction, and *O*-demethylation conditions.

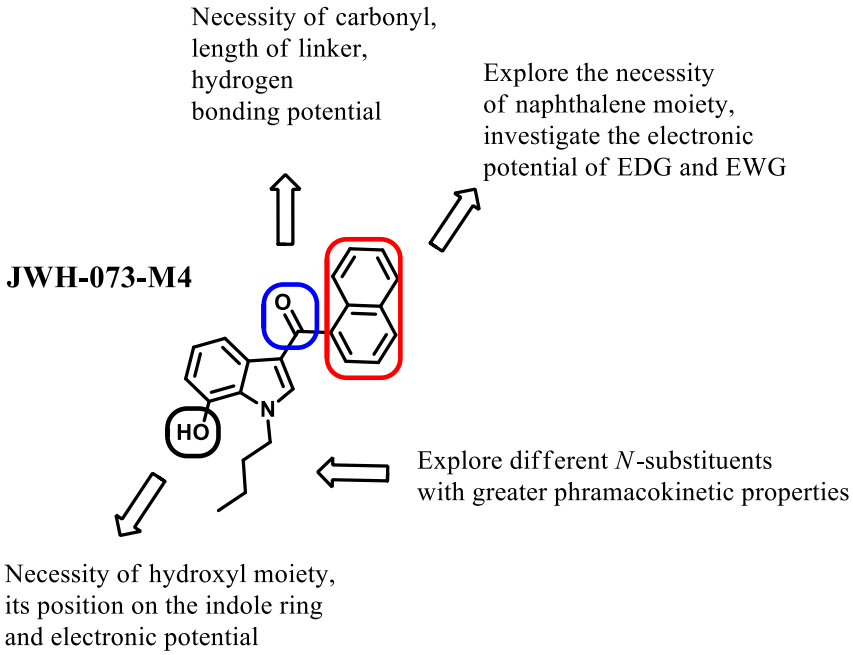

Figure 51. Rationale for the proposed SAR studies on the JWH-073-M4 scaffold

Synthesis

Synthesis of analogues based on the JWH-073-M4 scaffold began with the use of commercially available 7-methoxyindole **433**, which was subjected to mild alkylating conditions to afford compound **434**, an important intermediate in 74-93% yield for the different substituents, respectively (**Scheme 6**). In addition, commercially available 7-ethylindole was also subjected to the aforementioned conditions to yield compound **434** with an ethyl substitution at the 7-position of the indole ring in 93% yield. Intermediate **434** was then subjected to Friedel-Crafts like acylation conditions, using dimethyaluminum chloride and the appropriate acid chloride at 0°C to afford many of the analogues prepared, structurally represented as

intermediate **435**, in yields ranging from 9-68%. Compound **435** was shown to be a versatile intermediate that can undergo several reactions to yield various scaffolds. Specifically, it undergoes *O*-demethylation in the presence of BBr_3 to afford compound **436** in yields ranging from 38%-90% as well as LAH reduction conditions to afford compound **437** in 20% yield.

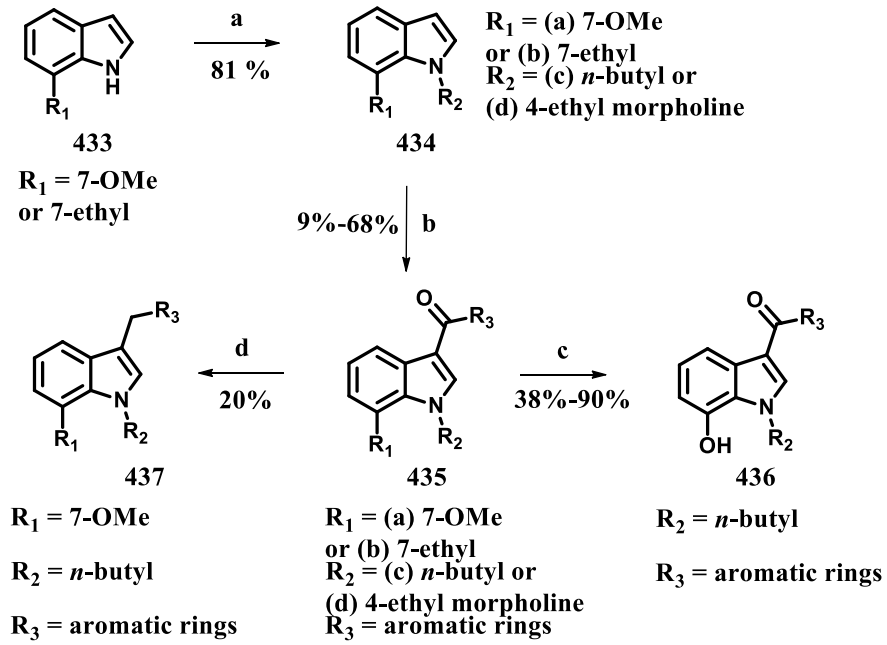

Scheme 6. Synthesis of JWH-073-M4 derived analogues - I. *Reagents and Conditions:* (a) 1-bromobutane or 4-(2-bromoethyl)morpholine, KOH, DMF, 50°C; (b) Me_2AlCl, RCOCl, DCM, 0°C; (c) BBr_3, DCM, -78°C; (d) $LiAlH_4$, $AlCl_3$, THF, 0°C

1-Butyl-5-methoxy-1*H*-indole, **439** synthesized from *N*-alkylation of commercially available 5-methoxyindole **438**, was subjected to Friedel-Crafts like acylation conditions to produce compound **440** in 58% yield, which was then *O*-demethylated using BBr_3 to afford compound **441** in 90% yield (**Scheme 7**). Compound **433** was additionally used in the synthesis of intermediate **442** utilizing a one-pot *N*-alkylation and 3-indole iodination in 69% yield. Intermediate **442** was then subjected to Suzuki coupling conditions utilizing different boronic acids to afford analogues **443** and **444** in 37% and 50% yield, respectively.

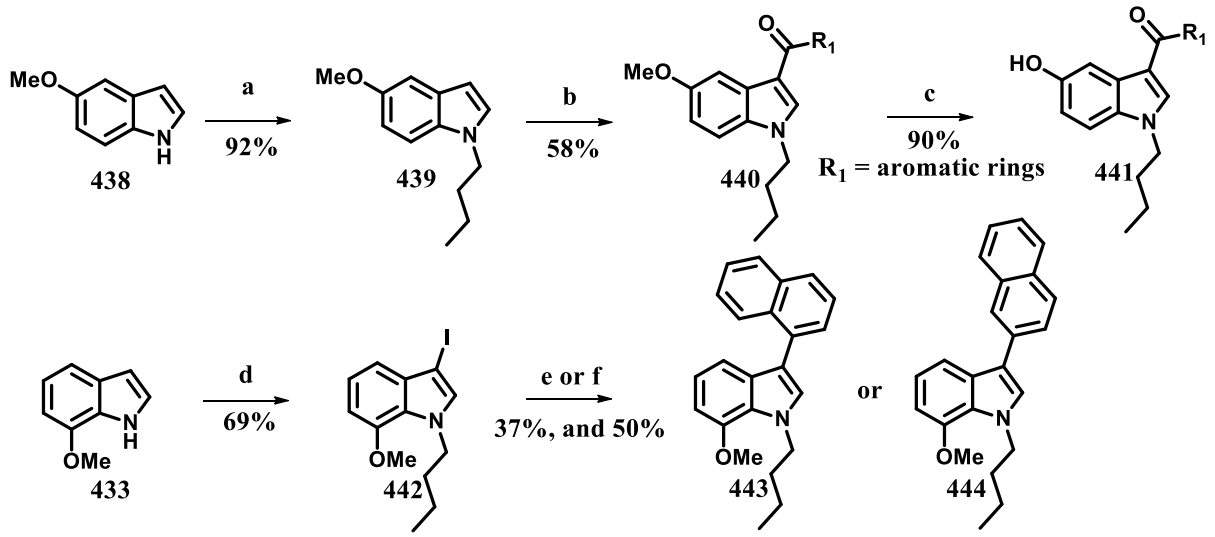

Scheme 7. Synthesis of JWH-073-M4 derived analogues - II. *Reagents and Conditions:* (a) 1-bromobutane, KOH, DMF, 50°C; (b) Me_2AlCl, RCOCl, DCM, 0°C; (c) BBr_3, DCM, -78°C; (d) 1-bromobutane, I_2, KOH, DMF, NaH, 50°C; (e) $Pd(PPh_3)_4$, 1-naphthaleneboronic acid, Na_2CO_3, DME, EtOH; (f) $Pd(OAc)_2$, SPhos, K_3PO_4, 2-naphthaleneboronic acid, toluene

In addition to the analogues synthesized by the methods reported above, analogue **450** was synthesized as represented in **Scheme 8**. Briefly, commercially available 1*H*-indole-7-carboxylic acid **445** was subjected to esterification conditions to yield intermediate **446** in 35% yield, which was then subjected to similar conditions as other *N*-alkylated analogues in this series to afford compound **447**, in 25% yield. Compound **447** has then subjected to Friedel-Crafts like conditions to afford aromatic ketone **448** in 71%. Subjection of intermediate **448** to *O*-ethylation with base afforded compound **449** in 77% yield, which was then exposed to amide bond formation with ammonia and peptide coupling reagents to afford analogue **450** in 53% yield.

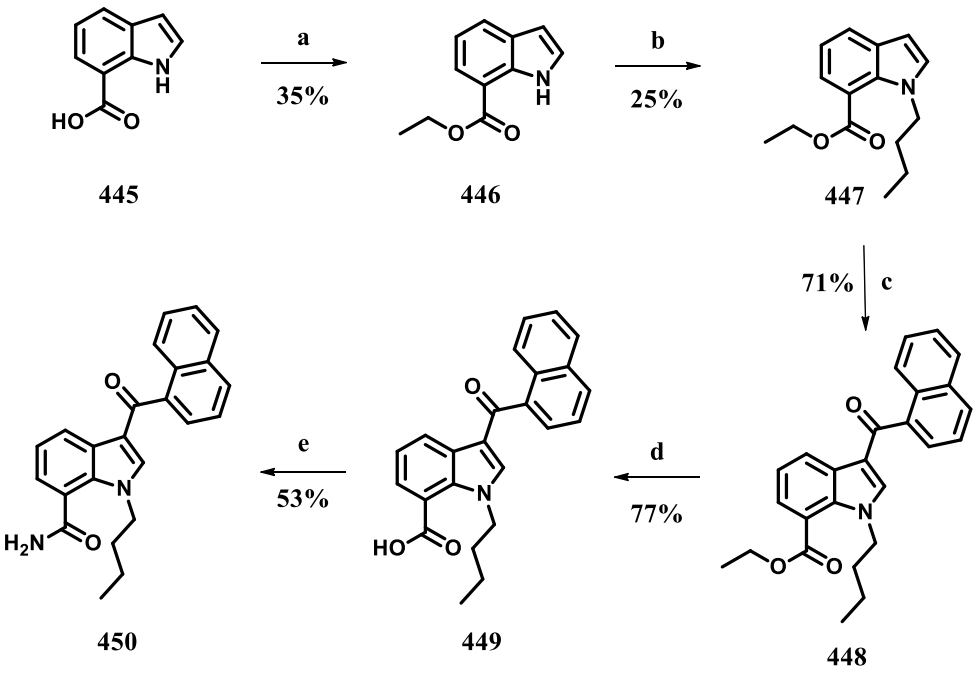

Scheme 8. Synthesis of JWH-073-M4 derived analogues - III. *Reagents and Conditions:* (a) EtOH, H_2SO_4; (b) 1-bromobutane, KOH, DMF, 50°C; (c) Me_2AlCl, RCOCl, DCM, 0°C; (d) 6M NaOH, MeOH, H_2O; (e) EDCI, HOBt, NH_3 (2M), DCM

The synthetic methods applied in the production of this series of JWH-073-M4 scaffold analogues afforded a group of 27 compounds, structurally represented in **Figure 52**.

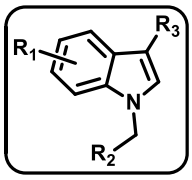

R_3 =

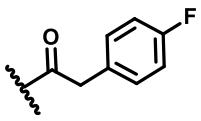

R_1 = 7-OMe
R_2 = *n*-butyl
451

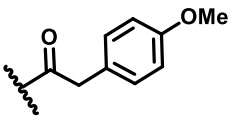

R_1 = 7-OMe
R_2 = *n*-butyl
452

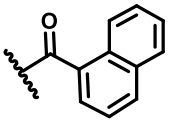

R_1 = 7-OMe
R_2 = *n*-butyl
453

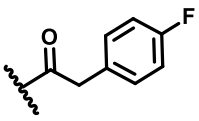

R_1 = 7-OH
R_2 = *n*-butyl
454

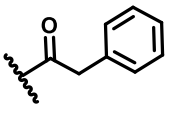

R_1 = 7-OMe
R_2 = *n*-butyl
455

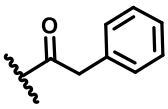

R_1 = 7-OH
R_2 = *n*-butyl
456

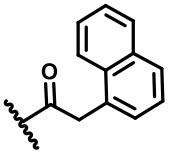

R_1 = 7-OMe
R_2 = *n*-butyl
457

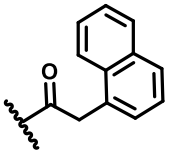

R_1 = 7-OH
R_2 = *n*-butyl
458

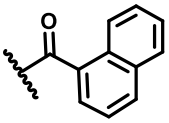

R_1 = 5-OMe
R_2 = *n*-butyl
459

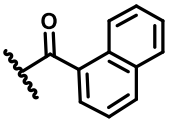

R_1 = 5-OH
R_2 = *n*-butyl
460

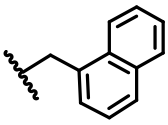

R_1 = 7-OMe
R_2 = *n*-butyl
461

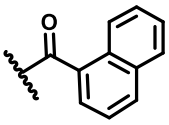

R_1 = 7-OMe
R_2 = 4-ethylmorpholine
462

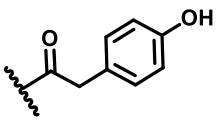

R_1 = 7-OH
R_2 = *n*-butyl
463

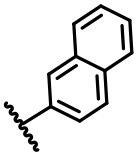

R_1 = 7-OMe
R_2 = *n*-butyl
444

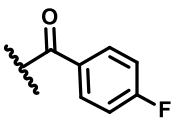

R_1 = 7-OMe
R_2 = *n*-butyl
464

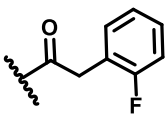

R_1 = 7-OMe
R_2 = *n*-butyl
465

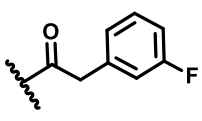

R_1 = 7-OMe
R_2 = *n*-butyl
466

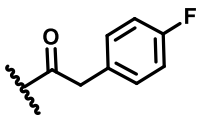

R_1 = 7-Ethyl
R_2 = *n*-butyl
467

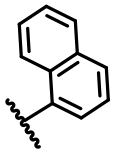

R_1 = 7-OMe
R_2 = *n*-butyl
443

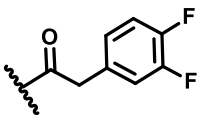

R_1 = 7-OMe
R_2 = *n*-butyl
468

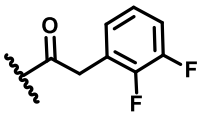

R_1 = 7-OMe
R_2 = *n*-butyl
469

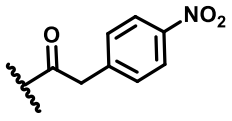

R_1 = 7-OMe
R_2 = *n*-butyl
470

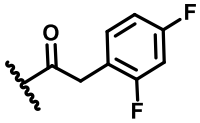

R_1 = 7-OMe
R_2 = *n*-butyl
471

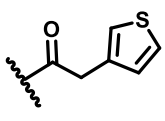

R_1 = 7-OMe
R_2 = *n*-butyl
472

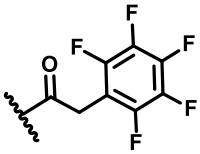

R_1 = 7-OMe
R_2 = *n*-butyl
473

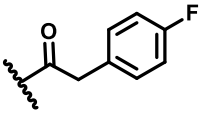

R_1 = 7-OMe
R_2 = 4-ethylmorpholine
474

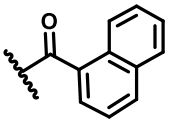

R_1 = 7-acetamide
R_2 = *n*-butyl
450

Figure 52. Sturtural represnetation of the analogues based on the JWH-073-M4 scaffold

Pharmacological Evaluation

In vitro Binding and Functional Assays

Analogues synthesized were then subjected to pharmacological testing for their activity at the cannabinoid receptors. Initial receptor binding screens for both CB1Rs and CB2Rs were conducted for all twenty-seven analogues prepared. These initial binding screens were conducted by examining the ability of a single analogue concentration of 1 μM to compete for receptor binding with the high affinity CB1R/CB2R agonist [^{3}H]CP-55,940.[474, 475] With this approach the approximate affinity of all the analogues was quickly attained. Compounds were selected for further assays to determine intrinsic activity at CB1R and CB2Rs if a 1 μM concentration produced over 50% displacement of a 0.2 nM concentration of [^{3}H]CP-55,940, indicating a relatively high sub-micromolar affinity. For example, employing the conditions used for this screen, it would be predicted by the Cheng-Prusoff equation that the concentration of a compound producing 50% displacement of [^{3}H]CP-55,940 from a receptor will estimate the compounds affinity for that receptor.[476] Data presented in **Table 21** shows that a 1μM concentration of most analogues examined produced greater than 50% displacement of [^{3}H]CP-55,940 from both CB1R and CB2Rs. Out of the twenty-seven analogues that were screened, seventeen bind to CB1R and twenty-three bind to CB2R with sub-micromolar affinity. Several analogues exhibited very high affinity for either of the two receptors tested, as seen from their near 100% displacement of [^{3}H]CP-55,940 from the receptors.

A functional assay to screen for the inhibition of AC-activity by CBRs was selected for determination of intrinsic activity of the analogues that demonstrated sub-micromolar affinity for CB1R and CB2Rs.[475] A 10 μM concentration of all compounds was used to achieve full-

receptor occupancy. It is assumed that full-receptor occupancy will produce maximal efficacy. The non-selective CB1R/CB2R full agonist CP-55,940 inhibited AC-activity via CB1Rs endogenously expressed in Neuro2A cells by 45% and 37% in CHO cells transfected with CB2Rs (**Table 21**). Most compounds examined exhibited levels of AC-inhibition similar to that produced by the full agonist CP-55,940. However, compounds **451**, **461**, and **444**, produced significantly less AC-inhibition via CB1Rs when compared to the full agonist CP-55,940 of -4, 18, and 16% inhibition, respectively. Despite little or no AC-inhibition when examined at CB1Rs, these compounds exhibited significantly different results when tested for activity at CB2Rs. Specifically, the three compounds **451**, **461**, and **444** produced levels of AC-inhibition that were similar to inhibition resulting from CP-55,940 administration of 22.1, 33.2, and 20.8%, respectively. These data indicate that compounds **451**, **461**, and **444** display only neutral antagonist to weak partial agonist activity at CB1Rs, while exhibiting partial to full agonist efficacy at CB2Rs. Despite the high binding affinities for the CB2Rs seen with analogues **450**, **470 – 474**, most of the analogues exhibited very little inhibition of AC-activity at the CB2Rs, however compounds **471** and **473** appeared to display inverse agonist activity at these receptors.

Table 21. Binding and activity of aminoalkylindole analogues **443**, **444**, **450** – **474**

Cmpd	% displacement of [^{3}H]CP-55,940 at CB1Rs	% displacement of [^{3}H]CP-55,940 at CB2Rs	% vehicle inhibition of AC-activity at CB1Rs	% vehicle inhibition of AC-activity at CB2Rs
	1 μM concentration of compounds used		*10 μM concentration of compounds used*	
CP-55,940	ND[a]	ND[a]	45	37
432	99	90	55	38
450	69	59	18	35
451	55	80	-4	22
452	38	64	ND[a]	ND[a]
453	93	100	51	52
454	29	10	ND[a]	ND[a]
455	69	91	34	16
456	21	20	ND[a]	ND[a]
457	81	91	34	-40
458	37	21	ND[a]	ND[a]
459	90	90	47	31
460	97	91	39	37
461	90	97	18	33
462	100	100	39	37
463	10	10	ND[a]	ND[a]
444	82	91	16	21
464	84	99	45	38
465	84	99	45	1
466	63	91	ND[a]	ND[a]
467	63	88	ND[a]	ND[a]
443	98	97	39	37
468	41	80	ND[a]	ND[a]
469	80	97	35	-6
470	29	62	-6	25
471	45	89	10	-25
472	70	92	16	5
473	5	69	0	-133
474	0	72	6	25

[a]ND = not determined

Based on efficacy predicted from the functional experiments examining AC-inhibition, together with the initial screen for sub-micromolar receptor affinity, several compounds were selected to determine actual K_i values by conducting full concentration effect curves for inhibition of [^{3}H]CP-55,940 binding to CBRs. Even though compound **451** produced minimal

AC-inhibition via CB1Rs, it was shown to bind to both CB1R and CB2Rs with a relatively low affinity of 387 and 281 nM, respectively (**Table 22**). However, analogue **453** demonstrated high affinity for CB1R and CB2Rs in the low nanomolar range of 1.7 nM and 0.81 nM, respectively. Compounds **461** and **444** displayed similar affinity for both receptors, however binding with slightly higher affinity to the CB2R. Specifically, **461** bound to CB1Rs with a K_i value of 15.4 nM, while binding to CB2Rs with a K_i value of 10.9 nM. Compound **444** demonstrated an affinity of 37.2 nM and 26.5 nM for CB1R and CB2Rs, respectively. Compounds **471** and **474** exhibited higher affinity for the CB2Rs than the CB1Rs, with K_i values of 71 and 148 nM, respectively. Compounds **471** and **474** were 14-fold and 136-fold more selective for the CB2Rs than the CB1Rs, respectively.

Table 22. Affinity of selected analogues for mouse CB1Rs and human CB2Rs

Cmpd	*m*CB1R K_i ± SEM, nM [a]	*h*CB2R K_i ± SEM, nM [a]
429	12.9 ± 3.4	9.8 ± 0.9
432	24.2 ± 17.2	78.3 ± 36.2
451	387 ± 77.0	281 ± 51.0
453	1.7 ± 0.3	0.81 ± 0.4
461	15.4 ± 2.2	10.9 ± 3.1
444	37.3 ± 11.8	26.5 ± 1.5
471	970 ± 180	71.4 ± 11.8
474	20,000 ± 12,800	147.7 ± 19.8

[a] Values represent mean ± standard error of mean, experiments performed in triplicate.

Compounds **451**, **453**, **461**, and **444** exhibited relatively high affinities as indicated by their K_i values were examined together with JWH-073-M4 (**432**) to determine their potency to inhibit AC-activity via CB1R and CB2Rs. Similar to data reported in the initial screen for AC-inhibition, **432** and **453** produced 50-60% inhibition of AC-activity via CB1Rs with IC_{50} values

of 225 and 45 nM, respectively. Conversely, **461** and **444** produced very little inhibition of AC-activity, which was only observed at very high concentrations of both analogues (**Figure 53A**). In support of the observed functional activity indicating neutral antagonism, the two lead compounds and the CB1R antagonist O-2050 (1 μM concentration) significantly antagonized AC-inhibition produced by the CB1R full agonist **429** (**Figure 53B**). In contrast to neutral antagonism at CB1Rs, all of the compounds examined produced 40-50% inhibition of AC-activity at CB2Rs in CHO-*h*CB2 cells with potency similar to their rank order of K_i values reported in **Table 21** (**Figure 54A**). To examine if the observed agonist activity in CHO-*h*CB2 cells is due to activation of CB2Rs, the AC-inhibition assay was conducted in CHO-WT cells not expressing CB2Rs. As observed in **Figure 54B**, neither **461** nor **444** significantly modified AC-activity in CHO-WT cells indicating that the agonist activity observed for both compounds in CHO-*h*CB2 cells is indeed due to their activation of CB2Rs.

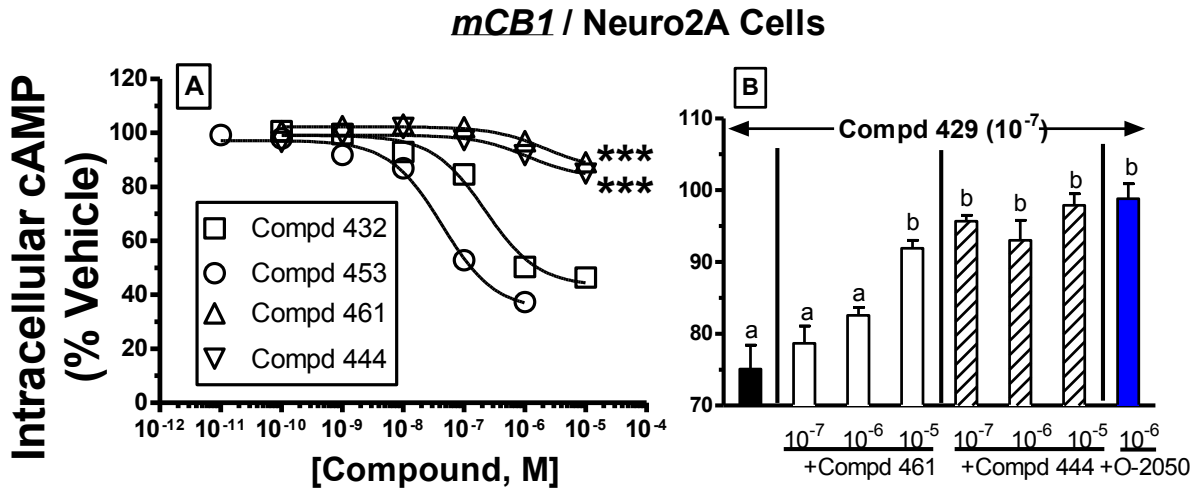

Figure 53. Inhibition of AC-activity at CB1Rs for analogues **461** and **444**. Compounds **461** and **444** produce very little inhibition of AC-activity when tested alone at high concentrations and antagonize AC-inhibition produced by CB1R-agonist (black bar in panel B represents inhibition of AC-activation of 10^{-7} M concentration of **429**)

***Lead compounds selected for testing in animals

[a,b] Different letters signify statistical differences between groups

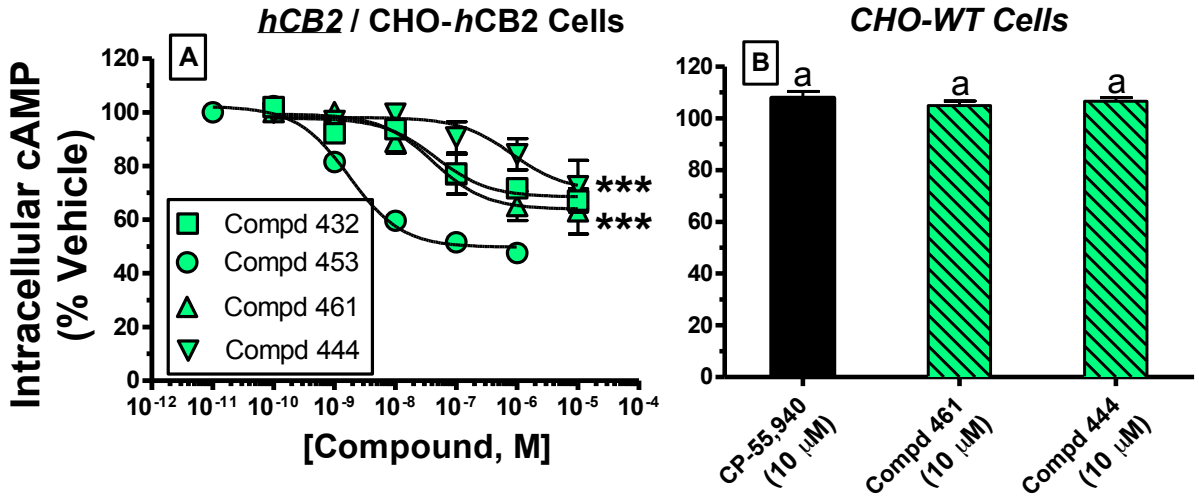

Figure 54. Inhibition of AC-activity at CB2Rs for analogues **461** and **444**. Compounds **461** and **444** produce concentration-dependent inhibition of adenylyl cyclase activity by activation of CB2Rs

***Lead compounds selected for testing in animals

[a] Letter signifies statistical differences between groups

From these results it can be concluded that the carbonyl moiety is not necessary of activity at the CBRs and that introduction of rotational bond at the C-3 position in the scaffold retained and improved activity at the CBRs. Furthermore, exploration of the electronic potential of the naphthalene moiety was well tolerated in that electron-withdrawing groups produced activity at the CBRs, however analogues containing electron-donating groups at this position need to be designed and synthesized in order for a full conclusion to be reached regarding the electronic potential of this substituent. It was also established that no linker or one carbon linker between the indole core the C-3 substituent is well tolerated retaining and significantly improving the activity at the CBRs. Additionally, different substitutions at the *N*-atom are tolerated; however *N*-butyl substituent is optimal of CB1R antagonist activity. Moreover, movement of the hydroxyl substituent around the indole core did not prove fruitful in that those

analogues that did not possess a C-7 substitution were not as active at the CBRs. Additionally, substitution of the 7-methoxy moiety with a 7-acetamide moiety was tolerated, however with lower activity at the CBRs than those analogues possessing a 7-methoxy substituent.

In vivo animal testing

The dual CB1R neutral antagonist/CB2R agonist activity displayed by compounds **461** and **444** in the *in vitro* assays prompted us to select these analogues for further evaluation *in vivo* using murine subjects in two complementary models relevant to alcohol abuse. These *in vivo* assay are based on the hypothesis that analogues with dual activity as CB1R neutral antagonist/CB2R agonist will reduce both the reinforcing effects of ethanol (EtOH) and the conditioned rewarding effects of EtOH in mice. Thermoregulation assay was used as an initial analysis that examines potential cannabinoid receptor antagonist activity. It is well known that cannabinoid agonists produce hypothermic effects, and are blunted by prior treatment with CB1R antagonists, allowing us to rapidly determine whether or not our selected compounds display *in vivo* effects consistent with CB1R antagonism.[477, 478] The assay was conducted using glass-encapsulated radiotelemetry probes surgically implanted into the peritoneal cavity of each mouse, which monitored core body temperature in response to drug administration.[473] Intraperitoneal administration of 10 mg/kg of the full CB1R agonist **429**, elicited a profound hypothermic effect as seen in **Figure 55** (black circles). Importantly, thirty minute pretreatment with either **461** (**Figure 55**, gray triangle) or **444** (**Figure 55**, white circles), significantly decreased the hypothermic effects elicited by subsequent administration of compound **429**,

confirming the *in vivo* cannabinoid activity of **461** and **444**, and illustrating apparent antagonist effects against CB1R agonist-induced hypothermia (**Figure 56**).

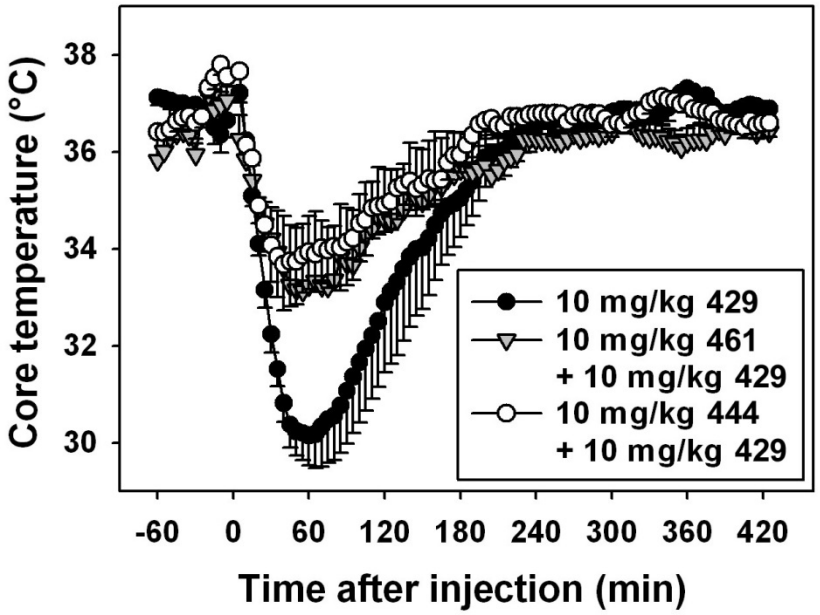

Figure 55. Thermoregulation assay for analogues **461** and **444**. Compounds **461** and **444** reduce agonist **429** induced hypothermic effects in rodents

Having established apparent *in vivo* antagonism, **461** and **444** were further tested in two complementary models of alcohol abuse: oral ethanol self-administration (SA) and ethanol conditioned place preference (CPP). Ethanol SA and CPP are important models for the study of alcoholism because they capture several aspects of this condition including voluntary EtOH drinking (SA) and conditioned EtOH reward (CPP).

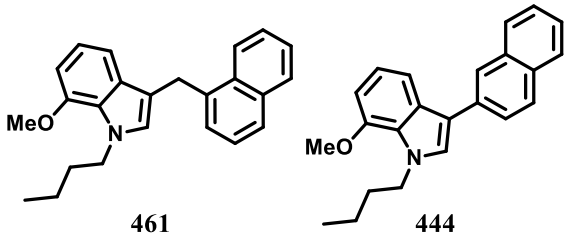

461 **444**

Figure 56. Structures of the two lead compounds, **461** and **444**

The effects of compounds **461** and **444** on voluntary 10% Procedure described by both Keane and coworkers and Cunningham and colleagues, where EtOH drinking was studied using a two-bottle choice procedure (ethanol vs. water) and where 10 mg/kg rimonabant was used as a positive control were employed.[479, 480] Across five observations conducted under baseline "no injection" conditions it can be observed in **Figures 57A**, and **Figure 57D** (black circles) that EtOH preference and total fluid consumption (**Figure 57B**, **Figure 57E**; black circles) were steadily maintained during the entire treatment period. Consistent with previous reports, daily treatment with 10 mg/kg rimonabant decreased EtOH preference (**Figure 57A**, **Figure 57D**, triangles) without altering total fluid intake (**Figure 57B**, **Figure 57E**, triangles).[481] However, as previously published reports have stated, rimonabant decreased body weight across the treatment period (**Figure 57C**, **Figure 57F**, triangles).[482, 483] After ten day treatment with rimonabant, mice were returned to baseline "no injection" conditions where their weights increased and voluntary EtOH drinking resumed. After five such observations, representing a two week drug "washout" period, daily treatments with 10 mg/kg of **461** or **444** were initiated. As previously observed with rimonabant, both compounds **461** and **444** reduced EtOH preference (**Figure 57A**, inverted triangles; **Figure 57D**, gray triangles, respectively) without affecting total fluid consumption (**Figure 57B**, inverted triangles; **Figure 57E**, gray triangles). However, unlike rimonabant, compounds **461** and **444** did not decrease body weight of mice tested (**Figure 57C**, inverted triangles; **Figure 57E**, gray triangles). The last treatment was a daily injection of the rimonabant/**461/444** vehicle, which was 8% Tween/92% sterile water. With the exception of the first observation period for compound **461** (perhaps representing a persistent effect of **461**), EtOH preference (**Figure 57A**, gray circles-compound **461**; **Figure 57D**, gray circles-compound **444**), total fluid consumption (**Figure 57B**, gray circles-compound **461**; **Figure 57E**, gray

circles-compound **444**), and mean body weight (**Figure 57C**, gray circles-compound **461**; **Figure 57F**, gray circles-compound **444**) were not affected by vehicle injections. This study demonstrates that a JWH-derived compound devoid of inverse agonist activity can replicate the effects of rimonabant on alcohol self-administration in mice.

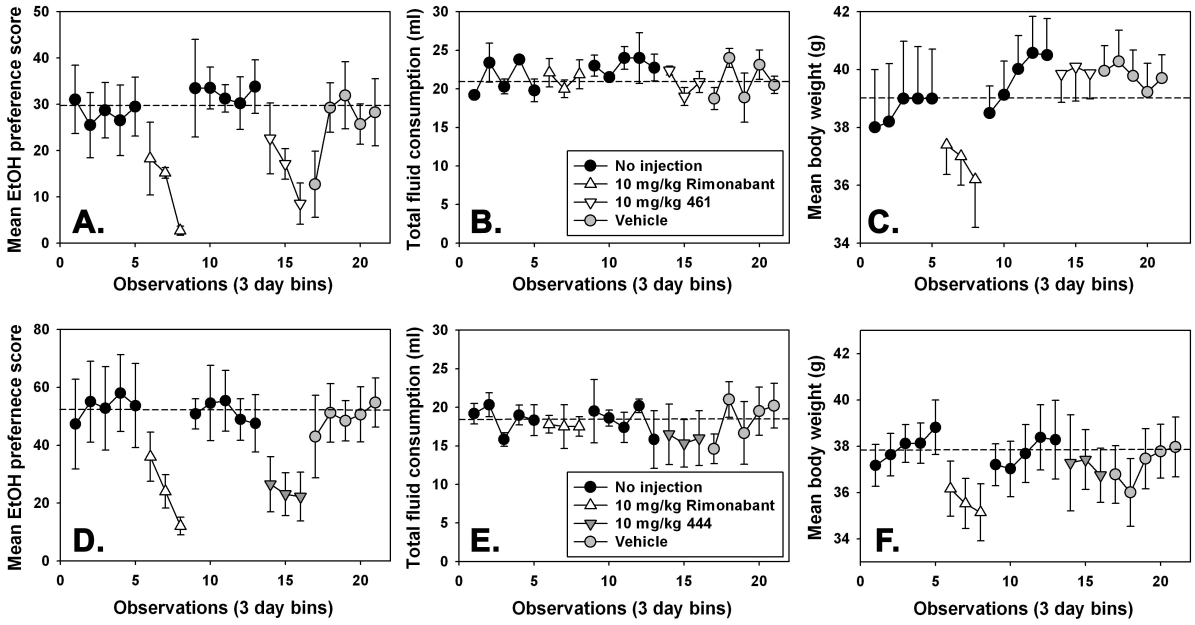

Figure 57. *In vivo* ethanols self-administration assay for analogues **461** and **444**. Reduction of EtOH self-administration with daily administration of 10 mg/kg rimonabant or compounds **461** and **444**. Dotted lines represent group means from the 10 "no injection" control periods

To further explore the *in vivo* effects of these compounds, an alcohol conditioned place preference assay was performed with compounds **461**, **444**, and rimonabant. The conditioned rewarding effects of ethanol are examine in this assay. Training of mice involved daily pairings of 2 mg/kg EtOH with novel contextual cues within a spatial conditioning chamber, and daily pairings of saline with distinct contextual cues within the same chamber. Following four such pairings, an increase in time spent in EtOH-paired chamber was observed, indicating the development of conditioned place preference (**Figure 58**, "No inj" bar). Separate groups of mice

were conditioned as previously described, with the exception that 10 mg/kg **461,** 10 mg/kg **444** or 10 mg/kg rimonabant were administered one hour before each EtOH pairing. In contrast to the ~400 sec preference elicited by EtOH in the absence of cannabinoid administration, mice treated with 10 mg/kg rimonabant prior to each EtOH pairing did not exhibit a significant preference for the EtOH-paired chamber, which is in agreement with previously reported data (**Figure 58**, "10 RIM" bar).[484, 485] Similar to the effects of rimonabant produced in the present study, the conditioned rewarding effects of EtOH were also blocked by the administration of either 10 mg/kg **461** or 10 mg/kg **444** prior to each EtOH pairing. In total, these studies demonstrate that a novel indole-derived compound with cannabinoid activity lacking inverse agonist activity can replicate the effects of rimonabant on alcohol induced CPP in mice.

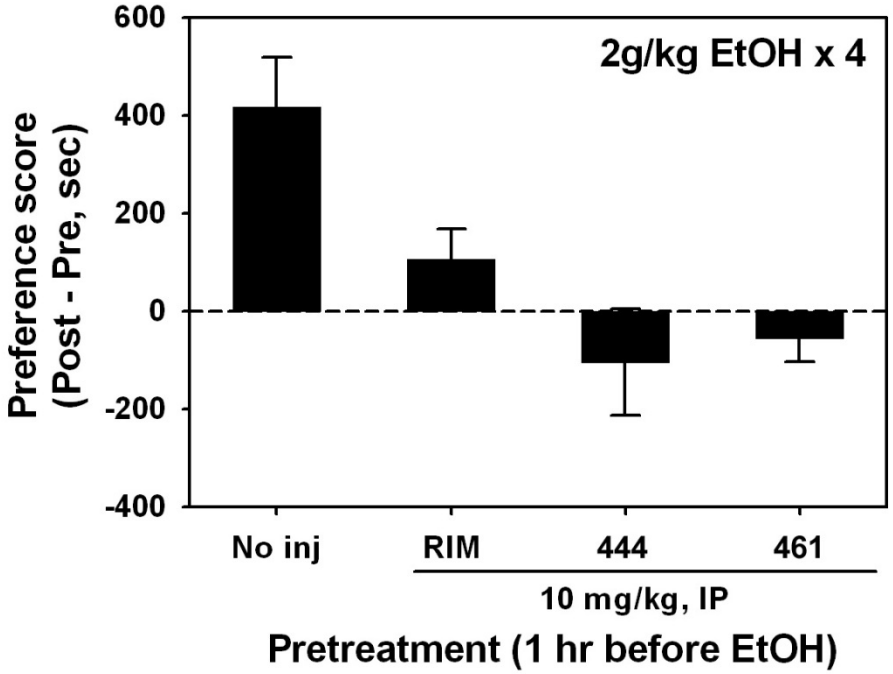

Figure 58. *In vivo* ethanol conditioned place preference for analogues **461** and **444**. Blockage of EtOH CPP with rimonabant and compounds **461** and **444**

Conclusions

Analogues of the JWH-073-M4 scaffold were designed and synthesized to gain a better understanding for the activity of this scaffold at the cannabinoid receptors. Analogues synthesized were designed to explore several different structural features in the molecule including the necessity of the carbonyl moiety, the optimal length of the linker from the indole core to the naphthalene ring, the electronic nature of the naphthalene substituent, the introduction of a rotatable bond at the C-3 position, the introduction of *N*-substituents with improved pharmacokinetic properties, and explore the optimal position of the substituent on the indole ring.

Upon synthesis, the designed analogues were subjected to an array of pharmacological assays for evaluation. As seen with the parent compound JWH-073, most of the analogues tested exhibited relatively high affinity for both CB1R and CB2Rs. Of all of the compounds tested, two analogues, **461** and **444**, appeared to have the most promise with affinities for the cannabinoid receptors in the low nanomolar range (**Figure 59**). In AC-inhibition assays, both compounds produced very little inhibition of AC-activity via CB1Rs, consistent with neutral antagonism. However, **461** and **444** both produced 40-50% inhibition of AC-activity via CB2Rs, similar to that of the full agonist CP-55,940 and thus consistent with partial to full agonism.

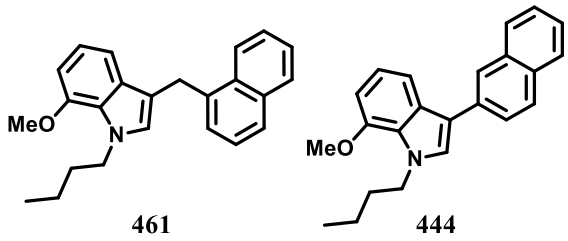

461 **444**

Figure 59. Structures of the two lead compounds, **461** and **444**

The promising *in vitro* pharmacological results for these to lead compounds prompted further evaluation in *in vivo* animal assays of alcohol abuse, namely ethanol SA and ethanol CPP. Similar to the actions produced by the CB1R antagonist/inverse agonist rimonabant, both **461** and **444** were shown to decrease alcohol self-administration, without affecting total fluid intake. Unlike rimonabant, **461** and **444** did not alter body weight during the treatment period. Both analogues **461** and **444** interestingly decreased ethanol CPP in a similar manner to rimonabant, despite not possessing any apparent inverse agonist activity *in vitro*. As previously reported for rimonabant, these results demonstrate that both the reinforcing and conditioning rewarding effects of alcohol can also be significantly blunted by treatment with novel JWH-derived cannabinoids, devoid of inverse agonist activity at CB1Rs.[486] Compounds with dual CB1R neutral antagonist/CB2R agonist activity such as analogues **461** and **444** may indeed represent potential leads in an ongoing search for new and improved alcohol abuse therapies.

Future Directions

The *in vivo* pharmacological results that were obtained utilizing murine models of alcohol abuse were very promising in the detection of two analogues with dual CB1R antagonists and CB2R agonist activities. A behavioral study completed in non-human primates would assist in the collection of behavioral effects that these compounds may have as well as to further examine the seen *in vivo* results of the two lead compounds **461** and **444**.

The positive results that were obtained from the present SAR study of the JWH-073-M4 scaffold can serve as the base for further SAR exploration of this scaffold at the cannabinoid receptors. Such studies can involve the design and synthesis of a series of analogues that explore

different structural features of the two lead compounds **461** and **444**. For example, analogues could be designed to explore the necessity of the naphthalene substituent off of the C-3 carbon on the indole core as well as explore the electronic potential at this position. Another series of analogues could explore different *N*-substituents varying in length of the alkyl chain as well as substituents with improved pharmacokinetic profiles. A third series of analogues could examine the positioning of the indole ring substituents as well as introduce substituents with different electronic profiles at various positions of the indole core. Lastly, explorations into alkyl substituents at the C-2 position as well as conformationaly constrained analogues could give us a new insight into the interactions of such molecules with the cannabinoid receptors.

CHAPTER 5: EXPERIMENTAL PROCEDURES FOR JWH-073-M4 ANALOGUES

Chemistry

General Procedures. Unless otherwise indicated, all reagents were purchased from commercial sources and were used without further purification. Melting points were determined on a Thomas-Hoover capillary melting apparatus. NMR spectra were recorded on a Bruker DRX-400 with qnp probe or a Bruker AV-500 with cryoprobe using δ values in ppm (TMS as internal standard) and *J* (Hz) assignments of ^{1}H resonance coupling. High resolution mass spectrometry data were collected on either a LCT Premier (Waters Corp., Milford, MA) time of flight mass spectrometer or an Agilent 6890 N gas chromatograph in conjunction with a quarto Micro GC mass spectrometer (Micromass Ltd, Manchester UK). Thin-layer chromatography (TLC) was performed on 0.25 mm plates Analtech GHLF silica gel plates using ethyl acetate/*n*-hexanes, in 20%:80% ratio as the solvent unless otherwise noted. Spots on TLC were visualized by UV (254 or 365 nm), or if applicable, phosphomolybdic acid in ethanol. Column chromatography was performed with silica gel (40-63 μ particle size) from Sorbent Technologies (Atlanta, GA). Analytical HPLC was carried out on an Agilent 1100 Series Capillary HPLC system with diode array detection at 254 nm on an Agilent Eclipse XDB-C18 column (250 x 10 mm, 5 μm) with isocratic elution in 80% CH_3CN/20% H_2O (0.1% formic acid) unless otherwise specified.

General Procedure A: Indole *N*-alkylation. To a suspension of KOH (5 equiv) in DMF (13 mL) was added 5-methoxyindole, 7-methoxyindole or 7-ethylindole (1 equiv). After stirring at 21 °C for an hour, 1-bromobutane (1.375 equiv) was added and the reaction mixture was

heated to 50 °C and stirred overnight. Upon completion, the resulting mixture was poured into H_2O (15 mL) and extracted with DCM (3 x 15 mL). Combined organic extracts were washed with water, dried over anhydrous Na_2SO_4, concentrated under reduced pressure and the resulting residue was purified by flash column chromatography on silica gel using EtOAc/*n*-hexanes.

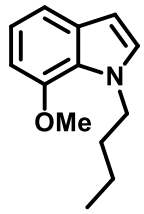

1-Butyl-7-methoxy-1H-indole (434ac). Compound **434ac** was synthesized from commercially available 7-methoxyindole using general procedure A and 1-bromobutane to afford 0.51 g (74% yield) as a clear oil. TLC system: 10% EtOAc/90% *n*-hexanes. Spectral data matched previously reported data.[487]

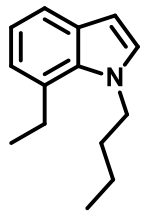

1-Butyl-7-ethyl-1H-indole (434bc). Compound **434bc** was synthesized from commercially available 7-ethylindole using general procedure A and 1-bromobutane to afford 0.64 g (93% yield) as a clear oil. TLC system: 10% EtOAc/90% *n*-hexanes. ^{1}H NMR (500 MHz, $CDCl_3$) δ 7.47 (dd, *J* = 7.6, 1.4 Hz, 1H), 7.05 – 6.95 (m, 3H), 6.47 (d, *J* = 3.1 Hz, 1H), 4.31 – 4.21 (m, 2H), 3.03 (q, *J* = 7.5 Hz, 2H), 1.83 – 1.69 (m, 2H), 1.35 (td, *J* = 7.6, 2.7 Hz, 5H),

0.94 (t, J = 7.4 Hz, 3H). ^{13}C NMR (126 MHz, $CDCl_3$) δ 133.57, 130.09, 129.60, 127.30, 122.42, 119.49, 119.00, 101.40, 48.75, 34.47, 25.67, 20.04, 16.08, 13.77. [M+H] calcd for $C_{14}H_{19}N$, 202.1590; found 202.1596.

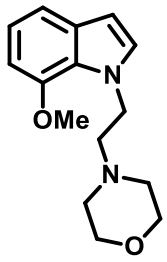

4-(2-(7-Methoxy-1H-indol-1-yl)ethyl)morpholine (434ad). Compound **434ad** was synthesized from commercially available 7-methoxyindole using general procedure A and 4-(2-bromoethyl)morpholine that was made utilizing conditions reported by Cai J., *et al*.[488] to afford 0.51 g (74% yield) as an oil with a slightly orange tint. TLC system: 40% EtOAc/60% *n*-hexanes. ^{1}H NMR (500 MHz, $CDCl_3$) δ 7.20 (dd, J = 7.9, 0.9 Hz, 1H), 7.01 – 6.99 (m, 1H), 6.97 (d, J = 7.8 Hz, 1H), 6.61 (dd, J = 7.8, 0.9 Hz, 1H), 6.42 (d, J = 3.1 Hz, 1H), 4.53 – 4.46 (m, 2H), 3.93 (s, 3H), 3.74 – 3.68 (m, 4H), 2.78 – 2.71 (m, 2H), 2.53 – 2.47 (m, 4H). ^{13}C NMR (126 MHz, $CDCl_3$) δ 147.33, 130.92, 129.19, 125.48, 119.75, 113.77, 102.14, 101.33, 67.02, 60.15, 55.15, 53.93, 46.65. [M+H] calcd for $C_{15}H_{21}N_2O_2$, 261.1598; found 261.1603.

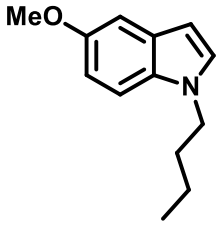

1-Butyl-5-methoxy-1H-indole (439). Compound **439** was synthesized from commercially available 5-methoxyindole using general procedure A and 1-bromobutane to afford 1.28 g (92% yield) as a clear oil. TLC system: 10% EtOAc/90% *n*-hexanes. ^{1}H NMR (500 MHz, $CDCl_3$) δ 7.18 (d, *J* = 8.9, 1H), 7.02 (dd, *J* = 2.7, 13.3, 2H), 6.81 (dd, *J* = 2.4, 8.9, 1H), 6.34 (dd, *J* = 0.7, 3.0, 1H), 4.02 (t, *J* = 7.1, 2H), 3.79 (s, 3H), 1.75 (ddd, *J* = 7.3, 11.2, 14.8, 2H), 1.32 – 1.23 (m, 2H), 0.87 (t, *J* = 7.4, 3H). ^{13}C NMR (126 MHz, $CDCl_3$) δ 154.09, 131.56, 129.06, 128.55, 111.93, 110.35, 102.71, 100.53, 56.12, 46.54, 32.63, 20.43, 13.95. [M+H] calcd for $C_{13}H_{18}NO$, 204.1383; found 204.1386.

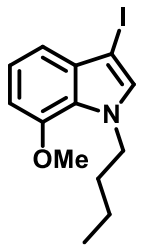

Preparation of 1-butyl-3-iodo-7-methoxy-1H-indole (442). A round bottom flask containing 7-methoxyindole (0.22 mL, 1.70 mmol, 1 equiv) in DMF at 21 °C was stirred with KOH (0.10 g, 1.78 mmol, 1.05 equiv) for 15 min and then treated with I_2 (0.44g, 1.73 mmol, 1.02 equiv). After 30 min, NaH (60% dispersion in mineral oil; 0.082 g, 2.04 mmol, 1.2 equiv) was added portion-wise. After an additional 15 min, 1-bromobutane (0.2 mL, 1.87 mmol, 1.1 equiv) was added and the reaction mixture was stirred until completion. Upon completion (TLC monitoring), water was added and allowed to stir for 15 min, upon which the mixture was extracted with DCM and the layers were separated. Aqueous layer was washed with DCM (3 x 15 mL) and the combined organic layers were washed with H_2O (2 x 15 mL), dried over anhydrous Na_2SO_4 and concentrated under reduced pressure. The resulting residue was purified

by silica gel column chromatography using EtOAc/*n*-hexanes to afford 0.45g (80% yield) as an clear oil with a yellow tint that was used immediately. TLC system: 10% EtOAc/90% *n*-hexanes. ^{1}H NMR (500 MHz, $CDCl_3$) δ 7.08 (t, *J* = 3.8, 2H), 7.04 (dd, *J* = 1.1, 8.0, 1H), 6.68 (d, *J* = 7.5, 1H), 4.38 (t, *J* = 7.2, 2H), 3.95 (s, 3H), 1.78 (dt, *J* = 7.5, 12.7, 2H), 1.33 (td, *J* = 7.5, 15.0, 2H), 0.94 (t, *J* = 7.4, 3H). ^{13}C NMR (126 MHz, CDCl3) δ 146.67, 132.31, 131.99, 125.18, 119.88, 113.27, 102.43, 54.80, 48.90, 33.67, 19.20, 13.13.

General Procedure B: *O*-Demethylation procedure. A solution of BBr_3 (1 M in DCM, 6 equiv) in DCM was added dropwise to a solution of methyl ether (1 equiv) in DCM at -78 °C. The mixture was then allowed to warm to 21 °C overnight, and upon completion, $NaHCO_3$ (6 equiv) was added. The resulting mixture was then cooled in an ice-bath and MeOH (20 mL) was added dropwise and then stirred for 30 min. The reaction mixture was then warmed up to 21 °C and stirred for an additional hour. The reaction was quenched with H_2O and the separated aqueous phase was extracted with DCM (3 x 15 mL). Combined organic extracts were dried over anhydrous Na_2SO_4, and concentrated under reduced pressure. The resulting residue was purified by flash chromatography on silica gel using mixtures of EtOAc/*n*-hexanes.

General Procedure C: Acid chloride formation. The appropriate acid (1 equiv) was placed in a round bottom flask and flushed twice with argon (Ar). Anhydrous DCM (7 mL) was then added followed by the dropwise addition of oxalyl chloride (2 M in DCM, 3.1 equiv). After 5 min, 3 drops of anhydrous DMF were added to the reaction mixture and once the fizzing stopped, the reaction was allowed to stir overnight at 21 °C. Solvent was then evaporated using reduced pressure and the crude residue was used immediately without any further purification.

General Procedure D: 3'-indole acylation. To a solution of the appropriate indole (1 equiv) in DCM at 0 °C under an Ar atmosphere was added Me_2AlCl (1.5 equiv) dropwise and the solution was allowed to stir at that temperature for 30 min, after which a solution of the appropriate acid chloride (1.2 equiv) in DCM was added dropwise. Reaction was monitored by TLC and upon completion, was carefully poured into an ice-cold 1N HCl solution and then extracted with DCM (3 x 15 mL). Combined organic layers were then washed with $NaHCO_3$ (2 x 15 mL), brine, and dried over anhydrous Na_2SO_4. The solvent was evaporated under reduced pressure and the resulting residue was purified by flash column chromatography on silica gel using mixtures of EtOAc/*n*-hexanes to afford the desired product.

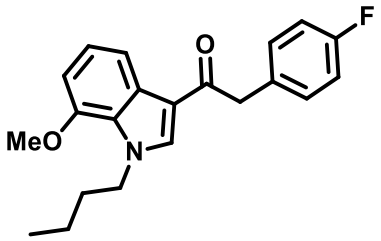

1-(1-Butyl-7-methoxy-1H-indol-3-yl)-2-(4-fluorophenyl)ethanone (451). Compound **451** was synthesized from compound **434** using general procedure D and 4-fluorophenylacetyl chloride to afford 0.08g (9% yield) isolated as a brown oil. ^{1}H NMR (500 MHz, $CDCl_3$) δ 7.98 (dd, *J* = 0.8, 8.1, 1H), 7.64 (s, 1H), 7.29 – 7.25 (m, 2H), 7.16 (t, *J* = 8.0, 1H), 7.02 – 6.96 (m, 2H), 6.71 (d, *J* = 7.5, 1H), 4.39 (t, *J* = 7.2, 2H), 4.09 (s, 2H), 3.93 (s, 3H), 1.85 – 1.77 (m, 2H), 1.36 – 1.27 (m, 2H), 0.94 (t, *J* = 7.4, 3H). ^{13}C NMR (126 MHz, $CDCl_3$) δ 192.32, 162.72, 160.77, 147.31, 135.78, 131.66 (d, *J* = 3.2 Hz), 130.95 (d, *J* = 7.9 Hz), 129.07, 126.33, 123.30, 115.70 (d, *J* = 21.4 Hz), 115.21, 115.12, 104.31, 55.36, 50.28, 45.87, 33.81, 19.78, 13.68.

HRMS (*m/z*): [M+K] calcd for $C_{21}H_{22}FKNO_2$, 378.1272; found 378.1315. HPLC t_R = 15.031 min; purity = 95.4% using 70% CH_3CN/30% H_2O (0.1% formic acid).

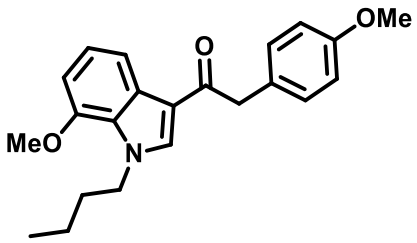

1-(1-Butyl-7-methoxy-1H-indol-3-yl)-2-(4-methoxyphenyl)ethanone (452).

Compound **452** was synthesized from compound **434** using general procedure D and 4-methoxyphenylacetyl chloride to afford 0.63 g (59.2% yield) isolated as a reddish solid, mp = 72-74 °C. ^{1}H NMR (500 MHz, $CDCl_3$) δ 8.00 (dd, *J* = 0.8, 8.1, 1H), 7.63 (s, 1H), 7.25 – 7.21 (m, 2H), 7.15 (t, *J* = 8.0, 1H), 6.87 – 6.81 (m, 2H), 6.70 (d, *J* = 7.8, 1H), 4.37 (t, *J* = 7.2, 2H), 4.06 (s, 2H), 3.92 (s, 3H), 3.77 (s, 3H), 1.84 – 1.76 (m, 2H), 1.35 – 1.26 (m, 2H), 0.93 (t, *J* = 7.4, 3H). ^{13}C NMR (126 MHz, $CDCl_3$) δ 193.44, 158.73, 147.69, 136.29, 130.73, 129.59, 128.50, 126.69, 123.58, 116.22, 115.62, 114.40, 104.62, 55.76, 55.69, 50.63, 46.48, 34.22, 20.19, 14.11. HRMS (*m/z*): [M+Na] calcd for $C_{22}H_{25}NNaO_3$, 374.1732; found 374.1783. HPLC t_R = 7.490 min; purity = 99.9%.

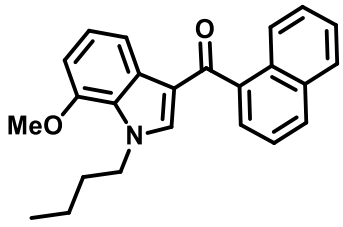

1-(1-Butyl-7-methoxy-1H-indol-3-yl)-2-(2,3-difluorophenyl)ethanone (453). Compound **453** was synthesized from compound **434** using general procedure D and 1-naphthoyl chloride to afford 2.00 g (53% yield) isolated as a pale brown solid, mp = 108-110 °C. ^{1}H NMR (500 MHz, $CDCl_3$) δ 8.19 (d, *J* = 8.4, 1H), 8.11 (d, *J* = 7.4, 1H), 7.96 (d, *J* = 8.2, 1H), 7.91 (d, *J* = 7.8, 1H), 7.65 (dd, *J* = 1.1, 7.0, 1H), 7.56 – 7.45 (m, 3H), 7.28 – 7.24 (m, 2H), 7.22 (s, 1H), 6.79 (d, *J* = 7.7, 1H), 4.30 (t, *J* = 7.3, 2H), 3.96 (s, 3H), 1.80 – 1.71 (m, 2H), 1.32 – 1.23 (m, 2H), 0.89 (t, *J* = 7.4, 3H). ^{13}C NMR (126 MHz, $CDCl_3$) δ 192.08, 147.45, 139.32, 139.07, 133.81, 130.89, 129.96, 129.46, 128.22, 126.79, 126.61, 126.34, 126.14, 125.89, 124.65, 123.60, 117.42, 115.35, 104.66, 55.50, 50.34, 33.86, 19.83, 13.73. HRMS (*m/z*): [M+Na+CH_3CN] calcd for $C_{26}H_{26}N_2NaO_2$ 421.1892; found 421.1843. HPLC t_R = 14.576; purity = 95.8%.

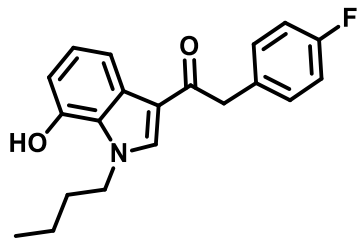

1-(1-Butyl-7-hydroxy-1H-indol-3-yl)-2-(4-fluorophenyl)ethanone (454). Compound **454** was synthesized from **435** using general procedure B to afford 0.10g (38% yield) isolated as an off-brown solid, mp = decomposition at 204-206 °C. ^{1}H NMR (500 MHz, DMSO) δ 9.91 (s, 1H), 8.44 (s, 1H), 7.62 (dd, *J* = 0.9, 8.0, 1H), 7.39 – 7.33 (m, 2H), 7.12 (ddd, *J* = 2.6, 5.9, 8.9, 2H), 6.94 (t, *J* = 7.8, 1H), 6.61 (dd, *J* = 0.9, 7.7, 1H), 4.44 (t, *J* = 7.0, 2H), 4.09 (s, 2H), 1.85 – 1.75 (m, 2H), 1.31 – 1.21 (m, 2H), 0.90 (t, *J* = 7.4, 3H). ^{13}C NMR (126 MHz, DMSO) δ 191.61, 161.72, 159.80, 144.49, 137.94, 132.17 (d, *J* = 3.1 Hz), 131.05, 130.69 (d, *J* = 8.0 Hz), 128.73, 125.46, 122.80, 114.76, 114.59, 114.50, 112.34, 108.26, 48.70, 44.52, 33.29, 18.97, 13.39.

HRMS (*m/z*): [M+Na+CH_3CN] calcd for $C_{22}H_{23}FN2NaO_2$, 389.1641; found 389.1711. HPLC t_R = 6.491 min; purity = 99.9% using 70% CH_3CN/30% H_2O (0.1% formic acid).

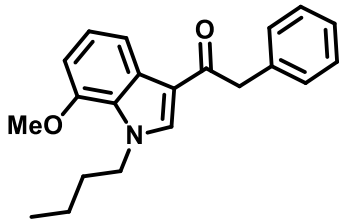

1-(1-Butyl-7-methoxy-1H-indol-3-yl)-2-phenylethanone (455). Compound **455** was synthesized from compound **434** using general procedure D and phenyacetyl chloride to afford 0.13 g (17% yield) isolated as an off-white solid with a pinkish tint, mp = 65-68 °C. ^{1}H NMR (500 MHz, $CDCl_3$) δ 8.03 (dd, *J* = 0.8, 8.1, 1H), 7.66 (s, 1H), 7.36 – 7.30 (m, 4H), 7.26 – 7.22 (m, 1H), 7.18 (t, *J* = 8.0, 1H), 6.72 (d, *J* = 7.8, 1H), 4.39 (t, *J* = 7.2, 2H), 4.14 (s, 2H), 3.94 (s, 3H), 1.87 – 1.77 (m, 2H), 1.32 (dq, *J* = 7.4, 14.8, 2H), 0.95 (t, *J* = 7.4, 3H). ^{13}C NMR (126 MHz, $CDCl_3$) δ 192.72, 147.37, 136.13, 136.06, 129.43, 129.25, 128.62, 126.64, 126.38, 123.30, 115.96, 115.30, 104.34, 55.44, 50.32, 47.09, 33.88, 19.86, 13.78. HRMS (*m/z*): [M+Na] calcd for $C_{21}H_{23}NNaO_2$, 344.1626; found 344.1656. HPLC t_R = 8.114 min; purity = 99.9%.

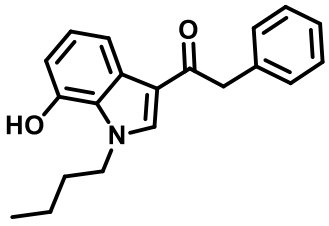

1-(1-Butyl-7-hydroxy-1H-indol-3-yl)-2-phenylethanone (456). Compound **456** was synthesized from compound **435** using general procedure B to afford 0.17 g (68% yield) isolated

as a fluffy brown solid, mp = decomposition at 197-200 °C. ^{1}H NMR (500 MHz, DMSO) δ 9.91 (s, 1H), 8.44 (s, 1H), 7.62 (dd, *J* = 0.9, 8.0, 1H), 7.36 – 7.31 (m, 2H), 7.28 (dd, *J* = 4.9, 10.3, 2H), 7.20 (dd, *J* = 4.3, 11.6, 1H), 6.93 (t, *J* = 7.8, 1H), 6.61 (dd, *J* = 0.9, 7.7, 1H), 4.44 (t, *J* = 7.0, 2H), 4.08 (s, 2H), 1.84 – 1.75 (m, 2H), 1.30 – 1.20 (m, 2H), 0.90 (t, *J* = 7.4, 3H). ^{13}C NMR (126 MHz, DMSO) δ 191.75, 144.49, 137.99, 136.39, 129.20, 128.76, 128.00, 126.01, 125.46, 122.77, 114.60, 112.35, 108.24, 48.67, 45.62, 33.28, 18.95, 13.38. HRMS (*m/z*): [M+Na] calcd for $C_{20}H_{21}NNaO_2$, 330.1470; found 330.1514. HPLC t_R = 6.458 min; purity = 99.8% using 70% CH_3CN/30% H_2O (0.1% formic acid).

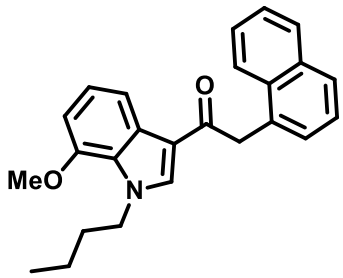

1-(1-Butyl-7-methoxy-1H-indol-3-yl)-2-(naphthalen-1-yl)ethanone (457). Compound **457** was synthesized from compound **434** using general procedure D and 1-naphthoylacetyl chloride to afford 0.09 g (12% yield) isolated as an amorphous yellow solid, mp = 110-113 °C. ^{1}H NMR (500 MHz, $CDCl_3$) δ 8.07 – 8.00 (m, 2H), 7.89 – 7.85 (m, 1H), 7.79 (dd, *J* = 2.4, 7.0, 1H), 7.72 (s, 1H), 7.51 – 7.46 (m, 2H), 7.46 – 7.43 (m, 2H), 7.18 (t, *J* = 8.0, 1H), 6.73 (d, *J* = 7.6, 1H), 4.61 (s, 2H), 4.38 (t, *J* = 7.1, 2H), 3.95 (s, 3H), 1.85 – 1.77 (m, 2H), 1.34 – 1.24 (m, 2H), 0.94 (t, *J* = 7.4, 3H). ^{13}C NMR (126 MHz, $CDCl_3$) δ 192.76, 147.41, 135.82, 133.97, 132.76, 132.55, 129.27, 128.76, 127.93, 127.63, 126.32, 126.30, 125.73, 125.57, 124.28, 123.31, 115.99,

115.33, 104.33, 55.45, 50.32, 44.80, 33.84, 19.84, 13.77. HRMS (*m/z*): [M+K] calcd for $C_{25}H_{25}KNO_2$, 410.1522; found 410.1527. HPLC t_R = 11.439 min; purity = 99.8%

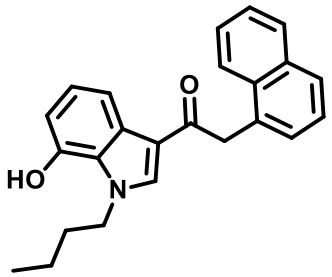

1-(1-Butyl-7-hydroxy-1H-indol-3-yl)-2-(naphthalen-1-yl)ethanone (458). Compound **458** was synthesized from compound **435** using general procedure B to afford 0.07 g (55% yield) isolated as an off brown solid, mp = decomposition at 213-216 °C. TLC system: 30% EtOAc/70% *n*-hexanes. ^{1}H NMR (500 MHz, DMSO) δ 9.32 (s, 1H), 8.85 (s, 1H), 8.65 – 8.58 (m, 1H), 8.39 – 8.33 (m, 1H), 8.28 (dt, *J* = 4.3, 8.6, 2H), 8.00 – 7.88 (m, 4H), 7.42 (t, *J* = 7.8, 1H), 7.15 (d, *J* = 7.6, 1H), 5.13 (s, 2H), 5.02 (t, *J* = 7.1, 2H), 2.41 – 2.33 (m, 2H), 1.81 (dq, *J* = 7.4, 14.9, 2H), 1.40 (t, *J* = 7.4, 3H). ^{13}C NMR (126 MHz, DMSO) δ 191.47, 144.32, 136.79, 133.93, 133.52, 132.76, 129.74, 128.34, 128.04, 127.00, 125.69, 125.40, 125.36, 124.74, 122.71, 115.59, 113.81, 108.35, 49.30, 43.73, 33.85, 19.44, 13.07. HRMS (*m/z*): [M+Na+CH_3CN] calcd for $C_{26}H_{26}N_2NaO_2$, 421.1892; found 421.1924. HPLC t_R = 6.458 min; purity = 99.8% using 70% CH_3CN/30% H_2O (0.1% formic acid).

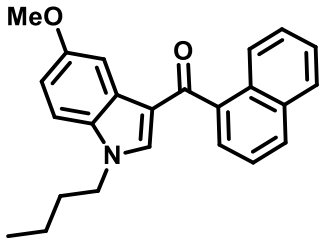

(1-Butyl-5-methoxy-1H-indol-3-yl)(naphthalen-1-yl)methanone (459). Compound **459** was synthesized from compound **439** using general procedure D and 1-naphthoylacetyl chloride to afford 0.36 g (16% yield) isolated as an amorphous yellow oil. ^{1}H NMR (500 MHz, $CDCl_3$) δ 8.18 (d, *J* = 8.5, 1H), 8.01 (d, *J* = 2.5, 1H), 7.96 (d, *J* = 8.2, 1H), 7.90 (d, *J* = 7.6, 1H), 7.64 (dd, *J* = 1.2, 7.0, 1H), 7.54 – 7.44 (m, 3H), 7.28 (d, *J* = 2.2, 1H), 7.25 (s, 1H), 6.98 (dd, *J* = 2.6, 8.9, 1H), 4.02 (t, *J* = 7.2, 2H), 3.92 (s, 3H), 1.81 – 1.71 (m, 2H), 1.32 – 1.22 (m, 2H), 0.88 (t, *J* = 7.4, 3H). ^{13}C NMR (126 MHz, $CDCl_3$) δ 192.12, 156.75, 139.25, 138.00, 133.81, 131.99, 130.88, 129.96, 128.24, 127.90, 126.80, 126.37, 126.11, 125.83, 124.65, 117.25, 114.28, 110.95, 103.99, 55.93, 47.23, 31.95, 20.11, 13.65. HRMS (*m/z*): [M+Na] calcd for $C_{26}H_{26}N_2NaO_2$, 421.1892; found 421.1930. HPLC t_R = 16.771 min; purity = 99.9% using 70% CH_3CN/30% H_2O (0.1% formic acid).

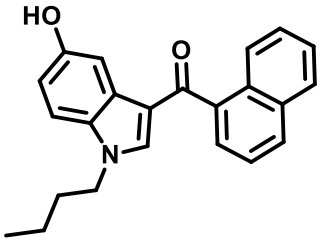

(1-Butyl-5-hydroxy-1H-indol-3-yl)(naphthalen-1-yl)methanone (460). Compound **460** was synthesized from compound **440** using general procedure B to afford 0.59 g (90% yield)

isolated as a lightly yellow solid, mp = 209-212 °C. TLC system: 30% EtOAc/70% *n*-hexanes. ^{1}H NMR (500 MHz, DMSO) δ 9.20 (s, 1H), 8.07 (d, *J* = 7.8, 1H), 8.02 (d, *J* = 7.9, 1H), 7.98 (d, *J* = 8.5, 1H), 7.74 (d, *J* = 2.4, 1H), 7.65 – 7.59 (m, 3H), 7.58 – 7.54 (m, 1H), 7.50 (ddd, *J* = 1.4, 6.8, 8.2, 1H), 7.41 (d, *J* = 8.8, 1H), 6.80 (dd, *J* = 2.4, 8.8, 1H), 4.11 (t, *J* = 7.2, 2H), 1.69 – 1.61 (m, 2H), 1.23 – 1.14 (m, 2H), 0.81 (t, *J* = 7.4, 3H). ^{13}C NMR (126 MHz, DMSO) δ 190.38, 153.63, 138.93, 138.61, 133.14, 130.83, 129.92, 129.30, 128.09, 127.39, 126.46, 126.06, 125.31, 125.20, 124.82, 115.24, 112.81, 111.40, 106.01, 45.86, 31.33, 19.16, 13.27. HRMS (*m/z*): [M+Na+CH_3CN] calcd for $C_{25}H_{24}N_2NaO_2$, 407.1735; found 407.1777. HPLC t_R = 13.460 min; purity = 100.0% using 60% CH_3CN/40% H_2O (0.1% formic acid).

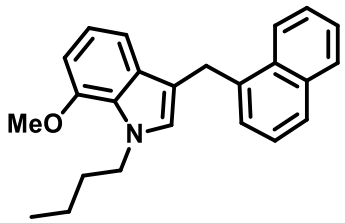

1-Butyl-7-methoxy-3-(naphthalen-1-ylmethyl)-1H-indole (461). $LiAlH_4$ (4.9 mL, 4.85 mmol, 4 equiv) was dissolved in THF (1M) and a solution of $AlCl_3$ (1.94 g, 14.5 mmol, 12 equiv) in THF (8 mL) was added dropwise at 0 °C. After 30 min, indole **435** (0.433 g, 1.21 mmol, 1 equiv) in THF (9 mL) was added to the reaction mixture and allowed to stir at 21 °C for 48 hrs. Upon completion, reaction mixture was cooled in an ice-bath and carefully quenched with H_2O and acidified with 1 N HCl to pH = 3. The organic phase was then separated and washed with $NaHCO_3$, brine, and dried over anhydrous Na_2SO_4. The solvent was evaporated under reduced pressure and the resulting residue was purified by flash column chromatography on silica gel using mixtures of EtOAc/*n*-hexanes to afford 0.07 g (18% yield) isolated as a

pinkish oil. TLC system: 10% EtOAc/90% *n*-hexanes. ^{1}H NMR (500 MHz, $CDCl_3$) δ 8.11 (d, *J* = 8.0, 1H), 7.91 – 7.85 (m, 1H), 7.76 (d, *J* = 8.0, 1H), 7.46 (tt, *J* = 3.5, 8.3, 2H), 7.42 – 7.34 (m, 2H), 7.21 (dd, *J* = 0.8, 8.0, 1H), 7.00 (t, *J* = 7.8, 1H), 6.65 (d, *J* = 7.5, 1H), 6.50 (s, 1H), 4.51 (s, 2H), 4.24 (t, *J* = 7.2, 2H), 3.94 (s, 3H), 1.70 (dt, *J* = 7.4, 14.8, 2H), 1.24 (dq, *J* = 7.4, 14.7, 2H), 0.87 (t, *J* = 7.4, 3H). ^{13}C NMR (126 MHz, $CDCl_3$) δ 147.93, 137.47, 134.22, 132.61, 130.65, 128.93, 128.32, 127.11, 126.92, 126.31, 126.09, 126.05, 125.83, 124.87, 119.55, 113.82, 112.31, 102.72, 55.68, 49.26, 34.70, 29.37, 20.24, 14.16. HRMS (*m/z*): [M^+] calcd for $C_{24}H_{25}NO$, 343.1936; found 343.1887. HPLC t_R = 12.038 min; purity = 99.9% using 90% CH_3CN/10% H_2O (0.1% formic acid).

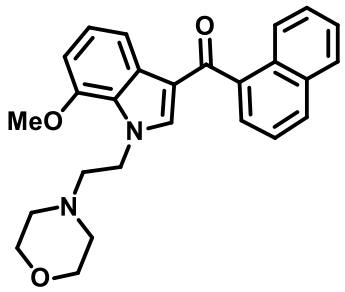

(7-Methoxy-1-(2-morpholinoethyl)-1H-indol-3-yl)(naphthalen-1-yl)methanone (462). Compound **462** was synthesized from compound **434** using general procedure D and 1-naphthoylacetyl chloride to afford 0.16 g (16% yield) isolated as a yellow solid, mp = 149-152 °C. TLC system: 50% EtOAc/50% *n*-hexanes. ^{1}H NMR (500 MHz, $CDCl_3$) δ 8.18 – 8.10 (m, 2H), 7.95 (d, *J* = 8.2, 1H), 7.89 (d, *J* = 7.5, 1H), 7.63 (dd, *J* = 1.2, 7.0, 1H), 7.54 – 7.41 (m, 3H), 7.27 – 7.23 (m, 3H), 6.77 (d, *J* = 7.4, 1H), 4.40 (t, *J* = 6.5, 2H), 3.94 (s, 3H), 3.60 – 3.49 (m, 4H), 2.67 (t, *J* = 6.6, 2H), 2.42 – 2.33 (m, 4H). ^{13}C NMR (126 MHz, $CDCl_3$) δ 192.18, 147.29, 140.00, 139.28, 133.80, 130.86, 130.00, 129.34, 128.26, 126.86, 126.45, 126.38, 126.06, 125.82,

124.55, 123.67, 117.60, 115.47, 104.70, 66.99, 59.29, 55.48, 53.77, 47.37. HRMS (*m/z*): [M+H] calcd for $C_{26}H_{27}N_2O_3^+$, 415.2016; found 415.1985. HPLC t_R = 7.049 min; purity = 95.0% using 30% CH_3CN/70% H_2O (0.1% formic acid).

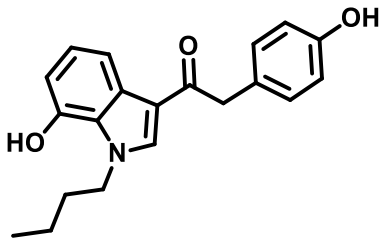

1-(1-Butyl-7-hydroxy-1H-indol-3-yl)-2-(4-hydroxyphenyl)ethanone (463).

Compound **463** was synthesized from compound **435** using general procedure B to afford 0.05 g (17% yield) isolated as an off-white solid, mp = decomposition at 197-200 °C. TLC system: 30% EtOAc/70% *n*-hexanes. ^{1}H NMR (500 MHz, Acetone) δ 8.86 (s, 1H), 8.23 (s, 1H), 8.16 (s, 1H), 7.86 (dd, *J* = 0.9, 8.0, 1H), 7.21 (d, *J* = 8.6, 2H), 6.98 (t, *J* = 7.8, 1H), 6.80 – 6.73 (m, 2H), 6.68 (dd, *J* = 0.9, 7.6, 1H), 4.54 (t, *J* = 7.1, 2H), 4.01 (s, 2H), 1.94 – 1.85 (m, 2H), 1.39 – 1.29 (m, 2H), 0.94 (t, *J* = 7.4, 3H). ^{13}C NMR (126 MHz, Acetone) δ 193.14, 156.81, 145.21, 137.93, 131.20, 130.75, 128.46, 126.87, 123.57, 116.43, 115.91, 115.82, 114.76, 109.25, 50.17, 46.31, 34.79, 20.37, 13.99. HRMS (*m/z*): [M+Na] calcd for $C_{22}H_{24}N_2NaO_3$, 387.1685; found 387.1658. HPLC t_R = 4.998 min; purity = 99.4% using 60% CH_3CN/40% H_2O (0.1% formic acid).

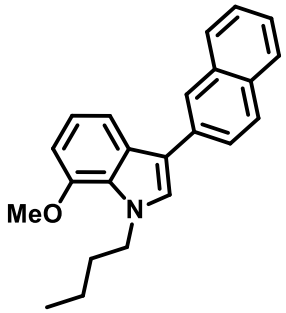

1-Butyl-7-methoxy-3-(naphthalen-2-yl)-1H-indole (444). $Pd(OAc)_2$ (2 mg, 0.01 mmol, 0.01 equiv), SPhos (7.4 mg, 0.02 mmol, 0.02 equiv), K_3PO_4 (379 mg, 1.79 mmol, 2 equiv), and 2-naphthaleneboronic acid (230 mg, 1.34 mmol, 1.5 equiv) were placed into a round bottom pressure flask and flushed with Ar. Intermediate **442** (294 mg, 0.89 mmol, 1 equiv) in toluene (1 mL) was then added and the reaction mixture was allowed to stir at 100 °C overnight. Reaction was monitored via TLC and upon completion, it was allowed to cool to 21 °C and diluted with Et_2O (10mL). Mixture was then filtered through a pad of Celite and concentrated under reduced pressure. The resulting residue was purified by flash column chromatography on silica gel using mixtures of DCM/*n*-hexanes, to afford 0.15 g (50% yield) isolated as a clear amorphous oil, TLC system: 15% DCM/85% *n*-hexanes. ^{1}H NMR (500 MHz, $CDCl_3$) δ 8.10 (s, 1H), 7.93 – 7.84 (m, 4H), 7.80 (dd, *J* = 1.8, 8.4, 1H), 7.65 (dt, *J* = 3.2, 6.3, 1H), 7.47 (dddd, *J* = 1.3, 6.9, 8.0, 16.2, 2H), 7.29 (s, 1H), 7.12 (t, *J* = 7.9, 1H), 6.72 (d, *J* = 7.7, 1H), 4.46 (t, *J* = 7.2, 2H), 3.99 (s, 3H), 1.92 – 1.83 (m, 2H), 1.45 – 1.36 (m, 2H), 0.98 (t, *J* = 7.4, 3H). ^{13}C NMR (126 MHz, $CDCl_3$) δ 147.84, 134.10, 133.46, 131.93, 128.72, 128.20, 127.80, 127.75, 127.51, 126.71, 126.56, 126.12, 125.11, 125.07, 120.43, 116.57, 112.74, 102.83, 55.45, 49.49, 34.43, 20.06, 13.91. HRMS (*m/z*): [M^+] calcd for $C_{23}H_{23}NO$, 329.1780; found 329.1747. HPLC t_R = 12.570 min; purity = 96.7% using 90% CH_3CN/10% H_2O (0.1% formic acid).

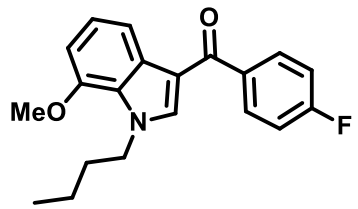

(1-Butyl-7-methoxy-1H-indol-3-yl)(4-fluorophenyl)methanone (464). Compound **464** was synthesized from compound **434** using general procedure D and 4-fluorobenzoyl chloride to afford 0.28 g (49% yield) isolated as a pinkish solid, mp = 91-94 °C. ^{1}H NMR (500 MHz, $CDCl_3$) δ 8.02 (dd, *J* = 0.8, 8.0, 1H), 7.89 – 7.84 (m, 2H), 7.45 (s, 1H), 7.26 (t, *J* = 8.0, 1H), 7.22 – 7.17 (m, 2H), 6.80 (d, *J* = 7.4, 1H), 4.44 (t, *J* = 7.2, 2H), 4.00 (s, 3H), 1.91 – 1.81 (m, 2H), 1.43 – 1.32 (m, 2H), 0.98 (t, *J* = 7.4, 3H). ^{13}C NMR (126 MHz, $CDCl_3$) δ 189.45, 165.64, 163.64, 147.43, 137.73, 137.64 (d, *J* = 3.1 Hz), 131.45 (d, *J* = 8.7 Hz), 129.80, 126.50, 123.39, 116.08 (d, *J* = 21.9 Hz), 115.28, 115.13, 104.57, 55.49, 50.37, 33.97, 19.90, 13.79. HRMS (*m/z*): [M+Na+CH_3CN] calcd for $C_{22}H_{23}FN_2NaO_2$, 389.1641; found 389.1608. HPLC t_R = 8.765 min; purity = 99.8%.

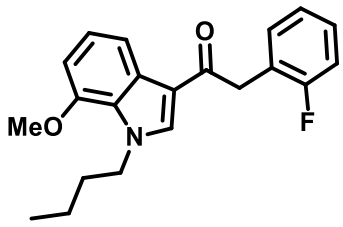

1-(1-Butyl-7-methoxy-1H-indol-3-yl)-2-(2-fluorophenyl)ethanone (465). Compound **465** was synthesized from compound **434** using general procedure D and an acid chloride made in situ from 2-(2-fluorophenyl)acetic acid[489] to afford 0.30 g (35% yield) isolated as a darker yellow solid, mp = 86-88 °C. ^{1}H NMR (500 MHz, $CDCl_3$) δ 8.04 (dd, *J* = 0.8, 8.1, 1H), 7.78 (s,

1H), 7.41 (td, *J* = 1.7, 7.6, 1H), 7.29 – 7.23 (m, 1H), 7.21 (t, *J* = 8.0, 1H), 7.16 – 7.07 (m, 2H), 6.75 (d, *J* = 7.4, 1H), 4.44 (t, *J* = 7.2, 2H), 4.20 (s, 2H), 3.97 (s, 3H), 1.91 – 1.82 (m, 2H), 1.42 – 1.32 (m, 2H), 0.99 (t, *J* = 7.4, 3H). ^{13}C NMR (126 MHz, $CDCl_3$) δ 190.37, 160.78, 158.83, 146.34, 135.03 (d, *J* = 1.9 Hz), 130.69 (d, *J* = 4.2 Hz), 128.14, 127.51 (d, *J* = 8.2 Hz), 125.39, 123.21 (d, *J* = 3.5 Hz), 122.30, 122.07 (d, *J* = 15.8 Hz), 114.61, 114.37, 114.19, 114.17, 103.31, 54.40, 49.30, 38.49, 38.48, 32.82, 18.80, 12.73. [M+Na] calcd for $C_{21}H_{22}FNNaO_2$, 362.1532; found 362.1513. HPLC t_R = 8.732 min; purity = 99.6%.

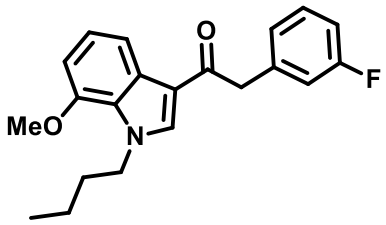

1-(1-Butyl-7-methoxy-1H-indol-3-yl)-2-(3-fluorophenyl)ethanone (466). Compound **466** was synthesized from compound **434** using general procedure D and an acid chloride made *in situ* from 2-(3-fluorophenyl)acetic acid[489] to afford 0.21 g (27% yield) isolated as a yellow oil. ^{1}H NMR (500 MHz, $CDCl_3$) δ 7.98 (dd, *J* = 0.8, 8.1, 1H), 7.63 (s, 1H), 7.28 – 7.21 (m, 2H), 7.16 (t, *J* = 8.0, 1H), 7.08 (d, *J* = 8.1, 1H), 7.03 (d, *J* = 9.8, 1H), 6.91 (td, *J* = 1.8, 8.3, 1H), 6.71 (d, *J* = 7.5, 1H), 4.38 (t, *J* = 7.2, 2H), 4.10 (s, 2H), 3.92 (s, 3H), 1.85 – 1.75 (m, 2H), 1.36 – 1.25 (m, 2H), 0.93 (t, *J* = 7.4, 3H). ^{13}C NMR (126 MHz, $CDCl_3$) δ 191.85, 163.92, 161.97, 147.41, 138.39 (d, *J* = 7.7 Hz), 138.36, 135.97, 129.97 (d, *J* = 8.3 Hz), 129.16, 126.44, 125.17 (d, *J* = 2.9 Hz), 123.45, 116.54, 116.37, 115.86, 115.21, 113.69, 113.52, 104.46, 55.46, 50.40, 46.55, 46.54, 33.88, 19.87, 13.77. HRMS (*m/z*): [M+Na] calcd for $C_{21}H_{22}FNNaO_2$, 362.1532; found

362.1503. HPLC t_R = 13.931 min; purity = 99.9% using 50% CH_3CN/50% H_2O (0.1% formic acid).

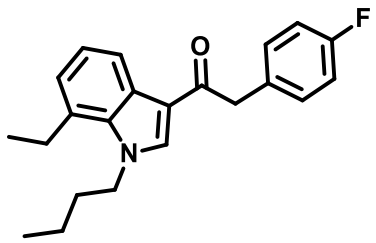

1-(1-Butyl-7-ethyl-1H-indol-3-yl)-2-(4-fluorophenyl)ethanone (467). Compound **467** was synthesized from compound **467** using general procedure D and 4-fluorophenylacetyl chloride to afford 0.34 g (39% yield) isolated as an white powder, mp = 67-70 °C. ^{1}H NMR (500 MHz, $CDCl_3$) δ 8.34 (dd, *J* = 1.2, 8.0, 1H), 7.72 (s, 1H), 7.32 – 7.27 (m, 2H), 7.25 – 7.20 (m, 1H), 7.10 (d, *J* = 6.5, 1H), 7.04 – 6.98 (m, 2H), 4.35 – 4.28 (m, 2H), 4.12 (s, 2H), 3.02 (q, *J* = 7.5, 2H), 1.87 – 1.78 (m, 2H), 1.42 – 1.32 (m, 5H), 0.98 (t, *J* = 7.4, 3H). ^{13}C NMR (126 MHz, $CDCl_3$) δ 192.35, 162.81, 160.87, 136.80, 134.58, 132.03 (d, *J* = 3.2 Hz), 131.23 (d, *J* = 7.9 Hz), 128.22, 127.79, 124.78, 123.06, 120.82, 115.82, 115.50, 115.33, 49.80, 46.00, 34.07, 25.52, 20.01, 16.28, 13.75. HRMS (*m/z*): [M+Na+CH_3CN] calcd for $C_{24}H_{27}FN_2NaO$, 401.2005; found 401.1976. HPLC t_R = 9.645 min; purity = 99.9%.

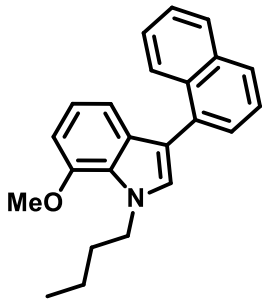

1-Butyl-7-methoxy-3-(naphthalen-1-yl)-1H-indole (443). Intermediate **443** (512 mg, 1.56 mmol, 1 equiv) and $Pd(PPh_3)_4$ (54 mg, 0.05 mmol, 0.03 equiv) were placed into a round bottom flask and flushed with Ar. Solvent (DME, 6 mL) was then added and allowed to stir for 10 min upon which the solution was degassed by bubbling with Ar for 15 min. Sodium carbonate (2M [1.06 g in 5 mL H_2O, 1.6 ml], 3.11mmol, 2 equiv) and 1-naphthaleboronic acid (401 mg, 2.33 mmol, 1.5 equiv) in EtOH (1 mL) were added and the reaction mixture was refluxed. Reaction was monitored via TLC and upon completion, it was allowed to cool to 21 °C and EtOAc was added. Mixture was then filtered through a pad of Celite and concentrated under reduced pressure. The resulting residue was purified by flash column chromatography on silica gel using 3% DCM/97% n-hexanes to afford 0.17 g (37% yield) isolated as a yellow solid, mp = 74-76 °C. TLC system: 10% DCM/90% n-hexanes. ^{1}H NMR (500 MHz, $CDCl_3$) δ 8.10 (d, J = 8.2, 1H), 7.92 (d, J = 8.2, 1H), 7.85 (d, J = 8.0, 1H), 7.53 (dddd, J = 1.3, 6.9, 8.1, 23.6, 3H), 7.41 (ddd, J = 1.3, 6.8, 8.2, 1H), 7.19 (s, 1H), 7.09 (dd, J = 0.9, 8.0, 1H), 7.00 (t, J = 7.8, 1H), 6.70 (d, J = 7.3, 1H), 4.50 (t, J = 7.1, 2H), 4.01 (s, 3H), 1.95 – 1.86 (m, 2H), 1.47 – 1.37 (m, 2H), 0.99 (t, J = 7.4, 3H). ^{13}C NMR (126 MHz, $CDCl_3$) δ 147.75, 134.08, 133.36, 132.64, 130.54, 128.76, 128.28, 127.75, 126.92, 126.80, 125.90, 125.70, 125.67, 125.65, 119.90, 114.86, 113.25, 102.56, 55.47, 49.36, 34.47, 20.08, 13.93. HRMS (*m/z*): [M^+] calcd for $C_{23}H_{23}NO$, 329.1780; found 329.1747. HPLC t_R = 11.727 min; purity = 95.4% using 90% CH_3CN/10% H_2O (0.1% formic acid).

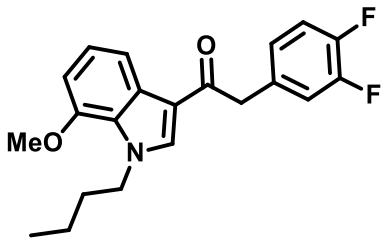

1-(1-Butyl-7-methoxy-1H-indol-3-yl)-2-(3,4-difluorophenyl)ethanone (468).

Compound **468** was synthesized from compound **434** using general procedure D and an acid chloride made *in situ* from 2-(3,4-difluorophenyl)acetic acid[489] to afford 0.07 g (8% yield) isolated as an off-white solid, mp = 88-90 °C. ^{1}H NMR (500 MHz, $CDCl_3$) δ 8.01 (dd, *J* = 0.8, 8.1, 1H), 7.68 (s, 1H), 7.21 (t, *J* = 8.0, 1H), 7.19 – 7.14 (m, 1H), 7.14 – 7.09 (m, 1H), 7.06 (d, *J* = 2.2, 1H), 6.76 (d, *J* = 7.8, 1H), 4.44 (t, *J* = 7.2, 2H), 4.11 (s, 2H), 3.97 (s, 3H), 1.92 – 1.79 (m, 2H), 1.37 (dq, *J* = 7.4, 14.8, 2H), 0.99 (t, *J* = 7.4, 3H). ^{13}C NMR (126 MHz, $CDCl_3$) δ 191.44 , 150.14 (dd, *J* = 247.8, 12.8 Hz), 149.30 (dd, *J* = 246.7, 12.6 Hz), 147.32 , 135.70 , 132.64 (dd, *J* = 6.0, 4.0 Hz), 128.98 , 126.38 , 125.38 (dd, *J* = 6.1, 3.6 Hz), 123.43 , 118.36 (d, *J* = 17.3 Hz), 117.08 (d, *J* = 17.1 Hz), 115.66 , 115.02 , 104.41 , 55.37 , 50.34 , 46.07 – 44.76 (m), 33.81 , 19.80 , 13.68 . HRMS (*m/z*): [M+Na+CH_3CN] calcd for $C_{23}H_{24}F_2N_2NaO_2$, 421.1704; found 421.1678. HPLC t_R = 8.678 min; purity = 100.0%.

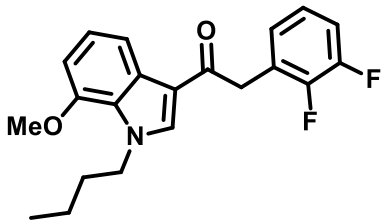

1-(1-Butyl-7-methoxy-1H-indol-3-yl)-2-(2,3-difluorophenyl)ethanone (469).

Compound **469** was synthesized from compound **434** using general procedure D and an acid chloride made *in situ* from 2-(2,3-difluorophenyl)acetic acid[489] to afford 0.23 g (24% yield) isolated as a yellow oil. ^{1}H NMR (500 MHz, $CDCl_3$) δ 8.02 (dd, *J* = 0.8, 8.1, 1H), 7.78 (s, 1H), 7.21 (t, *J* = 8.0, 1H), 7.16 (t, *J* = 6.7, 1H), 7.13 – 7.03 (m, 2H), 6.76 (d, *J* = 7.4, 1H), 4.45 (t, *J* = 7.2, 2H), 4.23 (d, *J* = 1.3, 2H), 3.98 (s, 3H), 1.92 – 1.83 (m, 2H), 1.43 – 1.33 (m, 2H), 0.99 (t, *J* =

7.4, 3H). ^{13}C NMR (126 MHz, $CDCl_3$) δ 190.40 , 150.68 (dd, *J* = 222.0, 13.0 Hz), 148.72 (dd, *J* = 220.5, 13.1 Hz), 147.32 , 135.89 (d, *J* = 1.6 Hz), 129.00 , 126.37 , 126.29 (t, *J* = 3.2 Hz), 125.38 (d, *J* = 12.6 Hz), 123.91 (dd, *J* = 6.9, 4.6 Hz), 123.37 , 115.65 (d, *J* = 17.1 Hz), 115.44 , 115.03 , 104.36 , 55.36 , 50.32 , 39.10 (t, *J* = 1.8 Hz), 33.78 , 19.76 , 13.67 . HRMS (*m/z*): [M+Na+CH_3CN] calcd for $C_{23}H_{24}F_2N_2NaO_2$, 421.1704; found 421.1687. HPLC t_R = 8.827 min; purity = 100.0%.

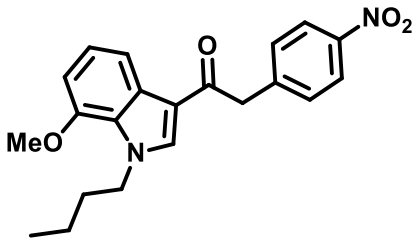

1-(1-butyl-7-methoxy-1H-indol-3-yl)-2-(4-nitrophenyl)ethanone (470). Compound **470** was synthesized from compound **434** using general procedure D and an acid chloride made *in situ* from 2-(4-nitrophenyl)acetic acid[489] to afford 0.41 g (46% yield) isolated as an off-brown solid. mp = 96-98 °C. ^{1}H NMR (500 MHz, $CDCl_3$) δ 8.22 – 8.15 (m, 2H), 7.96 (dd, *J* = 8.0, 0.9 Hz, 1H), 7.69 (s, 1H), 7.51 – 7.45 (m, 2H), 7.19 (t, *J* = 8.0 Hz, 1H), 6.74 (dd, *J* = 7.9, 0.9 Hz, 1H), 4.42 (t, *J* = 7.2 Hz, 2H), 4.25 (s, 2H), 3.94 (s, 3H), 1.89 – 1.78 (m, 2H), 1.39 – 1.29 (m, 2H), 0.96 (t, *J* = 7.4 Hz, 3H). ^{13}C NMR (126 MHz, $CDCl_3$) δ 190.44, 147.36, 146.81, 143.38, 135.73, 130.42, 128.90, 126.43, 123.63, 123.59, 115.70, 114.94, 104.53, 55.39, 50.41, 46.20, 33.82, 19.81, 13.69.HRMS (*m/z*): [2M+Na] calcd for $C_{42}H_{44}N_4NaO_8$, 755.3057; found 755.3074. HPLC t_R = 14.342 min; purity = 98.4% using 70% CH_3CN/30% H_2O.

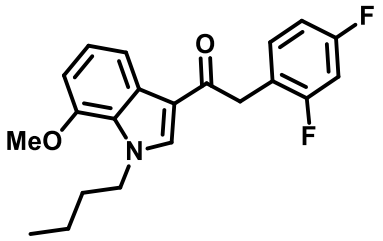

1-(1-butyl-7-methoxy-1H-indol-3-yl)-2-(2,4-difluorophenyl)ethanone (471).

Compound **471** was synthesized from compound **434** using general procedure D and an acid chloride made *in situ* from 2,4-difluorophenyl acetic acid[489] to afford 0.21 g (23% yield) isolated as a pinkish solid. mp = 113-115 °C. ^{1}H NMR (500 MHz, $CDCl_3$) δ 7.97 (dd, *J* = 8.0, 0.9 Hz, 1H), 7.73 (s, 1H), 7.33 (td, *J* = 8.4, 6.4 Hz, 1H), 7.17 (t, *J* = 8.0 Hz, 1H), 6.87 – 6.79 (m, 2H), 6.72 (dd, *J* = 7.9, 0.9 Hz, 1H), 4.41 (t, *J* = 7.2 Hz, 2H), 4.12 (d, *J* = 1.3 Hz, 2H), 3.94 (s, 3H), 1.88 – 1.79 (m, 2H), 1.39 – 1.29 (m, 2H), 0.95 (t, *J* = 7.4 Hz, 3H). ^{13}C NMR (126 MHz, $CDCl_3$) δ 190.91 , 161.95 (dd, *J* = 247.3, 12.1 Hz), 160.68 (dd, *J* = 247.2, 11.9 Hz), 147.31 , 135.81 (d, *J* = 1.7 Hz), 132.28 (dd, *J* = 9.5, 5.9 Hz), 129.00 , 126.36 , 123.34 , 118.79 (dd, *J* = 16.0, 3.9 Hz), 115.47 , 115.04 , 111.25 (dd, *J* = 21.1, 3.7 Hz), 104.32 , 103.62 (t, *J* = 25.8 Hz), 55.36 , 50.30 , 38.75 (d, *J* = 1.6 Hz), 33.79 , 19.77 , 13.68. HRMS (*m/z*): [M+Na+CH_3CN] calcd for $C_{23}H_{24}F_2N_2NaO_2$, 421.1704; found 421.1714. HPLC t_R = 9.087 min; purity = 99.9%.

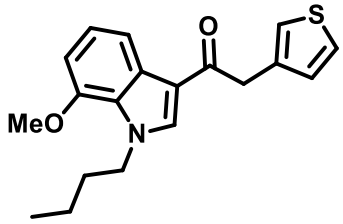

1-(1-butyl-7-methoxy-1H-indol-3-yl)-2-(thiophen-3-yl)ethanone (472). Compound **472** was synthesized from compound **434** using general procedure D and an acid chloride made *in situ* from 3-thiopheneacetic acid[489] to afford 0.21 g (38% yield) isolated as a brown-yellow solid. mp= 70-73 °C. ^{1}H NMR (500 MHz, $CDCl_3$) δ 8.01 (dd, *J* = 8.0, 0.9 Hz, 1H), 7.63 (s, 1H), 7.28 – 7.26 (m, 1H), 7.17 (t, *J* = 8.0 Hz, 1H), 7.14 (dq, *J* = 3.0, 1.0 Hz, 1H), 7.07 (dd, *J* = 4.9, 1.3 Hz, 1H), 6.71 (dd, *J* = 7.9, 0.9 Hz, 1H), 4.38 (t, *J* = 7.2 Hz, 2H), 4.15 – 4.13 (m, 2H), 3.93 (s, 3H), 1.81 (ddd, *J* = 8.7, 6.7, 1.4 Hz, 2H), 1.37 – 1.27 (m, 2H), 0.94 (t, *J* = 7.4 Hz, 3H). ^{13}C NMR (126 MHz, $CDCl_3$) δ 192.08, 147.28, 135.86, 135.76, 129.10, 128.72, 126.27, 125.50, 123.23, 122.21, 115.68, 115.13, 104.25, 55.35, 50.24, 41.54, 33.80, 19.77, 13.69. HRMS (*m/z*): [2M+Na] calcd for $C_{38}H_{42}N_2NaO_4S_2$, 677.2484; found 677.2466. HPLC t_R = 7.554 min; purity = 99.9%.

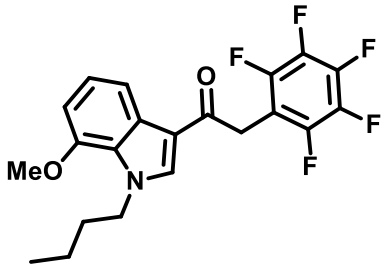

1-(1-butyl-7-methoxy-1H-indol-3-yl)-2-(perfluorophenyl)ethanone (473). Compound **473** was synthesized from compound **434** using general procedure D and an acid chloride made *in situ* from 2,3,4,5,6-pentafluororphenyl acetic acid[489] to afford 0.14 g (29% yield) isolated as a light brown solid. mp = 106-108 °C. ^{1}H NMR (500 MHz, $CDCl_3$) δ 7.90 (dd, *J* = 8.0, 0.9 Hz, 0H), 7.77 (s, 0H), 7.19 (t, *J* = 8.0 Hz, 0H), 6.74 (dd, *J* = 8.0, 0.9 Hz, 0H), 4.44 (t, *J* = 7.2 Hz, 1H), 4.28 (t, *J* = 1.5 Hz, 1H), 3.95 (s, 1H), 1.92 – 1.82 (m, 1H), 1.44 – 1.33 (m, 1H), 0.98 (t, *J* =

7.4 Hz, 1H). ^{13}C NMR (126 MHz, $CDCl_3$) δ 138.92 – 137.71 (m), 136.92 – 135.80 (m), 187.32 , 138.74 – 138.04 (m), 147.40 , 146.39 (t, *J* = 7.6 Hz), 144.41 (d, *J* = 11.3 Hz), 141.24 , 139.23 , 138.44 , 139.62 – 138.76 (m), 136.44 , 135.47 , 128.77 , 126.37 , 123.61 , 115.04 , 114.80 , 104.49 , 55.40 , 50.46 , 33.87 , 33.09 , 145.09 – 143.69 (m), 19.84 , 13.71 , 141.69 – 140.57 (m), 146.92 – 145.69 (m). HRMS (*m/z*): [M+Na+CH_3CN] calcd for $C_{23}H_{21}F_5N_2NaO_2$, 475.1421; found 475.1444. HPLC t_R = 12.530 min; purity = 99.2%.

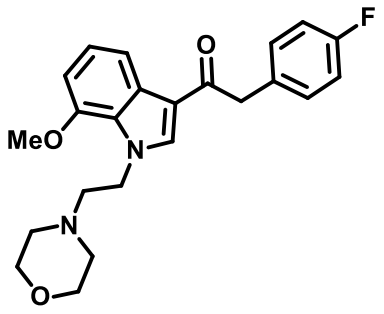

2-(4-fluorophenyl)-1-(7-methoxy-1-(2-morpholinoethyl)-1H-indol-3-yl)ethanone (474). Compound **474** was synthesized from compound **434** using general procedure D and an acid chloride made *in situ* from 4-fluorophenylacetic acid[489] to afford 0.11 g (14% yield) isolated as a brown oil. ^{1}H NMR (500 MHz, $CDCl_3$) δ 8.00 (dd, *J* = 8.1, 0.9 Hz, 1H), 7.72 (s, 1H), 7.30 – 7.26 (m, 2H), 7.18 (t, *J* = 8.0 Hz, 1H), 7.04 – 6.97 (m, 2H), 6.73 (dd, *J* = 7.9, 0.9 Hz, 1H), 4.53 (t, *J* = 6.7 Hz, 2H), 4.10 (s, 2H), 3.94 (s, 3H), 3.71 – 3.66 (m, 4H), 2.78 (t, *J* = 6.7 Hz, 2H), 2.53 – 2.46 (m, 4H). ^{13}C NMR (126 MHz, $CDCl_3$) δ 192.36, 162.73, 160.79, 147.08, 136.32, 131.43 (d, *J* = 3.2 Hz), 130.84, 130.77, 129.01, 126.14, 123.41, 116.04, 115.48 (d, *J* = 21.8 Hz), 115.25, 104.36, 66.88, 59.39, 55.33, 53.79, 47.53, 45.86.

HRMS (*m/z*): [M+Na] calcd for $C_{23}H_{25}FN_2NaO_3$, 419.1747; found 419.1757. HPLC t_R = 1.650 min; purity = 96.5% using 50% CH_3CN/50% H_2O (0.1% formic acid).

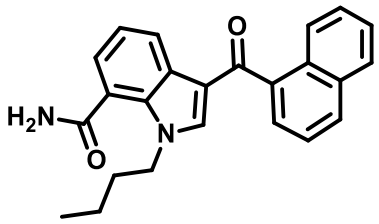

3-(1-naphthoyl)-1-butyl-1H-indole-7-carboxamide (450). To a solution of 3-(1-naphthoyl)-1-butyl-1H-indole-7-carboxylic acid (0.047 g, 0.127 mmol, 1 equiv) in DCM at ambient temperature were added EDCI (0.029 g, 0.152 mmol, 1.2 equiv), HOBt (0.021 g, 0.152 mmol, 1.2 equiv) and NH_3 (2.0 M in MeOH, 0.25 mL, 0.51 mmol, 4 equiv). The reaction mixture was allowed to stir at ambient temperature for 16 hours. Upon completion, the solvent was evaporated and the residue partitioned between EtOac (10 mL) and H_2O (10 mL). The aqueous layer was then washed with EtOAc (2x) and the combined organic extracts were dried over Na_2SO_4, filtered, and concentrated under reduced pressure. The resulting residue was purified by flash column chromatography on silica gel using of 50% EtOAc/50% *n*-hexanes, to afford 0.025 g (53% yield) isolated as a white solid, mp = 176-179 °C. TLC system: 40% EtOAc/60% *n*-hexanes. ^{1}H NMR (500 MHz, $CDCl_3$) δ 8.72 (dd, *J* = 8.0, 1.2 Hz, 1H), 8.17 (ddt, *J* = 8.4, 1.4, 0.8 Hz, 1H), 7.99 (dt, *J* = 8.4, 1.0 Hz, 1H), 7.95 – 7.89 (m, 1H), 7.65 (dd, *J* = 7.0, 1.3 Hz, 1H), 7.54 (ddd, *J* = 8.1, 6.8, 5.3 Hz, 2H), 7.51 – 7.46 (m, 2H), 7.37 – 7.35 (m, 2H), 6.12 – 6.04 (m, 1H), 5.81 (s, 1H), 4.33 – 4.25 (m, 2H), 1.70 – 1.61 (m, 2H), 1.25 – 1.17 (m, 2H), 0.85 (t, *J* = 7.4 Hz, 3H). ^{13}C NMR (126 MHz, $CDCl_3$) δ 192.05, 170.44, 140.61, 138.73, 133.73, 132.57, 130.73, 130.23, 129.32, 128.21, 126.86, 126.35, 126.06, 125.86, 125.79, 124.55, 123.23,

121.98, 121.07, 117.20, 49.75, 32.48, 19.80, 13.63. HRMS (*m/z*): [M+Na+CH_3CN] calcd for $C_{26}H_{25}N_3NaO_2$, 434.1844; found 434.1855. HPLC t_R = 8.227 min; purity = 100.0% using 60% CH_3CN/40% H_2O (0.1 % formic acid).

Binding and Efficacy Studies

Membrane preparation.[474] Mouse brain homogenates for *in vitro* assays were prepared as previously described.[474] Briefly, whole brains were harvested from B6SJL mice, snap-frozen in liquid nitrogen and stored at -80 °C. On the day membrane homogenates were to be prepared, brains were thawed on ice, then pooled in a 40 mL Dounce glass homogenizer and suspended in 5 volumes of ice-cold homogenization buffer (50mM HEPES, pH 7.4, 3 mM $MgCl_2$, and 1 mM EGTA). Brains were then subjected to 10 complete strokes with an A pestle, followed by centrifugation at 40,000 x g for 10 min at +4 °C. Resulting supernatants were discarded, and the pellet was resuspended, homogenized and centrifuged similarly twice more, with supernatants being discarded. For the final resuspension and homogenization with a B pestle, ice-cold 50 mM HEPES was used in place of homogenization buffer and homogenates were aliquoted and stored at -80 °C. Protein concentrations of homogenates were determined using the BCA™ Protein Assay (Thermo Scientific, Rockford, IL).

Competition receptor binding assay.[475] Competition receptor binding was performed as previously described.[475] Briefly, 50 μg of mouse brain homogenates were incubated for 90 min to attain equilibrium binding at room temperature with 0.2 nM [3H]CP-55,940, 5 mM $MgCl_2$, and either increasing cannabinoid concentrations (0.1 nM to 10 μM), 10 μM WIN-55,212-2 (for non-specific binding) or vehicle (for total binding), in triplicate, in a volume of 1

mL of buffer containing 50 mM Tris, 0.05% bovine serum albumin (BSA) and 0.1% ethanol vehicle. Reactions were terminated by rapid vacuum filtration through Whatman GF/B glass fiber filters, followed by five washes with ice-cold buffer (50 mM Tris, 0.05% BSA). Filters were immediately placed into 7 mL scintillation vials to which 4 mL of ScintiVerse™ BD Cocktail scintillation fluid (Fisher Scientific, Fair Lawn, NJ) was added. Bound radioactivity was determined after overnight incubation at room temperature and shaking, by liquid scintillation spectrophotometry with an efficiency of 44% (TriCarb 2100 TR Liquid Scintilation Analyzer, Packard Instrument Company, Meriden, CT). Specific binding is expressed as total binding minus non-specific binding, and is graphed for each data point as a percentage of specific binding occurring in the absence of any competitor.

Adenylyl cyclase assay.[475] Four million Neuro2AWT or CHO-*h*CB2 cells were plated into a 24-well plate and allowed to attach overnight. At 80-90% confluency (the following morning), 0.5 mL of warm incubation media composed of DMEM with 0.9g/L NaCl, 2.5 μCi/mL [^{3}H]Adenine and 0.5 mM IBMX was added to the cells. After a 4-hour incubation period at 37°C in a 5% CO_2 incubator, the media was removed and the plate was briefly floated on an ice-water bath while 0.5 mL of an assay mix was quickly added to the cells in triplicate. The assay mix consisted of a Krebs Ringer HEPES buffered saline solution containing 0.5 mM IBMX, 10 μM forskolin and either vehicle (0.2% ethanol) or at least 6 concentrations (0.1 nM to 10 μM) of each test compound. The plate was then transferred to a 37°C water bath for a 15 minute incubation and the reaction was terminated by addition of 50 μL of 2.2 N HCl. Intracellular [^{3}H]cAMP was separated by column chromatography employing acidic alumina. Four mL of the final eluent was added to 10 mL of ScintiVerse™ BD Cocktail Scintillation Fluid

(Fisher Scientific, Fair Lawn, NJ) and radioactivity was immediately measured employing liquid scintillation spectrophotometry (Tri Carb 2100 TR Liquid Scintillation Analyzer, Packard Instrument Company, Meriden, CT). Data are expressed as the percent of intracellular [^{3}H]cAMP relative to that observed in vehicle samples. In experiments where agonists and antagonists were co-incubated, antagonists were added 5 minutes prior to addition of agonists. Statistical comparison of mean IC_{50} and I_{MAX} values (± SEM) for test compounds was accomplished using one-way ANOVA followed by a Tukey's post- test.

In vivo mouse studies

Animal care and use. Prior to surgery (see below), male NIH Swiss mice (Harlan Sprague Dawley Inc., Indianapolis, IN), weighing approximately 25-30 g, were housed 3 animals per Plexiglass cage (15.24 x 25.40 x 12.70 cm) in a temperature-controlled room at the University of Arkansas for Medical Sciences, Little Rock, AR. Room conditions were maintained at an ambient temperature of 22 ± 2 °C at 45-50% humidity. Lights were set to a 12 h light/dark cycle. Animals were fed Lab Diet rodent chow (laboratory rodent Diet #5001, PMI Feeds, Inc., St. Louis, MO) and water *ad libitum* until immediately before testing. Animals were acclimated to the laboratory environment 2 days prior to experiments and were tested in groups of 4-8 mice per condition. All studies were carried out in accordance with the Declaration of Helsinki and with the Guide for Care and Use of Laboratory animals as adopted and promulgated by the National Institutes of Health. Experimental protocols were approved by the Animal care and Use Committee at the University of Arkansas for Medicinal Sciences.

Core temperature measurements. Following appropriate anesthetization with inhaled isoflurane, the abdominal area of each mouse was shaved and sanitized with iodine swabs. A rostral-caudal cut approximately 1.5 cm in length was made with skin scissors, providing access to the intraperitoneal cavity. A cylindrical glass encapsulated radiotelemetry probe (model ER-4000 E-Mitter, Mini Mitter, Bend, OR) was then inserted, and then incision was closed using absorbable 5-0 chromic gut suture material. At least 7 days were imposed between surgery and experimental observation of drug effects to allow incision to heal and mice to recover normal body weights. Following surgery, implanted mice were individually housed in Plexiglass mouse cages (15.24 x 25.40 x 12.70 cm) for the duration of all temperature experiments. Implanted transmitters produced temperature-modulated signals that were transmitted to a receiver (model ER-4000 receiver, Mini Mitter Co., Inc) underneath each mouse cage. Receivers were housed in light- and sound attenuating cubicles (med Associates model ENV-022MD, St. Albans, VT) equipped with exhaust fans, which further masked ambient laboratory noise. On experimental days, mice were weighted, marked, and returned to their individual cages for at least 1 hr of baseline data collection. Cannabinoid doses were then calculated and drugs were prepared for injection. Animals were subsequently removed from their cage and injected with various doses of drug or an equivalent volume of vehicle. Temperature data were collected at regular 5-min intervals and processed simultaneously by the Vital View data acquisition system (Mini Mitter Co., Inc.) for at least 8 hrs.

Oral EtOH self-administration (two-bottle EtOH choice).[490] The standard two-bottle EtOH choice protocol is a widely used oral self-administration model of ongoing EtOH drinking that captures aspects of voluntary alcohol consumption in humans. In our procedure, each home

cage contained two 25 mL Pyrex glass bottles, capped with rubber stoppers fitted with stainless steel tips. One bottle contained water while the other bottle contained a 10% ethanol solution (diluted with tap water). Volumetric consumption data were recorded from both drinking bottles every Monday and Thursday at approximately the same time. After recording consumption data, bottles were emptied, cleaned, refilled to 25 ml, and switched to eliminate a position preference. All animals were given unrestricted food access (Purina rodent lab diet) during testing, and all mice had 24 h access to 10% (v/v) EtOH and water for the duration of the study. Drinking preference was assessed as the amount of EtOH consumed divided by total fluid consumed × 100. Baseline drinking was established and considered stable when EtOH drinking varied by <10% for three consecutive days. After baseline criterion drinking was achieved, mice were injected (i.p.) with 10 mg/kg of the CB1 antagonist rimonabant for 10 consecutive days. After a two week drug "washout" period, mice were injected with 10 mg/kg **461** or 10 mg/kg **444**. After 10 days of treatment with either **461** or **444** was conducted, mice were injected with the drug vehicle solution for 10 consecutive days. Solutions were prepared fresh weekly with 8%tween and 92% distilled water.

Conditioned place preference.[491] Conditioned place preference (CPP) is one of the most popular models to study the motivational effects of drugs and non-drug treatments in experimental animals, and has been widely used to evaluate the appetitive effects of abused drugs in mice.[491] Our procedure for establishing CPP involved 3 distinct phases, using Panlab 3-compartment spatial discrimination chambers. Briefly, these chambers consist of a box with two equally-sized conditioning compartments connected by a rectangular corridor. The compartments are differentiated by visual pattern on the walls (dots vs. stripes), color (distinct

shades of grey), floor texture (smooth grid vs. rough), and shape (square vs. multi-angled), providing the subjects with multiple contextual dimensions across sensory modalities with which to differentiate the distinct compartments. During the pre-conditioning preference test, mice were allowed to explore the chamber for 30 min while their behavior was recorded and scored. These tests occurred on Friday afternoons, and on the next two days mice were housed in the colony room and not used experimentally. During this time, mice were assigned to receive EtOH pairings (see below) on their non-preferred side, and saline in their preferred compartment. On Monday, the conditioning phase began with all mice receiving a saline injection, then being placed in their preferred compartment for 30 min. During saline conditioning, the hallway was blocked so that mice could not leave the conditioning compartment. After the saline conditioning trial, mice were removed from the chamber and placed back in their home cage. Approximately 4 hours later, mice were injected with 2 g/kg EtOH, and then placed into their non-preferred compartment for 30 min. In this manner, mice were conditioned with both saline and drug each day, and these conditioning trials occurred Monday through Thursday. On Friday morning, the post-conditioning preference test was conducted in a manner identical to the pre-conditioning preference test. For studies involving CBR antagonists, mice were injected with 10 mg/kg rimonabant, 10 mg/kg **461**, or 10mg/kg **444** one hour before each EtOH pairing. To calculate a preference (or aversion) score, the time spent in the drug-paired side during the pre-conditioning test is subtracted from the time spent in that compartment during the post-conditioning test.

Statistical analysis. Curve fitting and statistical analyses for *in vitro* experiments were performed using GraphPad Prism version 5.0b (GraphPad Software, Inc., San Diego, CA). The

Cheng-Prusoff equation was used to convert the experimental IC_{50} values obtained from competition receptor binding experiments to *Ki* values, a quantitative measure of receptor binding.[476] Non-linear regression for one-site competition was used to determine the IC_{50} for competition binding. Data are expressed as mean ± SEM. A one-way ANOVA, followed by Tukey's Multiple Comparison post-hoc test, was used to determine statistical significance ($P<0.05$) between three or more groups. For core body temperature experiments, the area under the curve (AUC) was calculated using a trapezoidal rule from 0-10 hr. For temperature data, statistical significance ($P<0.05$) was determined using a one-way ANOVA, followed by Tukey's HSD post-hoc Test. All in vivo statistical calculations were performed using SigmaStat 3 (Systat Software, Inc., San Jose, CA).

CHAPTER 6: DISSERTATION CONCLUSIONS

It has been estimated that approximately 1.5 billion people worldwide are affected by CNS disorders, which accounts for a third of the global disease burden.[1] It has been estimated that by year 2050, the population of people older than 65 years will significantly increase yielding an additional 1 billion of elderly persons, thus increasing the need for CNS pharmaceuticals for the treatment of various CNS disorders.[2] In the United States and many countries around the world, CNS disorders will affect numerous people in years to come affecting health care systems and families of those in need. Aside from the overwhelming burden that neurological CNS disorders cause society, substance abuse and addiction are not to be forgotten as part of CNS disorders. Globally, the WHO estimated that in 2010, between 99,000 and 253,000 deaths were attributed to illicit drug use, accounting for 0.5 to 1.3% of all deaths affecting people aged 15-64 years.[492] Additionally, approximately 2.5 million people die of alcohol abuse each year among which 320,000 young adults between the ages of 15 and 29 die from alcohol-related causes.[460]

Treatments for most CNS disorders including substance addiction are currently available; however their use is hampered because of the increased appearance of unwanted side effects. The need for the discovery and development of novel CNS active ligands that have potential as CNS therapeutics continues to rise. In search for such agents, several studies were conducted.

The principal active component of *S. divinorum*, the neoclerodane diterpene salvinorin A (**83**), was investigated as a novel opioid receptor ligand. Salvinorin A was shown to be the first non-nitrogenous opioid ligand acting as potent and selective KOP receptor agonist.[124] Modification of the furan ring in order to gain additional knowledge of the interactions of the

furan ring binding pocket within the KOP receptor was the primary goal of this study. Analogues synthesized were designed to explore the changes at the C-13 position of the molecule and their effect on the activity at the KOP receptors. These modifications were designed to attain the optimal distance between the furan ring and the salvinorin A core and the steric requirements necessary for binding and activity at this position; the necessity of an aromatic substituent at the C-13 position; and the preferred orientation of the furan ring oxygen atom. Pharmacological evaluation of the synthesized analogues indicated that there is a preferred *O*-atom orientation in the salvinorin A-KOP receptor binding pocket in that the *cis* conformer (**236**) exhibited higher binding affinity than the *trans* conformer (**235**). Despite its similar affinity for the KOP receptor as salvinorin A, the *cis* –alkene analogue proved to be 34-fold less active at the KOP receptors than the parent molecule. The activity of the C-13 two carbon homologue of salvinorin A at the KOP receptors indicates that such modification is well tolerated, however additional studies need to be completed in order to determine the optimal distance between the furan ring and the diterpene core. Furthermore, it was also determined that an aromatic substituent at the C-13 position is not required for activity at the KOP receptors. Lastly, two carbon furan and tetrahydrofran homologs of salvinorin A were also well tolerated at the KOP receptor; nonetheless additional analogues need to be designed to determine the definite steric requirements at this position.

Further exploration of the salvinorin A core and investigation into the possibility to change the biological activity of salvinorin A was conducted. As basis for such studies, several quinone containing analogues of salvinorin A were designed and synthesized utilizing the structural similarity between the diterpene family of nakijiquinone marine natural products, the first naturally occurring Her-2/Neu kinase inhibitors and the neoclerodane diterpene salvinorin

A, whose BBB penetrating abilities have been well demonstrated.[279, 327] Such salvinorin A analogues would be interesting biological probes that could serve as diagnostic tool in various brain cancers. As expected, pharmacological evaluation of the quinone containing analogues of salvinorin A demonstrated that these analogues did not exhibit any significant opioid receptor activity. However, these analogues exhibited moderate antiproliferative activity in two breast cancer cell lines, representing the first report of salvinorin A analogues that exhibit antiproliferative activity.

The therapeutic potential of *Cannabis* has been known and well utilized throughout many centuries. The widespread distribution of the cannabinoid receptors within the CNS as well as in the periphery, may be the reason for the involvement of the endocannabinoid system in various physiological processes.[398] The recent discovery of the neutral antagonistic activity of a JWH-073 metabolite and the widely demonstrated therapeutic potential of CB1R antagonists, it was hypothesized that SAR modifications of the JWH-073-M4 scaffold would identify novel indole-based analogues with dual CB1R antagonist/CB2R agonist properties and potential as alcohol abuse therapies. Twenty-seven analogues were prepared using step-wise molecular investigation of the elements present in our lead scaffold JWH-073-M4. Analogues synthesized were designed to explore several positions in the JWH-073-M4 scaffold: (**a**) examine the necessity of the carbonyl moiety and the optimal length of the linker from the indole core to the naphthalene ring; (**b**) explore the possibility for addition of rotational bonds at this position of the molecule; (**c**) explore the requirement of the naphthalene ring through selective introduction of electron withdrawing and electron donating groups; (**d**) explore different substitution at the *N*-atom of the indole core; and (**e**) investigate the positioning of the hydroxyl moiety around the indole core and its necessity for activity at CBRs.

The designed analogues were subjected to an array of pharmacological assays for evaluation, where most of the analogues tested exhibited relatively high affinity for both CB1R and CB2Rs. From all the analogues tested, analogues **461** and **444**, showed the most promise with affinities for the cannabinoid receptors in the low nanomolar range. From the functional assay of inhibition of AC-activity, it was observed that both analogues exhibit very little inhibition of AC-activity via CB1Rs, which is consistent with neutral antagonism. Despite the seen antagonistic activity at the CB1Rs, both **461** and **444** produced 40-50% inhibition of AC-activity via CB2Rs, consistent with partial to full agonism.

The promising *in vitro* pharmacological results for these two lead compounds prompted further evaluation in *in vivo* animal assays of alcohol abuse, namely ethanol SA and ethanol CPP. Both analogues **461** and **444** exhibited similar actions to those seen with the CB1Rs antagonist rimonabant in that they both were shown to decrease ethanol self-administration, without affecting total fluid intake. However, unlike rimonabant, **461** and **444** did not alter body weight during the treatment period. Both analogues **461** and **444** interestingly decreased ethanol CPP in a similar manner to rimonabant, despite not possessing any apparent inverse agonist activity *in vitro*. In agreement with previous rimonabant reports, these results demonstrate that both the reinforcing and conditioning rewarding effects of ethanol can also be significantly blunted by treatment with novel JWH-derived cannabinoids, devoid of inverse agonist activity at CB1Rs.[486] Compounds with dual CB1R neutral antagonist/CB2R agonist activity such as analogues **461** and **444** may indeed represent potential leads in an ongoing search for new and improved alcohol abuse therapies.

Collectively, these studies emphasize the importance of the continuous search for novel CNS active ligands. The SAR of the furan ring of salvinorin A completed in this study can be used as the starting point in further SAR experiments that will allow for greater understating of the interaction between salvinorin A and the KOP receptor, as well as for further development of the salvinorin A scaffold as an useful biological tool. Furthermore, the dual activity CB1R antagonist/CB2R agonist ligands based on the JWH-073-M4 scaffold have the potential as alcohol abuse therapy, whose development is ongoing. The results from these studies confirm the utility and the use of novel scaffolds as CNS active agents.

References

1. Palmer, A. M. The role of the blood-CNS barrier in CNS disorders and their treatment. *Neurobiol. Dis.* **2010,** *37*, 3-12.
2. Alavijeh, M. S.; Chishty, M.; Qaiser, M. Z.; Palmer, A. M. Drug metabolism and pharmacokinetics, the blood-brain barrier, and central nervous system drug discovery. *NeuroRx* **2005,** *2*, 554-571.
3. PhRMA. New Report Shows Record Number of Medicines Currently in Development to Treat Mental Illness ; http://www.phrma.org/media/releases/new-report-shows-record-number-medicines-currently-development-treat-mental-illness; (2013).
4. Pangalos, M. N.; Schechter, L. E.; Hurko, O. Drug development for CNS disorders: strategies for balancing risk and reducing attrition. *Nat. Rev. Drug Discov.* **2007,** *6*, 521-532.
5. Kola, I.; Landis, J. Can the pharmaceutical industry reduce attrition rates? *Nat. Rev. Drug Discov.* **2004,** *3*, 711-715.
6. Palmer, A. M.; Alavijeh, M. S. Translational CNS medicines research. *Drug Discov. Today* **2012,** *17*, 1068-1078.
7. Di, L.; Rong, H.; Feng, B. Demystifying brain penetration in central nervous system drug discovery. Miniperspective. *J. Med. Chem.* **2013,** *56*, 2-12.
8. Jeffrey, P.; Summerfield, S. Assessment of the blood-brain barrier in CNS drug discovery. *Neurobiol. Dis.* **2010,** *37*, 33-37.
9. Di, L.; Kerns, E. H.; Carter, G. T. Strategies to assess blood-brain barrier penetration. *Expert opinion on drug discovery* **2008,** *3*, 677-687.
10. Abbott, N. J.; Patabendige, A. A. K.; Dolman, D. E. M.; Yusof, S. R.; Begley, D. J. Structure and function of the blood-brain barrier. *Neurobiol. Dis.* **2010,** *37*, 13-25.
11. Zhou, S. F. Structure, function and regulation of P-glycoprotein and its clinical relevance in drug disposition. *Xenobiotica* **2008,** *38*, 802-832.
12. Smith, D. A.; Di, L.; Kerns, E. H. The effect of plasma protein binding on in vivo efficacy: misconceptions in drug discovery. *Nat. Rev. Drug Discov.* **2010,** *9*, 929-939.
13. Liu, X.; Van Natta, K.; Yeo, H.; Vilenski, O.; Weller, P. E.; Worboys, P. D.; Monshouwer, M. Unbound drug concentration in brain homogenate and cerebral spinal fluid at steady state as a surrogate for unbound concentration in brain interstitial fluid. *Drug Metab. Dispos.* **2009,** *37*, 787-793.
14. Price, D. A.; Blagg, J.; Jones, L.; Greene, N.; Wager, T. Physicochemical drug properties associated with in vivo toxicological outcomes: a review. *Expert Opin. Drug Metab. Toxicol.* **2009,** *5*, 921-931.
15. Pajouhesh, H.; Lenz, G. R. Medicinal chemical properties of successful central nervous system drugs. *NeuroRx* **2005,** *2*, 541-553.
16. van de Waterbeemd, H.; Camenisch, G.; Folkers, G.; Chretien, J. R.; Raevsky, O. A. Estimation of blood-brain barrier crossing of drugs using molecular size and shape, and H-bonding descriptors. *J. Drug Target.* **1998,** *6*, 151-165.
17. Hansch, C.; Bjorkroth, J. P.; Leo, A. Hydrophobicity and central nervous system agents: on the principle of minimal hydrophobicity in drug design. *J. Pharm. Sci.* **1987,** *76*, 663-687.

18. Ghose, A. K.; Herbertz, T.; Hudkins, R. L.; Dorsey, B. D.; Mallamo, J. P. Knowledge-Based, Central Nervous System (CNS) Lead Selection and Lead Optimization for CNS Drug Discovery. *ACS Chem. Neurosci.* **2012,** *3*, 50-68.
19. Osterberg, T.; Norinder, U. Prediction of polar surface area and drug transport processes using simple parameters and PLS statistics. *J. Chem. Inf. Comput. Sci.* **2000,** *40*, 1408-1411.
20. Pardridge, W. M. CNS drug design based on principles of blood-brain barrier transport. *J. Neurochem.* **1998,** *70*, 1781-1792.
21. Kelder, J.; Grootenhuis, P. D.; Bayada, D. M.; Delbressine, L. P.; Ploemen, J. P. Polar molecular surface as a dominating determinant for oral absorption and brain penetration of drugs. *Pharm. Res.* **1999,** *16*, 1514-1519.
22. Wager, T. T.; Chandrasekaran, R. Y.; Hou, X.; Troutman, M. D.; Verhoest, P. R.; Villalobos, A.; Will, Y. Defining desirable central nervous system drug space through the alignment of molecular properties, in vitro ADME, and safety attributes. *ACS Chem. Neurosci.* **2010,** *1*, 420-434.
23. Didziapetris, R.; Japertas, P.; Avdeef, A.; Petrauskas, A. Classification analysis of P-glycoprotein substrate specificity. *J. Drug Target.* **2003,** *11*, 391-406.
24. de Graaf, C.; Vermeulen, N. P.; Feenstra, K. A. Cytochrome p450 in silico: an integrative modeling approach. *J. Med. Chem.* **2005,** *48*, 2725-2755.
25. Redfern, W. S.; Carlsson, L.; Davis, A. S.; Lynch, W. G.; MacKenzie, I.; Palethorpe, S.; Siegl, P. K. S.; Strang, I.; Sullivan, A. T.; Wallis, R.; Camm, A. J.; Hammond, T. G. Relationships between preclinical cardiac electrophysiology, clinical QT interval prolongation and torsade de pointes for a broad range of drugs: evidence for a provisional safety margin in drug development. *Cardiovasc. Res.* **2003,** *58*, 32-45.
26. Olesen, J.; Leonardi, M. The burden of brain diseases in Europe. *Eur. J. Neurol.* **2003,** *10*, 471-477.
27. Batsch, N. L., Mittelman, M. S. World Alzheimer's report 2012. Overcoming the stigma of dementia. Alzheimer's Disease International http://www.alz.org/documents_custom/world_report_2012_final.pdf.
28. World Health Organization. Dementia: a public health priority, 2012. http://apps.who.int/iris/bitstream/10665/75263/1/9789241564458_eng.pdf
29. Hardy, J. A hundred years of Alzheimer's disease research. *Neuron* **2006,** *52*, 3-13.
30. Hardy, J. A.; Higgins, G. A. Alzheimer's disease: the amyloid cascade hypothesis. *Science* **1992,** *256*, 184-185.
31. Corbett, A.; Smith, J.; Ballard, C. New and emerging treatments for Alzheimer's disease. *Expert Rev. Neurother.* **2012,** *12*, 535-543.
32. Corbett, A.; Ballard, C. New and emerging treatments for Alzheimer's disease. *Expert Opin Emerg Drugs* **2012,** *17*, 147-156.
33. Samii, A.; Nutt, J. G.; Ransom, B. R. Parkinson's disease. *Lancet* **2004,** *363*, 1783-1793.
34. Nussbaum, R. L. Alzheimer's disease and Parkinson's disease (vol 348, pg 1356, 2003). *N. Engl. J. Med.* **2003,** *348*, 2588-2588.
35. Kansara, S.; Trivedi, A.; Chen, S.; Jankovic, J.; Le, W. Early diagnosis and therapy of Parkinson's disease: can disease progression be curbed? *J. Neural Transm.* **2013,** *120*, 197-210.

36. Naoi, M.; Maruyama, W. Monoamine oxidase inhibitors as neuroprotective agents in age-dependent neurodegenerative disorders. *Curr. Pharm. Des.* **2010,** *16*, 2799-2817.
37. Mitchell, J. D.; Borasio, G. D. Amyotrophic lateral sclerosis. *Lancet* **2007,** *369*, 2031-2041.
38. Limpert, A. S.; Mattmann, M. E.; Cosford, N. D. Recent progress in the discovery of small molecules for the treatment of amyotrophic lateral sclerosis (ALS). *Beilstein J Org Chem* **2013,** *9*, 717-732.
39. Song, J. H.; Huang, C. S.; Nagata, K.; Yeh, J. Z.; Narahashi, T. Differential action of riluzole on tetrodotoxin-sensitive and tetrodotoxin-resistant sodium channels. *J. Pharmacol. Exp. Ther.* **1997,** *282*, 707-714.
40. Hubert, J. P.; Delumeau, J. C.; Glowinski, J.; Premont, J.; Doble, A. Antagonism by riluzole of entry of calcium evoked by NMDA and veratridine in rat cultured granule cells: evidence for a dual mechanism of action. *Br. J. Pharmacol.* **1994,** *113*, 261-267.
41. Kalmar, B.; Novoselov, S.; Gray, A.; Cheetham, M. E.; Margulis, B.; Greensmith, L. Late stage treatment with arimoclomol delays disease progression and prevents protein aggregation in the SOD1 mouse model of ALS. *J. Neurochem.* **2008,** *107*, 339-350.
42. Ito, H.; Wate, R.; Zhang, J.; Ohnishi, S.; Kaneko, S.; Ito, H.; Nakano, S.; Kusaka, H. Treatment with edaravone, initiated at symptom onset, slows motor decline and decreases SOD1 deposition in ALS mice. *Exp. Neurol.* **2008,** *213*, 448-455.
43. Rothstein, J. D.; Patel, S.; Regan, M. R.; Haenggeli, C.; Huang, Y. H.; Bergles, D. E.; Jin, L.; Dykes Hoberg, M.; Vidensky, S.; Chung, D. S.; Toan, S. V.; Bruijn, L. I.; Su, Z. Z.; Gupta, P.; Fisher, P. B. Beta-lactam antibiotics offer neuroprotection by increasing glutamate transporter expression. *Nature* **2005,** *433*, 73-77.
44. Rovini, A.; Carre, M.; Bordet, T.; Pruss, R. M.; Braguer, D. Olesoxime prevents microtubule-targeting drug neurotoxicity: Selective preservation of EB comets in differentiated neuronal cells. *Biochem. Pharmacol.* **2010,** *80*, 884-894.
45. A novel gene containing a trinucleotide repeat that is expanded and unstable on Huntington's disease chromosomes. The Huntington's Disease Collaborative Research Group. *Cell* **1993,** *72*, 971-983.
46. Walker, F. O. Huntington's disease. *Lancet* **2007,** *369*, 218-228.
47. Hersch, S. M.; Rosas, H. D. Neuroprotection for Huntington's disease: ready, set, slow. *Neurotherapeutics* **2008,** *5*, 226-236.
48. Goldberg, Y. P.; Kremer, B.; Andrew, S. E.; Theilmann, J.; Graham, R. K.; Squitieri, F.; Telenius, H.; Adam, S.; Sajoo, A.; Starr, E.; et al. Molecular analysis of new mutations for Huntington's disease: intermediate alleles and sex of origin effects. *Nat. Genet.* **1993,** *5*, 174-179.
49. Bonelli, R. M.; Wenning, G. K.; Kapfhammer, H. P. Huntington's disease: present treatments and future therapeutic modalities. *Int. Clin. Psychopharmacol.* **2004,** *19*, 51-62.
50. Dunkel, P.; Chai, C. L.; Sperlagh, B.; Huleatt, P. B.; Matyus, P. Clinical utility of neuroprotective agents in neurodegenerative diseases: current status of drug development for Alzheimer's, Parkinson's and Huntington's diseases, and amyotrophic lateral sclerosis. *Expert Opin Investig Drugs* **2012,** *21*, 1267-1308.
51. Lavu, S.; Boss, O.; Elliott, P. J.; Lambert, P. D. Sirtuins--novel therapeutic targets to treat age-associated diseases. *Nat. Rev. Drug Discov.* **2008,** *7*, 841-853.

52. Cen, Y. Sirtuins inhibitors: the approach to affinity and selectivity. *Biochim. Biophys. Acta* **2010,** *1804*, 1635-1644.
53. Mueser, K. T.; McGurk, S. R. Schizophrenia. *Lancet* **2004,** *363*, 2063-2072.
54. Jablensky, A. The 100-year epidemiology of schizophrenia. *Schizophr. Res.* **1997,** *28*, 111-125.
55. Wu, E. Q.; Birnbaum, H. G.; Shi, L.; Ball, D. E.; Kessler, R. C.; Moulis, M.; Aggarwal, J. The economic burden of schizophrenia in the United States in 2002. *J. Clin. Psychiatry* **2005,** *66*, 1122-1129.
56. Thaker, G. K.; Carpenter, W. T., Jr. Advances in schizophrenia. *Nat. Med.* **2001,** *7*, 667-671.
57. Meltzer, H. Y. Update on typical and atypical antipsychotic drugs. *Annu. Rev. Med.* **2013,** *64*, 393-406.
58. Borison, R. L.; Diamond, B. I. Neuropharmacology of the extrapyramidal system. *J. Clin. Psychiatry* **1987,** *48 Suppl*, 7-12.
59. Steck, H. [Extrapyramidal and diencephalic syndrome in the course of largactil and serpasil treatments]. *Ann. Med. Psychol. (Paris)* **1954,** *112*, 737-744.
60. Haddad, P. M.; Das, A.; Keyhani, S.; Chaudhry, I. B. Antipsychotic drugs and extrapyramidal side effects in first episode psychosis: a systematic review of head-head comparisons. *J Psychopharmacol* **2012,** *26*, 15-26.
61. Ghanizadeh, A.; Nikseresht, M. S.; Sahraian, A. The effect of zonisamide on antipsychotic-associated weight gain in patients with schizophrenia: a randomized, double-blind, placebo-controlled clinical trial. *Schizophr. Res.* **2013,** *147*, 110-115.
62. Duncan, J. S.; Sander, J. W.; Sisodiya, S. M.; Walker, M. C. Adult epilepsy. *Lancet* **2006,** *367*, 1087-1100.
63. Sander, J. W. The epidemiology of epilepsy revisited. *Curr. Opin. Neurol.* **2003,** *16*, 165-170.
64. Forsgren, L.; Beghi, E.; Oun, A.; Sillanpaa, M. The epidemiology of epilepsy in Europe - a systematic review. *Eur. J. Neurol.* **2005,** *12*, 245-253.
65. Sorensen, A. T.; Kokaia, M. Novel approaches to epilepsy treatment. *Epilepsia* **2013,** *54*, 1-10.
66. Fisher, R. S.; van Emde Boas, W.; Blume, W.; Elger, C.; Genton, P.; Lee, P.; Engel, J., Jr. Epileptic seizures and epilepsy: definitions proposed by the International League Against Epilepsy (ILAE) and the International Bureau for Epilepsy (IBE). *Epilepsia* **2005,** *46*, 470-472.
67. Sander, J. W. The use of antiepileptic drugs--principles and practice. *Epilepsia* **2004,** *45 Suppl 6*, 28-34.
68. Kwan, P.; Sander, J. W. The natural history of epilepsy: an epidemiological view. *J. Neurol. Neurosurg. Psychiatry* **2004,** *75*, 1376-1381.
69. Roiser, J. P.; Elliott, R.; Sahakian, B. J. Cognitive mechanisms of treatment in depression. *Neuropsychopharmacol.* **2012,** *37*, 117-136.
70. Chaki, S.; Ago, Y.; Palucha-Paniewiera, A.; Matrisciano, F.; Pilc, A. mGlu2/3 and mGlu5 receptors: potential targets for novel antidepressants. *Neuropharmacology* **2013,** *66*, 40-52.
71. Kessler, R. C.; Berglund, P.; Demler, O.; Jin, R.; Koretz, D.; Merikangas, K. R.; Rush, A. J.; Walters, E. E.; Wang, P. S.; National Comorbidity Survey, R. The epidemiology of

major depressive disorder: results from the National Comorbidity Survey Replication (NCS-R). *JAMA* **2003,** *289*, 3095-3105.
72. Wittchen, H. U.; Jacobi, F.; Rehm, J.; Gustavsson, A.; Svensson, M.; Jonsson, B.; Olesen, J.; Allgulander, C.; Alonso, J.; Faravelli, C.; Fratiglioni, L.; Jennum, P.; Lieb, R.; Maercker, A.; van Os, J.; Preisig, M.; Salvador-Carulla, L.; Simon, R.; Steinhausen, H. C. The size and burden of mental disorders and other disorders of the brain in Europe 2010. *Eur. Neuropsychopharmacol.* **2011,** *21*, 655-679.
73. Duric, V.; Duman, R. S. Depression and treatment response: dynamic interplay of signaling pathways and altered neural processes. *Cell. Mol. Life Sci.* **2013,** *70*, 39-53.
74. Schildkraut, J. J. The catecholamine hypothesis of affective disorders: a review of supporting evidence. *Am. J. Psychiatry* **1965,** *122*, 509-522.
75. Fekadu, A.; Wooderson, S. C.; Markopoulo, K.; Donaldson, C.; Papadopoulos, A.; Cleare, A. J. What happens to patients with treatment-resistant depression? A systematic review of medium to long term outcome studies. *J. Affect. Disord.* **2009,** *116*, 4-11.
76. Rosenzweig-Lipson, S.; Beyer, C. E.; Hughes, Z. A.; Khawaja, X.; Rajarao, S. J.; Malberg, J. E.; Rahman, Z.; Ring, R. H.; Schechter, L. E. Differentiating antidepressants of the future: efficacy and safety. *Pharmacol. Ther.* **2007,** *113*, 134-153.
77. Rush, A. J.; Trivedi, M. H.; Wisniewski, S. R.; Nierenberg, A. A.; Stewart, J. W.; Warden, D.; Niederehe, G.; Thase, M. E.; Lavori, P. W.; Lebowitz, B. D.; McGrath, P. J.; Rosenbaum, J. F.; Sackeim, H. A.; Kupfer, D. J.; Luther, J.; Fava, M. Acute and longer-term outcomes in depressed outpatients requiring one or several treatment steps: a STAR*D report. *Am. J. Psychiatry* **2006,** *163*, 1905-1917.
78. Nasca, C.; Xenos, D.; Barone, Y.; Caruso, A.; Scaccianoce, S.; Matrisciano, F.; Battaglia, G.; Mathe, A. A.; Pittaluga, A.; Lionetto, L.; Simmaco, M.; Nicoletti, F. L-acetylcarnitine causes rapid antidepressant effects through the epigenetic induction of mGlu2 receptors. *Proc. Natl. Acad. Sci. USA* **2013,** *110*, 4804-4809.
79. Li, J. X.; Zhang, Y. Emerging drug targets for pain treatment. *Eur. J. Pharmacol.* **2012,** *681*, 1-5.
80. National Institutes of Health: Fact Sheet, Pain Management. (2013). http://report.nih.gov/NIHfactsheets/ViewFactSheet.aspx?csid=57.
81. Xu, Q.; Yaksh, T. L. A brief comparison of the pathophysiology of inflammatory versus neuropathic pain. *Curr Opin Anaesthesiol* **2011,** *24*, 400-407.
82. Prisinzano, T.; Gebhart, G. F. Pain overview. *Comprehensive Medicinal Chemistry II* **2006,** *6*, 321-325.
83. Vane, J. R. The fight against rheumatism: from willow bark to COX-1 sparing drugs. *J. Physiol. Pharmacol.* **2000,** *51*, 573-586.
84. Sinha, M.; Gautam, L.; Shukla, P. K.; Kaur, P.; Sharma, S.; Singh, T. P. Current perspectives in NSAID-induced gastropathy. *Mediators Inflamm.* **2013,** *2013*, 258209.
85. Vane, J. R. Inhibition of prostaglandin synthesis as a mechanism of action for aspirin-like drugs. *Nat. New Biol.* **1971,** *231*, 232-235.
86. DeWitt, D. L.; Smith, W. L. Primary structure of prostaglandin G/H synthase from sheep vesicular gland determined from the complementary DNA sequence. *Proc. Natl. Acad. Sci. USA* **1988,** *85*, 1412-1416.
87. Chandrasekharan, N. V.; Dai, H.; Roos, K. L.; Evanson, N. K.; Tomsik, J.; Elton, T. S.; Simmons, D. L. COX-3, a cyclooxygenase-1 variant inhibited by acetaminophen and

other analgesic/antipyretic drugs: cloning, structure, and expression. *Proc. Natl. Acad. Sci. USA* **2002,** *99*, 13926-13931.
88. Xie, W. L.; Chipman, J. G.; Robertson, D. L.; Erikson, R. L.; Simmons, D. L. Expression of a mitogen-responsive gene encoding prostaglandin synthase is regulated by mRNA splicing. *Proc. Natl. Acad. Sci. USA* **1991,** *88*, 2692-2696.
89. Green, G. A. Understanding NSAIDs: from aspirin to COX-2. *Clin. Cornerstone* **2001,** *3*, 50-60.
90. Rao, P.; Knaus, E. E. Evolution of nonsteroidal anti-inflammatory drugs (NSAIDs): cyclooxygenase (COX) inhibition and beyond. *J. Pharm. Pharm. Sci.* **2008,** *11*, 81s-110s.
91. Payne, R. Limitations of NSAIDs for pain management: toxicity or lack of efficacy? *J Pain* **2000,** *1*, 14-18.
92. Prisinzano, T. E. Neoclerodanes as atypical opioid receptor ligands. *J. Med. Chem.* **2013,** *56*, 3435-3443.
93. Fries, D. S. Opioid Analgesiscs. In *In Foye's Principles of Medicinal Chemistry. 6 ed*, Lemke, T. L. W., D. A., Ed. Lippincott Williams & Wilkins: Baltimore, MD, 2008; pp 652-678.
94. McCurdy, C. R.; Prisinzano, T. E. Opioid Receptor Ligands. In *In Burger's Medicinal Chemistry, Drug Discovery and Development.*, John Wiley & Sons, Inc.: 2010; pp 1-168.
95. Gulland, J. M.; Robinson, R. The morphine group. Part I. A discussion of the constitutional problem. *J. Chem. Soc.* **1923,** *123*, 980-998.
96. Gulland, J. M.; Robinson, R. The morphine group. Part II. Thebainone, thebainol, and Dihydrothebainone. *J. Chem. Soc.* **1923,** *123*, 998-1011.
97. Gates, M.; Tschudi, G. The Synthesis of Morphine. *J. Am. Chem. Soc.* **1952,** *74*, 1109-1110.
98. Gates, M.; Tschudi, G. The Synthesis of Morphine. *J. Am. Chem. Soc.* **1956,** *78*, 1380-1393.
99. Iwamoto, E. T.; Martin, W. R. Multiple opioid receptors. *Med. Res. Rev.* **1981,** *1*, 411-440.
100. Dhawan, B. N.; Cesselin, F.; Raghubir, R.; Reisine, T.; Bradley, P. B.; Portoghese, P. S.; Hamon, M. International Union of Pharmacology. XII. Classification of opioid receptors. *Pharmacol. Rev.* **1996,** *48*, 567-592.
101. Kieffer, B. L.; Evans, C. J. Opioid tolerance-in search of the holy grail. *Cell* **2002,** *108*, 587-590.
102. Maudsley, S.; Martin, B.; Luttrell, L. M. The origins of diversity and specificity in g protein-coupled receptor signaling. *J. Pharmacol. Exp. Ther.* **2005,** *314*, 485-494.
103. Kieffer, B. L.; Gaveriaux-Ruff, C. Exploring the opioid system by gene knockout. *Prog. Neurobiol.* **2002,** *66*, 285-306.
104. Ko, M. C.; Lee, H.; Harrison, C.; Clark, M. J.; Song, H. F.; Naughton, N. N.; Woods, J. H.; Traynor, J. R. Studies of micro-, kappa-, and delta-opioid receptor density and G protein activation in the cortex and thalamus of monkeys. *J. Pharmacol. Exp. Ther.* **2003,** *306*, 179-186.
105. Mather, L. E.; Smith, M. T. Opioids in Pain Control: Basic and Clinical Aspects. In *In Clinical Pharmacology and Adverese Effects.*, Stein, C., Ed. Cambridge University Press: Cambridge, 1999; pp 188-211.
106. Goldstein, G. Pentazocine. *Drug Alcohol Depend.* **1985,** *14*, 313-323.

107. Tzschentke, T. M.; Christoph, T.; Kogel, B.; Schiene, K.; Hennies, H. H.; Englberger, W.; Haurand, M.; Jahnel, U.; Cremers, T. I.; Friderichs, E.; De Vry, J. (-)-(1R,2R)-3-(3-dimethylamino-1-ethyl-2-methyl-propyl)-phenol hydrochloride (tapentadol HCl): a novel mu-opioid receptor agonist/norepinephrine reuptake inhibitor with broad-spectrum analgesic properties. *J. Pharmacol. Exp. Ther.* **2007,** *323*, 265-276.
108. Brennan, M. J. Update on prescription extended-release opioids and appropriate patient selection. *J Multidiscip Healthc* **2013,** *6*, 265-280.
109. Woolf, C. J.; Hashmi, M. Use and abuse of opioid analgesics: potential methods to prevent and deter non-medical consumption of prescription opioids. *Curr Opin Investig Drugs* **2004,** *5*, 61-66.
110. National Institutes on Drug Abuse. The Drug Facts: Understanding Drug Abuse and Addiction (2012), http://www.drugabuse.gov/publications/drugfacts/understanding-drug-abuse-addiction#references.
111. National Drug Intelligence Center. The economic impact of illicit drug use on american society (2011), http://www.justice.gov/archive/ndic/pubs44/44731/44731p.pdf.
112. Adhikari, B. K., J.; Malaraner, A.; Pechacek, T; and Vong, T. Center for Disease Control and Prevention. Morbidity and mortality weekly report (2004), http://www.cdc.gov/mmwr/preview/mmwrhtml/mm5745a3.htm
113. Rehm, J.; Mathers, C.; Popova, S.; Thavorncharoensap, M.; Teerawattananon, Y.; Patra, J. Global burden of disease and injury and economic cost attributable to alcohol use and alcohol-use disorders. *Lancet* **2009,** *373*, 2223-2233.
114. Kreek, M. J.; LaForge, K. S.; Butelman, E. Pharmacotherapy of addictions. *Nat. Rev. Drug Discov.* **2002,** *1*, 710-726.
115. Savage, S. C., E. C.; Heit, H. A.; Hunt, J.; Joranson, D.; Schnoll, S. H. Definitions Related to the Use of Opioids for the Treatment of Pain. Americal Academy of Pain Medicine, American Pain Society, American Society of Addiction Medicine:. In Glenview, IL, 2001.
116. Prisinzano, T. E.; Tidgewell, K.; Harding, W. W. Kappa opioids as potential treatments for stimulant dependence. *AAPS J.* **2005,** *7*, E592-599.
117. Sturgess, J. E.; George, T. P.; Kennedy, J. L.; Heinz, A.; Muller, D. J. Pharmacogenetics of alcohol, nicotine and drug addiction treatments. *Addict. Biol.* **2011,** *16*, 357-376.
118. Volkow, N. D.; Skolnick, P. New medications for substance use disorders: challenges and opportunities. *Neuropsychopharmacol.* **2012,** *37*, 290-292.
119. Eguchi, M. Recent advances in selective opioid receptor agonists and antagonists. *Med. Res. Rev.* **2004,** *24*, 182-212.
120. Robson, M. J.; Noorbakhsh, B.; Seminerio, M. J.; Matsumoto, R. R. Sigma-1 receptors: potential targets for the treatment of substance abuse. *Curr. Pharm. Des.* **2012,** *18*, 902-919.
121. Justinova, Z.; Panlilio, L. V.; Goldberg, S. R. Drug addiction. *Curr. Top. Behav. Neurosci.* **2009,** *1*, 309-346.
122. Yang, P.; Wang, L.; Xie, X. Q. Latest advances in novel cannabinoid CB(2) ligands for drug abuse and their therapeutic potential. *Future Med. Chem.* **2012,** *4*, 187-204.
123. Borchardt, J. K. The Beginnings of Drug Therapy: Ancient Mesopotamian Medicine. *Drug News Perspect* **2002,** *15*, 187-192.

124. Roth, B. L.; Baner, K.; Westkaemper, R.; Siebert, D.; Rice, K. C.; Steinberg, S.; Ernsberger, P.; Rothman, R. B. Salvinorin A: a potent naturally occurring nonnitrogenous kappa opioid selective agonist. *Proc. Natl. Acad. Sci. USA* **2002,** *99*, 11934-11939.
125. Grothaus, P. G.; Cragg, G. M.; Newman, D. J. Plant Natural Products in Anticancer Drug Discovery. *Curr. Org. Chem.* **2010,** *14*, 1781-1791.
126. Borchardt, J. K. The beginnings of, drug therapy: Ancient Mesopotamian medicine. *Drug News & Perspectives* **2002,** *15*, 187-192.
127. Wasson, R. G.; Ingalls, D. H. The soma of the Rig Veda: what was it? *J Am Orient Soc* **1971,** *91*, 169-187.
128. Borchardt, J. K. Traditional Chinese drug therapy. *Drug News Perspect* **2003,** *16*, 698-702.
129. Rhizopoulou, S.; Katsarou, A. The plant material of medicine. *Adv. Nat. Appl. Sci.* **2008,** *2*, 94-98.
130. El-Seedi, H. R.; De Smet, P. A.; Beck, O.; Possnert, G.; Bruhn, J. G. Prehistoric peyote use: alkaloid analysis and radiocarbon dating of archaeological specimens of Lophophora from Texas. *J. Ethnopharmacol.* **2005,** *101*, 238-242.
131. World Health Organization. Traditional Medicines, fact sheet (2008), http://www.who.int/mediacentre/factsheets/fs134/en/.
132. Cragg, G. M.; Newman, D. J. Biodiversity: A continuing source of novel drug leads. *Pure Appl. Chem.* **2005,** *77*, 7-24.
133. Strohl, W. R. The role of natural products in a modern drug discovery program. *Drug Discov. Today* **2000,** *5*, 39-41.
134. Der Marderosian, A.; Beutler, J. A. The Review of Natural Products, 2nd ed. In *Facts and Comparisons*, Seattle, WA, 2002; pp 13-43.
135. Dias, D. A.; Urban, S.; Roessner, U. A historical overview of natural products in drug discovery. *Metabolites* **2012,** *2*, 303-336.
136. Cragg, G. M.; Newman, D. J. Natural products: a continuing source of novel drug leads. *Biochim. Biophys. Acta* **2013,** *1830*, 3670-3695.
137. Newman, D. J.; Cragg, G. M. Natural products as sources of new drugs over the 30 years from 1981 to 2010. *J. Nat. Prod.* **2012,** *75*, 311-335.
138. Demain, A. L.; Vaishnav, P. Natural products for cancer chemotherapy. *Microb Biotechnol* **2011,** *4*, 687-699.
139. Mitscher, L. A. Coevolution: mankind and microbes. *J. Nat. Prod.* **2008,** *71*, 497-509.
140. Newman, D. J.; Cragg, G. M.; Snader, K. M. The influence of natural products upon drug discovery. *Nat. Prod. Rep.* **2000,** *17*, 215-234.
141. Drews, J. Drug discovery: A historical perspective. *Science* **2000,** *287*, 1960-1964.
142. Newman, D. J.; Cragg, G. M. In *Natural products as drugs and leads to drugs: the historical perspective*, 2010; Royal Society of Chemistry: 2010; pp 3-27.
143. Newman, D. J.; Cragg, G. M. Natural product scaffolds as leads to drugs. *Future Med. Chem.* **2009,** *1*, 1415-1427.
144. American Cancer Society. Cancer Facts and Figures 2013, http://www.cancer.org/acs/groups/content/@epidemiologysurveilance/documents/document/acspc-036845.pdf.
145. Newman, D. J.; Cragg, G. M. Natural products as sources of new drugs over the last 25 years. *J. Nat. Prod.* **2007,** *70*, 461-477.

146. Baker, D. D.; Chu, M.; Oza, U.; Rajgarhia, V. The value of natural products to future pharmaceutical discovery. *Nat. Prod. Rep.* **2007,** *24*, 1225-1244.
147. Gordaliza, M. Natural products as leads to anticancer drugs. *Clin. Transl. Oncol.* **2007,** *9*, 767-776.
148. World Health Organization. Malaria Facts Sheet (2010), http://www.who.int/mediacentre/factsheets/fs094/en/index.html.
149. World Health Organization. World Malaria Report 2012, http://www.who.int/malaria/publications/world_malaria_report_2012/report/en/index.html.
150. Mutai, C.; Rukunga, G.; Vagias, C.; Roussis, V. In vivo screening of antimalarial activity of Acacia mellifera (benth) (leguminosae) on Plasmodium berghei in mice. *African Journal of Traditional Complementary and Alternative Medicines* **2008,** *5*, 46-50.
151. Wellems, T. E.; Plowe, C. V. Chloroquine-resistant malaria. *J. Infect. Dis.* **2001,** *184*, 770-776.
152. Wells, T. N. C. Natural products as starting points for future anti-malarial therapies: going back to our roots? *Malar. J.* **2011,** *10*.
153. Dewick, P. M. *Medicinal natural products : a biosynthetic approach*. 3rd ed.; Wiley: Hoboken, 2008.
154. Christianson, D. W. Unearthing the roots of the terpenome. *Curr. Opin. Chem. Biol.* **2008,** *12*, 141-150.
155. Christianson, D. W. Roots of biosynthetic diversity. *Science* **2007,** *316*, 60-61.
156. Ruzicka, L. The isoprene rule and the biogenesis of terpenic compounds. *Experientia* **1953,** *9*, 357-367.
157. Chinou, I. Labdanes of natural origin-biological activities (1981-2004). *Curr. Med. Chem.* **2005,** *12*, 1295-1317.
158. Breitmaier, E. *Terpenes: Flavors, Fragrances, Pharmaca, Pheromones*. 1st ed.; Wiley-VCH: Weinheim, Germany, **2006**.
159. Vardamides, J. C.; Sielinou, V. T.; Akone, S. H.; Nkengfack, A. E.; Abegaz, B. M. Terpenoids from Turraeanthus species. *Nat. Prod. Commun.* **2010,** *5*, 1535-1538.
160. Djemgou, P. C.; Gatsing, D.; Hegazy, M. E.; El-Hamd Mohamed, A. H.; Ngandeu, F.; Tane, P.; Ngadjui, B. T.; Fotso, S.; Laatsch, H. Turrealabdane, turreanone and an antisalmonellal agent from Turraeanthus africanus. *Planta Med.* **2010,** *76*, 165-171.
161. Schmidt, T. J.; Kaiser, M.; Brun, R. Complete structural assignment of serratol, a cembrane-type diterpene from Boswellia serrata, and evaluation of its antiprotozoal activity. *Planta Med.* **2011,** *77*, 849-850.
162. Hanson, J. R. Diterpenoids of terrestrial origin. *Nat. Prod. Rep.* **2011,** *28*, 1755-1772.
163. Tokoroyama, T. Synthesis of clerodane diterpenoids and related compounds - Stereoselective construction of the decalin skeleton with multiple contiguous stereogenic centers. *Synthesis-Stuttgart* **2000**, 611-633.
164. Lallemand, J. Y.; Six, Y.; Ricard, L. A concise synthesis of an advanced Clerodin intermediate through a Vaultier tandem reaction. *Eur. J. Org. Chem.* **2002**, 503-513.
165. Abdelwahab, S. I.; Koko, W. S.; Taha, M. M. E.; Mohan, S.; Achoui, M.; Abdulla, M. A.; Mustafa, M. R.; Ahmad, S.; Noordin, M. I.; Yong, C. L.; Sulaiman, M. R.; Othman, R.; Hassan, A. A. In vitro and in vivo anti-inflammatory activities of columbin through the inhibition of cycloxygenase-2 and nitric oxide but not the suppression of NF-kappa B translocation. *Eur. J. Pharmacol.* **2012,** *678*, 61-70.

166. Merritt, A. T.; Ley, S. V. Clerodane diterpenoids. *Nat. Prod. Rep.* **1992,** *9*, 243-287.
167. Rogers, D.; Unal, G. G.; Williams, D. J.; Ley, S. V.; Sim, G. A.; Joshi, B. S.; Ravindranath, K. R. Crystal-Structure of 3-Epicaryoptin and the Reversal of the Currently Accepted Absolute-Configuration of Clerodin. *Journal of the Chemical Society-Chemical Communications* **1979**, 97-99.
168. Lovell, K. M.; Prevatt-Smith, K. M.; Lozama, A.; Prisinzano, T. E. Synthesis of Neoclerodane Diterpenes and Their Pharamacological Effects. In *Chemistry of Opioids*, Nagase, H., Ed. Springer berlin Heidelberg: 2010; pp 141-181.
169. Hofmann, A. *LSD, My Problem Child*. McGraw-Hill: New York, 1980.
170. Valdes, L. J.; Diaz, J. L.; Paul, A. G. Ethnopharmacology of Ska-Maria-Pastora (Salvia, Divinorum, Epling and Jativa-M). *J. Ethnopharmacol.* **1983,** *7*, 287-312.
171. Valdes, L. J.; Butler, W. M.; Hatfield, G. M.; Paul, A. G.; Koreeda, M. Divinorin-a, a Psychotropic Terpenoid, and Divinorin-B from the Hallucinogenic Mexican Mint Salvia-Divinorum. *J. Org. Chem.* **1984,** *49*, 4716-4720.
172. Siebert, D. J. Salvia divinorum and salvinorin A: new pharmacologic findings. *J. Ethnopharmacol.* **1994,** *43*, 53-56.
173. Grundmann, O.; Phipps, S. M.; Zadezensky, I.; Butterweck, V. Salvia divinorum and salvinorin A: an update on pharmacology and analytical methodology. *Planta Med.* **2007,** *73*, 1039-1046.
174. Giroud, C.; Felber, F.; Augsburger, M.; Horisberger, B.; Rivier, L.; Mangin, P. Salvia divinorum: an hallucinogenic mint which might become a new recreational drug in Switzerland. *Forensic Sci. Int.* **2000,** *112*, 143-150.
175. Gonzalez, D.; Riba, J.; Bouso, J. C.; Gomez-Jarabo, G.; Barbanoj, M. J. Pattern of use and subjective effects of Salvia divinorum among recreational users. *Drug Alcohol Depend.* **2006,** *85*, 157-162.
176. Perron, B. E.; Ahmedani, B. K.; Vaughn, M. G.; Glass, J. E.; Abdon, A.; Wu, L. T. Use of Salvia divinorum in a Nationally Representative Sample. *Am. J. Drug Alcohol Abuse* **2012,** *38*, 108-113.
177. Valdes, L. J. Salvia-Divinorum and the Unique Diterpene Hallucinogen, Salvinorin (Divinorin)-A. *J. Psychoact. Drugs* **1994,** *26*, 277-283.
178. Prisinzano, T. E. Psychopharmacology of the hallucinogenic sage Salvia divinorum. *Life Sci.* **2005,** *78*, 527-531.
179. Eguchi, M. Recent advances in selective opioid receptor agonists and antagonists. *Med. Res. Rev.* **2004,** *24*, 182-212.
180. Lu, Y. X.; Weltrowska, G.; Lemieux, C.; Chung, N. N.; Schiller, P. W. Stereospecific synthesis of (2S)-2-methyl-3-(2 ',6 '-dimethyl-4 '-hydroxyphenyl)-propionic acid (Mdp) and its incorporation into an opioid peptide. *Bioorg. Med. Chem. Lett.* **2001,** *11*, 323-325.
181. Surratt, C. K.; Johnson, P. S.; Moriwaki, A.; Seidleck, B. K.; Blaschak, C. J.; Wang, J. B.; Uhl, G. R. -Mu Opiate Receptor - Charged Transmembrane Domain Amino-Acids Are Critical for Agonist Recognition and Intrinsic Activity. *J. Biol. Chem.* **1994,** *269*, 20548-20553.
182. Granier, S.; Manglik, A.; Kruse, A. C.; Kobilka, T. S.; Thian, F. S.; Weis, W. I.; Kobilka, B. K. Structure of the delta-opioid receptor bound to naltrindole. *Nature* **2012,** *485*, 400-404.

183. Manglik, A.; Kruse, A. C.; Kobilka, T. S.; Thian, F. S.; Mathiesen, J. M.; Sunahara, R. K.; Pardo, L.; Weis, W. I.; Kobilka, B. K.; Granier, S. Crystal structure of the micro-opioid receptor bound to a morphinan antagonist. *Nature* **2012,** *485*, 321-326.
184. Wu, H.; Wacker, D.; Mileni, M.; Katritch, V.; Han, G. W.; Vardy, E.; Liu, W.; Thompson, A. A.; Huang, X. P.; Carroll, F. I.; Mascarella, S. W.; Westkaemper, R. B.; Mosier, P. D.; Roth, B. L.; Cherezov, V.; Stevens, R. C. Structure of the human kappa-opioid receptor in complex with JDTic. *Nature* **2012,** *485*, 327-332.
185. Thompson, A. A.; Liu, W.; Chun, E.; Katritch, V.; Wu, H.; Vardy, E.; Huang, X. P.; Trapella, C.; Guerrini, R.; Calo, G.; Roth, B. L.; Cherezov, V.; Stevens, R. C. Structure of the nociceptin/orphanin FQ receptor in complex with a peptide mimetic. *Nature* **2012,** *485*, 395-399.
186. Martin, W. R.; Eades, C. G.; Thompson, J. A.; Huppler, R. E.; Gilbert, P. E. The effects of morphine- and nalorphine- like drugs in the nondependent and morphine-dependent chronic spinal dog. *J. Pharmacol. Exp. Ther.* **1976,** *197*, 517-532.
187. Gilbert, P. E.; Martin, W. R. The effects of morphine and nalorphine-like drugs in the nondependent, morphine-dependent and cyclazocine-dependent chronic spinal dog. *J. Pharmacol. Exp. Ther.* **1976,** *198*, 66-82.
188. Lord, J. A.; Waterfield, A. A.; Hughes, J.; Kosterlitz, H. W. Endogenous opioid peptides: multiple agonists and receptors. *Nature* **1977,** *267*, 495-499.
189. Pan, L.; Xu, J.; Yu, R.; Xu, M. M.; Pan, Y. X.; Pasternak, G. W. Identification and characterization of six new alternatively spliced variants of the human mu opioid receptor gene, Oprm. *Neuroscience* **2005,** *133*, 209-220.
190. Hampson, R. E.; Mu, J.; Deadwyler, S. A. Cannabinoid and kappa opioid receptors reduce potassium K current via activation of G(s) proteins in cultured hippocampal neurons. *J. Neurophysiol.* **2000,** *84*, 2356-2364.
191. Wang, H. Y.; Burns, L. H. Gbetagamma that interacts with adenylyl cyclase in opioid tolerance originates from a Gs protein. *J. Neurobiol.* **2006,** *66*, 1302-1310.
192. Satoh, M.; Minami, M. Molecular pharmacology of the opioid receptors. *Pharmacol. Ther.* **1995,** *68*, 343-364.
193. Hughes, J.; Smith, T. W.; Kosterlitz, H. W.; Fothergill, L. A.; Morgan, B. A.; Morris, H. R. Identification of two related pentapeptides from the brain with potent opiate agonist activity. *Nature* **1975,** *258*, 577-580.
194. Goldstein, A.; Fischli, W.; Lowney, L. I.; Hunkapiller, M.; Hood, L. Porcine pituitary dynorphin: complete amino acid sequence of the biologically active heptadecapeptide. *Proc. Natl. Acad. Sci. U. S. A.* **1981,** *78*, 7219-7223.
195. Li, C. H.; Chung, D. Isolation and structure of an untriakontapeptide with opiate activity from camel pituitary glands. *Proc. Natl. Acad. Sci. USA* **1976,** *73*, 1145-1148.
196. Kieffer, B. L.; Befort, K.; Gaveriaux-Ruff, C.; Hirth, C. G. The delta-opioid receptor: isolation of a cDNA by expression cloning and pharmacological characterization. *Proc. Natl. Acad. Sci. USA* **1992,** *89*, 12048-12052.
197. Evans, C. J.; Keith, D. E., Jr.; Morrison, H.; Magendzo, K.; Edwards, R. H. Cloning of a delta opioid receptor by functional expression. *Science* **1992,** *258*, 1952-1955.
198. Meng, F.; Xie, G. X.; Thompson, R. C.; Mansour, A.; Goldstein, A.; Watson, S. J.; Akil, H. Cloning and pharmacological characterization of a rat kappa opioid receptor. *Proc. Natl. Acad. Sci. USA* **1993,** *90*, 9954-9958.

199. Wang, J. B.; Johnson, P. S.; Persico, A. M.; Hawkins, A. L.; Griffin, C. A.; Uhl, G. R. Human mu opiate receptor. cDNA and genomic clones, pharmacologic characterization and chromosomal assignment. *FEBS Lett.* **1994,** *338*, 217-222.
200. Carlezon, W. A., Jr.; Beguin, C.; DiNieri, J. A.; Baumann, M. H.; Richards, M. R.; Todtenkopf, M. S.; Rothman, R. B.; Ma, Z.; Lee, D. Y.; Cohen, B. M. Depressive-like effects of the kappa-opioid receptor agonist salvinorin A on behavior and neurochemistry in rats. *J. Pharmacol. Exp. Ther.* **2006,** *316*, 440-447.
201. DeHaven-Hudkins, D. L.; Dolle, R. E. Peripherally restricted opioid agonists as novel analgesic agents. *Curr. Pharm. Des.* **2004,** *10*, 743-757.
202. Kivell, B.; Prisinzano, T. E. Kappa opioids and the modulation of pain. *Psychopharmacology* **2010,** *210*, 109-119.
203. Pfeiffer, A.; Brantl, V.; Herz, A.; Emrich, H. M. Psychotomimesis mediated by kappa opiate receptors. *Science* **1986,** *233*, 774-776.
204. Kumor, K. M.; Haertzen, C. A.; Johnson, R. E.; Kocher, T.; Jasinski, D. Human psychopharmacology of ketocyclazocine as compared with cyclazocine, morphine and placebo. *J. Pharmacol. Exp. Ther.* **1986,** *238*, 960-968.
205. Martin, W. R.; Fraser, H. F.; Gorodetzky, C. W.; Rosenberg, D. E. Studies of the dependence-producing potential of the narcotic antagonist 2-cyclopropylmethyl-2'-hydroxy-5,9-dimethyl-6,7-benzomorphan (cyclazocine, WIN-20,740, ARC II-c-3). *J. Pharmacol. Exp. Ther.* **1965,** *150*, 426-436.
206. Obara, I.; Parkitna, J. R.; Korostynski, M.; Makuch, W.; Kaminska, D.; Przewlocka, B.; Przewlocki, R. Local peripheral opioid effects and expression of opioid genes in the spinal cord and dorsal root ganglia in neuropathic and inflammatory pain. *Pain* **2009,** *141*, 283-291.
207. Xu, M.; Petraschka, M.; McLaughlin, J. P.; Westenbroek, R. E.; Caron, M. G.; Lefkowitz, R. J.; Czyzyk, T. A.; Pintar, J. E.; Terman, G. W.; Chavkin, C. Neuropathic pain activates the endogenous kappa opioid system in mouse spinal cord and induces opioid receptor tolerance. *J. Neurosci.* **2004,** *24*, 4576-4584.
208. Riviere, P. J. Peripheral kappa-opioid agonists for visceral pain. *Br. J. Pharmacol.* **2004,** *141*, 1331-1334.
209. Mello, N. K.; Negus, S. S. Interactions between kappa opioid agonists and cocaine - Preclinical studies. *New Medications for Drug Abuse* **2000,** *909*, 104-132.
210. Cami, J.; Farre, M. Drug addiction. *N. Engl. J. Med.* **2003,** *349*, 975-986.
211. Nestler, E. J.; Aghajanian, G. K. Molecular and cellular basis of addiction. *Science* **1997,** *278*, 58-63.
212. Margolis, E. B.; Hjelmstad, G. O.; Bonci, A.; Fields, H. L. Kappa-opioid agonists directly inhibit midbrain dopaminergic neurons. *J. Neurosci.* **2003,** *23*, 9981-9986.
213. Mysels, D.; Sullivan, M. A. The kappa-opiate receptor impacts the pathophysiology and behavior of substance use. *Am. J. Addict.* **2009,** *18*, 272-276.
214. Bruijnzeel, A. W. kappa-Opioid receptor signaling and brain reward function. *Brain Res. Rev.* **2009,** *62*, 127-146.
215. Wang, Y. H.; Sun, J. F.; Tao, Y. M.; Chi, Z. Q.; Liu, J. G. The role of kappa-opioid receptor activation in mediating antinociception and addiction. *Acta Pharmacol. Sin.* **2010,** *31*, 1065-1070.
216. Zhang, Y.; Butelman, E. R.; Schlussman, S. D.; Ho, A.; Kreek, M. J. Effect of the endogenous kappa opioid agonist dynorphin A(1-17) on cocaine-evoked increases in

striatal dopamine levels and cocaine-induced place preference in C57BL/6J mice. *Psychopharmacology (Berl)* **2004,** *172*, 422-429.
217. Koob, G. F.; Vaccarino, F. J.; Amalric, M.; Bloom, F. E. Neurochemical substrates for opiate reinforcement. *NIDA Res. Monogr.* **1986,** *71*, 146-164.
218. Xi, Z. X.; Fuller, S. A.; Stein, E. A. Dopamine release in the nucleus accumbens during heroin self-administration is modulated by kappa opioid receptors: an in vivo fast-cyclic voltammetry study. *J. Pharmacol. Exp. Ther.* **1998,** *284*, 151-161.
219. Glick, S. D.; Maisonneuve, I. M.; Raucci, J.; Archer, S. Kappa opioid inhibition of morphine and cocaine self-administration in rats. *Brain Res.* **1995,** *681*, 147-152.
220. Kuzmin, A. V.; Gerrits, M. A.; Van Ree, J. M. Kappa-opioid receptor blockade with nor-binaltorphimine modulates cocaine self-administration in drug-naive rats. *Eur. J. Pharmacol.* **1998,** *358*, 197-202.
221. Negus, S. S.; Henriksen, S. J.; Mattox, A.; Pasternak, G. W.; Portoghese, P. S.; Takemori, A. E.; Weinger, M. B.; Koob, G. F. Effect of antagonists selective for mu, delta and kappa opioid receptors on the reinforcing effects of heroin in rats. *J. Pharmacol. Exp. Ther.* **1993,** *265*, 1245-1252.
222. Kuzmin, A. V.; Semenova, S.; Gerrits, M. A.; Zvartau, E. E.; Van Ree, J. M. Kappa-opioid receptor agonist U50,488H modulates cocaine and morphine self-administration in drug-naive rats and mice. *Eur. J. Pharmacol.* **1997,** *321*, 265-271.
223. Schenk, S.; Partridge, B.; Shippenberg, T. S. U69593, a kappa-opioid agonist, decreases cocaine self-administration and decreases cocaine-produced drug-seeking. *Psychopharmacology* **1999,** *144*, 339-346.
224. Negus, S. S.; Mello, N. K.; Portoghese, P. S.; Lin, C. E. Effects of kappa opioids on cocaine self-administration by rhesus monkeys. *J. Pharmacol. Exp. Ther.* **1997,** *282*, 44-55.
225. Mello, N. K.; Negus, S. S. Effects of kappa opioid agonists on cocaine- and food-maintained responding by rhesus monkeys. *J. Pharmacol. Exp. Ther.* **1998,** *286*, 812-824.
226. Zhang, Y.; Butelman, E. R.; Schlussman, S. D.; Ho, A.; Kreek, M. J. Effects of the plant-derived hallucinogen salvinorin A on basal dopamine levels in the caudate putamen and in a conditioned place aversion assay in mice: agonist actions at kappa opioid receptors. *Psychopharmacology* **2005,** *179*, 551-558.
227. Suzuki, T.; Shiozaki, Y.; Masukawa, Y.; Misawa, M.; Nagase, H. The role of mu- and kappa-opioid receptors in cocaine-induced conditioned place preference. *Jpn. J. Pharmacol.* **1992,** *58*, 435-442.
228. Crawford, C. A.; McDougall, S. A.; Bolanos, C. A.; Hall, S.; Berger, S. P. The effects of the kappa agonist U-50,488 on cocaine-induced conditioned and unconditioned behaviors and Fos immunoreactivity. *Psychopharmacology* **1995,** *120*, 392-399.
229. Shippenberg, T. S.; LeFevour, A.; Heidbreder, C. kappa-Opioid receptor agonists prevent sensitization to the conditioned rewarding effects of cocaine. *J. Pharmacol. Exp. Ther.* **1996,** *276*, 545-554.
230. Zhang, Y.; Butelman, E. R.; Schlussman, S. D.; Ho, A.; Kreek, M. J. Effect of the kappa opioid agonist R-84760 on cocaine-induced increases in striatal dopamine levels and cocaine-induced place preference in C57BL/6J mice. *Psychopharmacology* **2004,** *173*, 146-152.

231. Mori, T.; Nomura, M.; Nagase, H.; Narita, M.; Suzuki, T. Effects of a newly synthesized kappa-opioid receptor agonist, TRK-820, on the discriminative stimulus and rewarding effects of cocaine in rats. *Psychopharmacology* **2002,** *161*, 17-22.
232. Hasebe, K.; Kawai, K.; Suzuki, T.; Kawamura, K.; Tanaka, T.; Narita, M.; Nagase, H.; Suzuki, T. Possible pharmacotherapy of the opioid kappa receptor agonist for drug dependence. *Ann. N. Y. Acad. Sci.* **2004,** *1025*, 404-413.
233. Funada, M.; Suzuki, T.; Narita, M.; Misawa, M.; Nagase, H. Blockade of morphine reward through the activation of kappa-opioid receptors in mice. *Neuropharmacology* **1993,** *32*, 1315-1323.
234. Ramarao, P.; Jablonski, H. I., Jr.; Rehder, K. R.; Bhargava, H. N. Effect of kappa-opioid receptor agonists on morphine analgesia in morphine-naive and morphine-tolerant rats. *Eur. J. Pharmacol.* **1988,** *156*, 239-246.
235. Tao, P. L.; Hwang, C. L.; Chen, C. Y. U-50,488 blocks the development of morphine tolerance and dependence at a very low dose in guinea pigs. *Eur. J. Pharmacol.* **1994,** *256*, 281-286.
236. Yamamoto, T.; Ohno, M.; Ueki, S. A selective kappa-opioid agonist, U-50,488H, blocks the development of tolerance to morphine analgesia in rats. *Eur. J. Pharmacol.* **1988,** *156*, 173-176.
237. Pan, Z. Z. mu-Opposing actions of the kappa-opioid receptor. *Trends Pharmacol. Sci.* **1998,** *19*, 94-98.
238. Wee, S.; Koob, G. F. The role of the dynorphin-kappa opioid system in the reinforcing effects of drugs of abuse. *Psychopharmacology* **2010,** *210*, 121-135.
239. Matthes, H. W.; Maldonado, R.; Simonin, F.; Valverde, O.; Slowe, S.; Kitchen, I.; Befort, K.; Dierich, A.; Le Meur, M.; Dolle, P.; Tzavara, E.; Hanoune, J.; Roques, B. P.; Kieffer, B. L. Loss of morphine-induced analgesia, reward effect and withdrawal symptoms in mice lacking the mu-opioid-receptor gene. *Nature* **1996,** *383*, 819-823.
240. Sora, I.; Takahashi, N.; Funada, M.; Ujike, H.; Revay, R. S.; Donovan, D. M.; Miner, L. L.; Uhl, G. R. Opiate receptor knockout mice define mu receptor roles in endogenous nociceptive responses and morphine-induced analgesia. *Proc. Natl. Acad. Sci. USA* **1997,** *94*, 1544-1549.
241. Tulunay, F. C.; Jen, M. F.; Chang, J. K.; Loh, H. H.; Lee, N. M. Possible regulatory role of dynorphin on morphine- and beta-endorphin-induced analgesia. *J. Pharmacol. Exp. Ther.* **1981,** *219*, 296-298.
242. Epstein, D. H.; Preston, K. L.; Stewart, J.; Shaham, Y. Toward a model of drug relapse: an assessment of the validity of the reinstatement procedure. *Psychopharmacology* **2006,** *189*, 1-16.
243. Gawin, F.; Kleber, H. Pharmacologic treatments of cocaine abuse. *Psychiatr. Clin. North Am.* **1986,** *9*, 573-583.
244. Carroll, I.; Thomas, J. B.; Dykstra, L. A.; Granger, A. L.; Allen, R. M.; Howard, J. L.; Pollard, G. T.; Aceto, M. D.; Harris, L. S. Pharmacological properties of JDTic: a novel kappa-opioid receptor antagonist. *Eur. J. Pharmacol.* **2004,** *501*, 111-119.
245. Beardsley, P. M.; Howard, J. L.; Shelton, K. L.; Carroll, F. I. Differential effects of the novel kappa opioid receptor antagonist, JDTic, on reinstatement of cocaine-seeking induced by footshock stressors vs cocaine primes and its antidepressant-like effects in rats. *Psychopharmacology* **2005,** *183*, 118-126.

246. Mague, S. D.; Pliakas, A. M.; Todtenkopf, M. S.; Tomasiewicz, H. C.; Zhang, Y.; Stevens, W. C., Jr.; Jones, R. M.; Portoghese, P. S.; Carlezon, W. A., Jr. Antidepressant-like effects of kappa-opioid receptor antagonists in the forced swim test in rats. *J. Pharmacol. Exp. Ther.* **2003,** *305*, 323-330.
247. McLaughlin, J. P.; Marton-Popovici, M.; Chavkin, C. kappa opioid receptor antagonism and prodynorphin gene disruption block stress-induced behavioral responses. *J. Neurosci.* **2003,** *23*, 5674-5683.
248. McLaughlin, J. P.; Land, B. B.; Li, S.; Pintar, J. E.; Chavkin, C. Prior activation of kappa opioid receptors by U50,488 mimics repeated forced swim stress to potentiate cocaine place preference conditioning. *Neuropsychopharmacol.* **2006,** *31*, 787-794.
249. Wee, S.; Orio, L.; Ghirmai, S.; Cashman, J. R.; Koob, G. F. Inhibition of kappa opioid receptors attenuated increased cocaine intake in rats with extended access to cocaine. *Psychopharmacology* **2009,** *205*, 565-575.
250. Shippenberg, T. S. The dynorphin/kappa opioid receptor system: a new target for the treatment of addiction and affective disorders? *Neuropsychopharmacol.* **2009,** *34*, 247.
251. McLaughlin, J. P.; Marton-Popovici, M.; Chavkin, C. Kappa opioid receptor antagonism and prodynorphin gene disruption block stress-induced behavioral responses. *J. Neurosci.* **2003,** *23*, 5674-5683.
252. Carlezon, W. A., Jr.; Thome, J.; Olson, V. G.; Lane-Ladd, S. B.; Brodkin, E. S.; Hiroi, N.; Duman, R. S.; Neve, R. L.; Nestler, E. J. Regulation of cocaine reward by CREB. *Science* **1998,** *282*, 2272-2275.
253. Pliakas, A. M.; Carlson, R. R.; Neve, R. L.; Konradi, C.; Nestler, E. J.; Carlezon, W. A. Altered responsiveness to cocaine and increased immobility in the forced swim test associated with elevated cAMP response element-binding protein expression in nucleus accumbens. *J. Neurosci.* **2001,** *21*, 7397-7403.
254. Shippenberg, T. S.; Rea, W. Sensitization to the behavioral effects of cocaine: modulation by dynorphin and kappa-opioid receptor agonists. *Pharmacol., Biochem. Behav.* **1997,** *57*, 449-455.
255. Spanagel, R.; Shippenberg, T. S. Modulation of morphine-induced sensitization by endogenous kappa opioid systems in the rat. *Neurosci. Lett.* **1993,** *153*, 232-236.
256. Chavkin, C.; Sud, S.; Jin, W.; Stewart, J.; Zjawiony, J. K.; Siebert, D. J.; Toth, B. A.; Hufeisen, S. J.; Roth, B. L. Salvinorin A, an active component of the hallucinogenic sage salvia divinorum is a highly efficacious kappa-opioid receptor agonist: structural and functional considerations. *J. Pharmacol. Exp. Ther.* **2004,** *308*, 1197-1203.
257. Wang, Y.; Tang, K.; Inan, S.; Siebert, D.; Holzgrabe, U.; Lee, D. Y.; Huang, P.; Li, J. G.; Cowan, A.; Liu-Chen, L. Y. Comparison of pharmacological activities of three distinct kappa ligands (Salvinorin A, TRK-820 and 3FLB) on kappa opioid receptors in vitro and their antipruritic and antinociceptive activities in vivo. *J. Pharmacol. Exp. Ther.* **2005,** *312*, 220-230.
258. Porter, J. H.; Prus, A. J. Discriminative stimulus properties of atypical and typical antipsychotic drugs: a review of preclinical studies. *Psychopharmacology* **2009,** *203*, 279-294.
259. Butelman, E. R.; Harris, T. J.; Kreek, M. J. The plant-derived hallucinogen, salvinorin A, produces kappa-opioid agonist-like discriminative effects in rhesus monkeys. *Psychopharmacology* **2004,** *172*, 220-224.

260. Willmore-Fordham, C. B.; Krall, D. M.; McCurdy, C. R.; Kinder, D. H. The hallucinogen derived from Salvia divinorum, salvinorin A, has kappa-opioid agonist discriminative stimulus effects in rats. *Neuropharmacology* **2007,** *53*, 481-486.
261. Fantegrossi, W. E.; Kugle, K. M.; Valdes, L. J., 3rd; Koreeda, M.; Woods, J. H. Kappa-opioid receptor-mediated effects of the plant-derived hallucinogen, salvinorin A, on inverted screen performance in the mouse. *Behav. Pharmacol.* **2005,** *16*, 627-633.
262. Baker, L. E.; Panos, J. J.; Killinger, B. A.; Peet, M. M.; Bell, L. M.; Haliw, L. A.; Walker, S. L. Comparison of the discriminative stimulus effects of salvinorin A and its derivatives to U69,593 and U50,488 in rats. *Psychopharmacology* **2009,** *203*, 203-211.
263. Li, J. X.; Rice, K. C.; France, C. P. Discriminative stimulus effects of 1-(2,5-dimethoxy-4-methylphenyl)-2-aminopropane in rhesus monkeys. *J. Pharmacol. Exp. Ther.* **2008,** *324*, 827-833.
264. Butelman, E. R.; Rus, S.; Prisinzano, T. E.; Kreek, M. J. The discriminative effects of the kappa-opioid hallucinogen salvinorin A in nonhuman primates: dissociation from classic hallucinogen effects. *Psychopharmacology* **2010,** *210*, 253-262.
265. Porsolt, R. D.; Le Pichon, M.; Jalfre, M. Depression: a new animal model sensitive to antidepressant treatments. *Nature* **1977,** *266*, 730-732.
266. Olds, J.; Milner, P. Positive reinforcement produced by electrical stimulation of septal area and other regions of rat brain. *J. Comp. Physiol. Psychol.* **1954,** *47*, 419-427.
267. Vlachou, S.; Markou, A. Intracranial self-stimulation. *Neuromethods* **2011,** *53*, 3-56.
268. Ebner, S. R.; Roitman, M. F.; Potter, D. N.; Rachlin, A. B.; Chartoff, E. H. Depressive-like effects of the kappa opioid receptor agonist salvinorin A are associated with decreased phasic dopamine release in the nucleus accumbens. *Psychopharmacology* **2010,** *210*, 241-252.
269. Braida, D.; Capurro, V.; Zani, A.; Rubino, T.; Vigano, D.; Parolaro, D.; Sala, M. Potential anxiolytic- and antidepressant-like effects of salvinorin A, the main active ingredient of Salvia divinorum, in rodents. *Br. J. Pharmacol.* **2009,** *157*, 844-853.
270. Harden, M. T.; Smith, S. E.; Niehoff, J. A.; McCurdy, C. R.; Taylor, G. T. Antidepressive effects of the kappa-opioid receptor agonist salvinorin A in a rat model of anhedonia. *Behav. Pharmacol.* **2012,** *23*, 710-715.
271. Baker, S. L.; Kentner, A. C.; Konkle, A. T.; Santa-Maria Barbagallo, L.; Bielajew, C. Behavioral and physiological effects of chronic mild stress in female rats. *Physiol. Behav.* **2006,** *87*, 314-322.
272. Willner, P. Chronic mild stress (CMS) revisited: consistency and behavioural-neurobiological concordance in the effects of CMS. *Neuropsychobiology* **2005,** *52*, 90-110.
273. Harding, W. W.; Tidgewell, K.; Byrd, N.; Cobb, H.; Dersch, C. M.; Butelman, E. R.; Rothman, R. B.; Prisinzano, T. E. Neoclerodane diterpenes as a novel scaffold for mu opioid receptor ligands. *J. Med. Chem.* **2005,** *48*, 4765-4771.
274. McCurdy, C. R.; Sufka, K. J.; Smith, G. H.; Warnick, J. E.; Nieto, M. J. Antinociceptive profile of salvinorin A, a structurally unique kappa opioid receptor agonist. *Pharmacol., Biochem. Behav.* **2006,** *83*, 109-113.
275. John, T. F.; French, L. G.; Erlichman, J. S. The antinociceptive effect of salvinorin A in mice. *Eur. J. Pharmacol.* **2006,** *545*, 129-133.
276. Fichna, J.; Dicay, M.; Lewellyn, K.; Janecka, A.; Zjawiony, J. K.; MacNaughton, W. K.; Storr, M. A. Salvinorin A has antiinflammatory and antinociceptive effects in

experimental models of colitis in mice mediated by KOR and CB1 receptors. *Inflamm. Bowel Dis.* **2012,** *18*, 1137-1145.
277. Ansonoff, M. A.; Zhang, J.; Czyzyk, T.; Rothman, R. B.; Stewart, J.; Xu, H.; Zjwiony, J.; Siebert, D. J.; Yang, F.; Roth, B. L.; Pintar, J. E. Antinociceptive and hypothermic effects of Salvinorin A are abolished in a novel strain of kappa-opioid receptor-1 knockout mice. *J. Pharmacol. Exp. Ther.* **2006,** *318*, 641-648.
278. Bowen, C. A.; Negus, S. S.; Kelly, M.; Mello, N. K. The effects of heroin on prolactin levels in male rhesus monkeys: use of cumulative-dosing procedures. *Psychoneuroendocrinology* **2002,** *27*, 319-336.
279. Butelman, E. R.; Mandau, M.; Tidgewell, K.; Prisinzano, T. E.; Yuferov, V.; Kreek, M. J. Effects of salvinorin A, a kappa-opioid hallucinogen, on a neuroendocrine biomarker assay in nonhuman primates with high kappa-receptor homology to humans. *J. Pharmacol. Exp. Ther.* **2007,** *320*, 300-306.
280. Butelman, E. R.; Prisinzano, T. E.; Deng, H.; Rus, S.; Kreek, M. J. Unconditioned behavioral effects of the powerful kappa-opioid hallucinogen salvinorin A in nonhuman primates: fast onset and entry into cerebrospinal fluid. *J. Pharmacol. Exp. Ther.* **2009,** *328*, 588-597.
281. Hooker, J. M.; Xu, Y.; Schiffer, W.; Shea, C.; Carter, P.; Fowler, J. S. Pharmacokinetics of the potent hallucinogen, salvinorin A in primates parallels the rapid onset and short duration of effects in humans. *NeuroImage* **2008,** *41*, 1044-1050.
282. Johnson, M. W.; MacLean, K. A.; Reissig, C. J.; Prisinzano, T. E.; Griffiths, R. R. Human psychopharmacology and dose-effects of salvinorin A, a kappa opioid agonist hallucinogen present in the plant Salvia divinorum. *Drug Alcohol Depend.* **2011,** *115*, 150-155.
283. Addy, P. H. Acute and post-acute behavioral and psychological effects of salvinorin A in humans. *Psychopharmacology* **2012,** *220*, 195-204.
284. Ranganathan, M.; Schnakenberg, A.; Skosnik, P. D.; Cohen, B. M.; Pittman, B.; Sewell, R. A.; D'Souza, D. C. Dose-Related Behavioral, Subjective, Endocrine, and Psychophysiological Effects of the kappa Opioid Agonist Salvinorin A in Humans. *Biol. Psychiat.* **2012,** *72*, 871-879.
285. MacLean, K. A.; Johnson, M. W.; Reissig, C. J.; Prisinzano, T. E.; Griffiths, R. R. Dose-related effects of salvinorin A in humans: dissociative, hallucinogenic, and memory effects. *Psychopharmacology* **2013,** *226*, 381-392.
286. Chartoff, E. H.; Potter, D.; Damez-Werno, D.; Cohen, B. M.; Carlezon, W. A., Jr. Exposure to the selective kappa-opioid receptor agonist salvinorin A modulates the behavioral and molecular effects of cocaine in rats. *Neuropsychopharmacol.* **2008,** *33*, 2676-2687.
287. Morani, A. S.; Kivell, B.; Prisinzano, T. E.; Schenk, S. Effect of kappa-opioid receptor agonists U69593, U50488H, spiradoline and salvinorin A on cocaine-induced drug-seeking in rats. *Pharmacol., Biochem. Behav.* **2009,** *94*, 244-249.
288. Schmidt, M. S.; Prisinzano, T. E.; Tidgewell, K.; Harding, W.; Butelman, E. R.; Kreek, M. J.; Murry, D. J. Determination of Salvinorin A in body fluids by high performance liquid chromatography-atmospheric pressure chemical ionization. *J. Chromatogr. B Analyt. Technol. Biomed. Life Sci.* **2005,** *818*, 221-225.
289. Schmidt, M. D.; Schmidt, M. S.; Butelman, E. R.; Harding, W. W.; Tidgewell, K.; Murry, D. J.; Kreek, M. J.; Prisinzano, T. E. Pharmacokinetics of the plant-derived

kappa-opioid hallucinogen salvinorin A in nonhuman primates. *Synapse* **2005,** *58*, 208-210.
290. Kutrzeba, L. M.; Karamyan, V. T.; Speth, R. C.; Williamson, J. S.; Zjawiony, J. K. In vitro studies on metabolism of salvinorin A. *Pharm. Biol.* **2009,** *47*, 1078-1084.
291. Pichini, S.; Abanades, S.; Farre, M.; Pellegrini, M.; Marchei, E.; Pacifici, R.; de la Torre, R.; Zuccaro, P. Quantification of the plant-derived hallucinogen Salvinorin A in conventional and non-conventional biological fluids by gas chromatography/mass spectrometry after Salvia divinorum smoking. *Rapid Commun. Mass Spectrom.* **2005,** *19*, 1649-1656.
292. Teksin, Z. S.; Lee, I. J.; Nemieboka, N. N.; Othman, A. A.; Upreti, V. V.; Hassan, H. E.; Syed, S. S.; Prisinzano, T. E.; Eddington, N. D. Evaluation of the transport, in vitro metabolism and pharmacokinetics of Salvinorin A, a potent hallucinogen. *Eur. J. Pharm. Biopharm.* **2009,** *72*, 471-477.
293. Tsujikawa, K.; Kuwayama, K.; Miyaguchi, H.; Kanamori, T.; Iwata, Y. T.; Inoue, H. In vitro stability and metabolism of salvinorin A in rat plasma. *Xenobiotica* **2009,** *39*, 391-398.
294. Cunningham, C. W.; Rothman, R. B.; Prisinzano, T. E. Neuropharmacology of the Naturally Occurring kappa-Opioid Hallucinogen Salvinorin A. *Pharmacol. Rev.* **2011,** *63*, 316-347.
295. Munro, T. A.; Rizzacasa, M. A.; Roth, B. L.; Toth, B. A.; Yan, F. Studies toward the pharmacophore of salvinorin A, a potent kappa opioid receptor agonist. *J. Med. Chem.* **2005,** *48*, 345-348.
296. Simpson, D. S.; Katavic, P. L.; Lozama, A.; Harding, W. W.; Parrish, D.; Deschamps, J. R.; Dersch, C. M.; Partilla, J. S.; Rothman, R. B.; Navarro, H.; Prisinzano, T. E. Synthetic studies of neoclerodane diterpenes from Salvia divinorum: preparation and opioid receptor activity of salvinicin analogues. *J. Med. Chem.* **2007,** *50*, 3596-3603.
297. Harding, W. W.; Schmidt, M.; Tidgewell, K.; Kannan, P.; Holden, K. G.; Dersch, C. M.; Rothman, R. B.; Prisinzano, T. E. Synthetic studies of neoclerodane diterpenes from Salvia divinorum: selective modification of the furan ring. *Bioorg. Med. Chem. Lett.* **2006,** *16*, 3170-3174.
298. Harding, W. W.; Schmidt, M.; Tidgewell, K.; Kannan, P.; Holden, K. G.; Gilmour, B.; Navarro, H.; Rothman, R. B.; Prisinzano, T. E. Synthetic studies of neoclerodane diterpenes from Salvia divinorum: semisynthesis of salvinicins A and B and other chemical transformations of salvinorin A. *J. Nat. Prod.* **2006,** *69*, 107-112.
299. Harding, W. W.; Tidgewell, K.; Schmidt, M.; Shah, K.; Dersch, C. M.; Snyder, J.; Parrish, D.; Deschamps, J. R.; Rothman, R. B.; Prisinzano, T. E. Salvinicins A and B, new neoclerodane diterpenes from Salvia divinorum. *Org. Lett.* **2005,** *7*, 3017-3020.
300. Beguin, C.; Duncan, K. K.; Munro, T. A.; Ho, D. M.; Xu, W.; Liu-Chen, L. Y.; Carlezon, W. A., Jr.; Cohen, B. M. Modification of the furan ring of salvinorin A: identification of a selective partial agonist at the kappa opioid receptor. *Bioorg. Med. Chem.* **2009,** *17*, 1370-1380.
301. Lozama, A.; Cunningham, C. W.; Caspers, M. J.; Douglas, J. T.; Dersch, C. M.; Rothman, R. B.; Prisinzano, T. E. Opioid receptor probes derived from cycloaddition of the hallucinogen natural product salvinorin A. *J. Nat. Prod.* **2011,** *74*, 718-726.
302. Lovell, K. M.; Vasiljevik, T.; Araya, J. J.; Lozama, A.; Prevatt-Smith, K. M.; Day, V. W.; Dersch, C. M.; Rothman, R. B.; Butelman, E. R.; Kreek, M. J.; Prisinzano, T. E.

Semisynthetic neoclerodanes as kappa opioid receptor probes. *Bioorg. Med. Chem.* **2012,** *20*, 3100-3110.
303. Yang, L.; Xu, W.; Chen, F.; Liu-Chen, L. Y.; Ma, Z.; Lee, D. Y. Synthesis and biological evaluation of C-12 triazole and oxadiazole analogs of salvinorin A. *Bioorg. Med. Chem. Lett.* **2009,** *19*, 1301-1304.
304. Beguin, C.; Potuzak, J.; Xu, W.; Liu-Chen, L. Y.; Streicher, J. M.; Groer, C. E.; Bohn, L. M.; Carlezon, W. A., Jr.; Cohen, B. M. Differential signaling properties at the kappa opioid receptor of 12-epi-salvinorin A and its analogues. *Bioorg. Med. Chem. Lett.* **2012,** *22*, 1023-1026.
305. Simpson, D. S.; Lovell, K. M.; Lozama, A.; Han, N.; Day, V. W.; Dersch, C. M.; Rothman, R. B.; Prisinzano, T. E. Synthetic studies of neoclerodane diterpenes from Salvia divinorum: role of the furan in affinity for opioid receptors. *Org. Biomol. Chem.* **2009,** *7*, 3748-3756.
306. Prisinzano, T. E. Natural products as tools for neuroscience: discovery and development of novel agents to treat drug abuse. *J. Nat. Prod.* **2009,** *72*, 581-587.
307. Kouzi, S. A.; McMurtry, R. J.; Nelson, S. D. Hepatotoxicity of germander (Teucrium chamaedrys L.) and one of its constituent neoclerodane diterpenes teucrin A in the mouse. *Chem. Res. Toxicol.* **1994,** *7*, 850-856.
308. Druckova, A.; Marnett, L. J. Characterization of the amino acid adducts of the enedial derivative of teucrin A. *Chem. Res. Toxicol.* **2006,** *19*, 1330-1340.
309. Druckova, A.; Mernaugh, R. L.; Ham, A. J.; Marnett, L. J. Identification of the protein targets of the reactive metabolite of teucrin A in vivo in the rat. *Chem. Res. Toxicol.* **2007,** *20*, 1393-1408.
310. Guengerich, F. P. Cytochrome P450s and other enzymes in drug metabolism and toxicity. *AAPS J.* **2006,** *8*, E101-111.
311. Tidgewell, K.; Harding, W. W.; Schmidt, M.; Holden, K. G.; Murry, D. J.; Prisinzano, T. E. A facile method for the preparation of deuterium labeled salvinorin A: synthesis of [2,2,2-2H3]-salvinorin A. *Bioorg. Med. Chem. Lett.* **2004,** *14*, 5099-5102.
312. Miyake, T.; Uda, K.; Kinoshita, M.; Fujii, M.; Akita, H. Concise syntheses of coronarin A, coronarin E, austrochaparol and pacovatinin A. *Chem. Pharm. Bull.* **2008,** *56*, 398-403.
313. Simpson, D. S.; Lovell, K. M.; Lozama, A.; Han, N.; Day, V. W.; Dersch, C. M.; Rothman, R. B.; Prisinzano, T. E. Synthetic studies of neoclerodane diterpenes from Salvia divinorum: role of the furan in affinity for opioid receptors. *Org. Biomol. Chem.* **2009,** *7*, 3748-3756.
314. Fontana, G.; Savona, G.; Rodriguez, B.; Dersch, C. M.; Rothman, R. B.; Prisinzano, T. E. Synthetic studies of neoclerodane diterpenoids from Salvia splendens and evaluation of Opioid Receptor affinity. *Tetrahedron* **2008,** *64*, 10041-10048.
315. Xu, H.; Hashimoto, A.; Rice, K. C.; Jacobson, A. E.; Thomas, J. B.; Carroll, F. I.; Lai, J.; Rothman, R. B. Opioid peptide receptor studies. 14. Stereochemistry determines agonist efficacy and intrinsic efficacy in the [(35)S]GTP-gamma-S functional binding assay. *Synapse* **2001,** *39*, 64-69.
316. Holden, K. G.; Tidgewell, K.; Marquam, A.; Rothman, R. B.; Navarro, H.; Prisinzano, T. E. Synthetic studies of neoclerodane diterpenes from Salvia divinorum: exploration of the 1-position. *Bioorg. Med. Chem. Lett.* **2007,** *17*, 6111-6115.

317. Molinski, T. F.; Dalisay, D. S.; Lievens, S. L.; Saludes, J. P. Drug development from marine natural products. *Nat. Rev. Drug Discov.* **2009,** *8*, 69-85.
318. Capon, R. J. Marine bioprospecting - Trawling for treasure and pleasure. *Eur. J. Org. Chem.* **2001**, 633-645.
319. Haefner, B. Drugs from the deep: marine natural products as drug candidates. *Drug Discov. Today* **2003,** *8*, 536-544.
320. Bergmann, W.; Feeney, R. J. The Isolation of a New Thymine Pentoside from Sponges. *J. Am. Chem. Soc.* **1950,** *72*, 2809-2810.
321. Newman, D. J.; Cragg, G. M. Marine natural products and related compounds in clinical and advanced preclinical trials. *J. Nat. Prod.* **2004,** *67*, 1216-1238.
322. Strohl, W. R. The role of natural products in a modern drug discovery program. *Drug Discov. Today* **2000,** *5*, 39-41.
323. Shigemori, H.; Madono, T.; Sasaki, T.; Mikami, Y.; Kobayashi, J. Nakijiquinone-a and Nakijiquinone-B, New Antifungal Sesquiterpenoid Quinones with an Amino-Acid Residue from an Okinawan Marine Sponge. *Tetrahedron* **1994,** *50*, 8347-8354.
324. Kobayashi, J.; Naitoh, K.; Sasaki, T.; Shigemori, H. Metachromins D-H, new cytotoxic sesquiterpenoids from the Okinawan marine sponge Hippospongia metachromia. *J. Org. Chem.* **1992,** *57*, 5773-5776.
325. Alvi, K. A.; Diaz, M. C.; Crews, P.; Slate, D. L.; Lee, R. H.; Moretti, R. Evaluation of New Sesquiterpene Quinones from 2 Dysidea Sponge Species as Inhibitors of Protein Tyrosine Kinase. *J. Org. Chem.* **1992,** *57*, 6604-6607.
326. Kondracki, M. L.; Guyot, M. Biologically-Active Quinone and Hydroquinone Sesquiterpenoids from the Sponge Smenospongia Sp. *Tetrahedron* **1989,** *45*, 1995-2004.
327. Kobayashi, J.; Madono, T.; Shigemori, H. Nakijiquinone-C and Nakijiquinone-D, New Sesquiterpenoid Quinones with a Hydroxy Amino-Acid Residue from a Marine Sponge Inhibiting C-Erbb-2 Kinase. *Tetrahedron* **1995,** *51*, 10867-10874.
328. Takahashi, Y.; Kubota, T.; Kobayashi, J. Nakijiquinones E and F, new dimeric sesquiterpenoid quinones from marine sponge. *Biorg. Med. Chem.* **2009,** *17*, 2185-2188.
329. Takahashi, Y.; Kubota, T.; Ito, J.; Mikami, Y.; Fromont, J.; Kobayashi, J. Nakijiquinones G-I, new sesquiterpenoid quinones from marine sponge. *Bioorg. Med. Chem.* **2008,** *16*, 7561-7564.
330. Takahashi, Y.; Ushio, M.; Kubota, T.; Yamamoto, S.; Fromont, J.; Kobayashi, J. Nakijiquinones J--R, sesquiterpenoid quinones with an amine residue from okinawan marine sponges. *J. Nat. Prod.* **2010,** *73*, 467-471.
331. Stahl, P.; Kissau, L.; Mazitschek, R.; Giannis, A.; Waldmann, H. Natural product derived receptor tyrosine kinase inhibitors: identification of IGF1R, Tie-2, and VEGFR-3 inhibitors. *Angew. Chem. Int. Ed. Engl.* **2002,** *41*, 1174-1178.
332. Stahl, P.; Kissau, L.; Mazitschek, R.; Huwe, A.; Furet, P.; Giannis, A.; Waldmann, H. Total synthesis and biological evaluation of the nakijiquinones. *J. Am. Chem. Soc.* **2001,** *123*, 11586-11593.
333. Stahl, P.; Waldmann, H. Asymmetric Synthesis of the Nakijiquinones-Selective Inhibitors of the Her-2/Neu Protooncogene. *Angew. Chem. Int. Ed. Engl.* **1999,** *38*, 3710-3713.
334. Kissau, L.; Stahl, P.; Mazitschek, R.; Giannis, A.; Waldmann, H. Development of natural product-derived receptor tyrosine kinase inhibitors based on conservation of protein domain fold. *J. Med. Chem.* **2003,** *46*, 2917-2931.

335. Ling, T.; Xiang, A. X.; Theodorakis, E. A. Enantioselective Total Synthesis of Avarol and Avarone. *Angew. Chem. Int. Ed. Engl.* **1999,** *38*, 3089-3091.
336. Tremblay, M. S.; Sames, D. A new fluorogenic transformation: development of an optical probe for coenzyme Q. *Org. Lett.* **2005,** *7*, 2417-2420.
337. Sutherland, H. S.; Higgs, K. C.; Taylor, N. J.; Rodrigo, R. Isobenzofurans and ortho-benzoquinone monoketals in syntheses of xestoquinone and its 9-and 10-methoxy derivatives. *Tetrahedron* **2001,** *57*, 309-317.
338. Di, L.; Kerns, E. H.; Fan, K.; McConnell, O. J.; Carter, G. T. High throughput artificial membrane permeability assay for blood-brain barrier. *Eur. J. Med. Chem.* **2003,** *38*, 223-232.
339. Konczol, A.; Muller, J.; Foldes, E.; Beni, Z.; Vegh, K.; Kery, A.; Balogh, G. T. Applicability of a blood-brain barrier specific artificial membrane permeability assay at the early stage of natural product-based CNS drug discovery. *J. Nat. Prod.* **2013,** *76*, 655-663.
340. Tidgewell, K.; Harding, W. W.; Schmidt, M.; Holden, K. G.; Murry, D. J.; Prisinzano, T. E. A facile method for the preparation of deuterium labeled salvinorin A: synthesis of [2,2,2-$^{2}H_3$]-salvinorin A. *Bioorg. Med. Chem. Lett.* **2004,** *14*, 5099-5102.
341. Kusuma, B. R.; Peterson, L. B.; Zhao, H.; Vielhauer, G.; Holzbeierlein, J.; Blagg, B. S. Targeting the heat shock protein 90 dimer with dimeric inhibitors. *J. Med. Chem.* **2011,** *54*, 6234-6253.
342. Ben Amar, M. Cannabinoids in medicine: A review of their therapeutic potential. *J. Ethnopharmacol.* **2006,** *105*, 1-25.
343. Seely, K. A.; Prather, P. L.; James, L. P.; Moran, J. H. Marijuana-based drugs: innovative therapeutics or designer drugs of abuse? *Mol. Interv.* **2011,** *11*, 36-51.
344. Touw, M. The religious and medicinal uses of Cannabis in China, India and Tibet. *J. Psychoact. Drugs* **1981,** *13*, 23-34.
345. Li, H. L. Archeological and Historical Account of Cannabis in China. *Econ. Bot.* **1974,** *28*, 437-448.
346. Bostwick, J. M. Blurred Boundaries: The Therapeutics and Politics of Medical Marijuana. *Mayo Clin. Proc.* **2012,** *87*, 172-186.
347. Zuardi, A. W. History of cannabis as a medicine: a review. *Rev Bras Psiquiatr* **2006,** *28*, 153-157.
348. Aggarwal, S. K.; Carter, G. T.; Sullivan, M. D.; ZumBrunnen, C.; Morrill, R.; Mayer, J. D. Medicinal use of cannabis in the United States: historical perspectives, current trends, and future directions. *J. Opioid Manag.* **2009,** *5*, 153-168.
349. Musto, D. F. The Marihuana Tax Act of 1937. *Arch. Gen. Psychiatry* **1972,** *26*, 101-108.
350. Banken, J. A. Drug abuse trends among youth in the United States. *Ann. N. Y. Acad. Sci.* **2004,** *1025*, 465-471.
351. Devane, W. A.; Dysarz, F. A., 3rd; Johnson, M. R.; Melvin, L. S.; Howlett, A. C. Determination and characterization of a cannabinoid receptor in rat brain. *Mol. Pharmacol.* **1988,** *34*, 605-613.
352. Matsuda, L. A.; Lolait, S. J.; Brownstein, M. J.; Young, A. C.; Bonner, T. I. Structure of a cannabinoid receptor and functional expression of the cloned cDNA. *Nature* **1990,** *346*, 561-564.
353. Munro, S.; Thomas, K. L.; Abu-Shaar, M. Molecular characterization of a peripheral receptor for cannabinoids. *Nature* **1993,** *365*, 61-65.

354. Guindon, J.; Hohmann, A. G. The endocannabinoid system and pain. *CNS Neurol. Disord. Drug Targets* **2009,** *8*, 403-421.
355. Begg, M.; Pacher, P.; Batkai, S.; Osei-Hyiaman, D.; Offertaler, L.; Mo, F. M.; Liu, J.; Kunos, G. Evidence for novel cannabinoid receptors. *Pharmacology & therapeutics* **2005,** *106*, 133-145.
356. Pertwee, R. G.; Howlett, A. C.; Abood, M. E.; Alexander, S. P.; Di Marzo, V.; Elphick, M. R.; Greasley, P. J.; Hansen, H. S.; Kunos, G.; Mackie, K.; Mechoulam, R.; Ross, R. A. International Union of Basic and Clinical Pharmacology. LXXIX. Cannabinoid receptors and their ligands: beyond CB(1) and CB(2). *Pharmacol. Rev.* **2010,** *62*, 588-631.
357. Goutopoulos, A.; Makriyannis, A. From cannabis to cannabinergics: new therapeutic opportunities. *Pharmacol. Ther.* **2002,** *95*, 103-117.
358. Thakur, G. A.; Tichkule, R.; Bajaj, S.; Makriyannis, A. Latest advances in cannabinoid receptor agonists. *Expert Opin. Ther. Pat.* **2009,** *19*, 1647-1673.
359. Ryberg, E.; Larsson, N.; Sjogren, S.; Hjorth, S.; Hermansson, N. O.; Leonova, J.; Elebring, T.; Nilsson, K.; Drmota, T.; Greasley, P. J. The orphan receptor GPR55 is a novel cannabinoid receptor. *Br. J. Pharmacol.* **2007,** *152*, 1092-1101.
360. Brown, A. J. Novel cannabinoid receptors. *Br. J. Pharmacol.* **2007,** *152*, 567-575.
361. Pertwee, R. G.; Ross, R. A. Cannabinoid receptors and their ligands. *Prostaglandins Leukot. Essent. Fatty Acids* **2002,** *66*, 101-121.
362. Jhaveri, M. D.; Sagar, D. R.; Elmes, S. J.; Kendall, D. A.; Chapman, V. Cannabinoid CB2 receptor-mediated anti-nociception in models of acute and chronic pain. *Mol. Neurobiol.* **2007,** *36*, 26-35.
363. Van Sickle, M. D.; Duncan, M.; Kingsley, P. J.; Mouihate, A.; Urbani, P.; Mackie, K.; Stella, N.; Makriyannis, A.; Piomelli, D.; Davison, J. S.; Marnett, L. J.; Di Marzo, V.; Pittman, Q. J.; Patel, K. D.; Sharkey, K. A. Identification and functional characterization of brainstem cannabinoid CB2 receptors. *Science* **2005,** *310*, 329-332.
364. Lambert, D. M.; Fowler, C. J. The endocannabinoid system: drug targets, lead compounds, and potential therapeutic applications. *J. Med. Chem.* **2005,** *48*, 5059-5087.
365. Devane, W. A.; Hanus, L.; Breuer, A.; Pertwee, R. G.; Stevenson, L. A.; Griffin, G.; Gibson, D.; Mandelbaum, A.; Etinger, A.; Mechoulam, R. Isolation and structure of a brain constituent that binds to the cannabinoid receptor. *Science* **1992,** *258*, 1946-1949.
366. Pertwee, R. G. Pharmacology of cannabinoid receptor ligands. *Curr. Med. Chem.* **1999,** *6*, 635-664.
367. Mechoulam, R.; Ben-Shabat, S.; Hanus, L.; Ligumsky, M.; Kaminski, N. E.; Schatz, A. R.; Gopher, A.; Almog, S.; Martin, B. R.; Compton, D. R.; et al. Identification of an endogenous 2-monoglyceride, present in canine gut, that binds to cannabinoid receptors. *Biochem. Pharmacol.* **1995,** *50*, 83-90.
368. Stella, N.; Schweitzer, P.; Piomelli, D. A second endogenous cannabinoid that modulates long-term potentiation. *Nature* **1997,** *388*, 773-778.
369. Di Marzo, V. 2-Arachidonoyl-glycerol as an "endocannabinoid": limelight for a formerly neglected metabolite. *Biochemistry (Mosc.)* **1998,** *63*, 13-21.
370. Bradshaw, H. B.; Walker, J. M. The expanding field of cannabimimetic and related lipid mediators. *Br. J. Pharmacol.* **2005,** *144*, 459-465.
371. Wang, J.; Ueda, N. Biology of endocannabinoid synthesis system. *Prostaglandins Other Lipid Mediat.* **2009,** *89*, 112-119.

372. Di, M. V. Endocannabinoids: synthesis and degradation. *Rev. Physiol., Biochem. Pharmacol.* **2008,** *160*, 1-24.
373. Cravatt, B. F.; Giang, D. K.; Mayfield, S. P.; Boger, D. L.; Lerner, R. A.; Gilula, N. B. Molecular characterization of an enzyme that degrades neuromodulatory fatty-acid amides. *Nature* **1996,** *384*, 83-87.
374. Giang, D. K.; Cravatt, B. F. Molecular characterization of human and mouse fatty acid amide hydrolases. *Proc. Natl. Acad. Sci. U. S. A.* **1997,** *94*, 2238-2242.
375. Dinh, T. P.; Carpenter, D.; Leslie, F. M.; Freund, T. F.; Katona, I.; Sensi, S. L.; Kathuria, S.; Piomelli, D. Brain monoglyceride lipase participating in endocannabinoid inactivation. *Proc. Natl. Acad. Sci. U. S. A.* **2002,** *99*, 10819-10824.
376. Poso, A.; Huffman, J. W. Targeting the cannabinoid CB2 receptor: modelling and structural determinants of CB2 selective ligands. *Br. J. Pharmacol.* **2008,** *153*, 335-346.
377. Padgett, L. W. Recent developments in cannabinoid ligands. *Life Sci.* **2005,** *77*, 1767-1798.
378. Huffman, J. W.; Lu, J.; Hynd, G.; Wiley, J. L.; Martin, B. R. A pyridone analogue of traditional cannabinoids. A new class of selective ligands for the CB(2) receptor. *Bioorg. Med. Chem.* **2001,** *9*, 2863-2870.
379. Thakur, G. A.; Palmer, S. L.; Harrington, P. E.; Stergiades, I. A.; Tius, M. A.; Makriyannis, A. Enantiomeric resolution of a novel chiral cannabinoid receptor ligand. *J. Biochem. Biophys. Methods* **2002,** *54*, 415-422.
380. Tius, M. A.; Hill, W. A.; Zou, X. L.; Busch-Petersen, J.; Kawakami, J. K.; Fernandez-Garcia, M. C.; Drake, D. J.; Abadji, V.; Makriyannis, A. Classical/non-classical cannabinoid hybrids; stereochemical requirements for the southern hydroxyalkyl chain. *Life Sci.* **1995,** *56*, 2007-2012.
381. Drake, D. J.; Jensen, R. S.; Busch-Petersen, J.; Kawakami, J. K.; Concepcion Fernandez-Garcia, M.; Fan, P.; Makriyannis, A.; Tius, M. A. Classical/nonclassical hybrid cannabinoids: southern aliphatic chain-functionalized C-6beta methyl, ethyl, and propyl analogues. *J. Med. Chem.* **1998,** *41*, 3596-3608.
382. Bourne, C.; Roy, S.; Wiley, J. L.; Martin, B. R.; Thomas, B. F.; Mahadevan, A.; Razdan, R. K. Novel, potent THC/anandamide (hybrid) analogs. *Bioorg. Med. Chem.* **2007,** *15*, 7850-7864.
383. D'Ambra, T. E.; Estep, K. G.; Bell, M. R.; Eissenstat, M. A.; Josef, K. A.; Ward, S. J.; Haycock, D. A.; Baizman, E. R.; Casiano, F. M.; Beglin, N. C.; et al. Conformationally restrained analogues of pravadoline: nanomolar potent, enantioselective, (aminoalkyl)indole agonists of the cannabinoid receptor. *J. Med. Chem.* **1992,** *35*, 124-135.
384. Bell, M. R.; D'Ambra, T. E.; Kumar, V.; Eissenstat, M. A.; Herrmann, J. L., Jr.; Wetzel, J. R.; Rosi, D.; Philion, R. E.; Daum, S. J.; Hlasta, D. J.; et al. Antinociceptive (aminoalkyl)indoles. *J. Med. Chem.* **1991,** *34*, 1099-1110.
385. Huffman, J. W.; Zengin, G.; Wu, M. J.; Lu, J.; Hynd, G.; Bushell, K.; Thompson, A. L.; Bushell, S.; Tartal, C.; Hurst, D. P.; Reggio, P. H.; Selley, D. E.; Cassidy, M. P.; Wiley, J. L.; Martin, B. R. Structure-activity relationships for 1-alkyl-3-(1-naphthoyl)indoles at the cannabinoid CB(1) and CB(2) receptors: steric and electronic effects of naphthoyl substituents. New highly selective CB(2) receptor agonists. *Bioorg. Med. Chem.* **2005,** *13*, 89-112.

386. Compton, D. R.; Gold, L. H.; Ward, S. J.; Balster, R. L.; Martin, B. R. Aminoalkylindole analogs: cannabimimetic activity of a class of compounds structurally distinct from delta 9-tetrahydrocannabinol. *The Journal of pharmacology and experimental therapeutics* **1992,** *263*, 1118-1126.
387. Huffmann, J. W.; Dai, D. Design, synthesis and pharmacology of cannabimimetic indoles. *Bioorg. Med. Chem. Lett.* **1994,** *4*, 563-566.
388. Eissenstat, M. A.; Bell, M. R.; D'Ambra, T. E.; Alexander, E. J.; Daum, S. J.; Ackerman, J. H.; Gruett, M. D.; Kumar, V.; Estep, K. G.; Olefirowicz, E. M.; et al. Aminoalkylindoles: structure-activity relationships of novel cannabinoid mimetics. *J. Med. Chem.* **1995,** *38*, 3094-3105.
389. D'Ambra, T. E.; Eissenstat, M. A.; Abt, J.; Ackerman, J. H.; Bacon, E. R.; Bell, M. R.; Carabateas, P. M.; Josef, K. A.; Kumar, V.; et, a. C-Attached aminoalkylindoles: potent cannabinoid mimetics. *Bioorg. Med. Chem. Lett.* **1996,** *6*, 17-22.
390. Wiley, J. L.; Compton, D. R.; Dai, D.; Lainton, J. A.; Phillips, M.; Huffman, J. W.; Martin, B. R. Structure-activity relationships of indole- and pyrrole-derived cannabinoids. *J. Pharmacol. Exp. Ther.* **1998,** *285*, 995-1004.
391. Huffman, J. W.; Lu, J.; Dai, D.; Kitaygorodskiy, A.; Wiley, J. L.; Martin, B. R. Synthesis and pharmacology of a hybrid cannabinoid. *Bioorg. Med. Chem.* **2000,** *8*, 439-447.
392. Deng, H.; Gifford, A. N.; Zvonok, A. M.; Cui, G.; Li, X.; Fan, P.; Deschamps, J. R.; Flippen-Anderson, J. L.; Gatley, S. J.; Makriyannis, A. Potent cannabinergic indole analogues as radioiodinatable brain imaging agents for the CB1 cannabinoid receptor. *J. Med. Chem.* **2005,** *48*, 6386-6392.
393. Willis, P. G.; Pavlova, O. A.; Chefer, S. I.; Vaupel, D. B.; Mukhin, A. G.; Horti, A. G. Synthesis and structure-activity relationship of a novel series of aminoalkylindoles with potential for imaging the neuronal cannabinoid receptor by positron emission tomography. *J. Med. Chem.* **2005,** *48*, 5813-5822.
394. Mazzoni, O.; Diurno, M. V.; di Bosco, A. M.; Novellino, E.; Grieco, P.; Esposito, G.; Bertamino, A.; Calignano, A.; Russo, R. Synthesis and pharmacological evaluation of analogs of indole-based cannabimimetic agents. *Chem. Biol. Drug Des.* **2010,** *75*, 106-114.
395. Frost, J. M.; Dart, M. J.; Tietje, K. R.; Garrison, T. R.; Grayson, G. K.; Daza, A. V.; El-Kouhen, O. F.; Yao, B. B.; Hsieh, G. C.; Pai, M.; Zhu, C. Z.; Chandran, P.; Meyer, M. D. Indol-3-ylcycloalkyl ketones: effects of N1 substituted indole side chain variations on CB(2) cannabinoid receptor activity. *J. Med. Chem.* **2010,** *53*, 295-315.
396. Ibrahim, M. M.; Deng, H.; Zvonok, A.; Cockayne, D. A.; Kwan, J.; Mata, H. P.; Vanderah, T. W.; Lai, J.; Porreca, F.; Makriyannis, A.; Malan, T. P., Jr. Activation of CB2 cannabinoid receptors by AM1241 inhibits experimental neuropathic pain: pain inhibition by receptors not present in the CNS. *Proc. Natl. Acad. Sci. U. S. A.* **2003,** *100*, 10529-10533.
397. Hynes, J., Jr.; Leftheris, K.; Wu, H.; Pandit, C.; Chen, P.; Norris, D. J.; Chen, B. C.; Zhao, R.; Kiener, P. A.; Chen, X.; Turk, L. A.; Patil-Koota, V.; Gillooly, K. M.; Shuster, D. J.; McIntyre, K. W. C-3 Amido-indole cannabinoid receptor modulators. *Bioorg. Med. Chem. Lett.* **2002,** *12*, 2399-2402.
398. Youssef, F. F.; Irving, A. J. From cannabis to the endocannabinoid system: refocussing attention on potential clinical benefits. *West Indian Med. J.* **2012,** *61*, 264-270.

399. Croxford, J. L. Therapeutic potential of cannabinoids in CNS disease. *CNS Drugs* **2003,** *17*, 179-202.
400. de Lago, E.; Gomez-Ruiz, M.; Moreno-Martet, M.; Fernandez-Ruiz, J. Cannabinoids, multiple sclerosis and neuroprotection. *Expert Rev. Clin. Pharmacol.* **2009,** *2*, 645-660.
401. Pretorius, P. M.; Quaghebeur, G. The role of MRI in the diagnosis of MS. *Clin. Radiol.* **2003,** *58*, 434-448.
402. Multiple Sclerosis Society. Multiple Sclerosis: Just the Facts (2012), http://www.google.com/url?sa=t&rct=j&q=&esrc=s&source=web&cd=3&ved=0CFYQFjAC&url=http%3A%2F%2Fwww.nationalmssociety.org%2Fdownload.aspx%3Fid%3D22&ei=UfwPUtPGMqqK2wWGtYGgBg&usg=AFQjCNFvg1d5r4SnWlFNzfV0NaXGcpMueQ&bvm=bv.50768961,d.b2I. **2012**.
403. Zajicek, J. P.; Apostu, V. I. Role of cannabinoids in multiple sclerosis. *CNS Drugs* **2011,** *25*, 187-201.
404. Di Marzo, V. Targeting the endocannabinoid system: to enhance or reduce? *Nat. Rev. Drug Discov.* **2008,** *7*, 438-455.
405. Eljaschewitsch, E.; Witting, A.; Mawrin, C.; Lee, T.; Schmidt, P. M.; Wolf, S.; Hoertnagl, H.; Raine, C. S.; Schneider-Stock, R.; Nitsch, R.; Ullrich, O. The endocannabinoid anandamide protects neurons during CNS inflammation by induction of MKP-1 in microglial cells. *Neuron* **2006,** *49*, 67-79.
406. Massi, P.; Valenti, M.; Bolognini, D.; Parolaro, D. Expression and function of the endocannabinoid system in glial cells. *Curr. Pharm. Des.* **2008,** *14*, 2289-2298.
407. Pertwee, R. G. Cannabinoids and multiple sclerosis. *Mol. Neurobiol.* **2007,** *36*, 45-59.
408. Maresz, K.; Pryce, G.; Ponomarev, E. D.; Marsicano, G.; Croxford, J. L.; Shriver, L. P.; Ledent, C.; Cheng, X.; Carrier, E. J.; Mann, M. K.; Giovannoni, G.; Pertwee, R. G.; Yamamura, T.; Buckley, N. E.; Hillard, C. J.; Lutz, B.; Baker, D.; Dittel, B. N. Direct suppression of CNS autoimmune inflammation via the cannabinoid receptor CB1 on neurons and CB2 on autoreactive T cells. *Nat. Med.* **2007,** *13*, 492-497.
409. Mechoulam, R.; Spatz, M.; Shohami, E. Endocannabinoids and neuroprotection. *Science's STKE : signal transduction knowledge environment* **2002,** *2002*, re5.
410. Sosin, D. M.; Sniezek, J. E.; Waxweiler, R. J. Trends in death associated with traumatic brain injury, 1979 through 1992. Success and failure. *JAMA* **1995,** *273*, 1778-1780.
411. Graham, D. I.; McIntosh, T. K.; Maxwell, W. L.; Nicoll, J. A. Recent advances in neurotrauma. *J. Neuropathol. Exp. Neurol.* **2000,** *59*, 641-651.
412. Faden, A. I. Neuroprotection and traumatic brain injury: the search continues. *Arch. Neurol.* **2001,** *58*, 1553-1555.
413. Muthian, S.; Rademacher, D. J.; Roelke, C. T.; Gross, G. J.; Hillard, C. J. Anandamide content is increased and CB1 cannabinoid receptor blockade is protective during transient, focal cerebral ischemia. *Neuroscience* **2004,** *129*, 743-750.
414. Panikashvili, D.; Simeonidou, C.; Ben-Shabat, S.; Hanus, L.; Breuer, A.; Mechoulam, R.; Shohami, E. An endogenous cannabinoid (2-AG) is neuroprotective after brain injury. *Nature* **2001,** *413*, 527-531.
415. Hansen, H. H.; Schmid, P. C.; Bittigau, P.; Lastres-Becker, I.; Berrendero, F.; Manzanares, J.; Ikonomidou, C.; Schmid, H. H.; Fernandez-Ruiz, J. J.; Hansen, H. S. Anandamide, but not 2-arachidonoylglycerol, accumulates during in vivo neurodegeneration. *J. Neurochem.* **2001,** *78*, 1415-1427.

416. van der Stelt, M.; Veldhuis, W. B.; van Haaften, G. W.; Fezza, F.; Bisogno, T.; Bar, P. R.; Veldink, G. A.; Vliegenthart, J. F.; Di Marzo, V.; Nicolay, K. Exogenous anandamide protects rat brain against acute neuronal injury in vivo. *J. Neurosci.* **2001,** *21*, 8765-8771.
417. Marsicano, G.; Goodenough, S.; Monory, K.; Hermann, H.; Eder, M.; Cannich, A.; Azad, S. C.; Cascio, M. G.; Gutierrez, S. O.; van der Stelt, M.; Lopez-Rodriguez, M. L.; Casanova, E.; Schutz, G.; Zieglgansberger, W.; Di Marzo, V.; Behl, C.; Lutz, B. CB1 cannabinoid receptors and on-demand defense against excitotoxicity. *Science* **2003,** *302*, 84-88.
418. Amantea, D.; Spagnuolo, P.; Bari, M.; Fezza, F.; Mazzei, C.; Tassorelli, C.; Morrone, L. A.; Corasaniti, M. T.; Maccarrone, M.; Bagetta, G. Modulation of the endocannabinoid system by focal brain ischemia in the rat is involved in neuroprotection afforded by 17beta-estradiol. *FEBS J.* **2007,** *274*, 4464-4775.
419. Hansen, H. H.; Azcoitia, I.; Pons, S.; Romero, J.; Garcia-Segura, L. M.; Ramos, J. A.; Hansen, H. S.; Fernandez-Ruiz, J. Blockade of cannabinoid CB(1) receptor function protects against in vivo disseminating brain damage following NMDA-induced excitotoxicity. *J. Neurochem.* **2002,** *82*, 154-158.
420. Mechoulam, R.; Lichtman, A. H. Neuroscience. Stout guards of the central nervous system. *Science* **2003,** *302*, 65-67.
421. Howlett, A. C.; Barth, F.; Bonner, T. I.; Cabral, G.; Casellas, P.; Devane, W. A.; Felder, C. C.; Herkenham, M.; Mackie, K.; Martin, B. R.; Mechoulam, R.; Pertwee, R. G. International Union of Pharmacology. XXVII. Classification of cannabinoid receptors. *Pharmacol. Rev.* **2002,** *54*, 161-202.
422. Walker, J. M.; Huang, S. M. Cannabinoid analgesia. *Pharmacol. Ther.* **2002,** *95*, 127-135.
423. Karst, M.; Wippermann, S.; Ahrens, J. Role of cannabinoids in the treatment of pain and (painful) spasticity. *Drugs* **2010,** *70*, 2409-2438.
424. Costa, B.; Colleoni, M.; Conti, S.; Parolaro, D.; Franke, C.; Trovato, A. E.; Giagnoni, G. Oral anti-inflammatory activity of cannabidiol, a non-psychoactive constituent of cannabis, in acute carrageenan-induced inflammation in the rat paw. *Naunyn Schmiedeberg's Arch. Pharmacol.* **2004,** *369*, 294-299.
425. Conti, S.; Costa, B.; Colleoni, M.; Parolaro, D.; Giagnoni, G. Antiinflammatory action of endocannabinoid palmitoylethanolamide and the synthetic cannabinoid nabilone in a model of acute inflammation in the rat. *Br. J. Pharmacol.* **2002,** *135*, 181-187.
426. Succar, R.; Mitchell, V. A.; Vaughan, C. W. Actions of N-arachidonyl-glycine in a rat inflammatory pain model. *Molecular pain* **2007,** *3*, 24.
427. Valenzano, K. J.; Tafesse, L.; Lee, G.; Harrison, J. E.; Boulet, J. M.; Gottshall, S. L.; Mark, L.; Pearson, M. S.; Miller, W.; Shan, S.; Rabadi, L.; Rotshteyn, Y.; Chaffer, S. M.; Turchin, P. I.; Elsemore, D. A.; Toth, M.; Koetzner, L.; Whiteside, G. T. Pharmacological and pharmacokinetic characterization of the cannabinoid receptor 2 agonist, GW405833, utilizing rodent models of acute and chronic pain, anxiety, ataxia and catalepsy. *Neuropharmacology* **2005,** *48*, 658-672.
428. Zogopoulos, P.; Vasileiou, I.; Patsouris, E.; Theocharis, S. E. The role of endocannabinoids in pain modulation. *Fundam. Clin. Pharmacol.* **2013,** *27*, 64-80.
429. Kraft, B. Is there any clinically relevant cannabinoid-induced analgesia? *Pharmacology* **2012,** *89*, 237-246.

430. Wallace, M.; Schulteis, G.; Atkinson, J. H.; Wolfson, T.; Lazzaretto, D.; Bentley, H.; Gouaux, B.; Abramson, I. Dose-dependent effects of smoked cannabis on capsaicin-induced pain and hyperalgesia in healthy volunteers. *Anesthesiology* **2007,** *107*, 785-796.
431. Abrams, D. I.; Jay, C. A.; Shade, S. B.; Vizoso, H.; Reda, H.; Press, S.; Kelly, M. E.; Rowbotham, M. C.; Petersen, K. L. Cannabis in painful HIV-associated sensory neuropathy: a randomized placebo-controlled trial. *Neurology* **2007,** *68*, 515-521.
432. Johnson, J. R.; Burnell-Nugent, M.; Lossignol, D.; Ganae-Motan, E. D.; Potts, R.; Fallon, M. T. Multicenter, double-blind, randomized, placebo-controlled, parallel-group study of the efficacy, safety, and tolerability of THC:CBD extract and THC extract in patients with intractable cancer-related pain. *J. Pain Symptom Manage.* **2010,** *39*, 167-179.
433. Viveros, M.-P.; Bermudez-Silva, F.-J.; Lopez-Rodriguez, A.-B.; Wagner, E. J. The endocannabinoid system as pharmacological target derived from its CNS role in energy homeostasis and reward. Applications in eating disorders and addiction. *Pharmaceuticals* **2011,** *4*, 1101-1136.
434. Maldonado, R.; Valverde, O.; Berrendero, F. Involvement of the endocannabinoid system in drug addiction. *Trends Neurosci.* **2006,** *29*, 225-232.
435. Arnold, J. C. The role of endocannabinoid transmission in cocaine addiction. *Pharmacol., Biochem. Behav.* **2005,** *81*, 396-406.
436. Cossu, G.; Ledent, C.; Fattore, L.; Imperato, A.; Bohme, G. A.; Parmentier, M.; Fratta, W. Cannabinoid CB1 receptor knockout mice fail to self-administer morphine but not other drugs of abuse. *Behav. Brain Res.* **2001,** *118*, 61-65.
437. Fattore, L.; Martellotta, M. C.; Cossu, G.; Mascia, M. S.; Fratta, W. CB1 cannabinoid receptor agonist WIN 55,212-2 decreases intravenous cocaine self-administration in rats. *Behav. Brain Res.* **1999,** *104*, 141-146.
438. Tanda, G. Modulation of the endocannabinoid system: therapeutic potential against cocaine dependence. *Pharmacol. Res.* **2007,** *56*, 406-417.
439. De Vries, T. J.; Shaham, Y.; Homberg, J. R.; Crombag, H.; Schuurman, K.; Dieben, J.; Vanderschuren, L. J.; Schoffelmeer, A. N. A cannabinoid mechanism in relapse to cocaine seeking. *Nat. Med.* **2001,** *7*, 1151-1154.
440. Anggadiredja, K.; Nakamichi, M.; Hiranita, T.; Tanaka, H.; Shoyama, Y.; Watanabe, S.; Yamamoto, T. Endocannabinoid system modulates relapse to methamphetamine seeking: Possible mediation by the arachidonic acid cascade. *Neuropsychopharmacol.* **2004,** *29*, 1470-1478.
441. Xi, Z. X.; Gilbert, J. G.; Peng, X. Q.; Pak, A. C.; Li, X.; Gardner, E. L. Cannabinoid CB1 receptor antagonist AM251 inhibits cocaine-primed relapse in rats: Role of glutamate in the nucleus accumbens. *J. Neurosci.* **2006,** *26*, 8531-8536.
442. Carr, G. D., Fibiger, H. C., Phillips, A. G. . The Neuropharmacological Basis Of Reward. In Copper, J. M. L. S. J., Ed. Clarendon Press, Oxford: 1989; pp 264-319.
443. Xi, Z. X.; Peng, X. Q.; Li, X.; Song, R.; Zhang, H. Y.; Liu, Q. R.; Yang, H. J.; Bi, G. H.; Li, J.; Gardner, E. L. Brain cannabinoid CB(2) receptors modulate cocaine's actions in mice. *Nat. Neurosci.* **2011,** *14*, 1160-1166.
444. Aracil-Fernandez, A.; Trigo, J. M.; Garcia-Gutierrez, M. S.; Ortega-Alvaro, A.; Ternianov, A.; Navarro, D.; Robledo, P.; Berbel, P.; Maldonado, R.; Manzanares, J. Decreased cocaine motor sensitization and self-administration in mice overexpressing cannabinoid CB(2) receptors. *Neuropsychopharmacol.* **2012,** *37*, 1749-1763.

445. Akbas, F.; Gasteyger, C.; Sjodin, A.; Astrup, A.; Larsen, T. M. A critical review of the cannabinoid receptor as a drug target for obesity management. *Obes. Rev.* **2009,** *10*, 58-67.
446. World Health Organization. Obesity and Overweight Fact Sheet, 2013. http://www.who.int/mediacentre/factsheets/fs311/en/index.html. **2013**.
447. Pataky, Z.; Bobbioni-Harsch, E.; Golay, A. Obesity: a complex growing challenge. *Exp. Clin. Endocrinol. Diabetes* **2010,** *118*, 427-433.
448. Bermudez-Silva, F. J.; Cardinal, P.; Cota, D. The role of the endocannabinoid system in the neuroendocrine regulation of energy balance. *J Psychopharmacol* **2012,** *26*, 114-124.
449. Trojniar, W.; Wise, R. A. Facilitory effect of delta 9-tetrahydrocannabinol on hypothalamically induced feeding. *Psychopharmacology* **1991,** *103*, 172-176.
450. Kirkham, T. C.; Williams, C. M.; Fezza, F.; Di Marzo, V. Endocannabinoid levels in rat limbic forebrain and hypothalamus in relation to fasting, feeding and satiation: stimulation of eating by 2-arachidonoyl glycerol. *Br. J. Pharmacol.* **2002,** *136*, 550-557.
451. Marco, E. M.; Romero-Zerbo, S. Y.; Viveros, M. P.; Bermudez-Silva, F. J. The role of the endocannabinoid system in eating disorders: pharmacological implications. *Behav. Pharmacol.* **2012,** *23*, 526-536.
452. Kunos, G.; Osei-Hyiaman, D.; Liu, J.; Godlewski, G.; Batkai, S. Endocannabinoids and the control of energy homeostasis. *J. Biol. Chem.* **2008,** *283*, 33021-33025.
453. Despres, J. P. The endocannabinoid system: a new target for the regulation of energy balance and metabolism. *Crit. Pathw. Cardiol.* **2007,** *6*, 46-50.
454. Heshmati, H.; Caplain, H.; Bellisle, F.; Mosse, M.; Fauveau, C.; Le Fur, G. SR141716, a selective cannabinoid CB1 receptor antagonist reduces hunger, caloric intake, and body weight in overweight or obese men. *Obes. Res.* **2001,** *9*, 70s-70s.
455. Janero, D. R.; Lindsley, L.; Vemuri, V. K.; Makriyannis, A. Cannabinoid 1 G protein-coupled receptor (periphero-)neutral antagonists: emerging therapeutics for treating obesity-driven metabolic disease and reducing cardiovascular risk. *Expert opinion on drug discovery* **2011,** *6*, 995-1025.
456. Kirilly, E.; Gonda, X.; Bagdy, G. CB1 receptor antagonists: new discoveries leading to new perspectives. *Acta physiologica* **2012,** *205*, 41-60.
457. Ishiguro, H.; Iwasaki, S.; Teasenfitz, L.; Higuchi, S.; Horiuchi, Y.; Saito, T.; Arinami, T.; Onaivi, E. S. Involvement of cannabinoid CB2 receptor in alcohol preference in mice and alcoholism in humans. *Pharmacogenomics J.* **2007,** *7*, 380-385.
458. Pava, M. J.; Woodward, J. J. A review of the interactions between alcohol and the endocannabinoid system: implications for alcohol dependence and future directions for research. *Alcohol* **2012,** *46*, 185-204.
459. Erdozain, A. M.; Callado, L. F. Involvement of the endocannabinoid system in alcohol dependence: the biochemical, behavioral and genetic evidence. *Drug Alcohol Depend.* **2011,** *117*, 102-110.
460. World Health Organization. Alcohol Fact Sheet, 2011. http://www.who.int/mediacentre/factsheets/fs349/en/index.html. **2011**.
461. Hungund, B. L.; Zheng, Z.; Lin, L.; Barkai, A. I. Ganglioside GM1 reduces ethanol induced phospholipase A2 activity in synaptosomal preparations from mice. *Neurochem. Int.* **1994,** *25*, 321-325.

462. Basavarajappa, B. S.; Hungund, B. L. Down-regulation of cannabinoid receptor agonist-stimulated [35S]GTP gamma S binding in synaptic plasma membrane from chronic ethanol exposed mouse. *Brain Res.* **1999,** *815*, 89-97.
463. Basavarajappa, B. S.; Hungund, B. L. Chronic ethanol increases the cannabinoid receptor agonist anandamide and its precursor N-arachidonoylphosphatidylethanolamine in SK-N-SH cells. *J. Neurochem.* **1999,** *72*, 522-528.
464. Wang, L.; Liu, J.; Harvey-White, J.; Zimmer, A.; Kunos, G. Endocannabinoid signaling via cannabinoid receptor 1 is involved in ethanol preference and its age-dependent decline in mice. *Proc. Natl. Acad. Sci. USA* **2003,** *100*, 1393-1398.
465. Hungund, B. L.; Szakall, I.; Adam, A.; Basavarajappa, B. S.; Vadasz, C. Cannabinoid CB1 receptor knockout mice exhibit markedly reduced voluntary alcohol consumption and lack alcohol-induced dopamine release in the nucleus accumbens. *J. Neurochem.* **2003,** *84*, 698-704.
466. Rodriguez de Fonseca, F.; Roberts, A. J.; Bilbao, A.; Koob, G. F.; Navarro, M. Cannabinoid receptor antagonist SR141716A decreases operant ethanol self administration in rats exposed to ethanol-vapor chambers. *Zhongguo Yao Li Xue Bao* **1999,** *20*, 1109-1114.
467. Cippitelli, A.; Bilbao, A.; Hansson, A. C.; del Arco, I.; Sommer, W.; Heilig, M.; Massi, M.; Bermudez-Silva, F. J.; Navarro, M.; Ciccocioppo, R.; de Fonseca, F. R.; European, T. C. Cannabinoid CB1 receptor antagonism reduces conditioned reinstatement of ethanol-seeking behavior in rats. *Eur. J. Neurosci.* **2005,** *21*, 2243-2251.
468. Gessa, G. L.; Serra, S.; Vacca, G.; Carai, M. A.; Colombo, G. Suppressing effect of the cannabinoid CB1 receptor antagonist, SR147778, on alcohol intake and motivational properties of alcohol in alcohol-preferring sP rats. *Alcohol Alcohol.* **2005,** *40*, 46-53.
469. Gallate, J. E.; Saharov, T.; Mallet, P. E.; McGregor, I. S. Increased motivation for beer in rats following administration of a cannabinoid CB1 receptor agonist. *Eur. J. Pharmacol.* **1999,** *370*, 233-240.
470. Colombo, G.; Serra, S.; Brunetti, G.; Gomez, R.; Melis, S.; Vacca, G.; Carai, M. M.; Gessa, L. Stimulation of voluntary ethanol intake by cannabinoid receptor agonists in ethanol-preferring sP rats. *Psychopharmacology* **2002,** *159*, 181-187.
471. Alen, F.; Moreno-Sanz, G.; Isabel de Tena, A.; Brooks, R. D.; Lopez-Jimenez, A.; Navarro, M.; Lopez-Moreno, J. A. Pharmacological activation of CB1 and D2 receptors in rats: predominant role of CB1 in the increase of alcohol relapse. *Eur. J. Neurosci.* **2008,** *27*, 3292-3298.
472. Rosenbaum, C. D.; Carreiro, S. P.; Babu, K. M. Here today, gone tomorrow...and back again? A review of herbal marijuana alternatives (K2, Spice), synthetic cathinones (bath salts), kratom, Salvia divinorum, methoxetamine, and piperazines. *J. Med. Toxicol.* **2012,** *8*, 15-32.
473. Brents, L. K.; Gallus-Zawada, A.; Radominska-Pandya, A.; Vasiljevik, T.; Prisinzano, T. E.; Fantegrossi, W. E.; Moran, J. H.; Prather, P. L. Monohydroxylated metabolites of the K2 synthetic cannabinoid JWH-073 retain intermediate to high cannabinoid 1 receptor (CB1R) affinity and exhibit neutral antagonist to partial agonist activity. *Biochem. Pharmacol.* **2012,** *83*, 952-961.
474. Prather, P. L.; Martin, N. A.; Breivogel, C. S.; Childers, S. R. Activation of cannabinoid receptors in rat brain by WIN 55212-2 produces coupling to multiple G protein alpha-subunits with different potencies. *Mol. Pharmacol.* **2000,** *57*, 1000-1010.

475. Shoemaker, J. L.; Joseph, B. K.; Ruckle, M. B.; Mayeux, P. R.; Prather, P. L. The endocannabinoid noladin ether acts as a full agonist at human CB2 cannabinoid receptors. *J. Pharmacol. Exp. Ther.* **2005,** *314*, 868-875.
476. Cheng, Y.; Prusoff, W. H. Relationship between the inhibition constant (K1) and the concentration of inhibitor which causes 50 per cent inhibition (I50) of an enzymatic reaction. *Biochem. Pharmacol.* **1973,** *22*, 3099-3108.
477. Martin, B. R.; Compton, D. R.; Thomas, B. F.; Prescott, W. R.; Little, P. J.; Razdan, R. K.; Johnson, M. R.; Melvin, L. S.; Mechoulam, R.; Ward, S. J. Behavioral, biochemical, and molecular modeling evaluations of cannabinoid analogs. *Pharmacology, biochemistry, and behavior* **1991,** *40*, 471-478.
478. Compton, D. R.; Johnson, M. R.; Melvin, L. S.; Martin, B. R. Pharmacological profile of a series of bicyclic cannabinoid analogs: classification as cannabimimetic agents. *J. Pharmacol. Exp. Ther.* **1992,** *260*, 201-209.
479. Keane, B.; Leonard, B. E. Rodent models of alcoholism: a review. *Alcohol Alcohol.* **1989,** *24*, 299-309.
480. Cunningham, C. L.; Fidler, T. L.; Hill, K. G. Animal models of alcohol's motivational effects. *Alcohol Res. Health* **2000,** *24*, 85-92.
481. Vinod, K. Y.; Yalamanchili, R.; Thanos, P. K.; Vadasz, C.; Cooper, T. B.; Volkow, N. D.; Hungund, B. L. Genetic and pharmacological manipulations of the CB(1) receptor alter ethanol preference and dependence in ethanol preferring and nonpreferring mice. *Synapse* **2008,** *62*, 574-581.
482. Ravinet Trillou, C.; Arnone, M.; Delgorge, C.; Gonalons, N.; Keane, P.; Maffrand, J. P.; Soubrie, P. Anti-obesity effect of SR141716, a CB1 receptor antagonist, in diet-induced obese mice. *Am. J. Physiol. Regul. Integr. Comp. Physiol.* **2003,** *284*, R345-353.
483. Kirkham, T. C. Endogenous cannabinoids: a new target in the treatment of obesity. *Am. J. Physiol-Reg I* **2003,** *284*, R343-344.
484. Biala, G.; Budzynska, B. Rimonabant attenuates sensitization, cross-sensitization and cross-reinstatement of place preference induced by nicotine and ethanol. *Pharmacol. Rep.* **2010,** *62*, 797-807.
485. Basavarajappa, B. S. The endocannabinoid signaling system: a potential target for next-generation therapeutics for alcoholism. *Mini Rev. Med. Chem.* **2007,** *7*, 769-779.
486. Maccioni, P.; Colombo, G.; Carai, M. A. Blockade of the cannabinoid CB1 receptor and alcohol dependence: preclinical evidence and preliminary clinical data. *CNS & neurological disorders drug targets* **2010,** *9*, 55-59.
487. Qi, T.; Qiu, W.; Liu, Y.; Zhang, H.; Gao, X.; Liu, Y.; Lu, K.; Du, C.; Yu, G.; Zhu, D. Synthesis, Structures, and Properties of Disubstituted Heteroacenes on One Side Containing Both Pyrrole and Thiophene Rings. *J. Org. Chem.* **2008,** *73*, 4638-4643.
488. Cai, J. C. C., S.; Chen, Y.; Chu , X.; Goodnow, R. A.; Le, K.; Luk, K.; Mischke, S. G.; Wovkulich, P. M. . Thiazolyl-Benzimidazoles; http://www.freepatentsonline.com/y2010/0160308.html. 2010.
489. Huang, Z.; Velazquez, C. A.; Abdellatif, K. R.; Chowdhury, M. A.; Reisz, J. A.; DuMond, J. F.; King, S. B.; Knaus, E. E. Ethanesulfohydroxamic acid ester prodrugs of nonsteroidal anti-inflammatory drugs (NSAIDs): synthesis, nitric oxide and nitroxyl release, cyclooxygenase inhibition, anti-inflammatory, and ulcerogenicity index studies. *J. Med. Chem.* **2011,** *54*, 1356-1364.

490. McBride, W. J.; Li, T. K. Animal models of alcoholism: neurobiology of high alcohol-drinking behavior in rodents. *Crit. Rev. Neurobiol.* **1998,** *12*, 339-369.
491. Tzschentke, T. M. Measuring reward with the conditioned place preference (CPP) paradigm: update of the last decade. *Addict. Biol.* **2007,** *12*, 227-462.
492. World Health Organization. Rescent Statistics and Trend Analysis of Illicit Drug Markets. Global Report, 2010. http://www.unodc.org/documents/data-and-analysis/WDR2012/WDR_2012_Chapter1.pdf

APPENDIX A: ^{1}H NMR SPECTRA

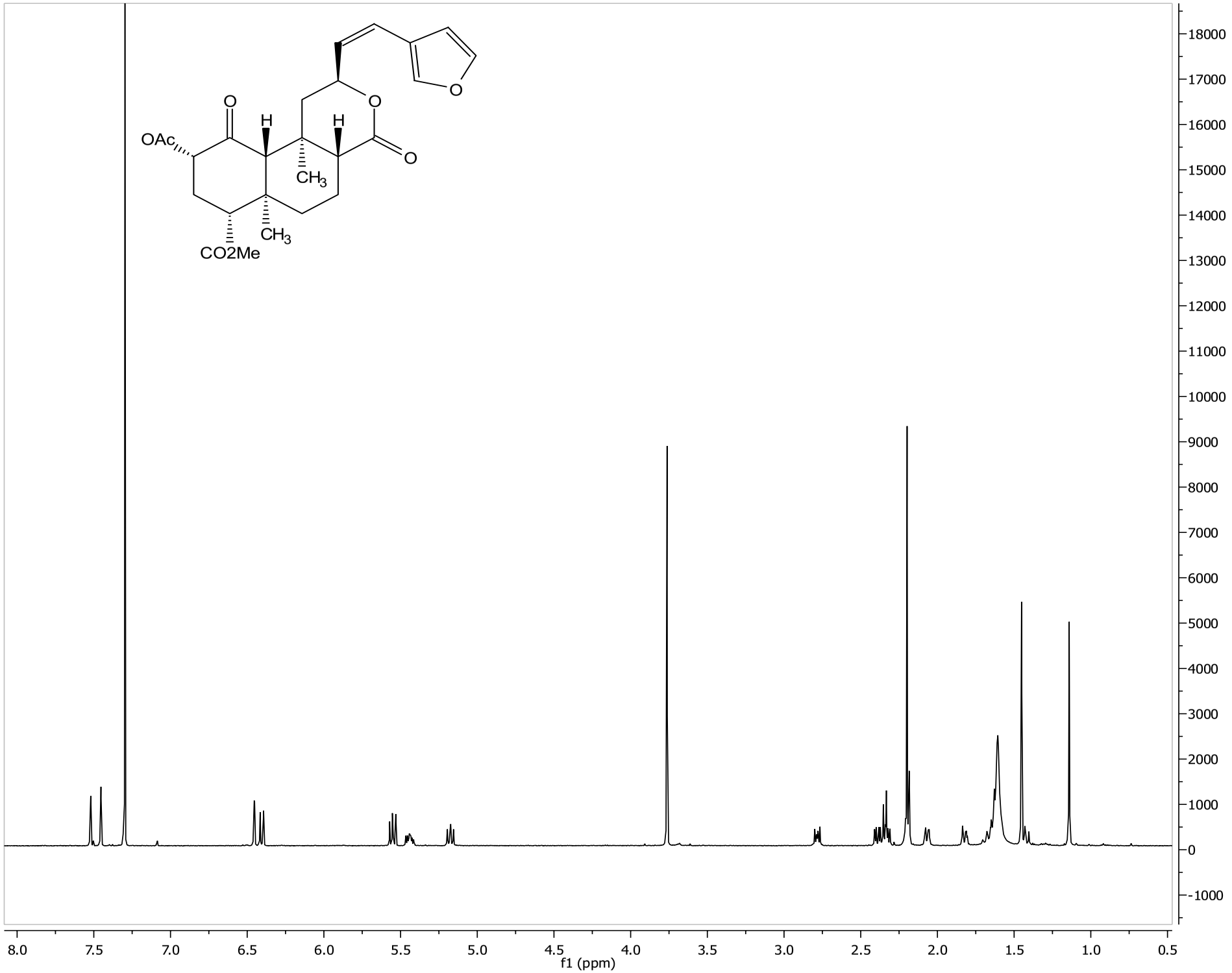
OAc
O
H
H
O
O
O
CH3
CH3
CO2Me
18000
17000
16000
15000
14000
13000
12000
11000
10000
9000
8000
7000
6000
5000
4000
3000
2000
1000
0
-1000
8.0
7.5
7.0
6.5
6.0
5.5
5.0
4.5
4.0
3.5
3.0
2.5
2.0
1.5
1.0
0.5
f1 (ppm)

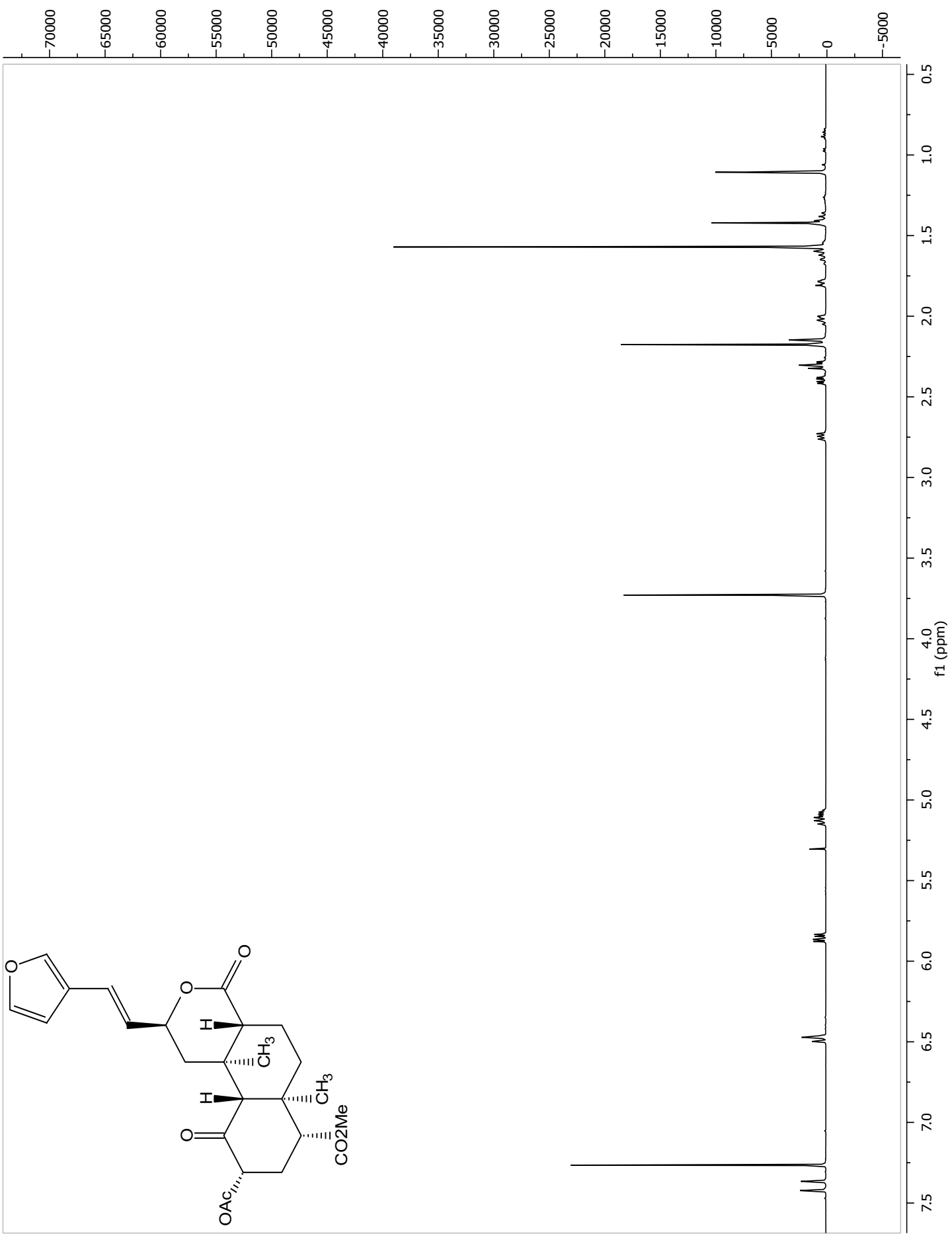
70000
65000
60000
55000
50000
45000
40000
35000
30000
25000
20000
15000
10000
5000
0
-5000
0.5
1.0
1.5
2.0
2.5
3.0
3.5
4.0
4.5
5.0
5.5
6.0
6.5
7.0
7.5
f1 (ppm)
O
O
O
H
CH3
H
CH3
O
CO2Me
OAc

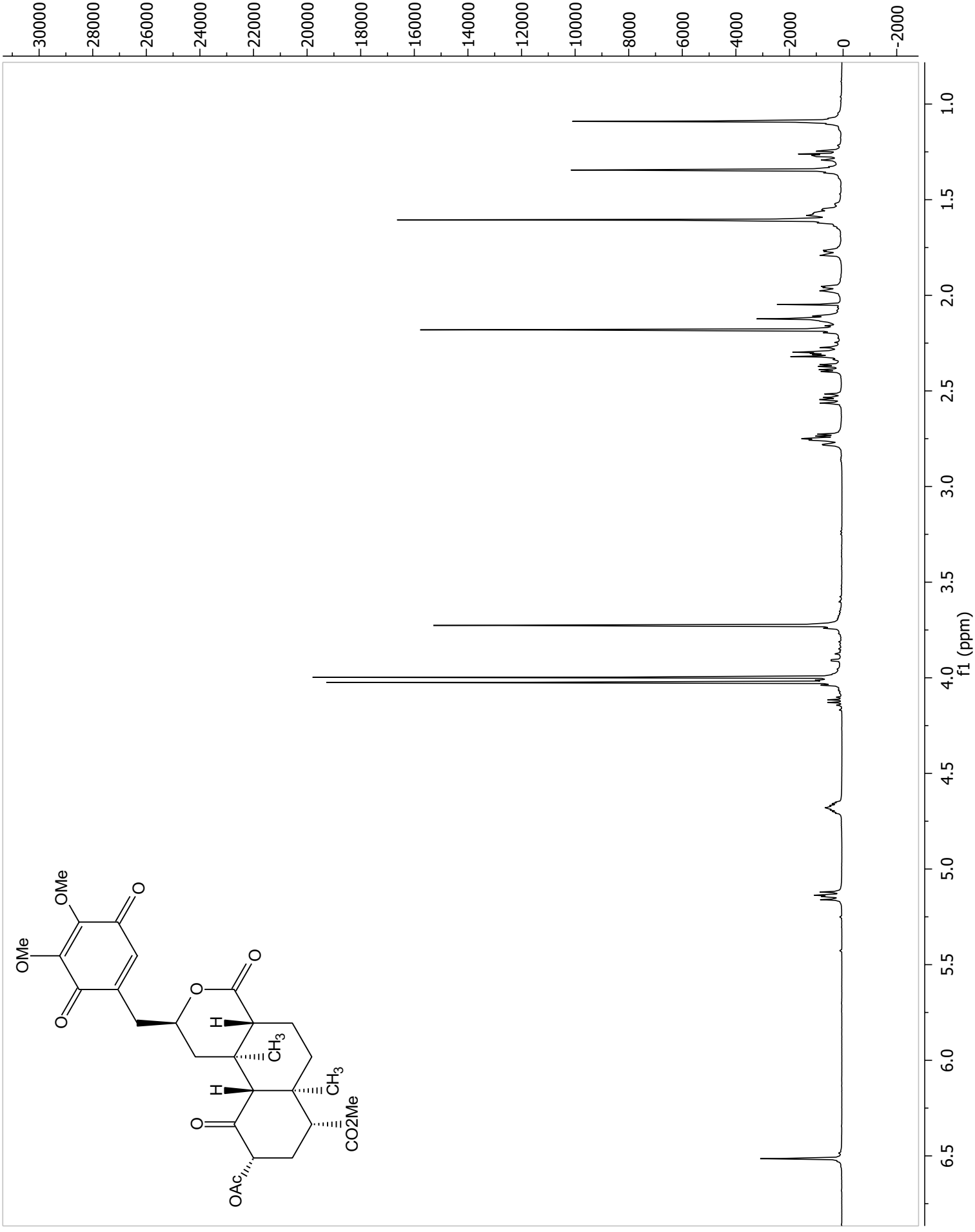
30000
28000
26000
24000
22000
20000
18000
16000
14000
12000
10000
8000
6000
4000
2000
0
-2000
1.0
1.5
2.0
2.5
3.0
3.5
4.0
4.5
5.0
5.5
6.0
6.5
f1 (ppm)
OMe
OMe
O
O
O
O
O
H
H
CH3
CH3
CO2Me
OAc

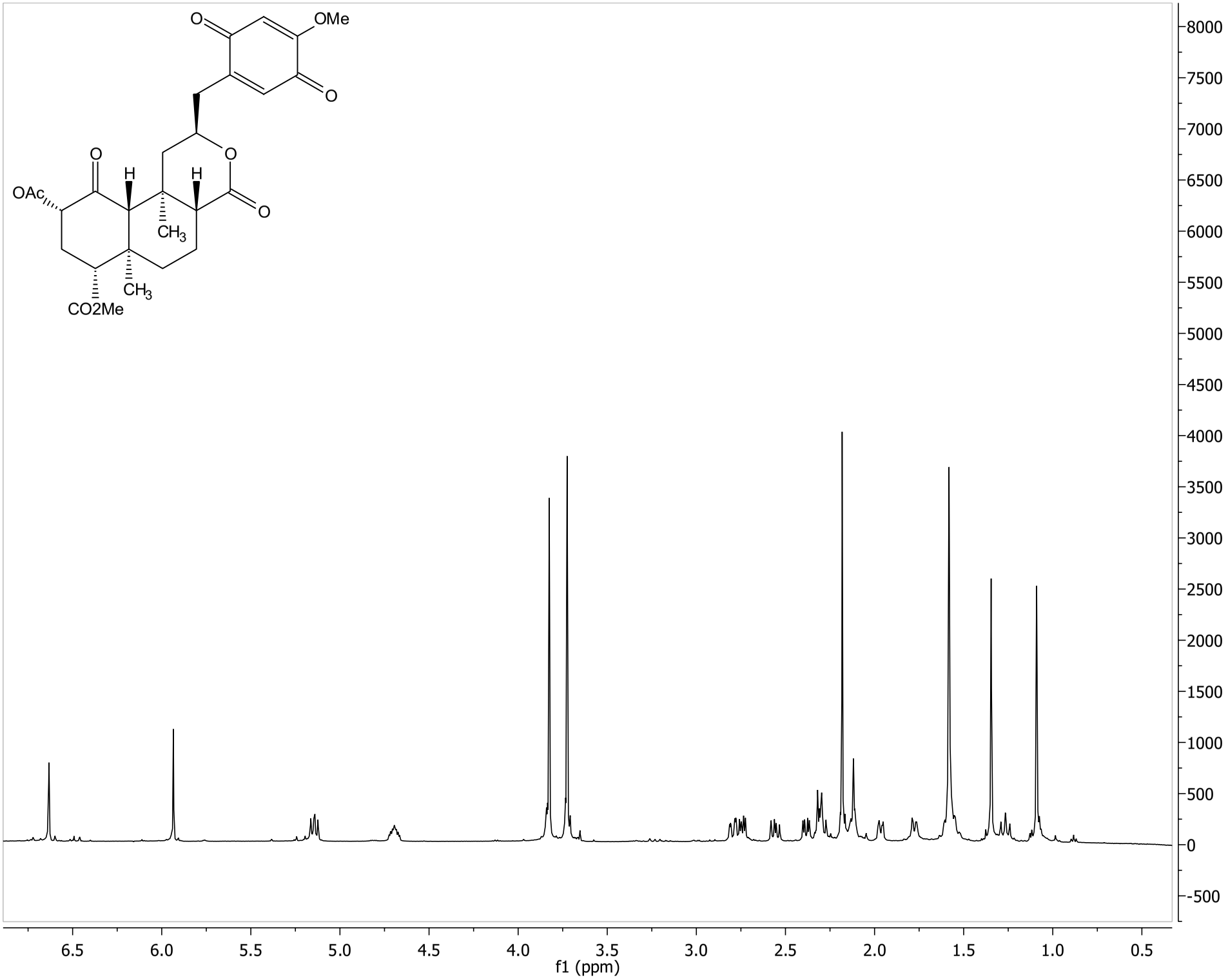
OMe
O
O
O
O
O
H
H
OAc
CH3
CH3
CO2Me
8000
7500
7000
6500
6000
5500
5000
4500
4000
3500
3000
2500
2000
1500
1000
500
0
-500
6.5
6.0
5.5
5.0
4.5
4.0
3.5
3.0
2.5
2.0
1.5
1.0
0.5
f1 (ppm)

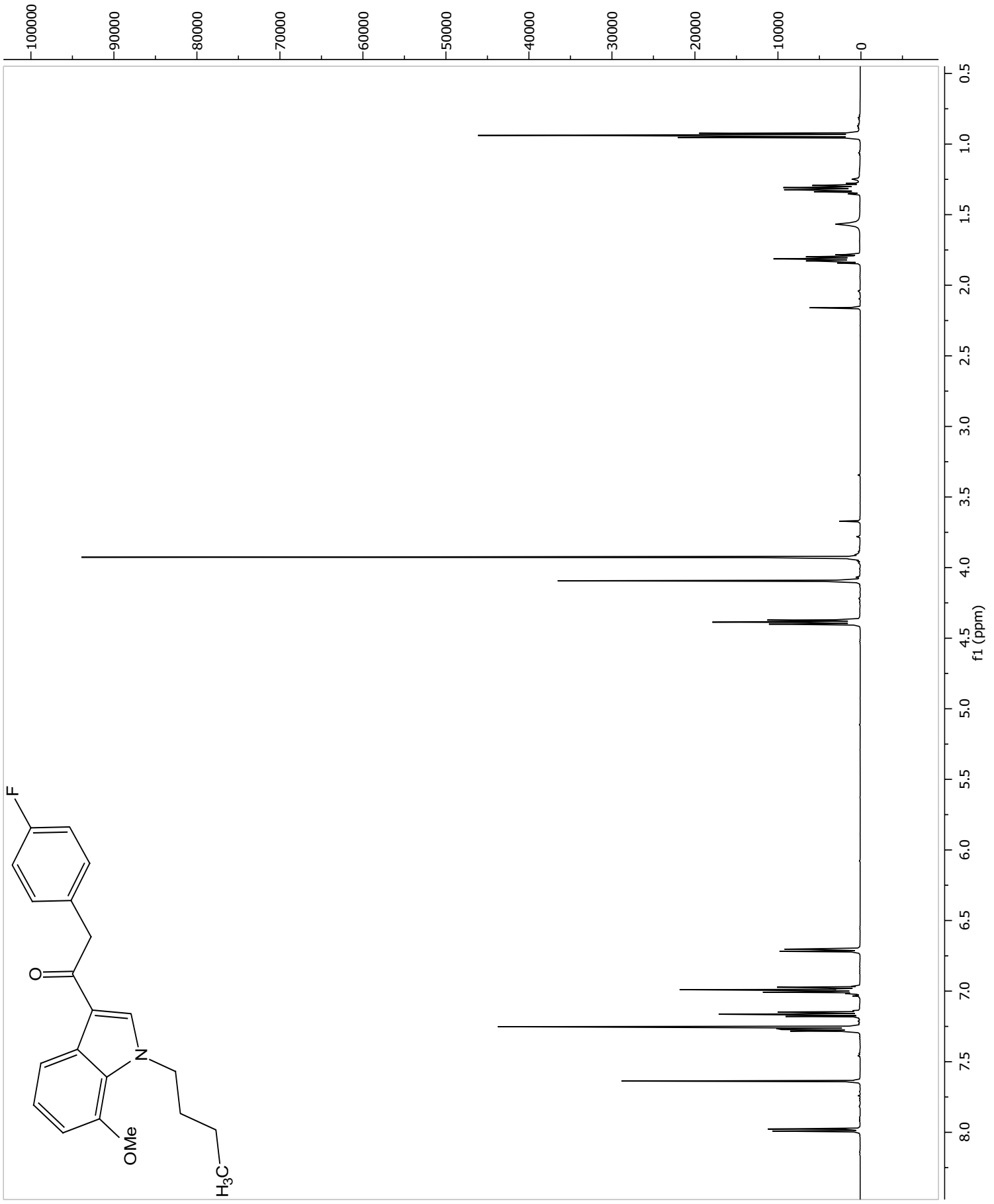
F
O
N
OMe
H3C
f1 (ppm)

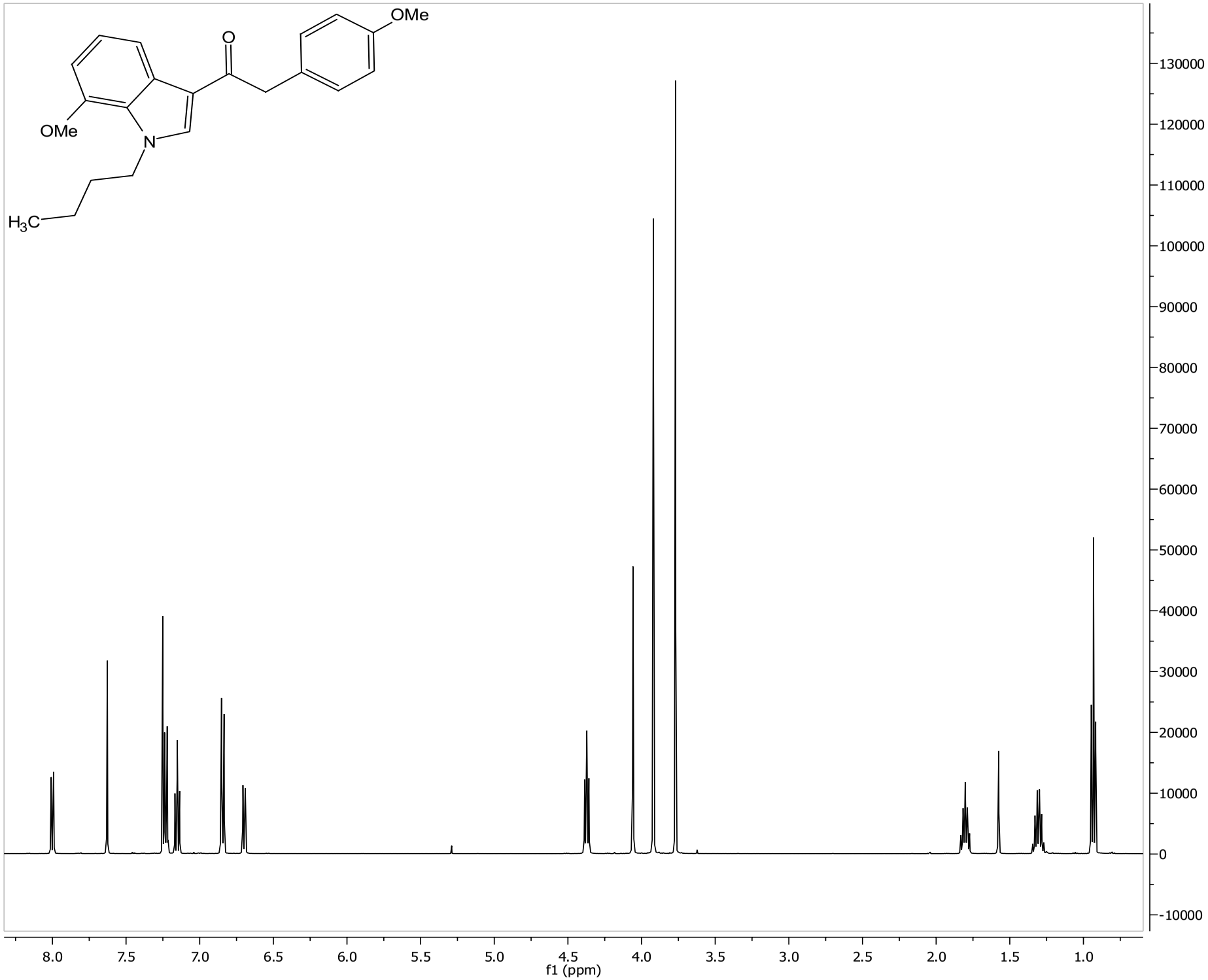
OMe
O
OMe
N
H3C
130000
120000
110000
100000
90000
80000
70000
60000
50000
40000
30000
20000
10000
0
-10000
8.0
7.5
7.0
6.5
6.0
5.5
5.0
4.5
4.0
3.5
3.0
2.5
2.0
1.5
1.0
f1 (ppm)

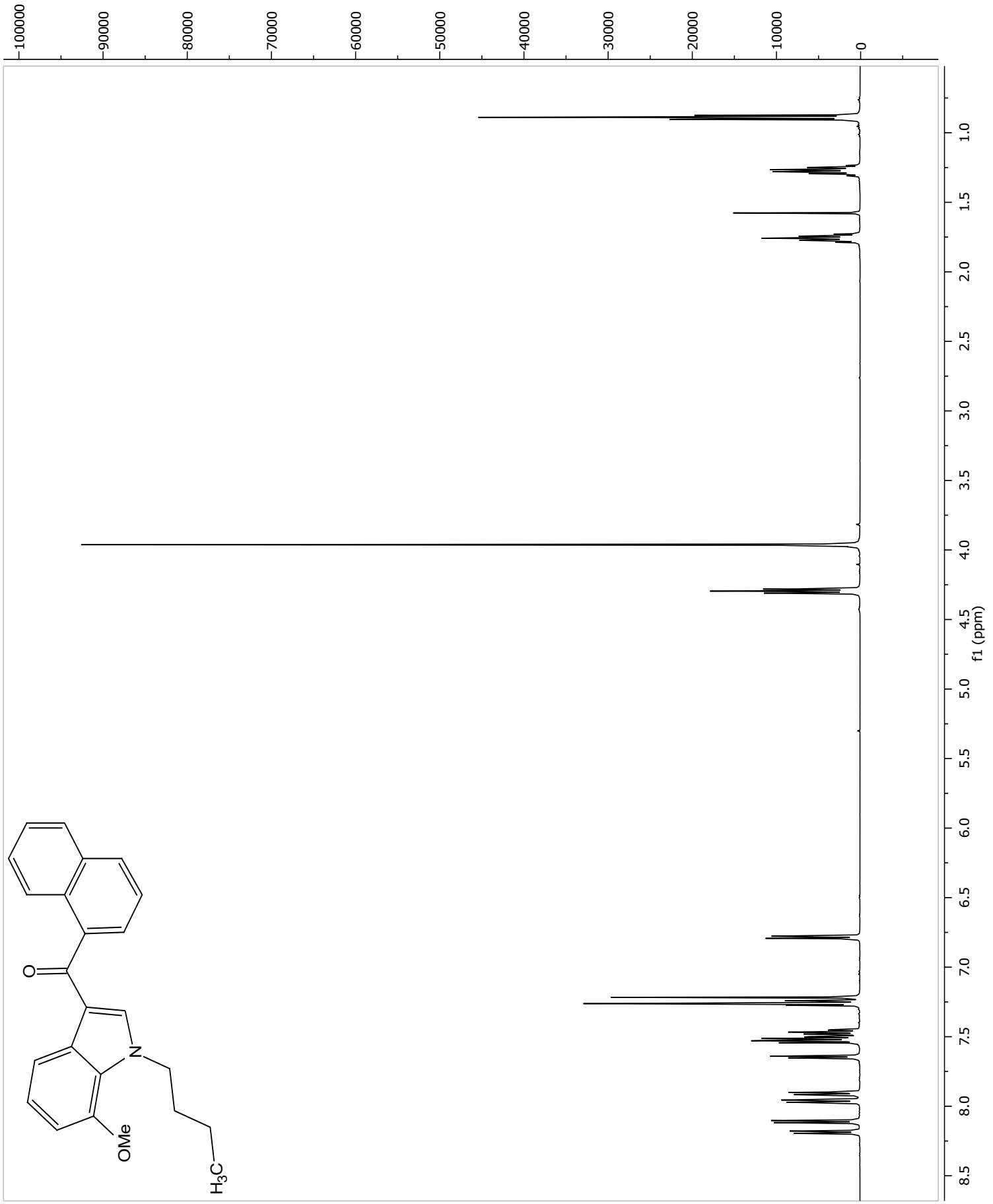
100000
90000
80000
70000
60000
50000
40000
30000
20000
10000
0
1.0
1.5
2.0
2.5
3.0
3.5
4.0
4.5
5.0
5.5
6.0
6.5
7.0
7.5
8.0
8.5
f1 (ppm)
O
N
OMe
H3C

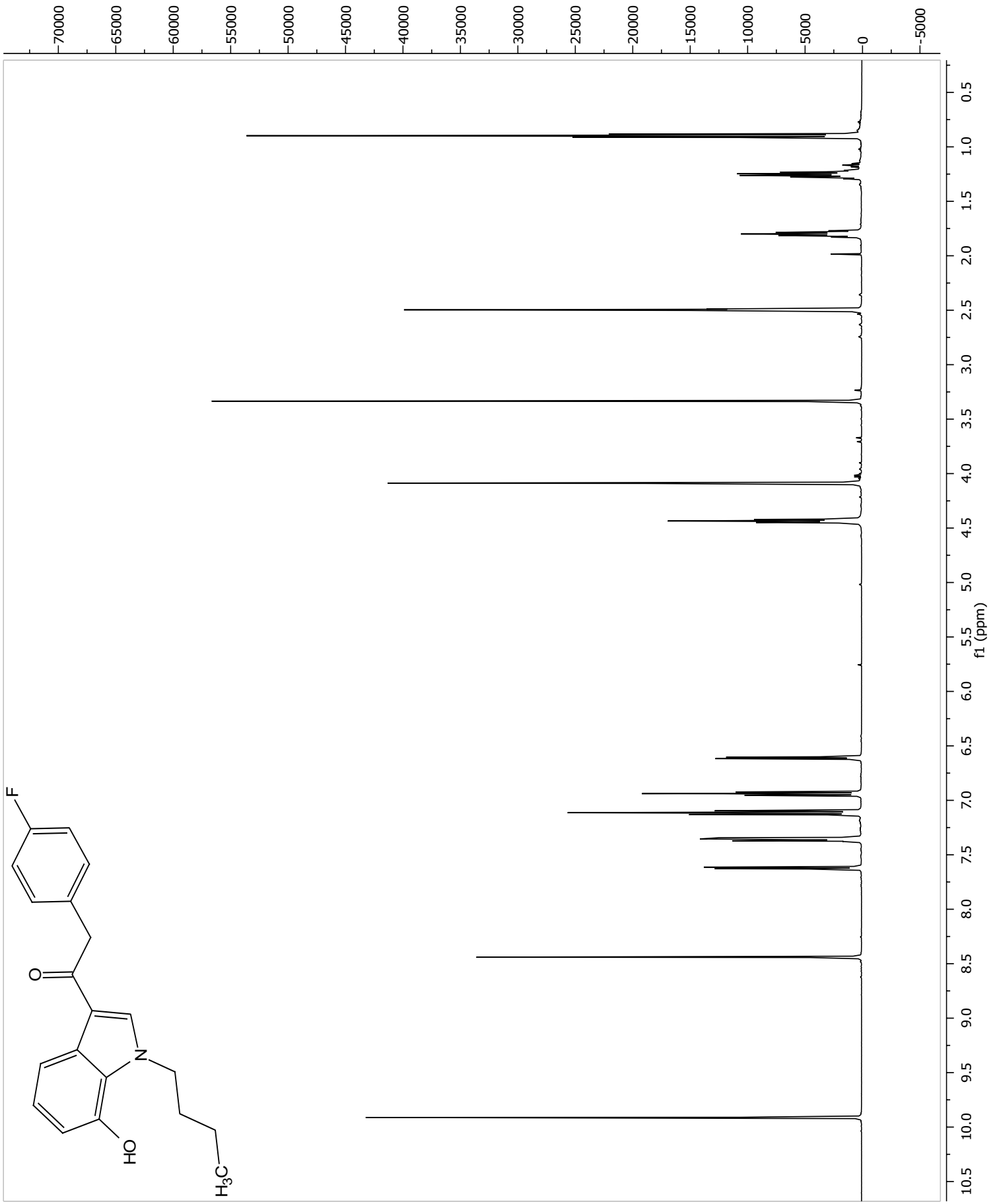
F
O
N
HO
H3C
f1 (ppm)

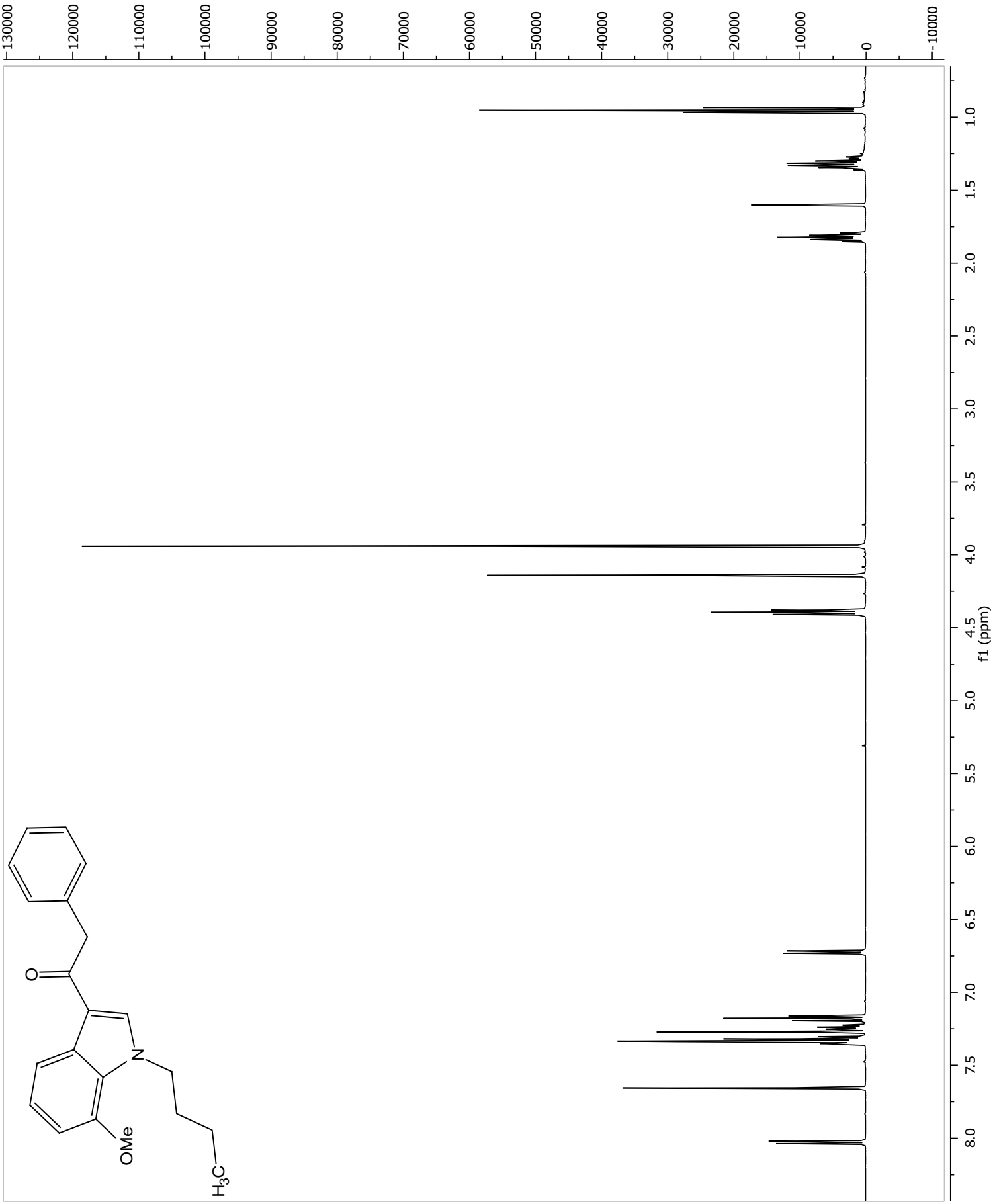
130000
120000
110000
100000
90000
80000
70000
60000
50000
40000
30000
20000
10000
0
-10000
1.0
1.5
2.0
2.5
3.0
3.5
4.0
4.5
f1 (ppm)
5.0
5.5
6.0
6.5
7.0
7.5
8.0
O
N
OMe
H3C

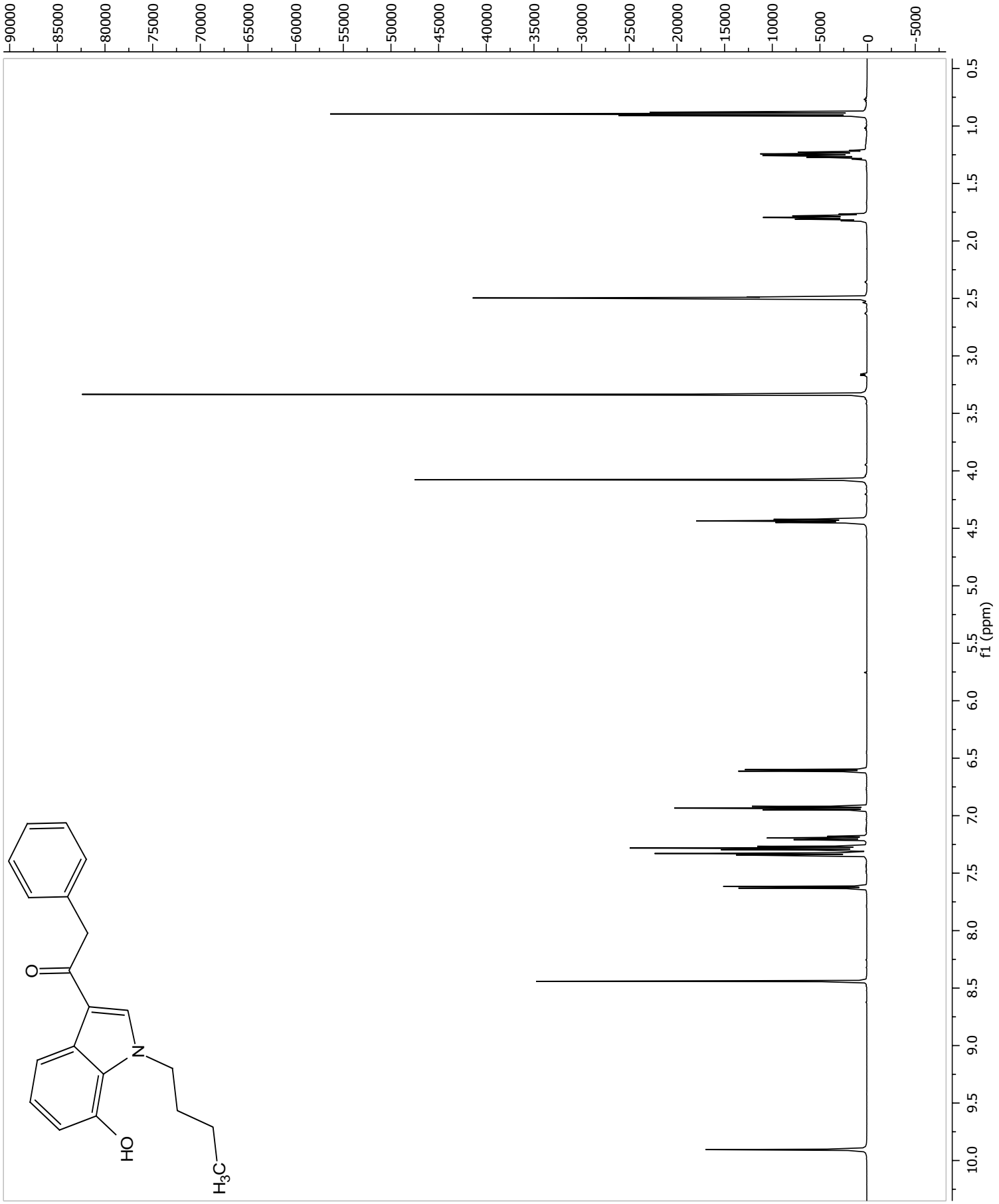
f1 (ppm)
O
N
HO
H3C

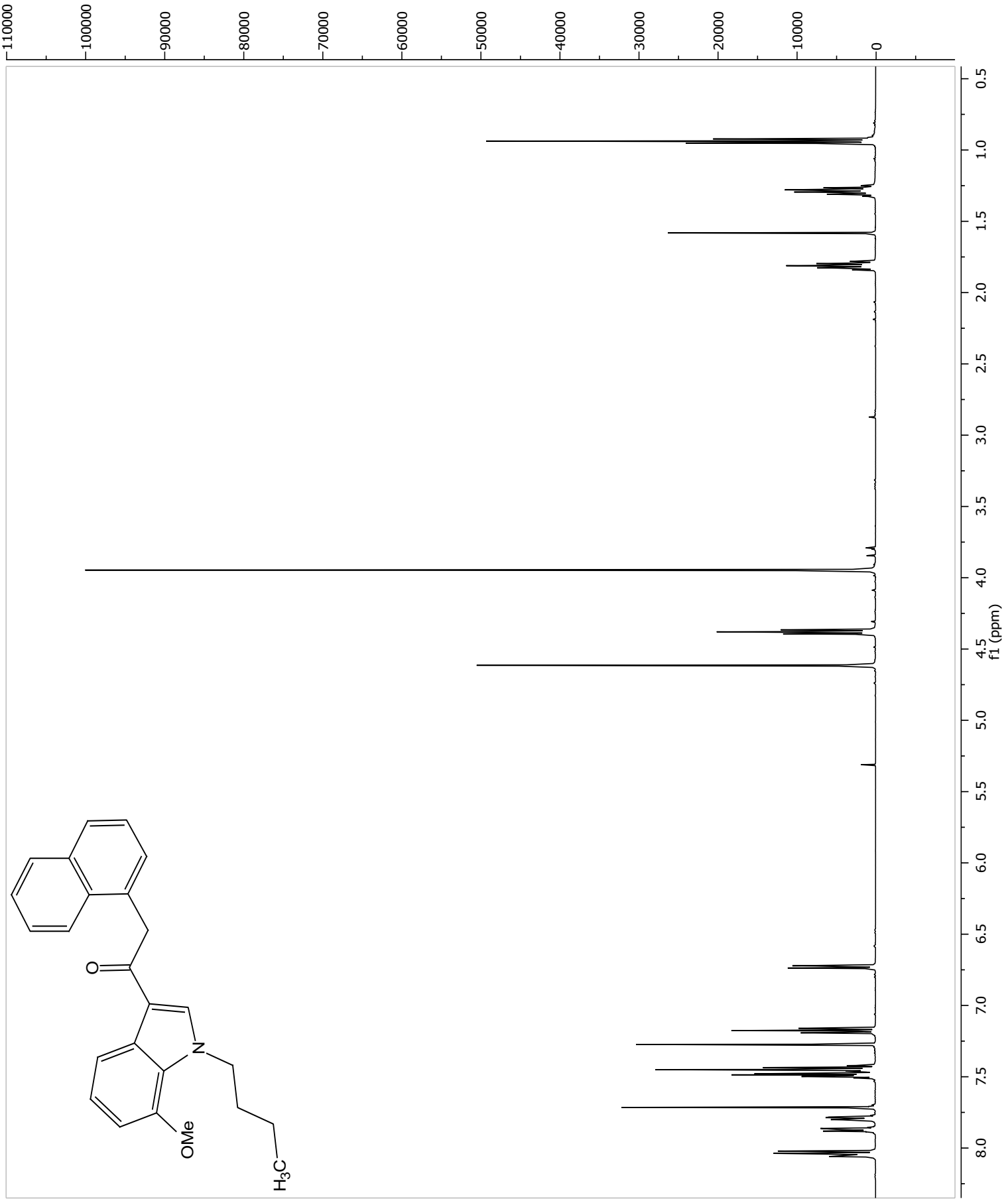
110000
100000
90000
80000
70000
60000
50000
40000
30000
20000
10000
0
0.5
1.0
1.5
2.0
2.5
3.0
3.5
4.0
4.5
5.0
5.5
6.0
6.5
7.0
7.5
8.0
f1 (ppm)
O
N
OMe
H3C

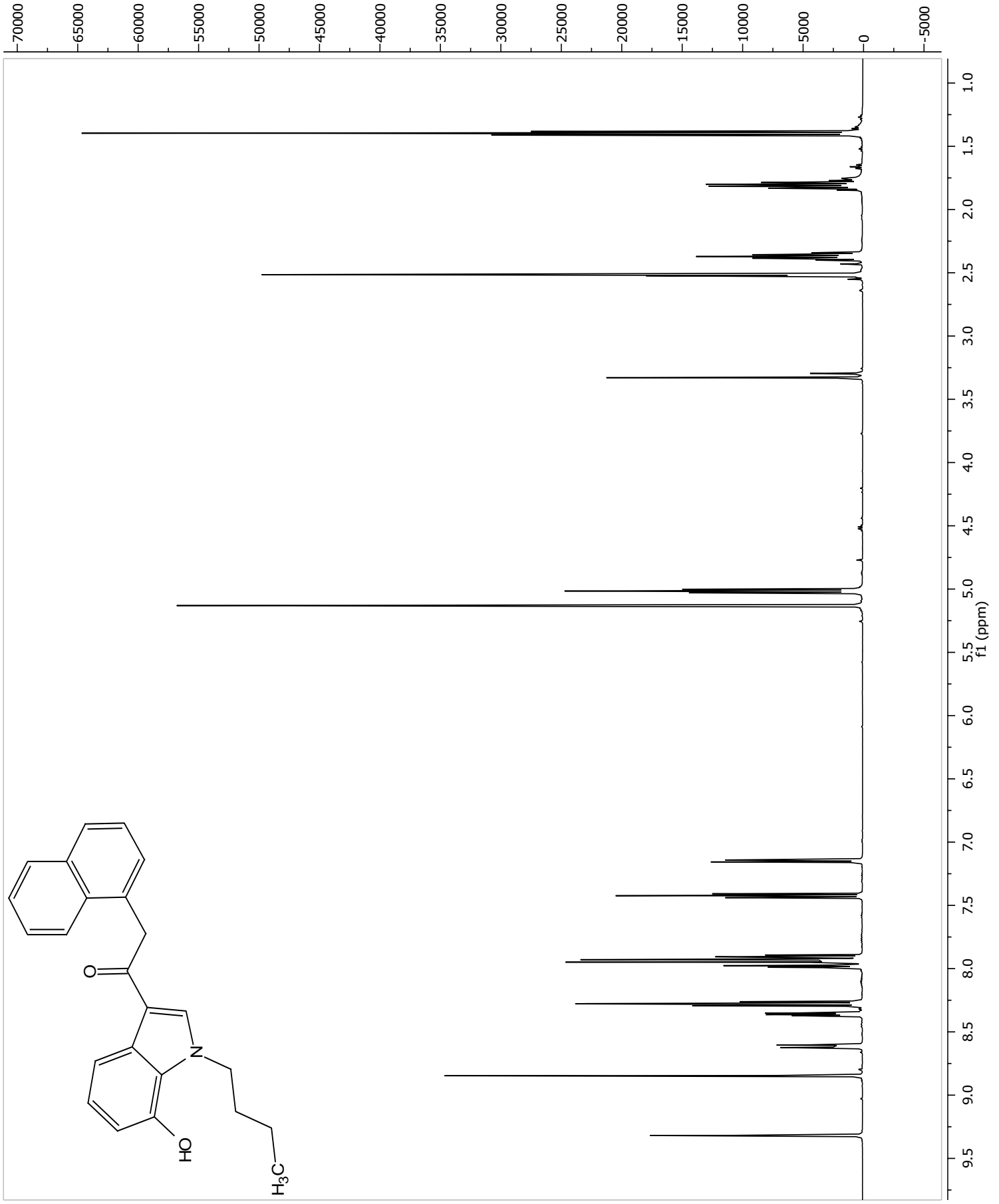
70000
65000
60000
55000
50000
45000
40000
35000
30000
25000
20000
15000
10000
5000
0
-5000
1.0
1.5
2.0
2.5
3.0
3.5
4.0
4.5
5.0
5.5
6.0
6.5
7.0
7.5
8.0
8.5
9.0
9.5
f1 (ppm)
O
N
HO
H3C

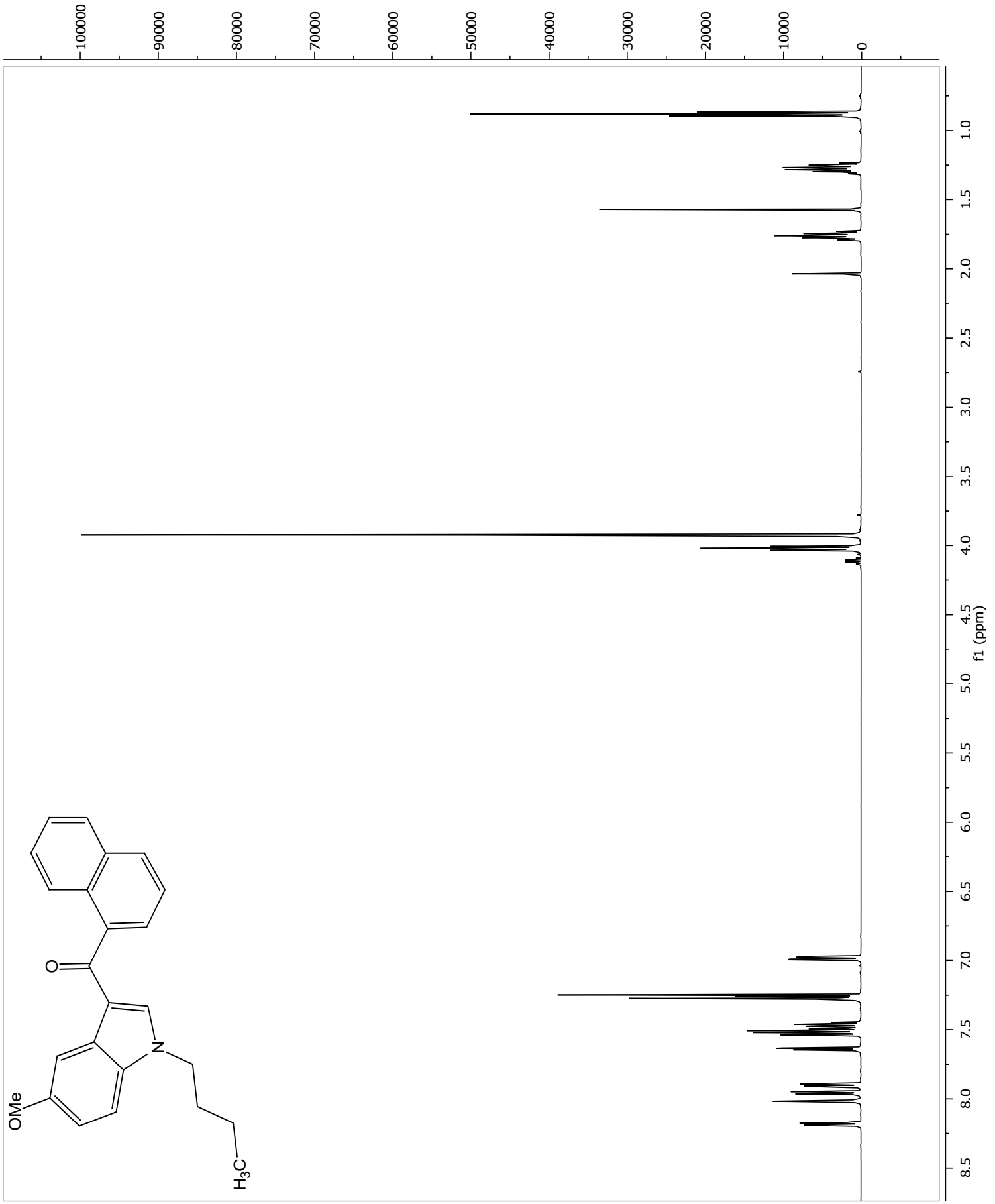
100000
90000
80000
70000
60000
50000
40000
30000
20000
10000
0
1.0
1.5
2.0
2.5
3.0
3.5
4.0
4.5
5.0
5.5
6.0
6.5
7.0
7.5
8.0
8.5
f1 (ppm)
O
N
OMe
H3C

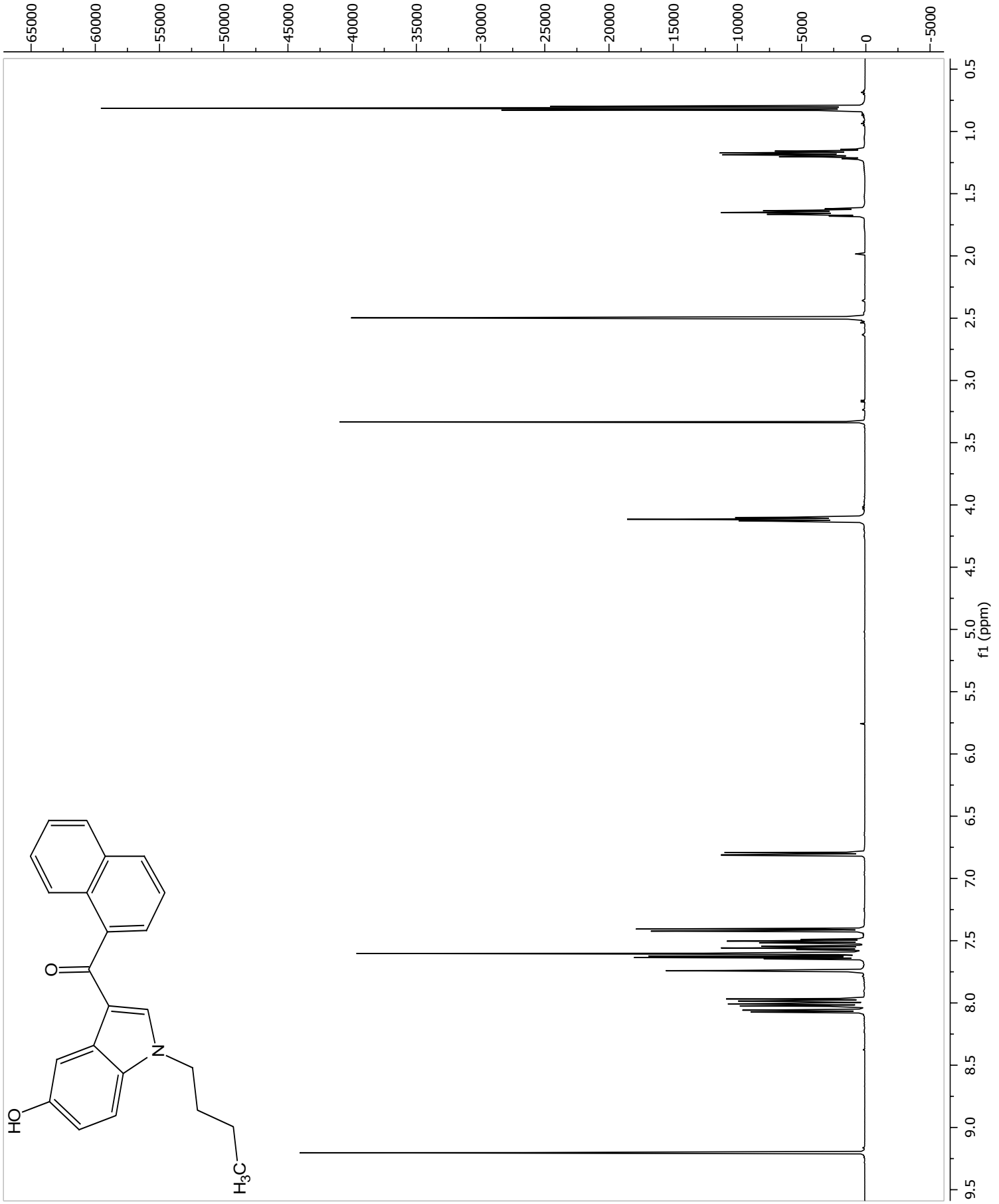
65000
60000
55000
50000
45000
40000
35000
30000
25000
20000
15000
10000
5000
0
-5000
0.5
1.0
1.5
2.0
2.5
3.0
3.5
4.0
4.5
5.0
5.5
6.0
6.5
7.0
7.5
8.0
8.5
9.0
9.5
f1 (ppm)
O
N
HO
H3C

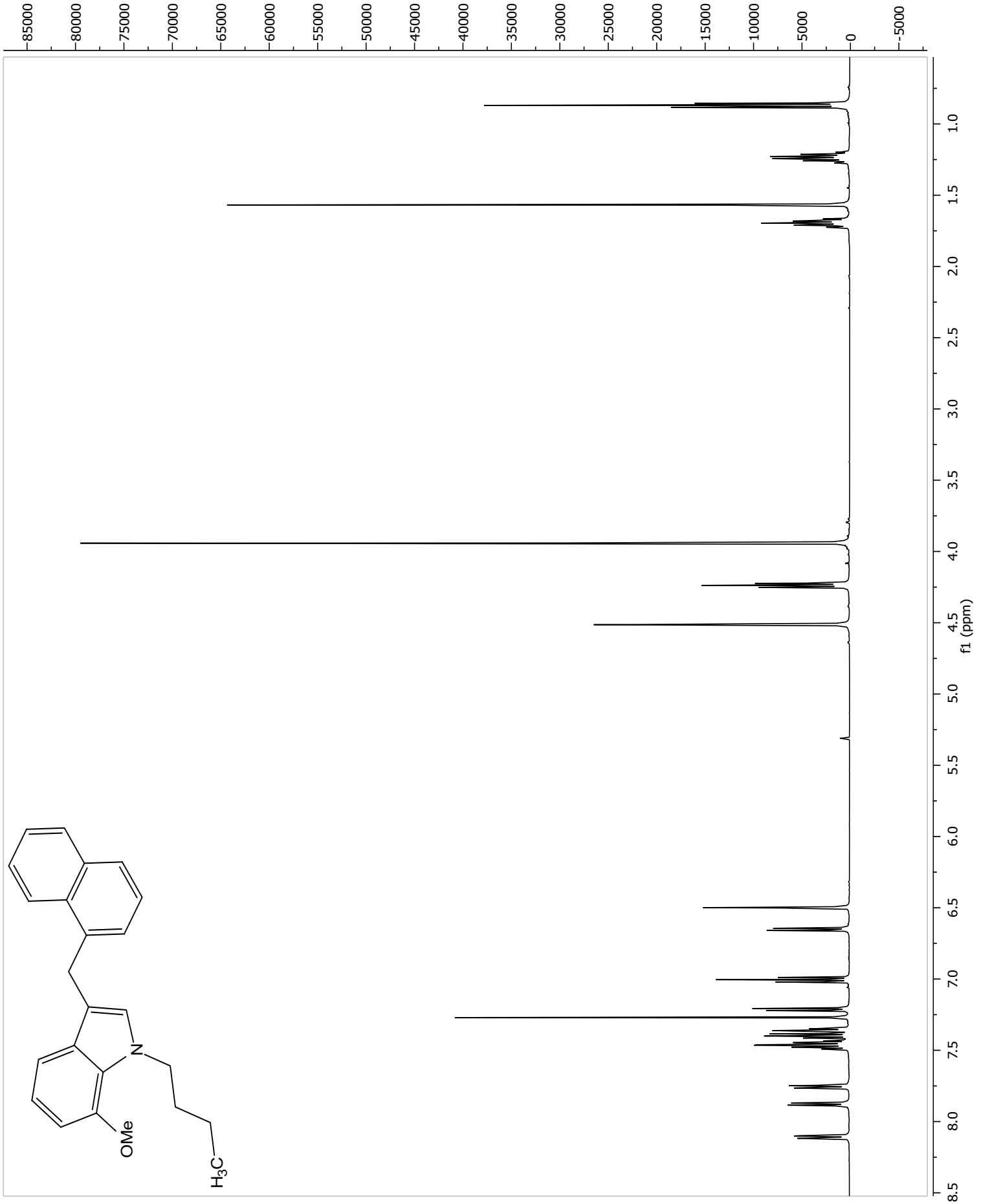
85000
80000
75000
70000
65000
60000
55000
50000
45000
40000
35000
30000
25000
20000
15000
10000
5000
0
-5000
1.0
1.5
2.0
2.5
3.0
3.5
4.0
4.5
5.0
5.5
6.0
6.5
7.0
7.5
8.0
8.5
f1 (ppm)
N
OMe
H3C

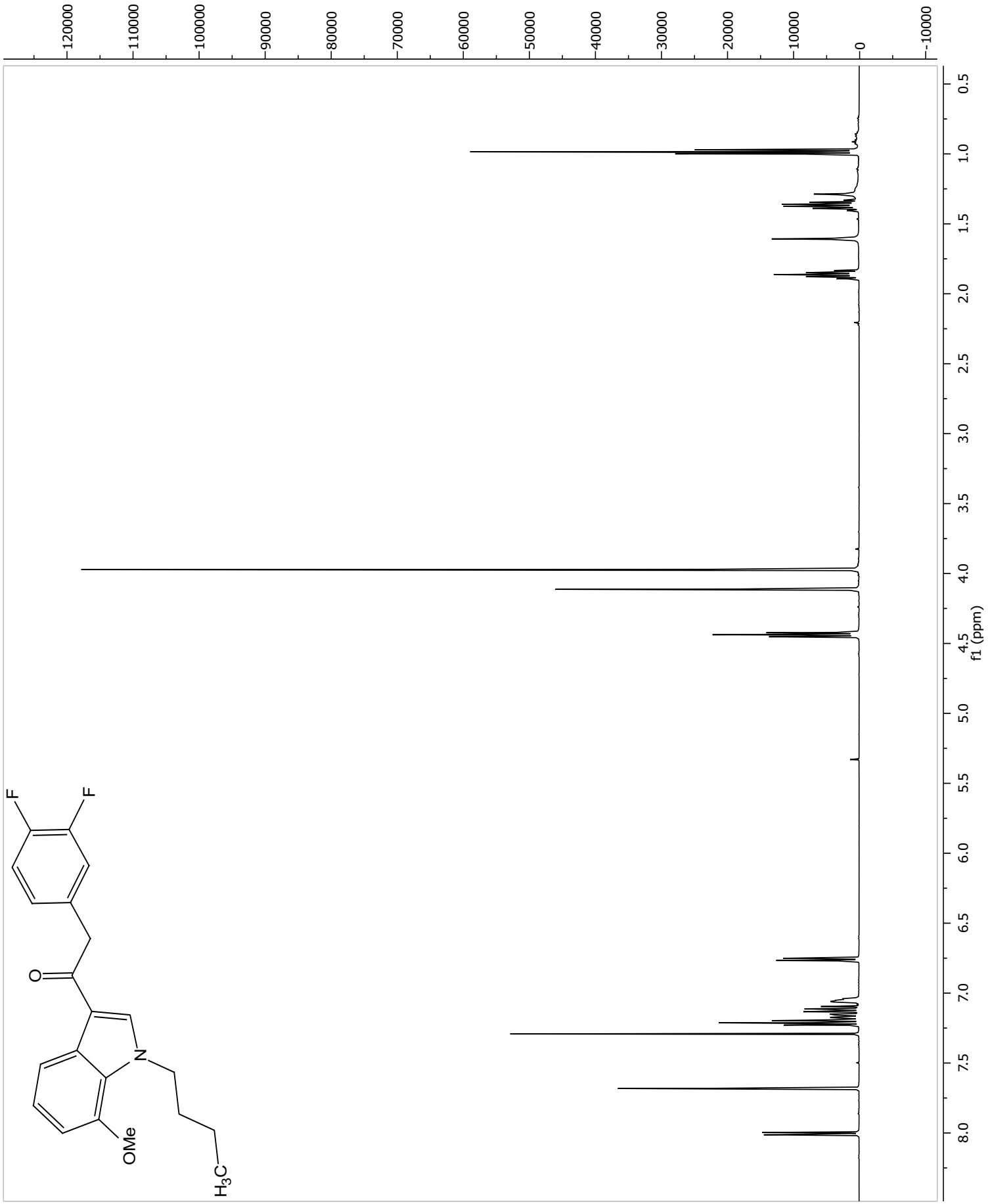
F
F
O
N
OMe
H3C
f1 (ppm)

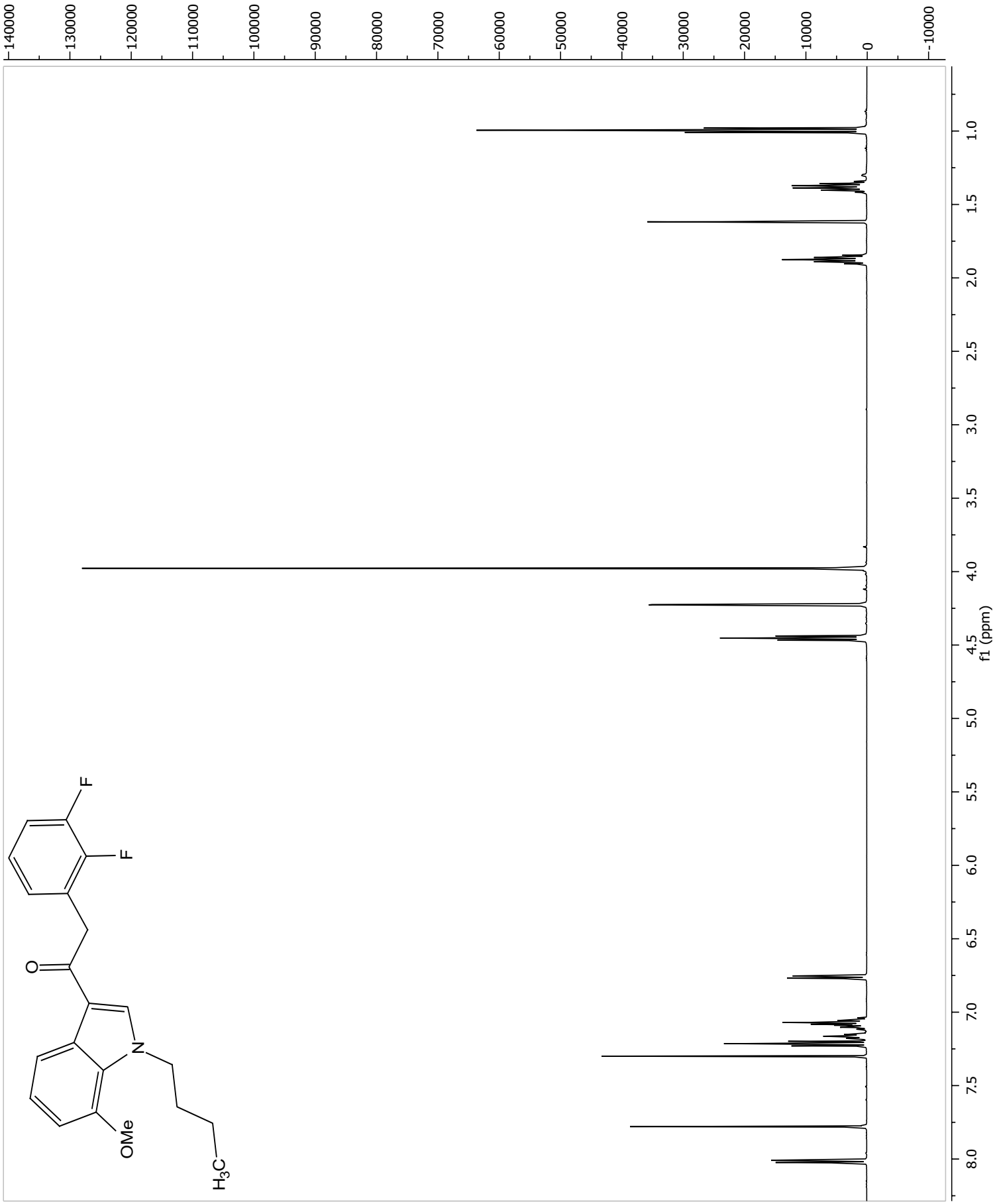
F
F
O
N
OMe
H3C
f1 (ppm)

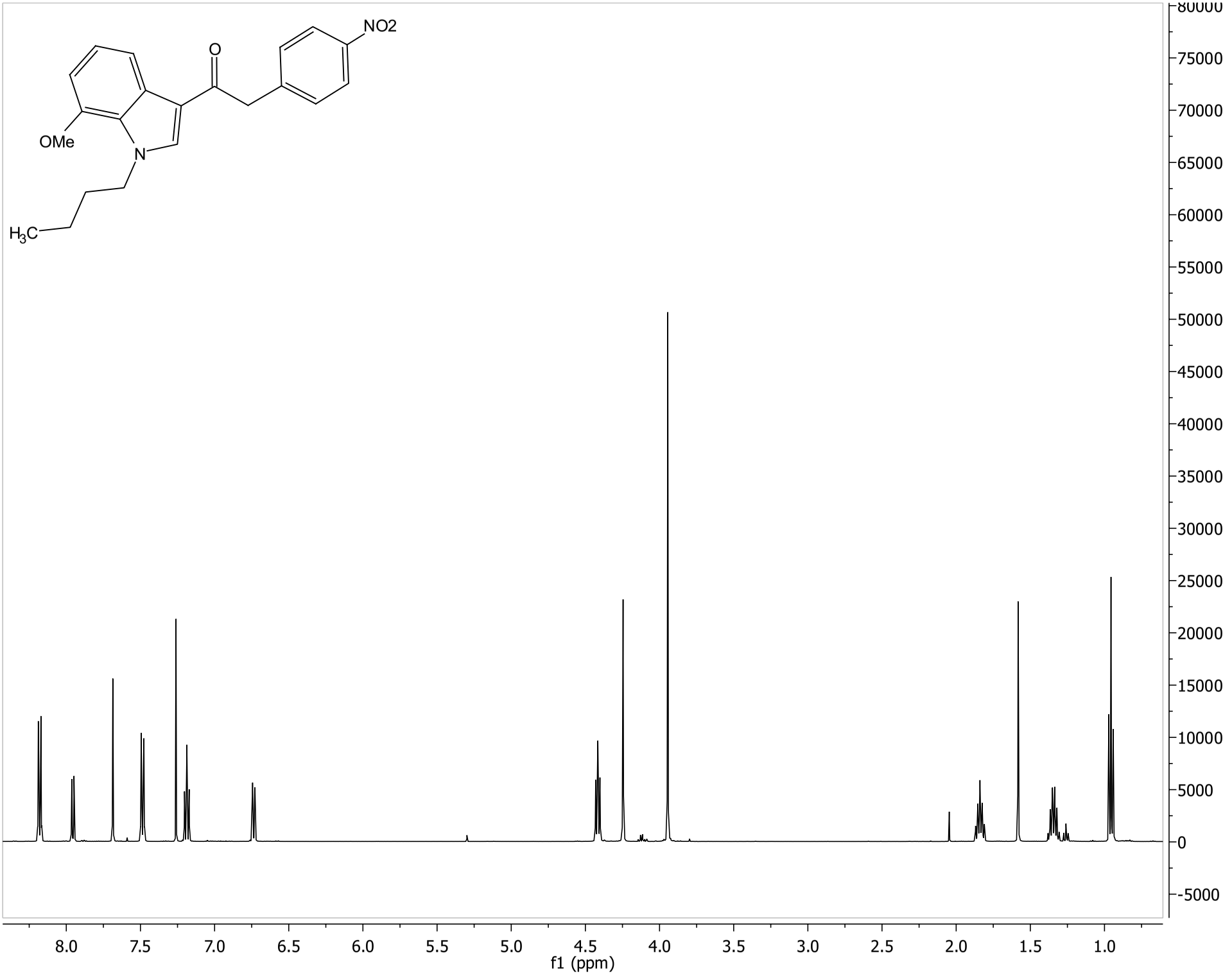
NO2
O
OMe
N
H3C
80000
75000
70000
65000
60000
55000
50000
45000
40000
35000
30000
25000
20000
15000
10000
5000
0
-5000
8.0
7.5
7.0
6.5
6.0
5.5
5.0
4.5
4.0
3.5
3.0
2.5
2.0
1.5
1.0
f1 (ppm)

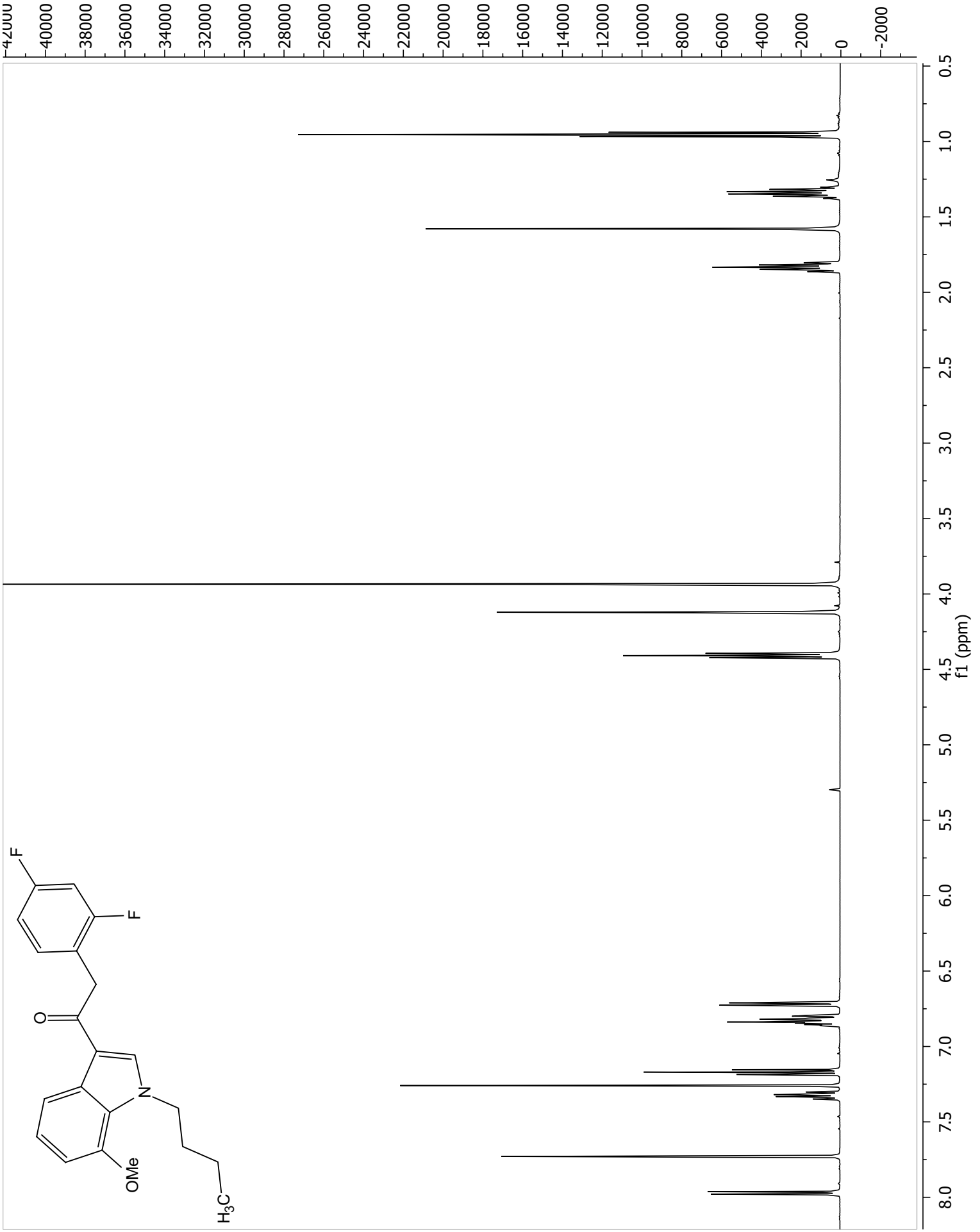
F
F
O
N
OMe
H3C
f1 (ppm)

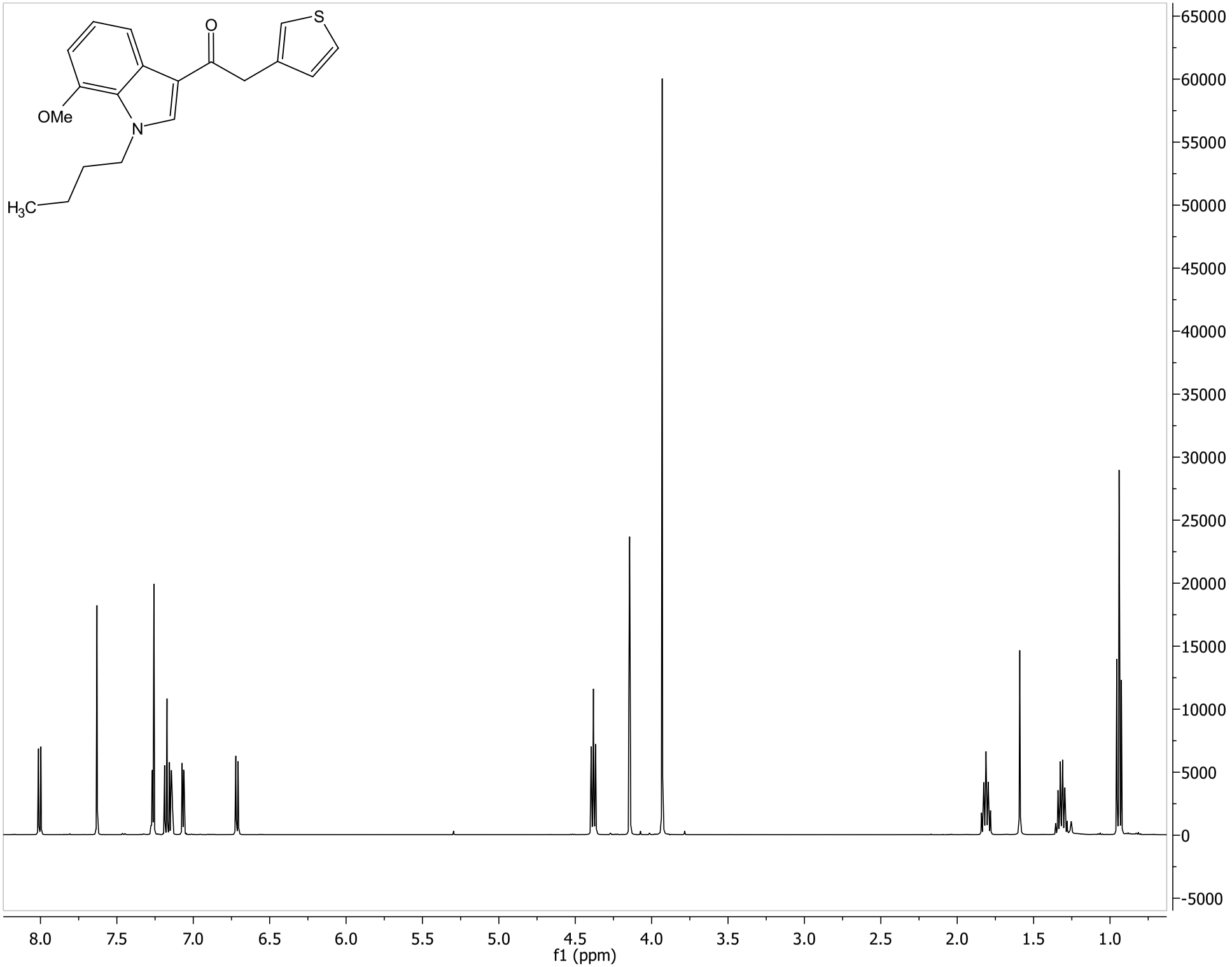
O
S
OMe
N
H3C
65000
60000
55000
50000
45000
40000
35000
30000
25000
20000
15000
10000
5000
0
-5000
8.0
7.5
7.0
6.5
6.0
5.5
5.0
4.5
4.0
3.5
3.0
2.5
2.0
1.5
1.0
f1 (ppm)

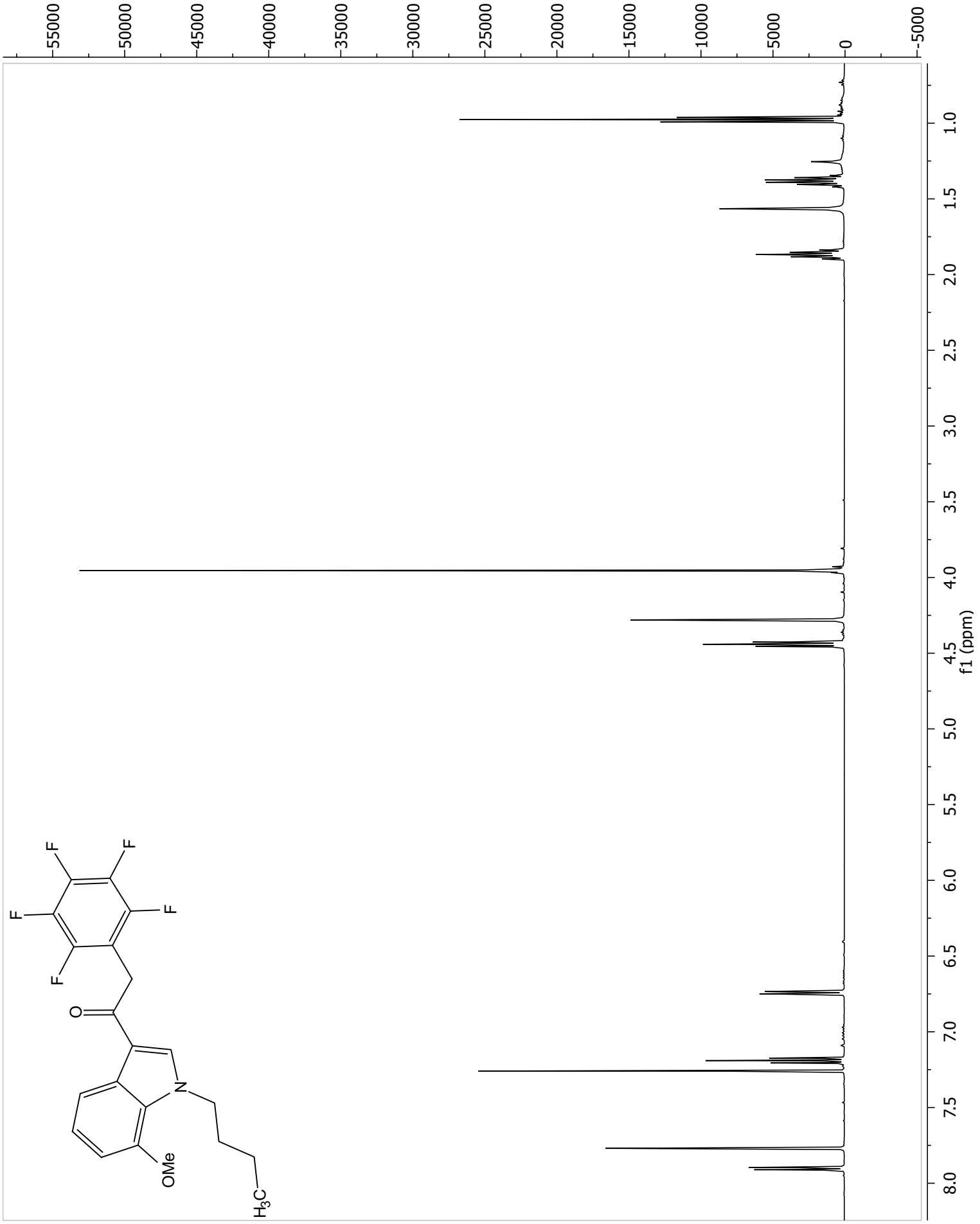
55000
50000
45000
40000
35000
30000
25000
20000
15000
10000
5000
0
-5000
1.0
1.5
2.0
2.5
3.0
3.5
4.0
4.5
5.0
5.5
6.0
6.5
7.0
7.5
8.0
f1 (ppm)
F
F
F
F
O
N
OMe
H3C

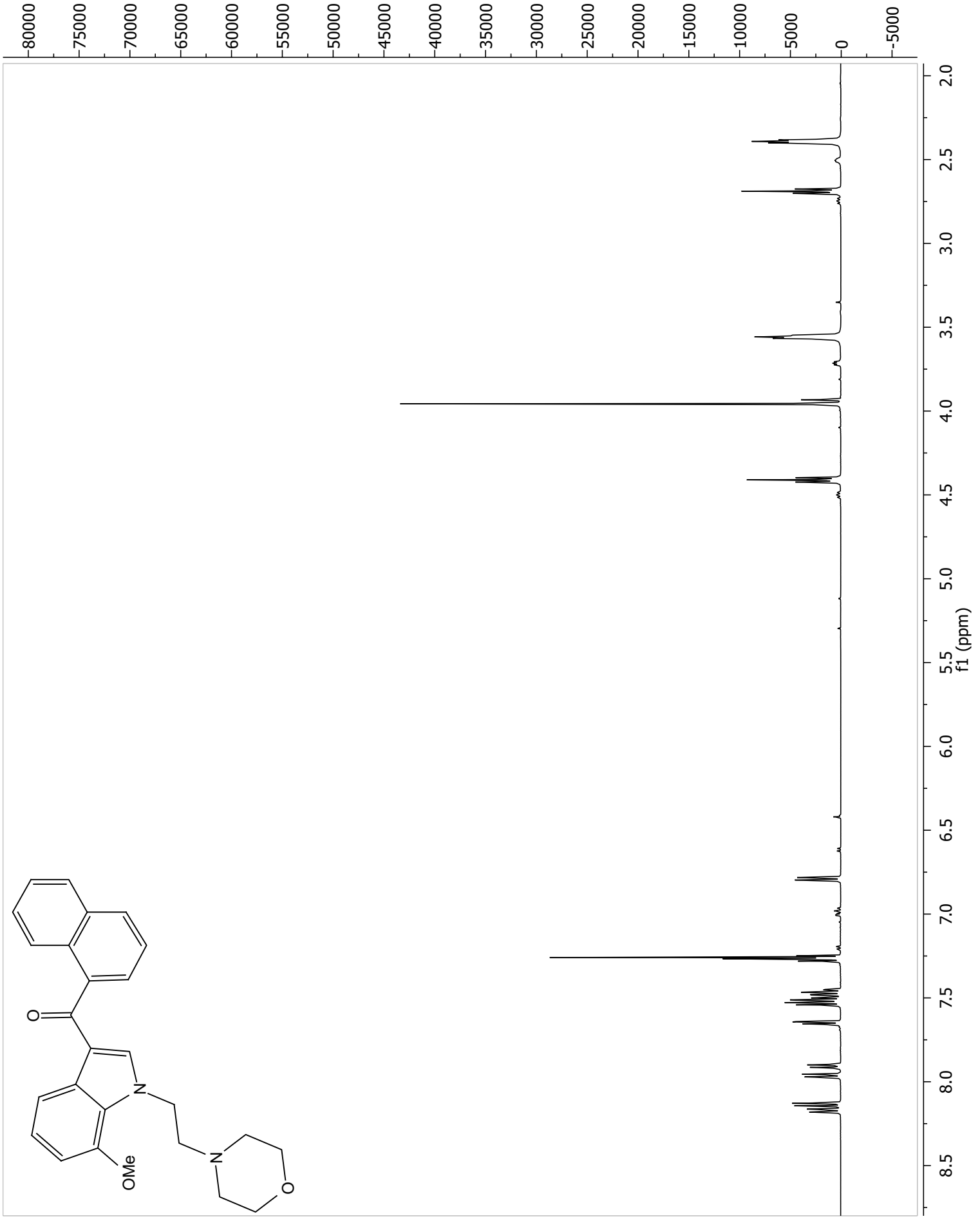
f1 (ppm)
OMe
O
N
N
O

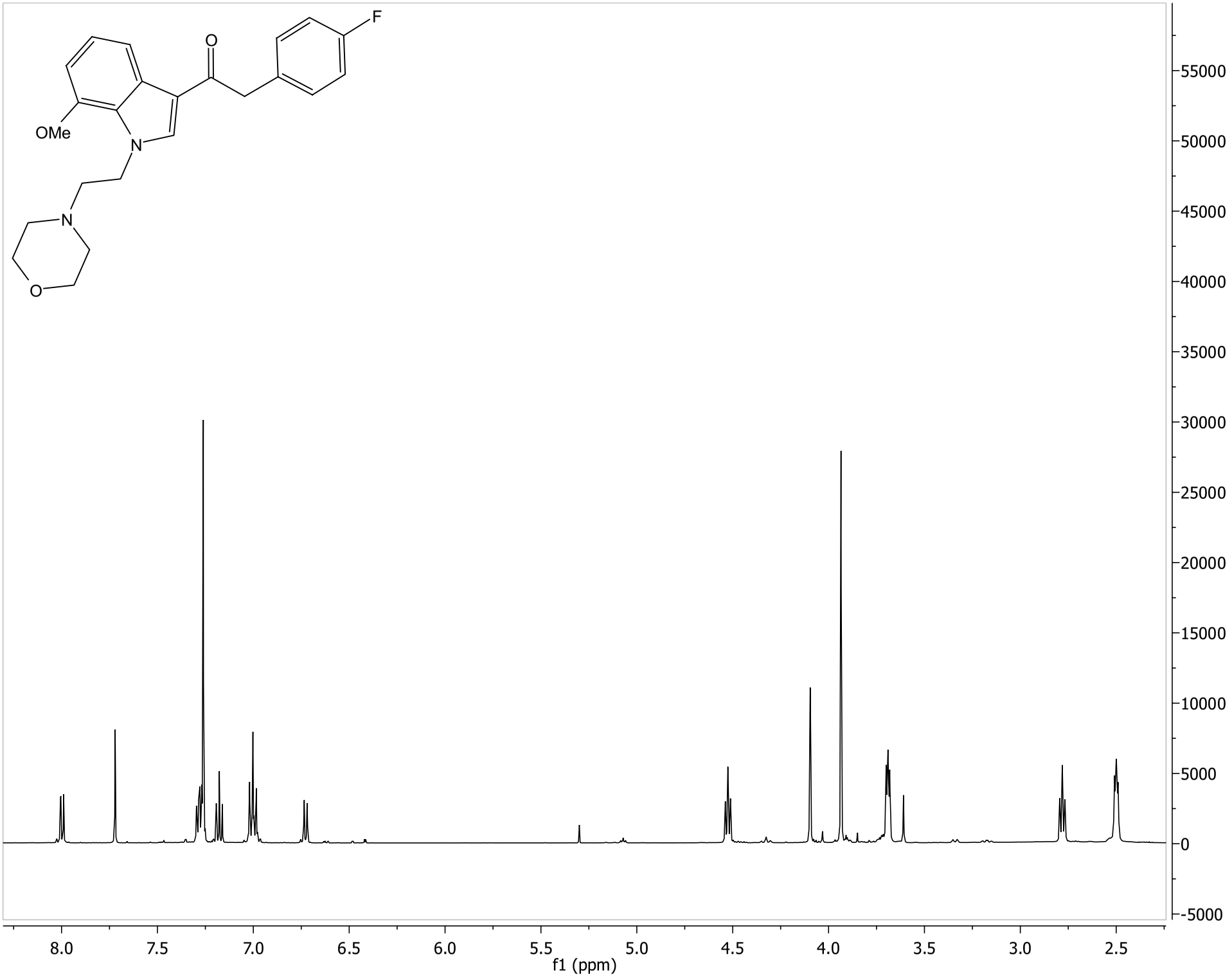
F
O
OMe
N
N
O
55000
50000
45000
40000
35000
30000
25000
20000
15000
10000
5000
0
-5000
8.0
7.5
7.0
6.5
6.0
5.5
5.0
4.5
4.0
3.5
3.0
2.5
f1 (ppm)

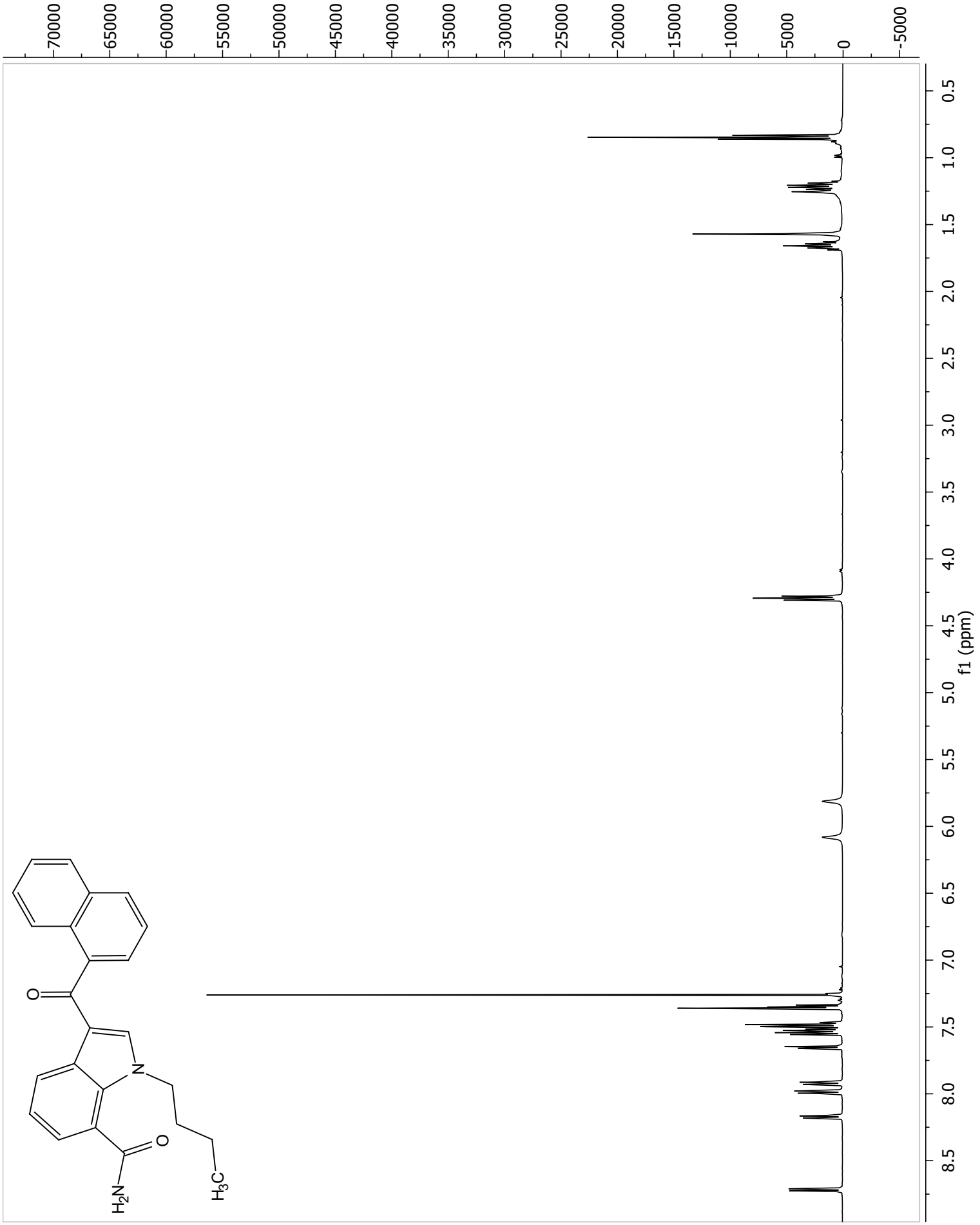
70000
65000
60000
55000
50000
45000
40000
35000
30000
25000
20000
15000
10000
5000
0
-5000
0.5
1.0
1.5
2.0
2.5
3.0
3.5
4.0
4.5
5.0
5.5
6.0
6.5
7.0
7.5
8.0
8.5
f1 (ppm)
O
N
O
H_2N
H_3C

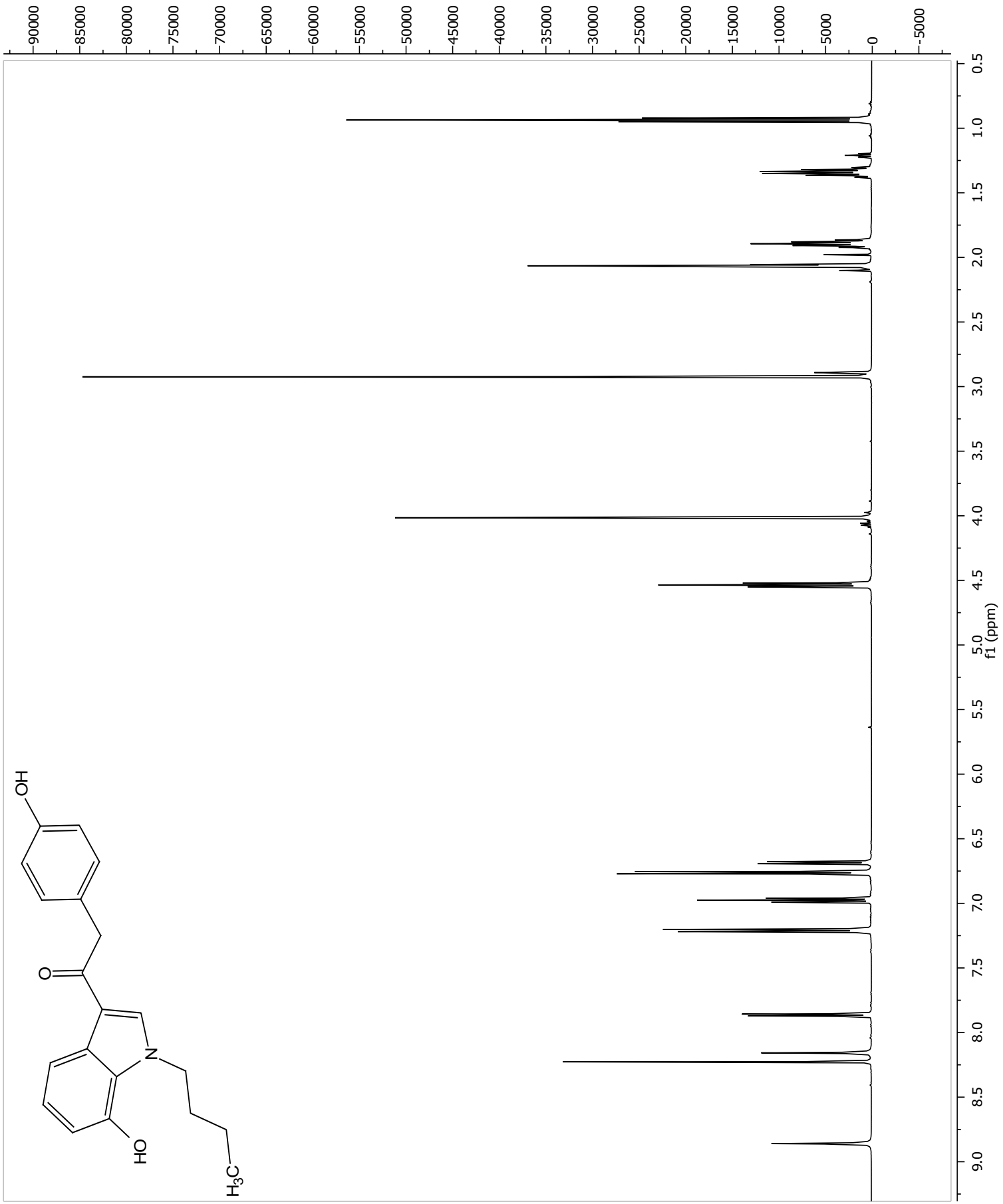
OH
O
N
HO
H3C
f1 (ppm)

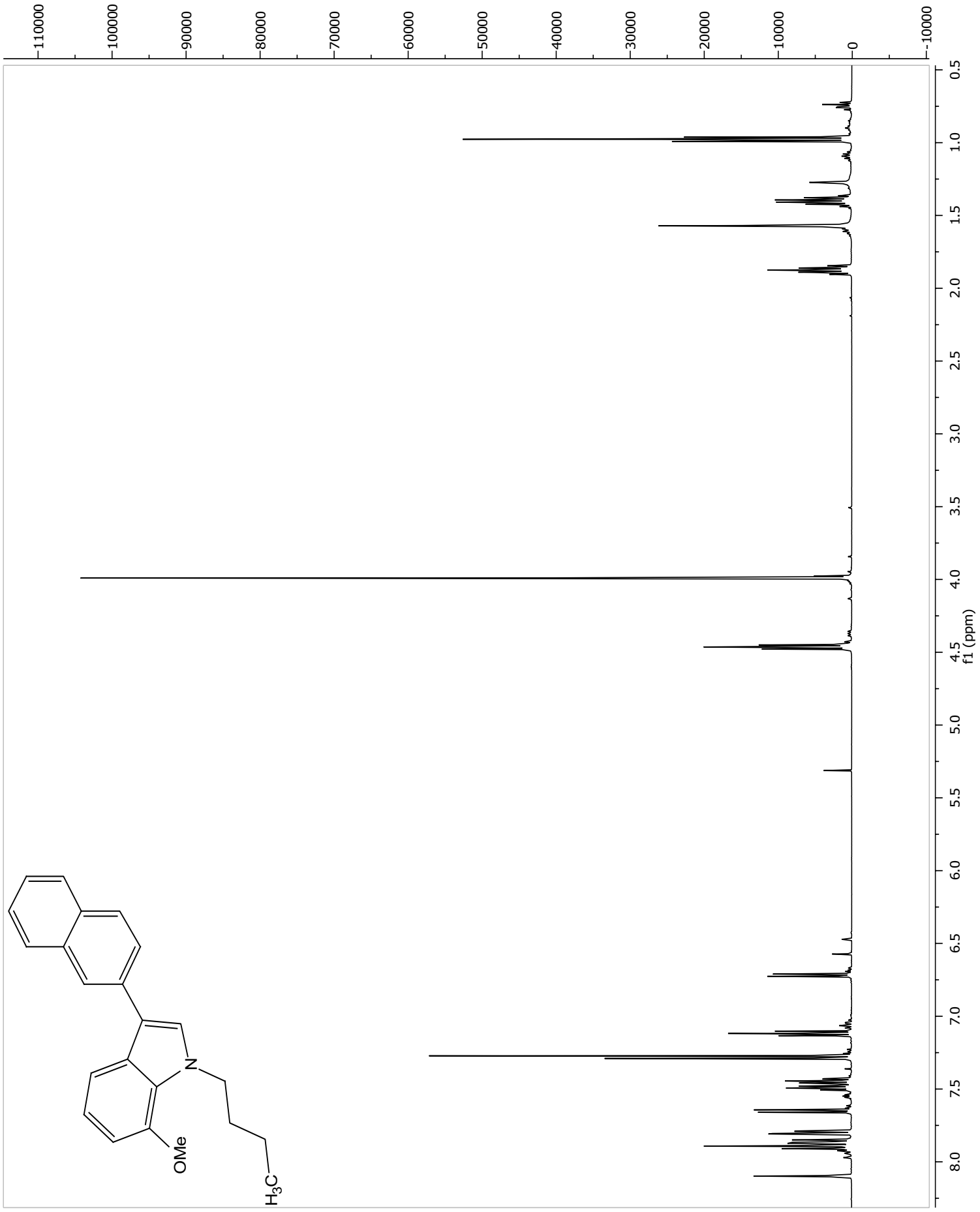
110000
100000
90000
80000
70000
60000
50000
40000
30000
20000
10000
0
-10000
0.5
1.0
1.5
2.0
2.5
3.0
3.5
4.0
4.5
5.0
5.5
6.0
6.5
7.0
7.5
8.0
f1 (ppm)
N
OMe
H3C

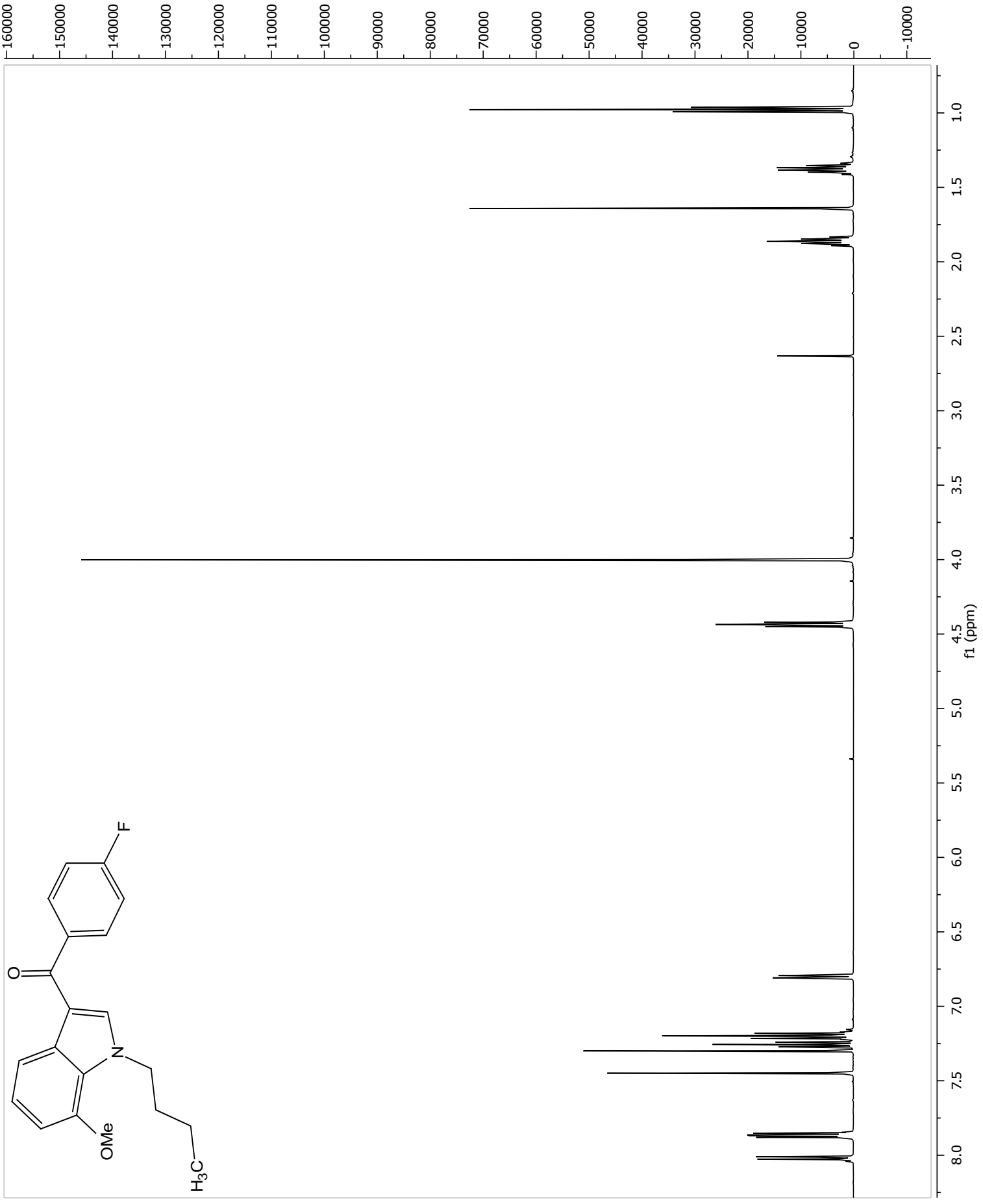
160000
150000
140000
130000
120000
110000
100000
90000
80000
70000
60000
50000
40000
30000
20000
10000
0
-10000
1.0
1.5
2.0
2.5
3.0
3.5
4.0
4.5
5.0
5.5
6.0
6.5
7.0
7.5
8.0
f1 (ppm)
F
O
N
OMe
H3C

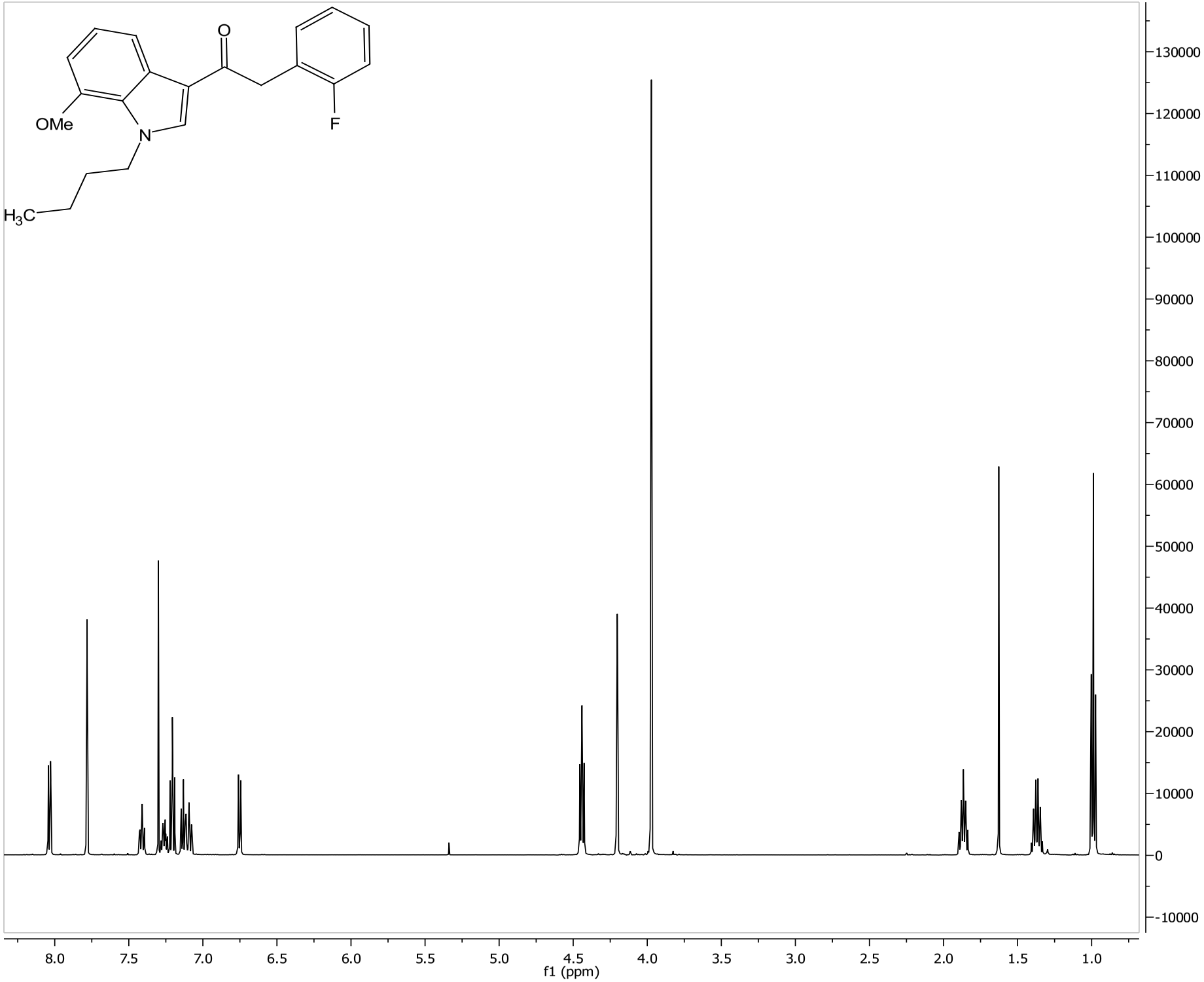
O
OMe
N
F
H3C
130000
120000
110000
100000
90000
80000
70000
60000
50000
40000
30000
20000
10000
0
-10000
8.0
7.5
7.0
6.5
6.0
5.5
5.0
4.5
4.0
3.5
3.0
2.5
2.0
1.5
1.0
f1 (ppm)

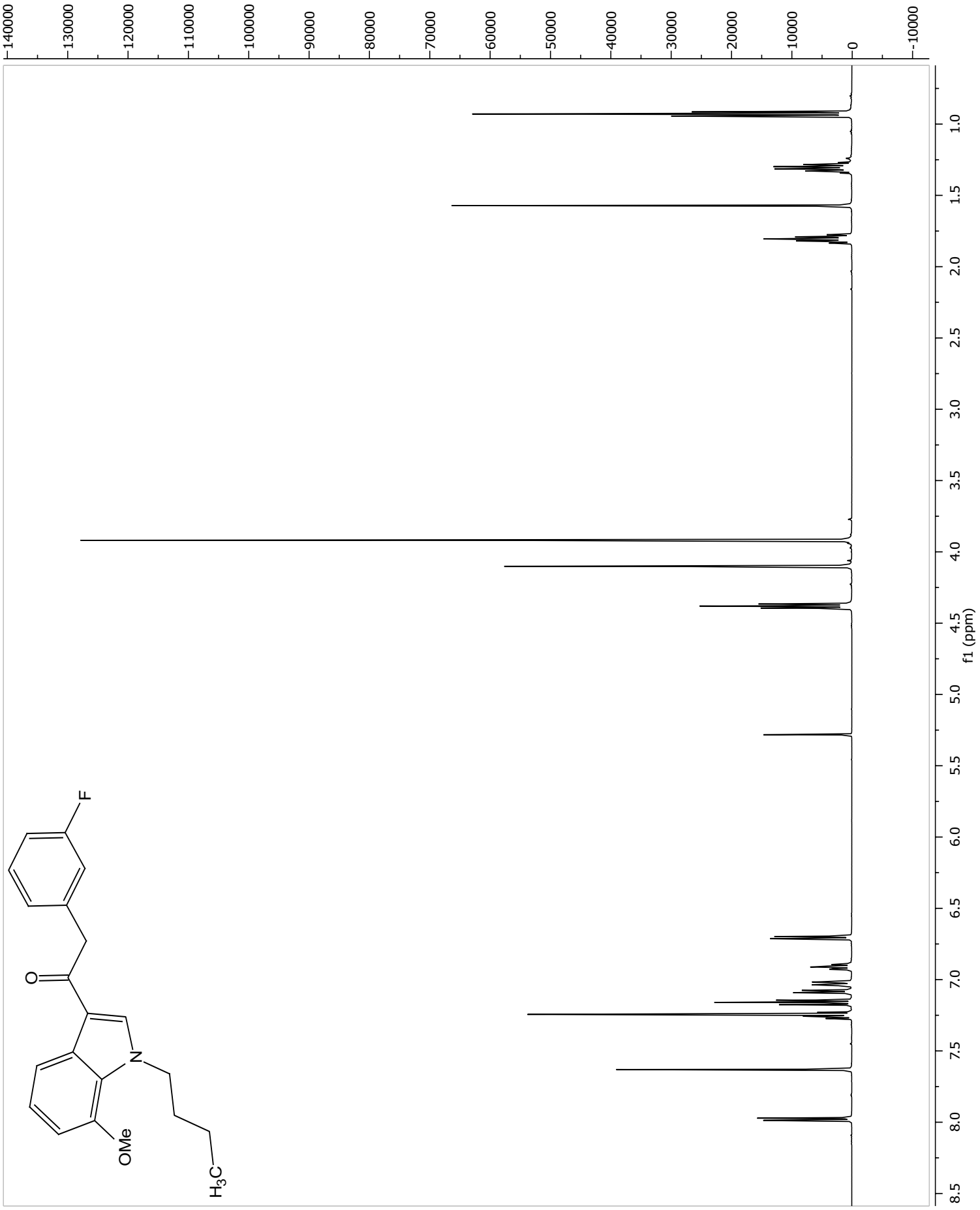
F
O
N
OMe
H3C
f1 (ppm)

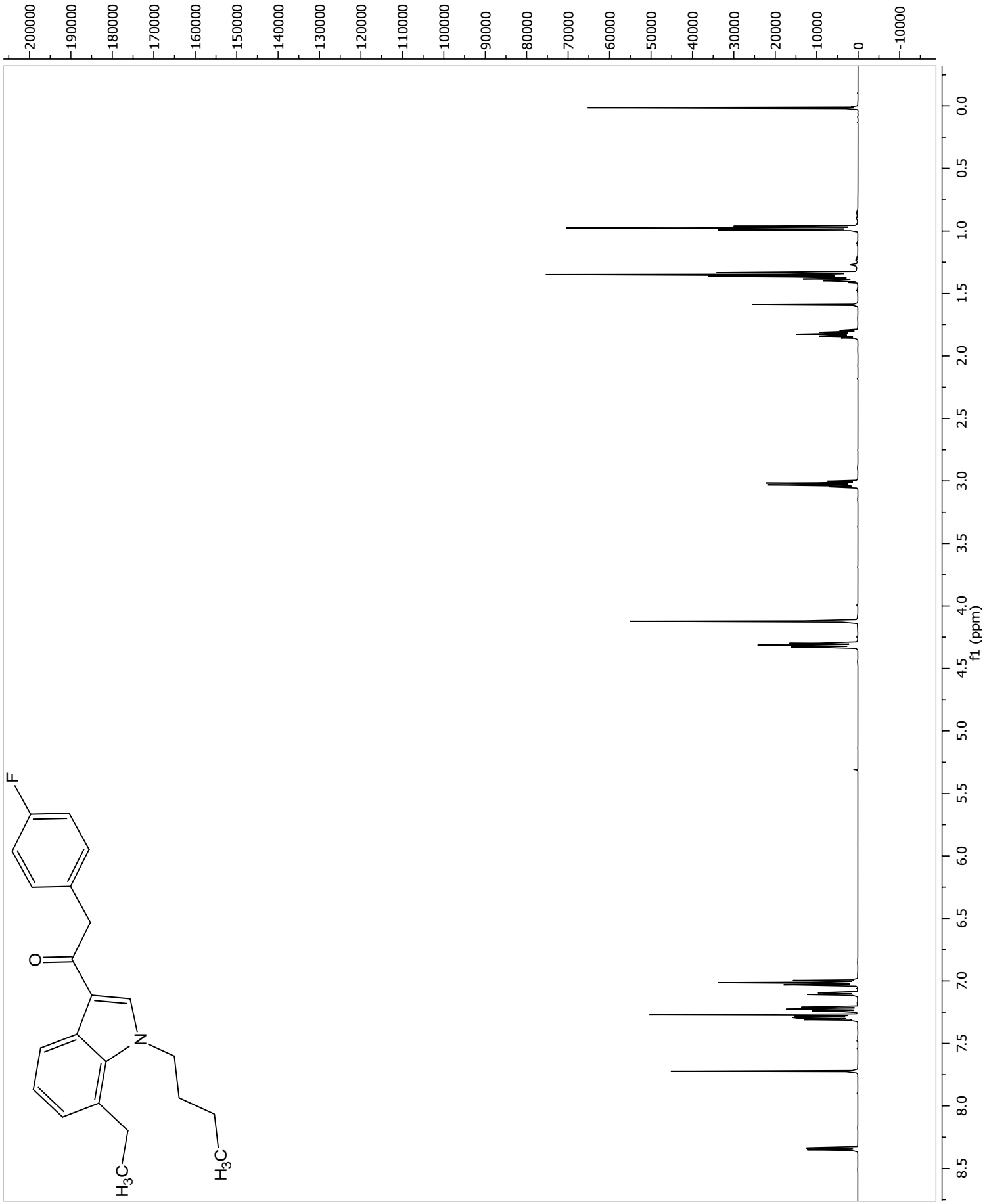
F
O
N
H3C
H3C
f1 (ppm)

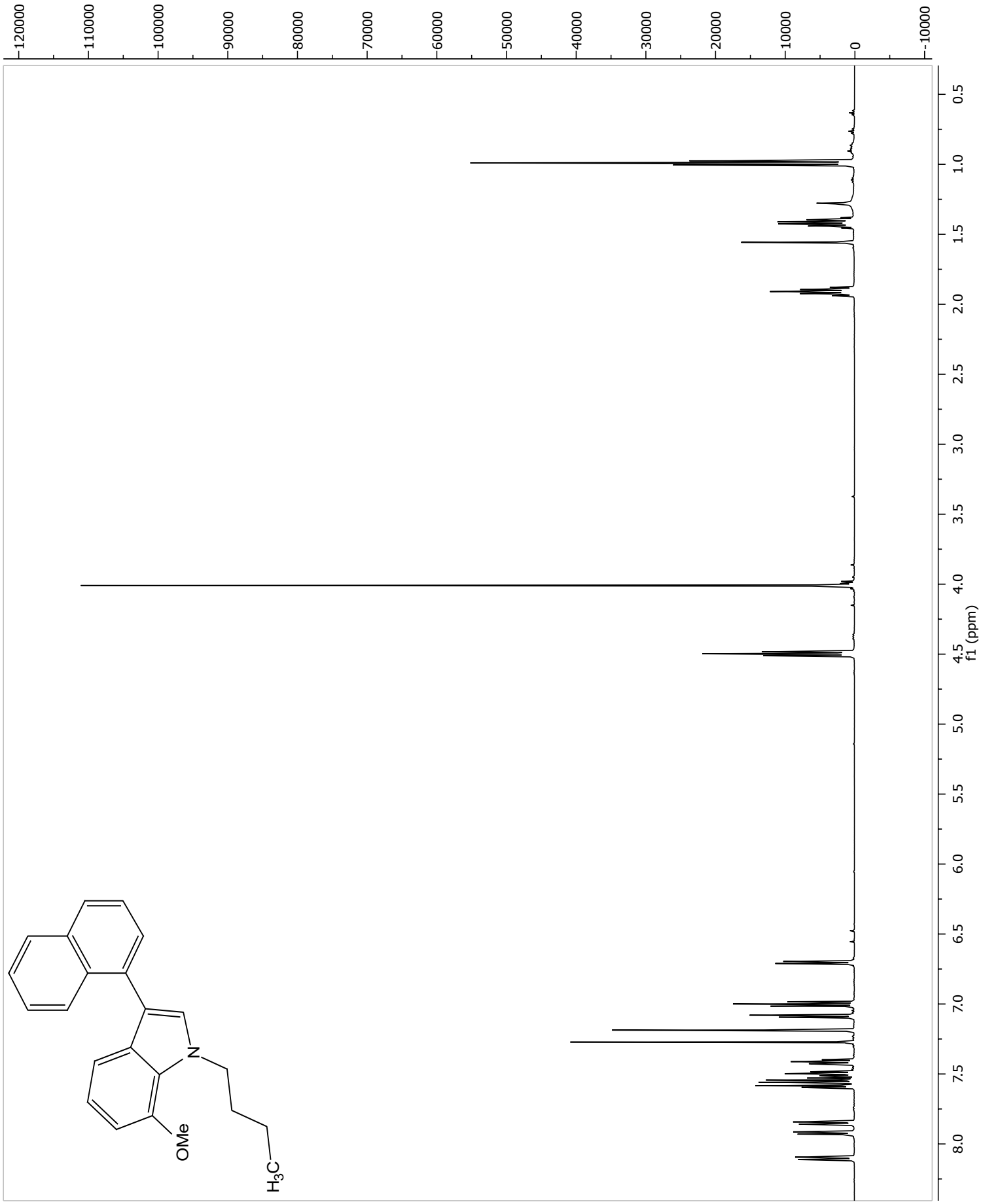
120000
110000
100000
90000
80000
70000
60000
50000
40000
30000
20000
10000
0
-10000
0.5
1.0
1.5
2.0
2.5
3.0
3.5
4.0
4.5
5.0
5.5
6.0
6.5
7.0
7.5
8.0
f1 (ppm)
N
OMe
H3C

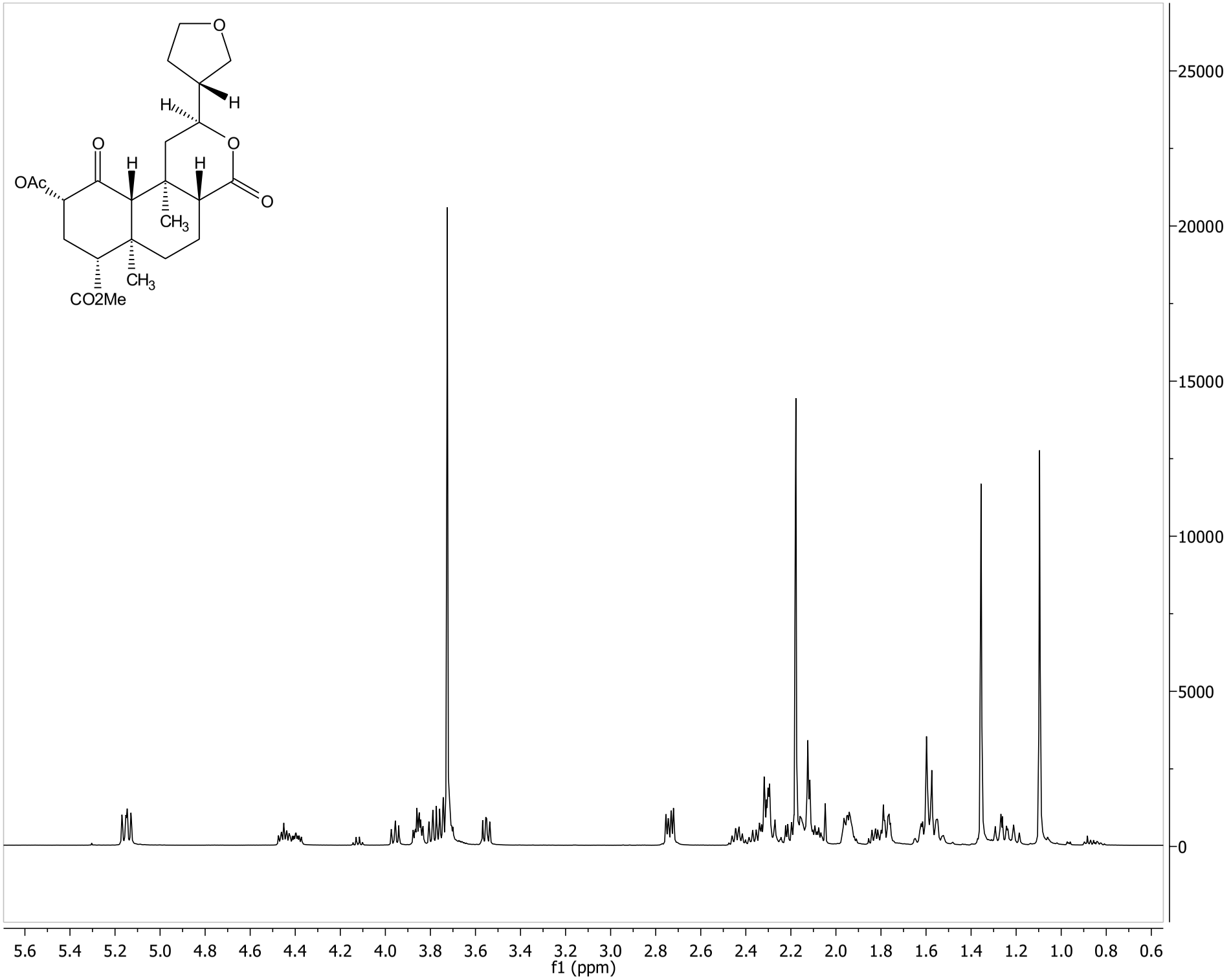
O
H
H
O
O
H
H
OAc
O
CH3
CH3
CO2Me
25000
20000
15000
10000
5000
0
5.6 5.4 5.2 5.0 4.8 4.6 4.4 4.2 4.0 3.8 3.6 3.4 3.2 3.0 2.8 2.6 2.4 2.2 2.0 1.8 1.6 1.4 1.2 1.0 0.8 0.6
f1 (ppm)

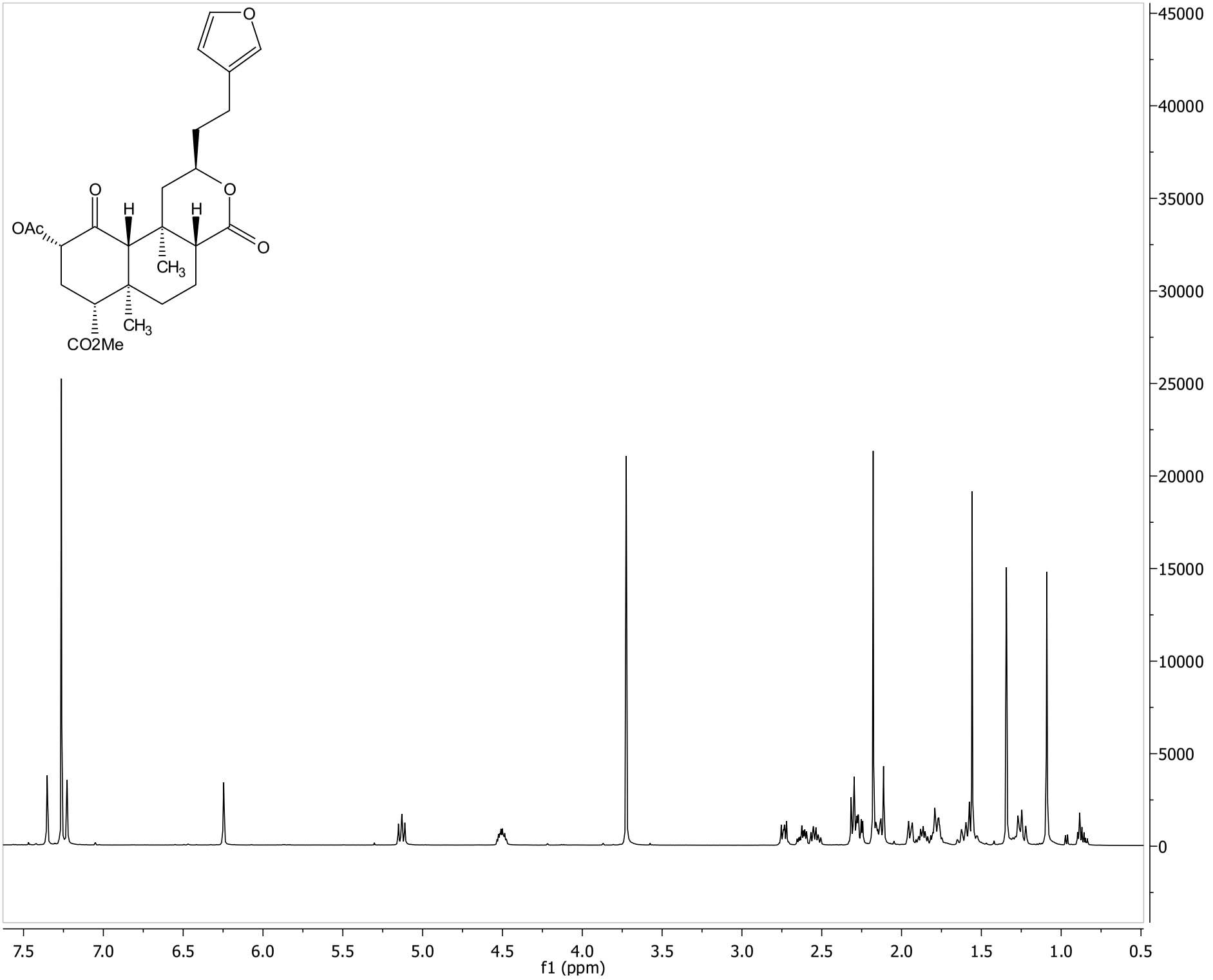
O
O
H
H
O
O
OAc
CH3
CH3
CO2Me
45000
40000
35000
30000
25000
20000
15000
10000
5000
0
7.5
7.0
6.5
6.0
5.5
5.0
4.5
4.0
3.5
3.0
2.5
2.0
1.5
1.0
0.5
f1 (ppm)

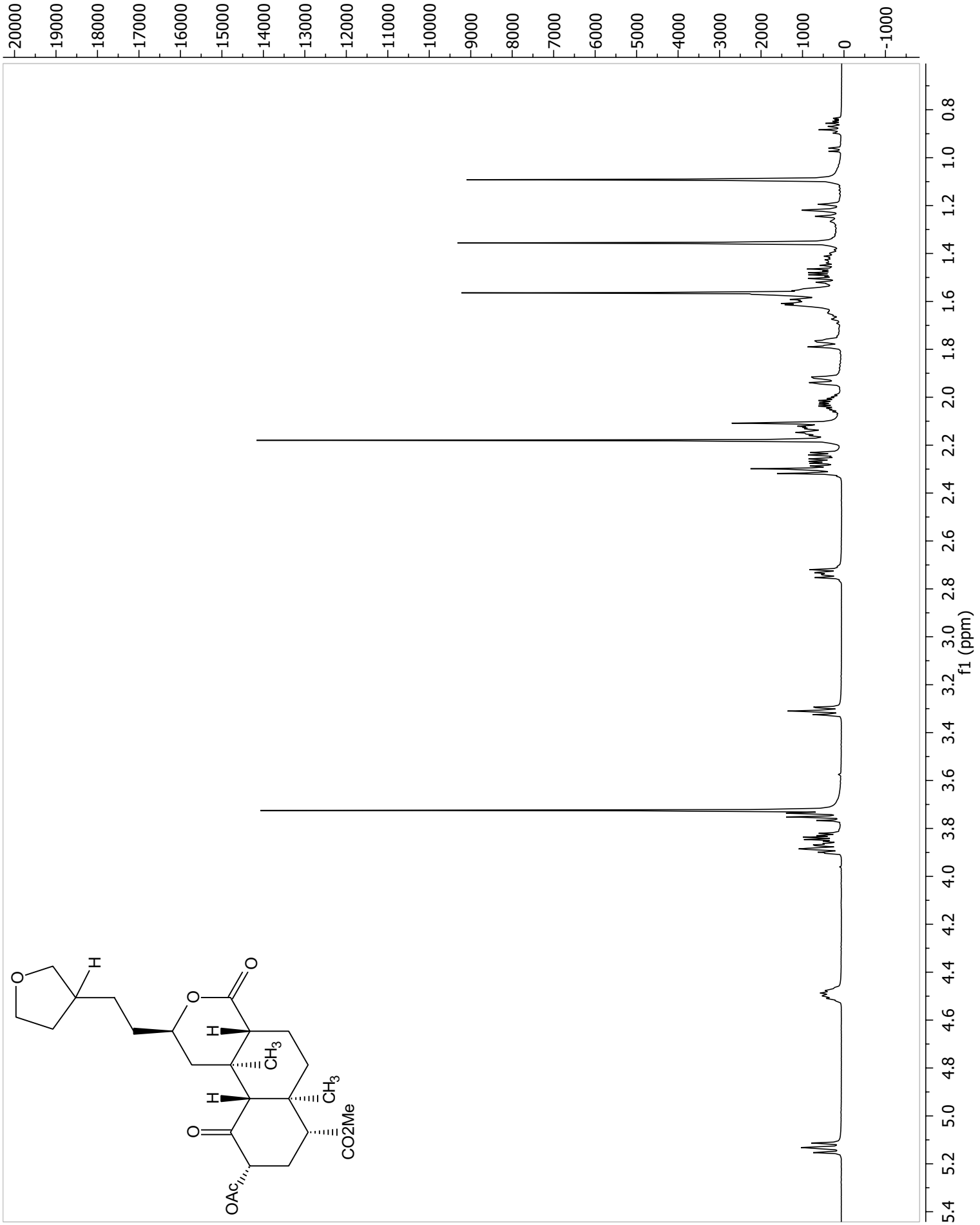
20000
19000
18000
17000
16000
15000
14000
13000
12000
11000
10000
9000
8000
7000
6000
5000
4000
3000
2000
1000
0
-1000
5.4
5.2
5.0
4.8
4.6
4.4
4.2
4.0
3.8
3.6
3.4
3.2
3.0
2.8
2.6
2.4
2.2
2.0
1.8
1.6
1.4
1.2
1.0
0.8
f1 (ppm)
O
H
O
O
H
CH3
H
CH3
O
CO2Me
OAc

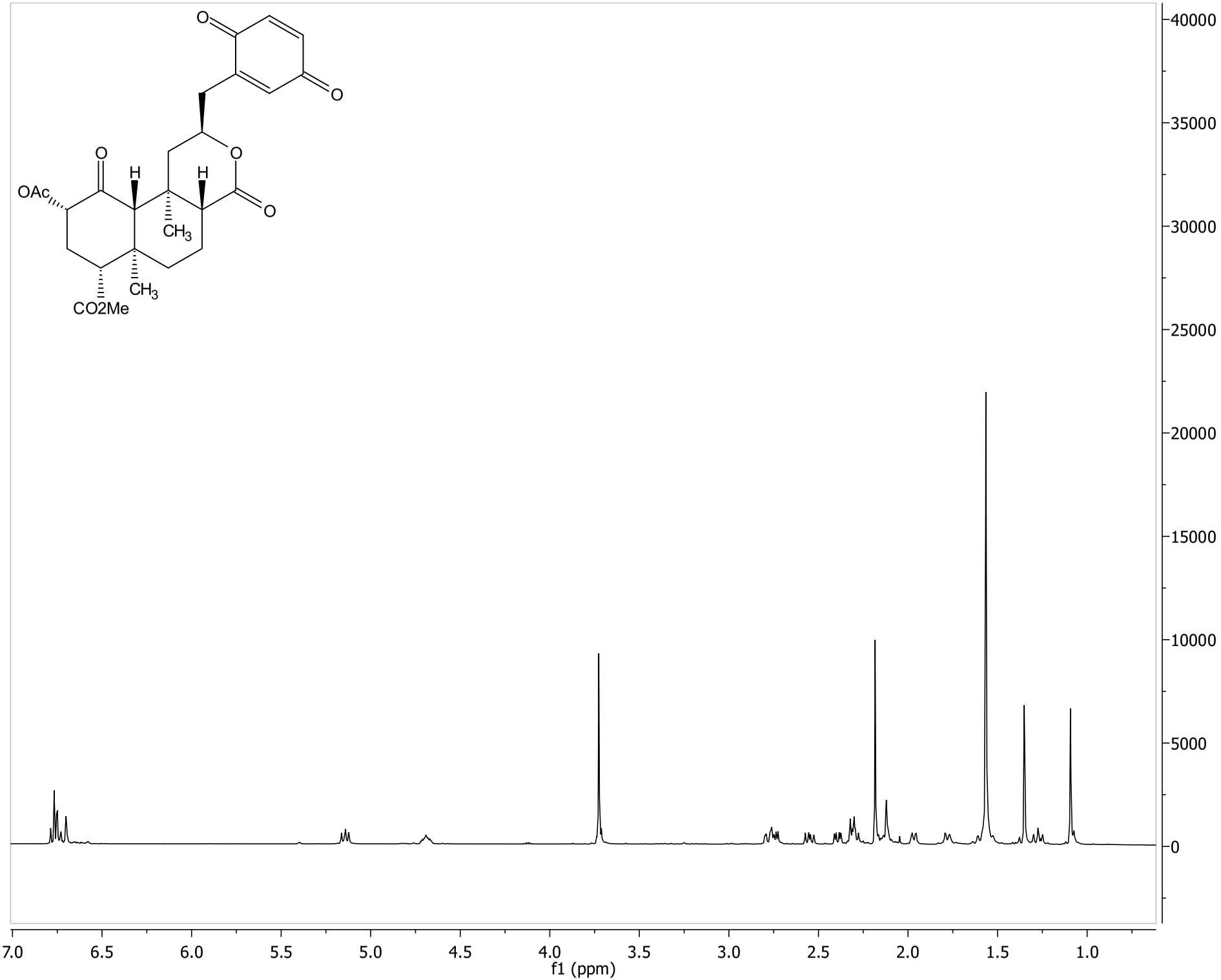
O
O
O
O
H
H
OAc
O
CH3
CH3
CO2Me
40000
35000
30000
25000
20000
15000
10000
5000
0
7.0
6.5
6.0
5.5
5.0
4.5
4.0
3.5
3.0
2.5
2.0
1.5
1.0
f1 (ppm)

APPENDIX B: HPLC CHROMATOGRAMS

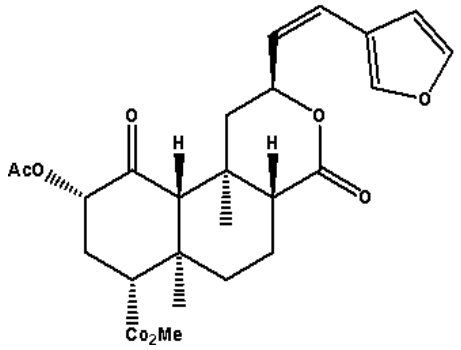

pump: Agilent 1100 series quaternary pump
column: Phenomenex Luna C-18, 5 micron, 10 x 250 mm
sample size: 100 microliters
sample concentration: 1.1 mg/mL
mobile phase: 60% acetonitrile - 40% water
flow rate: 5 mL/min
purity: 99.99%

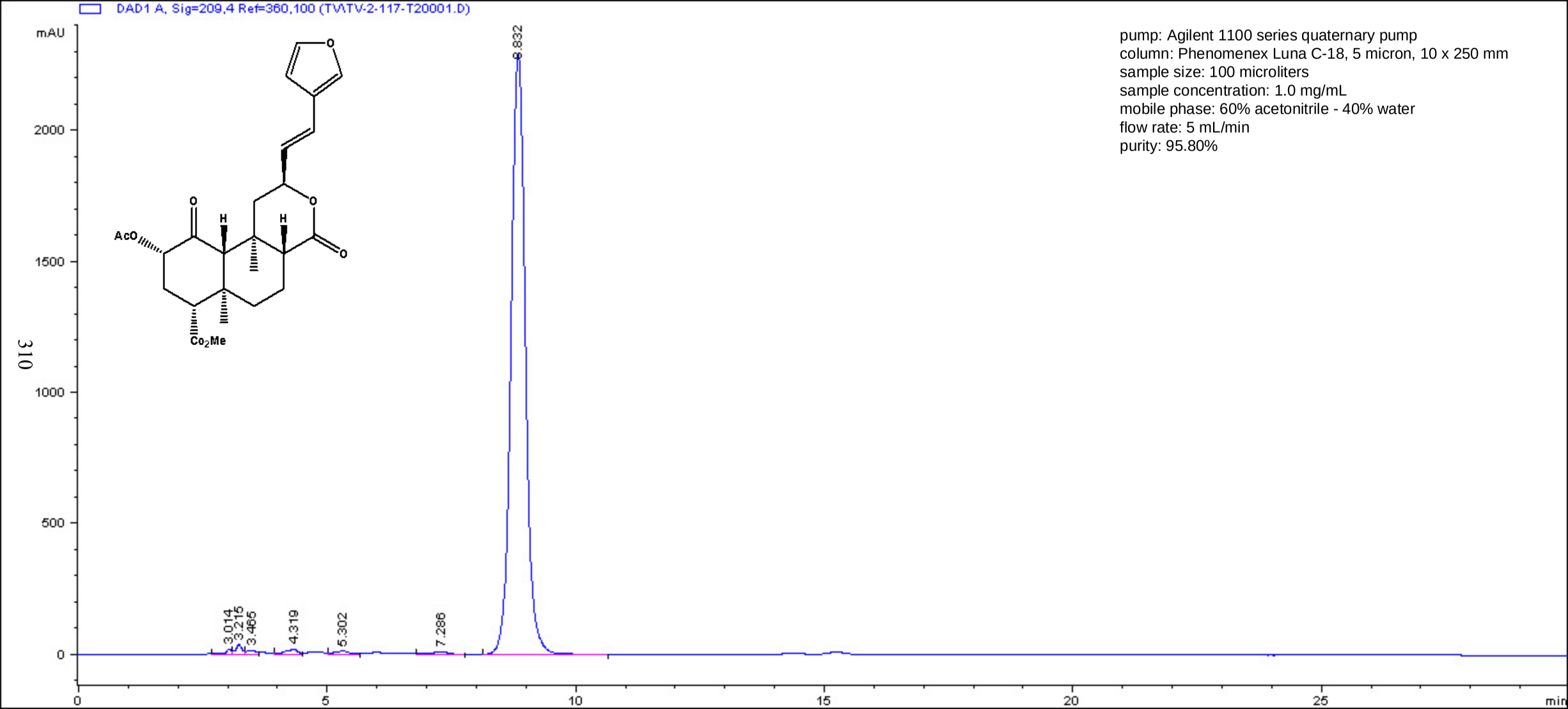

pump: Agilent 1100 series quaternary pump
column: Phenomenex Luna C-18, 5 micron, 10 x 250 mm
sample size: 100 microliters
sample concentration: 1.0 mg/mL
mobile phase: 60% acetonitrile - 40% water
flow rate: 5 mL/min
purity: 95.80%

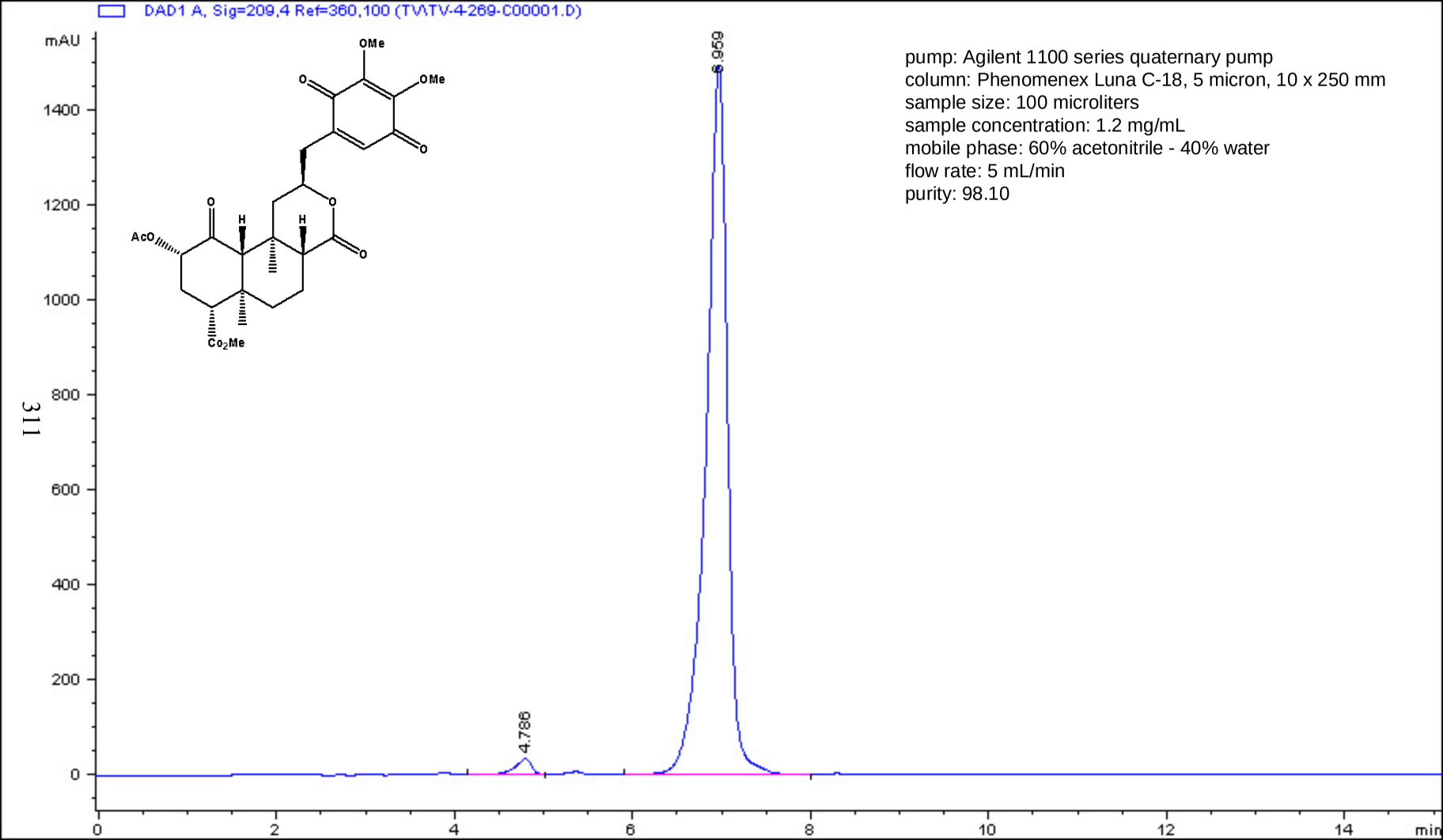
DAD1 A, Sig=209,4 Ref=360,100 (TV\TV-4-269-C00001.D)
mAU
1400
1200
1000
800
600
400
200
0
4.786
6.959
OMe
OMe
O
O
O
O
H
H
O
O
AcO
Co2Me
pump: Agilent 1100 series quaternary pump
column: Phenomenex Luna C-18, 5 micron, 10 x 250 mm
sample size: 100 microliters
sample concentration: 1.2 mg/mL
mobile phase: 60% acetonitrile - 40% water
flow rate: 5 mL/min
purity: 98.10
0
2
4
6
8
10
12
14
min

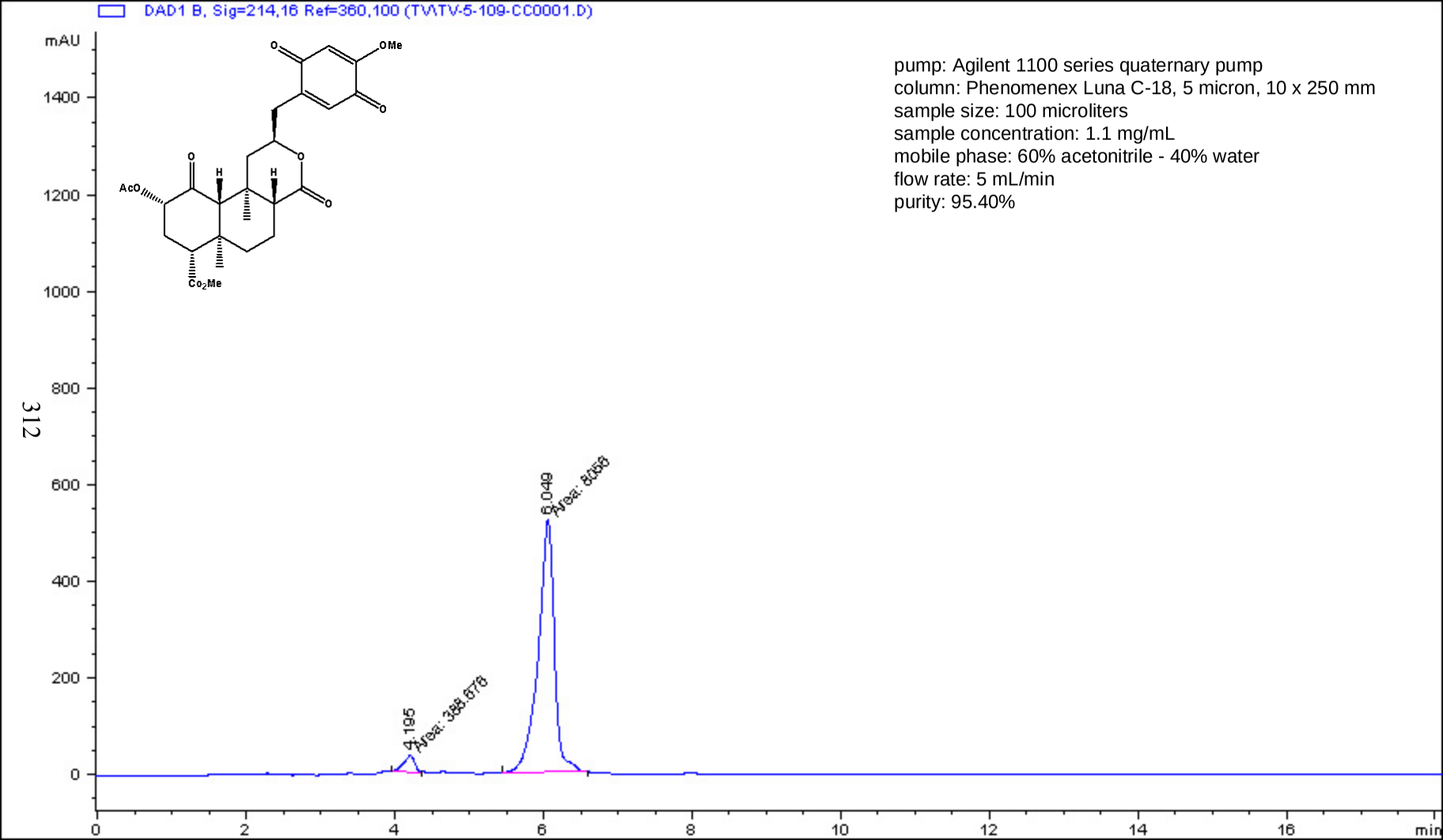

pump: Agilent 1100 series quaternary pump
column: Phenomenex Luna C-18, 5 micron, 10 x 250 mm
sample size: 100 microliters
sample concentration: 1.1 mg/mL
mobile phase: 60% acetonitrile - 40% water
flow rate: 5 mL/min
purity: 95.40%

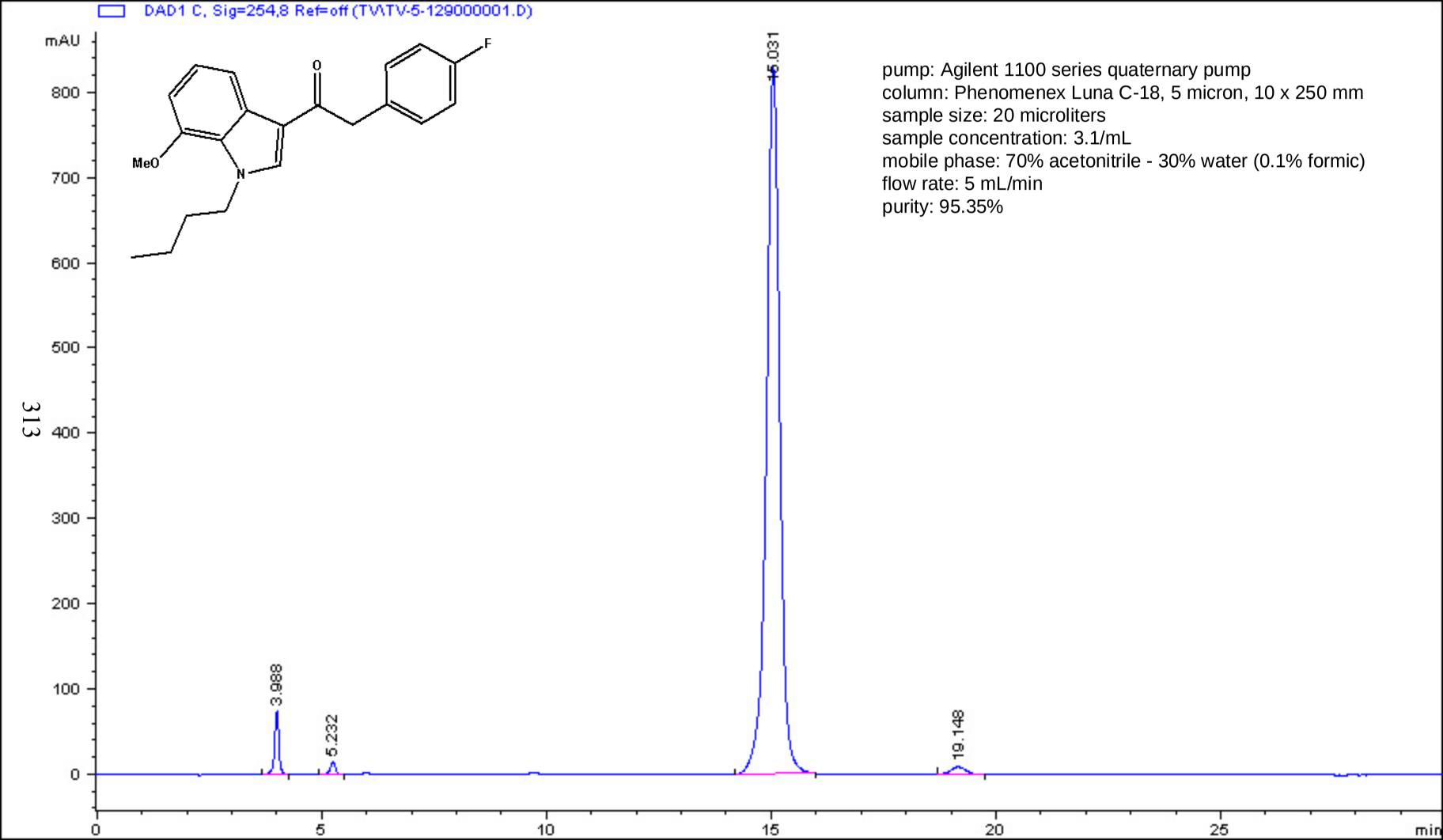
DAD1 C, Sig=254,8 Ref=off (TV\TV-5-129000001.D)
mAU
800
700
600
500
400
300
200
100
0
MeO
N
O
F
3.988
5.232
15.031
19.148
0
5
10
15
20
25
min
pump: Agilent 1100 series quaternary pump
column: Phenomenex Luna C-18, 5 micron, 10 x 250 mm
sample size: 20 microliters
sample concentration: 3.1/mL
mobile phase: 70% acetonitrile - 30% water (0.1% formic)
flow rate: 5 mL/min
purity: 95.35%

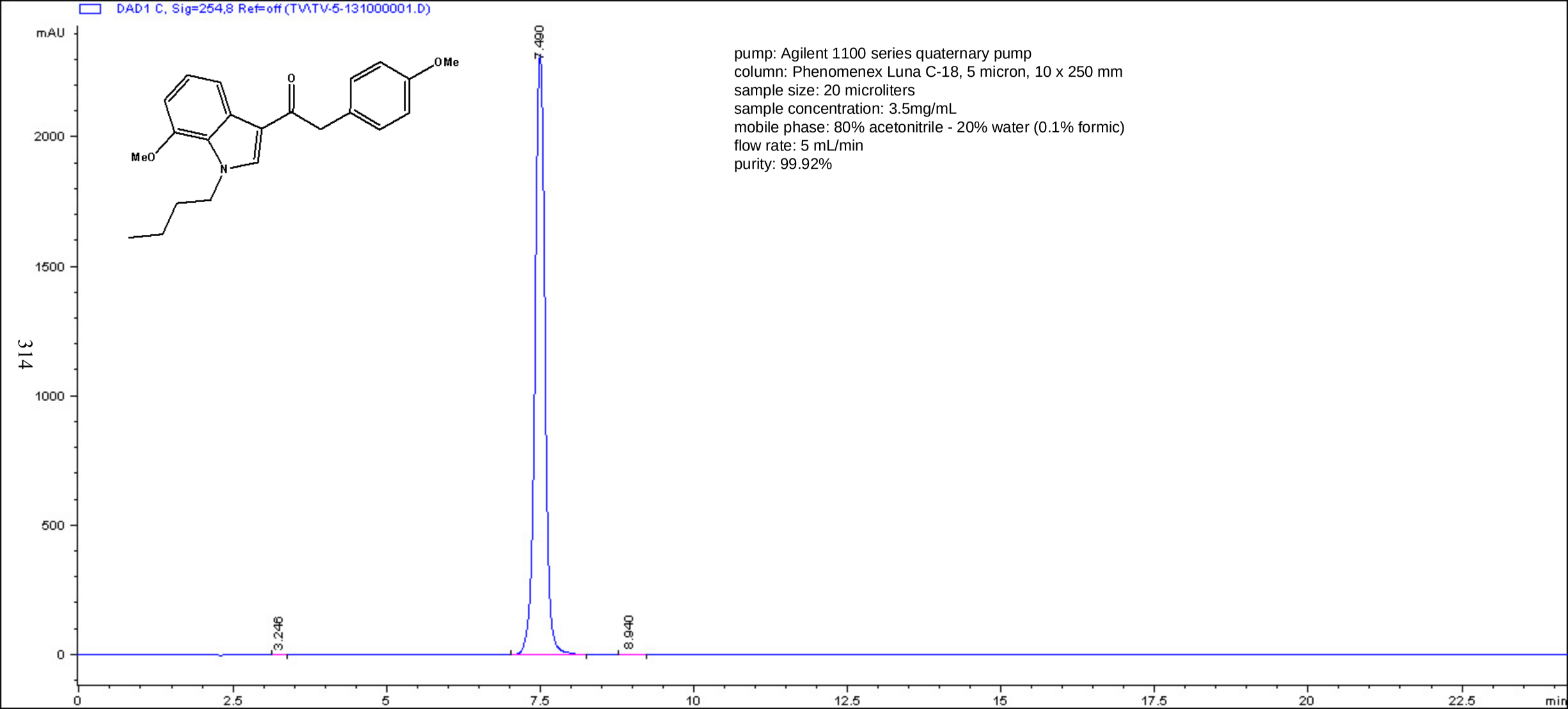
DAD1 C, Sig=254,8 Ref=off (TV\TV-5-131000001.D)
mAU
2000
1500
1000
500
0
7.490
3.246
8.940
0
2.5
5
7.5
10
12.5
15
17.5
20
22.5
min
O
OMe
MeO
N
pump: Agilent 1100 series quaternary pump
column: Phenomenex Luna C-18, 5 micron, 10 x 250 mm
sample size: 20 microliters
sample concentration: 3.5mg/mL
mobile phase: 80% acetonitrile - 20% water (0.1% formic)
flow rate: 5 mL/min
purity: 99.92%

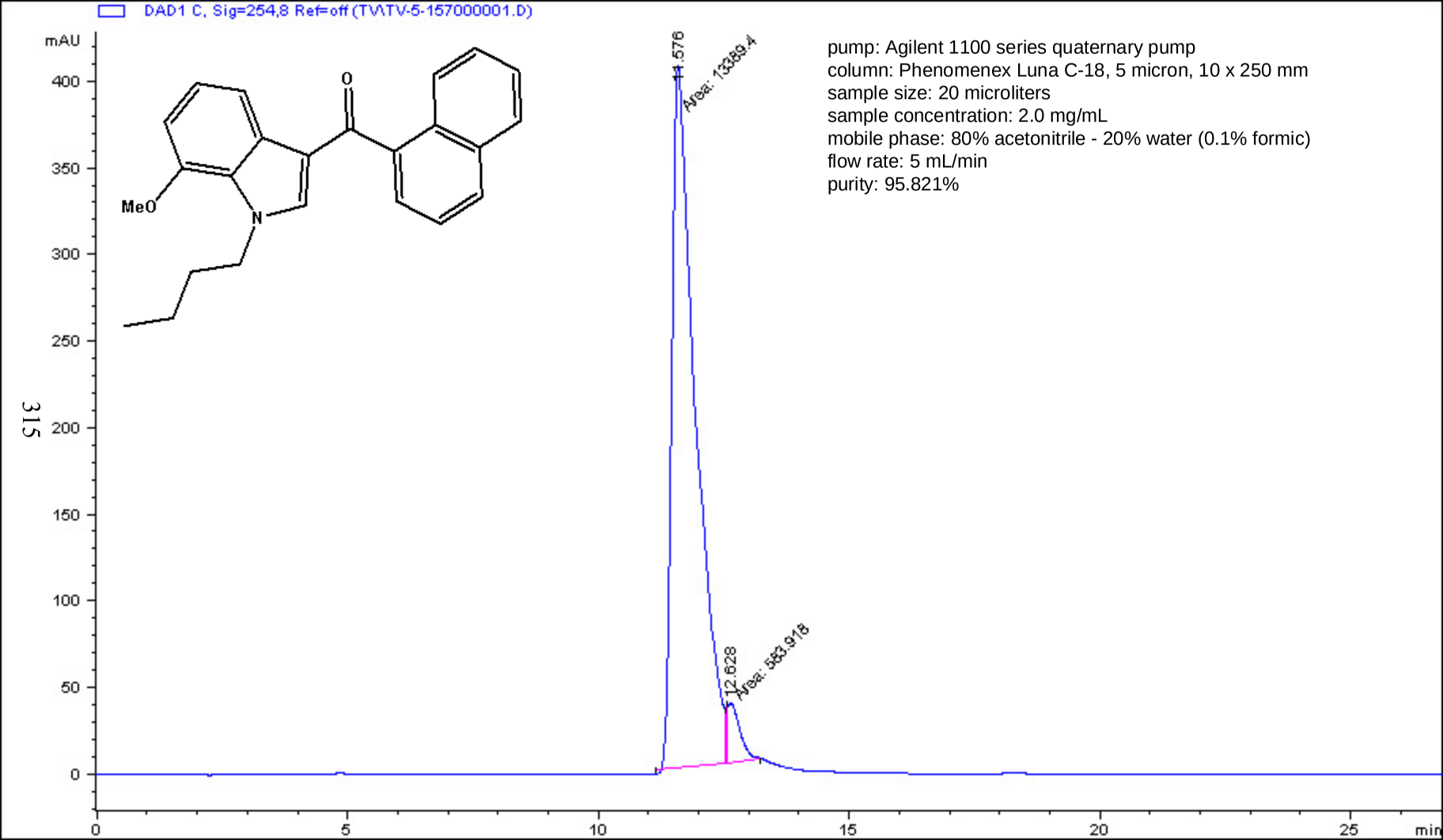
DAD1 C, Sig=254,8 Ref=off (TV\TV-5-157000001.D)
mAU
400
350
300
250
200
150
100
50
0
MeO
N
O
11.576
Area: 13389.4
12.628
Area: 583.918
pump: Agilent 1100 series quaternary pump
column: Phenomenex Luna C-18, 5 micron, 10 x 250 mm
sample size: 20 microliters
sample concentration: 2.0 mg/mL
mobile phase: 80% acetonitrile - 20% water (0.1% formic)
flow rate: 5 mL/min
purity: 95.821%
0
5
10
15
20
25
min

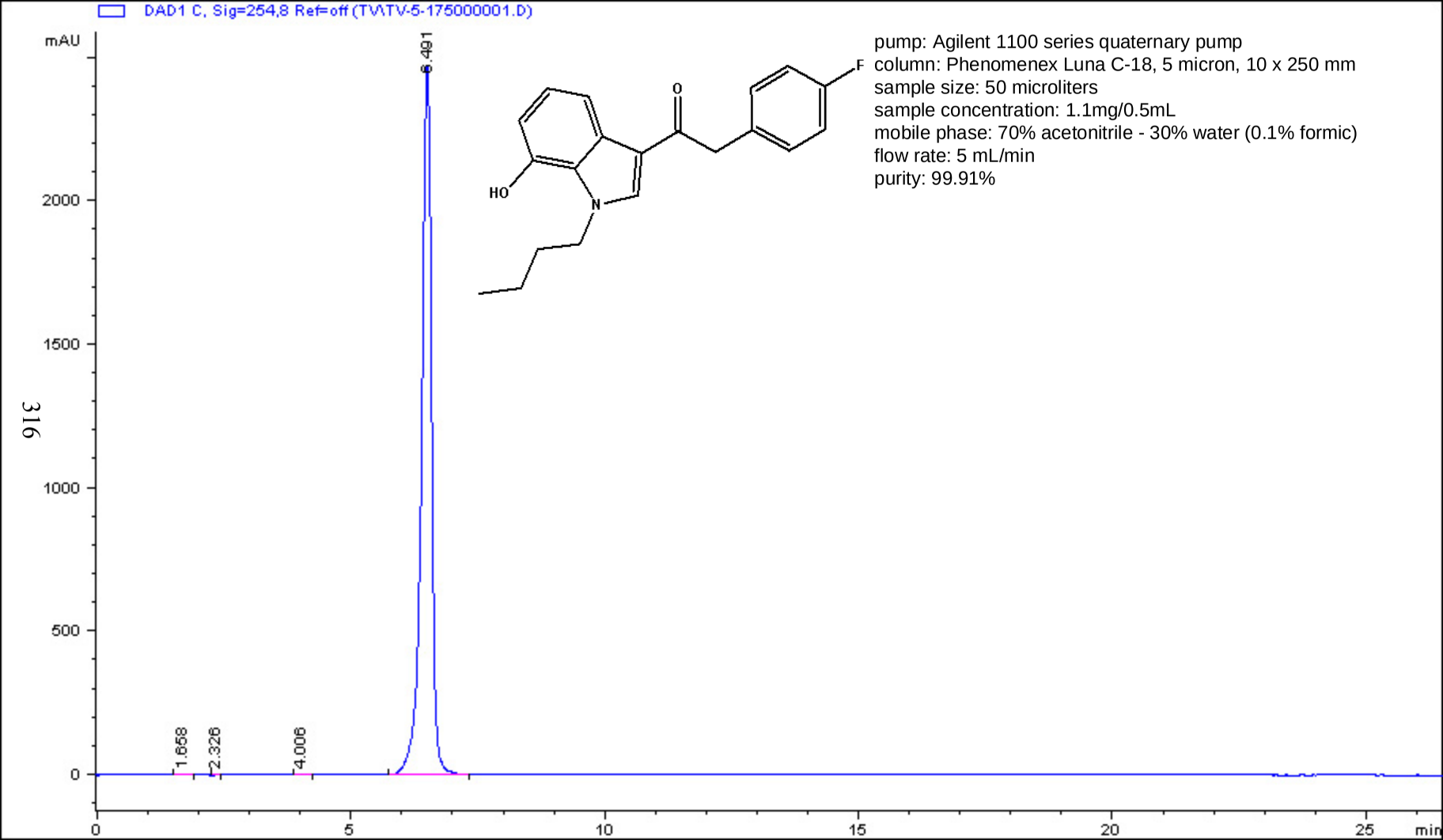
DAD1 C, Sig=254,8 Ref=off (TV\TV-5-175000001.D)
mAU
2000
1500
1000
500
0
6.491
1.658
2.326
4.006
HO
N
O
F
0
5
10
15
20
25
min
pump: Agilent 1100 series quaternary pump
column: Phenomenex Luna C-18, 5 micron, 10 x 250 mm
sample size: 50 microliters
sample concentration: 1.1mg/0.5mL
mobile phase: 70% acetonitrile - 30% water (0.1% formic)
flow rate: 5 mL/min
purity: 99.91%

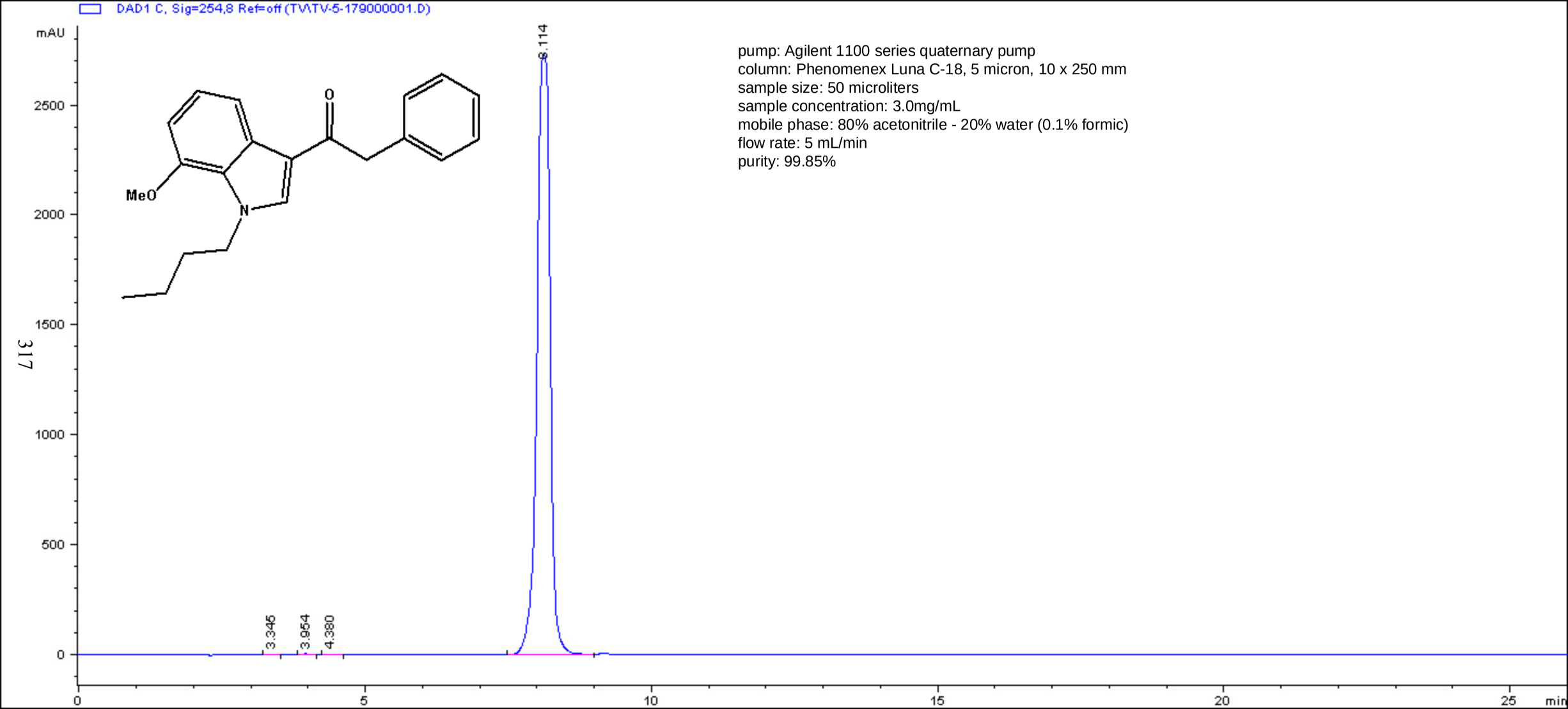
DAD1 C, Sig=254,8 Ref=off (TV\TV-5-179000001.D)
mAU
2500
2000
1500
1000
500
0
8.114
3.345
3.954
4.380
O
MeO
N
0
5
10
15
20
25
min
pump: Agilent 1100 series quaternary pump
column: Phenomenex Luna C-18, 5 micron, 10 x 250 mm
sample size: 50 microliters
sample concentration: 3.0mg/mL
mobile phase: 80% acetonitrile - 20% water (0.1% formic)
flow rate: 5 mL/min
purity: 99.85%

317

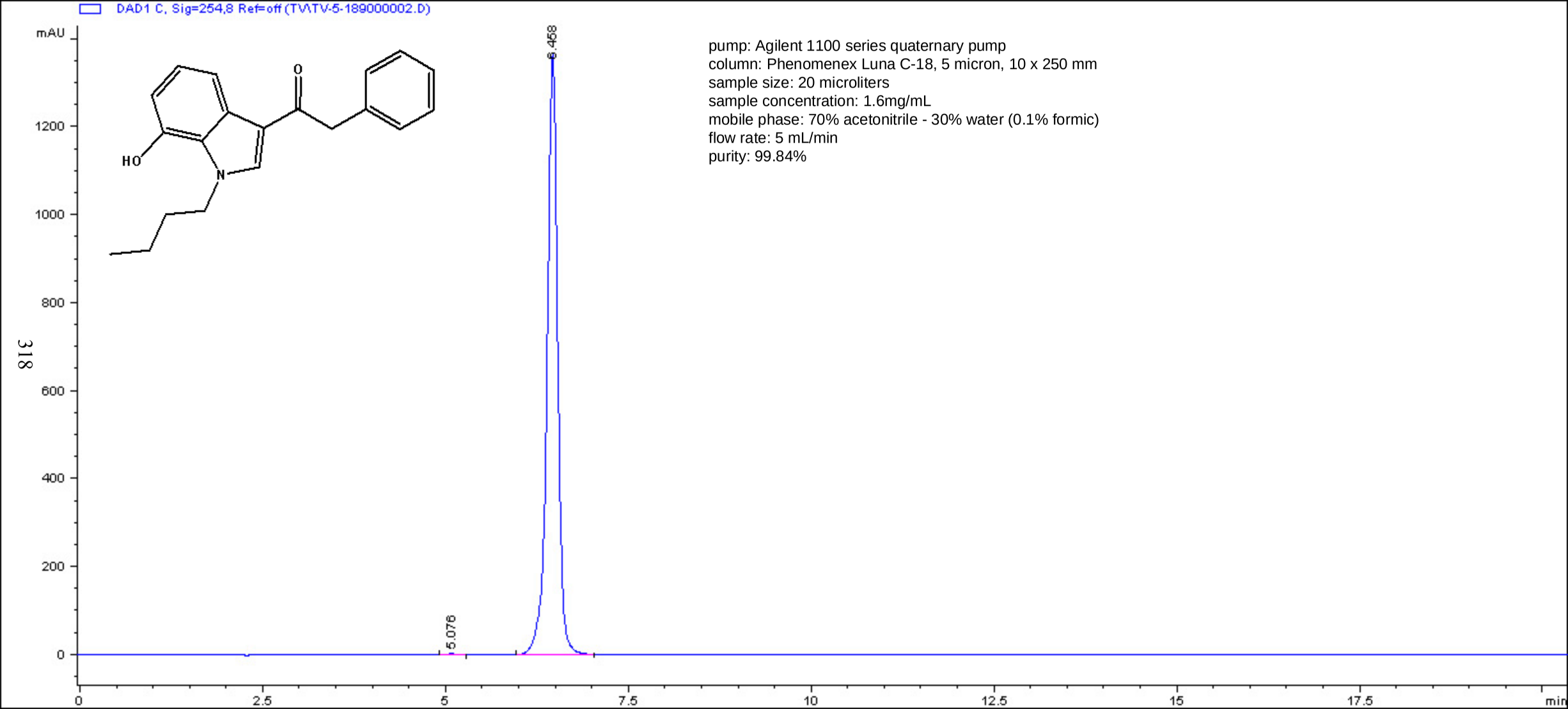
DAD1 C, Sig=254,8 Ref=off (TV\TV-5-189000002.D)
mAU
1200
1000
800
600
400
200
0
HO
O
N
6.458
5.076
0
2.5
5
7.5
10
12.5
15
17.5
min
pump: Agilent 1100 series quaternary pump
column: Phenomenex Luna C-18, 5 micron, 10 x 250 mm
sample size: 20 microliters
sample concentration: 1.6mg/mL
mobile phase: 70% acetonitrile - 30% water (0.1% formic)
flow rate: 5 mL/min
purity: 99.84%

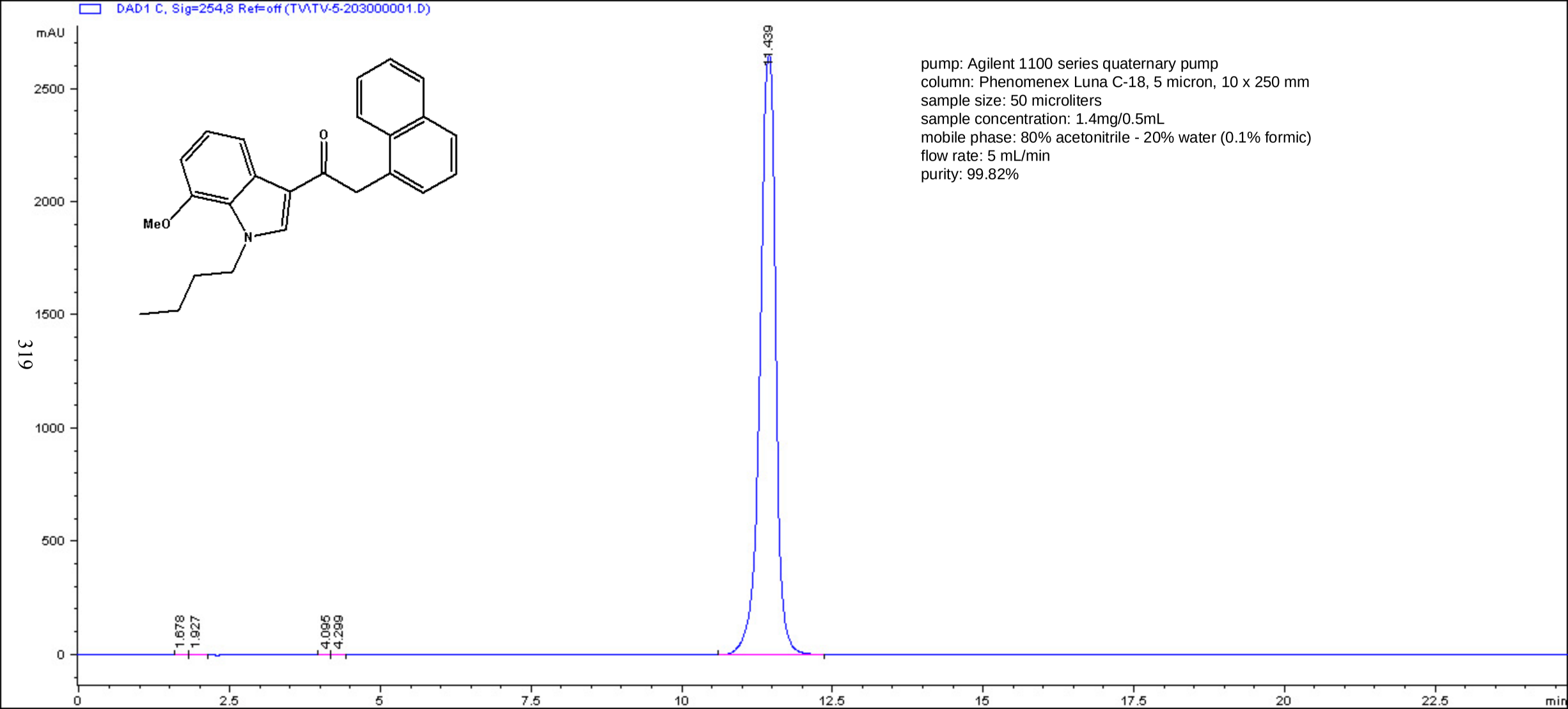
DAD1 C, Sig=254,8 Ref=off (TV\TV-5-203000001.D)
mAU
2500
2000
1500
1000
500
0
MeO
N
O
11.439
1.678
1.927
4.095
4.299
pump: Agilent 1100 series quaternary pump
column: Phenomenex Luna C-18, 5 micron, 10 x 250 mm
sample size: 50 microliters
sample concentration: 1.4mg/0.5mL
mobile phase: 80% acetonitrile - 20% water (0.1% formic)
flow rate: 5 mL/min
purity: 99.82%
0
2.5
5
7.5
10
12.5
15
17.5
20
22.5
min

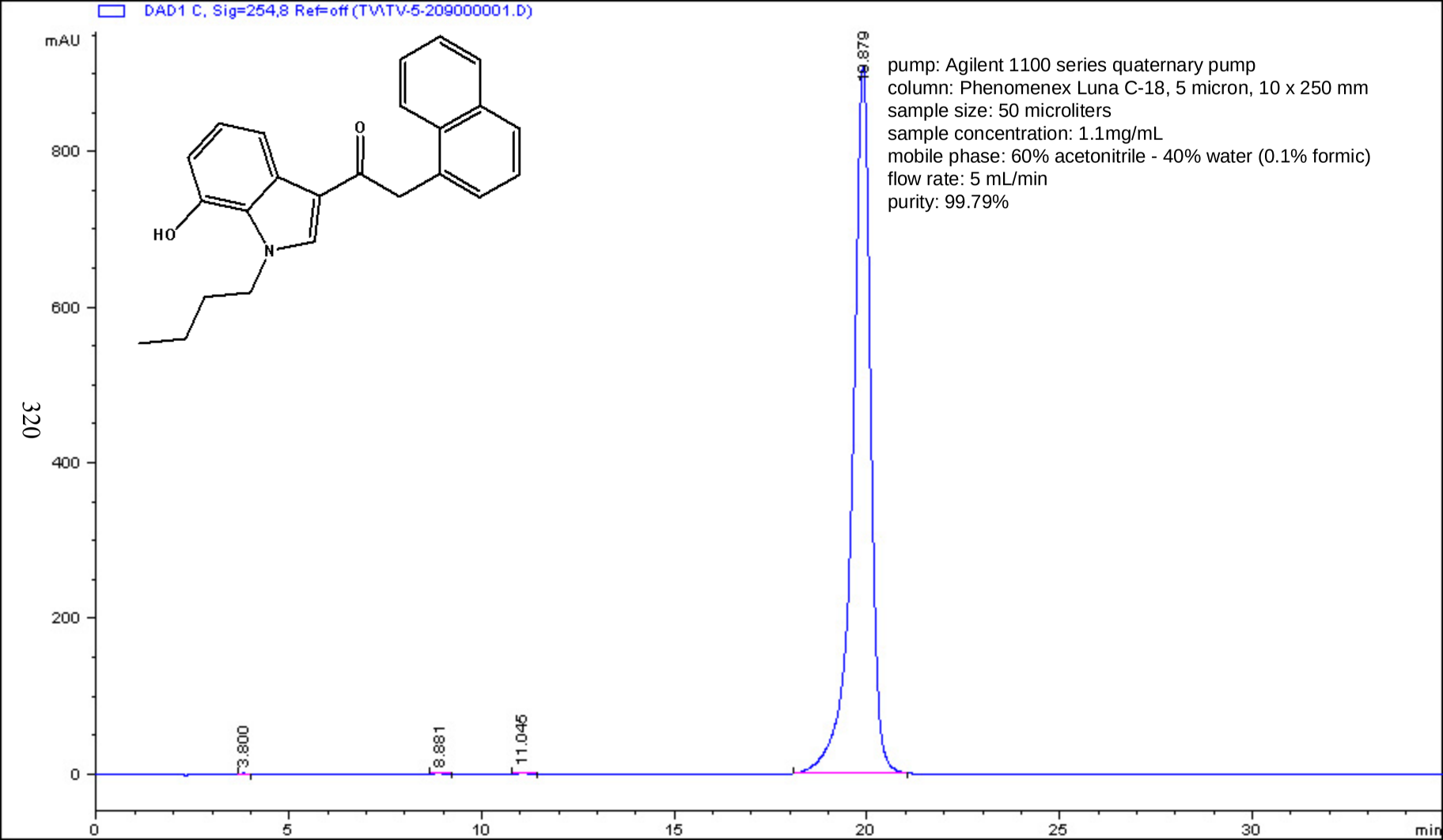
DAD1 C, Sig=254,8 Ref=off (TV\TV-5-209000001.D)
mAU
800
600
400
200
0
HO
O
N
3.800
8.881
11.045
19.879
pump: Agilent 1100 series quaternary pump
column: Phenomenex Luna C-18, 5 micron, 10 x 250 mm
sample size: 50 microliters
sample concentration: 1.1mg/mL
mobile phase: 60% acetonitrile - 40% water (0.1% formic)
flow rate: 5 mL/min
purity: 99.79%
0
5
10
15
20
25
30
min

320

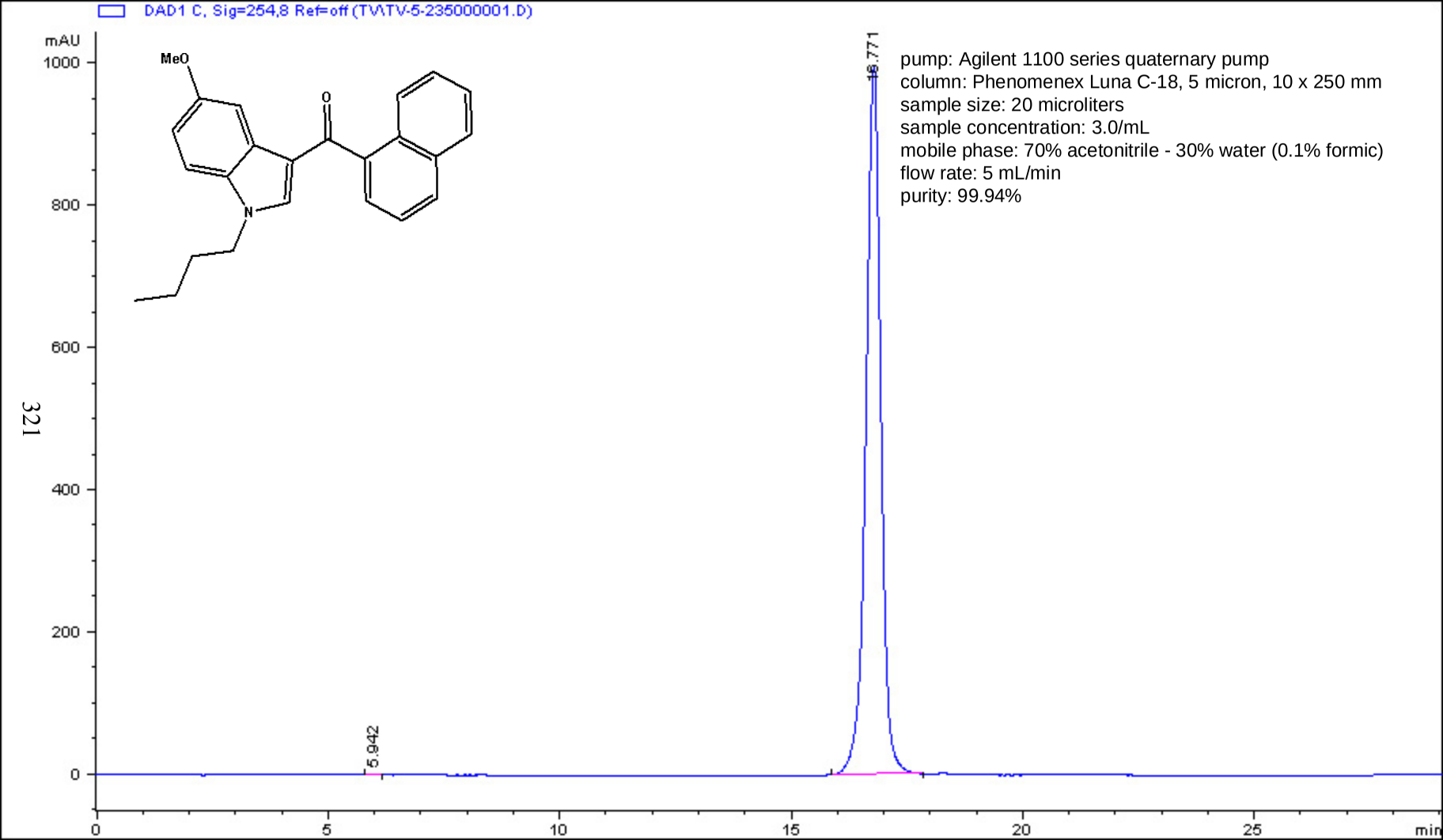
DAD1 C, Sig=254,8 Ref=off (TV\TV-5-235000001.D)
mAU
1000
800
600
400
200
0
MeO
O
N
5.942
16.771
pump: Agilent 1100 series quaternary pump
column: Phenomenex Luna C-18, 5 micron, 10 x 250 mm
sample size: 20 microliters
sample concentration: 3.0/mL
mobile phase: 70% acetonitrile - 30% water (0.1% formic)
flow rate: 5 mL/min
purity: 99.94%
0
5
10
15
20
25
min

321

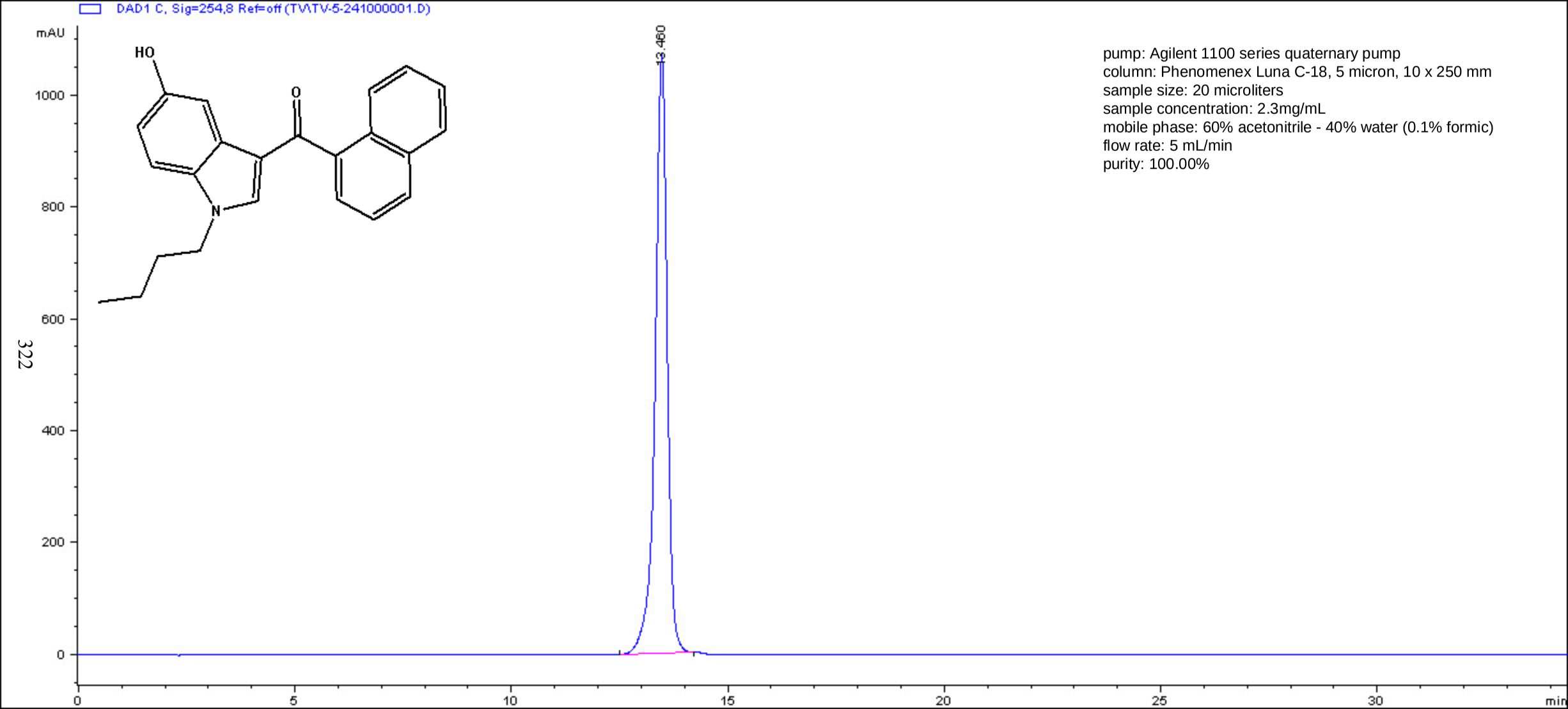
DAD1 C, Sig=254,8 Ref=off (TV\TV-5-241000001.D)
mAU
1000
800
600
400
200
0
HO
O
N
13.460
0
5
10
15
20
25
30
min
pump: Agilent 1100 series quaternary pump
column: Phenomenex Luna C-18, 5 micron, 10 x 250 mm
sample size: 20 microliters
sample concentration: 2.3mg/mL
mobile phase: 60% acetonitrile - 40% water (0.1% formic)
flow rate: 5 mL/min
purity: 100.00%

322

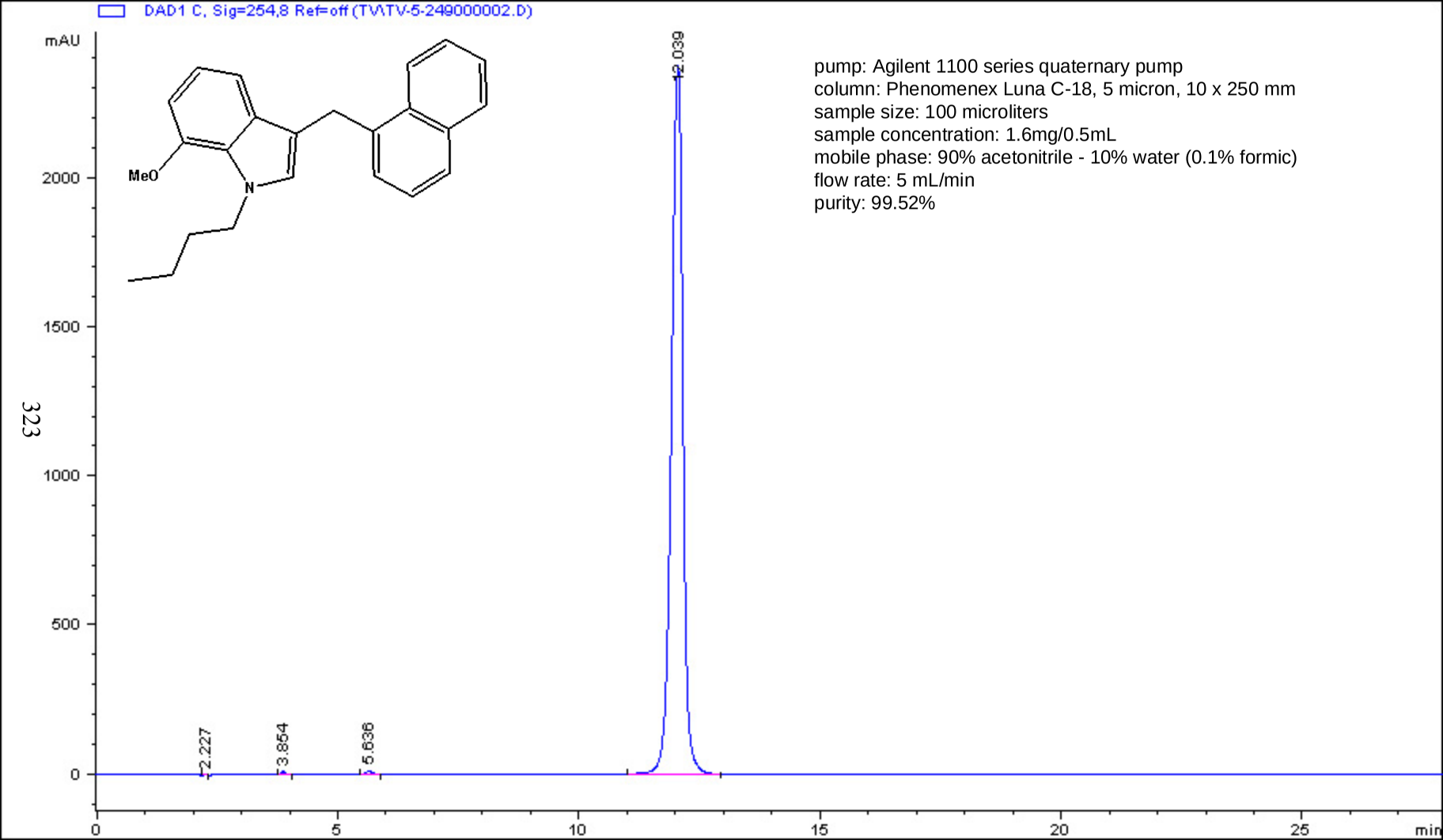
DAD1 C, Sig=254,8 Ref=off (TV\TV-5-249000002.D)
mAU
2000
1500
1000
500
0
MeO
N
12.039
2.227
3.854
5.636
0
5
10
15
20
25
min
pump: Agilent 1100 series quaternary pump
column: Phenomenex Luna C-18, 5 micron, 10 x 250 mm
sample size: 100 microliters
sample concentration: 1.6mg/0.5mL
mobile phase: 90% acetonitrile - 10% water (0.1% formic)
flow rate: 5 mL/min
purity: 99.52%

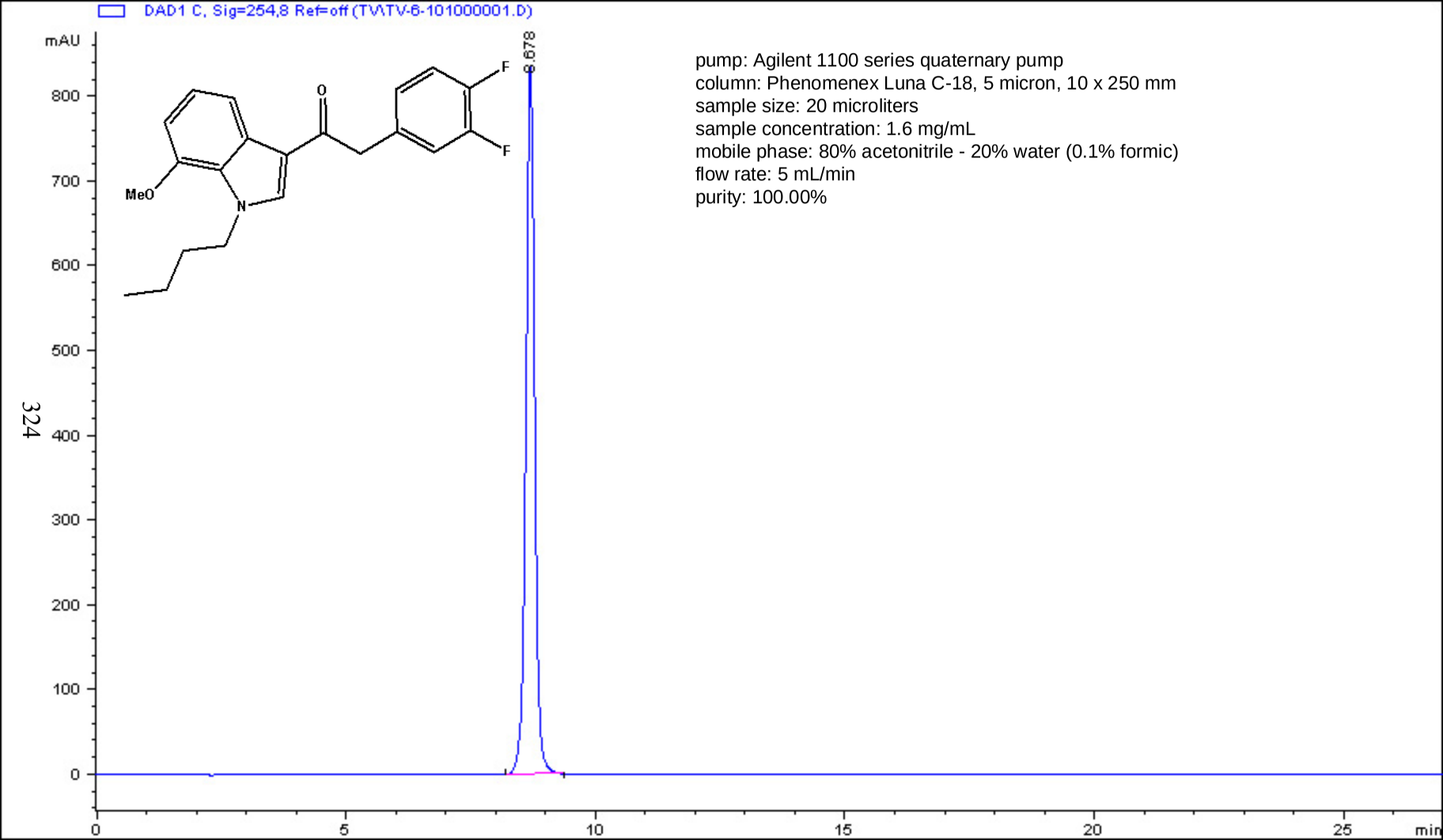

pump: Agilent 1100 series quaternary pump
column: Phenomenex Luna C-18, 5 micron, 10 x 250 mm
sample size: 20 microliters
sample concentration: 1.6 mg/mL
mobile phase: 80% acetonitrile - 20% water (0.1% formic)
flow rate: 5 mL/min
purity: 100.00%

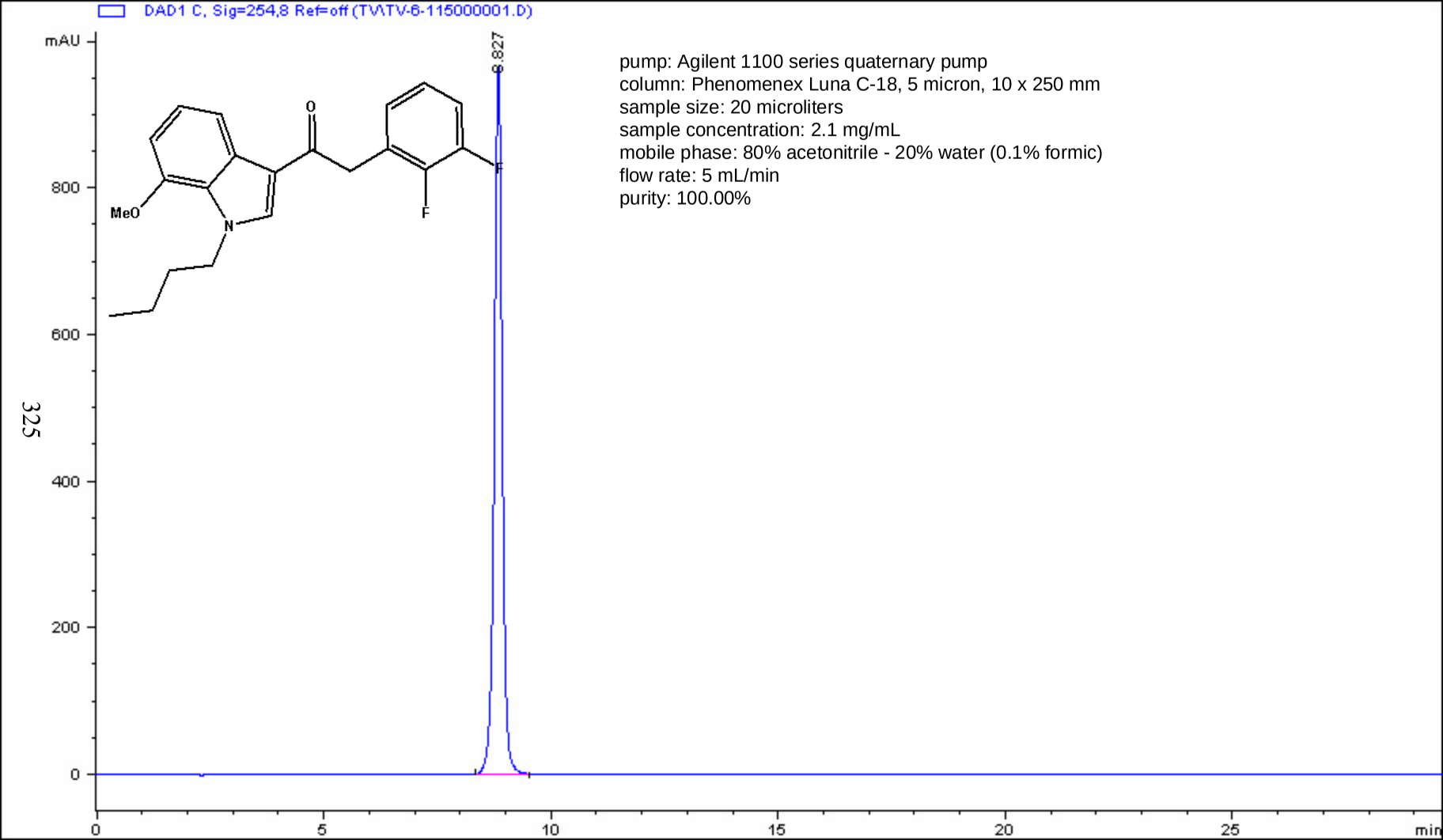

pump: Agilent 1100 series quaternary pump
column: Phenomenex Luna C-18, 5 micron, 10 x 250 mm
sample size: 20 microliters
sample concentration: 2.1 mg/mL
mobile phase: 80% acetonitrile - 20% water (0.1% formic)
flow rate: 5 mL/min
purity: 100.00%

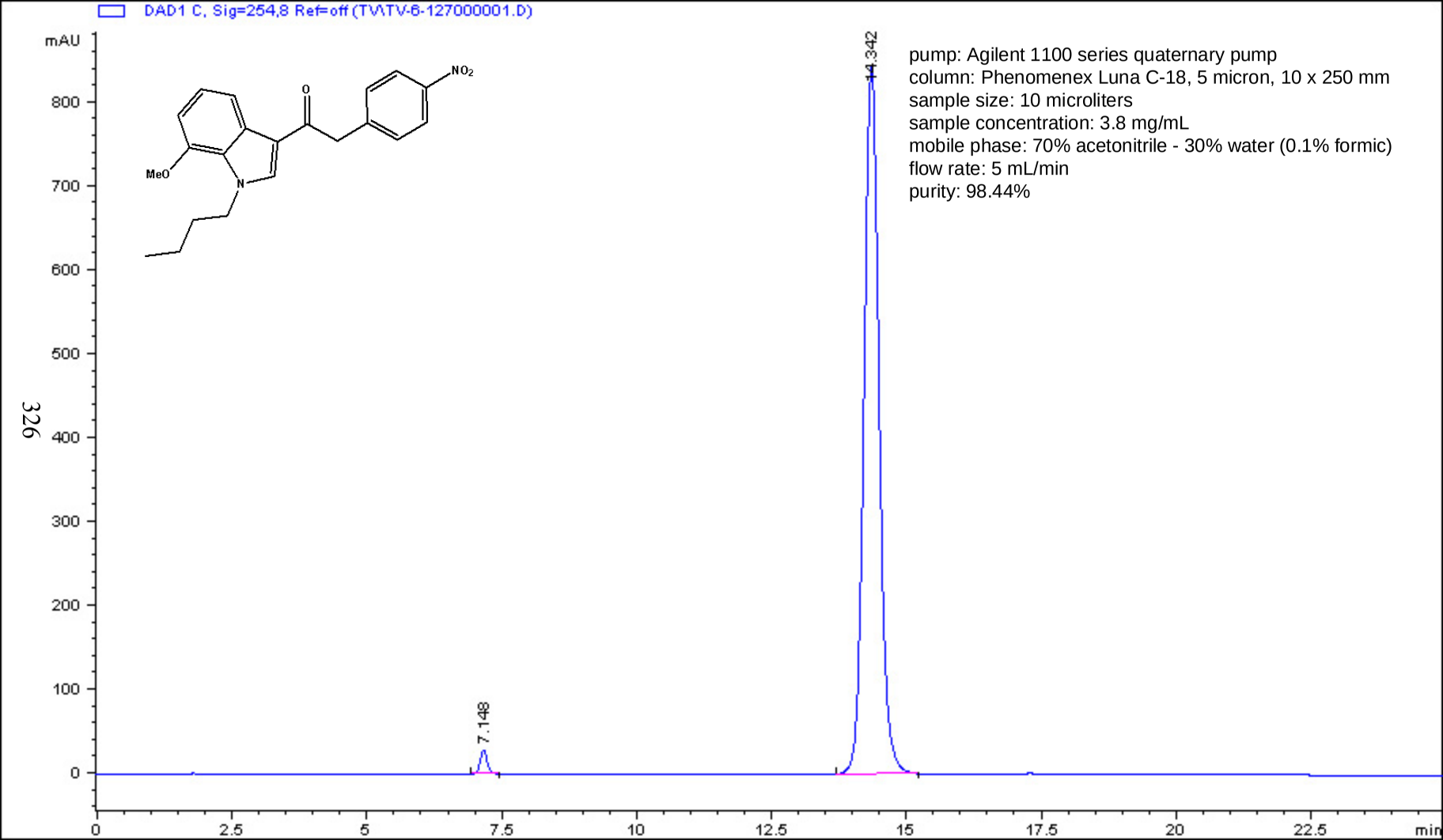
DAD1 C, Sig=254,8 Ref=off (TV\TV-6-127000001.D)
mAU
800
700
600
500
400
300
200
100
0
MeO
N
O
NO2
7.148
14.342
pump: Agilent 1100 series quaternary pump
column: Phenomenex Luna C-18, 5 micron, 10 x 250 mm
sample size: 10 microliters
sample concentration: 3.8 mg/mL
mobile phase: 70% acetonitrile - 30% water (0.1% formic)
flow rate: 5 mL/min
purity: 98.44%
0
2.5
5
7.5
10
12.5
15
17.5
20
22.5
min

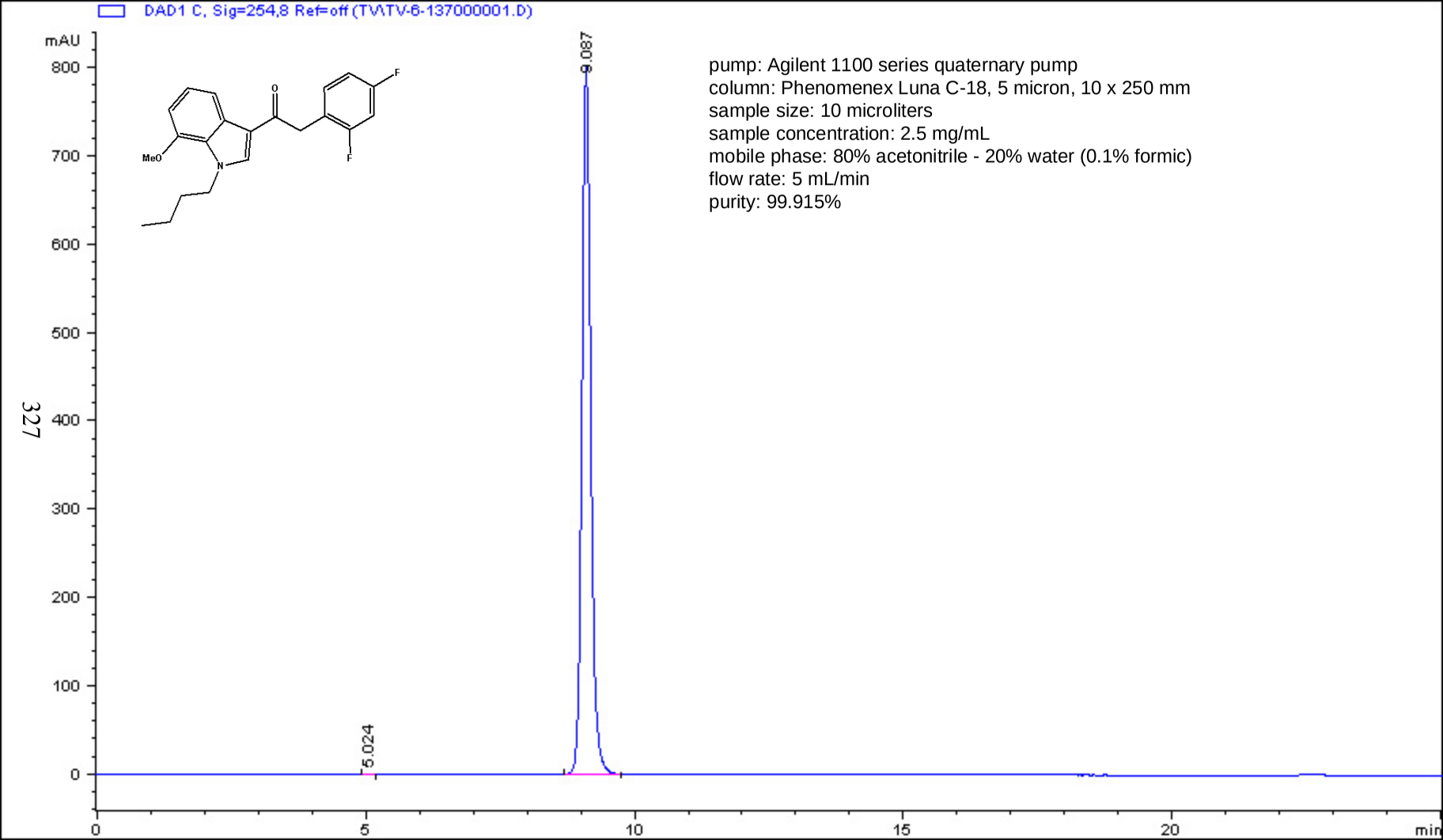
DAD1 C, Sig=254,8 Ref=off (TV\TV-6-137000001.D)
mAU
800
700
600
500
400
300
200
100
0
327
9.087
5.024
MeO
N
O
F
F
pump: Agilent 1100 series quaternary pump
column: Phenomenex Luna C-18, 5 micron, 10 x 250 mm
sample size: 10 microliters
sample concentration: 2.5 mg/mL
mobile phase: 80% acetonitrile - 20% water (0.1% formic)
flow rate: 5 mL/min
purity: 99.915%
0
5
10
15
20
min

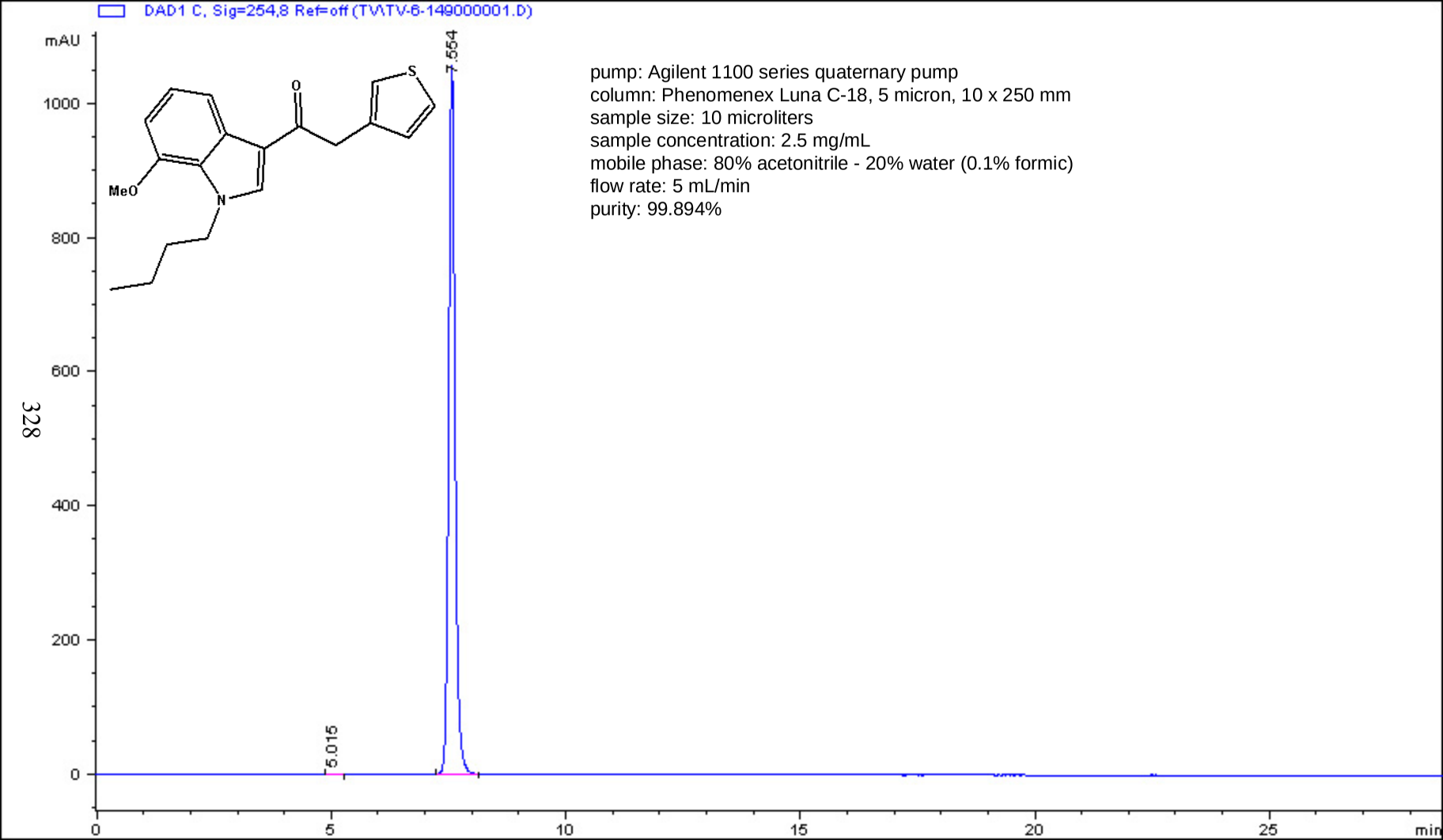

pump: Agilent 1100 series quaternary pump
column: Phenomenex Luna C-18, 5 micron, 10 x 250 mm
sample size: 10 microliters
sample concentration: 2.5 mg/mL
mobile phase: 80% acetonitrile - 20% water (0.1% formic)
flow rate: 5 mL/min
purity: 99.894%

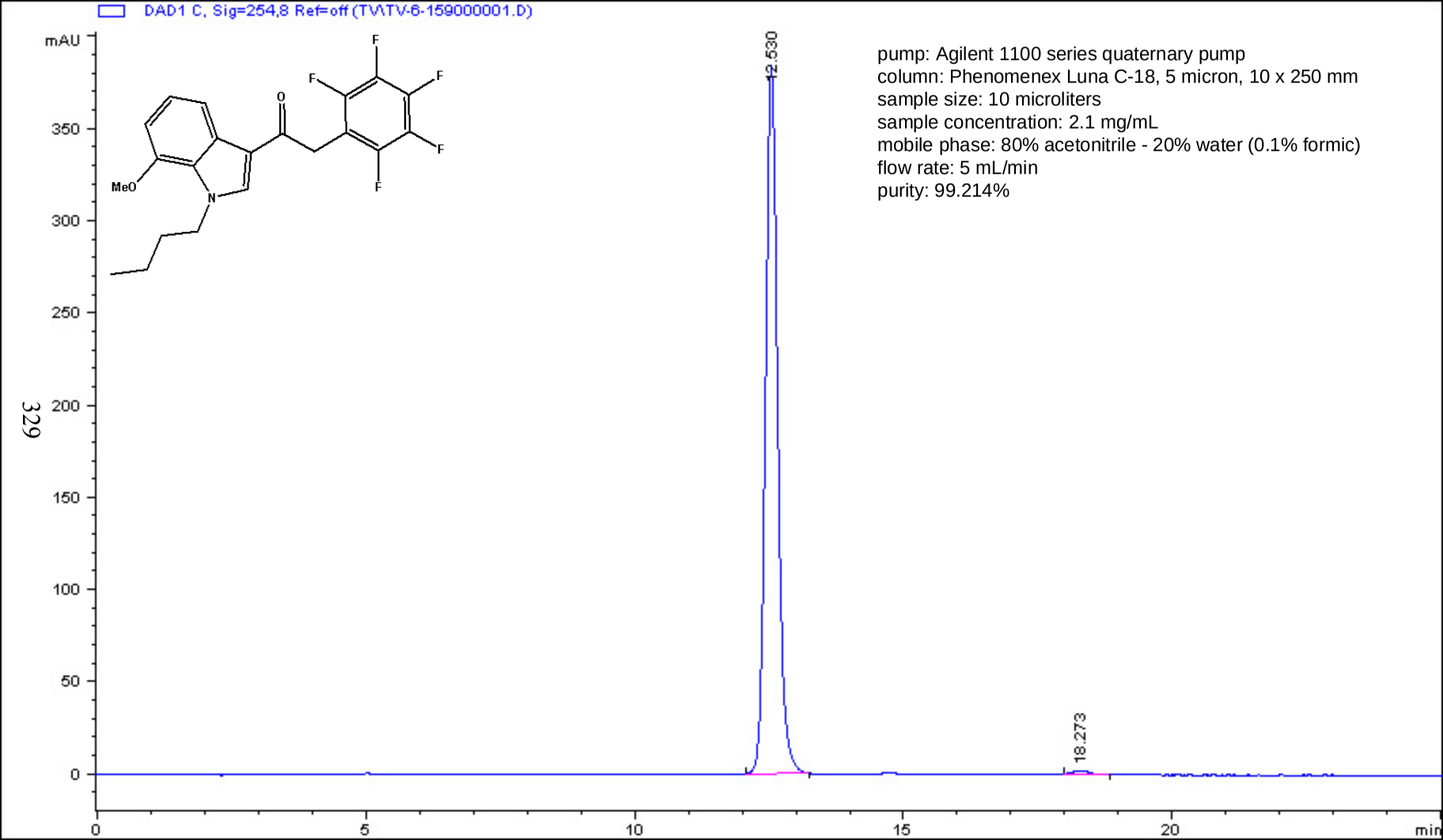
DAD1 C, Sig=254,8 Ref=off (TV\TV-6-159000001.D)
mAU
350
300
250
200
150
100
50
0
0
5
10
15
20
min
12.530
18.273
MeO
N
O
F
F
F
F
F
pump: Agilent 1100 series quaternary pump
column: Phenomenex Luna C-18, 5 micron, 10 x 250 mm
sample size: 10 microliters
sample concentration: 2.1 mg/mL
mobile phase: 80% acetonitrile - 20% water (0.1% formic)
flow rate: 5 mL/min
purity: 99.214%

329

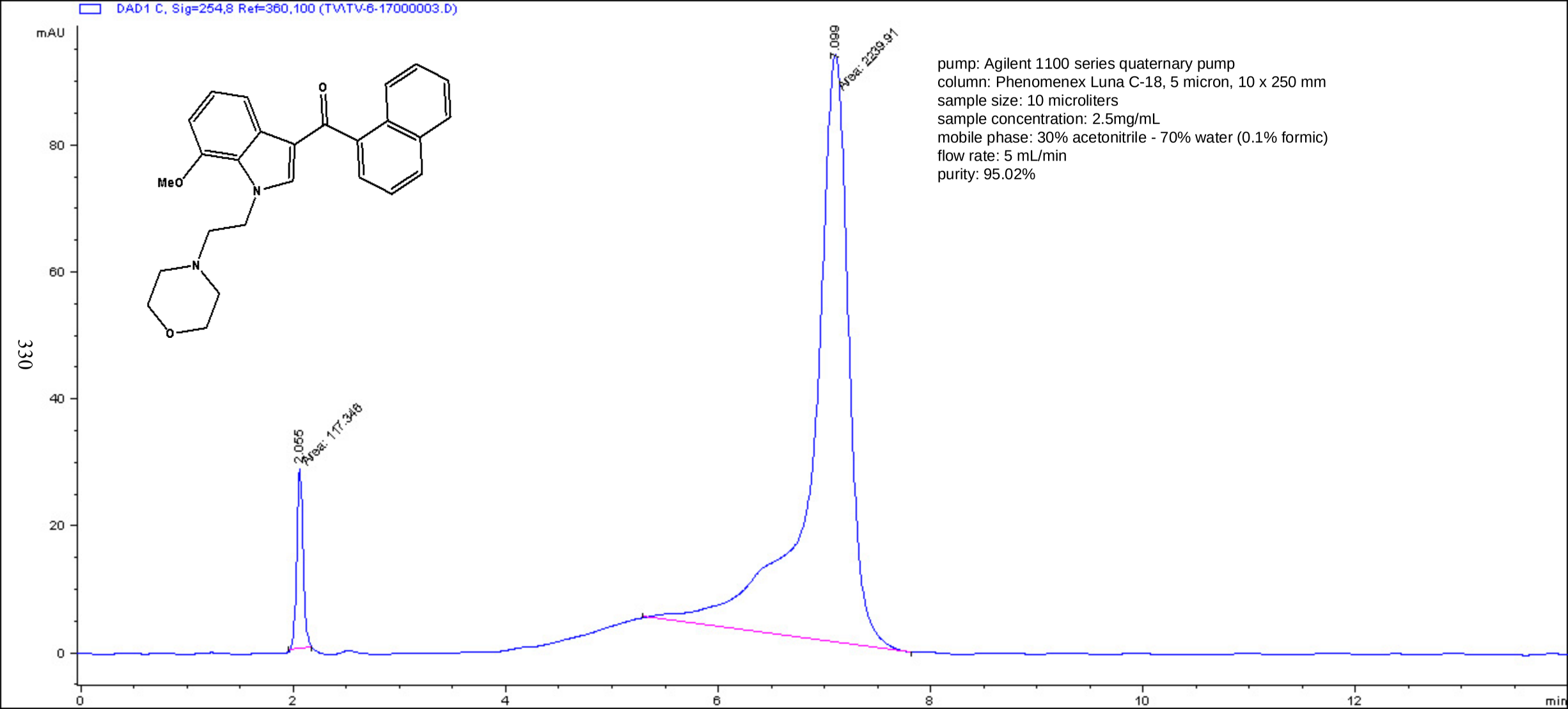
DAD1 C, Sig=254,8 Ref=360,100 (TV\TV-6-17000003.D)
mAU
80
60
40
20
0
MeO
N
O
N
O
2.055
Area: 177.348
7.069
Area: 2239.91
pump: Agilent 1100 series quaternary pump
column: Phenomenex Luna C-18, 5 micron, 10 x 250 mm
sample size: 10 microliters
sample concentration: 2.5mg/mL
mobile phase: 30% acetonitrile - 70% water (0.1% formic)
flow rate: 5 mL/min
purity: 95.02%
0
2
4
6
8
10
12
min

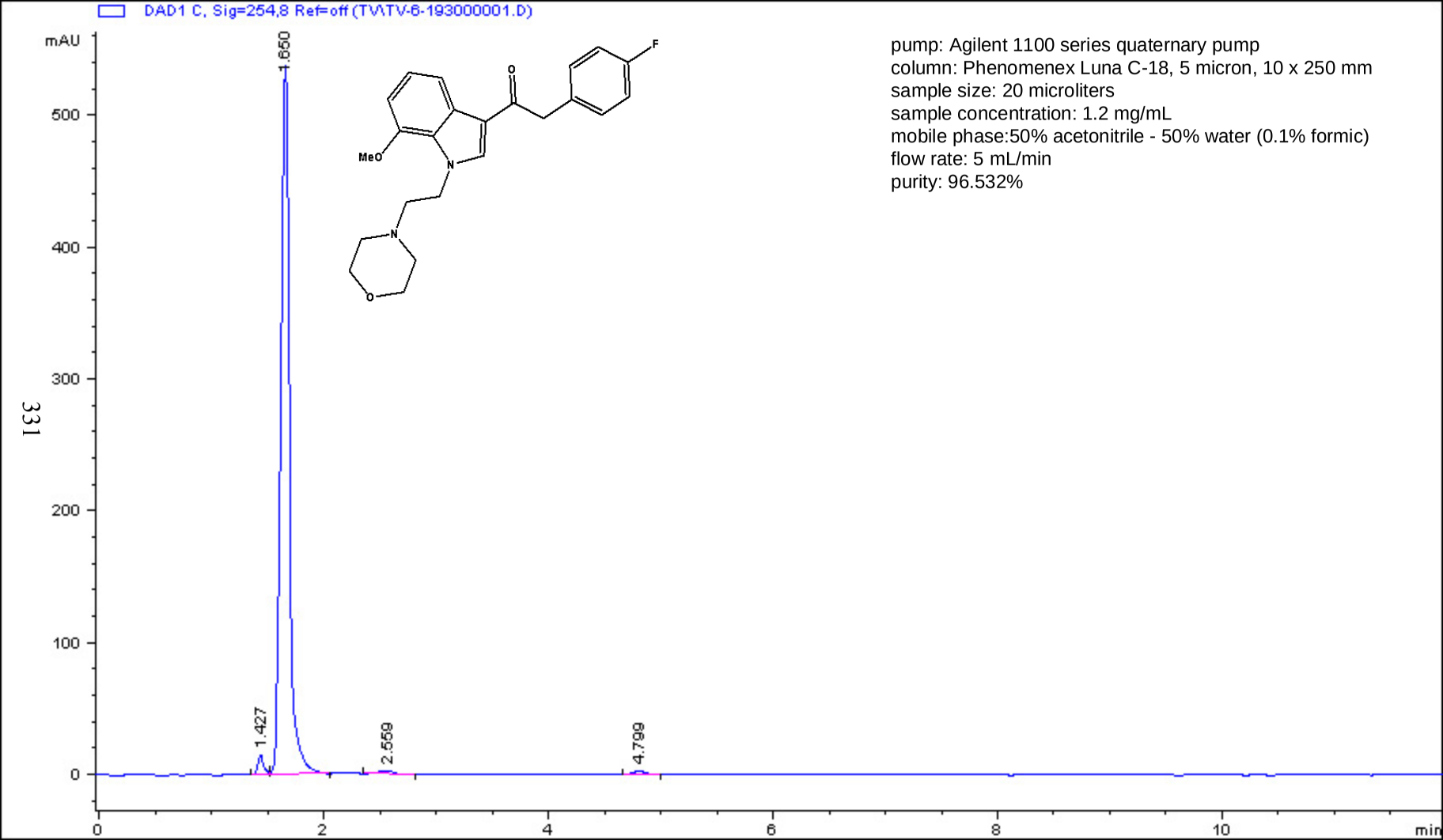

pump: Agilent 1100 series quaternary pump
column: Phenomenex Luna C-18, 5 micron, 10 x 250 mm
sample size: 20 microliters
sample concentration: 1.2 mg/mL
mobile phase:50% acetonitrile - 50% water (0.1% formic)
flow rate: 5 mL/min
purity: 96.532%

331

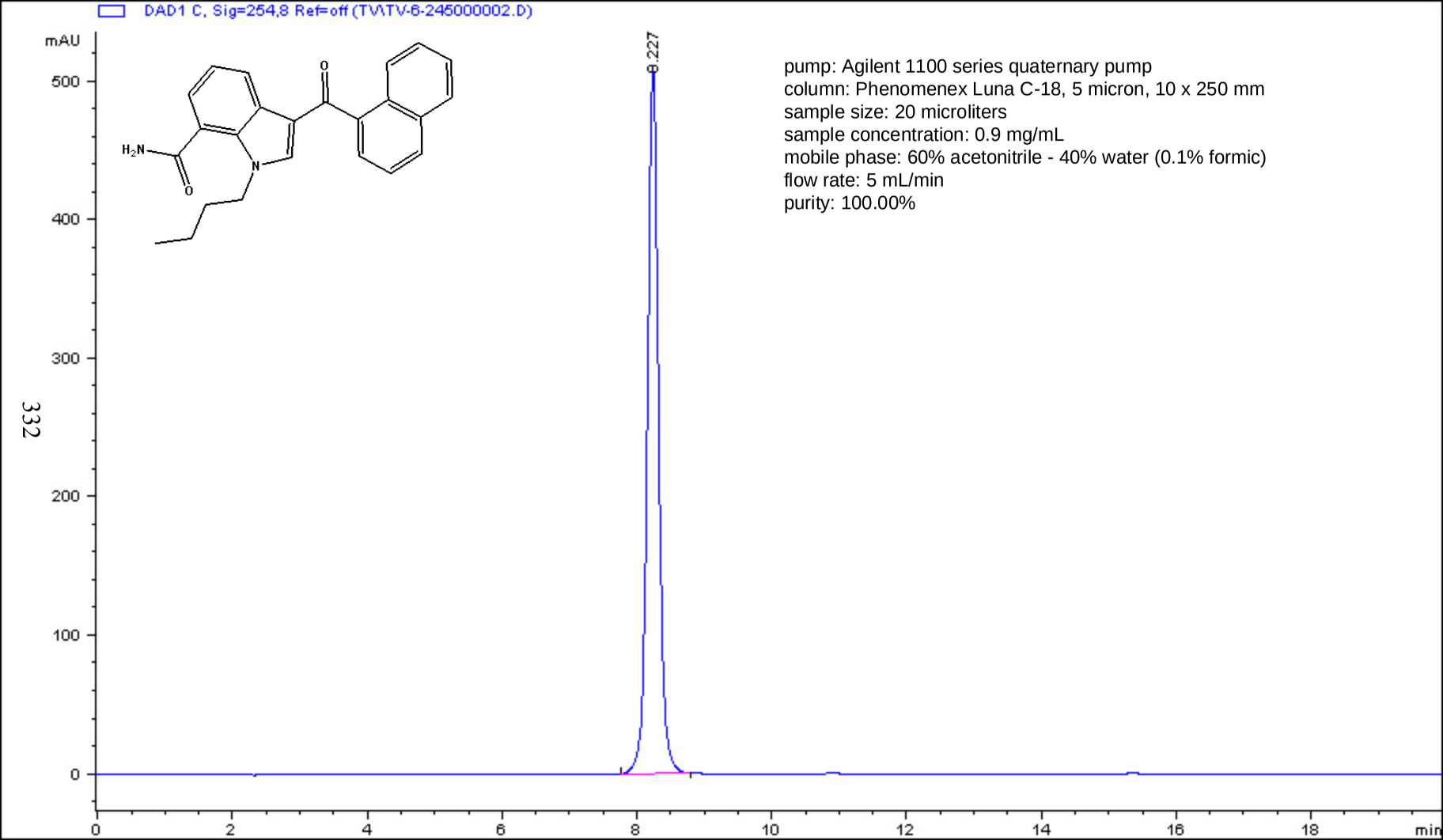
DAD1 C, Sig=254,8 Ref=off (TV\TV-6-245000002.D)
mAU
500
400
300
200
100
0
8.227
pump: Agilent 1100 series quaternary pump
column: Phenomenex Luna C-18, 5 micron, 10 x 250 mm
sample size: 20 microliters
sample concentration: 0.9 mg/mL
mobile phase: 60% acetonitrile - 40% water (0.1% formic)
flow rate: 5 mL/min
purity: 100.00%
0
2
4
6
8
10
12
14
16
18
min

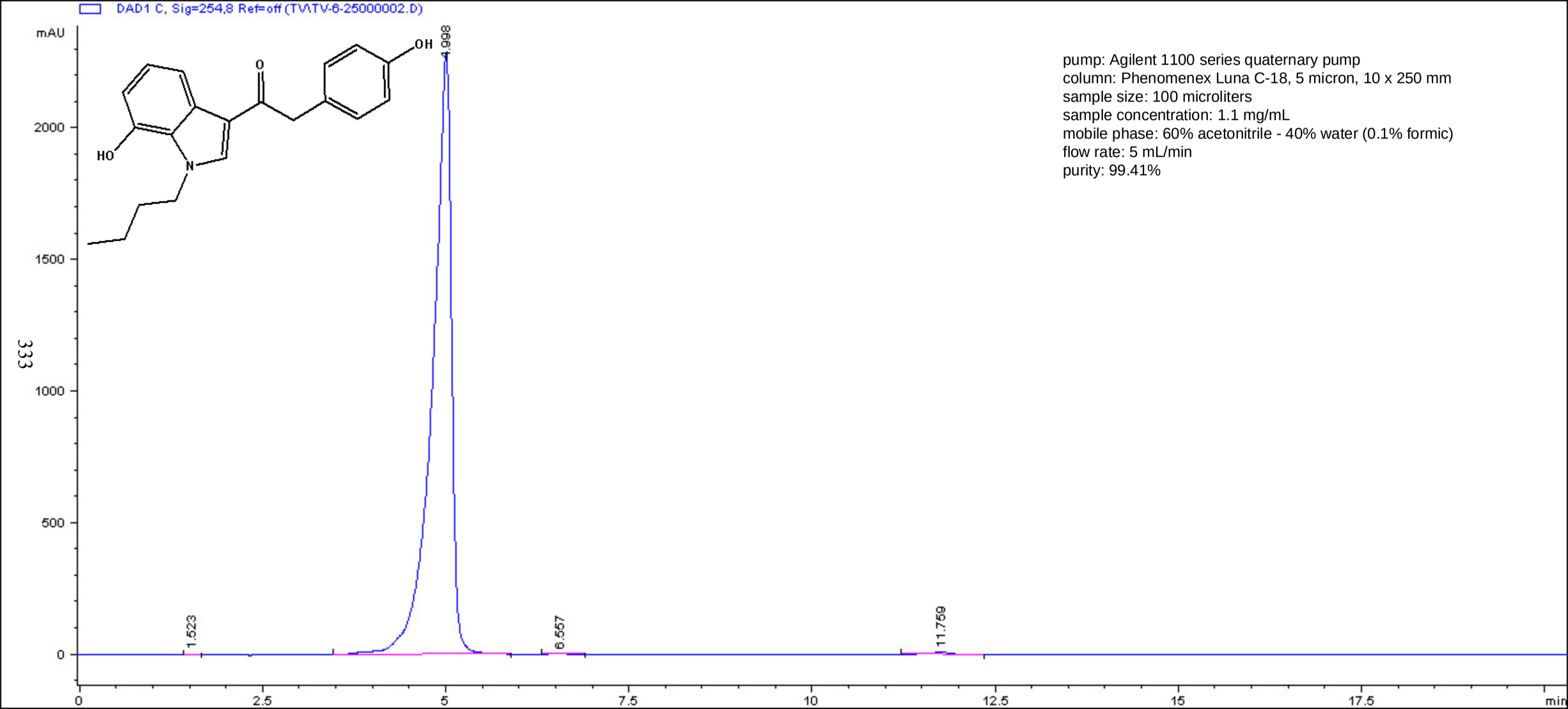
DAD1 C, Sig=254,8 Ref=off (TV\TV-6-25000002.D)
mAU
2000
1500
1000
500
0
4.998
1.523
6.557
11.759
OH
O
HO
N
0
2.5
5
7.5
10
12.5
15
17.5
min
pump: Agilent 1100 series quaternary pump
column: Phenomenex Luna C-18, 5 micron, 10 x 250 mm
sample size: 100 microliters
sample concentration: 1.1 mg/mL
mobile phase: 60% acetonitrile - 40% water (0.1% formic)
flow rate: 5 mL/min
purity: 99.41%

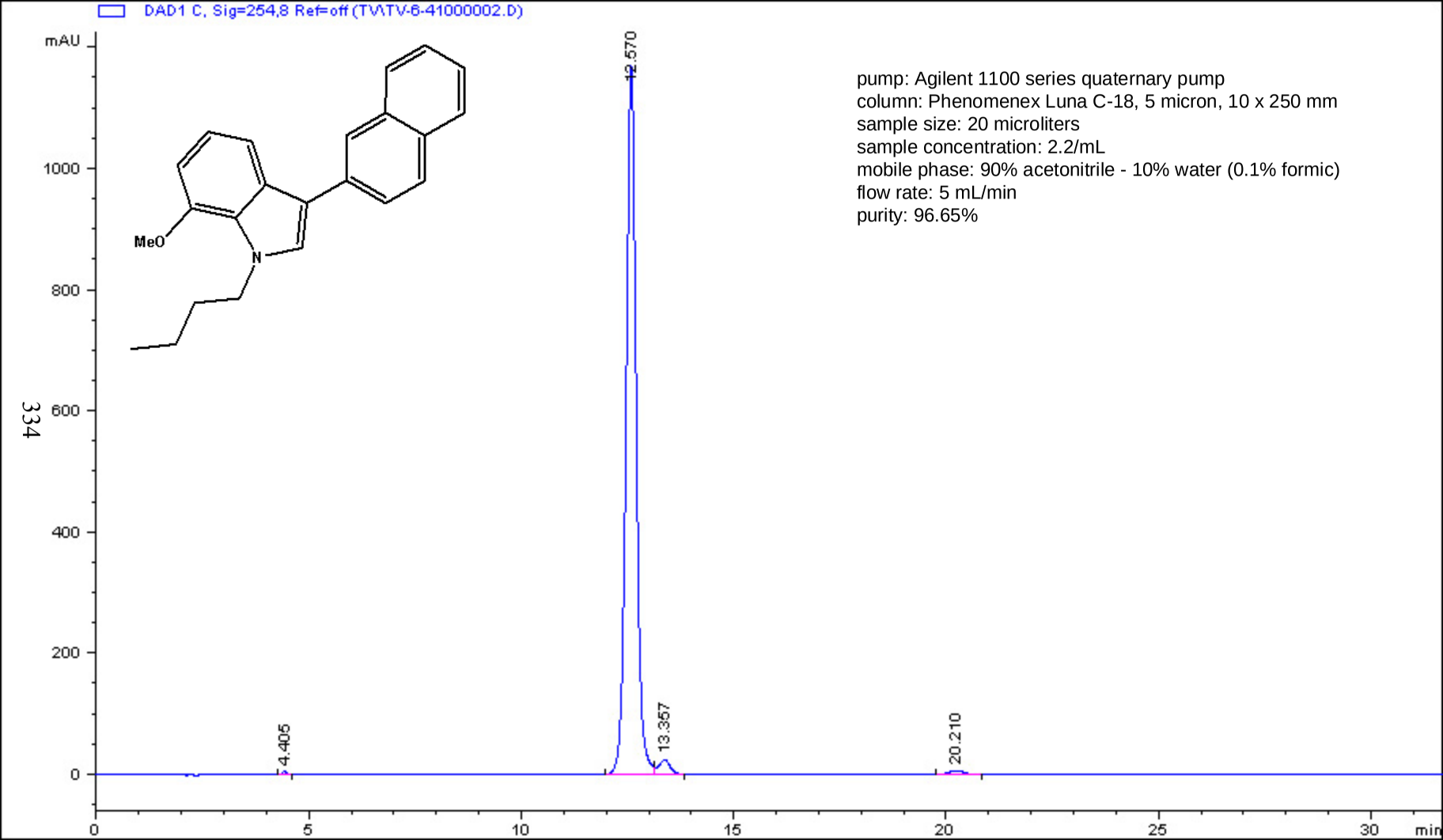
DAD1 C, Sig=254,8 Ref=off (TV\TV-6-41000002.D)
mAU
1000
800
600
400
200
0
MeO
N
12.570
4.405
13.357
20.210
0
5
10
15
20
25
30
min
pump: Agilent 1100 series quaternary pump
column: Phenomenex Luna C-18, 5 micron, 10 x 250 mm
sample size: 20 microliters
sample concentration: 2.2/mL
mobile phase: 90% acetonitrile - 10% water (0.1% formic)
flow rate: 5 mL/min
purity: 96.65%

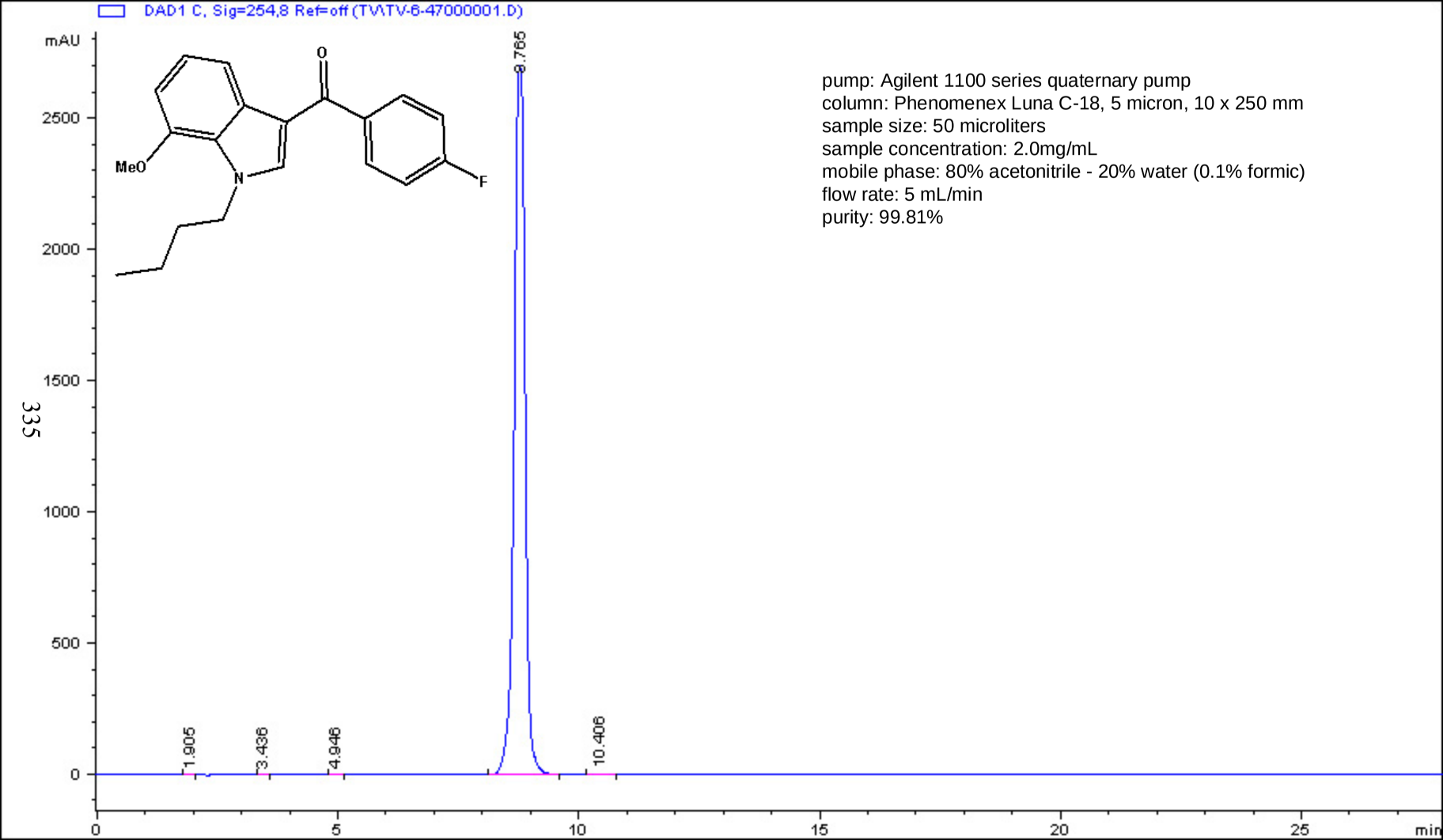

335

pump: Agilent 1100 series quaternary pump
column: Phenomenex Luna C-18, 5 micron, 10 x 250 mm
sample size: 50 microliters
sample concentration: 2.0mg/mL
mobile phase: 80% acetonitrile - 20% water (0.1% formic)
flow rate: 5 mL/min
purity: 99.81%

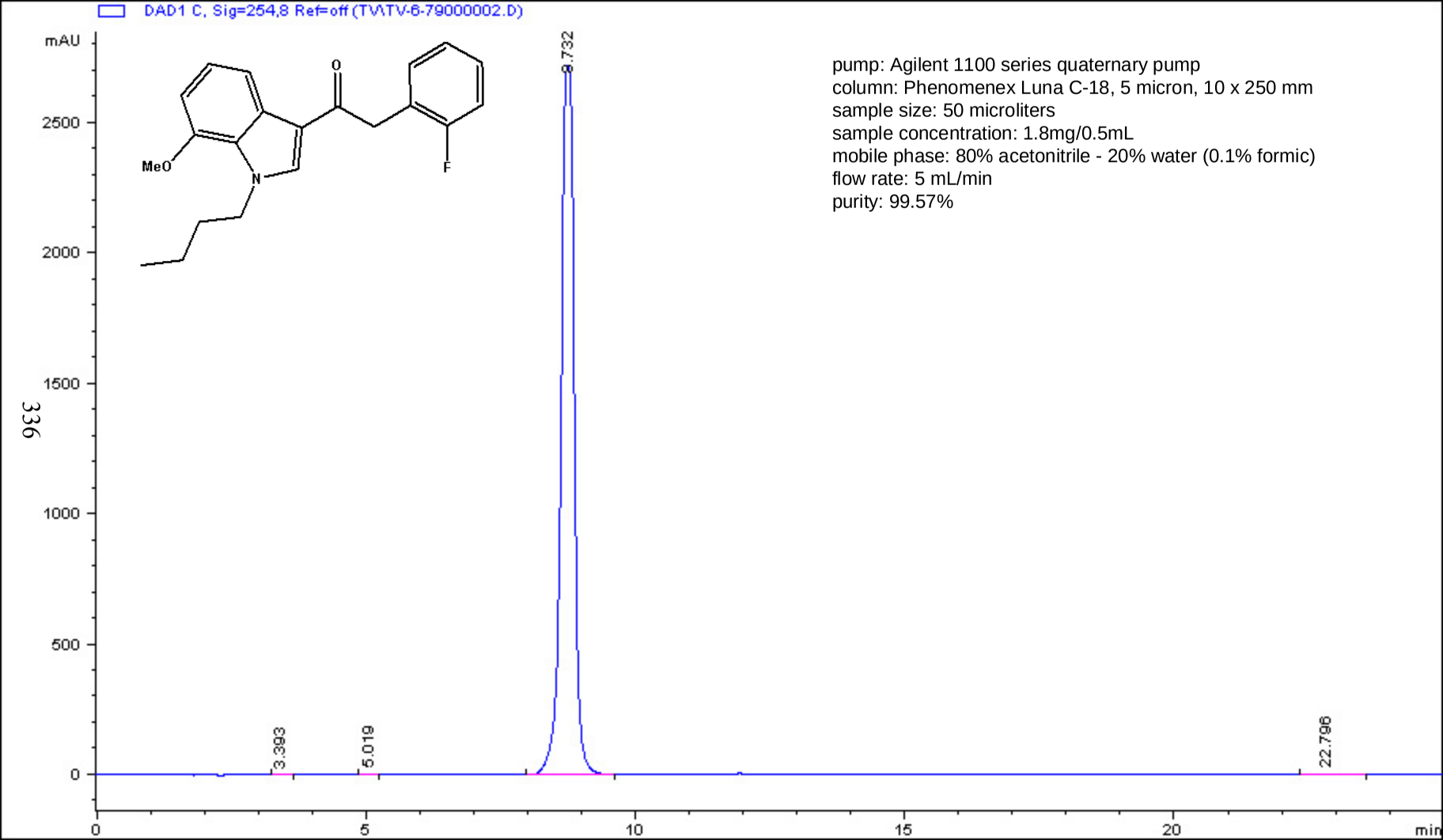
DAD1 C, Sig=254,8 Ref=off (TV\TV-6-79000002.D)
mAU
2500
2000
1500
1000
500
0
MeO
N
O
F
8.732
3.393
5.019
22.796
0
5
10
15
20
min
pump: Agilent 1100 series quaternary pump
column: Phenomenex Luna C-18, 5 micron, 10 x 250 mm
sample size: 50 microliters
sample concentration: 1.8mg/0.5mL
mobile phase: 80% acetonitrile - 20% water (0.1% formic)
flow rate: 5 mL/min
purity: 99.57%

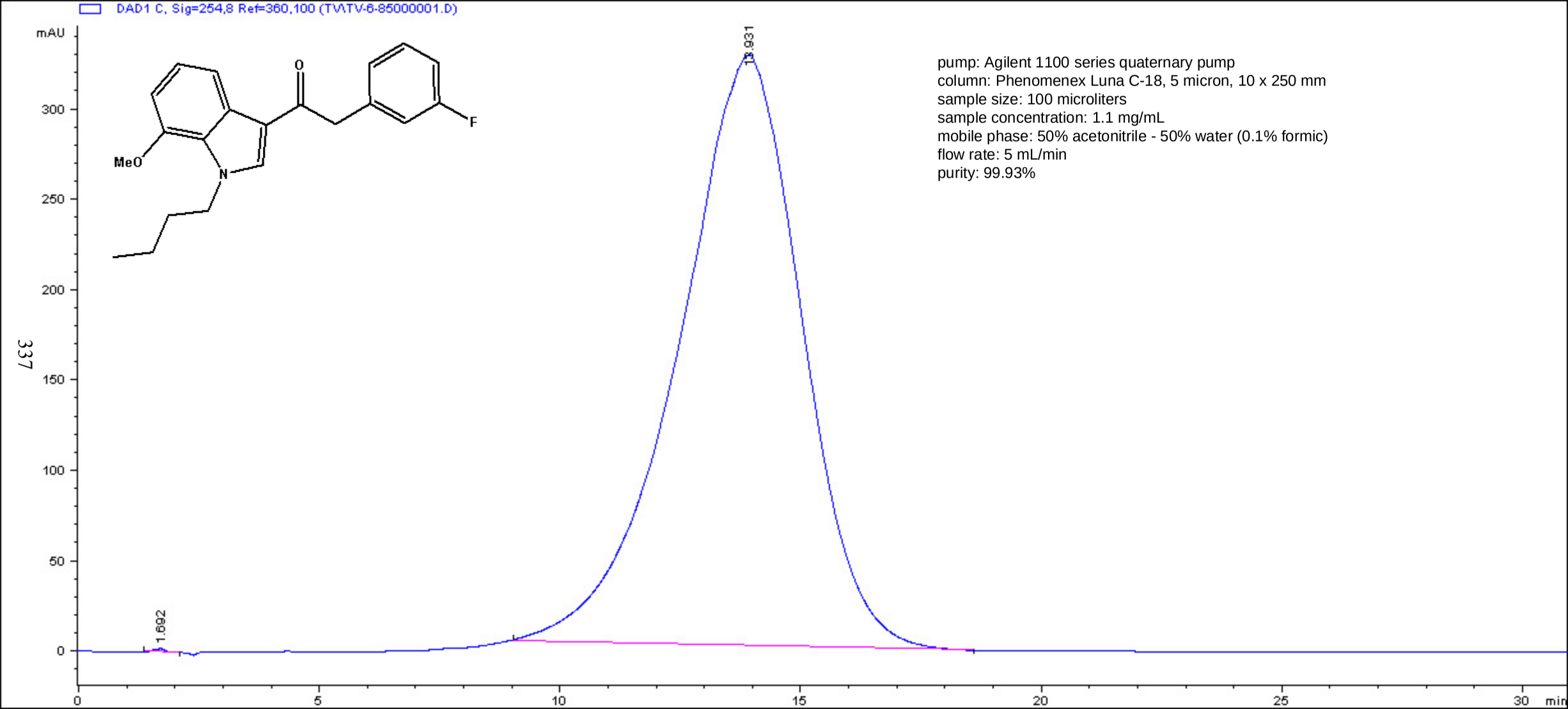
DAD1 C, Sig=254,8 Ref=360,100 (TV\TV-6-85000001.D)
mAU
300
250
200
150
100
50
0
MeO
O
N
F
1.692
13.931
pump: Agilent 1100 series quaternary pump
column: Phenomenex Luna C-18, 5 micron, 10 x 250 mm
sample size: 100 microliters
sample concentration: 1.1 mg/mL
mobile phase: 50% acetonitrile - 50% water (0.1% formic)
flow rate: 5 mL/min
purity: 99.93%
0
5
10
15
20
25
30
min

337

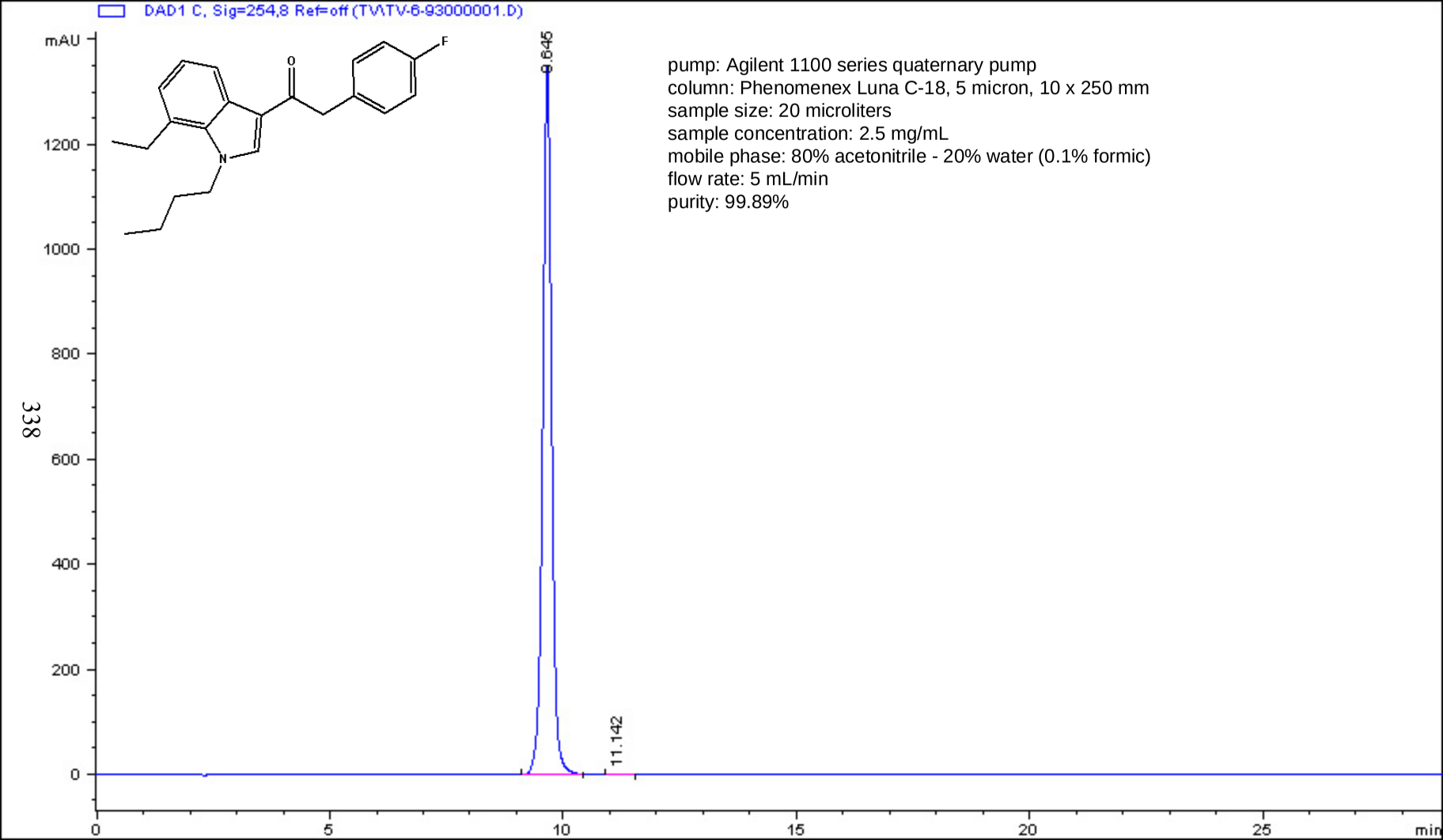

pump: Agilent 1100 series quaternary pump
column: Phenomenex Luna C-18, 5 micron, 10 x 250 mm
sample size: 20 microliters
sample concentration: 2.5 mg/mL
mobile phase: 80% acetonitrile - 20% water (0.1% formic)
flow rate: 5 mL/min
purity: 99.89%

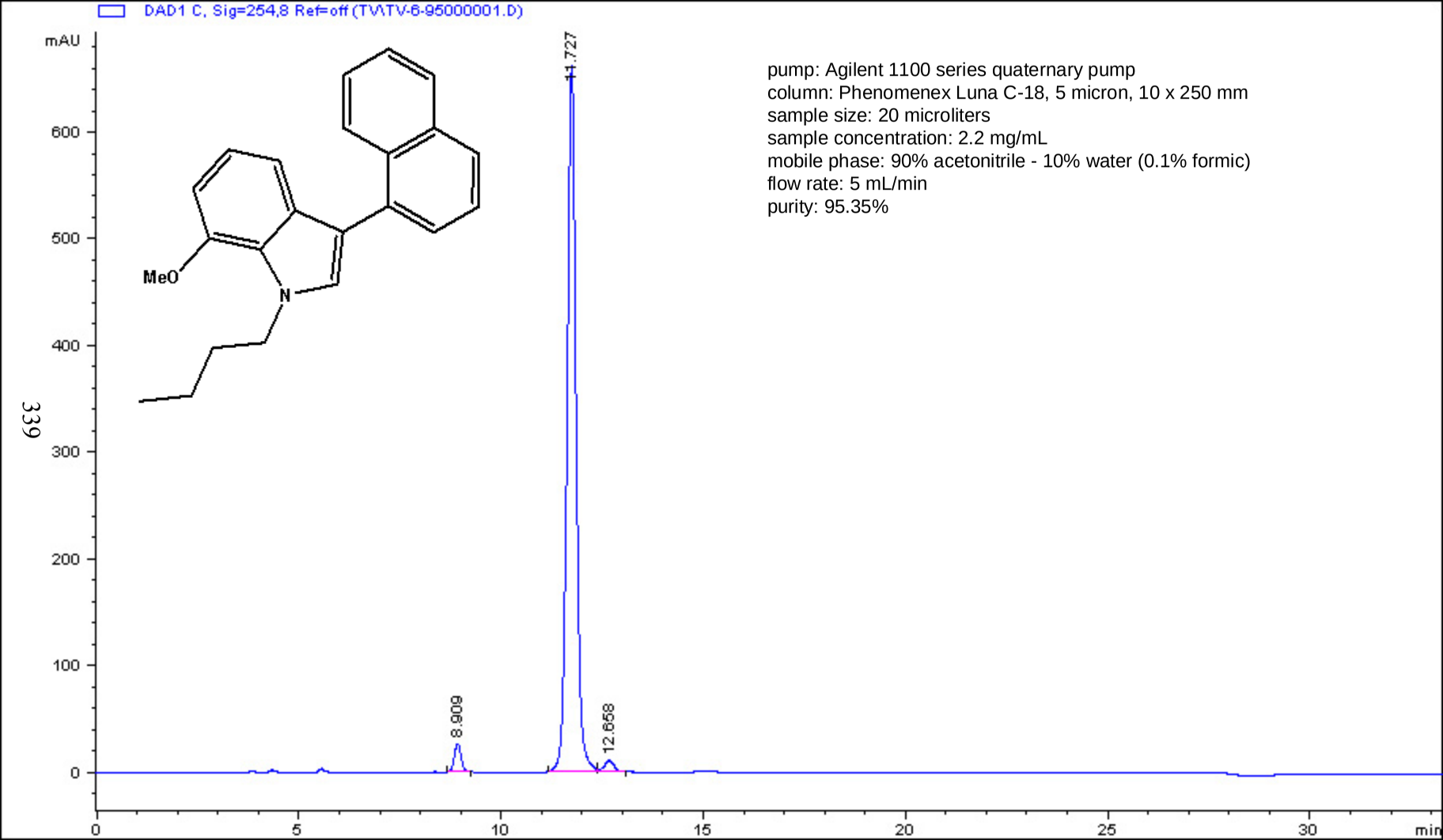
DAD1 C, Sig=254,8 Ref=off (TV\TV-6-95000001.D)
mAU
600
500
400
300
200
100
0
MeO
N
8.909
11.727
12.658
0
5
10
15
20
25
30
min
pump: Agilent 1100 series quaternary pump
column: Phenomenex Luna C-18, 5 micron, 10 x 250 mm
sample size: 20 microliters
sample concentration: 2.2 mg/mL
mobile phase: 90% acetonitrile - 10% water (0.1% formic)
flow rate: 5 mL/min
purity: 95.35%

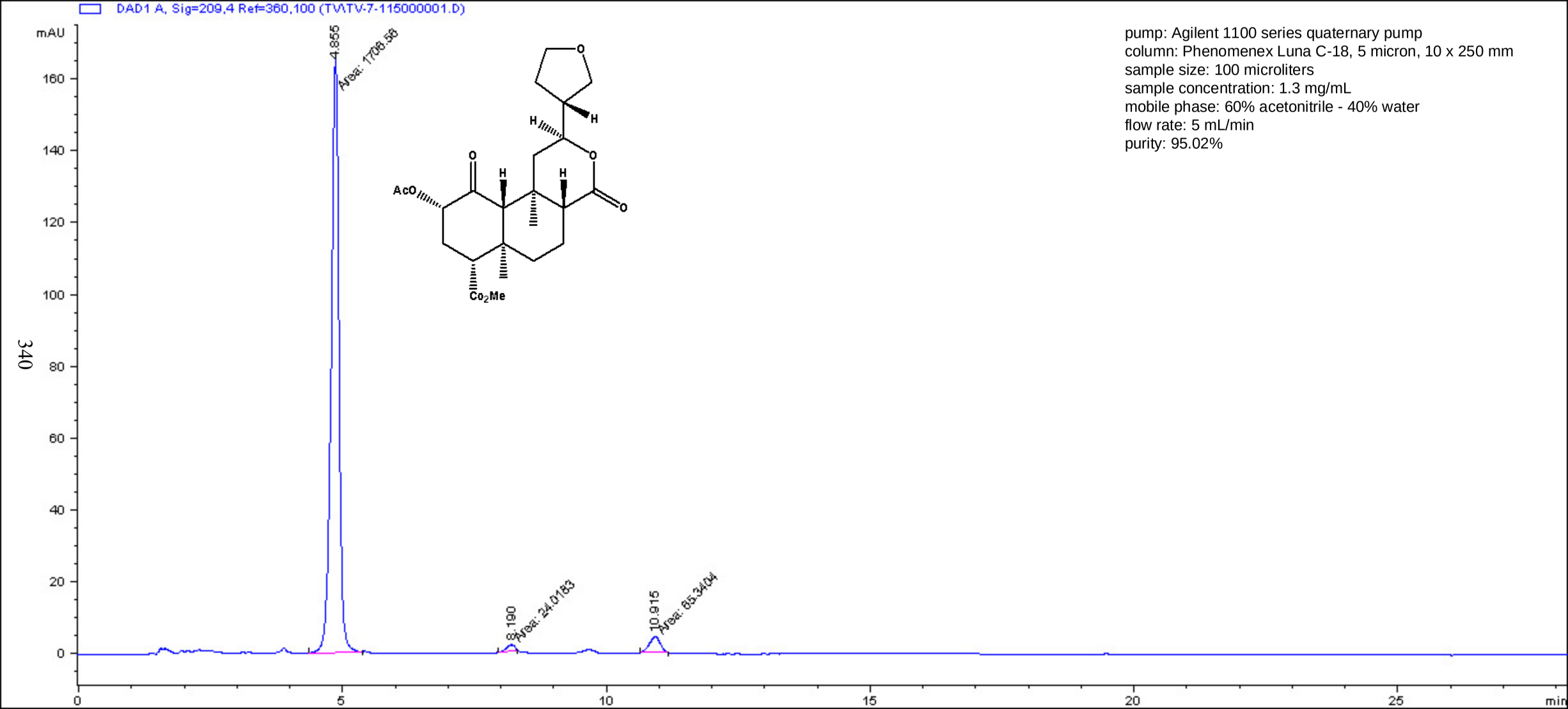
DAD1 A, Sig=209,4 Ref=360,100 (TV\TV-7-115000001.D)
mAU
4.855
Area: 1706.58
8.190
Area: 24.0183
10.915
Area: 65.3404
AcO
Co2Me
pump: Agilent 1100 series quaternary pump
column: Phenomenex Luna C-18, 5 micron, 10 x 250 mm
sample size: 100 microliters
sample concentration: 1.3 mg/mL
mobile phase: 60% acetonitrile - 40% water
flow rate: 5 mL/min
purity: 95.02%
min

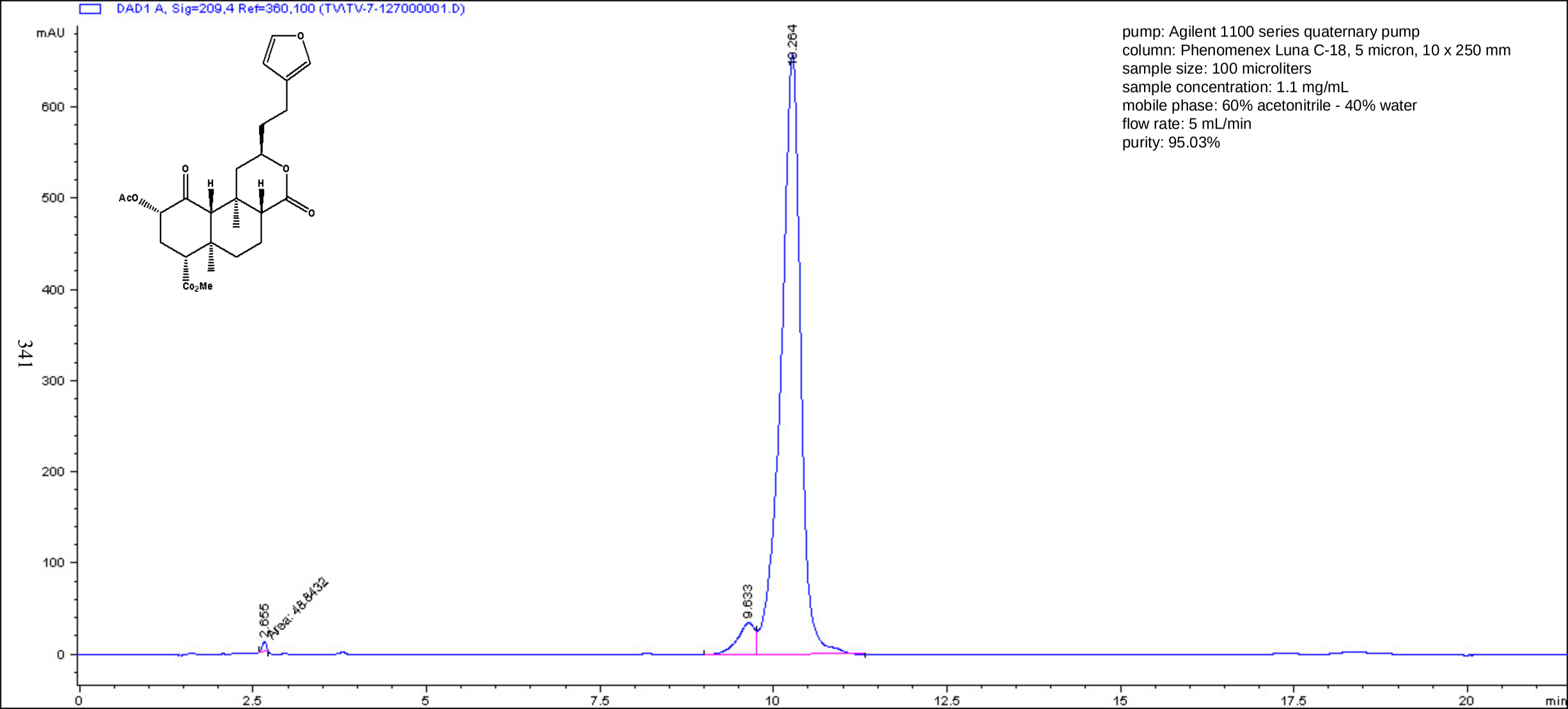
DAD1 A, Sig=209,4 Ref=360,100 (TV\TV-7-127000001.D)
mAU
600
500
400
300
200
100
0
AcO
O
H
H
O
O
O
Co2Me
2.655
Area: 48.84432
9.633
10.264
pump: Agilent 1100 series quaternary pump
column: Phenomenex Luna C-18, 5 micron, 10 x 250 mm
sample size: 100 microliters
sample concentration: 1.1 mg/mL
mobile phase: 60% acetonitrile - 40% water
flow rate: 5 mL/min
purity: 95.03%
0
2.5
5
7.5
10
12.5
15
17.5
20
min

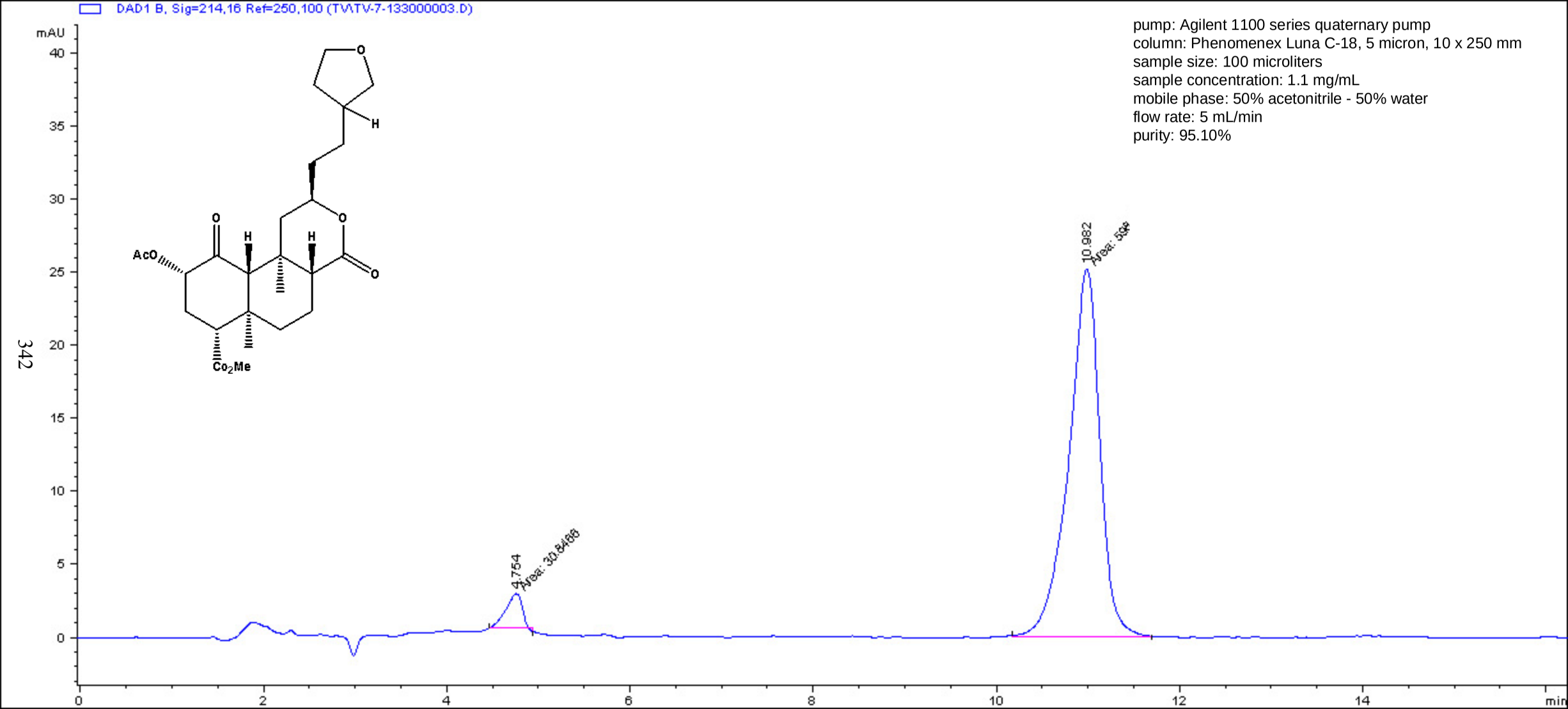
DAD1 B, Sig=214,16 Ref=250,100 (TV\TV-7-133000003.D)
mAU
40
35
30
25
20
15
10
5
0
AcO
O
H
H
O
O
O
O
H
Co2Me
4.754
Area: 30.8466
10.982
Area: 5qe
0
2
4
6
8
10
12
14
min
pump: Agilent 1100 series quaternary pump
column: Phenomenex Luna C-18, 5 micron, 10 x 250 mm
sample size: 100 microliters
sample concentration: 1.1 mg/mL
mobile phase: 50% acetonitrile - 50% water
flow rate: 5 mL/min
purity: 95.10%

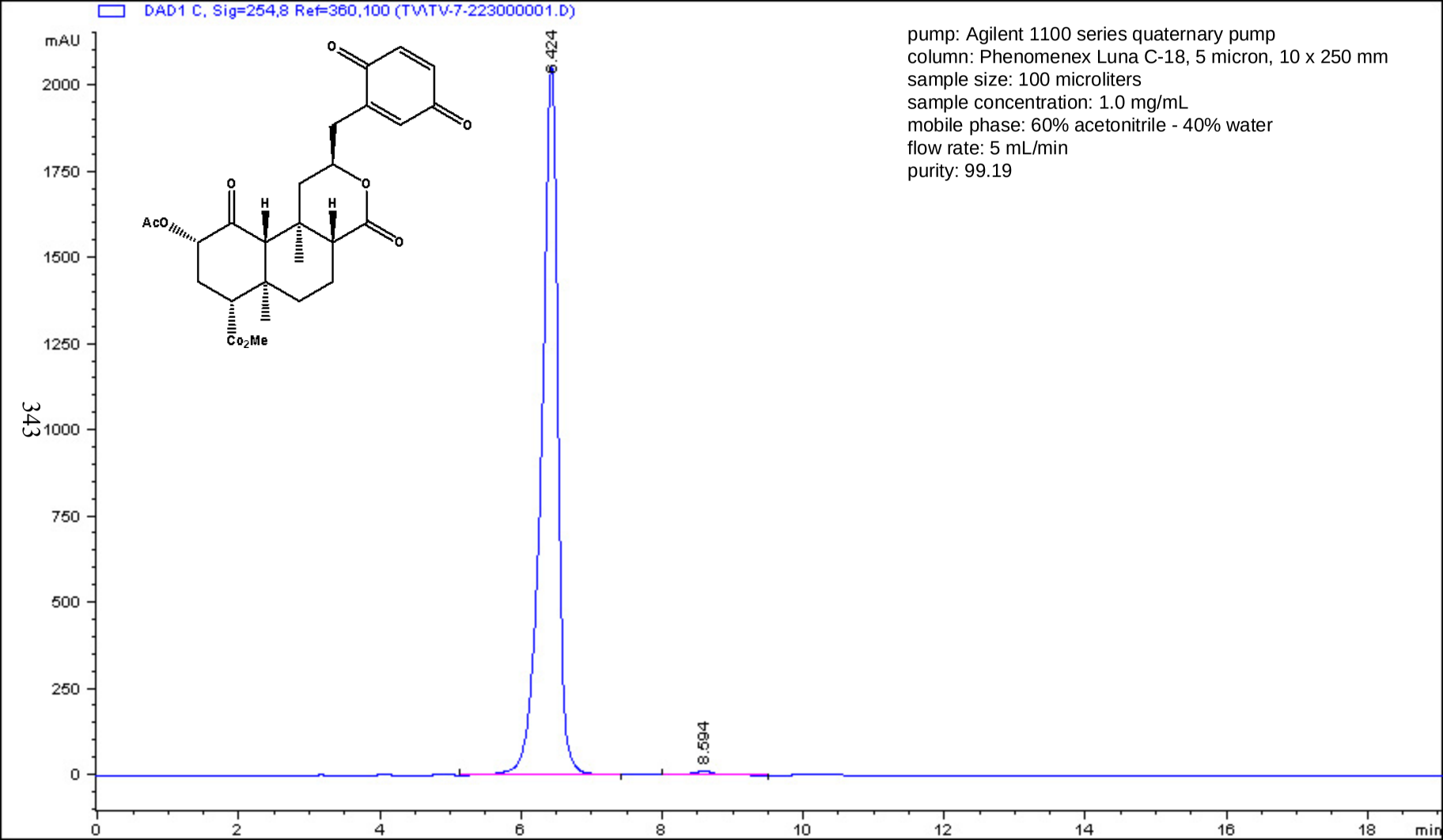
DAD1 C, Sig=254,8 Ref=360,100 (TV\TV-7-223000001.D)
mAU
2000
1750
1500
1250
1000
750
500
250
0
6.424
8.594
0
2
4
6
8
10
12
14
16
18
min
AcO
H
H
O
O
O
O
O
Co2Me
pump: Agilent 1100 series quaternary pump
column: Phenomenex Luna C-18, 5 micron, 10 x 250 mm
sample size: 100 microliters
sample concentration: 1.0 mg/mL
mobile phase: 60% acetonitrile - 40% water
flow rate: 5 mL/min
purity: 99.19